Eye in systemic diseases

Edited by
Anna Maria Roszkowska, Paolo Fogagnolo and Piergiorgio Neri

About Frontiers

Frontiers is more than just an open access publisher of scholarly articles: it is a pioneering approach to the world of academia, radically improving the way scholarly research is managed. The grand vision of Frontiers is a world where all people have an equal opportunity to seek, share and generate knowledge. Frontiers provides immediate and permanent online open access to all its publications, but this alone is not enough to realize our grand goals.

Frontiers journal series

The Frontiers journal series is a multi-tier and interdisciplinary set of open-access, online journals, promising a paradigm shift from the current review, selection and dissemination processes in academic publishing. All Frontiers journals are driven by researchers for researchers; therefore, they constitute a service to the scholarly community. At the same time, the *Frontiers journal series* operates on a revolutionary invention, the tiered publishing system, initially addressing specific communities of scholars, and gradually climbing up to broader public understanding, thus serving the interests of the lay society, too.

Dedication to quality

Each Frontiers article is a landmark of the highest quality, thanks to genuinely collaborative interactions between authors and review editors, who include some of the world's best academicians. Research must be certified by peers before entering a stream of knowledge that may eventually reach the public - and shape society; therefore, Frontiers only applies the most rigorous and unbiased reviews. Frontiers revolutionizes research publishing by freely delivering the most outstanding research, evaluated with no bias from both the academic and social point of view. By applying the most advanced information technologies, Frontiers is catapulting scholarly publishing into a new generation.

What are Frontiers Research Topics?

Frontiers Research Topics are very popular trademarks of the *Frontiers journals series*: they are collections of at least ten articles, all centered on a particular subject. With their unique mix of varied contributions from Original Research to Review Articles, Frontiers Research Topics unify the most influential researchers, the latest key findings and historical advances in a hot research area.

Find out more on how to host your own Frontiers Research Topic or contribute to one as an author by contacting the Frontiers editorial office: frontiersin.org/about/contact

Eye in systemic diseases

Topic editors

Anna Maria Roszkowska — University of Messina, Italy

Paolo Fogagnolo — University of Milan, Italy

Piergiorgio Neri — Cleveland Clinic Abu Dhabi, United Arab Emirates

Citation

Roszkowska, A. M., Fogagnolo, P., Neri, P., eds. (2023). *Eye in systemic diseases*. Lausanne: Frontiers Media SA. doi: 10.3389/978-2-83252-117-5

Table of contents

Check for updates

Editorial: Eye in systemic diseases

Anna M. Roszkowska[1,2]*, Paolo Fogagnolo[3] and
Piergiorgio Neri[4,5,6]

[1]Ophthalmology Clinic, Department of Biomedical Sciences, University of Messina, Messina, Italy,
[2]Ophthalmology Clinic, Faculty of Medicine and Health Sciences, Andrzej Frycz Modrzewski Kraków
University, Kraków, Poland, [3]Ophthalmology Clinic, University of Milan, Milan, Italy, [4]The Eye Institute,
Cleveland Clinic Abu Dhabi, Abu Dhabi, United Arab Emirates, [5]Cleveland Clinic Lerner College of
Medicine, Case Western Reserve University, Cleveland, OH, United States, [6]College of Medicine and
Health Sciences, Khalifa University, Abu Dhabi, United Arab Emirates

Editorial on the Research Topic
Eye in systemic diseases

The systemic diseases might involve the eyes in many ways, either with typical signs and symptoms or, often, with atypical presentation.

A rapid diagnosis may promote prompt treatment and a better clinical outcome in different cases.

Ocular involvement is present in metabolic, vascular, and rheumatologic diseases with retinopathy, inflammation, ocular surface, and corneal involvement. It may also be observed in different genetic syndromes. On the other hand, several systemic therapies may induce ocular changes, potentially affecting visual acuity.

This Research Topic aims to provide as comprehensive as possible information on ocular changes in systemic diseases, the signs, and symptoms that should be considered when systemic diseases are suspected. Additionally, it aims to evidence the ocular involvement in systemic disease and to highlight the necessity of the multidisciplinary approach for diagnosis and treatment.

Diabetes is undoubtedly the most common disease, with increasing prevalence worldwide, that involves different organs and tissues with diabetic angiopathy and neuropathy. It affects the eye with many degrees of severity diabetic retinopathy (DR) and cornea with tiny fibers neuropathy that affects the corneal sub-basal nerve plexus and may lead to severe visual impairment. In addition, it was reported that DR could be associated with cardiovascular involvement and stroke (1, 2).

Barrot et al. evaluated the role of diabetic retinopathy as a predictor of cardiovascular morbidity and mortality in subjects with type 2 diabetes in the Catalonia (Spain) population.

The authors investigated the predictive value of DR with its severity with the incidence of major cardiovascular events such as coronary heart disease, stroke, and all-cause mortality in subjects with T2DM in a Mediterranean region. They concluded that DR is related to coronary heart disease, macrovascular events, and all-cause mortality among persons with T2DM. The authors highlighted the importance of prompt screening and proper treatment of diabetic patients with DR to avoid cardiovascular complications leading to death.

Continuing with diabetes, another paper focused on the association between serum magnesium levels and diabetic macula edema (DME) in patients with DR (Xiang et al.). The systemic conditions that result from reduced serum magnesium might worsen the DR and promote DME with severe visual impairment (3).

The authors demonstrated that a higher serum magnesium level was associated with a lower risk of DME in patients with DR. These data open a new Research Topic to assess whether appropriate magnesium supplementation in diabetic patients reduces the risk of DME.

The relation between DR and Parkinson's disease (PD) as diabetes with DR and PD share some pathophysiological mechanisms related to stopped dopamine activity as both brain and retina are characterized by expression of D1like and D2-like dopamine receptors. So, the recognition of the DR as a marker of PD was hypothesized (4).

Mauricio et al. evaluated the primary health care large population in Catalonia (Spain) with type 2 diabetes and diabetic retinopathy for the risk of occurrence of PD. The authors concluded that DR was not associated with an increased risk of PD after adjusting for different risk factors such as age, male sex, and diabetes duration.

Dry eye is a multifactorial ocular surface disease affecting up to 50% of the population, significantly impacting the quality of life. Several risk factors for developing the disease and sleep apnea may dramatically impact ocular surface conditions (5). Pu et al. demonstrated a higher prevalence of DED in patients with obstructive sleep apnea syndrome (OSA), with a significant correlation between DED parameters worsening and OSA severity. This evident interaction should be addressed in patients with OSA, and proper ocular surface therapy should be considered.

Severe cornea and ocular surface disease are represented by neurotrophic keratitis (NK). Several systemic diseases, such as diabetes, rheumatoid arthritis, and atopia, might produce NK with severe visual impairment. Therefore, the patients should be monitored to promptly diagnose the early stage of corneal involvement to start the appropriate therapy to avoid, if possible, the progression that may lead to visual loss (6–10). In the paper related to NK in systemic diseases, Meduri et al. evidenced that the leading cause of NK was post-neuroma surgery (36%), followed by diabetes (18%). The remaining causes were rheumatoid arthritis (9%), post-traumatic (9%), post-surgery (9%), atopic (9%), and Graves' disease (9%). Additionally, the results of therapy with rh-NGF (Cenegermin) were presented, and the authors concluded that current knowledge of the pathogenesis of NK and the introduction of topical recombinant human Nerve Growth factor (rh-NGF) has significantly changed the natural history of the disease.

The effects of smoking on the microvascular system result in ocular complications (11).

The exciting paper of Xu et al. on the impact of chronic smoking on the microvascular system demonstrated the damage to the retinal vascular system. Furthermore, the authors highlighted the role of prevention and lifestyle improvement in preventing systemic diseases.

The research and validation of the new accurate and reliable tools to be used in the screening and assessment of systemic diseases are of extraordinary actuality, primarily due to the remarkable technological progress and availability of instruments increasingly sophisticated.

Retinal changes in different neurodegenerative diseases suggest its parallel involvement with significant differences. Therefore,

the retina was proposed as the window to the neurodegenerative changes in the central nervous system (12).

For this purpose, Deng et al. performed a systematic review and meta-analysis to evaluate retinal and microvascular parameters in patients with PD as compared to healthy controls. The authors considered RNFL, macular, GCL, vessel density, and optic disk area evaluated using OCT. The study evidenced that studied parameters were significantly lower in PD patients confirming that OCT and OCTA might play a role in detecting early morphological retinal changes in patients with PD and consequently support clinicians in diagnostic processes.

Additionally, OCT can classify PD patients accordingly to measure retinal changes. The authors speculated that in the next future, the OCT and OCTA might be used to assess the progression of PD based on variations of retinal parameters.

The last decades of exceptional technological progress have offered clinicians and researchers new diagnostic tools for visual disease assessment and follow-up.

And while OCT continuously improved and became essential for retinal examination, in corneal semiotics, AS-OCT and IVCM are now fundamental. Moreover, the use of IVCM to diagnose systemic diseases by corneal SBNP examination has become of growing interest, and its use in the assessment of diabetic peripheral polyneuropathy was widely documented (13–16).

Gu et al. performed a review of corneal confocal microscopy in the assessment of non-neurological autoimmune diseases. The authors concluded that IVCM parameters were altered in patients with NNAI affections compared to healthy subjects and highlighted the role of IVCM in early diagnosis and follow-up of affected patients.

The research to develop a more accurate analysis of IVCM data is the topic of the paper of Abicca et al., who presented the new algorithm for the evaluation of corneal nerves beadings in diabetic patients using IVCM. This new evaluation method adds a further possibility to investigate nerves changes in the early stage of peripheral neuropathy.

Lombardo et al. reports retinal imaging with new devices and a new approach to AMD.

Age-related macular degeneration is a visual threatening multifactorial disease with several systemic disorders such as hypertension, overweight, and low dietary intake of carotenoids act as decisive risk factors (17). In their report, the authors present a new system providing topical delivery of lutein into the retina using iontophoresis and show promising results of the pilot study on patients with AMD (18, 19). Furthermore, the authors discuss the advantage of using adaptive optics technology to improve the performance of optical systems by reducing the effects of optical distortions. Consequently, the improved resolution provides a more sensitive tool to study, detect, and track retinal diseases. Additionally, they present Resonance Raman spectroscopy (RRS) as one of the most promising technologies for measuring macular carotenoid levels from the human retina (20, 21).

Ocular adverse effects of systemic therapies were the topic of some papers.

The use of dupilomab, a targeted biological drug for atopic dermatitis (AD), is widely performed in adults and children. But the adverse effects could be expected, and they manifest with ocular

surface diseases (22). Jia et al. reviewed ocular adverse effects in patients treated with dupilumab for atopic dermatitis. The AE associated with the therapy manifested in up to 50% of patients with non-infectious conjunctivitis, followed by ocular pruritus, blepharitis, xerophthalmia, and keratitis. The cause is attributable to the inhibition of goblet cells through blocking IL-4 and IL-13 with dupilumab, which results in reduced mucin secretion. Another mechanism of conjunctivitis may be associated with serum IgE, thymus, and activation-regulated chemokine in dupilumab-treated patients (23). The authors reported good treatment results with fluorometholone or tacrolimus in affected patients providing dermatologists and ophthalmologists with diagnostic and therapeutic recommendations.

The widespread use of local and systemic corticosteroids might be controversial, and accurate estimation of risk and benefits should be consistently done (24). This problem emerges from the case report on the role of corticosteroids in treating acute ocular toxoplasmosis in an immunocompetent patient (25). Lin et al. showed that the early use of systemic corticosteroids in patients with acquired ocular toxoplasmosis might induce severe retinal visual-threatening complications. Therefore, they recommend accurate and continuous visual monitoring during therapy.

In conclusion, this special issue includes papers that provide information on ocular involvement in systemic disease that should be promptly diagnosed and treated. The multidisciplinary approach to diagnose, treat, and monitor the patients is recommended. Additionally, the issue highlights new possibilities to diagnose and follow up different systemic diseases by ophthalmic evaluation using the new examination tools. We hope that the content of this special issue will raise the level of understanding how the systemic diseases might impact on ocular health.

Author contributions

AR and PF drafted and wrote the paper. PN revised and wrote the paper. All authors contributed to the article and approved the final version.

Conflict of interest

The authors declare that the research was conducted in the absence of any commercial or financial relationships that could be construed as a potential conflict of interest.

Publisher's note

All claims expressed in this article are solely those of the authors and do not necessarily represent those of their affiliated organizations, or those of the publisher, the editors and the reviewers. Any product that may be evaluated in this article, or claim that may be made by its manufacturer, is not guaranteed or endorsed by the publisher.

References

1. Guo VY, Cao B, Wu X, Lee JJW, Zee BC. Prospective association between diabetic retinopathy and cardiovascular disease-a systematic review and meta-analysis of cohort studies. *J Stroke Cerebrovasc Dis.* (2016) 25:1688–95. doi: 10.1016/j.jstrokecerebrovasdis.2016.03.009

2. Hu K, Jiang M, Zhou Q, Zeng W, Lan X, Gao Q, et al. Association of diabetic retinopathy with stroke: a systematic review and meta-analysis. *Front Neurol.* (2021) 12:626996. doi: 10.3389/fneur.2021.626996

3. Xing B, Xu X, Li C, Zhao Y, Wang Y, Zhao W. Reduced serum magnesium levels are associated with the occurrence of retinopathy in patients with type 2 diabetes mellitus: a retrospective study. *Biol Trace Elem Res.* (2021) 200:2025–32. doi: 10.1007/s12011-021-02824-w

4. Cereda E, Barichella M, Pedrolli C, Klersy C, Cassani E, Caccialanza R, et al. Diabetes and risk of Parkinson's disease: a systematic review and meta-analysis. *Diabetes Care.* (2011) 34:2614–23. doi: 10.2337/dc11-1584

5. Magno MS, Utheim TP, Snieder H, Hammond CJ, Vehof J. The relationship between dry eye and sleep quality. *Ocul Surf.* (2021) 20:13–9. doi: 10.1016/j.jtos.2020.12.009

6. Bonini S, Lambiase A, Rama P, Sinigaglia F, Allegretti M et al. Phase II randomized, double-masked, vehicle-controlled trial of recombinant human nerve growth factor for neurotrophic keratitis. *Ophthalmology.* (2018) 125:1332–43. doi: 10.1016/j.ophtha.2018.02.022

7. Saad S, Abdelmassih Y, Saad R, Guindolet D, Khoury SE, Doan S, et al. Neurotrophic keratitis: frequency, etiologies, clinical management and outcomes. *Ocul Surf.* (2020) 18:231–6. doi: 10.1016/j.jtos.2019.11.008

8. Roszkowska AM, Inferrera L, Aragona E, Romina G, Postorino EI, Aragona P. Clinical and instrumental assessment of the corneal healing in moderate and severe neurotrophic keratopathy treated with rh-NGF (Cenegermin). *European J Ophthalmol.* (2022) 32:3402–10 doi: 10.1177/11206721221097584

9. Inferrera L, Aragona E, Wylegała A, Valastro A, Latino G, Postorino EI et al. The role of hi-tech devices in assessment of corneal healing in patients with neurotrophic keratopathy. *J Clin Med Ophthalmol.* (2022) 12:3924.

10. Fogagnolo P, Giannaccare G, Bolognesi F, Digiuni M, Tranchina L, Rossetti L et al. Direct versus indirect corneal neurotization for the treatment of neurotrophic keratopathy: a multicenter prospective comparative study. *Am J Ophthalmol.* (2020) 220:203–14. doi: 10.1016/j.ajo.2020.07.003

11. Galor A, Lee DJ. Effects of smoking on ocular health. *Curr Opin Ophthalmol.* (2011) 22:477–82. doi: 10.1097/ICU.0b013e32834bbe7a

12. Moreno-Ramos T, Benito-Leon J, Villarejo A, Bermejo-Pareja F. Retinal nerve fiber layer thinning in dementia associated with Parkinson's disease, dementia with Lewy bodies, and Alzheimer's disease. *J Alzheimers Dis.* (2013) 34:659–64. doi: 10.3233/JAD-121975

13. Patton N, Aslam T, Macgillivray T, Pattie A, Deary IJ, Dhillon B. Retinal vascular image analysis as a potential screening tool for cerebrovascular disease: a rationale based on homology between cerebral and retinal microvasculatures. *J Anat.* (2005) 206:319–48. doi: 10.1111/j.1469-7580.2005.00395.x

14. Roszkowska AM, Wylegała A, Gargiulo L, Inferrera L, Russo M, Mencucci R et al. Corneal sub-basal nerve plexus in non-diabetic small fiber polyneuropathies and the diagnosticrole of the in vivo corneal confocal microscopy. *J Clin Med.* (2023) 12:664. doi: 10.3390/jcm12020664

15. Cruzat A, Qazi Y, Hamrah P. In vivo confocal microscopy of corneal nerves in health and disease. *Ocul Surf.* (2017) 15:15–47. doi: 10.1016/j.jtos.2016.09.004

16. Roszkowska AM, Wylegala A, Inferrera L, Spinella R, Gargano R, Orzechowska-Wylegala B, et al. Impact of corneal parameters, refractive error and age on density and morphology of the subbasal nerve plexus fibers in healthy adults. *Sci Rep.* (2021) 11:6076. doi: 10.1038/s41598-021-85597-5

17. Roszkowska AM, Licitra C, Tumminello G, Postorino EI, Colonna MR, Aragona P. Corneal nerves in diabetes-The role of the in vivo corneal confocal microscopy of the subbasal nerve plexus in the assessment of peripheral small fiber neuropathy. *Surv Ophthalmol.* (2021) 66:493–513. doi: 10.1016/j.survophthal.2020.09.003

18. Colijn JM, Meester-Smoor M, Verzijden T, de Breuk A, Silva R, Merle BMJ, et al. Genetic risk, lifestyle, and age-related macular degeneration in europe: the EYE-RISK consortium. *Ophthalmology.* (2021) 128:1039–49. doi: 10.1016/j.ophtha.2020.11.024

19. Sousa-Martins D, Sousa S, Duarte J, Marta M, Lombardo M, Lombardo G. Lutein reaches the retina following iontophoresis application. *Invest Ophthalmol Vis Sci.* (2016) 57:106.

20. Lombardo M, Villari V, Micali N, Roy P, Sousa SH, Lombardo G. Assessment of trans-scleral iontophoresis delivery of lutein to the human retina. *J Biophotonics.* (2018) 11:jbio.201700095. doi: 10.1002/jbio.201700095

21. Lombardo M, Serrao S, Devaney N, Parravano M, Lombardo G. Adaptive optics technology for high-resolution retinal imaging. *Sensors.* (2013) 13:334–66. doi: 10.3390/s130100334

22. Bernstein PS, Yoshida MD, Katz NB, McClane RW, Gellermann W. Raman detection of macular carotenoid pigments in intact human retina. *Invest Ophthalmol Vis Sci.* (1998) 39:2003–11.

23. Akinlade B, Guttman-Yassky E, de Bruin-Weller M, Simpson EL, Blauvelt A, Cork MJ, et al. Conjunctivitis in dupilumab clinical trials. *Br J Dermatol.* (2019) 181:459–73. doi: 10.1111/bjd.18276

24. Uchida H, Kamata M, Nagata M, Fukaya S, Hayashi K, Fukuyasu A, et al. Conjunctivitis in patients with atopic dermatitis treated with dupilumab is associated with higher baseline serum levels of IgE and TARC but not clinical severity in a real-world setting. *J Am Acad Dermatol.* (2020) 82:1247–9. doi: 10.1016/j.jaad.2019.12.039

25. Oray M, Ozdal PC, Cebeci Z, Kir N, Tugal-Tutkun I. Fulminant ocular toxoplasmosis: the hazards of corticosteroid monotherapy. *Ocul Immunol Inflamm.* (2016) 24:637–46. doi: 10.3109/09273948.2015.1057599

Check for updates

Retinal Microvascular Reactivity in Chronic Cigarette Smokers and Non-smokers: An Observational Cross-Sectional Study

Huan Xu [1,2‡], Yuan Zong [1,2‡], Jian Yu [1,2], Chunhui Jiang [1,2*†], Haohao Zhu [3*†] and Xinghuai Sun [1,2]

[1] Department of Ophthalmology and Visual Science, Eye, Ear, Nose and Throat Hospital, Shanghai Medical College of Fudan University, Shanghai, China, [2] Key Laboratory of Myopia of State Health Ministry and Key Laboratory of Visual Impairment and Restoration of Shanghai, Shanghai, China, [3] Department of Ophthalmology, Shanghai Fifth People's Hospital, Fudan University, Shanghai, China

Purpose: To evaluate the changes in the retinal microvasculature and its reactivity in chronic cigarette smokers.

Methods: Thirty-four male chronic cigarette smokers and 18 male non-smokers were enrolled. Optical coherence tomography angiography was used to measure the perfused retinal vessel densities (PVDs) of the peripapillary and parafoveal areas at baseline and during phase IV of the Valsalva maneuver (VM-IV). Systemic blood pressure and intraocular pressure were also measured.

Results: The baseline PVD in the peripapillary area of the smokers was significantly lower than the non-smokers ($59.56 \pm 2.26\%$ vs. $61.67 \pm 3.58\%$, respectively; $P = 0.005$). However, there was no significant difference in the foveal avascular zone or parafoveal PVD between the two groups. During VM-IV, the peripapillary PVD of the smokers decreased by $1.13 \pm 3.50\%$, which was significantly less than that of the non-smokers ($-3.83 \pm 4.26\%$, $P < 0.05$). Similarly, the parafoveal PVD of the smokers decreased by $5.49 \pm 9.70\%$, which was significantly less than the percentage change of the non-smokers ($-13.01 \pm 8.39\%$, $P < 0.05$). There was no significant difference in the percentage change in systemic blood pressure parameters between the two groups.

Conclusion: The retinal microvasculature and its reactivity were impaired in chronic smokers compared with non-smokers. The extent of impairment differed among different regions of the fundus.

Keywords: retinal microvasculature, reactivity, optical coherence tomography angiography (OCTA), blood pressure, Valsalva maneuver (VM)

INTRODUCTION

Smoking is a global public health issue, which causes ~7 million deaths each year worldwide (1). Tobacco consumption in China accounts for 40% of global consumption (2). About 300 million individuals were reported to be current smokers in China in 2010, and over half (52.9%) of adult men (288 million) were smokers (3).

Cigarette smoke contains numerous compounds, many of which have toxic and deleterious effect on the vascular system of the human body (4). According to a World Health Organization report, cigarette smoking contributes to 10–30% of all cardiovascular deaths worldwide (5), and several epidemiological surveys have reported that smoking is also strongly associated with ocular vascular diseases, such as retinal ischemia and anterior ischemic optic neuropathy (6). Although the exact pathophysiological process remains unclear, endothelial dysfunction is thought to play a crucial role in the vascular diseases induced by smoking.

The retinal vasculature has an autoregulatory system to maintain constant blood flow and to ensure that the high metabolic needs of the retina are met under various conditions (7). Nesper et al. reported a significant, transient variation of retinal vessel density during the transition from dark adaptation to ambient light (8). Vascular reactivity is a well-known marker of endothelial function. Several studies have demonstrated that the reduction in vascular reactivity is an important and early sign of vascular endothelial dysfunction, which occurs before the appearance of pathological changes (9). Measuring this autoregulatory system involves analyzing the variation in the amplitudes of vascular hemodynamic indices in response to different stimuli, such as flicker stimulation (9–11), elevated blood pressure (BP) (12), inhalation hyperoxia (13), and handgrip test (14). In previous studies in smokers, Halloran et al. reported that the reactivity of retinal arteries was lower in chronic smokers than in non-smokers (15). Garhöfer et al. demonstrated that the response of retinal veins to flicker stimulation also significantly reduced in smokers compared with that in non-smokers (16).

Recently, it has been reported that the capillaries are crucial sites at which blood flow is controlled (17). However, because the techniques available were limited, most of previous studies assessed the reactivity of large vessels, and the reactivity of the capillaries of smokers have not been well-studied. In recent years, the development of optical coherence tomography angiography (OCTA) has allowed clear visualization of retinal capillaries and non-invasive quantification (18). Our previous study demonstrated that OCTA can be used to evaluate the retinal microvascular reactivity to the variations in BP during phase IV of the Valsalva maneuver (VM-IV) (19). In this study, using the same equipment and stimuli, the reactivity of the retinal microvasculature is compared between chronic smokers and non-smokers.

MATERIALS AND METHODS

All procedures in this study were reviewed and approved by the Institutional Review Board of the Eye, Ear, Nose, and Throat Hospital of Fudan University in Shanghai, China. The research conformed to the tenets of the Declaration of Helsinki, and the enrolled subjects read and signed a written informed consent form.

Study Subjects

Healthy subjects who underwent a routine health checkup annually were enrolled in this study. Detailed ophthalmologic examinations were performed in all subjects, including slit-lamp biomicroscopy and a fundus examination. We collected the following basic ophthalmologic data: best-corrected visual acuity (BCVA), intraocular pressure (CT-80A Computerized Tonometer; Topcon, Tokyo, Japan), refractive error (Auto Refractometer AR-610; Nidek Co, Ltd, Tokyo, Japan), and axial length (AL; IOLMaster®; Carl Zeiss, Inc., Jena, Germany). The inclusion criteria for the study were: (1) BCVA > 0.8; (2) IOP < 21 mmHg; (3) AL of 21–25 mm; (4) a spherical equivalent from −3 to +3 diopters; and (5) no retinopathy or other abnormal ophthalmologic signs. The exclusion criteria were: (1) systemic diseases such as diabetes, hypertension, or other cardiovascular diseases; (2) a history of ocular trauma; (3) inability to correctly perform or complete the VM. The smoking history of the subjects was asked and recorded in detail. Fifty-two healthy male subjects, including 18 non-smokers and 34 chronic smokers, were ultimately enrolled in the study. Non-smokers are defined as subjects who have no smoking history and live in smoke-free environment. Chronic smokers are defined as subjects who have a minimum 10-year smoking history with one or more pack-years. Up to now, the smokers still remain their smoking habits.

Optical Coherence Tomography Angiography

OCTA scanning of the macular (6.0×6.0 mm^2) and peripapillary regions (4.5×4.5 mm^2) was performed with a spectral-domain OCT system (RTVue-XR Avanti with AngioVue AngioAnalytics, version 2017.100.0.1; Optovue Inc., Fremont, CA, USA), as described in a previous study. The system automatically identifies the parafoveal superficial capillary plexus (signal projected from 3 μm below the internal limiting membrane to the outer boundary of the inner plexiform layer), and generates en face retinal angiograms. The perfused vessel densities (PVDs) in the peripapillary area (a 700-μm-wide elliptical annulus, extending outward from the optic disc boundary) and parafoveal area (an annulus formed by an outer circle with a diameter of 3 mm and an inner circle with a diameter of 1 mm) were automatically calculated with the software. The foveal avascular zone (FAZ) area was also obtained directly from the system. The quality of the OCTA scanning images was determined by the signal strength index (SSI). Finally, the images with an SSI~60 or less were excluded from the analysis. The OCTA system embraced the eye-tracking function to decrease the residual motion artifacts and improve the quality of scanning images.

Study Protocol

All the subjects were required to refrain from coffee and alcohol consumption for 24 h before the examinations. Before the test, the subjects were asked to rest in a sitting position for 20 min. The baseline retinal PVDs was acquired with the OCTA system, as described above. At the same time, the baseline BP parameters, including the systolic BP (SBP), diastolic BP (DBP), and heart rate (HR), were recorded with a fully automatic BP monitor (HEM-7130; OMRON, Dalian, China). The subjects were then

instructed to perform the modified VM by taking a deep breath and forcefully blowing out against the closed glottis while occluding the nose with their fingers. The maximum expiratory pressure had to be sustained for 15 s. The subjects were then required to open their glottis and breath normally. As previously described, phase III of VM started with the release of pressure and lasts for 1–2 s, with a transient fall in BP, and was followed by an overshoot of BP in phase IV, which last about 10–20 s [20]. To investigate the retinal microvascular response to the elevation in BP induced in VM-IV, OCTA images were obtained 5 s after VM release. Because it took 5–7 s to pressurize the cuff, the examiner pressed the "start" button of the BP monitor when the VM strain was released. Therefore, the BP parameters and retinal angiogram images were acquired at almost the same time. After resting for 1 h, the subjects performed a second VM, and IOP was measured 5 s after VM release.

Statistical Analysis

Spherical equivalence (SE) was calculated as the algebraic sum of the spherical value plus one half of the cylindrical value. The mean arterial pressure (MAP) and ocular perfusion pressure (OPP) were calculated with the following formulae:

$$MAP = 1/3 \ (2 \times DBP + SBP)$$
$$OPP = 2/3 \ MAP–IOP$$

The response of the retinal PVDs to VM-IV was expressed as "Δ," which was equal to the percentage change relative to the baseline level. The changes in the systemic parameters were calculated using similar methods. To investigate the effects of VM on the various parameters, paired t-tests were used to compare the differences in the parameters between baseline and during VM-IV in the same group. The one-sample Kolmogorov-Smirnov test and Levine's test were used to test the normality of distributions and the equality of variance, respectively, of all datasets. According to the results, the SE value, ΔFAZ, and ΔDBP were compared between the two groups with Mann-Whitney U-tests. All other baseline parameters were compared with two-tailed independent-samples t-tests. The differences of changes of the other parameters between the two groups (non-smokers vs. chronic smokers) were compared with the general linear model multivariate analysis, which could adjust for the potential confounders (age, AL, and BCVA). A linear regression model was used to analyze the correlation between pack-years and the response of the retinal PVDs to VM-IV in parafoveal and peripapillary regions. Data are presented as means ± standard deviations and statistical significance was set at $P < 0.05$. All statistical analyses were performed with SPSS software (version 20.0; SPSS, Inc., Chicago, IL, USA).

RESULTS

Subject Characteristics

The right eyes of 34 male chronic smokers and 18 male non-smokers were enrolled in the study. For chronic smokers, the mean smoking history last for 23.53 ± 7.95 years. The average amount of smoking cigarettes was 26.51 ± 12.15 pack-years. **Table 1** shows all the subjects' demographic and ocular characteristics. There was no significant difference between the

two groups in terms of their age or basic ocular indices, including BCVA, SE, AL, and IOP (all $P > 0.05$; **Table 1**).

Baseline BP and Retinal PVDs

Compared with the non-smokers, the smokers had similar baseline values in several systemic and ocular parameters, including SBP, DBP, HR, MAP, and OPP (all $P > 0.05$; **Table 2**). The peripapillary PVD was significantly lower in the smokers than in the non-smokers (59.56 ± 2.26% vs. 61.67 ± 3.58%, respectively; $P = 0.005$; **Table 3**). However, there was no significant difference in FAZ or parafoveal PVD between the smokers and non-smokers (both P > 0.05; **Table 3**).

Response to VM-IV

Compared with the baseline levels, there were significant increases in SBP, DBP, MAP, and OPP during VM-IV in the smokers and non-smokers (all $P < 0.05$; **Table 2**). However, IOP and HR did not significantly change in either group (both $P > 0.05$; **Table 2**). There was no significant difference between the two groups in the percentage change in SBP, DBP, MAP, OPP, IOP, or HR (**Table 2**).

During VM-IV, the peripapillary PVD and parafoveal PVD of the nonsmokers decreased significantly by 3.83 ± 4.26% and 13.01 ± 8.39%, respectively (both $P < 0.05$; **Figure 1**, **Table 3**). However, in the smokers, the peripapillary PVD remained unchanged ($-1.13 \pm 3.50\%$, $P > 0.05$) and only the parafoveal PVD significantly decreased ($-5.49 \pm 9.70\%$, $P < 0.05$; **Figure 1**, **Table 3**).

The percentage reductions in retinal PVDs (ΔPVD%) were compared between the two groups with the general linear model multivariate analysis. After adjusting for the potential confounders (age, AL and BCVA), the peripapillary ΔPVD% was significantly greater in the non-smokers than in the smokers (P = 0.036; **Figure 1**, **Table 3**). And the parafoveal ΔPVD% were also significantly greater in the non-smokers than in the smokers ($P = 0.017$; **Figure 1**, **Table 3**). Meanwhile, age was a significant factor that affected the comparison of parafoveal ΔPVD% between the two groups ($P = 0.028$). The FAZ area increased significantly in both the non-smokers and smokers (9.23 ± 16.51% vs. 8.74 ± 18.77%, respectively; both $P < 0.05$; **Table 3**), and ΔFAZ% was similar in both groups ($P = 0.413$; **Table 3**).

TABLE 1 | Subjects characteristics.

	Non-smokers	**Smokers**	**P**
Age (y)	43.88 ± 11.42	48.23 ± 9.94	0.165
BCVA (LogMAR) (Snellen)	0.01 ± 0.17 (20/20)	0.02 ± 0.11 (20/21)	0.823
SE (diopters)	−0.66 ± 1.49	−0.16 ± 0.92	0.093
AL (mm)	24.12 ± 0.91	23.65 ± 1.07	0.061
IOP (mmHg)	13.11 ± 3.23	12.85 ± 2.05	0.783

Data are presented as mean ± standard deviation.
BCVA, best-corrected visual acuity; SE, spherical equivalent; AL, axial length; IOP, intraocular pressure.
P, The SE values between the two group was compared with Mann-Whitney U-tests. All other parameters were compared with two-tailed independent sample t-tests.

TABLE 2 | Systemic parameter and other ocular findings before and after VM-IV in non-smokers and smokers.

	Baseline			VM-IV response (%)		
	Non-smokers	Smokers	P^a	Non-smokers	Smokers	P^b
SBP (mmHg)	119.33 ± 15.27	122.88 ± 13.39	0.390	$7.47 \pm 8.43^*$	$6.08 \pm 9.53^†$	0.606
DBP (mmHg)	76.29 ± 13.32	80.12 ± 9.09	0.282	$6.11 \pm 14.03^*$	$4.48 \pm 10.28^†$	0.635
MAP (mmHg)	90.93 ± 12.72	94.37 ± 10.01	0.288	$6.50 \pm 10.45^*$	$5.13 \pm 8.56^{††}$	0.613
IOP (mmHg)	13.11 ± 3.23	12.85 ± 2.05	0.783	1.24 ± 7.89	0.48 ± 6.38	0.707
OPP (mmHg)	47.56 ± 7.89	45.04 ± 10.20	0.366	$8.34 \pm 13.25^*$	$6.65 \pm 11.26^{††}$	0.630
HR (bpm)	72.67 ± 9.63	72.70 ± 9.00	0.991	-1.52 ± 2.87	-2.80 ± 8.51	0.437

VM-IV, phase IV of Valsalva maneuver; SBP, systolic blood pressure; DSP, diastolic blood pressure; MAP, mean arterial pressure; IOP, intraocular pressure; OPP, ocular perfusion pressure; HR, heart rate.

$^*P < 0.05$, Changes in parameters of non-smokers during VM-IV was tested with paired t-tests.

$^†P < 0.05$, $^{††}P < 0.01$, Changes in parameters of smokers during VM-IV was tested with paired t tests.

P^a, Comparison of baseline parameters between non-smokers and smokers, tested with two-tailed independent sample t-tests.

P^b, Comparison of percentage changes in parameters induced by VM-IV between non-smokers and smokers, tested with two-tailed independent sample t-tests and Mann–Whitney U-tests (DBP).

TABLE 3 | FAZ area and retinal PVDs before and after VM-IV in non-smokers and smokers.

	Baseline			VM-IV response (%)		
	Non-smokers	Smokers	P^a	Non-smokers	Smokers	P^b
FAZ area (mm^2)	0.33 ± 0.17	0.38 ± 0.12	0.232	$9.23 \pm 16.51^*$	$8.74 \pm 18.77^†$	0.413
Parafoveal PVD (%)	51.53 ± 0.98	51.95 ± 0.71	0.571	$-13.01 \pm 8.39^{**}$	$-5.49 \pm 9.70^{††}$	0.017#
Peripapillary PVD (%)	61.67 ± 3.58	59.56 ± 2.26	0.005	$-3.83 \pm 4.26^*$	-1.13 ± 3.50	0.036#

VM-IV, phase IV of Valsalva maneuver; FAZ, foveal avascular zone; PVD, perfused vessel density.

$^*P < 0.05$, $^{**}P < 0.01$, Changes in parameters of non-smokers during VM-IV was tested with paired t-tests.

$^†P < 0.05$, $^{††}P < 0.01$, Changes in parameters of smokers during VM-IV was tested with paired t-tests.

$P^a < 0.05$, Comparison of baseline parameters between non-smokers and smokers, tested with two-tailed independent-samples t-tests.

$^\#P^b < 0.05$, $^{\#\#}P^b < 0.01$, Comparison of percentage changes in parameters during VM-IV between non-smokers and smokers, tested with two-tailed independent-samples t-tests and Mann–Whitney U-tests (FAZ area).

For both smokers and non-smokers, the increase in BP during VM-IV induced a greater reduction in retinal PVD in the parafoveal region than in the peripapillary region (both $P < 0.05$; **Table 4**).

Linear regression analyses revealed that there was no significant correlation between pack-years and retinal microvascular response induced by VM-IV in either peripapillary region ($\beta = 0.444$, $P = 0.553$) or parafoveal region ($\beta = 0.415$, $P = 0.058$; **Figure 2**).

DISCUSSION

This study used OCTA to assess the potential damage of the retinal microvasculature and its reactivity in smokers. Compared with the non-smokers, the retinal microvasculature and its reactivity were impaired in the smokers, and the extent of impairment differed in different regions of the fundus.

The retinal PVD in the peripapillary area was lower in smokers than in non-smokers. A previous study found that nicotine, a major ingredient of tobacco, has direct toxic effect on the endothelium and smooth muscle cells (SMCs), leading to the loss of capillary vessels (21, 22). Several studies have also indicated that smoking increases the release of vasoconstrictive agents, such as endothelin (23). Consequently, vasoconstriction or the loss of retinal vessels may contribute to the reduced PVD detected in smokers.

Interestingly, no significant difference was found in the baseline parafoveal PVD between smokers and non-smokers. Although the detailed mechanism is still unclear, some inferences can be drawn from this phenomenon. First, four major retinal arteries and veins are located in the peripapillary region, whereas the parafoveal region mainly contains capillaries. In the retina, the larger vessels, such as arteries and arterioles, are encircled by vascular smooth muscle cells (VSMCs), whereas the capillaries are not fully covered by pericytes and their processes (24). Therefore, the major cells controlling the vascular tone differ in the parafoveal and peripapillary regions. Wang et al. found that chronic nicotine exposure elevated the resting intracellular calcium ion concentration and upregulated the expression of the canonical transient receptor potential channels in cultured VSMCs, which are responsible for
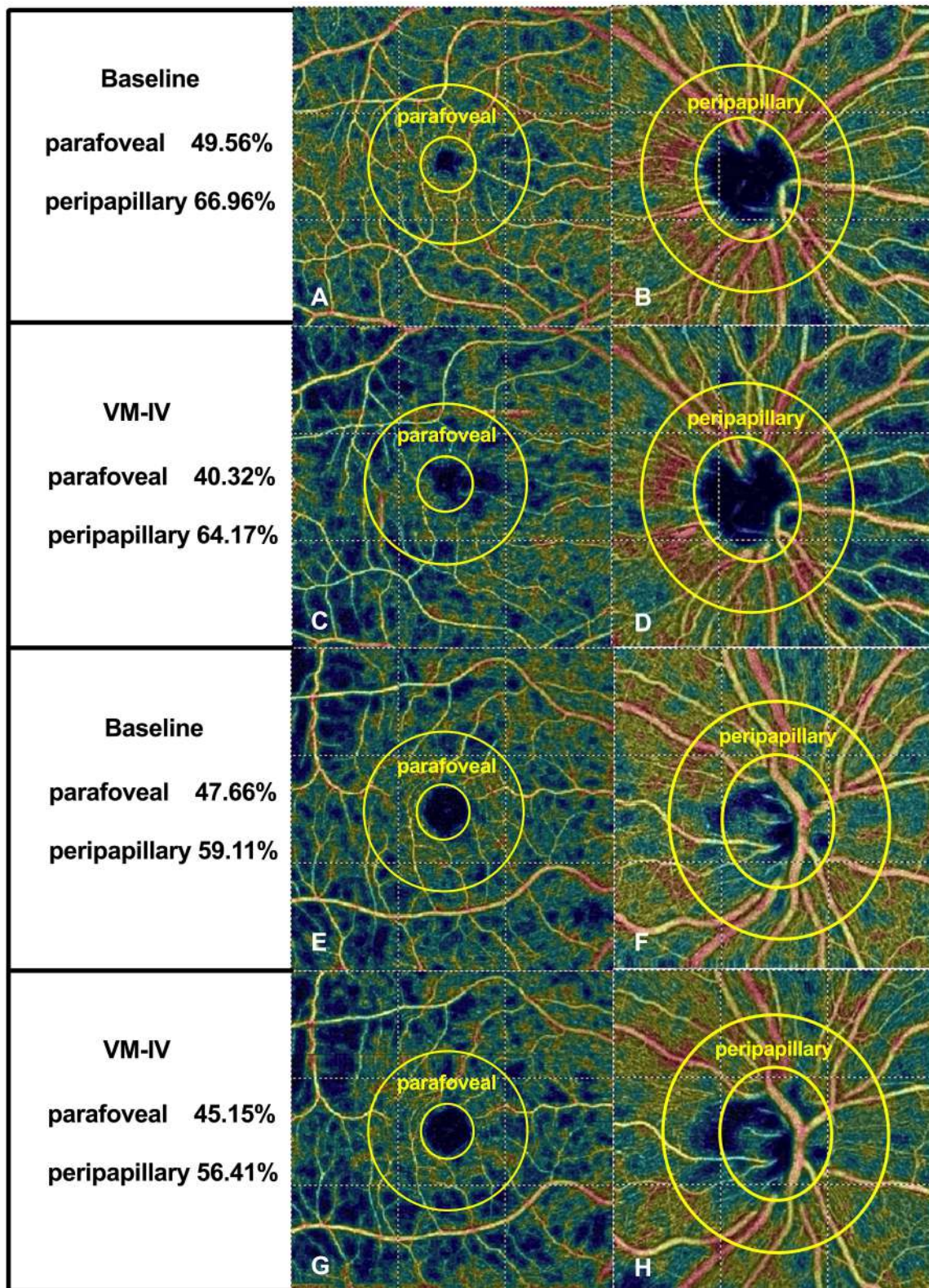
FIGURE 1 | Typical optical coherence tomography angiographic scanning images of non-smokers **(A–D)** and smokers **(E–H)** at baseline and during phase IV of the Valsalva maneuver.

the increased vascular tone (25).Thus, this may cause a difference in the extent of vessel contraction in different regions of the retina, explaining the different changes in vessel density in smokers.

The evaluation of retinal vascular reactivity is a sensitive diagnostic method because it reflects endothelial function; and retinal vascular reactivity is often impaired in the early stage of diseases, even before vascular structural damage is apparent (26). Using handgrip test, Sousa et al. found an early impairment of the retinal vascular reactivity in patients with type 1 diabetes without clinical diabetic retinopathy (27). VM is a simple, effective, and non-invasive method that is widely used as a diagnostic procedure in several disciplines (28, 29). The VM is divided into four physiological phases according to the BP response. The "overshoot" of BP occurs during VM-IV and lasts for ∼10–20 s as a result of the sustained vasoconstriction commencing in phase II. Therefore, VM is also used as a standard stimulus to evaluate the regulatory ability of the cardiac and cerebral vascular systems during variations in BP (29). The present study was designed to investigate the retinal microvascular reactivity to the elevation in BP during VM-IV.

Our study revealed that the retinal microvascular response to VM-IV in the peripapillary and parafoveal areas was significantly lower in smokers than in non-smokers. This result is consistent with previous reports. O'Halloran et al. reported that the magnitude of vasoconstriction in the retinal arteriole response to hyperoxia reduced in smokers compared to non-smokers (30). Similarly, Garhöfer et al. demonstrated that the hemodynamic response of retinal veins induced by flicker stimulation reduced in chronic smokers (16). However, the exact mechanism underlying impaired vascular reactivity has not been fully clarified. Our results show that VM-IV induced increases in BP and the ocular perfusion pressure. Under normal conditions, the retinal hemodynamic response to increasing OPP is caused by an increase in vascular resistance (12). This behavior is called the "myogenic response," and is controlled by VSMCs (7).The active contraction of VSMCs is responsible for counteracting the increased transmural pressure. Neymar et al. provided experimental evidence that chronic smoking induces hypoxemia and hypercapnia (31), and a recent study demonstrated that hypercapnia impairs the myogenic regulation of retinal vessels in response to changes in BP (32). Exposure to nicotine also induced the phenotypic transformation of SMCs from the contractile type to a synthetic-like type, which might attenuate the sensitivity of the myogenic response (22). These lines of evidence may partly explain the present findings.

The result showed that age was a significant factor affecting the comparison of parafoveal ΔPVD% between the two groups. This result could be explained by the previous study. Yu et al. demonstrated that age was negatively associated with baseline macular vessel density (33). Additionally, our group reported that age also has negative correlation with the change in parafoveal vessel density during VM-IV (19). In the present study, the average age of smokers was slightly higher than the non-smokers, although there was no statistical difference between the two groups. Thus, age become a significant confounder affecting the difference in parafoveal ΔPVD% in the multivariate analysis.

TABLE 4 | Comparisons of retinal microvascular reactivity to VM-IV between parafoveal region and peripapillary region.

	ΔParafoveal PVD (%)	ΔPeripapillary PVD (%)	P
Non-smokers	−13.01 ± 8.39	−3.83 ± 4.26	<0.001**
Smokers	−5.49 ± 9.70	−1.13 ± 3.50	0.005**

VM-IV, phase IV of Valsalva maneuver; PVD, perfused vessel density.
Δ, equal to a percentage change during VM-IV relative to the baseline levels.
**P < 0.01, tested with paired t-tests.

FIGURE 2 | Correlation between pack-years and percentage changes of perfused vessel density induced by Valsalva maneuver in parafoveal **(A)** and peripapillary **(B)** regions.
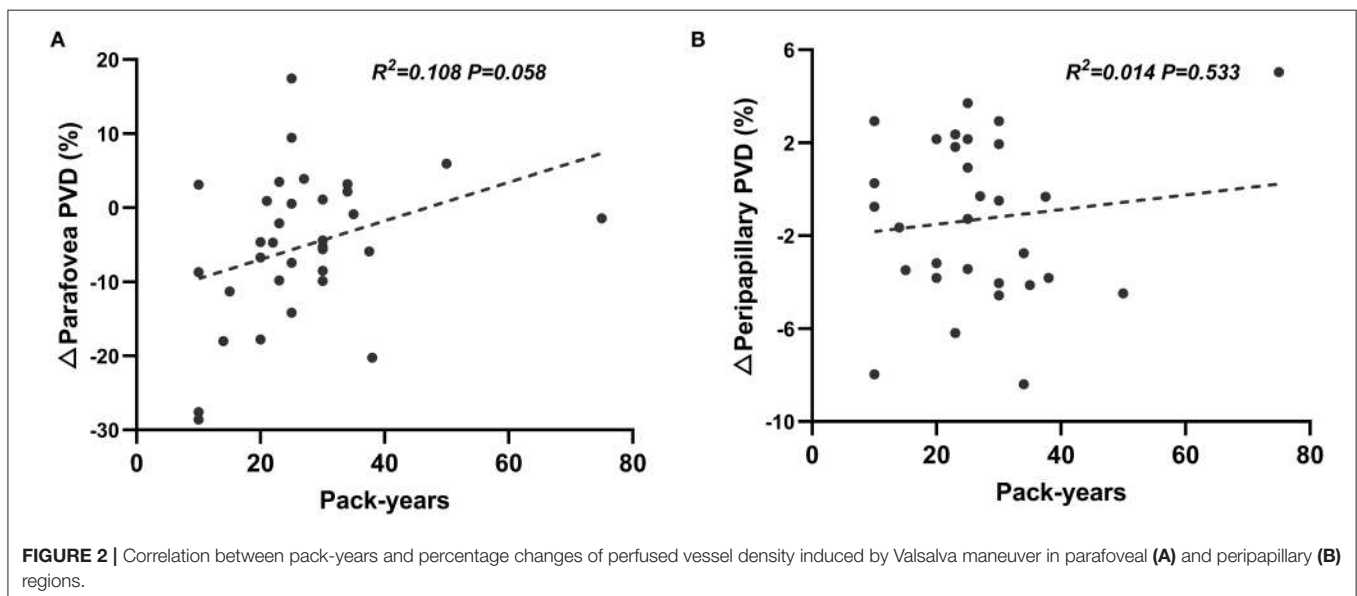
For smokers, the borderline level of statistical significance ($P = 0.058$) was obtained from linear regression analysis of the correlation between pack-years and retinal parafoveal ΔPVDs. This result might be due to the limited number of enrolled subjects. However, to some extent, it could reveal that the increasing cigarette consumption has strong tendency to be negatively correlated with the retinal microvascular reactivity. Future research with larger sample size will be conducted to validate this finding.

For both smokers and non-smokers, the increase in BP induced a greater reduction in retinal PVD in the parafoveal region than in the peripapillary region. This result is consistent with previous studies, which demonstrated differential vascular reactivity in different regions. Assam et al. demonstrated that the changes in the hemodynamic parameters are smaller in the nasal region than in the temporal region, which contains the macular area (34). In previous studies using OCTA, the retinal microvascular response to VM is greater in the parafoveal region than in the peripapillary region (19, 35). All of these results indicate that the greater vascular autoregulatory capacity of the macular vessels may better adapt them to various conditions or stimuli, in order to maintain the relatively constant blood flow required to supply the highly metabolic macula tissue.

There are several drawbacks in this study. Firstly, only a small group of Chinese males was included in this study, so the findings may not be generalizable to other populations. Further studies that include more subjects of different ages, sexes, and backgrounds are required. The exact mechanisms of the damage caused by smoking and the potential benefits of quitting smoking will be evaluated in the further. Secondly, this study was conducted in 2017, when the OCTA image acquisition system has not been updated. Thus, in parafoveal region, only the superficial capillary plexus could be identified and the perfused vessel density in this layer could be automatically quantified. In the future, we will compare the difference of retinal vascular reactivity in different capillary layer using the updated OCTA system. Lastly, due to the limited space between the subject's head and the instrument, we chose a modified VM instead of the classical VM developed by Levin (36). A modified VM is done by forcefully expiring against a closed glottis. As the pressure of forceful expiration could not be measured numerically, the repeatability and reproducibility of the modified VM might be lower than that of the classical method.

In conclusion, the results presented here, together with previous findings, demonstrate the potential damage to the retinal vascular system caused by smoking, although the degree of impairment may differ in different regions of the retina. Further studies in this field are required, and particular attention should be paid to potential variations in the sizes and locations of the affected vessels.

DATA AVAILABILITY STATEMENT

The raw data supporting the conclusions of this article will be made available by the authors, without undue reservation.

ETHICS STATEMENT

The studies involving human participants were reviewed and approved by Institutional Review Board of the Eye, Ear, Nose, and Throat Hospital of Fudan University in Shanghai, China. The patients/participants provided their written informed consent to participate in this study.

AUTHOR CONTRIBUTIONS

HX: conception and design. CJ, XS, and HZ: administrative support. CJ and HZ: provision of study materials or patients. HX, YZ, and JY: collection and assembly of data. HX and YZ: data analysis and interpretation. All authors wrote the manuscript and final approval of manuscript.

FUNDING

ACKNOWLEDGMENTS

REFERENCES

1. GBD 2015 Tobacco Collaborators. Smoking prevalence and attributable disease burden in 195 countries and territories, 1990-2015: a systematic analysis from the Global Burden of Disease Study 2015. *Lancet Lund Engl.* (2017) 389:1885–906. doi: 10.1016/S0140-6736(17)30819-X
2. Yang G, Wang Y, Wu Y, Yang J, Wan X. The road to effective tobacco control in China. *Lancet.* (2015) 385:1019–28. doi: 10.1016/S0140-6736(15)60174-X
3. Iovino GA, Mirza SA, Same JM, Gupta PC, Jarvis MJ, Bhava N, et al. Tobacco use in 3 billion individuals from 16 countries: an analysis of nationally representative cross-sectional household surveys. *Lancet.* (2012) 380:668–79. doi: 10.1016/S0140-6736(12)61085-X
4. Ricotta NA, Clair C. Managing tobacco use: the neglected cardiovascular disease risk factor. *Eur Heart J.* (2013) 34:3259–67. doi: 10.1093/eurheartj/eht352
5. Mathers C, World Health Organization. *WHO Global Report: Mortality Attributable to Tobacco.* Geneva: World Health Organization (2012). Available online at: http://whqlibdoc.who.int/publications/2012/9789241564434_eng.pdf (accessed August 17, 2019).
6. Galor A, Lee DJ. Effects of smoking on ocular health. *Curr Opin Ophthalmol.* (2011) 22:477–82. doi: 10.1097/ICU.0b013e32834bbe7a
7. Kur J, Newman EA, Chan-Ling T. Cellular and physiological mechanisms underlying blood flow regulation in the retina and choroid in health and disease. *Prog Retin Eye Res.* (2012) 31:377–406. doi: 10.1016/j.preteyeres.2012.04.004

8. Nesper PL, Lee HE, Fayed AE, Schwartz GW, Yu F, Fawzi AA. Hemodynamic response of the three macular capillary plexuses in dark adaptation and flicker stimulation using optical coherence tomography angiography. *Investig Opthalmology Vis Sci.* (2019) 60:694. doi: 10.1167/iovs.18-25478

9. Mandecka A, Dawczynski J, Blum M, Müller N, Kloos C, Wolf G, et al. Influence of flickering light on the retinal vessels in diabetic patients. *Diabetes Care.* (2007) 30:3048–52. doi: 10.2337/dc07-0927

10. Kallab M, Hommer N, Tan B, Pfister M, Schlatter A, Werkmeister RM, et al. Plexus-specific effect of flicker-light stimulation on the retinal microvasculature assessed with optical coherence tomography angiography. *Am J Physiol Heart Circ Physiol.* (2021) 320:H23–8. doi: 10.1152/ajpheart.00495.2020

11. Polak K, Schmetterer L, Riva CE. Influence of flicker frequency on flicker-induced changes of retinal vessel diameter. *Invest Ophthalmol Vis Sci.* (2002) 43:2721–6.

12. Jeppesen P, Sanye-Hajari J, Bek T. Increased blood pressure induces a diameter response of retinal arterioles that increases with decreasing arteriolar diameter. *Invest Ophthalmol Vis Sci.* (2007) 48:328–31. doi: 10.1167/iovs.06-0360

13. Jean-Louis S, Lovasik JV, Kergoat H. Systemic hyperoxia and retinal vasomotor responses. *Investig Opthalmology Vis Sci.* (2005) 46:1714. doi: 10.1167/iovs.04-1216

14. Sousa DC, Leal I, Moreira S, do Vale S, Silva-Herdade AS, Aguiar P, et al. A protocol to evaluate retinal vascular response using optical coherence tomography angiography. *Front Neurosci.* (2019) 13:566. doi: 10.3389/fnins.2019.00566

15. Holló G. Valsalva maneuver and peripapillary OCT angiography vessel density. *J Glaucoma.* (2018) 27:e133–6. doi: 10.1097/IJG.0000000000000983

16. Garhöfer G, Resch H, Sacu S, Weigert G, Schmidl D, Lasta M, et al. Effect of regular smoking on flicker induced retinal vasodilatation in healthy subjects. *Microvasc Res.* (2011) 82:351–5. doi: 10.1016/j.mvr.2011.07.001

17. Hall CN, Reynell C, Gesslein B, Hamilton NB, Mishra A, Sutherland BA, et al. Capillary prices regulate cerebral blood flow in health and disease. *Nature.* (2014) 508:55–60. doi: 10.1038/nature13165

18. Jia Y, Morrison JC, Tokayer J, Tan O, Lombardi L, Baumann B, et al. Quantitative OCT angiography of optic nerve head blood flow. *Biomed Opt Express.* (2012) 3:3127–37. doi: 10.1364/BOE.3.003127

19. Zong Y, Xu H, Yu J, Jiang C, Kong X, He Y, et al. Retinal vascular autoregulation during phase iv of the valsalva maneuver: an optical coherence tomography angiography study in healthy Chinese adults. *Front Physiol.* (2017) 8:553. doi: 10.3389/fphys.2017.00553

20. Novak P. Assessment of sympathetic index from the valsalva maneuver. *Neurology.* (2011) 76:2010–6. doi: 10.1212/WNL.0b013e31821e5563

21. Makwana O, Flockton H, Smith GA, Watters GP, Nisar R, Fields W. Mechanisms of whole smoke conditioned media induced cytotoxicity to human aortic endothelial cells. *Toxicol Vitro.* (2019) 58:239–44. doi: 10.1016/j.tiv.2019.03.011

22. Yoshiyama S, Chen Z, Okagaki T, Kohama K, Nasu-Kawaharada R, Izumi T, et al. Nicotine exposure alters human vascular smooth muscle cell phenotype from a contractile to a synthetic type. *Atherosclerosis.* (2014) 237:464–70. doi: 10.1016/j.atherosclerosis.2014.10.019

23. Wright JL, Tai H, Churg A. Cigarette smoke induces persisting increases of vasoactive mediators in pulmonary arteries. *Am J Respir Cell Mol Biol.* (2004) 31:501–9. doi: 10.1165/rcmb.2004-0051OC

24. Hamilton NB, Attwell D, Hall CN. Pericyte-mediated regulation of capillary diameter: a component of neurovascular coupling in health and disease. *Front Neuroenergetics.* (2010) 2:5. doi: 10.3389/fnene.2010.00005

25. Wang J, Chen Y, Lin C, Jia J, Tian L, Yang K, et al. Effects of chronic exposure to cigarette smoke on canonical transient receptor potential expression in rat pulmonary arterial smooth muscle. *Am J Physiol Cell Physiol.* (2014) 306:C364–73. doi: 10.1152/ajpcell.00048.2013

26. Lott MEJ, Slocomb JE, Shivkumar V, Smith B, Quillen D, Gabbay RA, et al. Impaired retinal vasodilator responses in prediabetes and type 2 diabetes. *Acta Ophthalmol.* (2013) 91:e462–9. doi: 10.1111/aos.12129

27. Sousa DC, Leal I, Moreira S, do Vale S, Silva-Herdade AS, Aguiar P, et al. Retinal vascular reactivity in type 1 diabetes patients without retinopathy using optical coherence tomography angiography. *Investig Opthalmology Vis Sci.* (2020) 61:49. doi: 10.1167/iovs.61.6.49

28. Pstras L, Thomaseth K, Waniewski J, Balzani I, Bellavere F. The valsalva manoeuvre: physiology and clinical examples. *Acta Physiol.* (2016) 217:103–19. doi: 10.1111/apha.12639

29. Perry BG, Cotter JD, Mejuto G, Mündel T, Lucas SJE. Cerebral hemodynamics during graded valsalva maneuvers. *Front Physiol.* (2014) 5:349. doi: 10.3389/fphys.2014.00349

30. O'Halloran M, O'Donoghue E, Dainty C. Measurement of the retinal arteriolar response to a hyperoxic provocation in nonsmokers and smokers, using a high-resolution confocal scanning laser ophthalmoscope. *J Biomed Opt.* (2014) 19:076012. doi: 10.1117/1.JBO.19.7.076012

31. Neymar A, Al-Salam S, Yuvaraju P, Beegam S, Yasin J, Ali BH. Chronic exposure to water-pipe smoke induces cardiovascular dysfunction in mice. *Am J Physiol Heart Circ Physiol.* (2017) 312:H329–39. doi: 10.1152/ajpheart.00450.2016

32. Liu G, Cull G, Wang L, Bui BV. Hypercapnia impairs vasoreactivity to changes in blood pressure and intraocular pressure in rat retina. *Optom Vis Sci Off Publ Am Acad Optom.* (2019) 96:470–6. doi: 10.1097/OPX.00000000000 01400

33. Yu J, Jiang C, Wang X, Zhu L, Gu R, Xu H, et al. Macular perfusion in healthy Chinese: an optical coherence tomography angiogram study. *Invest Ophthalmol Vis Sci.* (2015) 56:3212–7. doi: 10.1167/iovs.14-16270

34. Assam SM, Patel V, Chen HC, Kohner EM. Regional retinal blood flow and vascular autoregulation. *Eye Lund Engl.* (1996) 10 (Pt 3):331–7. doi: 10.1038/eye.1996.69

35. Ozcan SC, Kurtul BE, Ozarslan Ozcan D. Evaluation of microvascular changes in optic disc and retina by optical coherence tomography angiography during valsalva maneuver. *Int Ophthalmol.* (2020) 40:2743–9. doi: 10.1007/s10792-020-01461-x

36. Levin AB. A simple test of cardiac function based upon the heart rate changes induced by the valsalva maneuver. *Am J Cardiol.* (1966) 18:90–99. doi: 10.1016/0002-9149(66)90200-1

Associations Between Diabetic Retinopathy and Parkinson's Disease: Results From the Catalonian Primary Care Cohort Study

Didac Mauricio [1,2,3,4*†], Bogdan Vlacho [1†], Joan Barrot de la Puente [1,5],
Xavier Mundet-Tudurí [1,6], Jordi Real [1,4], Jaime Kulisevsky [7], Emilio Ortega [1,8,9],
Esmeralda Castelblanco [1,10], Josep Julve [11*] and Josep Franch-Nadal [1,4,12]

[1] DAP-Cat Group, Unitat de Suport a la Recerca Barcelona, Fundació Institut Universitari per a la recerca a l'Atenció Primària de Salut Jordi Gol i Gurina, Barcelona, Spain, [2] Departament of Medicine, University of Vic-Central University of Catalonia, Catalonia, Spain, [3] Department of Endocrinology and Nutrition, Hospital de la Santa Creu i Sant Pau, Barcelona, Spain, [4] CIBER of Diabetes and Associated Metabolic Diseases, Instituto de Salud Carlos III, Madrid, Spain, [5] Primary Health Care Center Dr. Jordi Nadal i Fàbregas (Salt), Gerència d'Atenció Primaria, Institut Català de la Salut, Girona, Spain, [6] Faculty of Medicine, Department of Medicine, Autonomous University of Barcelona, Barcelona, Spain, [7] Movement Disorders Unit, Neurology Department, Hospital de la Santa Creu i Sant Pau, Barcelona, Spain, [8] Department of Endocrinology and Nutrition, Institut d'Investigacions Biomèdiques August Pi i Suñer, Hospital Clinic, Barcelona, Spain, [9] CIBER of Physiopathology of Obesity and Nutrition, Instituto de Salud Carlos III, Madrid, Spain, [10] Division of Endocrinology, Metabolism and Lipid Research, Washington University School of Medicine in St. Louis, St. Louis, MO, United States, [11] Institut de Recerca de l'Hospital de la Santa Creu i Sant Pau, Barcelona, Spain, [12] Primary Health Care Center Raval Sud, Gerència d'Atenció Primaria, Institut Català de la Salut, Barcelona, Spain

The purpose of this study was to assess the risk of occurrence of Parkinson's disease (PD) among subjects with type 2 diabetes and diabetic retinopathy (DR) in our large primary health care database from Catalonia (Spain). A retrospective cohort study with pseudo-anonymized routinely collected health data from SIDIAP was conducted from 2008 to 2016. We calculated the number of events, time to event, cumulative incidence, and incidence rates of PD for subjects with and without DR and for different stages of DR. The proportional hazards regression analysis was done to assess the probability of occurrence between DR and PD. In total, 26,453 type 2 diabetic subjects with DR were identified in the database, and 216,250 subjects without DR at inclusion. During the follow-up period, 1,748 PD events occurred. PD incidence rate and cumulative incidence were higher among subjects with DR (16.95 per 10,000 person-years and 0.83%, respectively). In the unadjusted analysis, subjects with DR were at 1.25 times higher risk (hazard ratio: 1.22, 95% confidence interval: 1.06; 1.41) of developing PD during the study period. However, we did not find any statistically significant HR for DR in any models after adjusting for different risk factors (age, sex, duration of diabetes, smoking, body mass index, glycosylated hemoglobin, comorbidities). In conclusion, in our primary health care population database, DR was not associated with an increased risk of PD after adjusting for different risk factors. In our retrospective cohort study, age, male sex, and diabetes duration were independent risk factors for developing PD.

Keywords: age, diabetic retinopathy, diabetes type 2, Parkinson's disease, primary care, real world data (RWD)

INTRODUCTION

Diabetes mellitus (DM) is a metabolic disorder that may result in an unfavorable impact in different organs and leading to numerous complications (1). The complications of diabetes are generally classified as macrovascular and microvascular. Large blood vessels are affected by macrovascular complications, and depending on the location, three types of complications exist: coronary artery disease, peripheral artery disease, and cerebrovascular disease. On the other hand, microvascular complications affect blood microvessels, leading to complications such as diabetic peripheral neuropathy, diabetic nephropathy, and diabetic retinopathy (DR). However, unlike classical vascular complications, DM may affect almost every organ system and damage other tissues or cell types (1). In addition to vascular tissue, damage to non-vascular tissue also happens in DR, one of the most common complications among subjects with DM. Due to the retina's particular neurovascular structure, neuro-dysfunction and neurodegeneration caused by DM is an important component of this complication. For example, it was previously reported that different neuronal damage and functional changes could occur in the retina due to poor DM control. These changes include loss of dendrites and synaptic activity, neural apoptosis, thinning of the inner retina, ganglion cell loss, reactive microglial activation, and deficits in the retina's electrophysiological activity, dark adaptation, contrast sensitivity, or color vision (2, 3). Overall, the complications of diabetes are far from vascular only, and there are a lot of other non-classical chronic complications of diabetes, including neurodegenerative complications (1).

Parkinson's disease (PD) is the second most common neurodegenerative disease. Generally, this chronic disease is more prevalent among older adults and Hispanic people (4). So far, many risk factors have been reported to be related to PD, such as pesticides, dietary factors, melanoma, traumatic brain injury, and diabetes (4–7). The role of DM as a risk factor for neurodegenerative diseases involves different pathways of cellular metabolic injury such as impaired insulin signaling and inflammatory and oxidative stress, which can lead to mitochondrial dysfunction, neuroinflammation, synaptic plasticity and other neuronal dysfunction and degeneration (8). So far, different studies have been conducted to evaluate the risk of DM on PD. In cohort studies from Finland, Denmark, UK, Taiwan, and South Korea (9–14), type 2 diabetes mellitus (T2DM) was a risk factor for PD. However, no such associations were found in cohort studies in the US (15, 16).

The results related to the association between DM and PD reported in meta-analyses have also been heterogeneous. In one meta-analysis with 11 observational studies (four cohort and seven case-control studies) on the association of diabetes as a risk factor for PD, the authors concluded that diabetes appears to be a risk factor for PD (6). Another meta-analysis with observational studies indicated that T2DM increases the risk of future PD; however, no associations were found when the authors changed the exposure definition to any type of diabetes (7). Moreover, the authors pointed out that the association between DM and PD tended to change depending on the study design since a possible effect of survivor bias among the patients with diabetes may interfere with the results (7).

Evidence suggests that DR and PD share similar pathophysiological characteristics and mechanisms (dopamine reduction, increased α-Synuclein expression, and abnormal neurotrophic factors expression) related to disrupted dopamine activity since both brain and retina express D1-like and D2-like dopamine receptors (17). The phosphorylation of α-Synuclein as a result of the dopamine in abnormal regulation in the retinal layers may be a reason for neurodegeneration in the retina and brain (18). Therefore, a close association between pathophysiological mechanisms of DR and PD may be expected.

To our knowledge, there is only one large population database study from South Korea aimed to investigate this association. The authors found that the incidence of PD was higher among DM subjects and even higher among subjects with DM and DR; however, they acknowledged that important variables related to the DM were not available for the analysis, such as duration of diabetes, and glycated hemoglobin (19). On this background, we undertook the current study to assess the risk of occurrence of PD among subjects with DR in our large primary health care database from Catalonia (Spain).

MATERIALS AND METHODS

Study Design and Data Source

We used a retrospective cohort of subjects with T2DM attended in primary health care centers from the Catalonian Health Institute–ICS, using the pseudo-anonymized routinely collected health data from the SIDIAP (Sistema d'Informació per al desenvolupament de la Investigació en Atenció Primària) database. This database is a well-validated data source for the study of diabetes in Spain (20, 21), collecting different data related to health problems, clinical and diagnostic procedures, laboratory parameters, and information on medication prescribed and dispensed. The data were collected for the period between January 1, 2008, and December 31, 2016.

Definition of Eligibility Criteria

We included all subjects aged 30 years or above, with a register of T2DM defined as the presence of relevant ICD-10 (International Classification of Diseases, 10th Revision) diagnostic codes and sub-codes (E11 and E14). Subjects with diagnostic codes for other types of diabetes (type 1, gestational or other) or without T2DM codes were excluded from the analysis. Those subjects with preexisting primary and secondary Parkinson's disease (ICD-10: G20 and G21) were also excluded from the study population.

Definition of Variables

At inclusion, variables related to DR and clinical characteristics of the subjects were collected. DR was defined as the presence of diagnostic codes and sub-codes (ICD-10: E11.3, E14.3, and H36) and/or abnormal (pathologic) results for fundus photography. In those with available fundus photography data, DR was stratified in different stages using the Early Treatment Diabetic Retinopathy Study (ETDRS) classification: no apparent retinopathy (NDR), mild non-proliferative retinopathy (NPDR),

TABLE 1 | Code list.

Variable	Definition
Codes used for definition of the study variables	
Type 2 diabetes mellitus	ICD-10-CM Codes: E11.xx; E14.xx
Cardiovascular diseases	ICD-10-CM Codes: I21.xx; I22.xx; I23.xx; I25.xx; G45.xx; G46.xx; I60.xx; I61.xx I62.xx; I63.xx; I64.xx
Diabetic retinopathy	ICD-10-CM Codes: E11.3; E14.3; H36;H36.0;H36.8 and/or fundus photography: mild non-proliferative retinopathy (NPDR), moderate NPDR, severe NPDR, proliferative diabetic retinopathy (PRD), and diabetic macular edema (DME)
Dyslipidemia	ICD-10-CM Codes: E78;E78.9 and/or Lipid-lowering drugs
Hypertension	ICD-10-CM Codes: 10 and/or Antihypertensive agents
Parkinson's disease as event	ICD-10-CM Codes: G20
Parkinson's disease as exclusion criteria	ICD-10-CM Codes: G20;G21.xx
Chronic kidney disease	CKD-EPI glomerular filtration rate <60 ml/min/1.73 m^2 and or albumin/creatinine ratio>30 mg/g
Antithrombotic agents	ATC/DDD codes: B01A
Antihypertensive agents	ATC/DDD codes: C02; C03; C07; C08; C09
Antidiabetics agents	ATC/DDD codes: A10
Lipid-Lowering agents	ATC/DDD codes: C10

xx, sub codes.

moderate NPDR, severe NPDR, proliferative diabetic retinopathy (PRD), and diabetic macular edema (DME) [22]. We also collected variables related to sociodemographic characteristics (age, sex) and toxic habits (tobacco use). Duration of T2DM was calculated. Due to the under-reporting in our database, dyslipidemia and hypertension were identified as a combination of diagnostic code and/or treatment for these diseases. In addition, chronic kidney disease (CKD) was defined as a combination of CKD-EPI glomerular filtration rate <60 ml/min/1.73 m^2 and/or an albumin/creatinine ratio >30 mg/g. To identify cardiovascular disease, we used diagnostic codes alone. Moreover, concomitant medication (antihypertensive, antiplatelet, lipid-lowering, antidiabetic drugs), laboratory parameters [lipid profile, renal profile, glycated hemoglobin (HbA1c)], and clinical variables [systolic and diastolic blood pressure, body mass index (BMI)] were collected. The detailed information on the different codes used in defining the study variables is included as **Table 1** code list.

During follow-up, we collected data related to PD as a primary study event. PD was defined as the presence of a diagnostic code for Parkinson's disease (ICD-10: G20). The follow-up period was defined as the time between the inclusion in the study and the primary study event.

Statistical Analysis

For the variables collected at inclusion, we used descriptive statistics. The number and frequencies for the qualitative variables were calculated, while we estimated the means and standard deviation for the quantitative variables.

At follow-up, for the primary study event (PD), we calculated the number of subjects and events for each group (presence/absence of DR and each stage of DR), time to event (time to a diagnosis of PD after a diagnosis of DR), cumulative incidence and incidence rates (person/year). To assess the probability of occurrence between DR and PD, we used proportional hazards regression analysis. The hazard ratios (HR) for the primary outcome event were calculated with corresponding 95% confidence intervals (CI), and statistical significance was established as a $p < 0.05$. Additionally, adjusted HRs were calculated using different clinically important variables as risk factors. Gradually we added different risk factors to the model, starting with age and sex in the first model, adding T2DM duration, smoking status, hypertension, dyslipidemia, and BMI in the second model, and adding CKD, CVD, and HbA1c in the third model. Moreover, to assess the effect of diabetes duration and HbA1c on the association of DR with risk of incident PD, we performed additional models with different combinations of these two variables with the other relevant variables from the first model. We also performed a sensitivity analysis with the estimates from different models and, also, stratification for diabetes duration and HbA1c. Data management and all analyses were performed using R statistical software, version 3.6.1.

Institutional Review Board Statement

The study was conducted according to the guidelines of the Declaration of Helsinki and approved by the Institutional Review Board (or Ethics Committee) of IDIAP Jordi Gol i Gurina Foundation (protocol code P13/028 and date of approval 03/04/2013).

RESULTS

Subjects Characteristics

From 2008 until 2016, 250,363 subjects with T2DM were identified in the SIDIAP database. We excluded 1,850 individuals who had a previous diagnostic category of PD and 5,838 individuals without T2DM diagnostic codes. In total, 216,250 subjects did not have DR at baseline, while 26,453 had DR by diagnostic code and/or diagnosis by fundus photography. The study flowchart is presented in **Figure 1**.

The clinical characteristics of the cohort and different groups at inclusion are presented in **Table 2**. The mean age of the study subjects was 65.3 years. There were more males (57.5%), and the average duration of T2DM was 5.35 years. There were differences between the study groups regarding age, comorbidities, laboratory parameters, and concomitant drug use. Subjects with DR were, on average, 2.7 years older and with more comorbidity, especially cardiovascular diseases and CKD, compared with those without DR. We also observed higher mean values for HbA1c, lower glomerular filtration ratios, and slightly lower BMI among subjects with DR. Regarding concomitant

FIGURE 1 | Study flowchart.
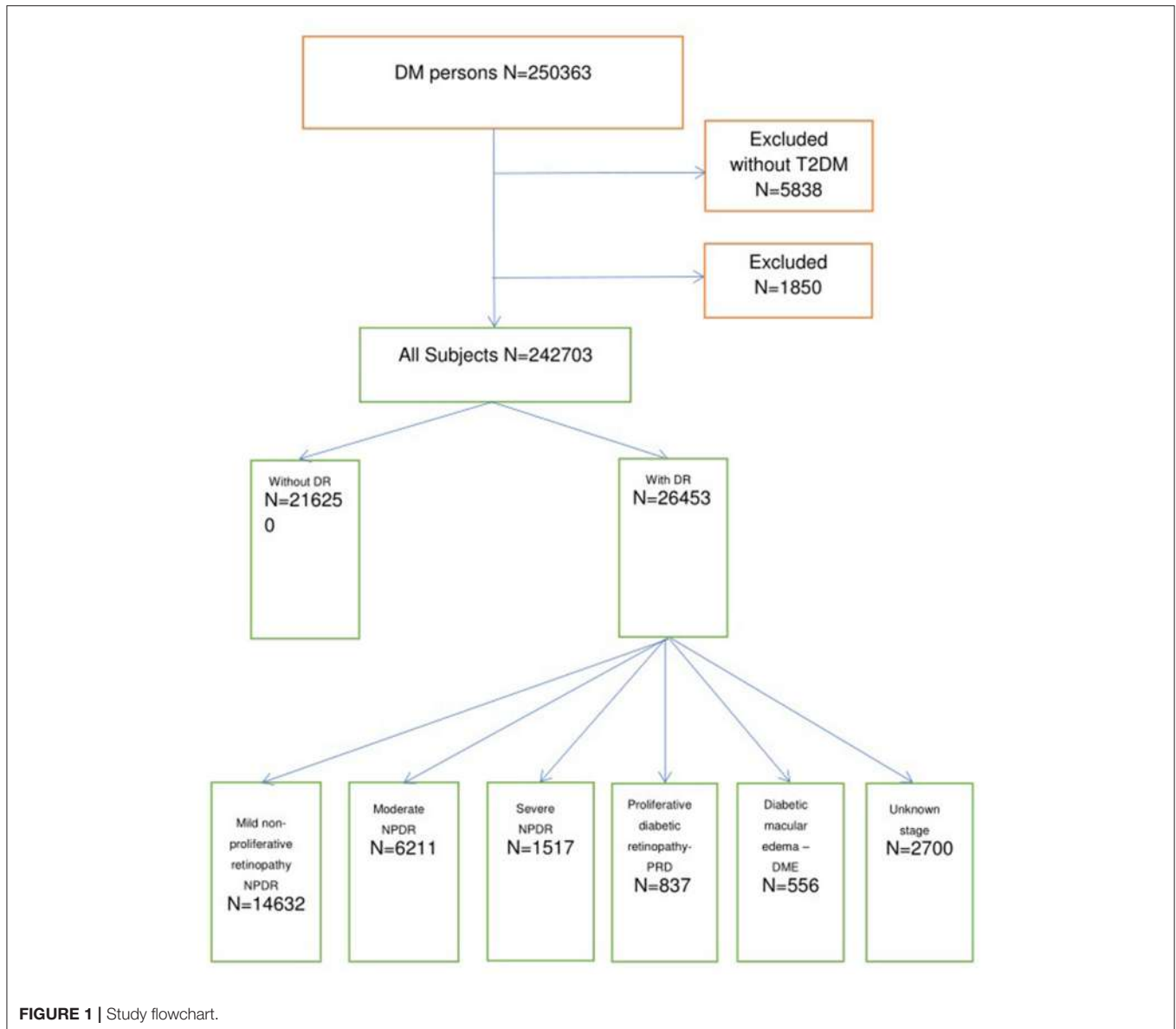
drug use, higher percentages were also observed for all drug classes of interest in the DR group.

Parkinson's Disease Incidence Among the Groups

Information on the time of follow-up, events, and cumulative incidence are presented in **Table 3**. The average time to the event among study subjects was 4.8 years. In total, 1,748 PD events occurred, with an incidence rate of 14.25 per 10,000 person-years and a cumulative incidence of 0.72%. PD incidence and cumulative incidence were higher among subjects with DR (16.95 per 10,000 person-years and 0.82%, respectively). When the different stages of DR were compared, the highest incidence rate and cumulative incidence of PD was observed among those with moderate non-proliferative retinopathy (20.73 per 10,000

person-years and 0.99%, respectively). High incidence rate and cumulative incidence were observed among individuals with DR identified by diagnostic code but without grading of DR according to fundus photography (27.77 per 10,000 person-years and 1.33%, respectively).

Factors Predicting Parkinson's Disease

We observed statistically significant un-adjusted HR (Unadj-HR) for the primary study event between the groups (**Table 3**). The subjects with DR had a 1.22 times higher risk of developing PD during the study period. Additionally, we also calculated the Unadj-HR considering the stage of DR. The highest Unadj-HR was observed among the subjects with moderate NPDR. These subjects were at a 1.50 times higher risk of developing PD compared with those without DR. Further, a higher risk (Unadj-HR: 2.02) of developing PD was observed for the group with

	All subjects $N = 242,703$	Group without DR $N = 216,250$	Group with DR $N = 26,453$	p-value
Age, mean (SD), years	65.3 (11.5)	65.0 (11.5)	67.7 (11.5)	<0.001
Sex (male), n (%)	142,749 (57.4)	127,534 (57.5)	15,215 (56.7)	
Smoking habit, n (%)				<0.001
No smoker	140,585 (57.9)	124,530 (57.6)	16,055 (60.7)	
Ex-smoker	32,843 (13.5)	29,782 (13.8)	3,061 (11.6)	
Current smoker	69,275 (28.5)	61,938 (28.6)	7,337 (27.7)	
Comorbidities, n (%)				
Dyslipidemia	125,617 (51.8)	111,117 (51.4)	14,500 (54.8)	<0.001
Hypertension	155,115 (63.9)	136,395 (63.1)	18,720 (70.8)	<0.001
Cardiovascular diseases	30,014 (12.4)	25,424 (11.8)	4,590 (17.4)	<0.001
Chronic kidney disease	37,804 (15.6)	31,529 (14.6)	6,275 (23.7)	0.000
Clinical variables, mean, (SD)				
Diabetes duration, (years)	5.35 (5.39)	4.98 (5.04)	8.41 (6.92)	0.000
BMI (kg/m^2)	30.6 (5.16)	30.6 (5.15)	30.2 (5.24)	<0.001
SBP (mmHg)	134 (14.9)	134 (14.7)	137 (16.3)	<0.001
DBP (mmHg)	76.7 (9.72)	76.9 (9.62)	75.4 (10.4)	<0.001
Laboratory parameters, mean, (SD)				
HbA1c (%)	7.18 (1.52)	7.12 (1.48)	7.74 (1.72)	0.000
HbA1c (mmol/mol)	55.0 (16.6)	54.3 (16.2)	61.1 (18.8)	
Total cholesterol (mg/dl)	195 (41.1)	195 (40.9)	188 (42.5)	<0.001
HDL cholesterol (mg/dl)	48.6 (12.8)	48.6 (12.8)	48.8 (13.2)	0.005
LDL cholesterol (mg/dl)	114 (34.3)	115 (34.2)	109 (34.9)	<0.001
Triglycerides (mg/dl)	167 (121)	168 (123)	159 (109)	<0.001
Creatinine (mg/dl)	0.91 (0.30)	0.90 (0.28)	0.96 (0.43)	<0.001
Albumin / Creatinine ratio (mg/g)	35.9 (142)	31.2 (123)	74.0 (239)	<0.001
Glomerular filtration (ml/min/1.73 m^2)	76.7 (20.5)	77.5 (20.1)	69.4 (22.8)	<0.001
Concomitant medications, n (%)				
Antithrombotic	76,507 (31.5)	64,823 (30.0)	11,684 (44.2)	0.000
Antihypertensive	154,166 (63.5)	135,576 (62.7)	18,590 (70.3)	<0.001
Antidiabetics	181,237 (74.7)	158,665 (73.4)	22,572 (85.3)	0.000
Lipid-lowering	123,969 (51.1)	109,697 (50.7)	14,272 (54.0)	<0.001

BMI, body mass index; SBP, systolic blood pressure; DBP, diastolic blood pressure; HbA1c, glycosylated hemoglobin; SD, standard deviation.

DR identified by diagnostic code, but without grading of DR compared with the group without DR.

Figure 2 and **Table 4** show the results of the different multivariable proportional hazards analysis models. In the proportional hazards analysis adjusting the models for different risk factors, we did not find any statistically significant HRs for DR in any models. Age and male sex were independent risk factors in all of the models. T2DM duration was a risk factor in the second and third models, especially for subjects with T2DM duration of more than 20 years. In contrast, having a BMI over 39 kg/m^2 and being an ex-smoker decreased the risk of PD. In the additional models, adjusting only for age, sex, and diabetes duration and/or HbA1c, we did not find a significant association of DR with PD. The age, sex and diabetes duration remained risk

factors for PD in these models. **Table 5** shows the results of these additional models.

Sensitivity Analysis

In the sensitivity analysis, stratifying by diabetes duration or HbA1c, similar tendencies were observed for the HRs for DR observed in the previously described models. However, having an HbA1c between 9.1 and 10% and DR was negatively associated with PD when including additional relevant variables in this additional model (age, sex, T2DM duration) or variables in model 3 (age, sex, smoking, T2DM duration, dyslipidemia, CVD, HTA, CKD, IMC). The results of this sensitivity analysis are shown in **Table 6** and **Figure 3**.

TABLE 3 | Parkinson's disease events among the study groups, stage of diabetic retinopathy and un-adjusted hazards ratios.

Variable	N subjects	Person-years	Time free from the event (years)	Parkinson's disease events	Incidence rate per 10000-Year	Cumulative incidence	Un-adjusted HR 95% CI [LI; UI]
All subjects	242,703	1226699.67	4.82	1,748	14.25	0.72	–
Group without DR	216,250	1097519.23	4.86	1,529	13.93	0.71	Ref
Group with DR	26,453	129180.43	4.56	219	16.95	0.83	1.22 [1.06; 1.41]
Stage of DR							
No apparent diabetic retinopathy (NDR)	216,250	1097519.23	4.86	1,529	13.93	0.71	Ref
Mild non-proliferative diabetic retinopathy (NPDR)	14,632	72673.13	4.63	109	14.99	0.75	1.08 [0.89; 1.31]
Moderate (NPDR)	6,211	29900.12	4.48	62	20.74	0.99	1.50 [1.16; 1.93]
Severe (NPDR)	1,517	7669.25	4.91	3	3.91	0.20	0.28 [0.09; 0.87]
Proliferative diabetic retinopathy (PRD)	837	3736.21	4.11	5	13.38	0.60	0.98 [0.41; 2.35]
Diabetic macular edema (DME)	556	2238.91	3.56	4	17.87	0.72	1.33 [0.50; 3.54]
Unknown stage*	2,700	12962.82	4.65	36	27.77	1.33	2.02 [1.45; 2.81]

DR, diabetic retinopathy; NDR, no apparent diabetic retinopathy; NPDR, non-proliferative diabetic retinopathy; PRD, proliferative diabetic retinopathy; DME, diabetic macular edema; ref, reference group; HR, hazard ratio; 95% CI, 95% confidence interval; LI, lower limit; UI, upper limit.
*Subjects having diabetic retinopathy by diagnostic code but without fundus photography/stage of DR.

DISCUSSION

The results from our retrospective cohort study from a primary care database from 2008 until 2016 showed no increased risk for developing PD among subjects with previous diabetic retinopathy in fully adjusted models. Instead, age, male gender, and longer T2DM duration conferred an increased risk of PD over time independently among T2DM subjects.

To date only one similar observational study with routinely collected health data from South Korea investigated the relationship between T2DM retinopathy and PD (16). Comparing the clinical characteristics of the DR subjects in both studies, subjects from our study were on average 6.7 years older, with a higher proportion of males (8.5%), 14.3% more smokers, and were also more obese (average difference 5.7 kg/m^2). The differences found between subjects with DR from the two studies are not surprising. It is well reported that the characteristics of eastern Asian people with T2DM are different from European T2DM subjects (23). In Asian countries, T2DM subjects are younger and have a lower BMI than those from the US or European countries. Compared to Caucasians, Asians have more lipotoxicity and insulin resistance due to the greater visceral adiposity, which is more metabolically adverse (23). People with T2DM from Asia also tend to have a higher incidence of renal complications and ischemic strokes but lower coronary heart disease or peripheral arterial disease (24). Our study observed a higher percentage of subjects with CKD in the DR group (23.7%). However, these data cannot be compared to the South Korea study due differences in the definition of these variables. For instance, in the South Korean study, end-stage renal disease was defined by diagnostic code, while in our study, we defined CKD by values of CKD-EPI glomerular filtration rate <60 ml/min/1.73 m^2 and/or an albumin/creatinine ratio >30 mg/g. Regarding the differences in the events of PD between

the two studies, the incidence rate was slightly higher among subjects with DR in our study (16.95 vs. 15.51 per 10,000 person-years, respectively). Comparing groups without DR between the two studies, we observed a higher incidence rate than in the South Korea study (13.93 vs. 8.39 per 10,000 person-years, respectively). An explanation for this difference could be that our non-DR population was older than the South Korean population, and it is well known that PD increases rapidly with age (4). In general, our T2DM population was relatively older, and we had smaller differences between the groups in age (with or without DR). In particular, this could also explain the differences in the unadjusted HR observed in our study (Unadj-HR: 1.22 95% CI: 1.06; 1.41) compared with the South Korean study, where more pronounced differences in un-adjusted HR were observed (Unadj-HR: 5.72, 95% CI: 5.41; 6.05) (19). For our definition of DR, we intentionally included fundus photography, which is a gold standard screening method with a high sensitivity to detect DR, which could prevent possible misclassification of this condition (25). Possible overestimation of DR due to the utilization of only one diagnostic code related to DR (ICD-10: H36) in the South Korean study could be one of the reasons for significant associations found between DR and PD in the multivariable proportional hazards regression analysis models.

In our multivariable model, besides basic clinical factors such as age and sex, we evaluated the effect of duration of T2DM, BMI, smoking status and HbA1c. Longer diabetes duration has been previously established as a strong risk factor for microvascular complications, especially DR (26, 27). Indeed, we also observed that T2DM duration was an independent risk factor for the development of PD in our multivariable model analysis. Other similar studies have also reported that diabetes is an independent risk factor for PD. For example, a recently published observational study with the same database as ours reported an increased risk of PD among T2DM subjects (adj-HR

FIGURE 2 | Unadjusted and adjusted hazard ratios for Parkinson's disease according to diabetic retinopathy status and stage of diabetic retinopathy. **(A)** Unadjusted hazard ratios for Parkinson's disease for different stages of diabetic retinopathy. DR, diabetic retinopathy; NDR, no apparent diabetic retinopathy; NPDR, non-proliferative diabetic retinopathy; PRD, proliferative diabetic retinopathy; DME, diabetic macular edema. **(B)** Unadjusted and adjusted hazards ratios for Parkinson's disease for subjects with and without diabetic retinopathy; Model 1: adjusted for age and sex; Model 2: adjusted for, age, sex, diabetes duration, smoking status, hypertension, dyslipidemia and body mass index; Model 3: adjusted for age, sex, diabetes duration, smoking status, hypertension, dyslipidemia, CKD, CVD and BMI and HbA1c.

TABLE 4 | Adjusted hazard ratios for different variables.

	Model 1	Model 2	Model 3
Predictor	HR 95% CI [LI; UI]	HR 95% CI [LI; UI]	HR 95% CI [LI; UI]
Group with DR, ref: Group without DR	1.06 0.92; 1.22	1.01 0.87; 1.17	1.01 0.88; 1.17
Sex (male)	**1.35 1.22; 1.48**	**1.07 1.07; 1.08**	**1.38 1.24; 1.54**
Age (years)	**1.08 1.07; 1.08**	**1.39 1.25; 1.55**	**1.07 1.07; 1.08**
T2DM duration 6–10 years		**1.23 1.10; 1.37**	**1.22 1.10; 1.36**
T2DM duration 11–15 years		**1.24 1.07; 1.43**	**1.23 1.06; 1.43**
T2DM duration 16–20 years		**1.34 1.07; 1.68**	**1.33 1.06; 1.68**
T2DM duration more than 20 years		**1.57 1.20; 2.05**	**1.56 1.19; 2.04**
Ex-smoker		**0.69 0.56; 0.84**	**0.69 0.56; 0.84**
Current smoker		0.93 0.82; 1.05	0.92 0.82; 1.04
Dyslipidemia		1.07 0.97; 1.18	1.06 0.96; 1.17
Hypertension		0.94 0.85; 1.05	0.93 0.84; 1.04
BMI 24.9–29.9 kg/m^2		1.02 0.86; 1.22	1.02 0.86; 1.22
BMI 30.0–34.9 kg/m^2		0.94 0.78; 1.13	0.93 0.77; 1.12
BMI 35.0–39.9 kg/m^2		0.90 0.70; 1.14	0.89 0.70; 1.14
BMI more than 39.9 kg/m^2		**0.63 0.41; 0.95**	**0.63 0.41; 0.94**
BMI (missing)		0.93 0.77; 1.11	0.93 0.78;1.12
HbA1c 6.5–7%			0.98 0.85; 1.14
HbA1c 7.1–8%			1.00 0.87; 1.14
HbA1c 8.1–9%			1.08 0.90; 1.30
HbA1c 9.1–10%			0.96 0.73; 1.26
HbA1c more than 10%			**0.73 0.53; 1.00**
HbA1c (missing)			0.93 0.81; 1.08
CKD			1.03 0.91; 1.17
CVD			1.08 0.95; 1.24
Observations	242,703	242,703	242,703
R2 Nagelkerke	0.026	0.027	0.027

BMI, body mass index; CKD, chronic kidney disease; CVD, Cardiovascular disease; DR, diabetic retinopathy; HbA1c, glycosylate hemoglobin; HR, hazard ratio; 95% CI, 95% confidence interval; LI, lower limit; UI, upper limit; T2DM, type 2 diabetes mellitus. Bold values means statistically significant Hazard ratios.

TABLE 5 | Additional models for adjusted hazard ratios for different variables.

	Model 1.1	Model 1.2	Model 1.3
Predictor	HR 95% CI [LI; UI]	HR 95% CI [LI; UI]	HR 95% CI [LI; UI]
Group with DR, ref: Group without DR	1.01 0.88; 1.17	1.01 0.87; 1.16	1.06 0.92; 1.23
Sex (male)	**1.35** **1.23; 1.49**	**1.35** **1.23; 1.49**	**1.35** **1.23; 1.49**
Age (years)	**1.07** **1.07; 1.08**	**1.07** **1.07; 1.08**	**1.08** **1.07; 1.08**
T2DM duration 6–10 years	**1.23** **1.10; 1.38**	**1.23** **1.11; 1.38**	
T2DM duration 11–15 years	**1.25** **1.08; 1.44**	**1.36** **1.08; 1.70**	
T2DM duration 16–20 years	**1.36** **1.08; 1.70**	**1.25** **1.08; 1.44**	
T2DM duration more than 20 years	**1.59** **1.22; 2.08**	**1.59** **1.22; 2.08**	
HbA1c 6.5–7%	0.98 0.85; 1.13		1.00 0.87; 1.15
HbA1c 7.1–8%	0.99 0.87; 1.14		1.04 0.91; 1.19
HbA1c 8.1–9%	1.07 0.89; 1.29		1.14 0.95; 1.37
HbA1c 9.1–10%	0.95 0.72; 1.25		1.00 0.76; 1.32
HbA1c more than 10%	**0.72** **0.52; 0.99**		0.75 0.54; 1.03
HbA1c (missing)	0.92 0.80; 1.06		0.94 0.82; 1.08
Observations	242,703	242,703	242,703
R2 Nagelkerke	0.026	0.026	0.026

HbA1c, glycosylate hemoglobin; HR, hazard ratio; 95% CI, 95% confidence interval; LI, lower limit; UI, upper limit; T2DM, type 2 diabetes mellitus.
Bold values means statistically significant Hazard ratios.

of 1.19, 95% CI: 1.13; 1.25) and subjects with prediabetes (adj-HR of 1.07, 95% CI: 1.00; 1.14) compared to those subjects without these conditions (28). Despite the different periods of observation and definition of the study outcome, as well as the variable of exposure (prediabetes state and T2DM), a similar number of events for PD were observed in this study (PD among T2DM, 1,789 events) compared with our study (PD with and without DR, 1,748 events) (28). Knowing the fact that subjects with prediabetes are at an increased risk of developing T2DM (29), that the diagnosis of T2DM is usually delayed by between 4 and 7 years (30), and that both prediabetes and T2DM increase with age (31), could explain findings in our model that subjects with longer T2DM duration had a higher risk for PD. Similar results were also reported in a recently published case-control study from Denmark, in which the authors did not find an association between DR and PD; further, it should be pointed out that in this study subjects with Parkinson's disease had a longer duration of diabetes (32). In our sensitivity analysis, when we stratified for diabetes duration, the HRs remained in the same direction; however, there was no association of DR with the development of PD. Stratification for HbA1c revealed that a value between 9.1 and 10% in the presence of DR was negatively associated with PD. This finding has to be taken cautiously as it was only found for this HbA1c interval; additionally, there is no clear clinical explanation for this based on current knowledge.

The results from studies examining an association between BMI/obesity and PD have so far been inconsistent. For most of the longitudinal studies, according to a recent review on the epidemiology of PD, no associations between BMI and PD were observed (4). However, in a Spanish retrospective study, overweight and obese individuals were associated with higher PD risk (adj-HR: 1.21; 95% CI 1.15–1.27), compared with normal weight (28). This could be explained due to the different population characteristics or different variables considered in the HR analysis. Another prospective study from Finland reported that overweight or obese subjects were more at risk of developing PD than those with a BMI <23 kg/m^2 (33). We observed surprising results in our multivariable models, where those subjects with a BMI >39.9 kg/m^2 had a 41% decreased risk of developing PD compared with subjects with a BMI <24.9 kg/m^2. We do not have an explanation for this association which was otherwise only restricted to the highest stratum of body weight. Therefore, further studies are warranted to address this question.

So far one recent systemic review and meta-analysis, including 27 observational studies, addressed the relationship between DR and systemic neurodegeneration (34). The authors reported that systemic neurodegeneration was statistically associated with DR. However, in a smaller subgroup meta-analysis related to the severity of DR, the authors did not observe associations with systemic neurodegeneration. Moreover, they only included one study that analyzed the relationship between DR and PD that was summarized but not included in the quantitative review (34). Another systematic review on the potential association between diabetic retinopathy and hyperkinetic disorders found that DR could be indirectly related with striatopallidal microangiopathy; further, the authors suggested that the severity of the DR and glycemic fluctuation could be associated with increased risk or worse prognosis of hyperkinetic disorders (35).

The results of our study should be interpreted with caution, keeping in mind potential limitations. Firstly, this was a retrospective observational study with pseudo-anonymized routinely collected health data where the presence of missing data is inherent. There is a possibility that not all subjects with DR were captured. For this reason, we used the fundus photography results and combined them with diagnostic codes. Secondly, a numerical imbalance between the different groups occurred due to the study design and lack of randomization. Thirdly, we did not have information on the treatment of PD; therefore, we only used the diagnostic code to define the main study event. Besides these limitations, our study includes a large population of subjects attended in primary health care centers which increases the statistical power. Moreover, in our multivariable hazard ratio models, we considered more potentially confounding variables (T2DM duration) related to PD than previously published studies.

TABLE 6 | Sensitivity analysis.

Stratum	Subgroup	Model	HR	95% CI LI	95% CI UI	p	Adjusted by	N
Overall		1	1.06	0.92	1.23	0.40	Sex (male) + Age (years)	242,703
Overall		1.1	1.01	0.88	1.17	0.85	Sex (male) + Age (years) + T2DM duration + HbA1c	242,703
Overall		1.2	1.01	0.87	1.16	0.92	Sex (male) + Age (years) + T2DM duration	242,703
Overall		1.3	1.06	0.92	1.23	0.41	Sex (male) + Age (years) + HbA1c	242,703
Overall		2	1.01	0.86	1.17	0.89	Sex (male) + Age (years) + Smoking + T2DM duration + Dyslipidemia + HTA + BMI	242,703
Overall		3	1.01	0.88	1.17	0.88	Sex (male) + Age (years) + Smoking + T2DM duration + Dyslipidemia + CVD + HTA + CKD + HbA1c + BMI	242,703
T2DM duration	T2DM duration less 6 years	1.1	1.06	0.82	1.37	0.65	Sex (male) + Age (years) + HbA1c	138,553
T2DM duration	T2DM duration 6–10 years	1.1	1.03	0.81	1.31	0.79	Sex (male) + Age (years) + HbA1c	64,161
T2DM duration	T2DM duration 11–15 years	1.1	0.81	0.57	1.15	0.23	Sex (male) + Age (years) + HbA1c	27,449
T2DM duration	T2DM duration 16–20 years	1.1	1.04	0.63	1.71	0.89	Sex (male) + Age (years) + HbA1c	8,140
T2DM duration	T2DM duration more than 20 years	1.1	1.23	0.71	2.12	0.46	Sex (male) + Age (years) + HbA1c	4,400
HbA1c	HbA1c less 6.5%	1.1	1.10	0.84	1.45	0.49	Sex (male) + Age (years) + T2DM duration	79,068
HbA1c	HbA1c 6.5–7%	1.1	1.09	0.75	1.60	0.63	Sex (male) + Age (years) + T2DM duration	37,778
HbA1c	HbA1c 7.1–8%	1.1	1.22	0.91	1.64	0.18	Sex (male) + Age (years) + T2DM duration	41,252
HbA1c	HbA1c 8.1–9%	1.1	1.18	0.79	1.75	0.42	Sex (male) + Age (years) + T2DM duration	18,471
HbA1c	HbA1c 9.1–10%	1.1	0.21	0.06	0.66	0.01	Sex (male) + Age (years) + T2DM duration	9,607
HbA1c	HbA1c more than 10%	1.1	0.73	0.32	1.67	0.45	Sex (male) + Age (years) + T2DM duration	11,957
HbA1c	HbA1c (missing)	1.1	0.82	0.57	1.19	0.31	Sex (male) + Age (years) + T2DM duration	44,570
T2DM duration	T2DM duration less 6 years	3	1.06	0.82	1.38	0.64	Sex (male) + Age (years) + Smoking + Dyslipidemia + CVD + HTA + CKD + HbA1c + BMI	138,553
T2DM duration	T2DM duration 6–10 years	3	1.02	0.80	1.29	0.87	Sex (male) + Age (years) + Smoking + Dyslipidemia + CVD + HTA + CKD + HbA1c + BMI	64,161
T2DM duration	T2DM duration 11–15 years	3	0.80	0.57	1.16	0.25	Sex (male) + Age (years) + Smoking + Dyslipidemia + CVD + HTA + CKD + HbA1c + BMI	27,449
T2DM duration	T2DM duration 16–20 years	3	1.03	0.62	1.69	0.91	Sex (male) + Age (years) + Smoking + Dyslipidemia + CVD + HTA + CKD + HbA1c + BMI	8,140
T2DM duration	T2DM duration more than 20 years	3	1.22	0.70	2.11	0.48	Sex (male) + Age (years) + Smoking + Dyslipidemia + CVD + HTA + CKD + HbA1c + BMI	4,400
HbA1c	HbA1c less 6.5%	3	1.10	0.84	1.45	0.48	Sex (male) + Age (years) + Smoking + T2DM duration + Dyslipidemia + CVD + HTA + CKD + BMI	79,068
HbA1c	HbA1c 6.5–7%	3	1.10	0.75	1.61	0.61	Sex (male) + Age (years) + Smoking + T2DM duration + Dyslipidemia + CVD + HTA + CKD + BMI	37,778
HbA1c	HbA1c 7.1–8%	3	1.23	0.92	1.65	0.17	Sex (male) + Age (years) + Smoking + T2DM duration + Dyslipidemia + CVD + HTA + CKD + BMI	41,252
HbA1c	HbA1c 8.1–9%	3	1.17	0.78	1.73	0.45	Sex (male) + Age (years) + Smoking + T2DM duration + Dyslipidemia + CVD + HTA + CKD + BMI	18,471
HbA1c	HbA1c 9.1–10%	3	0.20	0.06	0.66	0.01	Sex (male) + Age (years) + Smoking + T2DM duration + Dyslipidemia + CVD + HTA + CKD + BMI	9,607
HbA1c	HbA1c more than 10%	3	0.71	0.31	1.62	0.41	Sex (male) + Age (years) + Smoking + T2DM duration + Dyslipidemia + CVD + HTA + CKD + BMI	11,957
HbA1c	HbA1c (missing)	3	0.82	0.57	1.19	0.31	Sex (male) + Age (years) + Smoking + T2DM duration + Dyslipidemia + CVD + HTA + CKD + BMI	44,570

BMI, body mass index; CKD, chronic kidney disease; CVD, Cardiovascular disease; DR, diabetic retinopathy; HbA1c, glycosylate hemoglobin; HR, hazard ratio; 95% CI, 95% confidence interval; LI, lower limit; UI, upper limit; T2DM, type 2 diabetes mellitus.

FIGURE 3 | Hazard ratios for Parkinson's disease according retinopathy status. Sensitivity analysis. M1: Sex (male) + Age (years). M 1.1 Sex (male) + Age (years) + Diabetes duration + HbA1c. M1.2 Sex (male) + Age (years) + Diabetes duration. M1.3 Sex (male) + Age (years) + HbA1c. M2: Sex (male) + Age (years) + Smoking + Diabetes duration + Dyslipidemia + HTA + BMI. M3: Sex (male) + Age (years) + Smoking + Diabetes duration + Dyslipidemia + HTA +CKD + HbA1c + BMI.
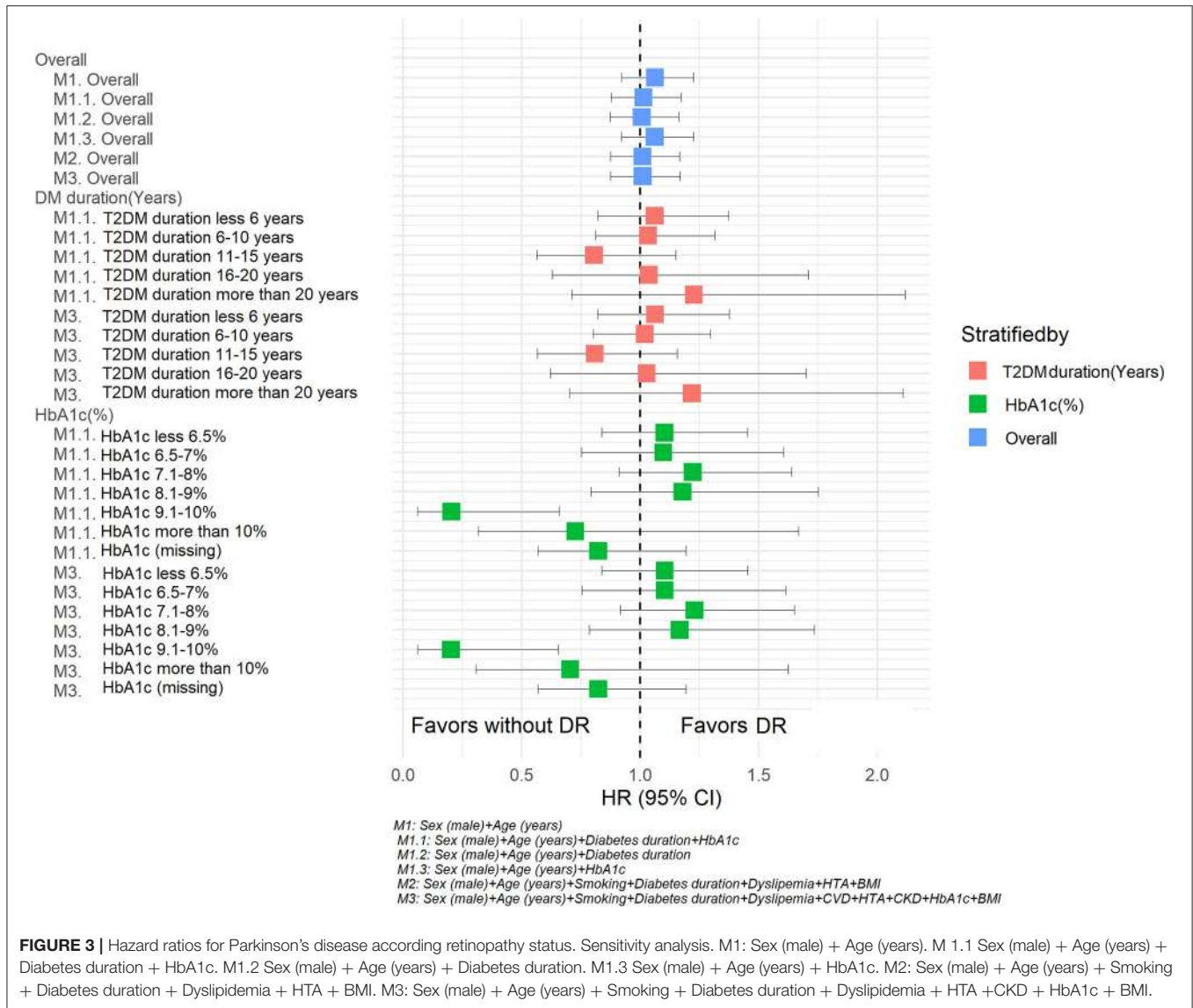
In conclusion, in our primary health care population database, DR was not associated with an increased risk of PD after adjusting for different risk factors. The detection of DR is mainly based on retinal vascular changes that do not always coincide with retinal neurodegeneration (33). Even though a strong biological background exists between DR and PD, further mechanistic studies and well-designed clinical studies are needed to investigate the possible relationship between these two neurodegenerative conditions.

DATA AVAILABILITY STATEMENT

The data analyzed in this study is subject to the following licenses/restrictions: restrictions apply to the availability of some or all data generated or analyzed during this study because they were used under license. The corresponding author will on request detail the restrictions and any conditions under which access to some data may be provided.

Requests to access these datasets should be directed to Dídac Mauricio, didacmauricio@gmail.com.

ETHICS STATEMENT

The studies involving human participants were reviewed and approved by IDIAP Jordi Gol i Gurina Foundation (protocol code P13/028 and date of approval 03/04/2013). Written informed consent for participation was not required for this study in accordance with the national legislation and the institutional requirements.

AUTHOR CONTRIBUTIONS

DM: conceptualization and methodology. JR: software, formal analysis, and data curation. JR, BV, and DM: validation. XM-T: resources. BV: writing—original draft

preparation. BV and DM: writing—review and editing. DM, JJ, JR, EO, EC, JB, JK, and JF-N: supervision. All authors have read and agreed to the published version of the manuscript.

REFERENCES

1. Mauricio D, Alonso N, Gratacòs M. Chronic diabetes complications: the need to move beyond classical concepts. *Trends Endocrinol Metab.* (2020) 31:287–95. doi: 10.1016/j.tem.2020.01.007

2. Lynch SK, Abràmoff MD. Diabetic retinopathy is a neurodegenerative disorder. *Vision Res.* (2017) 139:101–7. doi: 10.1016/j.visres.2017.03.003

3. Simó R, Stitt AW, Gardner TW. Neurodegeneration in diabetic retinopathy: does it really matter? *Diabetologia.* (2018) 61:1902–12. doi: 10.1007/s00125-018-4692-1

4. Ascherio A, Schwarzschild MA. The epidemiology of Parkinson's disease: risk factors and prevention. *Lancet Neurol.* (2016) 15:1257–72. doi: 10.1016/S1474-4422(16)30230-7

5. Bellou V, Belbasis L, Tzoulaki I, Evangelou E, Ioannidis JPA. Environmental risk factors and Parkinson's disease: an umbrella review of meta-analyses. *Park Relat Disord.* (2016) 23:1–9. doi: 10.1016/j.parkreldis.2015.12.008

6. Cereda E, Barichella M, Pedrolli C, Klersy C, Cassani E, Caccialanza R, et al. Diabetes and risk of Parkinson's disease: a systematic review and meta-analysis. *Diabetes Care.* (2011) 34:2614–23. doi: 10.2337/dc11-1584

7. Chohan H, Senkevich K, Patel RK, Bestwick JP, Jacobs BM, Bandres Ciga S, et al. Type 2 diabetes as a determinant of Parkinson's disease risk and progression. *Mov Disord.* (2021) 36:1420–9. doi: 10.1002/mds.28551

8. Verdile G, Fuller SJ, Martins RN. The role of type 2 diabetes in neurodegeneration. *Neurobiol Dis.* (2015) 84:22–38. doi: 10.1016/j.nbd.2015.04.008

9. Hu G, Jousilahti P, Bidel S, Antikainen R, Tuomilehto J. Type 2 diabetes and the risk of Parkinson's disease. *Diabetes Care.* (2007) 30:842–7. doi: 10.2337/dc06-2011

10. Schernhammer E, Hansen J, Rugbjerg K, Wermuth L, Ritz B. Diabetes and the risk of developing Parkinson's disease in Denmark. *Diabetes Care.* (2011) 34:1102–8. doi: 10.2337/dc10-1333

11. De Pablo-Fernandez E, Goldacre R, Pakpoor J, Noyce AJ, Warner TT. Association between diabetes and subsequent Parkinson disease. *Neurology.* (2018) 91:e139–42. doi: 10.1212/WNL.0000000000005771

12. Sun Y, Chang YH, Chen HF, Su YH, Su HF, Li CY. Risk of Parkinson disease onset in patients with diabetes: a 9-year population-based cohort study with age and sex stratifications. *Diabetes Care.* (2012) 35:1047–9. doi: 10.2337/dc11-1511

13. Xu Q, Park Y, Huang X, Hollenbeck A, Blair A, Schatzkin A, et al. Diabetes and risk of Parkinson's disease. *Diabetes Care.* (2011) 34:910–5. doi: 10.2337/dc10-1922

14. Rhee SY, Han KD, Kwon H, Park SE, Park YG, Kim YH, et al. Association between glycemic status and the risk of Parkinson disease: a nationwide population based study. *Diabetes Care.* (2020) 43:2169–75. doi: 10.2337/dc19-0760

15. Simon KC, Chen H, Schwarzschild M, Ascherio A. Hypertension, hypercholesterolemia, diabetes, and risk of Parkinson disease. *Neurology.* (2007) 69:1688–95. doi: 10.1212/01.wnl.0000271883.45010.8a

16. Palacios N, Gao X, McCullough ML, Jacobs EJ, Patel AV, Mayo T, et al. Obesity, diabetes, and risk of Parkinson's disease. *Mov Disord.* (2011) 26:2253–9. doi: 10.1002/mds.23855

17. Zhang Z, Zhou Y, Zhao H, Xu J, Yang X. Association between pathophysiological mechanisms of diabetic retinopathy and Parkinson's disease. *Cell Mol Neurobiol.* (2020). doi: 10.1007/s10571-020-00953-9

18. Mohana Devi S, Mahalaxmi I, Aswathy NP, Dhivya V, Balachandar V. Does retina play a role in Parkinson's Disease? *Acta Neurol Belg.* (2020) 120:257–65. doi: 10.1007/s13760-020-01274-w

19. Lee SE, Han K, Baek JY, Ko KS, Lee KU, Koh EH. Association between diabetic retinopathy and parkinson disease: the Korean national health insurance service database. *J Clin Endocrinol Metab.* (2018) 103:3231–8. doi: 10.1210/jc.2017-02774

20. Mata-Cases M, Mauricio D, Real J, Bolíbar B, Franch-Nadal J. Is diabetes mellitus correctly registered and classified in primary care? a population-based study in Catalonia, Spain. *Endocrinol Nutr.* (2016) 63:440–8. doi: 10.1016/j.endonu.2016.07.004

21. Mata-Cases M, Franch-Nadal J, Mauricio D, Bolíbar B. Investigar en diabetes desde una base de datos de atención primaria: la experiencia del Sistema de Información para el Desarrollo de la Investigación en Atención Primaria (SIDIAP). *Av en Diabetol.* (2013) 29:169–74. doi: 10.1016/j.avdiab.2013.09.002

22. Wu L. Classification of diabetic retinopathy and diabetic macular edema. *World J Diabetes.* (2013) 4:290. doi: 10.4239/wjd.v4.i6.290

23. Ma RCW, Chan JCN. Type 2 diabetes in East Asians: similarities and differences with populations in Europe and the United States. *Ann N Y Acad Sci.* (2013) 1281:64–91. doi: 10.1111/nyas.12098

24. Clarke PM, Glasziou P, Patel A, Chalmers J, Woodward M, Harrap SB, et al. Event rates, hospital utilization, and costs associated with major complications of diabetes: a multicountry comparative analysis. *PLoS Med.* (2010) 7:e1000236. doi: 10.1371/journal.pmed.1000236

25. Manuel DG, Rosella LC, Stukel TA. Importance of accurately identifying disease in studies using electronic health records. *BMJ.* (2010) 341:c4226. doi: 10.1136/bmj.c4226

26. Zoungas S, Woodward M, Li Q, Cooper ME, Hamet P, Harrap S, et al. Impact of age, age at diagnosis and duration of diabetes on the risk of macrovascular and microvascular complications and death in type 2 diabetes. *Diabetologia.* (2014) 57:2465–74. doi: 10.1007/s00125-014-3369-7

27. Jerneld B, Algvere P. Relationship of duration and onset of diabetes to prevalence of diabetic retinopathy. *Am J Ophthalmol.* (1986) 102:431–7. doi: 10.1016/0002-9394(86)90069-3

28. Sánchez-Gómez A, Díaz Y, Duarte-Salles T, Compta Y, Martí MJ. Prediabetes, type 2 diabetes mellitus and risk of Parkinson's disease: a population-based cohort study. *Parkinsonism Relat Disord.* (2021) 89:22–7. doi: 10.1016/j.parkreldis.2021.06.002

29. Aroda VR, Ratner R. Approach to the patient with prediabetes. *J Clin Endocrinol Metab.* (2008) 93:3259–65. doi: 10.1210/jc.2008-1091

30. Harris MI, Klein R, Welborn TA, Knuiman MW. Onset of NIDDM occurs at Least 4-7 yr before clinical diagnosis. *Diabetes Care.* (1992) 15:815–9. doi: 10.2337/diacare.15.7.815

31. Chang AM, Halter JB. Aging and insulin secretion. *Am J Physiol Metab.* (2003) 284:E7–E12. doi: 10.1152/ajpendo.00366.2002

32. Larsen MEC, Thykjaer AS, Pedersen FN, Laugesen CS, Andersen N, Andresen J, et al. Diabetic retinopathy as a potential marker of Parkinson' s disease: a register-based cohort study. (2021) 3:fcab262. doi: 10.1093/braincomms/fcab262

33. Hu G, Jousilahti P, Nissinen A, Antikainen R, Kivipelto M, Tuomilehto J. Body mass index and the risk of Parkinson disease. *Neurology.* (2006) 67:1955–9. doi: 10.1212/01.wnl.0000247052.18422.e5

34. Pedersen HE, Sandvik CH, Subhi Y, Grauslund J, Pedersen FN. Relationship between diabetic retinopathy and systemic neurodegenerative diseases: a systematic review and meta-analysis. *Ophthalmol Retin.* (2021). S2468-6530(21)00225-6. doi: 10.1016/j.oret.2021.07.002

35. Lizarraga KJ, Chunga N, Yannuzzi NA, Flynn HW, Singer C, Lang AE. The retina as a window to the basal ganglia: systematic review

of the potential link between retinopathy and hyperkinetic disorders in diabetes. *Park Relat Disord.* (2020) 80:194–8. doi: 10.1016/j.parkreldis.2020. 10.025

Conflict of Interest: DM and JF-N received advisory and/or speaking fees from Astra-Zeneca. Ascensia. Boehringer Ingelheim. GSK. Lilly. MSD. Novartis. Novo Nordisk. and Sanofi and received research grants to the institution from Astra-Zeneca. GSK. Lilly. MSD. Novartis. Novo Nordisk. Sanofi. and Boehringer. EO has received advisory and or speaking fees from Astra-Zeneca, Boehringer Ingelheim, Lilly, MSD, Novo Nordisk, Sanofi, and Amgen; he has received research grants to the institution from MSD and Amgen.

The remaining authors declare that the research was conducted in the absence of any commercial or financial relationships that could be construed as a potential conflict of interest.

Publisher's Note: All claims expressed in this article are solely those of the authors and do not necessarily represent those of their affiliated organizations, or those of the publisher, the editors and the reviewers. Any product that may be evaluated in this article, or claim that may be made by its manufacturer, is not guaranteed or endorsed by the publisher.

Check for updates

Ocular Adverse Effects in Atopic Dermatitis Patients Treated With Dupilumab: A Bibliometric Analysis

Qian-Nan Jia, Ju Qiao, Kai Fang and Yue-Ping Zeng*

Department of Dermatology, State Key Laboratory of Complex Severe and Rare Diseases, Peking Union Medical College Hospital, Chinese Academy of Medical Science and Peking Union Medical College, National Clinical Research Center for Dermatologic and Immunologic Diseases, Beijing, China

Background: Atopic dermatitis (AD) is one of the most common chronic inflammatory skin disorders. Dupilumab, the first targeted biological drug approved for the treatment of AD, has been widely used, along with increasing ocular adverse effects (AEs).

Objective: To perform a bibliometric analysis of all the qualified literature involving ocular AEs during the treatment of AD with dupilumab.

Methods: Relevant studies were extracted from the Web of Science database and screened by researchers. The bibliographic analysis was performed using the VOSviewer.

Results: A total of 138 articles were enrolled in this study. The first study was published in 2016 by Oregon Health and Science University from the United States. The majority of publications were published in the past 3 years. *British Journal of Dermatology* published the highest number of articles. The United States was the country with the most publications. Sanofi (France) and Regeneron Pharmaceuticals (USA) were the leading organizations with the most contributions. Conjunctivitis was the most common ocular AE. The management of AD will continue to be the research hotspot and development trend in this area. The milestone research is the first article "Two Phase 3 Trials of Dupilumab vs. Placebo in Atopic Dermatitis" published in the *New England Journal of Medicine*. Most of the top 10 papers were mainly randomized, placebo-controlled phase 2 and phase 3 clinical trials and real-life large cohort studies.

Conclusions: This study may help better understand ocular AEs in the dupilumab treatment of AD, and grasp the research trends and most influential topics in this field.

Keywords: atopic dermatitis, dupilumab, ocular adverse effects, bibliometric, conjunctivitis

INTRODUCTION

Atopic dermatitis (AD) is one of the most common chronic inflammatory skin disorders, and affects patients of all ages in all aspects, from physical health to psychological condition and economic burden (1, 2). The prevalence of AD is up to 25% in children (3) and 7–10% in adults (4). Most patients have an early disease onset by the age of 5 years and may last for a lifetime. Clinically, AD is characterized by erythema and severe pruritus, and had a strong tendency to relapse. Patients with AD suffer from intense itching, pain, sleep disturbance, anxiety, depression, and psychosocial stress (5, 6). With increased prevalence for years, AD has been becoming a health-threatening disease with severe impacts on the patient's quality of life.

Atopic dermatitis is believed to be the result of complex interactions between genetic and environmental factors that affect the immune system and epidermal barrier function (7). The inflammatory reaction in AD is generally considered due to the activation of T helper cell type 2 (Th2) immune response, in which related cytokines interleukin-4 (IL-4), IL-13, and IL-31 are quite essential (8). The treatment of AD remains to be a clinical challenge, especially for patients with moderate-to-severe AD. Moderate-to-severe AD may require systemic agents, such as immunosuppressant drugs and dupilumab (9). Dupilumab is a fully-human monoclonal antibody that is against IL-4 receptor α and blocks crucial pathways from both IL-4 and IL-13 in AD (10). The safety profile and adverse effects (AEs) are required in the long-term dupilumab treatment of patients with AD.

In 2014, Beck et al. (11) first reported that patients with moderate-to-severe AD had marked and rapid improvement after the treatment with dupilumab in a randomized, double-blind, placebo-controlled trial. Moreover, 2 years later, two-phase 3 trials of dupilumab vs. placebo in AD investigated the effectiveness and safety of dupilumab, and revealed that dupilumab improved the signs and symptoms of AD in all aspects (12). Since then, articles involving the safety of patients with AD treated with dupilumab have been published increasingly. With the approval of dupilumab for the treatment of moderate-to-severe AD adults by the FDA in 2017, dupilumab has been used widespread, along with increasing AEs reported in the literature. AEs induced by dupilumab in AD clinical trials were mainly ocular diseases and increased eosinophil counts. Other AEs reported later in the real world were as follows: psoriasis-like lesions, head and neck erythematous lesions, rosacea-like skin symptoms, alopecia, muscular pain, and arthritis (13–19). In detail, ocular AEs mainly included conjunctivitis, keratitis, keratoconjunctivitis, blepharitis, eye pruritus, and dry eye. The prominent clinical manifestation of ocular AEs was redness of the conjunctiva in both eyes, and especially hyperemia and nodular swelling of the limbus. Other clinical symptoms included itching, tearing, stinging, burning, and foreign body sensation. Bibliometrics is a quantitative analysis of the published literature in a specific scientific field using mathematical and statistical methods. The application of bibliometric analysis could help better understand the knowledge structure and significant advances in a certain research field, and is thus rapidly increasing in several diseases for the past few years. However, there are few bibliometric studies referring to AD. Therefore, we aimed to perform a bibliometric analysis of all the qualified literature involving ocular AEs during the treatment of AD with dupilumab. The present study described the characteristics of articles and the collaboration network of authors, organizations, and countries/regions, and revealed the research dynamics, especially evaluating research focus and emerging trends in this field.

METHODS

Data Extraction and Screening

Relevant studies in relation to dupilumab in the treatment of atopic dermatitis were extracted from the Web of Science Core Collection database on August 30, 2021. The detailed search strategy was as follows: TOPIC: (dupilumab) *AND* TOPIC: (atopic dermatitis) *AND* DOCUMENT TYPES: (Article OR Letter) *AND* LANGUAGE: (English).

Two researchers (QN Jia and J Qiao) further performed literature screening of the title and abstract independently, with full text downloaded if necessary. Research regarding ocular adverse events in the treatment of atopic dermatitis with dupilumab were retrieved and collected, such as research letters and case letters. Articles that meet the following criteria were excluded: (1) ocular adverse events were uninvolved in the main topic of article; (2) the article was a review, systematic review, meta-analysis, correspondence, expert opinion, retracted article, conference article, or guideline. With the guidance of a senior expert (YP Zeng), a final agreement was reached on the literature screening.

For articles that met the criteria, we recorded all the available information, such as title, authors, institutions, funding organization, country/region, abstract, keywords, journal of publication, year of publication, citations, and cited references. Journal impact factor (IF) was queried from the 2020 Journal Citation Reports.

Data Analysis and Visualization

The bibliographic information was analyzed using the VOSviewer (version 1.6.17). The co-occurrence analyses of authors, organizations, countries/regions, and keywords were performed with VOSviewer, as well as the analyses of reference citations, and co-citations. The related maps of the above analyses were produced.

RESULTS

We extracted 494 articles on the topic of patients with AD treated with dupilumab from the Web of Science Core Collection database following our search strategy. After literature screening by researchers, a total of 138 articles reported the occurrence of ocular AEs and were enrolled in this study. By document type, 138 articles were categorized into 97 original articles and 41 letters. The flow diagram of the present study is shown in **Figure 1**.

Evolution of Scientific Production

All 138 articles were published between 2016 and 2021. The number of publications of each year are displayed in **Figure 2**. There were a few articles sporadically published from 2016 to 2018. However, the number of publications abruptly rose in 2019 and 2020, accounting for nearly two-thirds of the total amount, when added together. It should be noted that data extraction was performed in August 30, 2021, and thus publications in 2021 were incomplete.

Journals of Publication

All the articles analyzed in this study were published in 47 journals, including 22 Dermatological journals. The other 25 journals were classified into Ophthalmology (9 journals), Medicine, General & Internal (6 journals), Immunology

FIGURE 1 | The flow diagram of this study.

FIGURE 2 | The number of publications of each year in this area.

TABLE 1 | The top 10 journals with the largest number of published articles in the study area.

Journal	Publication number	Journal IF*	WoS# Categories
Br J Dermatol	18	9.302	DERMATOLOGY
J Am Acad Dermatol	15	11.527	DERMATOLOGY
Dermatol Ther	13	2.851	DERMATOLOGY
J Eur Acad Dermatol Venereol	11	6.166	DERMATOLOGY
JAMA Dermatol	7	10.282	DERMATOLOGY
Am J Clin Dermatol	5	7.403	DERMATOLOGY
Int J Dermatol	5	2.736	DERMATOLOGY
J Dermatol Treat	5	3.359	DERMATOLOGY
Allergy	4	13.146	ALLERGY, IMMUNOLOGY
J Clin Med	4	4.241	MEDICINE, GENERAL & INTERNAL

*Journal impact factor (IF) was queried from the 2020 Journal Citation Reports. #Web of Science.

Analysis of Countries/Regions, Organizations, and Authors

There were 33 countries/regions reporting ocular AEs during the treatment of AD with dupilumab. The United States published the highest number of publications (53, 38.41%), followed by France (27, 19.57%), Germany (27, 19.57%), Italy (27, 19.57%), and Netherlands (22, 15.94%). The collaborative network among the major countries/regions was generated by VOSviewer and presented in **Figure 3**. There were 15 nodes and 80 links. The larger the circle, the more publications the country/region. A line is corresponding to a connection between two countries/regions. The length of a line represented the cooperation intensity of two countries/regions. The shorter the line, the stronger the relatedness. As shown in **Figure 3B**, the geographical distribution changed over time. The foremost contributing countries were the United States, Germany, Denmark, and Canada, followed by France, UK, Netherlands, Japan, etc. Italy subsequently caught up in 2020 with 27 publications.

In total, 326 organizations had made contributions in this study area. Regeneron Pharmaceuticals Inc. made the most contributions with 21 articles (15.22%), followed by Sanofi (20, 14.49%), University Medical Center Utrecht (17, 12.32%), Oregon Health and Science University (16, 11.59%), and Northwestern University (14, 10.14%). Oregon Health and Science University was the first to report ocular AEs in this medication field, subsequently with Oregon Medical Research Center, Sanofi, Ludwig-Maximilians-University Munchen, and Aarhus University Hospital, etc. When it comes to the cooperation network, there were 20 nodes and 158 links (**Figure 4**). The organizations presented in **Figure 4** were mainly from the United States and Italy, while others were from the UK, Denmark, and the Netherlands.

A total of 788 authors participated in this research field. Both Graham NMH (Regeneron Pharmaceuticals Inc., USA)

(6 journals), Allergy (5 journals), Pharmacology & Pharmacy (2 journals), Medicine, Research & Experimental (1 journal), and Multidisciplinary Sciences (1 journal) (Five journals were classified into both Allergy and Immunology categories.). The number of publications varied from 1 to 18 in these journals. The journal IF was distributed between 0.22 and 91.245. **Table 1** showed that top 10 journals with the largest number of published articles, comprising nearly two-thirds of the total publications. Of the 10 journals, four journals had smaller IF than 5, three journals with an IF between 5 and 10, while three journals (*Allergy, Journal of the American Academy of Dermatology* and *JAMA Dermatology*) had an IF higher than 10. Eight out of the 10 journals belonged to a dermatologic field (80%). *British Journal of Dermatology* took the lead and had the highest number of publications (18, 13.04%, IF 2020 = 9.302), followed by *Journal of the American Academy of Dermatology* (15, 10.87%, IF 2020 = 11.527), *Dermatologic Therapy* (13, 9.42%, IF 2020 = 2.851), *Journal of the European Academy of Dermatology and Venereology* (11, 7.97%, IF 2020 =6.166), and *JAMA Dermatology* (7, 5.07%, IF 2020 = 10.282).

and Simpson EL (Oregon Health and Science University, USA) published the largest number of articles in this study area (10, 7.25%), followed by de Bruin-Weller M (9, 6.52%, University Medical Center, Netherlands), Blauvelt A (8, 5.80%, Oregon Medical Research Center Utrecht, USA), and Chen Z (8, 5.80%, Regeneron Pharmaceuticals Inc., USA). Co-authorship analysis revealed 34 nodes and 300 links (**Figure 5**). The top 10 authors with the most publications were mainly from the United States, with only three authors from the Netherlands, Germany, and France, respectively.

Co-occurrence Analysis of Keywords

As shown in **Figure 6**, the co-occurrence analysis of keywords was conducted and revealed 26 keywords and 182 links. The top keywords with the highest frequency were as follows: prevalence, conjunctivitis, 2-phase 3 trials, persistent asthma, safety, efficacy, quality of life, care, severity, daily practice, eczema herpeticum, epidemiology, IL-13, risk, allergic conjunctivitis, asthma, azathioprine, biomarkers, IL-4, long-term, monoclonal antibody, and reliability. Conjunctivitis was the main ocular AE detected in this analysis. Prevalence is the most popular phrase, besides AD and dupilumab. Two-Phase 3 Trials of Dupilumab vs. Placebo in Atopic Dermatitis published in the New England Journal of Medicine were the most frequently mentioned clinical trials. Keywords regarding the management of AD made up the largest proportion, such as the safety and efficacy of dupilumab, quality of life and care of the patients, and daily practice. The mechanism of dupilumab in the treatment of AD was also commonly mentioned with the following keywords: IL-13, IL-4, biomarker, and monoclonal antibody.

Reference Citations and Co-Citations

Of the 138 papers, the analysis of reference citations discovered 134 nodes and 686 links (**Figure 7A**). The vast majority of studies were published in 2019, 2020, and 2021, with only a few in 2016, 2017, 2018. The top 10 papers with most citations were uniformly distributed between 2016 and 2020. "Two-Phase 3 Trials of Dupilumab vs. Placebo in Atopic Dermatitis" (12) (2016), which was also detected as a popular keyword, had 741 citations. Other top papers were as follows: "Long-term management of moderate-to-severe atopic dermatitis with dupilumab and concomitant topical corticosteroids (LIBERTY AD CHRONOS): a 1-year, randomized, double-blinded, placebo-controlled, phase 2 trial" (20) (2017, 443 citations); "Efficacy and safety of dupilumab in adults with moderate-to-severe atopic dermatitis inadequately controlled by topical treatments: a randomized, placebo-controlled, dose-ranging phase 2b trial" (9) (2016, 315 citations). The above papers were published in the *New England Journal of Medicine* and *Lancet* with an IF of 91.245 and 79.321.

The co-citation analysis is performed with 20 citations set as the minimum number of a cited reference. Of the 1,348 cited references, 16 papers met the threshold with 120 links (**Figure 7B**, **Table 2**). All the papers were published between 2013 and 2019, with the majority between 2016 and 2019. More than half of these papers were published in the *New England Journal of Medicine* (5, 31.25%), *Lancet* (3, 18.75%), and *British Journal*

of Dermatology (3, 18.75%). Other journals were the *Journal of the American Academy of Dermatology, Journal of Allergy and Clinical Immunology-In Practice, JAMA Dermatology,* and *JAMA.* The top 2 papers were identical to those in the analysis of citations, and were undoubtedly the most co-cited papers with 87 and 82 citations, respectively. "Dupilumab with concomitant topical corticosteroid treatment in adults with atopic dermatitis with an inadequate response or intolerance to ciclosporin A or when this treatment is medically inadvisable: a placebo-controlled, randomized phase III clinical trial" (21) (2018) ranked third with 49 citations; followed by "Dupilumab treatment in adults with moderate-to-severe atopic dermatitis" (11) (2014, 39 citations), and "Conjunctivitis in dupilumab clinical trials" (19) (2019, 35 citations).

DISCUSSION

Dupilumab which is the first targeted biological drug approved for the treatment of AD, has been generally administrated in both adults and children. Ocular AEs reported during the treatment of AD with dupilumab have been increasing sharply, and were proposed to be under the definition "dupilumab induced ocular surface disease" (DIOSD) by Zirwas et al. (22).

In recent years, bibliometric analysis has been gradually applied in a variety of medical fields, such as respiratory medicine, ocular disease, and cancer. In dermatology, several research fields have been analyzed with bibliometric methods, such as general dermatology, melanoma, psoriasis, psoriatic arthritis, toxic epidermal necrolysis, and Stevens-Johnson syndrome (23–25).

To the best of our knowledge, this is the first bibliometric analysis focusing on ocular AEs during the treatment of AD with dupilumab. In this study, we investigated published documents involving dupilumab in the treatment of AD, identified all the related ocular AEs, and systematically analyzed the basic characteristics of literature, such as the journals, collaborative networks of countries/regions, organizations and authors, co-occurrence of keywords, and citation network.

The analysis of document type showed that less than one-third of documents were case letters or research letters, and most papers were original research studies. With regard to the publication time, the earliest study was published in 2016, and the majority (89.86%) of publications were published in the past 3 years (2019–2021), indicating research on ocular AEs is a novel and emerging field.

The bibliometric analysis of journals found a total of 47 journals of publication. Dermatologic journals (22, 46.81%) and ophthalmologic journals (9, 19.15%) were undoubtedly the top 2 categories, followed by Medicine, General & Internal and Immunology/Allergy categories. The reason why Medicine, General & Internal journals published quite a few papers might be that some general medicine journals (*New England Journal of Medicine and Lancet*) have higher IFs than dermatologic journals. The top 6 journals were the *British Journal of Dermatology, Journal of the American Academy of Dermatology, Dermatologic Therapy, Journal of the European Academy of Dermatology*

FIGURE 3 | The collaborative network among the major countries/regions. **(A)** Network visualization; **(B)** overlay visualization.

FIGURE 4 | The collaborative network of organizations.
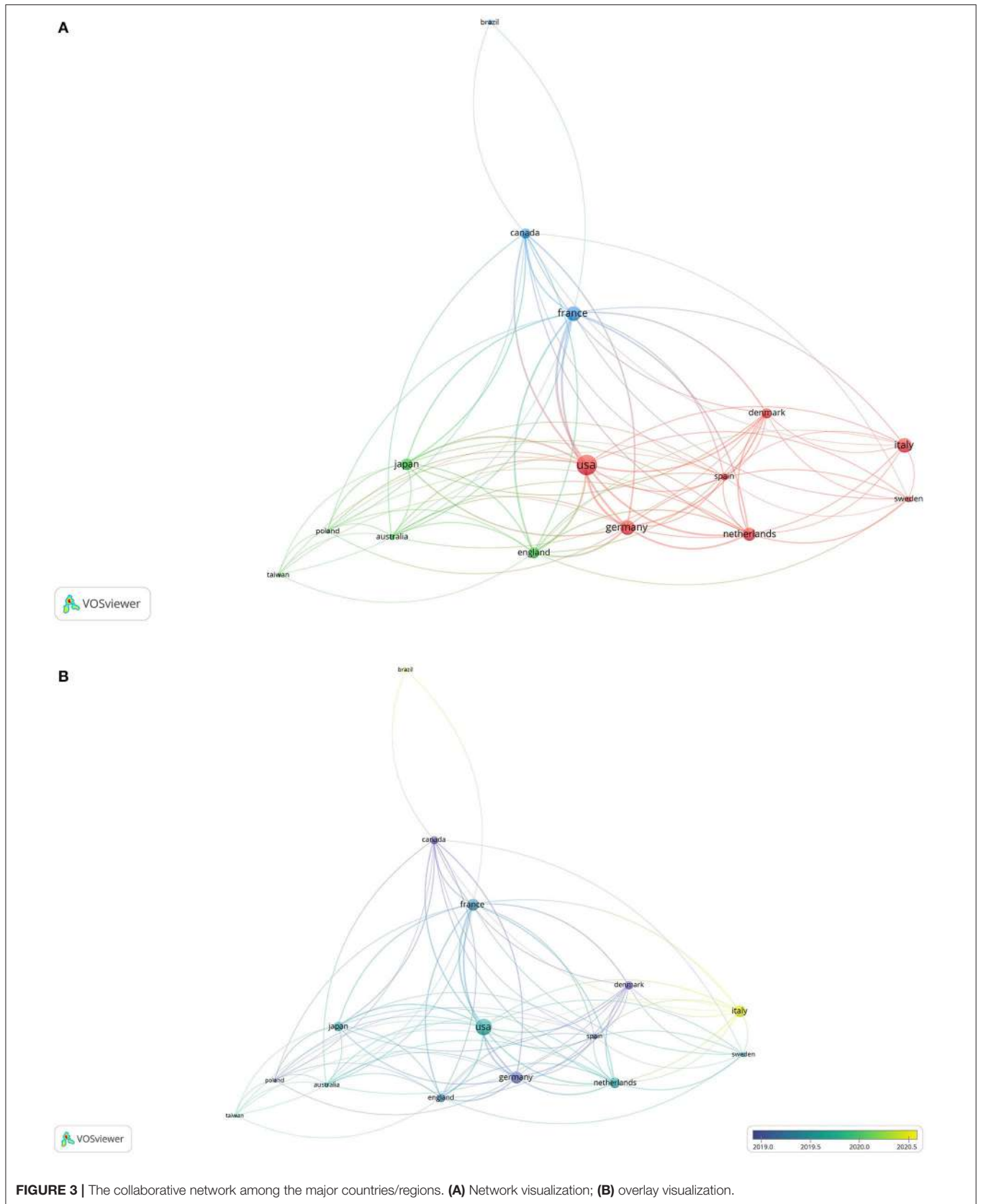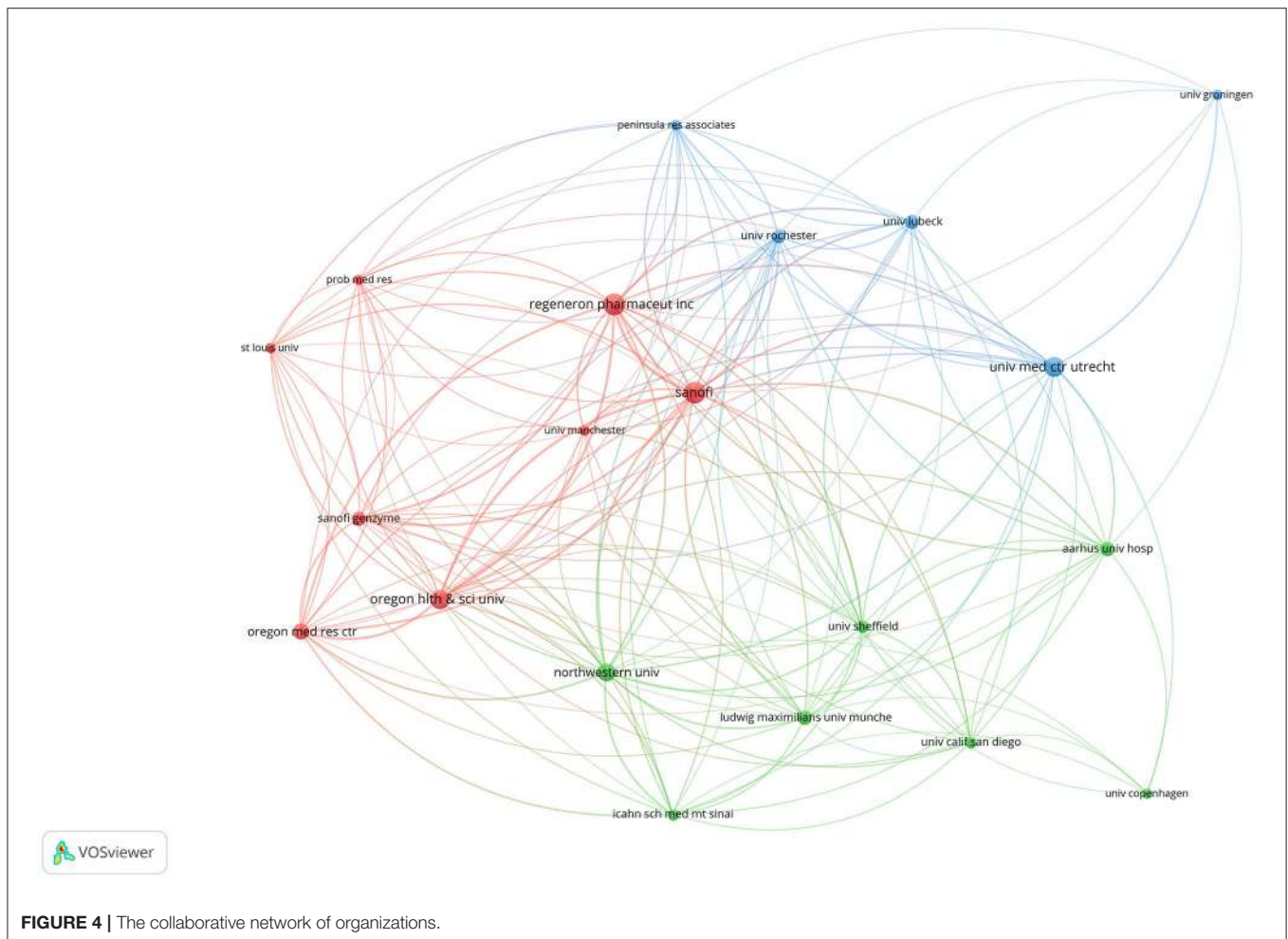
and Venereology, JAMA Dermatology, and *American Journal of Clinical Dermatology.* All of them were dermatologic journals, and 5 out of 6 journals were world-class dermatologic journals with IFs higher than 6.

Our study showed that 33 countries/regions had reported ocular AEs during the treatment of AD with dupilumab. The United States published the earliest article and the highest number of publications and was far ahead of other countries/regions. In the collaborative network, the United States had the strongest total link strength, suggesting a highest cooperation intensity with others. Although Italy tied for second with France and Germany in the publication number, Italy ranked 13th in the total link strength, which might be because studies from Italy were mainly published after 2020 with limited time for citations. These countries/regions presented in the collaboration network were mainly distributed in Europe (9/15), followed by North America (2), East Asia (2), Australia (1), and South America (1). The vast majority (86.67%) of countries/regions were in the Northern Hemisphere. Except for Brazil, all the other countries/regions were developed countries/regions.

In the bibliometric analysis of organizations, 326 organizations had made contributions in this study area. Oregon Health and Science University published the first article reporting ocular AEs during the treatment of AD with dupilumab. Most organizations were universities and research centers. However, organizations leading the way were Sanofi (France) and Regeneron Pharmaceuticals Inc. (USA), since dupilumab was jointly developed by them. University Medical Center Utrecht (Netherlands) was the leading university, followed by Oregon Health and Science University (USA), and Northwestern University (USA). Thus, the main forms of research group were biopharmaceutical companies, universities, and research centers. Regarding the cooperation network, Sanofi containing Sanofi Genzyme ranked first in the cooperation intensity with the highest total link strength, followed by Regeneron Pharmaceuticals Inc., demonstrating the dominant position in the development of dupilumab. Half of the top 10 organizations with the most citations were from the United States, reflecting the great influence on this research field.

On the subject of authors, we summarized a total of 788 authors participating in this research field. Concerning first authors, Graham NMH (Regeneron Pharmaceuticals Inc.) and

FIGURE 5 | The collaborative network of authors.

FIGURE 6 | The co-occurrence network of keywords.
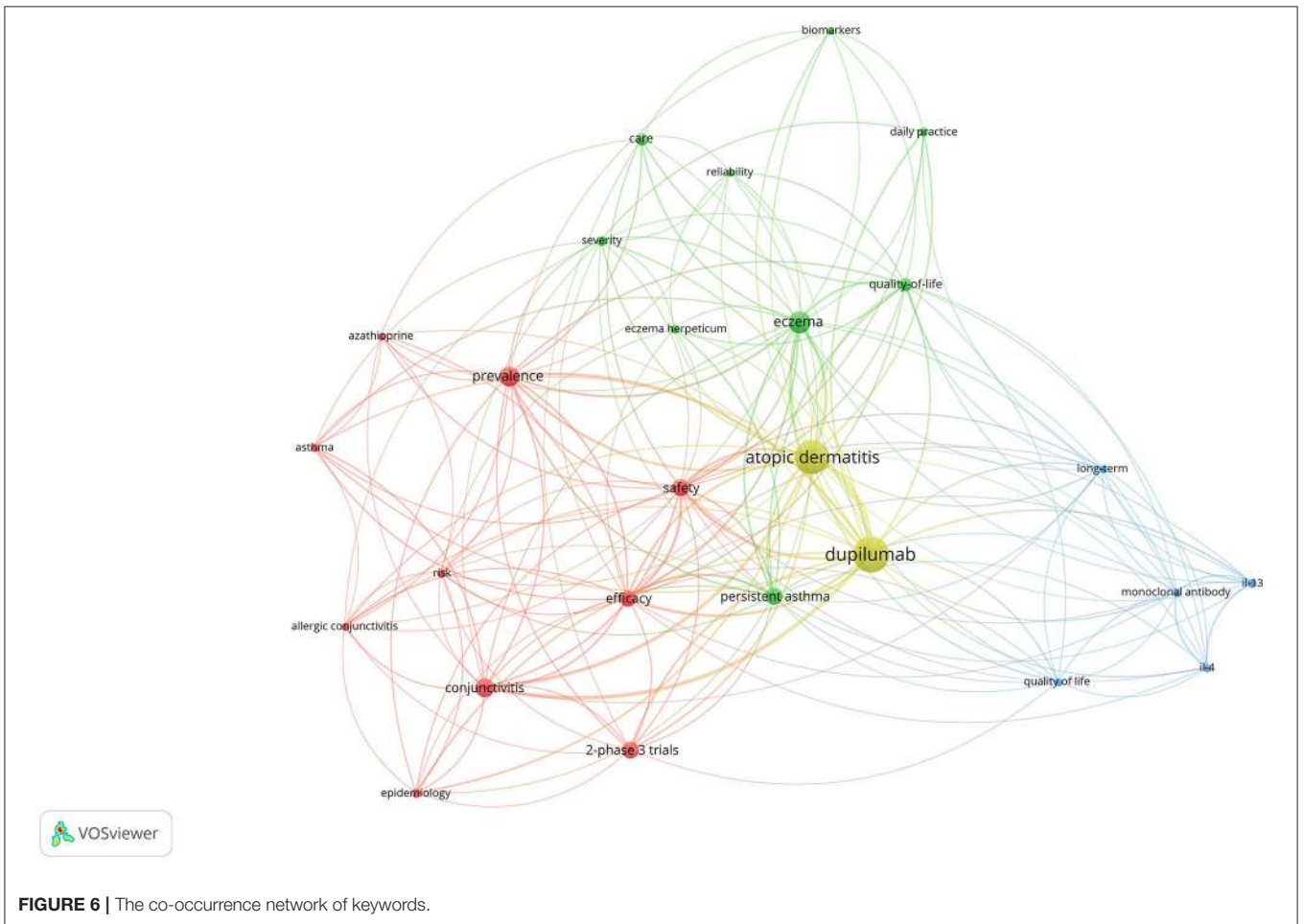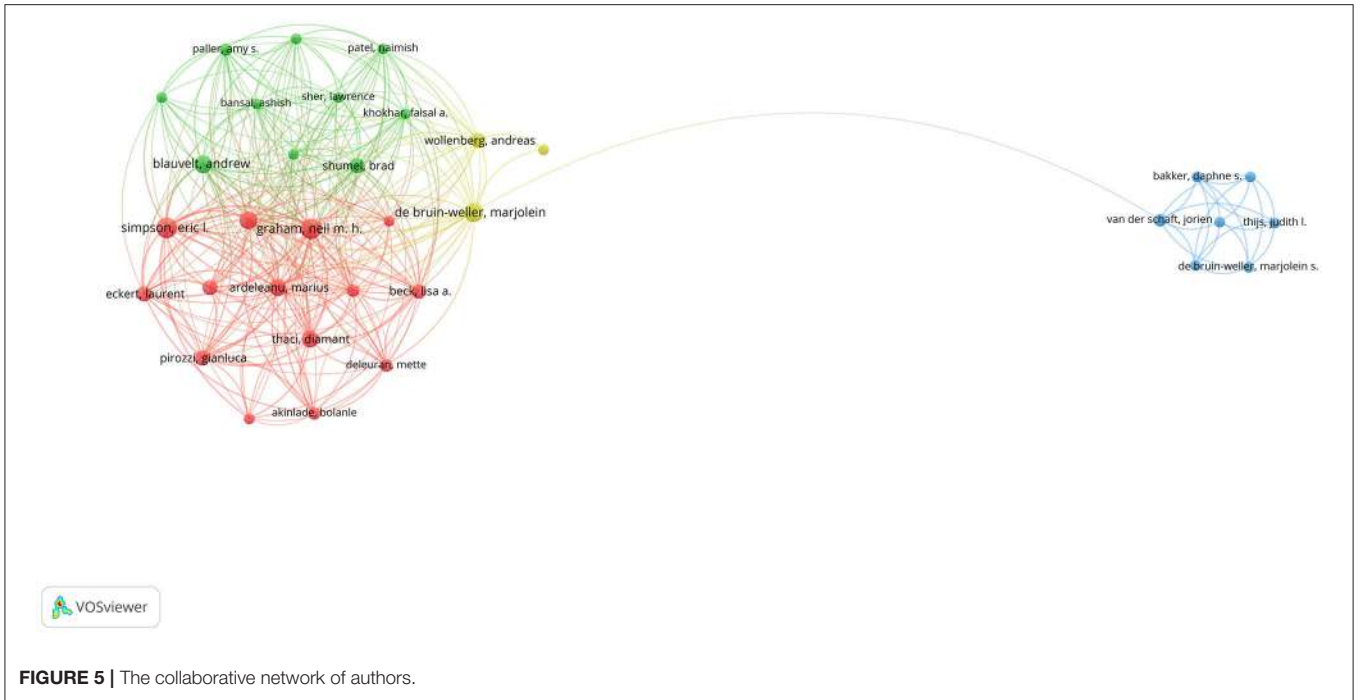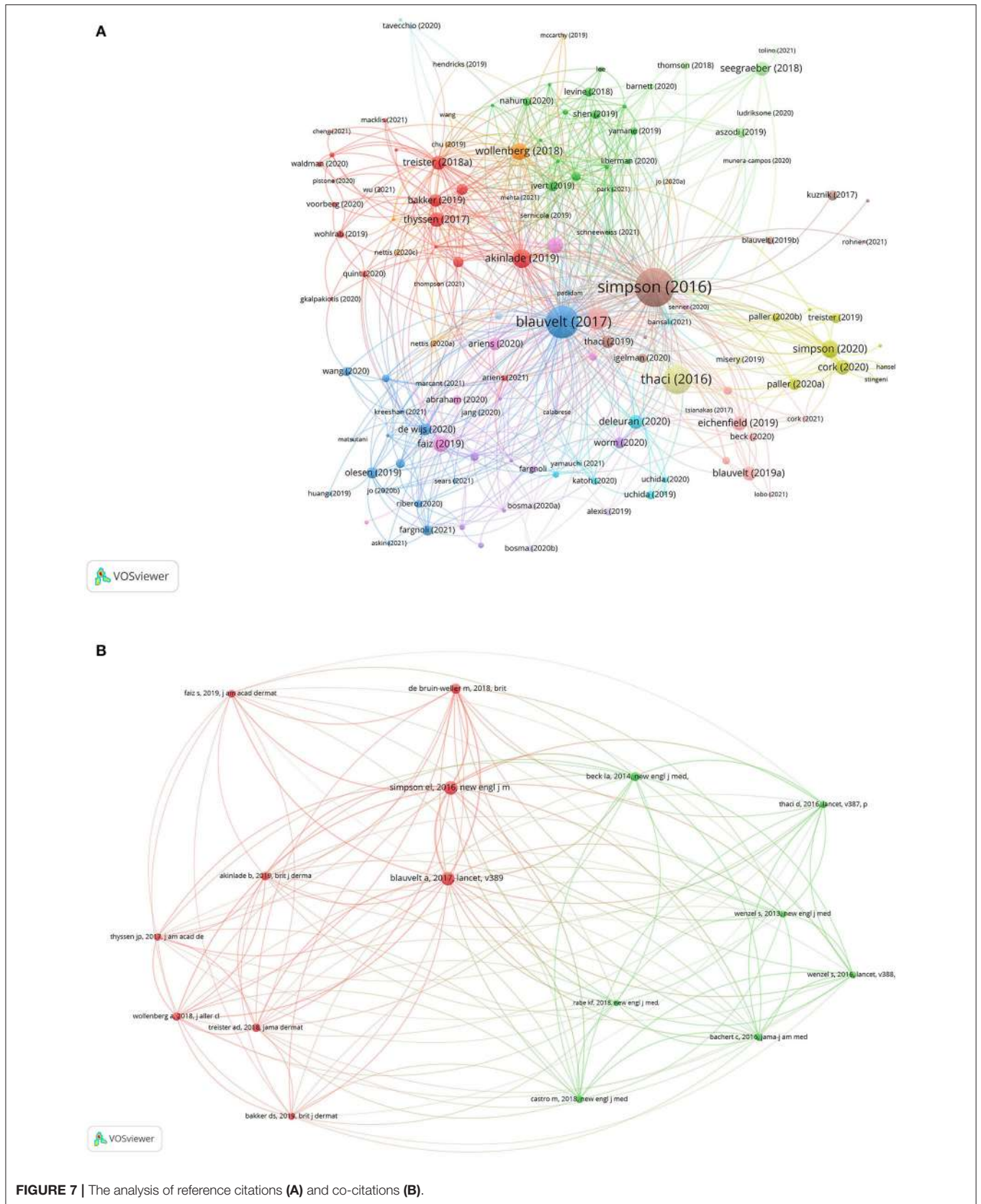
FIGURE 7 | The analysis of reference citations **(A)** and co-citations **(B)**.

Year	Journal	References	Article title	Citations	Total link strength
2016	New Engl J Med	Simpson et al. (12)	Two Phase 3 Trials of Dupilumab versus Placebo in Atopic Dermatitis	87	385
2017	Lancet	Blauvelt et al. (20)	Long-term management of moderate-to-severe atopic dermatitis with dupilumab and concomitant topical corticosteroids (LIBERTY AD CHRONOS): a 1-year, randomized, double-blinded, placebo-controlled, phase 2 trial	82	367
2018	Brit J Dermatol	de Bruin-Weller et al. (21)	Dupilumab with concomitant topical corticosteroid treatment in adults with atopic dermatitis with an inadequate response or intolerance to ciclosporin A or when this treatment is medically inadvisable: a placebo-controlled, randomized phase III clinical trial	49	252
2014	New Engl J Med	Beck et al. (11)	Dupilumab treatment in adults with moderate-to-severe atopic dermatitis	39	230
2019	Brit J Dermatol	Akinlade et al. (19)	Conjunctivitis in dupilumab clinical trials	35	169

Simpson EL (Oregon Health and Science University) were the most prolific authors with the most citations. In the co-authorship network, the top 10 authors with the highest link strength mainly came from organizations of the United States, in which Regeneron Pharmaceuticals Inc. made up the largest proportion. Additionally, the contributions of ophthalmology specialists are significant in the correct classification and management of eye involvement in the treatment of AD, and several articles have highlighted the significance of the cooperation between dermatologists and ophthalmologists (26).

With respect to the co-occurrence analysis of keywords, conjunctivitis was the most common ocular AE identified in this study. Plenty of clinical trials have demonstrated that AD patients treated with dupilumab had a higher incidence of conjunctivitis than those treated with placebo. The term "conjunctivitis" contained the following diseases: conjunctivitis, conjunctivitis allergic, conjunctivitis bacterial, conjunctivitis viral, and atopic keratoconjunctivitis, with all being reported as AEs in the literature. Other ocular AEs, such as dry eyes, eye pruritus, blepharitis, blepharoconjunctivitis, and cicatricial ectropion, were also reported.

Notably, in our study, allergic conjunctivitis, blepharitis, keratitis, and atopic keratoconjunctivitis were also complications at baseline in some cases. Previous studies have proved that the above ocular diseases are common comorbidities occurring in nearly half of patients with AD (27). Moreover, Akinlade et al. (19) has found that prior conjunctivitis history is associated with the increased incidence of conjunctivitis in AD patients treated with dupilumab. The mechanism of ocular AEs remains unknown. The possible causes of ocular AEs may be the inhibition of goblet cells through blocking IL-4 and IL-13 with dupilumab, resulting in decreased mucin secretion and mucosal epithelial barrier dysfunction (28). Other studies have found that the increased risk of conjunctivitis may be associated with serum IgE, thymus and activation-regulated chemokine in dupilumab treated patients (29). It is worth exploratory whether conjunctivitis results from the blockade of IL-4 and IL-13 with dupilumab or

that conjunctivitis, in the first place, is part of this systemic allergic disorder.

Furthermore, keywords regarding the management of AD made up the largest proportion in the co-occurrence network of keywords, such as the safety and efficacy of dupilumab, quality of life and care of the patients, and daily practice. Clinical lesions of AD usually tend to be recurrent and may last for a lifetime. Moreover, topical treatments have relatively limited efficiency for moderate-to-severe AD, and systemic therapy with long-term significant efficiency and safety is required for treatment. Therefore, for a long time, the management of AD is one of the great concerns in dermatology, and remains to be a therapeutic challenge for clinicians. The occurrence network of keywords indicated that the management of AD will continue to be the research hotspot and development trend in this medical area.

Reference citation links are undirected links between two articles where one cites the other. The article "Two Phase 3 Trials of Dupilumab vs. Placebo in Atopic Dermatitis" published in the top-tier journal *New England Journal of Medicine,* took the lead with 741 citations, such as both citing and cited conditions. This article was the first study discovering ocular AEs of dupilumab in the treatment of AD, and thus became the milestone research in this field. The top papers with the most citations were mainly randomized, placebo-controlled phase 2, and phase 3 clinical trials. Except for clinical trials, real-life evidence and clinical reports have also provided fundamental evidence for future studies. A clinical report "Conjunctivitis occurring in atopic dermatitis patients treated with dupilumab-clinical characteristics and treatment" (30), ranked the seventh with 75 citations. This article reported conjunctivitis occurring in 25 and 50% of dupilumab-treated patients with AD in two centers from 2016 to 2017, with a focus on the detailed clinical characteristics. More importantly, the authors reported successful treatment of all the 13 patients with fluorometholone or tacrolimus, and gave dermatologists and ophthalmologists useful and fundamental recommendations. A large retrospective cohort study "Effectiveness and safety of dupilumab for the treatment of atopic dermatitis in a real-life French multicenter

adult cohort" (31), ranked at the eighth position with 65 citations. This real-life study revealed high frequency (107/220, 48.6%) of non-infectious ophthalmologic AEs. Non-infectious conjunctivitis was the most common ocular AE, followed by ocular pruritus, blepharitis, xerophthalmia, and keratitis. Ocular AEs are well tolerated in most of patients, and only a small proportion of patients (10/238, 4.2%) discontinued the treatment of dupilumab at 6-month follow-up endpoint. A long-term real-life evidence entitled "A 48-week update of a multicentre real-life experience of dupilumab in adult patients with moderate-to-severe atopic dermatitis" (32), ocular AEs related to dupilumab were well tolerated with frequent remission in most cases.

Information about co-citation analysis were exhibited in **Table 2**, **Figure 7B**. Reference co-citation links represent the connection between two references that are both cited by the same article. The top 2 articles were the same as those in citation analysis, and had the highest co-citation times and total link strength, indicating a strong connection and close relatedness with other articles. This might be because the top-tier journal *New England Journal of Medicine* and *Lancet* preferred frontier research and innovative articles, and in return, these journals would bring a more influential and broader readership to the articles.

There were several limitations of this study. First, the data source was limited to the Web of Science Core Collection database, and only documents published in English were extracted, which may result in the inclusion bias. Moreover, to recognize contributions accurately, only original articles, case letters, and research letters were included in this study. Second, newly published articles have less time of exposure to allow for citations, which may lead to the underestimation of potential significant articles.

In summary, the present study presented a comprehensive bibliometric analysis concerning ocular AEs during the treatment of AD patients with dupilumab. The first study was published in 2016 by Oregon Health and Science University from the United States; the majority of publications were published in the past 3 years; *British Journal of Dermatology* published the highest number of articles; the United States was the country with the most publications; Sanofi (France) and Regeneron Pharmaceuticals (USA) were the leading organizations with most contributions; conjunctivitis was the most common ocular AE; the management of AD will continue to be the research hotspot and development trend in this area; the milestone research is the first article "Two Phase 3 Trials of Dupilumab vs. Placebo in Atopic Dermatitis" published in *New England Journal of Medicine*; most of the top 10 papers were mainly randomized, placebo-controlled phase 2 and phase 3 clinical trials and real-life large cohort studies.

Our results predicted that research on ocular AEs was the frontiers and promising field, and the management of AD was the great concern and difficulty and would be the future research direction. In conclusion, this study may help better understand ocular AEs in the dupilumab treatment of AD, and grasp the research trends and most influential topics in this field.

DATA AVAILABILITY STATEMENT

The raw data supporting the conclusions of this article will be made available by the authors, without undue reservation.

AUTHOR CONTRIBUTIONS

QNJ, JQ, and YPZ contributed to concept, design, literature search, and edited the manuscript. QNJ and KF contributed to data acquisition and analysis and statistical analysis. QNJ drafted the manuscript. QNJ, JQ, KF, and YPZ reviewed the manuscript. All authors contributed to the article and approved the submitted version.

REFERENCES

1. Langan SM, Irvine AD, Weidinger S. Atopic dermatitis. *Lancet.* (2020) 396:345–60. doi: 10.1016/S0140-6736(20)31286-1
2. Laughter MR, Maymone MBC, Mashayekhi S, Arents BWM, Karimkhani C, Langan SM, et al. The global burden of atopic dermatitis: lessons from the global burden of disease study 1990-2017. *Br J Dermatol.* (2021) 184:304–9. doi: 10.1111/bjd.19580
3. Odhiambo JA, Williams HC, Clayton TO, Robertson CF, Asher MI, ISAAC Phase Three Study Group. Global variations in prevalence of eczema symptoms in children from ISAAC phase three. *J Allergy Clin Immunol.* (2009) 124:1251–8. doi: 10.1016/j.jaci.2009.10.009
4. Weidinger S, Beck LA, Bieber T, Kabashima K, Irvine AD. Atopic dermatitis. *Nat Rev Dis Primers.* (2018) 4:1. doi: 10.1038/s41572-018-0001-z
5. Eckert L, Gupta S, Amand C, Gadkari A, Mahajan P, Gelfand JM. The burden of atopic dermatitis in US adults: health care resource utilization data from the 2013 national health and wellness survey. *J Am Acad Dermatol.* (2018) 78:54–61. doi: 10.1016/j.jaad.2017.08.002
6. Silverberg JI, Gelfand JM, Margolis DJ, Boguniewicz M, Fonacier L, Grayson MH, et al. Patient burden and quality of life in atopic dermatitis in US adults: a population-based cross-sectional study. *Ann Allergy Asthma Immunol.* (2018) 121:340–7. doi: 10.1016/j.anai.2018.07.006

7. Leung DY. New insights into atopic dermatitis: role of skin barrier and immune dysregulation. *Allergol Int.* (2013) 62:151–61. doi: 10.2332/allergolint.13-RAI-0564
8. Paton DM. Dupilumab: human monoclonal antibody against IL-4Rα for moderate to severe atopic dermatitis. *Drugs Today.* (2017) 53:477–87. doi: 10.1358/dot.2017.53.9.2693150
9. Thaçi D, Simpson EL, Beck LA, Bieber T, Blauvelt A, Papp K, et al. Efficacy and safety of dupilumab in adults with moderate-to-severe atopic dermatitis inadequately controlled by topical treatments: a randomised, placebo-controlled, dose-ranging phase 2b trial. *Lancet.* (2016) 387:40–52. doi: 10.1016/S0140-6736(15)00388-8
10. D'Erme AM, Romanelli M, Chiricozzi A. Spotlight on dupilumab in the treatment of atopic dermatitis: design, development, and potential place in therapy. *Drug Des Devel Ther.* (2017) 11:1473–80. doi: 10.2147/DDDT.S113192
11. Beck LA, Thaçi D, Hamilton JD, Graham NM, Bieber T, Rocklin R, et al. Dupilumab treatment in adults with moderate-to-severe atopic dermatitis. *N Engl J Med.* (2014) 371:130–9. doi: 10.1056/NEJMoa1314768
12. Simpson EL, Bieber T, Guttman-Yassky E, Beck LA, Blauvelt A, Cork MJ, et al. Two phase 3 trials of dupilumab versus placebo in atopic dermatitis. *N Engl J Med.* (2016) 375:2335–48. doi: 10.1056/NEJMoa1610020

13. Wang Y, Jorizzo JL. Retrospective analysis of adverse events with dupilumab reported to the United States food and drug administration. *J Am Acad Dermatol*. (2021) 84:1010–4. doi: 10.1016/j.jaad.2020.11.042

14. Ou Z, Chen C, Chen A, Yang Y, Zhou W. Adverse events of Dupilumab in adults with moderate-to-severe atopic dermatitis: a meta-analysis. *Int Immunopharmacol*. (2018) 54:303–10. doi: 10.1016/j.intimp.2017.11.031

15. Ludriksone L, Elsner P, Schliemann S. Acquired hypersensitivity to dupilumab: first case report. *J Eur Acad Dermatol Venereol*. (2019) 33:e482–3. doi: 10.1111/jdv.15807

16. Brumfiel CM, Patel MH, Zirwas MJ. Development of psoriasis during treatment with dupilumab: a systematic review. *J Am Acad Dermatol*. (2021). S0190-9622(00)995-6. doi: 10.1016/j.jaad.2021.05.013

17. Zhu GA, Kang KJW, Chen JK, Novoa RA, Brown RA, Chiou AS, et al. Inflammatory alopecia in patients on dupilumab: a retrospective cohort study at an academic institution. *J Eur Acad Dermatol Venereol*. (2020) 34:e159–61. doi: 10.1111/jdv.16094

18. Chrétien B, Dolladille C, Alexandre J, Fedrizzi S, Lelong-Boulouard V, Lambert JC, et al. Dupilumab-associated arthralgia: an observational retrospective study in VigiBase. *Br J Dermatol*. (2021) 185:464–5. doi: 10.1111/bjd.20138

19. Akinlade B, Guttman-Yassky E, de Bruin-Weller M, Simpson EL, Blauvelt A, Cork MJ, et al. Conjunctivitis in dupilumab clinical trials. *Br J Dermatol*. (2019) 181:459–73. doi: 10.1111/bjd.17869

20. Blauvelt A, de Bruin-Weller M, Gooderham M, Cather JC, Weisman J, Pariser D, et al. Long-term management of moderate-to-severe atopic dermatitis with dupilumab and concomitant topical corticosteroids (LIBERTY AD CHRONOS): a 1-year, randomised, double-blinded, placebo-controlled, phase 3 trial. *Lancet*. (2017) 389:2287–303. doi: 10.1016/S0140-6736(17)31191-1

21. de Bruin-Weller M, Thaçi D, Smith CH, Reich K, Cork MJ, Radin A, et al. Dupilumab with concomitant topical corticosteroid treatment in adults with atopic dermatitis with an inadequate response or intolerance to ciclosporin A or when this treatment is medically inadvisable: a placebo-controlled, randomized phase III clinical trial (LIBERTY AD CAFÉ). *Br J Dermatol*. (2018) 178:1083–101. doi: 10.1111/bjd.16156

22. Zirwas MJ, Wulff K, Beckman K. Lifitegrast add-on treatment for dupilumab-induced ocular surface disease (DIOSD): a novel case report. *JAAD Case Rep*. (2018) 5:34–6. doi: 10.1016/j.jdcr.2018.10.016

23. Maymone MBC, Laughter M, Vashi NA, Jones JD, Hugh J, Dunnick CA, et al. The most cited articles and authors in dermatology: a bibliometric analysis of 1974-2019. *J Am Acad Dermatol*. (2020) 83:201–5. doi: 10.1016/j.jaad.2019.06.1308

24. Bickers DR, Modlin RL. A review of the journal of investigative dermatology's most cited publications over the past 25 years and the use of developing bibliometric methodologies to assess journal quality. *J Invest Dermatol*. (2012) 132:1050–60. doi: 10.1038/jid.2011.391

25. Zhang H, Wang Y, Zheng Q, Tang K, Fang R, Wang Y, et al. Research interest and public interest in melanoma: a bibliometric and google trends analysis. *Front Oncol*. (2021) 11:629–87. doi: 10.3389/fonc.2021.629687

26. Sernicola A, Gattazzo I, Di Staso F, Giordano D, Capalbo A, Persechino F, et al. Treatment of refractory conjunctivitis associated to dupilumab with topical pimecrolimus applied to the eyelid skin. *Dermatol Ther*. (2019) 32:e13134. doi: 10.1111/dth.13134

27. Thyssen JP, Toft PB, Halling-Overgaard AS, Gislason GH, Skov L, Egeberg A, et al. Incidence, prevalence, and risk of selected ocular disease in adults with atopic dermatitis. *J Am Acad Dermatol*. (2017) 77:280–6. doi: 10.1016/j.jaad.2017.03.003

28. Tukler Henriksson J, Coursey TG, Corry DB, De Paiva CS, Pflugfelder SC. IL-13 stimulates proliferation and expression of mucin and immunomodulatory genes in cultured conjunctival goblet cells. *Invest Ophthalmol Vis Sci*. (2015) 56:4186–97. doi: 10.1167/iovs.14-15496

29. Uchida H, Kamata M, Nagata M, Fukaya S, Hayashi K, Fukuyasu A, et al. Conjunctivitis in patients with atopic dermatitis treated with dupilumab is associated with higher baseline serum levels of IgE and TARC but not clinical severity in a real-world setting. *J Am Acad Dermatol*. (2020) 82:1247–9. doi: 10.1016/j.jaad.2019.12.039

30. Wollenberg A, Ariens L, Thurau S, van Luijk C, Seegräber M, de Bruin-Weller M. Conjunctivitis occurring in atopic dermatitis patients treated with dupilumab-clinical characteristics and treatment. *J Allergy Clin Immunol Pract*. (2018) 6:1778–80. doi: 10.1016/j.jaip.2018.01.034

31. Faiz S, Giovannelli J, Podevin C, Jachiet M, Bouaziz JD, Reguiai Z, et al. Effectiveness and safety of dupilumab for the treatment of atopic dermatitis in a real-life French multicenter adult cohort. *J Am Acad Dermatol*. (2019) 81:143–51. doi: 10.1016/j.jaad.2019.02.053

32. Fargnoli MC, Esposito M, Ferrucci S, Girolomoni G, Offidani A, Patrizi A, et al. A 48-week update of a multicentre real-life experience of dupilumab in adult patients with moderate-to-severe atopic dermatitis. *J Dermatolog Treat*. (2020). doi: 10.1080/09546634.2020.1773379. [Epub ahead of print].

Conflict of Interest: The authors declare that the research was conducted in the absence of any commercial or financial relationships that could be construed as a potential conflict of interest.

Publisher's Note: All claims expressed in this article are solely those of the authors and do not necessarily represent those of their affiliated organizations, or those of the publisher, the editors and the reviewers. Any product that may be evaluated in this article, or claim that may be made by its manufacturer, is not guaranteed or endorsed by the publisher.

Orbital Apex Syndrome: A Case Series in a Tertiary Medical Center in Southern Taiwan

Peng-Hsuan Lee[1], Shih-Chieh Shao[2,3] and Wan-Ju Annabelle Lee[3,4,5]*

[1] Department of Ophthalmology, National Cheng Kung University Hospital, College of Medicine, National Cheng Kung University, Tainan, Taiwan, [2] Department of Pharmacy, Keelung Chang Gung Memorial Hospital, Keelung, Taiwan, [3] School of Pharmacy, Institute of Clinical Pharmacy and Pharmaceutical Sciences, College of Medicine, National Cheng Kung University, Tainan, Taiwan, [4] Department of Ophthalmology, Chi Mei Medical Center, Tainan, Taiwan, [5] Department of Optometry, Chung Hwa University of Medical Technology, Tainan, Taiwan

Background: Orbital apex syndrome (OAS) is a rare ocular complication following by infection, inflammation, trauma, neoplasms, and vascularity. The epidemiological features of OAS remained limited, so this study aimed to present ophthalmic clinical features, determine the causes to evaluate the visual prognosis of orbital apex syndrome (OAS) patients in Taiwan.

Methods: This was a retrospective study by reviewing the electronic medical records from National Cheng Kung University Hospital in Taiwan during 2017–2019. We included patients diagnosed with OAS to review their ocular symptoms and signs, visual acuity, ocular images, etiologies, treatment and visual prognosis.

Results: Twenty cases (mean age: 65.55 ± 13.06; male: 75%) with the diagnosis of OAS were included in this study. All patients presented as unilateral involvement, but the initial ocular presentations and etiologies varied. For example, blurred vision was reported in 80% of these patients, and tumor-related compression (55%) and infection (15%) were the most frequent causes for the OAS. After the follow-up, we found 35% of patients' visions declined or worsened to the blindness, 15% of patients' visions remained stable, 20% of patients' visions had mild improvement, and 35% of patients' visions were not measured because of debilitating clinical condition. We identified three OAS patients with mortality (15%), and all of them were attributed to the underlying malignancies.

Conclusion: The clinical magnifications and etiologies of OAS are heterogeneous in Taiwan. Our findings indicated the tumor-related compression is the most frequent causes of OAS in Taiwan, and it is also related to poor clinical outcomes.

Keywords: orbital apex syndrome, OAS, ophthalmoplegia, proptosis, case series

INTRODUCTION

The orbital apex is an area that includes structures from the tendinous annulus of Zinn, optic nerve, and ophthalmic artery through the optic canal (1). Orbital apex syndrome (OAS) is defined as a collection of dysfunctions involving multiple cranial nerves (CNs), including the optic, oculomotor, trochlear, and abducens nerves, and the ophthalmic branch of the trigeminal nerve. OAS results from disease processes occurring in the region of the optic canal, superior orbital fissure, or cavernous sinus. The hallmarks of OAS are vision loss from optic neuropathy and ophthalmoplegia involving multiple CNs (2).

OAS can be attributed to a variety of clinical conditions, such as neoplastic diseases (3, 4) (e.g., local tumor invasion and distant metastatic tumors), inflammatory processes (5) (e.g., systemic lupus erythematosus, sarcoidosis, and Tolosa-Hunt syndrome), infections (6–8) (e.g., bacterial or fungal sinusitis and herpes zoster), traumatic injuries (9) (e.g., iatrogenic and craniomaxillofacial fracture), and vascular conditions (10) (e.g., carotid cavernous fistula, carotid cavernous aneurysms, and cavernous sinus thrombosis).

Detailed patient history with a review of the systems and thorough physical examination assessing neurological dysfunctions is important in narrowing the differential diagnosis. Imaging modalities, such as computed tomography (CT), magnetic resonance imaging (MRI), and endoscopy, are usually warranted. Surgical biopsy for histopathological examination is sometimes required for definitive diagnosis. Treatment should be directed toward the underlying process and usually involves a multidisciplinary approach.

The severity and prognosis of OAS vary widely due to the large variety of disease conditions. Furthermore, disease prevalence varies across countries and continents. Given the lack of data regarding the ophthalmic presentations of patients with OAS in the Chinese population, we aimed to delineate the clinical features, possible etiology, potential management, visual prognosis, and systemic prognosis of OAS in Taiwan.

METHOD

Patient Enrolment

Two ophthalmologists (PH Lee and WA Lee) retrospectively identified patients diagnosed with OAS by reviewing the electronic medical records from the National Cheng Kung University Hospital, a tertiary referral hospital in Taiwan, between January 1, 2017, and December 31, 2019.

Medical History

We performed descriptive analyses by recording the patients' demographics (e.g., sex and age), disease characteristics (e.g., laterality of the involved eyes, clinical manifestations, imaging findings, histopathologic results, initial and final best-corrected visual acuity, and etiologies), treatment patterns (e.g., surgery, medications, and radiotherapy), prognosis, and mortality.

Diagnosis

Diagnoses of OAS were based on the patients' clinical signs and symptoms. Medical imaging, such as CT and MRI, was performed in all patients except for in case No. 18 due to loss to follow-up. Furthermore, histopathologic specimens were obtained from certain patients who underwent surgical intervention.

Prognosis

Visual outcomes and mortality were evaluated in this study. The best-corrected visual acuity was assessed using the Landolt C chart with autorefraction. A visual acuity worse than 20/200 was deemed poor in this study.

Statistical Analysis

Categorical variables are presented as number and percentage values and were analyzed using Fisher's exact test due to the relatively small sample size. Continuous variables are presented as the mean and standard deviation (SD) and were analyzed using Student's *t-test*. A *P*-value of < 0.05 was considered the threshold for statistical significance. The study data were analyzed using SPSS V.20.0 (IBM; Chicago, Illinois, USA) and the Excel software program (Office 2010, Microsoft Corp, Redmond, WA, USA). This study was conducted in accordance with the Declaration of Helsinki and was approved by the Institutional Review Board of the National Cheng Kung University Hospital, Taiwan (IRB A-ER-109-077).

RESULTS

Patient Characteristics

We included twenty patients with OAS in this study. Their mean age was 65.6 (SD: 13.1) years, and most of them were male (75%). The follow-up period of these patients ranged from 0 to 24 months, with a mean of 8.8 (SD: 8.6) months.

Disease Characteristics

On initial presentation, all patients had single-eye involvement of OAS with a wide variety of ocular manifestations (**Table 2**). Initially, the most common manifestations in these patients included blurring of vision (80%), ptosis (55%), and proptosis (40%). Other less frequent symptoms included diplopia, headache, facial numbness, redness, and periorbital pain.

The limitation of extraocular movement was observed in 90% of the patients, and 80% had documented CN III, IV, or VI involvement. The ophthalmic division of CN V was affected in three (15%) patients, among whom one also had maxillary division involvement. Hertel exophthalmometer measurements were taken in 25% of the patients and showed an average of 2.8 $\pm$ 1.5 mm proptosis on the lesion side. Ocular hypertension was recorded in 20% of the cases.

The initial visual acuity of the twenty patients was evaluated using the Landolt C chart and ranged from no light perception to 20/30. Half (ten patients) of the patients had a visual acuity worse than 20/200 upon presentation, and within which half of them (five patients) had no light perception. Positive relative afferent papillary defects were detected in 60% of the patients.

Diagnostic Tools

All the patients underwent imaging investigations, including eight patients with CT only, five patients with MRI only, and six patients with both CT and MRI. However, one patient received no imaging evaluation due to loss to follow-up.

Eleven patients underwent tissue biopsy for definitive diagnosis, and the histopathologic results showed infection in three patients and neoplasm in eight. Six patients were diagnosed by typical imaging examinations along with a comprehensive

systemic work-up and detailed medical history review, which revealed that three had autoimmune-related inflammatory processes, two had vascular tumors, and one had a trauma-related condition. Direct invasion or metastatic malignant neoplasm was presumed to be the cause of OAS in three cases in which tissue biopsy was not performed in view of the surgical risks and poor general condition of the patients due to advanced cancer. Therefore, the diagnosis was made based on typical imaging, a medical history review, or previous evidence of central nervous system metastasis in other locations.

Etiology of OAS

Among the twenty patients, neoplasm was the leading cause of OAS, accounting for 55% (11/20), followed by inflammatory causes accounting for 15% (3/20), infectious causes for 15% (3/20), vascular causes for 10% (2/20), and trauma-related causes for 5% (1/20) (**Figure 1**).

Among the eleven patients with neoplastic causes, eight were diagnosed by a histopathology examination, and three by typical imaging only. The neoplasms leading to OAS observed in our study were found to be malignant in 90.9% (10/11)

of cases, with only one meningioma being considered benign. The pathophysiology of malignant neoplastic causes of OAS in our study could be categorized into direct local invasion from head and neck cancers (6/10) or metastasis from distant sites (4/10). The pathology of metastatic tumors included breast cancer (2), bladder cancer (1), and prostate cancer (1). As for advanced head and neck cancer, tongue (1), palate (1), buccal (2), nasopharyngeal (1), and paranasal sinus cancers (1) were diagnosed. The different etiologies for OAS in our study are shown in **Table 1**; **Figure 1**.

Treatment

Treatment options were determined based on the definite etiology and patients' medical conditions. Infectious causes were treated with surgical debridement and antimicrobial therapy, inflammatory causes were treated with systemic corticosteroids with dose of intravenous 1 g of methylprednisolone for consecutive 3 days followed by oral prednisolone with dose of 1 mg/kg of body weight with slow tapering, vascular causes were treated with endovascular embolization, and neoplastic causes were treated with surgical resection, chemotherapy, or

FIGURE 1 | Etiology of orbital apex syndrome.
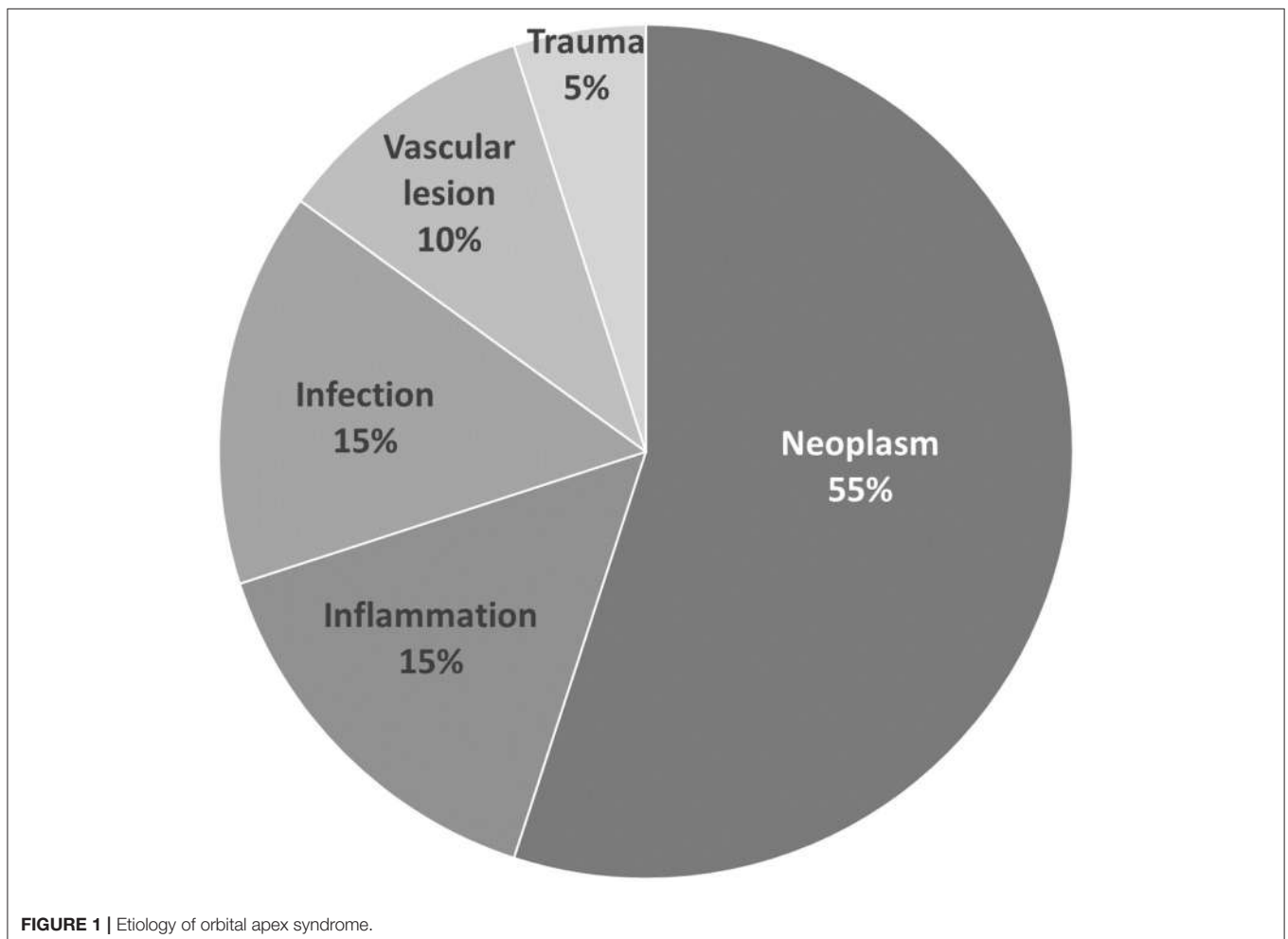
TABLE 1 | Basic information of each patient with orbital apex syndrome.

No.	Age	Sex	OD/OS	Cause	Clinical manifestation										Initial VA	Final VA
					Redness	Pain	Blurred vision	Headache	Facial numbness	Elevated IOP	Proptosis	Ptosis	Limited EOM	RAPD		
1	89	M	OS	Unspecified inflammation	−	−	+	−	+	−	−	+	+	−	20/50	20/63
2	80	F	OD	Systemic lupus erythematosus	+	+	−	−	−	+	−	−	+	−	20/63	20/63
3	75	M	OD	Urothelial carcinoma with bone metastasis	−	−	+	−	−	−	+, 3 mm	+	+	+	NLP	LP
4	47	M	OD	Tongue cancer with local invasion	−	−	+	−	−	+	+		+	+	20/50	20/32
5	83	M	OS	Fungal sinusitis	−	+	+	+	−	−	+, 2 mm	+	+	−	20/200	LP
6	52	M	OD	Fungal sinusitis	−	+	−	−	−	−	−	−	−	−	20/63	20/50
7	69	M	OS	Prostate cancer with brain metastasis	−	−	−	+	−	−	+, 1 mm	+	+	−	20/63	N/A
8	60	M	OS	Buccal cancer with local invasion	+	−	+	+	−	+	−	−	+	+	20/100	N/A
9	54	F	OD	Breast cancer with brain metastasis	−	−	+	+	−	−	−	−	+	+	NLP	NLP
10	55	M	OD	Carotid carvenous fistula	+	−	+	−	−	−	+, 5 mm	+	+	+	20/32	20/20
11	57	M	OD	NPC with local invasion	−	−	+	−	+	−	+	+	−	−	CF	NLP
12	59	M	OD	Palatal cancer with local invasion	−	−	+	−	−	−	+		+	+	20/2000	LP
13	75	F	OS	Breast cancer with brain metastasis	−	−	+	−	−	−	−	+	+	+	CF	NLP
14	75	F	OD	Meningioma	−	−	+	−	−	−	+	−	+	−	LP	N/A
15	57	F	OD	Cavernous ICA out-pouch	−	−	+	+	+	−	−	+	+	−	20/32	20/400
16	84	M	OS	Trauma	−	−	+	−	−	−	−	−	+	+	LP	N/A
17	61	M	OD	Sinusitis	−	−	−	−	−	+	+, 3 mm	+	+	+	20/100	20/200
18	69	M	OD	suspected GPA	−	−	+	−	+	−	−	+	+	+	NLP	N/A
19	42	M	OS	Buckle cancer with local invasion	+	−	+	−	−	−	+	−	+	+	NLP	N/A
20	69	M	OS	Sinus cancer with local invasion	−	−	+	−	−	−	−	+	+	+	NLP	NLP

IOP, intraocular pressure; EOM, extraocular motility, RAPD, relative afferent pupillary defect; LP, positive light perception; NLP, no light perception, GPA, granulomatosis with polyangiitis; OD, Oculus Dexter, right eye; OS, Oculus Sinister, left eye; CF, counting finger; HM, hand motion; NPC, nasopharyngeal carcinoma; ICA, internal carotid artery; N/A, not applicable.

Mean of age = 65.55.

The amount of proptosis was quantified by Hertel exophthalmometer.

Cases No. 3, No. 4 and No. 7 died within 1 year after orbital apex syndrome occurred.

radiotherapy. In our study, thirteen patients received treatment, while seven patients only received palliative management. Of those who received no specific treatment for OAS, only one patient experienced improvement in visual acuity. Of those who received various treatments aimed at the underlying etiologies, six experienced preserved or improved visual acuity.

Among patients with neoplastic causes, three patients underwent surgical resection or debulking of the tumor masses, two received radiotherapy with total doses around 20–24 Gray in multiple fractions, two received combined radiotherapy and chemotherapy, one received chemotherapy alone, and three received no further treatment.

Visual Prognosis

The initial visual acuity at diagnosis ranged from no light perception to 20/30, whereas the final visual acuity at the last follow-up visit ranged from no light perception to 20/20. Among the fourteen patients with documented final visual acuity, eight (57.1%) had a visual acuity worse than 20/200, in which five had no light perception. In patients with a final visual acuity worse than 20/200, malignancies accounted for 75% of the disease conditions. Among those with documented initial and final visual acuity, seven (50%) had worsened, three (21.4%) had stable, and four (28.6%) had improved visual acuity. Thorough statistical analysis by a paired t-test failed to demonstrate significant differences between initial visual acuity and post-treatment final visual acuity ($p = 0.44$) (**Figures 2A,B**). The reason for that **Figure 2B** shows different data is because only those with documented both initial and final visual acuity were included in the **Figure 2B** (which was fourteen patients out of all twenty patients). Among the fourteen patients, six patients had initial visual acuity < 20/200, which was 43%, as shown in **Figure 2B**. The 0.0% in bar 2 in **Figure 2B** represents those with initial VA 0.5–1.0 in group 1 (neoplastic OAS). The 0.0% in bar 3 in **Figure 2B** represents those with initial VA < 0.1 in group 2 (non-neoplastic OAS). Therefore, neoplastic causes seemed to correlate with poor visual acuity.

Our data show a relationship revealed by Fisher's exact test between the causes of the disease (neoplastic or non-neoplastic) and visual prognosis. Neoplastic causes tended to correlate with poor initial visual acuity ($p = 0.035$) and final visual acuity ($p = 0.051$).

The peripapillary retinal nerve fiber layer (RNFL) thickness was measured by optical coherence tomography in ten patients. Overall, the initial RNFL thickness was within 43 and $114\,\mu m$ (mean $\pm$ SD: $80.7 \pm 27.6\,\mu m$). The final RNFL thickness was documented in five patients with overall thickness within 30 and $113\,\mu m$ (mean $\pm$ SD: $74.2 \pm 34.4\,\mu m$). For those five patients with serial follow-ups of RNFL thickness, three patient demonstrated progressive thinning of RNFL thickness with an average of $-7.7\,\mu m$ decline (SD: $5.5\,\mu m$).

Automated perimetry was performed for visual field evaluation in case No. 2, 5, 6, 9, 10, 11, 17. Three patients demonstrated generalized depression, two showed paracentral scotoma. Case No. 6 presented as nasal defect respect the vertical midline, which was more likely attributed to his underlying history of subarachnoid hemorrhage due to head trauma.

Mortality

During follow-up, mortality occurred in three (15%) patients, and the intervals between the onset of OAS and mortality were 6, 9, and 24 weeks, respectively. All mortalities documented in our study were attributable to underlying malignancies (**Table 2**).

DISCUSSION

The literature on OAS related to ocular diseases is scarce and involves mostly small-scale studies, possibly due to the rarity of this disease entity (11–13) and heterogeneity of underlying etiologies that require experienced specialists for accurate diagnosis. The literature on OAS in Taiwan is limited to case reports only (14, 15). Therefore, our study collected more cases and aimed at providing a more general overview of the ophthalmic clinical features, etiologies, and visual prognosis of OAS.

The hallmarks of OAS are blurred vision and ophthalmoplegia. In our study, the most common complaints upon initial presentation were blurring of vision (80%), ptosis (55%), and proptosis (50%). The most common clinical signs included limited extraocular movement and positive relative afferent pupillary defects.

All our patients exhibited unilateral involvement of OAS, but bilateral involvement is still possible. Yusuke et al. reported a rare case of bilateral OAS caused by granulomatosis with polyangiitis (16). Although the limitation of extraocular movement was documented through a physical examination in 90% of the patients, only 30% reported subjective diplopia. This discrepancy might be due to poor visual acuity in the affected eyes, which failed to produce double vision; missing data due to the retrospective study design; or unreliable patient statements.

The underlying causes of OAS vary among inflammatory, neoplastic, traumatic, infectious, and vascular causes. Detailed clinical examination, appropriate imaging modalities, and sometimes tissue biopsy for histopathological examinations are crucial for establishing an accurate diagnosis. Aryasit et al. (16) reported 80 cases of OAS in which carotid-cavernous fistula was the leading cause, accounting for 37.5% of cases. Twenty-four (30%) patients had neoplasia, and the most common diagnosis was lymphoma (nine patients), followed by meningioma (seven patients). The results of our study are very different from those of previous studies in which malignant neoplasms accounted for over half of the cases. Furthermore, the neoplasms leading to OAS found in our study were mostly malignant, and direct local invasion from head and neck cancers accounted for the majority of cases. This disparity might be partly related to differences in the prevalence rates of certain malignancies in different countries. Taiwan has the highest incidence of oral cancer (17, 18) worldwide, and nasopharyngeal carcinoma (19) is more common in Asian populations.

Our study demonstrates that the overall visual prognosis of OAS is poor despite vigorous multidisciplinary management. More than half of our patients were legally blind, and only 28.6% experienced an improvement in visual acuity after

FIGURE 2 | Fourteen eyes with documented initial vs. final visual acuity. Group 1 comprises the eyes in which orbital apex syndrome was attributed to neoplastic causes. Group 2 comprises the eyes in which orbital apex syndrome was attributed to non-neoplastic causes. **(A)** Categorization of visual improvement. **(B)** Categorization of visual acuity as good (0.5–1.0), fair (0.1–0.4), and poor (< 0.1).

treatment. A meta-analysis of traumatic OAS also revealed poor overall visual prognosis, with only 51.7% of patients experiencing improvement in vision despite various medical and surgical interventions (20). The even worse visual outcome in our study may be related to different etiologies of OAS, as the disease in more than half of our cases was attributed to neoplastic causes. In addition, our results showed that neoplastic causes of OAS correlated with poor initial and post-treatment visual prognosis ($p = 0.035$ and 0.051, respectively). There was no significant correlation between the initial and post-treatment visual acuity. While Aryasit et al. (16)

reported no significant relationship between the causes of the disease and visual prognosis, there was no statistically significant relationship between the initial and post-treatment visual acuity.

In our study, mortality was documented in three patients, which occurred 6, 9, and 24 weeks after the diagnosis of OAS. All deaths were attributed to the underlying malignancies. Brain or skull metastases of cancers usually represent advanced disease stages with poor prognosis, and patients are often treated with palliative therapy. Prado-Ribeiro et al. (21) reported four cases of OAS caused by head and neck

TABLE 2 | Details of clinical presentation, etiology, visual change, diagnostic tools and mortality in our case series.

Items	Number (n)	Percentage (%)
Gender		
Male	15	75
Female	5	25
Laterality		
Right eye	12	60
Left eye	8	40
Original S/S		
Ptosis	11	55
Proptosis	8	40
Diplopia	6	30
Blurred vision	16	80
Facial numbness	4	20
Headache	5	25
Others (red eye, eye pain)	2	10
VA change		
Better	4	20
Worse	7	35
No change	3	15
Others (no records)	6	30
Diagnostic image tools		
CT	8	40
MRI	5	25
CT/ MRI both	6	30
Loss to follow-up	1	5
Mortality		
Yes	3	15
No	16	80
Loss to follow-up	1	5

VA, visual acuity; S/S, symptoms and signs; CT, computed tomography; MRI, magnetic resonance image.

cancer, and the average survival after the diagnosis of OAS was 9.5 months. The incidence of OAS in cancer patients and its correlation with overall prognosis have not yet been established. However, our results clearly indicate that the occurrence of OAS can serve as an indicator of advanced disease status in cancer patients and may indicate foreseeable mortality.

Our study had several limitations. First, we frequently use Landolt C for visual acuity testing in Taiwan's hospitals because most patients fail to read English letters from Snellen chart. Second, due to the retrospective nature of our study, the pupil sizes or changes were not documented in the medical records. Patients with mydriasis due to compression of the oculomotor nerve were not found in our study. This important clinical manifestation should be carefully recorded in further large-scaled study. Third, this was a retrospective study; therefore, the issue of missing data was inevitably encountered. Since our study was based on data from a tertiary referral center, the patients tended to have greater disease severity and complexity, which may have contributed to the overall poor prognosis in our study. Therefore,

the findings in our study population may not be generalizable to the entire population of Taiwan. Further studies involving multiple medical centers and larger sample sizes are necessary to overcome these limitations.

Nevertheless, our study is the first case series of OAS in Taiwan. We aimed to provide an overview of the typical clinical features, possible etiologies, potential management, visual prognosis, and overall prognosis of OAS. The factors related to poor visual outcomes were also addressed. We believe that our data can be beneficial to ophthalmologists, general practitioners, otolaryngologists, or even oncologists who are not familiar with this disease entity but need to be aware of the typical clinical manifestations, as some of the causes may lead to significant morbidity and mortality.

In conclusion, OAS may result from various etiologies, including traumatic, inflammatory, infectious, neoplastic, and vascular conditions. Our data showed that malignant neoplasms are the most common cause of OAS in Taiwan. Generally, most patients with OAS experience vision loss despite aggressive multidisciplinary management. In terms of visual acuity, patients with non-neoplastic causes may have more favorable outcomes. OAS caused by malignancies usually indicates late-stage underlying tumors and thus may indicate a poor systemic prognosis.

DATA AVAILABILITY STATEMENT

The original contributions presented in the study are included in the article/supplementary material, further inquiries can be directed to the corresponding authors.

ETHICS STATEMENT

The studies involving human participants were reviewed and approved by Institutional Review Board of the National Cheng Kung University Hospital, Taiwan (IRB A-ER-109-077). Written informed consent for participation was not required for this study in accordance with the national legislation and the institutional requirements.

AUTHOR CONTRIBUTIONS

P-HL conceptualized and designed the study, drafted the initial manuscript, designed the data collection instruments, collected data, and carried out the initial analyses. S-CS had reviewed the literature and helped to edit the references. W-JL conceptualized and designed the study and reviewed and revised the manuscript. All authors approved the final manuscript as submitted and agree to be accountable for all aspects of the work.

FUNDING

Half of publication fee will be funded by Chi Mei Medical Center after acceptance.

REFERENCES

1. Badakere A, Patil-Chhablani P. Orbital apex syndrome: a review. *Eye Brain*. (2019) 11:63–72. doi: 10.2147/EB.S180190

2. Borchard NA, Nayak JV. Orbital apex syndrome. *N Engl J Med*. (2018) 378:e23. doi: 10.1056/NEJMicm1703770

3. Ganesh A, Dondey J, Forte V, Drake JM, Gentili F, Armstrong D, et al. Orbital involvement by nasopharyngeal angiofibroma. *J Pediatr Ophthalmol Strabismus*. (2004) 41:116–21. doi: 10.3928/0191-3913-20040301-15

4. Shindler KS, Liu GT, Womer RB. Long-term follow-up and prognosis of orbital apex syndrome resulting from nasopharyngeal rhabdomyosarcoma. *Am J Ophthalmol*. (2005) 140:236–41. doi: 10.1016/j.ajo.2005.02.054

5. Yuen SJ, Rubin PA. Idiopathic orbital inflammation: distribution, clinical features, and treatment outcome. *Arch Ophthalmol*. (2003) 121:491–9. doi: 10.1001/archopht.121.4.491

6. Jun LH, Gupta A, Milea D, Jaufeerally FR. More than meets the eye: varicella zoster virus-related orbital apex syndrome. *Indian J Ophthalmol*. (2018) 66:1647–9. doi: 10.4103/ijo.IJO_592_18

7. Pfeiffer ML, Merritt HA, Bailey LA, Richani K, Phillips ME. Orbital apex syndrome from bacterial sinusitis without orbital cellulitis. *Am J Ophthalmol Case Rep*. (2018) 10:84–6. doi: 10.1016/j.ajoc.2018.01.041

8. Aydin E, Balikoglu-Yilmaz M, Imre SS, Koc F, Kazanci L, Ozturk AT, et al. Rare patient with orbital apex syndrome, anterior uveitis, and necrotizing scleritis due to herpes zoster ophthalmicus. *J Craniofac Surg*. (2016) 27:e750–e2. doi: 10.1097/SCS.0000000000003098

9. Shokri T, Zacharia BE, Lighthall JG. Traumatic orbital apex syndrome: an uncommon sequela of facial trauma. *Ear Nose Throat J*. (2019) 98:609–12. doi: 10.1177/0145561319860526

10. Huang Y, Gui L. Cavernous sinus-orbital apex aspergillus infection in a diabetic patient: a case report. *Medicine*. (2019) 98:e15041. doi: 10.1097/MD.0000000000015041

11. Besada E, Hunter M, Bittner B. An uncommon presentation of orbital apex syndrome. *Optometry (St Louis, Mo)*. (2007) 78:339–43. doi: 10.1016/j.optm.2007.04.086

12. Zafar MA, Waheed SS, Enam SA. Orbital aspergillus infection mimicking a tumour: a case report. *Cases J*. (2009) 2:7860. doi: 10.4076/1757-1626-2-7860

13. Chaudhary A, Ramchand T, Frohman LP, Liu JK, Eloy JA. Miller Fisher variant of Guillain-Barre syndrome masquerading as acute sphenoid sinusitis with orbital apex syndrome. *Laryngoscope*. (2012) 122:970–2. doi: 10.1002/lary.23248

14. Yip CM, Hsu SS, Liao WC, Chen JY, Liu SH, Chen CH. Orbital apex syndrome due to aspergillosis with subsequent fatal subarachnoid hemorrhage. *Surg Neurol Int*. (2012) 3:124. doi: 10.4103/2152-7806.102349

15. Lim CC, Liao IC, Lee WA. Orbital apex syndrome secondary to fungal sinusitis. *QJM*. (2020) 113:205–6. doi: 10.1093/qjmed/hcz279

16. Aryasit O, Preechawai P, Aui-Aree N. Clinical presentation, aetiology and prognosis of orbital apex syndrome. *Orbit*. (2013) 32:91–4. doi: 10.3109/01676830.2013.764439

17. Chuang SL, Su WW, Chen SL, Yen AM, Wang CP, Fann JC, et al. Population-based screening program for reducing oral cancer mortality in 2,334,299 Taiwanese cigarette smokers and/or betel quid chewers. *Cancer*. (2017) 123:1597–609. doi: 10.1002/cncr.30517

18. Chou HC, Lin HW, Yang JH, Lin PY, Cheng SJ, Wu YH, et al. Clinical outcomes of oral cancer patients who survive for more than 5 years in Taiwan. *Taiwan yi zhi*. (2019) 118:1616–22. doi: 10.1016/j.jfma.2019.07.022

19. Shu CH, Tu TY. Prevalence of the Taiwan variant of the Epstein-Barr virus in nasopharyngeal carcinoma patients and normal individuals. *Zhonghua yi xue za zhi*. (2000) 63:288–93.

20. Talwar AA, Ricci JA. A meta-analysis of traumatic orbital apex syndrome and the effectiveness of surgical and clinical treatments. *J Craniofac Surg*. (2021) 32:2176–9. doi: 10.1097/SCS.0000000000007629

21. Prado-Ribeiro AC, Luiz AC, Montezuma MA, Mak MP, Santos-Silva AR, Brandão TB. Orbital apex syndrome affecting head and neck cancer patients: a case series. *Med Oral Patol Oral Cir Bucal*. (2017) 22:e354–e8. doi: 10.4317/medoral.21506

Corneal *in vivo* Confocal Microscopy for Assessment of Non-Neurological Autoimmune Diseases: A Meta-Analysis

Yuxiang Gu [1,2†], Xin Liu [1,2†], Xiaoning Yu [1,2], Qiyu Qin [1,2], Naiji Yu [1,2], Weishaer Ke [1,2], Kaijun Wang [1,2‡] and Min Chen [1,2*‡]*

[1] Eye Center of the Second Affiliated Hospital, School of Medicine, Zhejiang University, Hangzhou, China, [2] Zhejiang Provincial Key Lab of Ophthalmology, Hangzhou, China

Purpose: This study aimed to evaluate the features of corneal nerve with *in vivo* confocal microscopy (IVCM) among patients with non-neurological autoimmune (NNAI) diseases.

Methods: We systematically searched PubMed, Web of Science, and Cochrane Central Register of Controlled Trials for studies published until May 2021. The weighted mean differences (WMDs) of corneal nerve fiber length (CNFL), corneal nerve fiber density (CNFD), corneal nerve branch density (CNBD), tortuosity, reflectivity, and beadings per 100 μm with a 95% CI between NNAI and control group were analyzed using a random-effects model.

Results: The results showed 37 studies involving collective totals of 1,423 patients and 1,059 healthy controls were ultimately included in this meta-analysis. The pooled results manifested significantly decreased CNFL (WMD: −3.94, 95% CI: −4.77−−3.12), CNFD (WMD: −6.62, 95% CI: −8.4−−4.85), and CNBD (WMD: −9.89, 95% CI: −14−−5.79) in NNAI patients. In addition, the NNAI group showed more tortuous corneal nerve (WMD: 1.19, 95% CI:0.57–1.81). The comparison between NNAI patients and healthy controls in beadings per 100 μm corneal nerve length was inconsistent. No significant difference was found in the corneal nerve fiber reflectivity between NNAI and the control group (WMD: −0.21, 95% CI: −0.65–0.24, $P = 0.361$).

Conclusions: The parameters and morphology of corneal nerves observed by IVCM proved to be different in NNAI patients from healthy controls, suggesting that IVCM may be a non-invasive technique for identification and surveillance of NNAI diseases.

Keywords: corneal nerve, confocal microscopy, non-neurological autoimmune diseases, type 1 diabetes, Sjögren's syndrome

INTRODUCTION

Autoimmune diseases are a range of diseases characterized by increased activity of the immune system which results in organ damage or dysfunction (1). According to research, autoimmune diseases affect approximately 7.6–9.4% of the general population and impose huge burdens not only on patients themselves but also on the whole society (2). Genetic, microbial, environmental, lifestyle, and psychological factors are thought as contributing elements to autoimmune diseases

although the underlying etiology remains to be explored (3). Despite impressive advances in the management of autoimmune diseases, they are still impossible to cure. A definitive diagnosis as early as possible can increase the efficiency and efficacy of the treatment strategy and also help to avoid complications (4, 5). In this case, an early diagnosis can play a decisive role in improving the patient's quality of life as well as life expectancies.

The cornea is a transparent part covering the front portion of the eyewall and is regarded as the most densely innervated tissue in the human body. With a density of approximately 7,000 epithelial-free nerve endings per square millimeter, the cornea is about 300–600 times more sensitive than skin (6). A review has concluded that changes in corneal innervation can occur for many reasons, including keratitis, corneal dystrophies, corneal degenerations, corneal ecstasies, glaucoma, medical treatment, etc (7). Corneal nerve alternation is not only a window to observe some ocular diseases, but also a potential window to observe systemic diseases. In this article, we focus on non-neurological autoimmune (NNAI) diseases which exclude autoimmune diseases that affect the central nervous system mostly or present obvious psychiatric manifestations. This is a range of autoimmune diseases admitted by the American Autoimmune and Related Diseases Association and excluded from the list of known neurological disorders by the American Academy of Neurology. Some of the NNAI diseases have been discovered to be associated with the human cornea and peripheral neurological manifestations as early as the 1980's. Keratitis was found may be a presenting sign of rheumatoid arthritis or sarcoidosis (8); immune deposits in the cornea were found in patients with systemic lupus erythematosus by immunopathological staining (9). People with NNAI diseases are at high risk of innervation alternation and have a high incidence of various kinds of neuropathy. For instance, it is reported that up to 86% of patients with sarcoidosis present with typical small-fiber neuropathy symptoms (10), over 60% of patients with Sjögren's syndrome suffer from peripheral neuropathy (11, 12), higher prevalence of NNAI diseases including rheumatoid arthritis, systemic lupus erythematosus, Sjögren's syndrome suffer from fibromyalgia and so on (13). Innervation alternation may be progressing soon after the onset of NNAI because of the high sensitivity of the nerves. The corneal nerve may have undergone a long time when observable changes appear, but no symptoms or discomfort are perceived by the patient. For this reason, corneal signs may be the first manifestation of autoimmune diseases. Alteration of corneal nerve parameters is of great significance beyond ocular diseases, it can provide clinicians with thought-provoking insight into the clinical diagnosis or management of many diseases like type 1 diabetes, Parkinson's disease, Friedreich ataxia before organ damages is manifested (14–16). Many researchers showed significant associations between the reduction in corneal innervation and increasing disease severity in neurological autoimmune diseases like multiple sclerosis (17, 18). However, studies present conflicting results on the effect of NNAI diseases on corneal innervation. Moreover, previous studies focus on histopathology results rather than non-invasive analysis. *In vivo* confocal microscopy (IVCM), with its ease of clinical set-up and a 800-fold magnification of cellular level, is becoming a promising as well as a non-invasive tool to view and quantify corneal nerve parameters directly (19). In this way, IVCM may provide a non-invasive potential biomarker for NNAI. Hence, we collected data from different studies about the corneal nerve parameters measured by IVCM in various NNAI diseases and conduct a meta-analysis to evaluate the potential application of this technique as an indicator of NNAI diseases.

METHODS

Search Strategy

A systematic literature search was conducted in PubMed, Web of Science, and Cochrane Central Register of Controlled Trials (updated to May 2021). No constraints were applied regarding the language or the publication time of works of literature. Search terms included confocal microscopy or IVCM or cornea* nerve with a combination of autoimmune diseases or autoimmune diseases or XXX, the last-mentioned representing 36 individual NNAI diseases (**Figure 1**). The selection of NNAI diseases referred to Alexis E. Cullen's study (20). All autoimmune diseases searched were selected a priori from the American Autoimmune and Related Diseases Association and were cross-checked against known neurological disorders, as listed by the American Academy of Neurology. We excluded uveitis for it is essentially a type of eye disease and would, to some extent, affects corneal structure and function. Neither did we adopt data among type 1 diabetes peripheral neuropathy and type 1 diabetic retinopathy, for they had been proved to be related to corneal nerve changes (21–23).

Inclusion and Exclusion Criteria

We included studies that met the following criteria: (1) at least 10 adults with a definite diagnosis of NNAI diseases in the test group; (2) a healthy population as the control group; (3) reporting at least corneal nerve fiber density (CNFD) or corneal nerve fiber length (CNFL). Exclusion Criteria were as follows: (1) inappropriate types of articles, such as reviews, case reports, editorials, conference papers and abstracts, short surveys, or letters; (2) studies which subjects with NNAI diseases were divided into irrelevant subgroups, for instance, dividing patients with type 1 diabetes by erectile dysfunction; (3) studies assessing only animals; (4) studied based or partially based on the same population (studies with the most sufficient data were selected); (5) articles without sufficient data (i.e., mean and *SD*).

Data Extraction

All publications searched were exported to Endnote (version X9.3; The Thomson Corporation Corp, Stanford, CT, USA). Then, duplicate publications were collated and removed. Two researchers (YG and XL) assessed the titles and abstracts independently for potential eligibility, and the full-text articles were retrieved which appeared relevant. Final eligibility was performed by assessing full-text articles and disagreements on eligibility were resolved via discussion and, if necessary, by consulting a third researcher (XY). Studies that were in accord with the inclusion/exclusion criteria were read, and the following information was extracted from the eligible articles: study details

Non-Neurological Autoimmune Diseases

- Addison disease
- Alopecia areata
- Ankylosing spondylitis
- Autoimmune hepatitis or chronic active hepatitis or primary biliary cirrhosis
- Autoimmune thyroiditis, thyrotoxicosis or hyperthyroidism or hypothyroidism or thyroid disorder or Graves' disease
- Behcet's disease
- Celiac or coeliac disease
- Crohn's disease
- Dermatomyositis
- Endometriosis
- Goodpasture syndrome
- Hereditary haemolytic anaemia
- Hypersensitivity vasculitis
- Idiopathic thrombocytopenic purpura
- Interstitial cystitis
- Juvenile arthritis or juvenile idiopathic arthritis or arthritis or rheumatoid arthritis or seropositive rheumatoid arthritis or seronegative arthritis
- Kawasaki disease
- Mixed connective tissue disease
- Myositis
- Pemphigoid
- Pemphigus vulgaris
- Pernicious anaemia
- Polymyalgia rheumatica
- Primary adrenocortical disease
- Primary sclerosing cholangitis
- Psoriasis or psoriasis vulgaris
- Psoriatic arthritis
- Purpura
- Sarcoidosis
- Sjorgen's syndrome
- Systemic lupus erythematosus
- Systemic sclerosis or scleroderma
- Type 1 diabetes or diabetes type 1 or insulin dependent diabetes or diabetes mellitus
- Ulcerative colitis
- Vitiligo
- Wegener granulomatosis

FIGURE 1 | Search terms used to identify non-neurological autoimmune diseases.

FIGURE 2 | Flow diagram of article selection.
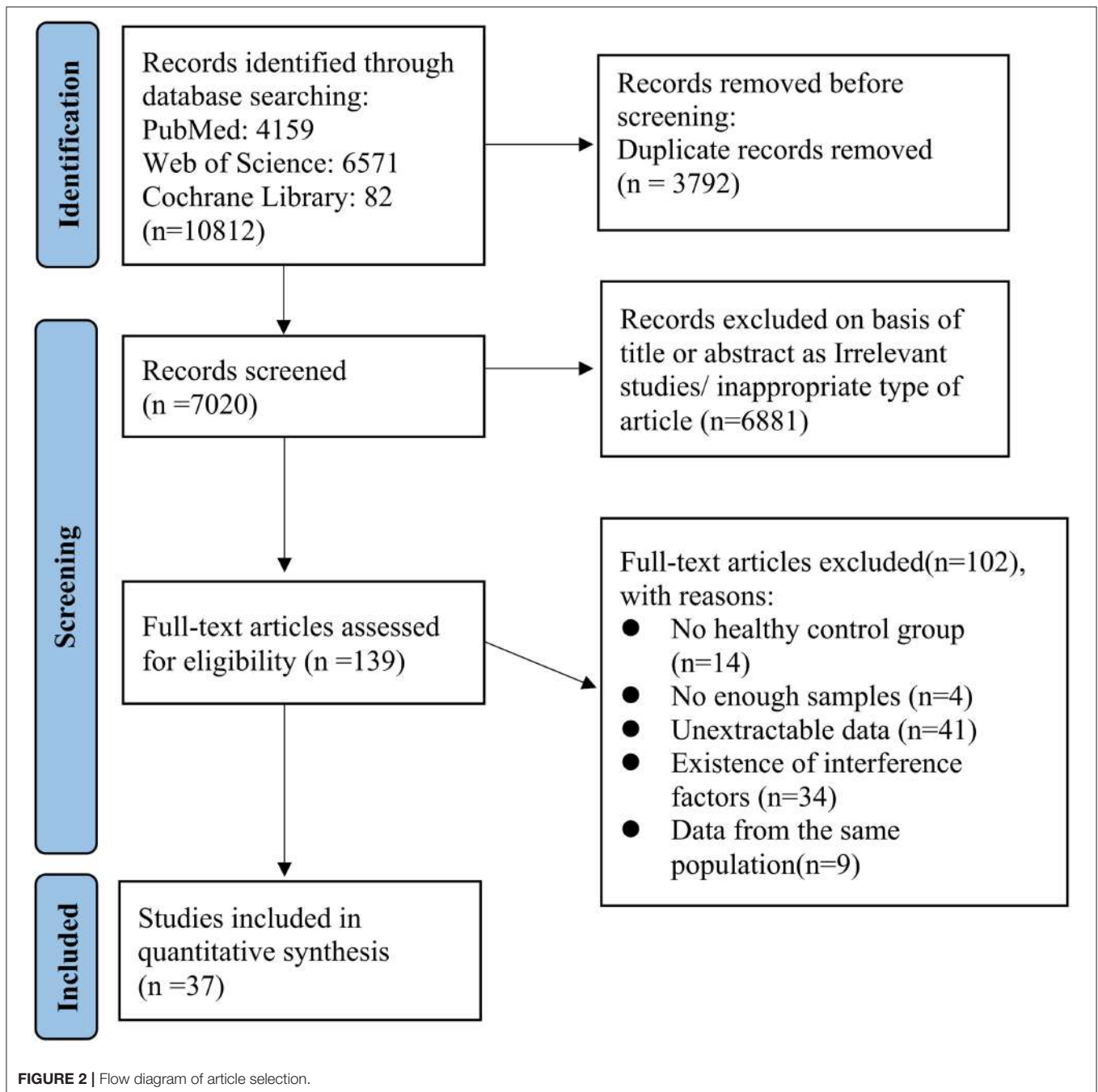
(such as the first author's name, year of acceptance, type of IVCM, and software used to measure corneal nerve parameters) and subjects' information (such as mean age, subjects' sex, duration of NNAI diseases, type of diseases, and corneal nerve parameters). The screening process and protocol are summarized and described in the flow diagram.

Assessments of Article Quality

The Newcastle-Ottawa Scale, covering three methodological domains (selection criteria, comparability, and measurement of exposure and/or outcome), was used to rate article quality. With a maximum score of 9, we defined the article as low quality if the numeric score was 0–3, moderate quality if the score was 4–6, and high quality if the score was 7–9. Low-quality articles were excluded.

Statistical Analysis

This meta-analysis was conducted using the Stata (version 15.1; StataCorp LLC, College Station, TX, USA), a p-value of <0.05 was considered statistically significant. We extracted the mean,

TABLE 1 | Characteristics of the included studies ($n = 37$).

References	Country	Duration (Years)	Groups	Number	Age	Type of IVCM	Sex (F/M)	Software used	Quality scores	CN			T	B	R
										FD	FL	BD			
Ahmed et al. (54)	Canada	17.60 ± 14.00	Type 1 diabetes	56	34.90 ± 14.80	LSCM	29/27	CCMetrics	7	√	√	√	√		
		–	Healthy controls	64	38.90 ± 17.60		34/30								
Alam et al. (45)	UK	17.20 ± 12.00	Type 1 diabetes	30	38.80 ± 12.50	LSCM	17/13	CCMetrics	6	√	√	√			
		–	Healthy controls	27	41.00 ± 14.90		11/16								
Ceská Burdová et al. (39)	Czech Republic	13.50 ± 7.20	Type 1 diabetes	24	37.70 ± 12.30	SSCM	NA	Built-in software	7	√	√	√	√		
		–	Healthy controls	20	32.20 ± 9.90		11/9								
Chen et al. (38)	UK	20.00 ± 11.10 11.10	Type 1 diabetes	63	44.00 ± 15.00	LSCM	NA	CCMetrics	5	√	√	√			
		–	Healthy controls	84	46.00 ± 15.00		NA								
Chen et al. (50)	UK	23.00 ± 15.00	Type 1 diabetes	46	44.00 ± 13.00	LSCM	NA	CCMetrics	9	√	√	√			
		–	Healthy controls	26	44.00 ± 15.00		NA								
Cozzini et al. (29)	Italy	8.70 ± 4.20	Type 1 diabetes	150	16.60 ± 4.00	LSCM	77/73	ACCMetrics	7	√	√	√			
		–	Healthy controls	51	16.30 ± 2.90		25/26								
D'Onofrio et al. (28)	Italy	19.40 ± 7.60	Type 1 diabetes	25	53.30 ± 11.70	LSCM	8/17	CCMetrics	6		√				
		–	Healthy controls	23	54.10 ± 11.10		12/11								
Ferdousi et al. (35)	UK	9.10 ± 2.70	Type 1 diabetes	64	14.60 ± 2.50	LSCM	31/33	CCMetrics	8	√	√	√	√		
		–	Healthy controls	55	13.60 ± 3.10		33/22								
Ferdousi et al. (37)	USA	29.98 ± 2.64	Type 1 diabetes	42	49.21 ± 2.53	LSCM	15/27	ACCMetrics	6	√	√	√			
		–	Healthy controls	25	48.70 ± 2.84		14/11								
Gad et al. (27)	Qatar	4.08 ± 2.91	Type 1 diabetes	20	14.47 ± 2.43	LSCM	NA	CCMetrics	8	√	√	√	√		
		–	Healthy controls	20	12.83 ± 1.91		NA								
Hertz et al. (55)	Canada	NA	Type 1 diabetes	12	NA	LSCM	NA	CCMetrics	8	√	√	√	√		
		–	Healthy controls	20	41.40 ± 17.30		15/5								
Schiano Lomoriello et al. (34)	Italy	12.47 ± 8.29	Type 1 diabetes	19	37.42 ± 8.99	SSCM	10/9	CS4 software	8	√	√	√	√	√	
		–	Healthy controls	19	40.31 ± 11.15		10/9								
Misra et al. (48)	New Zealand	25.8 ± 11.3	Type 1 diabetes	53	48.60 ± 11.80	LSCM	27/26	Analysis 3.1	7		√				
		–	Healthy controls	40	44.30 ± 14.70		23/17								
Pritchard et al. (52)	Australia	20.00 ± 15.00	Type 1 diabetes	168	43.00 ± 16.00	LSCM	83/85	CCMetrics	8		√	√			
		–	Healthy controls	154	46.00 ± 15.00		84/70								
Scarr et al. (43)	Canada	23.50 ± 14.40	Type 1 diabetes	139	42.00 ± 16.00	LSCM	73/66	CCMetrics	7		√				
		–	Healthy controls	68	38.00 ± 16.00		36/32								
Stem et al. (51)	USA	13.50 ± 6.70	Type 1 diabetes	25	38.70 ± 14.20	LSCM	18/7	Image J	8		√				
		–	Healthy controls	9	43.90 ± 10.20		6/3								
Szalai et al. (16)	Hungary	5.79 ± 2.58	Type 1 diabetes	18	16.45 ± 2.59	LSCM	NA	ACCMetrics	5	√	√	√			

(Continued)

TABLE 1 | Continued

References	Country	Duration	Groups	Number	Age	Type of IVCM	Sex (F/M)	Software used	Quality scores	CN			T	B	R
										FD	FL	BD			
		–	Healthy controls	17	26.53 ± 2.43		8/9								
Tummanapalli et al. (31)	Australia	15.00 ± 9.00	Type 1 diabetes	27	32.00 ± 10.00	LSCM	10/17	ACCMetrics	8	√	√	√			
		–	Healthy controls	29	37.00 ± 11.00		13/16								
Barcelos et al. (30)	Portugal	11.70 ± 7.70	Sjögren's Syndrome	55	57.80 ± 11.80	LSCM	NA	Image J	8	√	√				
		–	Healthy controls	20	51.00 ± 6.50		NA								
Castillo et al. (59)	Spain	8.60 ± 3.20	Sjögren's Syndrome	11	61.30 ± 11.30	SSCM	10/1	NA	8		√	√		√	
		–	Healthy controls	10	65.40 ± 3.20		8/2								
Benítez del Castillo et al. (60)	Spain	10.40 ± 3.20	Sjögren's Syndrome	11	52.90 ± 8.70	SSCM	10/1	NA	8		√	√	√	√	√
		–	Healthy controls	10	68.70 ± 7.10		8/2								
Chen et al. (56)	China	NA	Sjögren's Syndrome	26	42.30 ± 9.70	LSCM	25/1	Analysis 3.1	7	√				√	
		–	Healthy controls	26	40.80 ± 9.30		21/5								
Levy et al. (44)	France	NA	Sjögren's Syndrome	30	58.90 ± 15.40	LSCM	20/10	Image J	6	√	√			√	√
		–	Healthy controls	15	59.30 ± 12.30		9/6								
Matsumoto et al. (32)	Japan	NA	Sjögren's Syndrome	23	65.40 ± 11.40	LSCM	23/0	Image J	8	√	√			√	√
		–	Healthy controls	13	68.80 ± 9.80		13/0								
McNamara et al. (47)	USA	NA	Sjögren's Syndrome	10	56.50 ± 8.71	SSCM	9/1	CC Metrics	8	√	√	√	√		
		–	Healthy controls	10	58.20 ± 8.44		9/1								
Semeraro et al. (46)	Italy	12.29 ± 6.37	Sjögren's Syndrome	24	54.31 ± 11.49	NA	24/0	Image J	7	√	√	√	√	√	
		–	Healthy controls	24	48.88 ± 6.50		24/0								
Tepelus et al. (42)	USA	NA	Sjögren's Syndrome	22	57.50 ± 8.60	LSCM	21/1	Image J	8		√		√		√
		–	Healthy controls	7	59.30 ± 12.70		6/1								
Tuisku et al. (57)	Finland	NA	Sjögren's Syndrome	20	54.50 ± 7.00	SSCM	19/1	Built-in software	5	√					
		–	Healthy controls	10	49.80 ± 5.00		9/1								
Tuominen et al. (61)	Finland	8.00 ± 4.60	Sjögren's Syndrome	10	50.10 ± 13.50	TSCM	9/1	NA	6	√					
		–	Healthy controls	10	48.30 ± 14.50		9/1								

(Continued)

TABLE 1 | Continued

References	Country	Duration	Groups	Number	Age	Type of IVCM	Sex (F/M)	Software used	Quality scores	CN			T	B	R
										FD	FL	BD			
Villani et al. (53)	Italy	NA	Sjögren's Syndrome	15	52.10 ± 15.40	LSCM	11/4	Cell Count software	8	√			√	√	
	–		Healthy controls	15	45.20 ± 15.90		10/5								
Villani et al. (58)	Italy	NA	Sjögren's Syndrome	15	52.30 ± 10.30	SSCM	12/3	Cell Count software	8	√			√		√
	–		Healthy controls	20	51.20 ± 18.20		13/7								
Bitirgen et al. (40)	Turkey	NA	Bechet's disease	49	39.90 ± 11.20	LSCM	32/17	ACCMetrics	8	√	√	√			
	–		Healthy controls	30	41.20 ± 11.50		20/10								
Gad et al. (33)	Qatar	4.49 ± 4.02	Coeliac disease	20	11.78 ± 1.74	LSCM	NA	CCMetrics	8	√	√	√	√		
	–		Healthy controls	20	12.83 ± 1.91		NA								
Kocabeyoglu et al. (49)	Turkey	0.87 ± 0.63	Graves' disease	40	35.40 ± 11.20	SSCM	29/11	Image J	7	√	√	√	√		
	–		Healthy controls	40	33.80 ± 10.30		26/14								
Sharma et al. (36)	UK	NA	Hypothyroidism	20	49.55 ± 13.34	LSCM	11/9	CCMetrics	8	√	√	√			
	–		Healthy controls	20	44.95 ± 14.29		12/8								
Tepelus et al. (41)	USA	NA	Mucous Membrane Pemphigoid	23	76.40 ± 13.80	LSCM	NA	Image J	8		√		√		√
	–		Healthy controls	8	74.30 ± 7.50		NA								
Barcelos et al. (30)	Portugal	11.70 ± 7.70	Rheumatoid arthritis	18	55.30 ± 13.70	LSCM	NA	Image J	6	√	√				
	–		Healthy controls	20	51.00 ± 6.50		NA								

F/M, female/male; CN, corneal nerve; FD, fiber density; FL, fiber length; BD, branch density; T, tortuosity; B, beadings; R, reflectivity; NA, not available.

standard deviation, and sample size for continuous corneal nerve parameters, and the Random-effects model was applied to calculate the weighted mean difference (WMD) with 95% CI. In order to facilitate comparison, we defined the total length of the corneal nerve fibers as CNFL, the total number of corneal nerve fibers per mm^2 as CNFD, and the number of branches originating from major nerve trunks per mm^2 as corneal nerve branch density (CNBD). Nerve length or nerve density was divided by image area, if necessary, in order to unify the units of corneal nerve parameters. Besides the parameters above, we also recorded nerve tortuosity, reflectivity, and beadings. Nerve tortuosity and nerve reflectivity were presented as four grades according to previously validated grading scales ([24]). Beadings were defined as the number of bead-like formations in $100 \mu m$ of the nerve fiber. It should be mentioned that some works of research evaluated corneal nerve tortuosity with tortuosity coefficient, which is not adopted in this meta-analysis for a reliable comparison. We performed a sensitivity analysis by omitting one study at a time and calculating a pooled estimate for the remaining studies to evaluate the contribution of each individual study to the results. The I^2 statistic was used to estimate heterogeneity among the studies. To explore the potential confounding factors, we performed subgroup analysis by age, type of IVCM, software used to measure corneal nerve parameters, and types of NNAI diseases. Publication bias was estimated by funnel plot, as well as Egger's linear regression test and Begg's rank association test with significance set to $P < 0.1$ ([25], [26]).

RESULTS

Search Process

The selection of studies is shown in **Figure 2**. Potential references were screened from PubMed ($n = 4,159$), Web of Science ($n = 6,571$) and Cochrane Library ($n = 82$). After duplicate publications were removed, the titles and abstracts of 7,020 remaining studies were assessed for potential eligibility. For final eligibility, a total of 139 full-text articles were screened thoroughly and 102 studies were excluded due to reasons listed in **Figure 2**. No articles were excluded because of low quality. Quality rating scores ranged from 5 to 9 (mean: 7.24, *SD*: 1.04). Thus, a total of 37 studies were eligible for the final meta-analysis which included 1,423 patients and 1,059 healthy controls ([16], [27]–[61]).

Study Characteristics

Among the 37 included studies, 18 were related to type 1 diabetes, 13 were related to Sjögren's Syndrome, 1 was related to Bechet's disease, 1 was related to coeliac disease, 1 was related to Graves' disease, 1 was related to hypothyroidism, 1 was related to mucous membrane pemphigoid, and 1 was related to rheumatoid arthritis. As shown in **Table 1**, different studies reported different corneal nerve parameters. Most of the studies used laser scanning confocal microscopy (LSCM) or slit scanning confocal microscopy (SSCM) as IVCM appliances, except for tandem scanning confocal microscopy (TSCM) in one study and unspecified appliance in another. As for IVCM image

analysis software, CCMetrics, ACCMetrics, and Image J were commonly used. Other characteristics of the included studies such as demographics, research groups, disease durations are also summarized in **Table 1**. Representative IVCM images of the cornea in patients with healthy controls and patients with NNAI diseases are listed in **Figure 3**.

Corneal Nerve Parameters (CNFL, CNFD, CNBD)

Including 2,335 participants (1,337 in the NNAI group and 998 in the control group), thirty-two studies reported on CNFL. The WMD in CNFL between NNAI and control groups was -3.94 (95% CI: $-4.77-−3.12$, $P < 0$), with significant heterogeneity across studies (I$^2 = 93.2\%$, **Figure 4**). The results showed CNFL (mm/mm^2) was obviously lower in the NNAI group.

Furthermore, twenty-eight studies with a total of 1,696 participants (946 in the NNAI group and 750 in the control group) reported on CNFD. The weighted mean difference was -6.62 (95% CI: $-8.4-−4.85$, $P < 0$), with significant heterogeneity across studies (I$^2 = 90.6\%$, **Figure 5**), showing that CNFD (no./mm^2) of the NNAI group was significantly lower than that of the control group.

Finally, twenty-two studies with a total of 1,699 participants (924 in the NNAI group and 775 in the control group) reported on CNBD. The weighted mean difference was -9.89 (95% CI: $-14-−5.79$, $P < 0$), with significant heterogeneity across studies (I$^2 = 88.4\%$, **Figure 6**). Consistently, CNBD (no./mm2) of NNAI patients was significantly lower than that of healthy controls.

Publication Bias

The publication bias of the studies was shown by funnel plots (**Figure 7**). The symmetrical funnel plot showed no significant publication bias in the publications reported on CNFD and CNBD. However, the results revealed that studies reported CNFL was mild asymmetry visually, suggesting a publication bias. In addition, Egger linear regression tests and the Begg's rank association tests were performed (**Table 2**). All other results demonstrated no evidence of significant publication bias except for Egger's test on CNFL. After recalculating the WMD on CNFL using the trim and fill methods, the pooled results were similar to the original results, which means the observed publication bias did not influence the overall results.

Sensitivity Analysis and Subgroup Analysis

To explore the source of heterogeneity, sensitivity analysis was performed. The results revealed that no individual study had an excessive influence on the above-mentioned pooled effect (**Figure 8**).

Stratifications by age, type of IVCM, software used to measure corneal nerve parameters, and type of NNAI diseases were analyzed due to high heterogeneity. Among studies that reported CNFL, subgroup analysis demonstrated that heterogeneity was reduced for studies grouped by type of IVCM only when using SSCM to record CNFL (I$^2 = 26.1\%$). Among studies that reported CNFD, subgroup analysis demonstrated that heterogeneity was reduced for studies grouped by the software used only when using built-in software to assess CNFD (I$^2 = 43.1\%$). And among
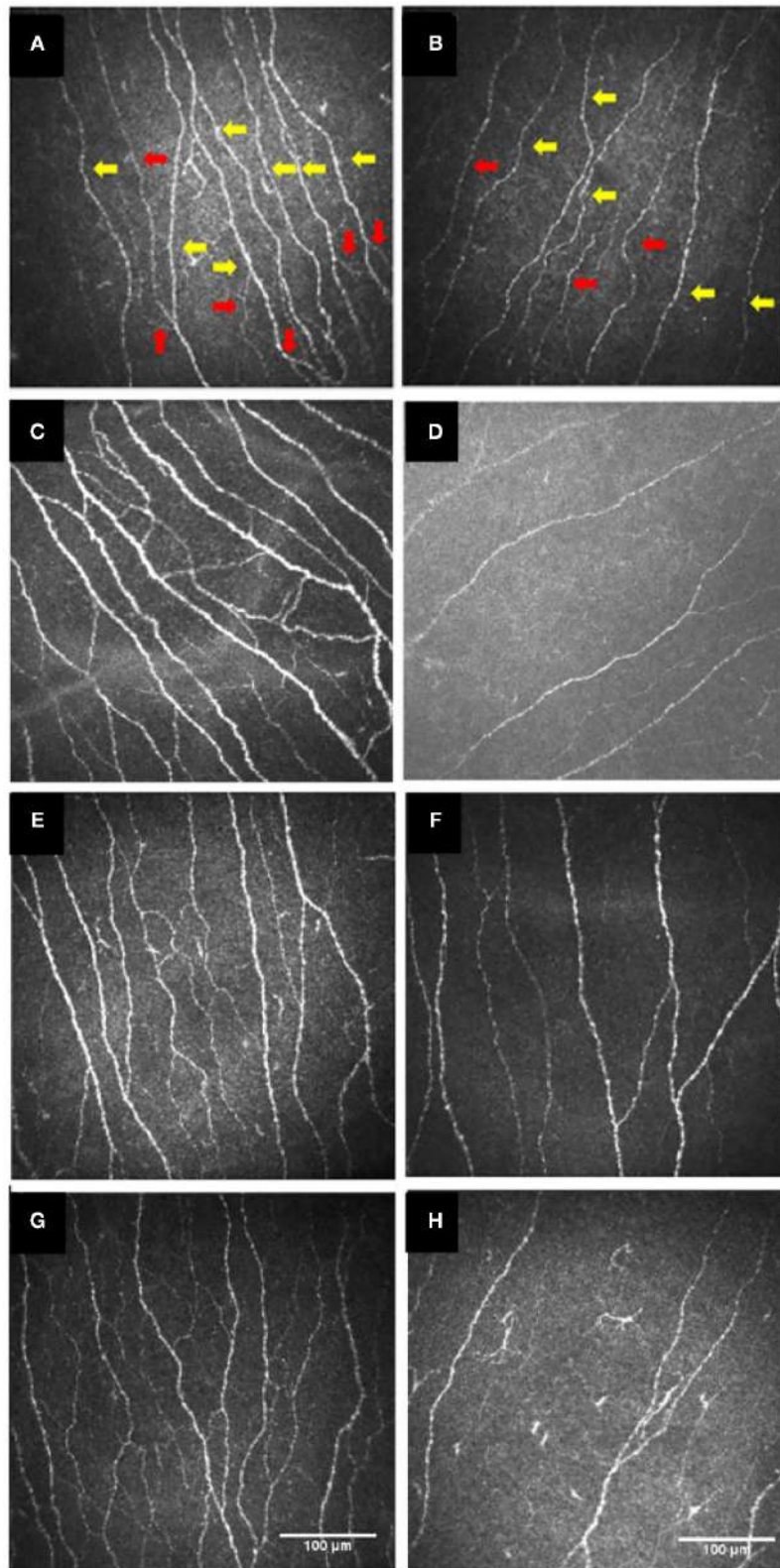
FIGURE 3 | IVCM images of the cornea in the healthy controls **(A,C,E,G)** and patients with type 1 diabetes **(B)**, or with Sjögren's syndrome **(D)**, or with celiac disease **(F)**, or with Behçet's disease **(H)**. Red arrows show corneal nerve branches and yellow arrows show corneal nerve fibers. **(A,B)** were re-organized with permission from (45), copyright 2017, Public Library of Science. **(C,D)** were re-organized with permission from (62), copyright 2021, BioMed Central. **(E,F)** were re-organized with permission from (33), copyright 2020, Public Library of Science. **(G,H)** were re-organized with permission from (40), copyright 2018, Frontiers. IVCM, *in vivo* confocal microscopy.
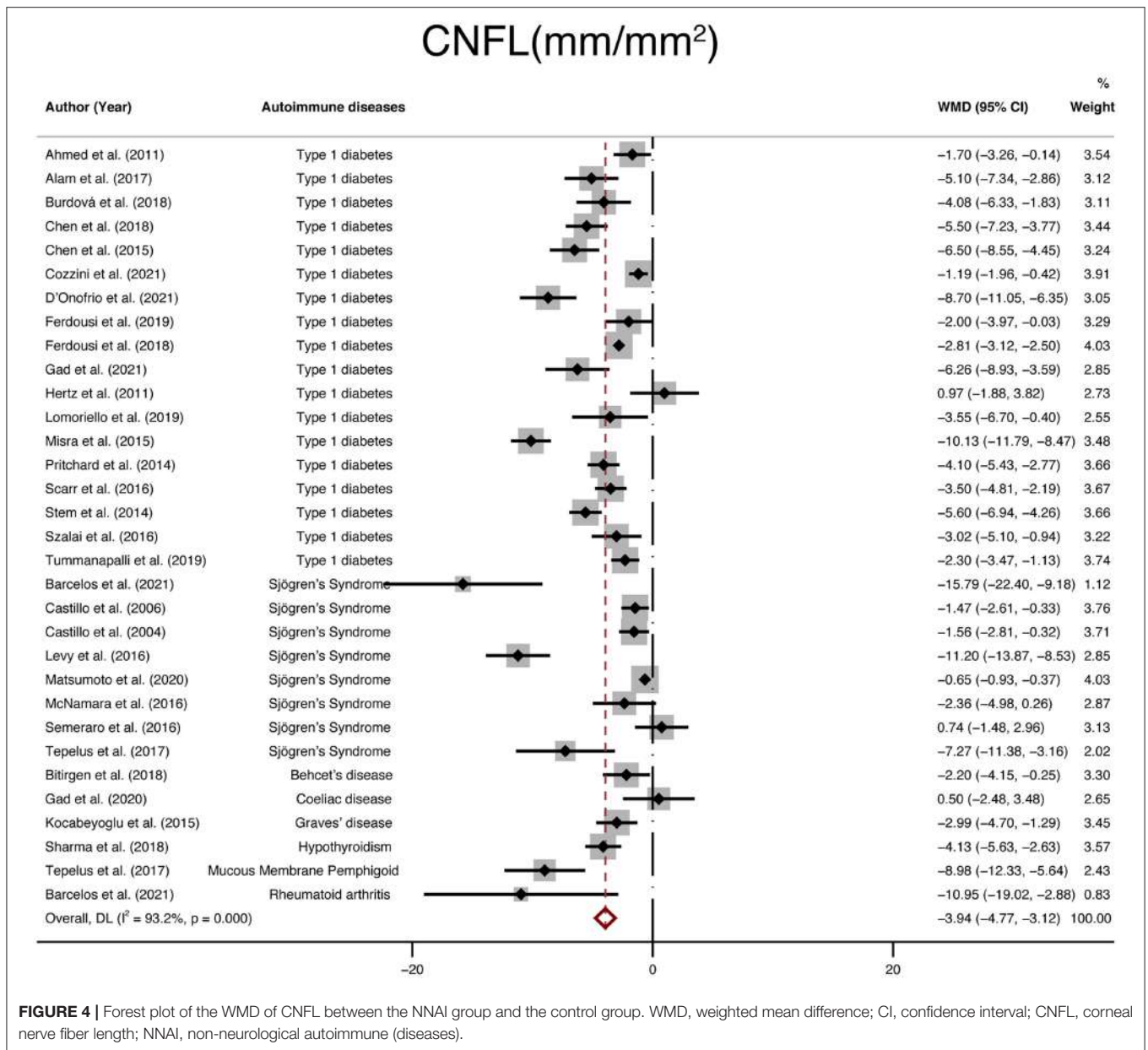
FIGURE 4 | Forest plot of the WMD of CNFL between the NNAI group and the control group. WMD, weighted mean difference; CI, confidence interval; CNFL, corneal nerve fiber length; NNAI, non-neurological autoimmune (diseases).

studies that reported CNBD, heterogeneity was significantly reduced for studies grouped by the software used only when using Image J to assess CNBD ($I^2 = 0\%$). The detailed results of subgroup analysis are depicted in **Table 3**.

Tortuosity, Reflectivity, and Beadings

In addition, IVCM enabled en-face examination of corneal nerves. Therefore, tortuosity, reflectivity, and beadings are also widely used to quantify corneal nerve morphology. We collected 11 studies that reported tortuosity, 6 studies that reported reflectivity, 6 studies that reported beadings and performed a meta-analysis. The results demonstrated that the differences in tortuosity (WMD: 1.19, 95% CI:0.57–1.81) and beadings (WMD: 19.91, 95% CI: 11.92–27.9) between the NNAI group and the

control group were statistically significant, while the reflectivity (WMD: −0.21, 95% CI: −0.65–0.24) of NNAI patients showed no statistical difference from healthy controls (**Figure 9**).

To further assess the reliability of our results, we also performed funnel plots (**Figure 10**), as well as Egger's linear regression tests and Begg's rank association tests (**Table 4**) to estimated publication bias. Sensitivity analysis of studies that reported beadings of corneal nerve per $100\,\mu m$ showed that four out of six studies may have excessive influence on the above-mentioned pooled effect, and results of tortuosity and reflectivity showed that no individual study had an excessive influence on the above-mentioned pooled effect (**Figure 11**). Funnel plots of tortuosity and beadings were visually asymmetric, suggesting possible publication bias. Egger's test also showed
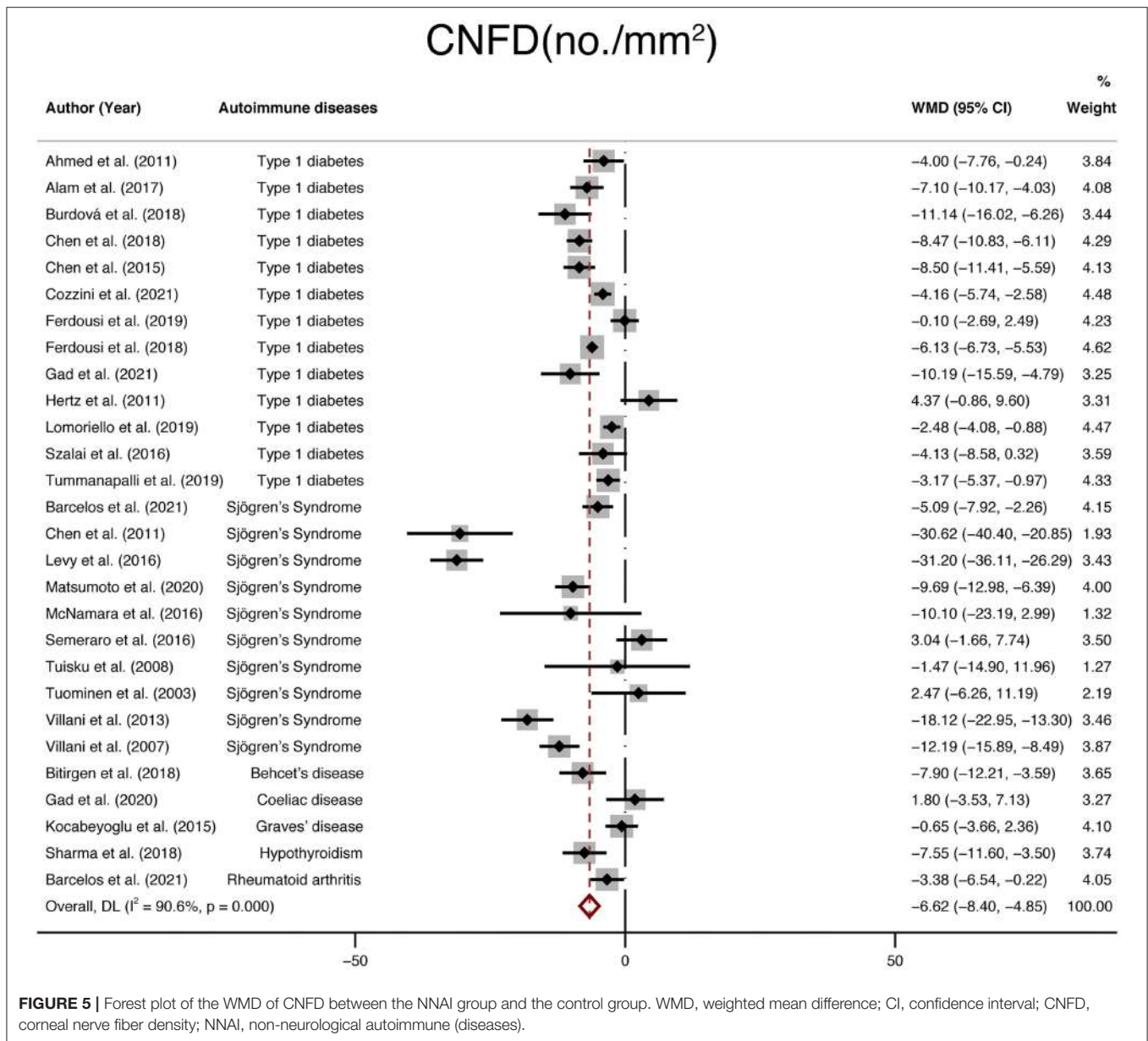
FIGURE 5 | Forest plot of the WMD of CNFD between the NNAI group and the control group. WMD, weighted mean difference; CI, confidence interval; CNFD, corneal nerve fiber density; NNAI, non-neurological autoimmune (diseases).

that there may be a publication bias on studies reported on tortuosity and beadings. After using the trim and fill methods, the pooled result of tortuosity was not changed while that of beadings was quite different from the original results. According to our study, the publication bias did not influence the overall results of tortuosity but did interfere with the overall result of beadings.

DISCUSSION

The cornea, as the front portion of the ocular surface, plays an important role in the visual system. Its integrity is crucial for the health and normal function of the eye, and its delicate mucosal immune system was extremely vulnerable to autoimmune dysregulation so that the cornea is able to

detect and repair the damage promptly. It was reported that assessment of corneal nerve parameters has become one of the most common clinical tests to evaluate ocular surface symptoms in many kinds of diseases (63). IVCM provides a direct and non-invasive tool to observe corneal nerve morphology and assess corneal nerve parameters. NNAI diseases, to our knowledge, are a range of diseases with abnormal autoimmune reactions including varied manifestations on the ocular surface. Many researchers reported that the involvement of the cornea may be an initial manifestation of some of the autoimmune diseases and may be sight-threatening if not well treated (64–66). As one of the most densely innervated parts of the human body, the corneal nerve may serve as a marker of some diseases with its morphological alternation.

FIGURE 6 | Forest plot of the WMD of CNBD between the NNAI group and the control group. WMD, weighted mean difference; CI, confidence interval; CNBD, corneal nerve branch density; NNAI, non-neurological autoimmune (diseases).
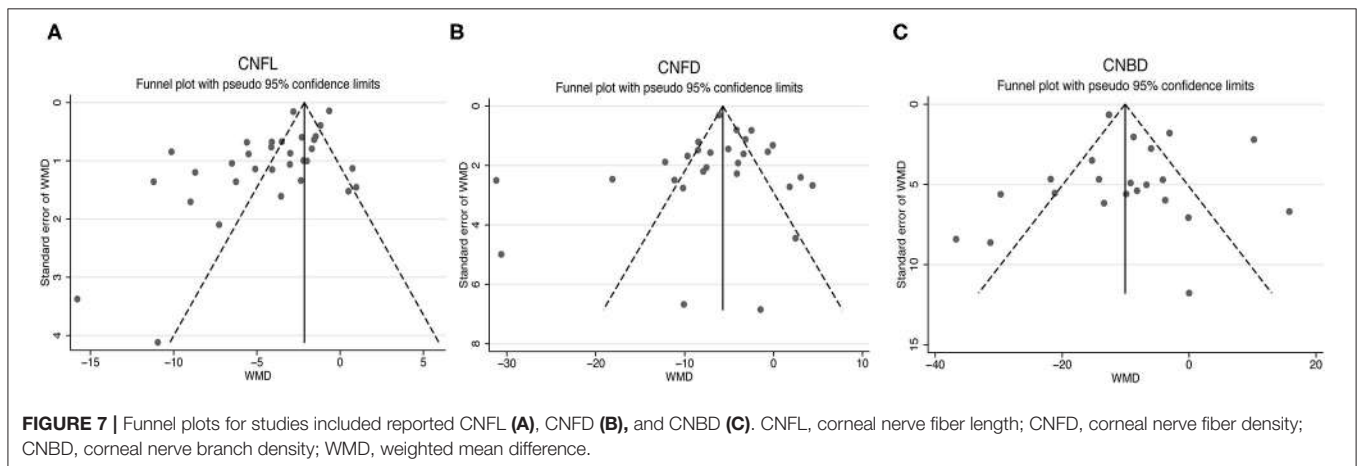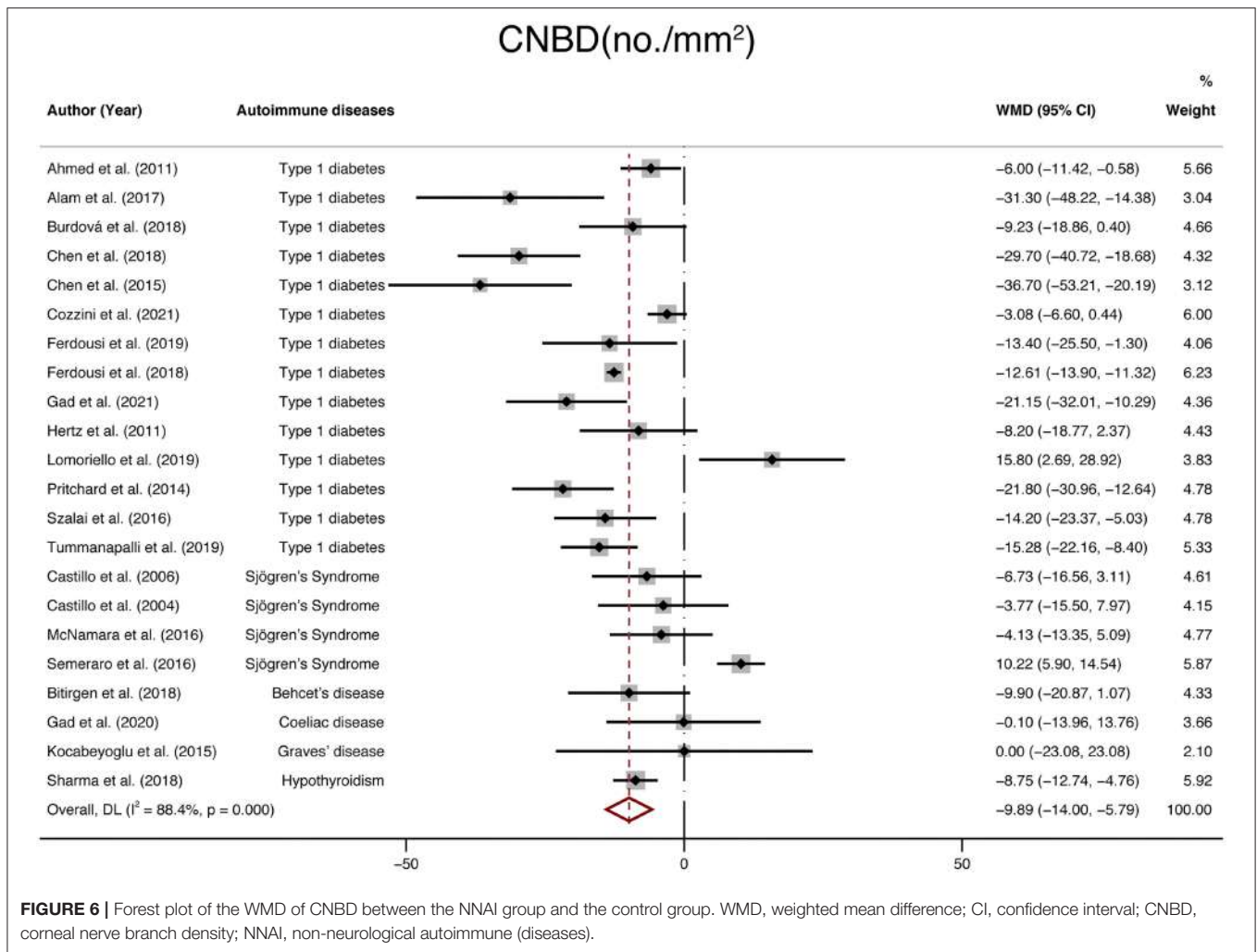

FIGURE 7 | Funnel plots for studies included reported CNFL **(A)**, CNFD **(B)**, and CNBD **(C)**. CNFL, corneal nerve fiber length; CNFD, corneal nerve fiber density; CNBD, corneal nerve branch density; WMD, weighted mean difference.

In the pathology of NNAI diseases, the exact etiological and pathophysiological mechanisms are often unknown. However, many researchers found that elevating inflammatory mediators, such as IL1-beta, IL6, IL8, and TNF-alpha might play an important role in autoimmune patients with small fiber neuropathy. Reducing mechanical nociceptive thresholds and dysesthesias were also found to be associated with higher IL1-beta and TNF-alpha concentrations (67–69). The corneal nerves,

Subject	CNFL	CNFD	CNBD
Begg's test	0.195	0.323	0.554
Egger's test	0.001	0.548	0.657
WMD1 (95% CI) [†]	−3.94 (−4.77, −3.12)	−6.62 (−8.40, −4.85)	−9.89 (−14.00, −5.79)
WMD2 (95% CI) ‡	−3.81 (−4.64, −2.99)	NA	NA

CNFL, corneal nerve fiber length; CNFD, corneal nerve fiber density; CNBD, corneal nerve branch; WMD, weighted mean difference; CI, confidence interval; NA, not available.
[†] Original WMD and 95% CI.
‡WMD and 95% CI after using the trim and fill method.

as one kind of small nerve fibers, may share the same mechanisms to some extent. Patients with Sjögren's syndrome, systemic lupus erythematosus, or rheumatoid arthritis, for instance, were found to have local increasing lymphocytes in the cornea which implied inflammatory infiltration in corneal nerve fibers (70). Recently, researchers using Mouse models of type 1 diabetes found that decreasing neutrophil infiltration and reducing expression of IL1-beta and TNF-alpha could prevent corneal nerve loss (71, 72). In this way, we speculate that inflammatory mediators may be one reason why a similar pattern of corneal nerve loss occurs in NNAI diseases. Other mechanisms such as metabolic, infectious, and genetic factors may also take part, but the exact pathophysiological mechanisms would need future explorations.

Various works of research had proved that corneal IVCM could be a sensitive evaluation tool in early diabetic peripheral neuropathy and might be clinically useful to diagnosis and surveillance of other neuropathies (48, 73, 74). It is plausible that the alteration of the corneal nerve under IVCM may be a tool to identify NNAI diseases. The other way around, the effect of NNAI diseases on the corneal nerve might be the reason why ocular symptoms were commonly presented among NNAI patients. It is well acknowledged that the corneal nerve helps maintain a well-lubricated and smooth eye surface not only by inducing tear production but also by stimulating the blinking reflex through an elaborate interaction between the corneal surface and lacrimal glands (75). Therefore, damage of the corneal nerve may be associated with the ocular sicca symptoms usually seen and more severe in many NNAI diseases (76–78).

However, many of the previous studies are limited in sample size and their results were contradictory. There is a lack of analytical summary to evaluate the change of corneal nerves in a certain spectrum of NNAI diseases. In this case, a meta-analysis is a powerful tool to summarize results from different studies by providing a more objective evaluation of the major effect with enhanced accuracy and to explain the heterogeneity between different studies. To the best of our knowledge, this is the first meta-analysis to investigate the corneal nerve parameters using IVCM in patients with NNAI and control groups. Our analysis showed significantly decreased CNFL (WMD: −3.94, 95% CI: −4.77−−3.12), CNFD (WMD: −6.62, 95% CI: −8.4−−4.85), CNBD (WMD: −9.89, 95% CI: −14−−5.79) in NNAI

groups. However, there was significant heterogeneity of three sets of parameters mentioned above among the studies included. Sensitivity analysis, creation of funnel plots, Egger's test, Begg's test, and the trim and fill methods were performed to confirm the reliability of the results. And the analysis stratified by age, type of IVCM, software used, and types of NNAI diseases, were performed to assess between-study heterogeneity. However, subgroup results showed no potential source of heterogeneity. In the article of Roszkowska et al., it was concluded that corneal nerve changes in diabetes examined by IVCM are related to HbA1c level, diabetes duration, the progress of diabetic retinopathy, and race (79). It is possible that factors such as the severity or duration of NNAI, racial differences in participants, male-female distribution, the acquisition mode with IVCM, or the number of images analyzed per participant, might cause heterogeneity. Due to the incomparability and incompleteness of data, the effect of these above-mentioned potential factors on between-study heterogeneity could not be further examined. All in all, our meta-analysis included thirty-seven studies and with analysis of a large sample size, had shown a significant decrease in CNFL, CNFD, and CNBD among NNAI patients.

In addition, it is interesting that results showed patients with Sjögren's syndrome had a greater reduction in CNFD and minimal impact on CNBD, and consequent comparable reduction in CNFL. In many diseases affecting corneal nerves, CNBD was found to be elevated rather than reduced as subconsciously assumed. For instance, the pattern of corneal nerves appeared to be unique in Parkinson's disease with reduced CNFD and a markedly increased CNBD (80, 81). Similarly, a study demonstrated enhanced CNBD and reduced CNFD and CNFL in patients with painful diabetic neuropathy (82). In addition, increased CNBD was also found to be the first sign to indicate regeneration after simultaneous pancreas and kidney transplantation or continuous subcutaneous insulin infusion in type 1 diabetes (83, 84). All studies mentioned above supported the hypothesis that enhanced CNBD signified some preserved susceptibility of corneal nerve fibers toward regeneration and attempts to repair, but the attempts as yet appeared insufficient to culminate in an increased CNFD or CNFL. Consequently, we consider that CNBD's attempt at regeneration may to some extent compensate for the reduced CNBD by injury. As for CNFL and CNFD, to our knowledge, it is proved that CNFL has been shown to have the best reproducibility and consistency compared to CNFD and CNBD for detecting early preclinical small fiber damage (54, 79, 85, 86). This may indicate that CNFL is most susceptible to damage from various diseases, but our results presented contradictory. It is strange and hard to explain, and maybe knowing the exact pathology of Sjögren's syndrome would help explain it. However, at present, studies on corneal nerve alternation of patients are mainly *in vivo* studies, which means that we can basically only carry out some non-invasive detections like corneal confocal, corneal sensation, biological fluid detection, etc. Although these detections prove to be very promising ways to an early small fiber neuropathy diagnosis (87), the exact pathophysiology and signaling pathways activated in diseases remain unknown due to invasive procedures that cannot be
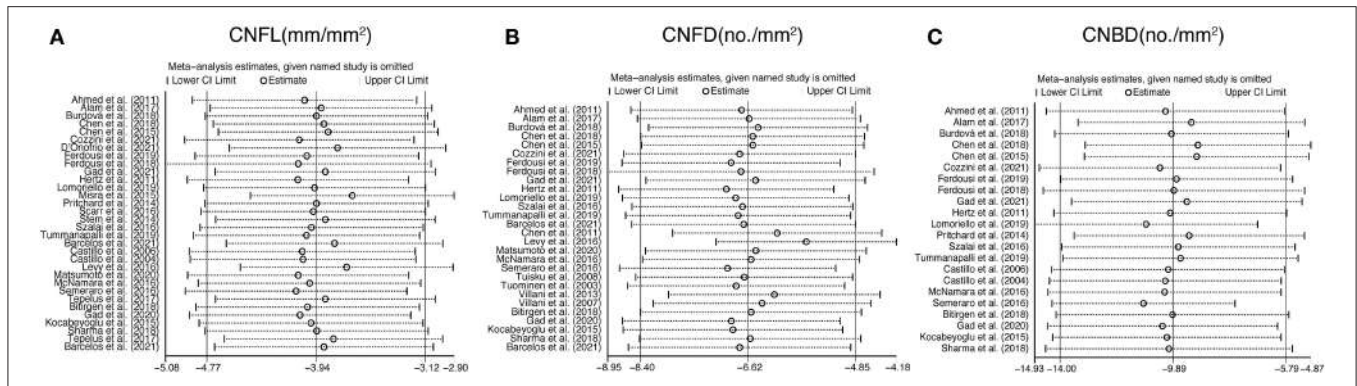
FIGURE 8 | Sensitivity analysis data for studies included reported CNFL **(A)**, CNFD **(B),** and CNBD **(C)**. CNFL, corneal nerve fiber length; CNFD, corneal nerve fiber density; CNBD, corneal nerve branch density.

TABLE 3 | Subgroup analysis of CNFL, CNFD, and CNBD by age, type of IVCM, software used, and types of NNAI diseases.

| Subgroup	Group by	CNFL			CNFD			CNBD		
		N	WMD (95%CI)	I^2	N	WMD (95%CI)	I^2	N	WMD (95%CI)	I^2
Age										
	10–20	5	−2.32 (−4.06, −0.59)	76.0	5	−3.18 (−6.27, −0.08)	76.3	5	−10.13 (−18.03, −2.24)	73.9
	30–40	8	−3.39 (−4.52, 2.26)	68.9	7	−4.72 (−6.93, −2.52)	74.7	7	−8.14 (−16.10, −0.18)	76.3
	40–50	6	−4.22 (−5.33, −3.12)	80.6	5	−9.38 (−12.59, −6.17)	86.5	5	−18.30 (−24.61, −11.99)	83.9
	50–60	9	−7.01 (−10.47, −3.55)	94.3	9	−8.75 (−15.62, −1.87)	94.6	3	1.61 (−9.44, 12.66)	81.6
	>60	3	−2.85 (−5.26, −0.44)	92.1	/	/	/	/	/	/
Type of IVCM										
	LSCM	25	−4.51 (−5.49, −3.52)	94.6	20	−7.44 (−9.50, −5.38)	91.6	15	−13.56 (−17.22, −9.90)	79.3
	SSCM	6	−2.26 (−3.10, −1.43)	26.1	6	−6.25 (−10.84, −1.66)	86.2	6	−2.34 (−9.13, 4.46)	50.9
Software used										
	CCMetrics	13	−3.80 (−5.02, −2.58)	80.7	10	−4.81 (−7.75, −1.87)	83.2	11	−15.16 (−21.00, −9.32)	77.2
	Built-in software	/	/	/	2	−8.41 (−16.94, 0.11)	43.1	/	/	/
	ACCMetrics	5	−2.24 (−3.10, −1.39)	73.6	5	−4.98 (−6.53, −3.43)	67.1	5	−10.64 (−16.04, −5.24)	84.8
	Image J	9	−6.19 (−9.04, −3.34)	95.3	5	−7.35 (−16.32, 1.62)	96.9	2	9.87 (5.63, 14.12)	0.0
	Cell Count software	/	/	/	2	−14.95 (−20.75, −9.14)	72.7	/	/	/
Types of NNAI diseases										
	Type 1 diabetes	18	−4.14 (−5.14, −3.14)	90.3	13	−4.95 (−6.53, −3.37)	84.1	14	−13.49 (−17.93, −9.05)	83.7
	Sjögren's Syndrome	8	−3.74 (−5.71, −1.78)	92.6	10	−11.45 (−18.02, −4.87)	94.1	4	−0.42 (−10.32, 9.48)	82.3

N, number; CNFL, corneal nerve fiber length; CNFD, corneal nerve fiber density; CNBD, corneal nerve branch density; WMD, weighted mean difference; CI, confidence interval; IVCM, in vivo confocal microscopy; LSCM, laser scanning confocal microscopy; SSCM, slit scanning confocal microscopy; NNAI, non-neurological autoimmune (diseases).

performed *in vivo*. Moving forward, more future research is needed for a deeper understanding.

Besides CNFL, CNFD, and CNBD, tortuosity, reflectivity, and beadings are also important parameters to describe corneal nerve morphology. According to our analysis, the corneal nerve of the NNAI group presented more beadings per 100 μm (WMD: 19.91, 95% CI: 11.92–27.9) and was more tortuous (WMD: 1.19, 95% CI:0.57–1.81) than that of the control group, while there seemed to be no statistical difference on corneal nerve reflectivity (WMD: −0.21, 95% CI: −0.65−0.24, *P* = 0.361) between two groups. However, the results of subjective parameters like tortuosity and beadings in our analysis seem to be less convincing according to publication bias analysis. There could be due to many reasons. One of the reasons may be that these subjective parameters are infrequently reported

in the included literature, resulting in a small sample size of data. Another reason may be that measurement of subjective parameters is not uniform across studies. For instance, some studies reported corneal nerve tortuosity according to previously validated grading scales, while others used tortuosity coefficient (47). Besides, the interpretations of the results by these subjective parameters rely a lot on researchers' subjective judgment and observers' experience, which made the results less comparable.

Nevertheless, we can't deny the promising function of subjective parameters in predicting corneal nerve neuropathy. Indeed, according to research examining corneal nerves in patients with type 2 diabetes (88), the size and number of beadings had the best sensitivity and specificity to predict the dysfunctions of the peripheral neuropathy compared with CNFD, CNFL. Similarly, a previous study among glaucoma patients
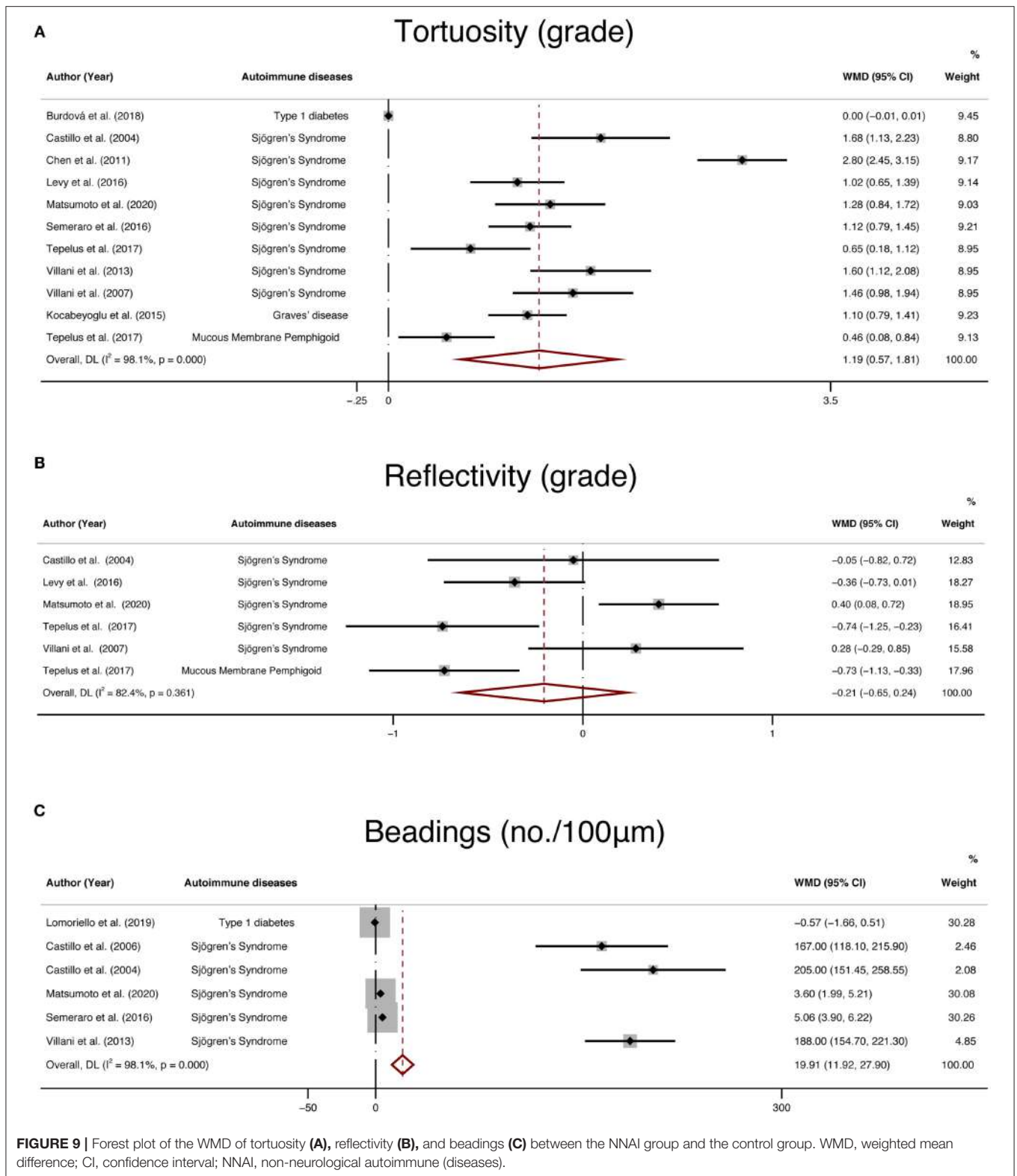
FIGURE 9 | Forest plot of the WMD of tortuosity **(A)**, reflectivity **(B),** and beadings **(C)** between the NNAI group and the control group. WMD, weighted mean difference; CI, confidence interval; NNAI, non-neurological autoimmune (diseases).

showed that tortuosity and beadings directly correlated with corneal nerve function (89). In recent years, software and methods have been developed to obtain more objective and

reproducible evaluations of tortuosity (90, 91). For example, a study proposed an automatic algorithm that was able to correctly trace more than 80% of the recognizable nerve
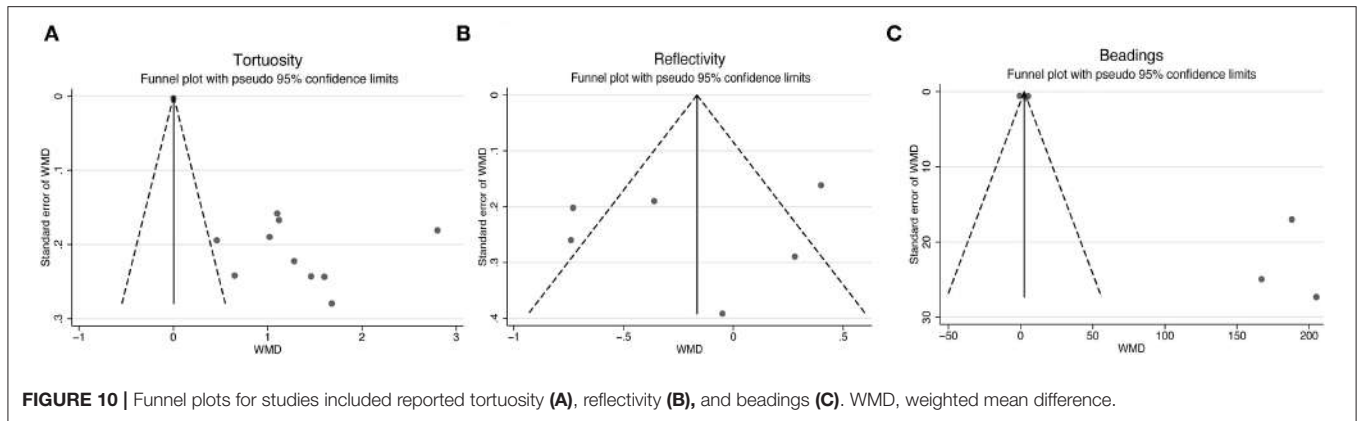
FIGURE 10 | Funnel plots for studies included reported tortuosity **(A)**, reflectivity **(B),** and beadings **(C)**. WMD, weighted mean difference.

FIGURE 11 | Sensitivity analysis data for studies included reported tortuosity **(A)**, reflectivity **(B),** and beadings **(C)**.

TABLE 4 | Publication bias measured by Begg's and Egger's test, WMD (95% CI) recalculated with trim and fill method.

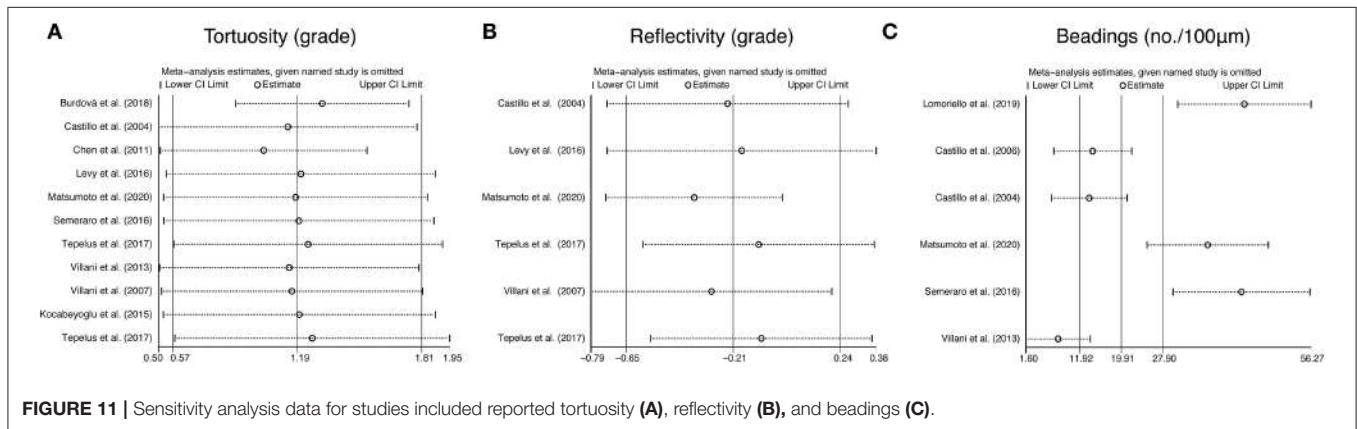| Subject	Tortuosity	Reflectivity	Beadings
Begg's test	0.815	0.851	0.091
Egger's test	0.000	0.706	0.017
WMD1 (95% CI) [†]	1.19 (0.58, 1.81)	−0.21 (−0.65, 0.24)	19.91 (11.92, 27.90)
WMD2 (95% CI) [‡]	1.19 (0.58, 1.81)	NA	8.40 (−1.09, 17.88)

WMD, weighted mean difference; CI, confidence interval.
[†] Original WMD and 95% CI.
‡WMD and 95% CI after using the trim and fill method.

fibers in the images and proved its clinical validity regarding tortuosity measure (92). We believe that in the future, more accurate software will help make these subjective parameters more comparable among various studies and more practical in clinical performance.

The present study has some limitations that should be considered. Firstly, the types of NNAI included in our study were mostly typed 1 diabetes and Sjögren's Syndrome, which might not be representative of NNAI in general. Many other NNAI diseases were reported presenting ocular manifestation as the initial manifestation like rheumatoid arthritis and systemic lupus erythematosus. It is reasonable to infer that alteration in corneal innervation also occurs in these diseases, but it is a pity that we did not find qualified studies for every NNAI disease that could be included in the meta-analysis. And we look forward to more research about morphological alternation of the corneal nerve of NNAI so we may draw a more reliable conclusion. Secondly, although IVCM has already been widely used in clinical practice, there is still a lack of a gold standard for corneal nerve parameters. For example, the majority of studies have defined CNFL as the total length of nerves visible within a defined area in mm/mm^2 while some only measured nerve branches longer than 50 μm or analyzed the total length of nerves within a frame (93–97). Other factors contributing to the non-uniform assessment may include. (1) Each image captured by IVCM represents only approximately 0.2% of the average corneal surface which might give out non-representative images and result in misleading inferences (7, 98). (2) A possible correlation between myopic refractive error and CNFL might be neglected among our included articles that assess corneal nerves (99). (3) According to instrument design, IVCM can be generally divided into tandem scanning confocal microscopy, laser scanning confocal microscopy, and slit scanning confocal microscopy (100). Different kinds of confocal microscopy are equipped with different field brightness and contrast which may affect the apparent thickness of corneal nerves, particularly when they approach the limit of resolution, thus influencing the uniformity among different studies (97, 101). (4) IVCM image processing could be performed by different methods, including manual

tracing, ImageJ, the CCMetrics system, the ACCMetrics system, etc (102, 103). The inconsistency of image-processing methods and the subjectivity during the image-analyzing procedure among different studies may also result in significant discrepancy and heterogeneity.

In conclusion, this meta-analysis suggested that corneal nerve parameters (CNFL, CNFD, CNBD) might be clinical markers for NNAI diseases, while our analysis of other morphology indicators (tortuosity, reflectivity, beadings) lack reliable conclusion from the included studies. Future longitudinal studies could delve into the role of IVCM as a promising way to diagnose and evaluate NNAI diseases.

DATA AVAILABILITY STATEMENT

The original contributions presented in the study are included in the article/supplementary material, further inquiries can be directed to the corresponding authors.

AUTHOR CONTRIBUTIONS

YG, XL, and XY conceived of the study, carried out the literature search, extracted the data, and performed the statistical analysis. NY and WK conducted the quality assessment. YG, XL, and QQ were involved in revising and modification of the manuscript. KW and MC directed the project, reviewed, and revised the manuscript. All authors have contributed significantly and agree with the content of the manuscript. All authors read and approved the final manuscript.

FUNDING

REFERENCES

1. Karagianni P, Tzioufas AG. Epigenetic perspectives on systemic autoimmune disease. *J Autoimmun.* (2019) 104:102315. doi: 10.1016/j.jaut.2019.102315

2. Cooper GS, Bynum ML, Somers EC. Recent insights in the epidemiology of autoimmune diseases: improved prevalence estimates and understanding of clustering of diseases. *J Autoimmun.* (2009) 33:197–207. doi: 10.1016/j.jaut.2009.09.008

3. Stojanovich L, Marisavljevich D. Stress as a trigger of autoimmune disease. *Autoimmun Rev.* (2008) 7:209–13. doi: 10.1016/j.autrev.2007.11.007

4. Saccucci M, Di Carlo G, Bossù M, Giovarruscio F, Salucci A, Polimeni A. Autoimmune diseases and their manifestations on oral cavity: diagnosis and clinical management. *J Immunol Res.* (2018) 2018:6061825. doi: 10.1155/2018/6061825

5. Bodolay E, Dérfalvi B, Gergely P, Poór G. When does an autoimmune disease begin? Importance of the early diagnosis. *Orv Hetil.* (2007) 148 Suppl 1:25–30. doi: 10.1556/oh.2007.28031

6. Yang AY, Chow J, Liu J. Corneal Innervation and Sensation: the eye and beyond. *Yale J Biol Med.* (2018) 91:13–21.

7. Kokot J, Wylegała A, Wowra B, Wójcik Ł, Dobrowolski D, Wylegała E. Corneal confocal sub-basal nerve plexus evaluation: a review. *Acta Ophthalmol.* (2018) 96:232–42. doi: 10.1111/aos.13518

8. Freissler KA, Lang GE. The cornea and systemic diseases. *Curr Opin Ophthalmol.* (1996) 7:22–7. doi: 10.1097/00055735-199608000-00005

9. Karpik AG, Schwartz MM, Dickey LE, Streeten BW, Roberts JL. Ocular immune reactants in patients dying with systemic lupus erythematosus. *Clin Immunol Immunopathol.* (1985) 35:295–312. doi: 10.1016/0090-1229(85)90091-1

10. Basantsova NY, Starshinova AA, Dori A, Zinchenko YS, Yablonskiy PK, Shoenfeld Y. Small-fiber neuropathy definition, diagnosis, and treatment. *Neurol Sci.* (2019) 40:1343–50. doi: 10.1007/s10072-019-03871-x

11. Harboe E, Tjensvoll AB, Maroni S, Gøransson LG, Greve OJ, Beyer MK, et al. Neuropsychiatric syndromes in patients with systemic lupus erythematosus and primary Sjögren syndrome: a comparative population-based study. *Ann Rheum Dis.* (2009) 68:1541–6. doi: 10.1136/ard.2008.098301

12. Lopate G, Pestronk A, Al-Lozi M, Lynch T, Florence J, Miller T, et al. Peripheral neuropathy in an outpatient cohort of patients with Sjögren's syndrome. *Muscle Nerve.* (2006) 33:672–6. doi: 10.1002/mus.20514

13. Ryabkova VA, Churilov LP, Shoenfeld Y. Neuroimmunology: What Role for Autoimmunity, Neuroinflammation, and Small Fiber Neuropathy in Fibromyalgia, Chronic Fatigue Syndrome, and Adverse Events after Human Papillomavirus Vaccination? *Int J Mol Sci.* (2019) 20:5164. doi: 10.3390/ijms20205164

14. Lim SH, Ferdousi M, Kalteniece A, Kass-Iliyya L, Petropoulos IN, Malik RA, et al. Corneal confocal microscopy detects small fibre neurodegeneration in Parkinson's disease using automated analysis. *Sci Rep.* (2020) 10:20147. doi: 10.1038/s41598-020-76768-x

15. Pagovich OE, Vo ML, Zhao ZZ, Petropoulos IN, Yuan M, Lertsuwanroj B, et al. Corneal confocal microscopy: Neurologic disease biomarker in Friedreich ataxia. *Ann Neurol.* (2018) 84:893–904. doi: 10.1002/ana.25355

16. Szalai E, Deák E, Módis L Jr, Németh G, Berta A, Nagy A, et al. Early Corneal Cellular and Nerve Fiber Pathology in Young Patients With Type 1 Diabetes Mellitus Identified Using Corneal Confocal Microscopy. *Invest Ophthalmol Vis Sci.* (2016) 57:853–8. doi: 10.1167/iovs.15-18735

17. Bitirgen G, Akpinar Z, Uca AU, Ozkagnici A, Petropoulos IN, Malik RA. Progressive loss of corneal and retinal nerve fibers in patients with multiple sclerosis: a 2-year follow-up study. *Transl Vis Sci Technol.* (2020) 9:37. doi: 10.1167/tvst.9.13.37

18. Bitirgen G, Akpinar Z, Malik RA, Ozkagnici A. Use of corneal confocal microscopy to detect corneal nerve loss and increased dendritic cells in patients with multiple sclerosis. *JAMA Ophthalmol.* (2017) 135:777–82. doi: 10.1001/jamaophthalmol.2017.1590

19. Cruzat A, Qazi Y, Hamrah P. In Vivo Confocal Microscopy of Corneal Nerves in Health and Disease. *Ocul Surf.* (2017) 15:15–47. doi: 10.1016/j.jtos.2016.09.004

20. Cullen AE, Holmes S, Pollak TA, Blackman G, Joyce DW, Kempton MJ, et al. Associations between non-neurological autoimmune disorders and psychosis: a meta-analysis. *Biol Psychiatry.* (2019) 85:35–48. doi: 10.1016/j.biopsych.2018.06.016

21. Tavakoli M, Quattrini C, Abbott C, Kallinikos P, Marshall A, Finnigan J, et al. Corneal confocal microscopy: a novel noninvasive test to diagnose and stratify the severity of human diabetic neuropathy. *Diabetes Care.* (2010) 33:1792–7. doi: 10.2337/dc10-0253

22. Messmer EM, Schmid-Tannwald C, Zapp D, Kampik A. In vivo confocal microscopy of corneal small fiber damage in diabetes mellitus. *Graefes Arch Clin Exp Ophthalmol.* (2010) 248:1307–12. doi: 10.1007/s00417-010-1396-8

23. Chang PY, Carrel H, Huang JS, Wang IJ, Hou YC, Chen WL, et al. Decreased density of corneal basal epithelium and subbasal corneal nerve bundle changes in patients with diabetic retinopathy. *Am J Ophthalmol.* (2006) 142:488–90. doi: 10.1016/j.ajo.2006.04.033

24. Oliveira-Soto L, Efron N. Morphology of corneal nerves using confocal microscopy. *Cornea.* (2001) 20:374–84. doi: 10.1097/00003226-200105000-00008

25. Egger M, Davey Smith G, Schneider M, Minder C. Bias in meta-analysis detected by a simple, graphical test. *BMJ.* (1997) 315:629–34. doi: 10.1136/bmj.315.7109.629

26. Begg CB, Mazumdar M. Operating characteristics of a rank correlation test for publication bias. *Biometrics*. (1994) 50:1088–101. doi: 10.2307/2533446

27. Gad H, Al-Jarrah B, Saraswathi S, Mohamed S, Kalteniece A, Petropoulos IN, et al. Corneal confocal microscopy identifies a reduction in corneal keratocyte density and sub-basal nerves in children with type 1 diabetes mellitus. *Br J Ophthalmol*. (2021). doi: 10.1136/bjophthalmol-2021-319057

28. D'Onofrio L, Kalteniece A, Ferdousi M, Azmi S, Petropoulos IN, Ponirakis G, et al. Small Nerve Fiber Damage and Langerhans Cells in Type 1 and Type 2 Diabetes and LADA Measured by Corneal Confocal Microscopy. *Invest Ophthalmol Vis Sci*. (2021) 62:5. doi: 10.1167/iovs.62.6.5

29. Cozzini T, Piona C, Marchini G, Merz T, Brighenti T, Bonetto J, et al. In vivo confocal microscopy study of corneal nerve alterations in children and youths with Type 1 diabetes. *Pediatr Diabetes*. (2021) 22:780–6. doi: 10.1111/pedi.13219

30. Barcelos F, Hipólito-Fernandes D, Martins C, Ângelo-Dias M, Cardigos J, Monteiro R, et al. Corneal sub-basal nerve plexus assessment and its association with phenotypic features and lymphocyte subsets in Sjögren's Syndrome. *Acta Ophthalmol*. (2021) 99:e1315. doi: 10.1111/aos.14811

31. Tummanapalli SS, Issar T, Kwai N, Poynten A, Krishnan AV, Willcox M, et al. Association of corneal nerve loss with markers of axonal ion channel dysfunction in type 1 diabetes. *Clin Neurophysiol*. (2020) 131:145–54. doi: 10.1016/j.clinph.2019.09.029

32. Matsumoto Y, Ibrahim OMA, Kojima T, Dogru M, Shimazaki J, Tsubota K. Corneal In Vivo Laser-Scanning Confocal Microscopy Findings in Dry Eye Patients with Sjögren's Syndrome. *Diagnostics (Basel)*. (2020) 10:497. doi: 10.3390/diagnostics10070497

33. Gad H, Saraswathi S, Al-Jarrah B, Petropoulos IN, Ponirakis G, Khan A, et al. Corneal confocal microscopy demonstrates minimal evidence of distal neuropathy in children with celiac disease. *PLoS ONE*. (2020) 15:e0238859. doi: 10.1371/journal.pone.0238859

34. Schiano Lomoriello D, Abicca I, Parravano M, Giannini D, Russo B, Frontoni S, et al. Early Alterations of Corneal Subbasal Plexus in Uncomplicated Type 1 Diabetes Patients. *J Ophthalmol*. (2019) 2019:9818217. doi: 10.1155/2019/9818217

35. Ferdousi M, Romanchuk K, Mah JK, Virtanen H, Millar C, Malik RA, et al. Early corneal nerve fibre damage and increased Langerhans cell density in children with type 1 diabetes mellitus. *Sci Rep*. (2019) 9:8758. doi: 10.1038/s41598-019-45116-z

36. Sharma S, Tobin V, Vas PRJ, Rayman G. The LDIFLARE and CCM methods demonstrate early nerve fiber abnormalities in untreated hypothyroidism: a prospective study. *J Clin Endocrinol Metab*. (2018) 103:3094–102. doi: 10.1210/jc.2018-00671

37. Ferdousi M, Petropoulos IN, Kalteniece A, Azmi S, Ponirakis G, Efron N, et al. No Relation between the severity of corneal nerve, epithelial, and keratocyte cell morphology with measures of dry eye disease in type 1 diabetes. *Invest Ophthalmol Vis Sci*. (2018) 59:5525–30. doi: 10.1167/iovs.18-25321

38. Chen X, Graham J, Petropoulos IN, Ponirakis G, Asghar O, Alam U, et al. Corneal nerve fractal dimension: a novel corneal nerve metric for the diagnosis of diabetic sensorimotor polyneuropathy. *Invest Ophthalmol Vis Sci*. (2018) 59:1113–8. doi: 10.1167/iovs.17-23342

39. Ceská Burdová M, Kulich M, Dotrelová D, Mahelková G. Effect of diabetes mellitus type 1 diagnosis on the corneal cell densities and nerve fibers. *Physiol Res*. (2018) 67:963–74. doi: 10.33549/physiolres.933899

40. Bitirgen G, Tinkir Kayitmazbatir E, Satirtav G, Malik RA, Ozkagnici A. In Vivo Confocal Microscopic Evaluation of Corneal Nerve Fibers and Dendritic Cells in Patients With Behçet's Disease. *Front Neurol*. (2018) 9:204. doi: 10.3389/fneur.2018.00204

41. Tepelus TC, Huang J, Sadda SR, Lee OL. Characterization of Corneal Involvement in Eyes With Mucous Membrane Pemphigoid by In Vivo Confocal Microscopy. *Cornea*. (2017) 36:933–41. doi: 10.1097/ICO.0000000000001201

42. Tepelus TC, Chiu GB, Huang J, Huang P, Sadda SR, Irvine J, et al. Correlation between corneal innervation and inflammation evaluated with confocal microscopy and symptomatology in patients with dry eye syndromes: a preliminary study. *Graefes Arch Clin Exp Ophthalmol*. (2017) 255:1771–8. doi: 10.1007/s00417-017-3680-3

43. Scarr D, Lovblom LE, Ostrovski I, Kelly D, Wu T, Farooqi MA, et al. Agreement between automated and manual quantification of corneal nerve fiber length: Implications for diabetic neuropathy research. *J Diabetes Complications*. (2017) 31:1066–73. doi: 10.1016/j.jdiacomp.2016.07.024

44. Levy O, Labbé A, Borderie V, Hamiche T, Dupas B, Laroche L, et al. Increased corneal sub-basal nerve density in patients with Sjögren syndrome treated with topical cyclosporine A. *Clin Exp Ophthalmol*. (2017) 45:455–63. doi: 10.1111/ceo.12898

45. Alam U, Jeziorska M, Petropoulos IN, Asghar O, Fadavi H, Ponirakis G, et al. Diagnostic utility of corneal confocal microscopy and intra-epidermal nerve fibre density in diabetic neuropathy. *PLoS ONE*. (2017) 12:e0180175. doi: 10.1371/journal.pone.0180175

46. Semeraro F, Forbice E, Nascimbeni G, Taglietti M, Romano V, Guerra G, et al. Effect of Autologous Serum Eye Drops in Patients with Sjögren Syndrome-related Dry Eye: Clinical and In Vivo Confocal Microscopy Evaluation of the Ocular Surface. *In Vivo*. (2016) 30:931–8. doi: 10.21873/invivo.11016

47. McNamara NA, Ge S, Lee SM, Enghauser AM, Kuehl L, Chen FY, et al. Reduced Levels of Tear Lacritin Are Associated With Corneal Neuropathy in Patients With the Ocular Component of Sjögren's Syndrome. *Invest Ophthalmol Vis Sci*. (2016) 57:5237–43. doi: 10.1167/iovs.16-19309

48. Misra SL, Craig JP, Patel DV, McGhee CN, Pradhan M, Ellyett K, et al. In vivo confocal microscopy of corneal nerves: an ocular biomarker for peripheral and cardiac autonomic neuropathy in type 1 diabetes mellitus. *Invest Ophthalmol Vis Sci*. (2015) 56:5060–5. doi: 10.1167/iovs.15-16711

49. Kocabeyoglu S, Mocan MC, Cevik Y, Irkec M. Ocular Surface Alterations and In Vivo Confocal Microscopic Features of Corneas in Patients With Newly Diagnosed Graves' Disease. *Cornea*. (2015) 34:745–9. doi: 10.1097/ICO.0000000000000426

50. Chen X, Graham J, Dabbah MA, Petropoulos IN, Ponirakis G, Asghar O, et al. Small nerve fiber quantification in the diagnosis of diabetic sensorimotor polyneuropathy: comparing corneal confocal microscopy with intraepidermal nerve fiber density. *Diabetes Care*. (2015) 38:1138–44. doi: 10.2337/dc14-2422

51. Stem MS, Hussain M, Lentz SI, Raval N, Gardner TW, Pop-Busui R, et al. Differential reduction in corneal nerve fiber length in patients with type 1 or type 2 diabetes mellitus. *J Diabetes Complications*. (2014) 28:658–61. doi: 10.1016/j.jdiacomp.2014.06.007

52. Pritchard N, Edwards K, Dehghani C, Fadavi H, Jeziorska M, Marshall A, et al. Longitudinal assessment of neuropathy in type 1 diabetes using novel ophthalmic markers (LANDMark): study design and baseline characteristics. *Diabetes Res Clin Pract*. (2014) 104:248–56. doi: 10.1016/j.diabres.2014.02.011

53. Villani E, Magnani F, Viola F, Santaniello A, Scorza R, Nucci P, et al. In vivo confocal evaluation of the ocular surface morpho-functional unit in dry eye. *Optom Vis Sci*. (2013) 90:576–86. doi: 10.1097/OPX.0b013e318294c184

54. Ahmed A, Bril V, Orszag A, Paulson J, Yeung E, Ngo M, et al. Detection of diabetic sensorimotor polyneuropathy by corneal confocal microscopy in type 1 diabetes: a concurrent validity study. *Diabetes Care*. (2012) 35:821–8. doi: 10.2337/dc11-1396

55. Hertz P, Bril V, Orszag A, Ahmed A, Ng E, Nwe P, et al. Reproducibility of in vivo corneal confocal microscopy as a novel screening test for early diabetic sensorimotor polyneuropathy. *Diabet Med*. (2011) 28:1253–60. doi: 10.1111/j.1464-5491.2011.03299.x

56. Chen Q, Zhang X, Cui L, Huang Q, Chen W, Ma H, et al. Upper and lower tear menisci in Sjögren's syndrome dry eye. *Invest Ophthalmol Vis Sci*. (2011) 52:9373–8. doi: 10.1167/iovs.11-7431

57. Tuisku IS, Konttinen YT, Konttinen LM, Tervo TM. Alterations in corneal sensitivity and nerve morphology in patients with primary Sjögren's syndrome. *Exp Eye Res*. (2008) 86:879–85. doi: 10.1016/j.exer.2008.03.002

58. Villani E, Galimberti D, Viola F, Mapelli C, Ratiglia R. The cornea in Sjogren's syndrome: an in vivo confocal study. *Invest Ophthalmol Vis Sci*. (2007) 48:2017–22. doi: 10.1167/iovs.06-1129

59. Benítez-Del-Castillo JM, Acosta MC, Wassfi MA, Díaz-Valle D, Gegúndez JA, Fernandez C, et al. Relation between corneal innervation with confocal microscopy and corneal sensitivity with noncontact esthesiometry in patients with dry eye. *Invest Ophthalmol Vis Sci*. (2007) 48:173–81. doi: 10.1167/iovs.06-0127

60. Benítez del Castillo JM, Wasfy MA, Fernandez C, Garcia-Sanchez J. An in vivo confocal masked study on corneal epithelium and subbasal nerves in patients with dry eye. *Invest Ophthalmol Vis Sci.* (2004) 45:3030–5. doi: 10.1167/iovs.04-0251

61. Tuominen IS, Konttinen YT, Vesaluoma MH, Moilanen JA, Helintö M, Tervo TM. Corneal innervation and morphology in primary Sjögren's syndrome. *Invest Ophthalmol Vis Sci.* (2003) 44:2545–9. doi: 10.1167/iovs.02-1260

62. Li F, Zhang Q, Ying X, He J, Jin Y, Xu H, et al. Corneal nerve structure in patients with primary Sjögren's syndrome in China. *BMC Ophthalmol.* (2021) 21:211. doi: 10.1186/s12886-021-01967-7

63. Palomar APD, Montolío A, Cegoñino J, Dhanda SK, Lio CT, Bose T. The Innate Immune Cell Profile of the Cornea Predicts the Onset of Ocular Surface Inflammatory Disorders. *J Clin Med.* (2019) 8:2110. doi: 10.3390/jcm8122110

64. McCluskey P, Powell RJ. The eye in systemic inflammatory diseases. *Lancet.* (2004) 364:2125–33. doi: 10.1016/S0140-6736(04)17554-5

65. Ladas JG, Mondino BJ. Systemic disorders associated with peripheral corneal ulceration. *Curr Opin Ophthalmol.* (2000) 11:468–71. doi: 10.1097/00055735-200012000-00014

66. Messmer EM, Foster CS. Vasculitic peripheral ulcerative keratitis. *Surv Ophthalmol.* (1999) 43:379–96. doi: 10.1016/S0039-6257(98)00051-4

67. Uçeyler N, Kafke W, Riediger N, He L, Necula G, Toyka KV, et al. Elevated proinflammatory cytokine expression in affected skin in small fiber neuropathy. *Neurology.* (2010) 74:1806–13. doi: 10.1212/WNL.0b013e3181e0f7b3

68. Ferreira SH, Lorenzetti BB, Bristow AF, Poole S. Interleukin-1 beta as a potent hyperalgesic agent antagonized by a tripeptide analogue. *Nature.* (1988) 334:698–700. doi: 10.1038/334698a0

69. Cunha FQ, Poole S, Lorenzetti BB, Ferreira SH. The pivotal role of tumour necrosis factor alpha in the development of inflammatory hyperalgesia. *Br J Pharmacol.* (1992) 107:660–4. doi: 10.1111/j.1476-5381.1992.tb14503.x

70. Wang H, Wang PB, Chen T, Zou J, Li YJ, Ran XF, et al. Analysis of clinical characteristics of immune-related dry eye. *J Ophthalmol.* (2017) 2017:8532397. doi: 10.1155/2017/8532397

71. Zhang Z, Hu X, Qi X, Di G, Zhang Y, Wang Q, et al. Resolvin D1 promotes corneal epithelial wound healing and restoration of mechanical sensation in diabetic mice. *Mol Vis.* (2018) 24:274–85.

72. Hou Y, Xin M, Li Q, Wu X. Glycyrrhizin micelle as a genistein nanocarrier: Synergistically promoting corneal epithelial wound healing through blockage of the HMGB1 signaling pathway in diabetic mice. *Exp Eye Res.* (2021) 204:108454. doi: 10.1016/j.exer.2021.108454

73. Tavakoli M, Petropoulos IN, Malik RA. Corneal confocal microscopy to assess diabetic neuropathy: an eye on the foot. *J Diabetes Sci Technol.* (2013) 7:1179–89. doi: 10.1177/193229681300700509

74. Petropoulos IN, Green P, Chan AW, Alam U, Fadavi H, Marshall A, et al. Corneal confocal microscopy detects neuropathy in patients with type 1 diabetes without retinopathy or microalbuminuria. *PLoS ONE.* (2015) 10:e0123517. doi: 10.1371/journal.pone.0123517

75. Stern ME, Gao J, Siemasko KF, Beuerman RW, Pflugfelder SC. The role of the lacrimal functional unit in the pathophysiology of dry eye. *Exp Eye Res.* (2004) 78:409–16. doi: 10.1016/j.exer.2003.09.003

76. Turk MA, Hayworth JL, Nevskaya T, Pope JE. Ocular manifestations in rheumatoid arthritis, connective tissue disease, and vasculitis: a systematic review and metaanalysis. *J Rheumatol.* (2021) 48:25–34. doi: 10.3899/jrheum.190768

77. Palejwala NV, Walia HS, Yeh S. Ocular manifestations of systemic lupus erythematosus: a review of the literature. *Autoimmune Dis.* (2012) 2012:290898. doi: 10.1155/2012/290898

78. Marsovszky L, Resch MD, Németh J, Toldi G, Medgyesi E, Kovács L, et al. In vivo confocal microscopic evaluation of corneal Langerhans cell density, and distribution and evaluation of dry eye in rheumatoid arthritis. *Innate Immun.* (2013) 19:348–54. doi: 10.1177/1753425912461677

79. Roszkowska AM, Licitra C, Tumminello G, Postorino EI, Colonna MR, Aragona P. Corneal nerves in diabetes-The role of the in vivo corneal confocal microscopy of the subbasal nerve plexus in the assessment of peripheral small fiber neuropathy. *Surv Ophthalmol.* (2021) 66:493–513. doi: 10.1016/j.survophthal.2020.09.003

80. Nolano M, Provitera V, Estraneo A, Selim MM, Caporaso G, Stancanelli A, et al. Sensory deficit in Parkinson's disease: evidence of a cutaneous denervation. *Brain.* (2008) 131(Pt 7):1903–11. doi: 10.1093/brain/awn102

81. Kass-Iliyya L, Javed S, Gosal D, Kobylecki C, Marshall A, Petropoulos IN, et al. Small fiber neuropathy in Parkinson's disease: a clinical, pathological and corneal confocal microscopy study. *Parkinsonism Relat Disord.* (2015) 21:1454–60. doi: 10.1016/j.parkreldis.2015.10.019

82. Püttgen S, Bönhof GJ, Strom A, Müssig K, Szendroedi J, Roden M, et al. Augmented corneal nerve fiber branching in painful compared with painless diabetic neuropathy. *J Clin Endocrinol Metab.* (2019) 104:6220–8. doi: 10.1210/jc.2019-01072

83. Tavakoli M, Mitu-Pretorian M, Petropoulos IN, Fadavi H, Asghar O, Alam U, et al. Corneal confocal microscopy detects early nerve regeneration in diabetic neuropathy after simultaneous pancreas and kidney transplantation. *Diabetes.* (2013) 62:254–60. doi: 10.2337/db12-0574

84. Azmi S, Ferdousi M, Petropoulos IN, Ponirakis G, Fadavi H, Tavakoli M, et al. Corneal confocal microscopy shows an improvement in small-fiber neuropathy in subjects with type 1 diabetes on continuous subcutaneous insulin infusion compared with multiple daily injection. *Diabetes Care.* (2015) 38:e3–4. doi: 10.2337/dc14-1698

85. Petropoulos IN, Manzoor T, Morgan P, Fadavi H, Asghar O, Alam U, et al. Repeatability of in vivo corneal confocal microscopy to quantify corneal nerve morphology. *Cornea.* (2013) 32:e83–9. doi: 10.1097/ICO.0b013e3182749419

86. Edwards K, Pritchard N, Vagenas D, Russell A, Malik RA, Efron N. Utility of corneal confocal microscopy for assessing mild diabetic neuropathy: baseline findings of the LANDMark study. *Clin Exp Optom.* (2012) 95:348–54. doi: 10.1111/j.1444-0938.2012.00740.x

87. Terkelsen AJ, Karlsson P, Lauria G, Freeman R, Finnerup NB, Jensen TS. The diagnostic challenge of small fibre neuropathy: clinical presentations, evaluations, and causes. *Lancet Neurol.* (2017) 16:934–44. doi: 10.1016/S1474-4422(17)30329-0

88. Ishibashi F, Kojima R, Taniguchi M, Kosaka A, Uetake H, Tavakoli M. The Expanded Bead Size of Corneal C-Nerve Fibers Visualized by Corneal Confocal Microscopy Is Associated with Slow Conduction Velocity of the Peripheral Nerves in Patients with Type 2 Diabetes Mellitus. *J Diabetes Res.* (2016) 2016:3653459. doi: 10.1155/2016/3653459

89. Martone G, Frezzotti P, Tosi GM, Traversi C, Mittica V, Malandrini A, et al. An in vivo confocal microscopy analysis of effects of topical antiglaucoma therapy with preservative on corneal innervation and morphology. *Am J Ophthalmol.* (2009) 147:725–35.e1. doi: 10.1016/j.ajo.2008.10.019

90. Scarpa F, Colonna A, Ruggeri A. Multiple-image deep learning analysis for neuropathy detection in corneal nerve images. *Cornea.* (2020) 39:342–7. doi: 10.1097/ICO.0000000000002181

91. Kim J, Markoulli M. Automatic analysis of corneal nerves imaged using in vivo confocal microscopy. *Clin Exp Optom.* (2018) 101:147–61. doi: 10.1111/cxo.12640

92. Scarpa F, Zheng X, Ohashi Y, Ruggeri A. Automatic evaluation of corneal nerve tortuosity in images from in vivo confocal microscopy. *Invest Ophthalmol Vis Sci.* (2011) 52:6404–8. doi: 10.1167/iovs.11-7529

93. Zhang M, Chen J, Luo L, Xiao Q, Sun M, Liu Z. Altered corneal nerves in aqueous tear deficiency viewed by in vivo confocal microscopy. *Cornea.* (2005) 24:818–24. doi: 10.1097/01.ico.0000154402.01710.95

94. Erie JC, McLaren JW, Hodge DO, Bourne WM. The effect of age on the corneal subbasal nerve plexus. *Cornea.* (2005) 24:705–9. doi: 10.1097/01.ico.0000154387.51355.39

95. Patel DV, McGhee CN. In vivo confocal microscopy of human corneal nerves in health, in ocular and systemic disease, and following corneal surgery: a review. *Br J Ophthalmol.* (2009) 93:853–60. doi: 10.1136/bjo.2008.150615

96. Patel DV, Ku JY, Johnson R, McGhee CN. Laser scanning in vivo confocal microscopy and quantitative aesthesiometry reveal decreased corneal innervation and sensation in keratoconus. *Eye (Lond).* (2009) 23:586–92. doi: 10.1038/eye.2008.52

97. Patel DV, McGhee CN. Quantitative analysis of in vivo confocal microscopy images: a review. *Surv Ophthalmol.* (2013) 58:466–75. doi: 10.1016/j.survophthal.2012.12.003

98. Vagenas D, Pritchard N, Edwards K, Shahidi AM, Sampson GP, Russell AW, et al. Optimal image sample size for corneal nerve morphometry. *Optom Vis Sci.* (2012) 89:812–7. doi: 10.1097/OPX.0b013e31824ee8c9

99. Roszkowska AM, Wylegała A, Gargano R, Spinella R, Inferrera L, Orzechowska-Wylegała B, et al. Impact of corneal parameters, refractive error and age on density and morphology of the subbasal nerve plexus fibers in healthy adults. *Sci Rep.* (2021) 11:6076. doi: 10.1038/s41598-021-85597-5

100. Guthoff RF, Zhivov A, Stachs O. In vivo confocal microscopy, an inner vision of the cornea - a major review. *Clin Exp Ophthalmol.* (2009) 37:100–17. doi: 10.1111/j.1442-9071.2009.02016.x

101. Erie EA, McLaren JW, Kittleson KM, Patel SV, Erie JC, Bourne WM. Corneal subbasal nerve density: a comparison of two confocal microscopes. *Eye Contact Lens.* (2008) 34:322–5. doi: 10.1097/ICL.0b013e31818 b74f4

102. Baltrusch S. Confocal microscope examination of the corneal nerve plexus as biomarker for systemic diseases : View from the corneal nerve plexus on diabetes mellitus disease. *Ophthalmologe.* (2017) 114:592–600. doi: 10.1007/s00347-017-0 480-4

103. Petroll WM, Robertson DM. In Vivo Confocal Microscopy of the Cornea: New Developments in Image Acquisition, Reconstruction, and Analysis Using the HRT-Rostock Corneal Module. *Ocul Surf.* (2015) 13:187–203. doi: 10.1016/j.jtos.2015.05.002

Publisher's Note: All claims expressed in this article are solely those of the authors and do not necessarily represent those of their affiliated organizations, or those of the publisher, the editors and the reviewers. Any product that may be evaluated in this article, or claim that may be made by its manufacturer, is not guaranteed or endorsed by the publisher.

Check for updates

Case Report: A Neuro-Ophthalmological Assessment of Vision Loss in a Pediatric Case of McCune-Albright Syndrome

Jordan D. Lemme[1], Anthony Tucker-Bartley[1,2], Laura A. Drubach[3], Nehal Shah[4], Laura Romo[5], Mariesa Cay[1], Stephan Voss[3], Neha Kwatra[3], Leonard B. Kaban[6], Adam S. Hassan[7], Alison M. Boyce[8] and Jaymin Upadhyay[1,9]*

[1] Department of Anesthesiology, Critical Care and Pain Medicine, Boston Children's Hospital and Harvard Medical School, Boston, MA, United States, [2] Department of Anesthesiology, Critical Care and Pain Medicine, Massachusetts General Hospital and Harvard Medical School, Boston, MA, United States, [3] Department of Radiology, Boston Children's Hospital, Hospital and Harvard School, Boston, MA, United States, [4] Department of Radiology, Brigham and Women's Hospital, Hospital and Harvard School, Boston, MA, United States, [5] Head and Neck Imaging, Department of Radiology, Massachusetts Eye and Ear and Harvard Medical School, Boston, MA, United States, [6] Department of Oral & Maxillofacial Surgery, Massachusetts General Hospital, Harvard School of Dental Medicine, Boston, MA, United States, [7] Eye Plastic and Facial Cosmetic Surgery, Grand Rapids, MI, United States, [8] Metabolic Bone Disorders Unit, National Institute of Dental and Craniofacial Research, National Institutes of Health, Bethesda, MD, United States, [9] Department of Psychiatry, McLean Hospital and Harvard Medical School, Belmont, MA, United States

Patients diagnosed with McCune-Albright Syndrome (MAS) frequently manifest craniofacial fibrous dysplasia (FD). Craniofacial FD can impinge nerve fibers causing visual loss as well as craniofacial pain. Surgical decompression of affected nerves is performed, with variable efficacy, in an attempt to restore function or alleviate symptoms. Here, we present a case of a 12-year-old MAS patient with visual deficits, particularly in the left eye (confirmed by enlarged blind spots on Goldmann visual field testing), and craniofacial pain. Decompression surgery of the left optic nerve mildly improved vision, while persistent visual deficits were noted at a 3-month follow-up assessment. An in-depth, imaging-based evaluation of the visual system, including the retinal nerve fiber layer, optic nerves, and central nervous system (CNS) visual pathways, revealed multiple abnormalities throughout the visual processing stream. In the current FD/MAS patient, a loss of white matter fiber density within the left optic radiation and functional changes involving the left primary visual cortex were observed. Aberrant structural and functional abnormalities embedded within central visual pathways may play a role in facilitating deficits in vision in FD/MAS and contribute to the variable outcome following peripheral nerve decompression surgery.

Keywords: McCune-Albright Syndrome, craniofacial lesions, vision loss, headache, central nervous system

INTRODUCTION

Fibrous dysplasia (FD) is a rare, non-inherited bone disease arising from a R201 missense mutation of the *GNAS* gene (1–3). A key pathological feature of FD includes the formation of bony lesions within a single bone (monostotic FD) or multiple bones (polyostotic FD) (4–6). Skeletal disease may occur in isolation or in conjunction with endocrinopathies and hyperpigmented macules, termed

McCune-Albright Syndrome (MAS). FD lesions readily pervade the axial-appendicular skeleton and craniofacial structures, with the latter frequently leading to craniofacial nerve compression, neuropathy, and vision loss (7–12).

Symptomatic patients with evidence of optic nerve impingement often undergo decompression surgery, yet there is variable efficacy of the procedure in terms of improving or preserving vision (13–16). Moreover, decompression surgery may cause thermal and ischemic injury to the optic nerve, resulting in neuropathy (17). We hypothesized that factors outside of isolated optic nerve impingement may facilitate visual impairment in FD/MAS patients, including those embedded within the central nervous system (CNS). To date, however, the visual processing pathways in the CNS remain unexplored in FD/MAS. We further hypothesized that in FD/MAS, the use of advanced imaging techniques that allow for characterization of CNS white matter pathways (i.e., optic radiation) and visual cortex function in parallel would provide an improved understanding of how visual deficits and, by extension, other neurological phenotypes are generated. Here, we present a pediatric MAS patient with craniofacial FD and a history of bilateral visual deficits, craniofacial pain, and headaches. In this patient, optic nerve decompression surgery in the left hemisphere improved but did not fully correct his visual deficits. To investigate the abnormalities in the visual pathway, from the retinal nerve fiber layer (RNFL) to the visual cortex, the current MAS patient was evaluated using a combination of (i) ^{18}F-sodium fluoride positron emission tomography/computed tomography (^{18}F-NaF PET/CT), (ii) optic coherence tomography (OCT), (iii) non-contrast, magnetic resonance imaging (MRI) of peripheral nerves, and (iv) functional and structural MRI of the CNS. This unique case and a multimodal approach provide insights into the effects of craniofacial FD on a developing biological system in addition to the complex pathophysiology of the associated neurological signs and symptoms. This report points to the importance of using a multimodal approach as early as possible upon diagnosis of pediatric FD/MAS.

PATIENT OVERVIEW

A 12-year-old boy with MAS and craniofacial FD presented with worsening vision. He was diagnosed with MAS at age 8. At age 10, the patient developed visual complaints including blurry vision and decreased acuity, particularly in the left eye, which worsened over the subsequent 2 years. Functional evaluation performed with Goldmann visual field testing revealed enlarged blind spots bilaterally, with a more significant effect for the left eye than the right. Of note, he also developed bilateral chronic tension type headache pain covering regions above the eye and the posterior surface of the external ear. At age 12, visual acuity testing showed 20/70 vision and 20/100 in the right and left eye, respectively. Color testing with Ishihara was 1/11 and 0/11 in the right and left eye, respectively. OCT showed declining RNFL starting at age 10 (see **Supplemental Information**).

Due to concerns of declining visual acuity, the patient underwent a left orbital decompression surgery (performed by ASH) at age 12 years. The surgical procedure relieved pressure on the left optic nerve by removing a portion of the left lateral orbital

wall and opening the periosteum allowing for orbital fat and the lateral rectus muscle to prolapse into the newly created space. Conservative bone removal was performed in order to reduce the likelihood of the patient developing enophthalmos. The patient had an unremarkable post-operative course. Post-operatively his vision improved to 20/40 and 20/50 in the right and left eyes, respectively, while color testing was 1/11 in both eyes. Improvements in vision were reported by the patient following surgery, but with sustained visual deficits. 3 months after the surgery, the patient presented for a multidisciplinary study of FD/MAS consisting of behavioral testing, imaging, and clinical evaluation. This study was approved by the Boston Children's Hospital and the Massachusetts General Brigham, Institutional Review Boards. The patient and patient's legal guardian provided informed consent.

Craniofacial Pain Evaluation

At post-surgery evaluation, his craniofacial pain and headache was described as burning, shooting, stabbing, or cramping and was often triggered by bright lights, psychological stress, or physical exertion. Craniofacial pain varied between 2 and 4 on a 0–10 scale and over a one-week period. Quantitative sensory testing (QST) revealed higher cold pain threshold and tolerance temperatures in the left relative to the right craniofacial regions, specifically the V2 and V3 distribution of the trigeminal system, suggesting more cold pain sensitivity in the left hemisphere. Further details on QST procedures and findings have been provided in **Supplemental Information**.
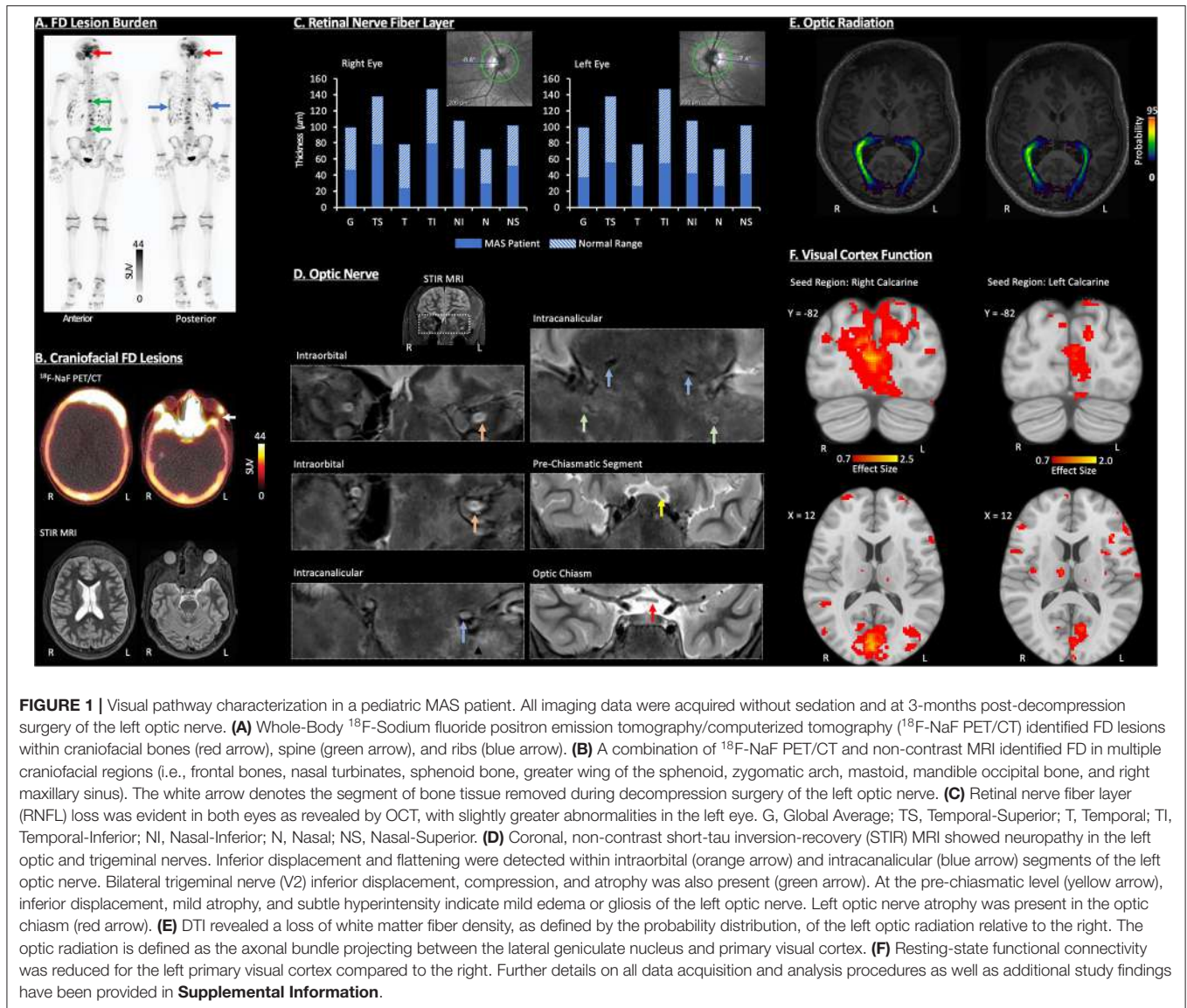
Craniofacial FD Burden

^{18}F-NaF PET/CT was performed to characterize FD lesion burden and activity (**Figures 1A,B**). There were multiple intense foci of uptake within the skull and facial bones associated with ground-glass CT abnormalities of FD, including the frontal bone, occipital bone, right maxillary sinus, nasal turbinates, clivus, bilateral sphenoid bone, right zygomatic arch, left mastoid bone, and mandible. Furthermore, acquisition of multisequence and multiplanar, non-contrast magnetic resonance imaging (MRI) data further defined the distribution of craniofacial FD and revealed inter- and intra-lesion heterogeneity in terms of fluid content, volume, and disruption of cranial nerves (**Figure 1B**).

RNFL

OCT was performed and compared to previous studies prior to surgery (**Figure 1C**). Following the patient's initial decline in RNFL thicknesses, at 3 months post-surgery, levels (global mean and individual quadrants) remained within the 1% thickness percentiles of the reference database. Overall, reduction in RNFL was evident in right and left eyes with, sub-regions of the temporal RNFL (i.e., Temporal-Inferior) showing more involvement in the left vs. right.

Optic Nerve and Optic Radiation

The condition of the optic nerve and V2 division of the trigeminal system were primarily evaluated using STIR MRI (**Figure 1D**). At the intraorbital and intracanalicular levels, an abnormal inferior displacement of the left optic nerve was observed, and as compared to the right optic nerve, the left optic nerve was

FIGURE 1 | Visual pathway characterization in a pediatric MAS patient. All imaging data were acquired without sedation and at 3-months post-decompression surgery of the left optic nerve. **(A)** Whole-Body ^{18}F-Sodium fluoride positron emission tomography/computerized tomography (^{18}F-NaF PET/CT) identified FD lesions within craniofacial bones (red arrow), spine (green arrow), and ribs (blue arrow). **(B)** A combination of ^{18}F-NaF PET/CT and non-contrast MRI identified FD in multiple craniofacial regions (i.e., frontal bones, nasal turbinates, sphenoid bone, greater wing of the sphenoid, zygomatic arch, mastoid, mandible occipital bone, and right maxillary sinus). The white arrow denotes the segment of bone tissue removed during decompression surgery of the left optic nerve. **(C)** Retinal nerve fiber layer (RNFL) loss was evident in both eyes as revealed by OCT, with slightly greater abnormalities in the left eye. G, Global Average; TS, Temporal-Superior; T, Temporal; TI, Temporal-Inferior; NI, Nasal-Inferior; N, Nasal; NS, Nasal-Superior. **(D)** Coronal, non-contrast short-tau inversion-recovery (STIR) MRI showed neuropathy in the left optic and trigeminal nerves. Inferior displacement and flattening were detected within intraorbital (orange arrow) and intracanalicular (blue arrow) segments of the left optic nerve. Bilateral trigeminal nerve (V2) inferior displacement, compression, and atrophy was also present (green arrow). At the pre-chiasmatic level (yellow arrow), inferior displacement, mild atrophy, and subtle hyperintensity indicate mild edema or gliosis of the left optic nerve. Left optic nerve atrophy was present in the optic chiasm (red arrow). **(E)** DTI revealed a loss of white matter fiber density, as defined by the probability distribution, of the left optic radiation relative to the right. The optic radiation is defined as the axonal bundle projecting between the lateral geniculate nucleus and primary visual cortex. **(F)** Resting-state functional connectivity was reduced for the left primary visual cortex compared to the right. Further details on all data acquisition and analysis procedures as well as additional study findings have been provided in **Supplemental Information**.

flattened, with partial effacement of the normal T2 hyperintense cerebral spinal fluid (CSF) signal within the optic nerve sheath. Intracanalicular segments of both optic nerves and V2 trigeminal nerves through foramen rotundum, showed complete effacement of the normal T2 hyperintense CSF signal along both optic nerves. There was also moderate narrowing and compression of the foramen rotundum bilaterally with atrophy of the V2 divisions of both trigeminal nerves. The pre-chiasmatic segments of both optic nerves showed a relatively smaller, inferiorly displaced left optic nerve with mild intrinsic T2 hyperintensity consistent with relative atrophy and gliosis of the left optic nerve as compared to the right. The optic chiasm showed a slightly smaller left optic nerve compared to the right consistent with left sided optic nerve atrophy.

Diffusion tensor imaging (DTI) and probabilistic tractography were performed to map the right and left optic radiation (**Figure 1E**). The probability density, a measure of white matter

fiber density, was lower in the left optic radiation relative to the right, especially as the optic radiation nears the primary visual cortex.

Visual Cortex Function

Functional connectivity of resting state functional MRI data was performed to evaluate primary visual cortex function (**Figure 1F**). In this patient, seed (right or left calcarine cortex) to voxel connectivity analysis revealed more robust connectivity for the right calcarine cortex (5,212 voxels; maximum effect size = 2.5) compared to the left calcarine cortex (1,385 voxels; maximum effect size = 2.0). The loss of functional connectivity involving the left hemisphere visual cortex reflects functional disturbance or perhaps reorganization within central visual pathways in the current MAS patient.

DISCUSSION

Vision loss in patients with FD/MAS is likely driven by multiple neuro-ophthalmological abnormalities and cannot be explained purely by physical optic nerve compression alone (18–20). While several case reports note improved visual function following decompression surgery (8, 9, 21), other patients with craniofacial FD fail to experience a substantial benefit (22, 23). Lastly, patients may note improved visual function without surgical decompression (24).

In many cases, the primary objective of incorporating cranial imaging in patients with FD/MAS with vison loss is to define the extent of craniofacial lesions or lesion burden, and determine whether FD structurally alters optic nerves. The impact of craniofacial FD lesions can have an affect along multiple points along the visual processing stream including those portions residing in the CNS. Here, white matter changes particularly those localized to the left optic radiation and likely maladaptive plasticity anchored within the primary visual cortex are believed to work in concert with upstream, optic nerve and RNFL abnormalities to produce the full array of visual deficits. Moreover, we hypothesize that for the current MAS patient, the impact of the craniofacial FD lesions on the left eye temporal retina as shown on OCT and downstream optic pathway (i.e., left optic radiation) alterations contributed to vision loss (see **Supplemental Information**). A more detailed and necessary determination of the underlying neurobiological changes causing left or right hemisphere anopia may be obtained with retinotopic mapping. A further limitation of the current study is indeed the absence of pre- *and* post-surgical DTI and fMRI datasets. With the availability of multi-timepoint neuroimaging assessments, the associations and interactions among peripheral and central visual system changes in cases of craniofacial FD could be better ascertained. The current results now provide the rationale for longitudinally incorporating DTI- and fMRI in FD/MAS studies alongside more conventional imaging methods (i.e., OCT and structural MRI of craniofacial structures) and behavioral testing of visual function. This report also details the course of a single individual with MAS; therefore, additional studies in larger and more heterogeneous populations are required to determine the generalizability of these results.

The presence of structural and functional changes between the RNFL and visual cortex may underpin vision loss either before or after decompression surgery, and relatedly the variable outcomes following surgical intervention. Moreover, while further investigation is required, the impact of craniofacial lesions on visual pathways may be unique in pediatric cases considering involvement of a developing neurobiological system. Even a mild level of FD may lead to more severe signs and symptoms, yet early and careful intervention combined with inherent neurobiological plasticity of a maturing system may facilitate better long-term outcome.

A multimodal, imaging-based assessment of the collective visual apparatus including the optic nerve, but also the orbit, RNFL, visual tracts, and the visual cortex provides an opportunity to objectively characterize the visual system and identify abnormalities that drive vision loss in FD/MAS. This complementary approach may be particularly informative when the level of patient reported visual deficit is discordant with the severity of objective FD craniofacial lesions or optic nerve compression. This strategy may be ideal to employ when there is a need to more accurately pinpoint causes of vison loss either before or after decompression surgery. Furthermore, persistent extra-skeletal abnormalities may in part explain the frequent failure of decompression surgery in alleviating visual deficits in FD; however, much work remains to thoroughly explore this perspective.

DATA AVAILABILITY STATEMENT

The original contributions presented in the study are included in the article/**Supplementary Material**, further inquiries can be directed to the corresponding author.

ETHICS STATEMENT

The studies involving human participants were reviewed and approved by Boston Children's Hospital Institutional Review Board. Written informed consent to participate in this study was provided by the participant's legal guardian/next of kin.

AUTHOR CONTRIBUTIONS

JL, AT-B, and MC analyzed data, drafted the initial manuscript, and reviewed and revised the manuscript. LD, NS, LR, SV, and NK designed the study, acquired and analyzed data, and reviewed and revised the manuscript. LK reviewed and revised the manuscript. AH provide patient care, acquired and analyzed data, drafted the initial manuscript, and reviewed and revised the manuscript. AB designed the study, analyzed data, drafted the initial manuscript, and reviewed and revised the manuscript. JU designed the study, acquired and analyzed data, drafted the initial manuscript, and reviewed and revised the manuscript. All authors approved the final manuscript as submitted and agree to be accountable for all aspects of the work.

FUNDING

ACKNOWLEDGMENTS

SUPPLEMENTARY MATERIAL

The Supplementary Material for this article can be found online at: https://www.frontiersin.org/articles/10.3389/fmed.2022.857079/full#supplementary-material

REFERENCES

1. Boyce AM, Florenzano P, de Castro LF, Collins MT. Fibrous Dysplasia/McCune-Albright Syndrome, In: Adam MP, Ardinger HH, Pagon RA, Wallace SE, Bean LJH, Stephens K, et al. (Eds.), Seattle (WA):GeneReviews((R)) (1993).

2. Riminucci M, Liu B, Corsi A, Shenker A, Spiegel AM, Robey PG, et al. The histopathology of fibrous dysplasia of bone in patients with activating mutations of the Gs alpha gene: site-specific patterns and recurrent histological hallmarks. *J Pathol.* (1999) 187:249–58. doi: 10.1002/(SICI)1096-9896(199901)187:2<249::AID-PATH222>3.0. CO;2-J

3. Ramaswamy G, Kim H, Zhang D, Lounev V, Wu JY, Choi Y, et al. Gsalpha controls cortical bone quality by regulating osteoclast differentiation via cAMP/PKA and beta-catenin pathways. *Sci Rep.* (2017) 7:45140. doi: 10.1038/srep45140

4. Tucker-Bartley A, Lemme J, Gomez-Morad A, Shah N, Veliu MF, et al. Upadhyay, pain phenotypes in rare musculoskeletal and neuromuscular diseases. *Neurosci Biobehav Rev.* (2021) 124:267Biob doi: 10.1016/j.neubiorev.2021.02.009

5. Hartley I, Zhadina M, Collins MT, Boyce AM. Fibrous dysplasia of bone and mccune-albright syndrome: a bench to bedside review. *Calcif Tissue Int.* (2019) 104:517–29. doi: 10.1007/s00223-019-00550-z

6. Robinson C, Collins MT, Boyce AM. Fibrous dysplasia/mccune-albright syndrome: clinical and translational perspectives. *Curr Osteoporos Rep.* (2016) 14:178–86. doi: 10.1007/s11914-016-0317-0

7. Hu AC, Lee CJ, Hsu FPK, Vyas RM. Extensive polyostotic craniofacial fibrous dysplasia with optic nerve impingement, *J Craniofac Surg.* (2021) 32:e435–7. doi: 10.1097/SCS.0000000000007241

8. Bland LI, Marchese MJ, McDonald JV. Acute monocular blindness secondary to fibrous dysplasia of the skull: a case report. *Ann Ophthalmol.* (1992) 24:263–6.

9. Papadopoulos MC, Casey AT, Powell M. Craniofacial fibrous dysplasia complicated by acute, reversible visual loss: report of two cases. *Br J Neurosurg.* 12 (1998):159–61. doi: 10.1080/02688699845320

10. Utriainen P, Valta H, Bjornsdottir S, Makitie OE. Horemuzova, polyostotic fibrous dysplasia with and without mccune-albright syndrome-clinical features in a nordic pediatric cohort. *Front Endocrinol (Lausanne).* (2018) 9:96. doi: 10.3389/fendo.2018.00096

11. Sarihan F, Kasius KM. Teaching neuroimages: craniofacial fibrous dysplasia: loss of vision after head trauma. *Neurology.* (2017) 89:e236–7. doi: 10.1212/WNL.0000000000 004625

12. Kim D, Wysong A, Lai J, Alcorn DM, Benjamin LT. Sudden onset vision loss in an 8-year-old female with McCune-Albright syndrome. *Pediatr Dermatol.* (2014) 31:80–2. doi: 10.1111/j.1525-1470.2012. 01800.x

13. Seiff SR. Optic nerve decompression in fibrous dysplasia: indications, efficacy, and safety. *Plast Reconstr Surg.* (1997) 100:1611–2. doi: 10.1097/00006534-199711000-00045

14. Chen YR, Breidahl A, Chang CN. Optic nerve decompression in fibrous dysplasia: indications, efficacy, and safety. *Plast Reconstr Surg.* (1997) 99:22–30. doi: 10.1097/00006534-199701000-00004

15. Katz BJ, Nerad JA. Ophthalmic manifestations of fibrous dysplasia: a disease of children and adults. *Ophthalmology.* (1998) 105:2207–15. doi: 10.1016/S0161-6420(98)91217-9

16. Gabbay JS, Yuan JT, Andrews BT, Kawamoto HK, Bradley JP. Fibrous dysplasia of the zygomaticomaxillary region: outcomes of surgical intervention. *Plast Reconstr Surg.* (2013) 13:1329–38. doi: 10.1097/PRS.0b013e31828bd70c

17. Shaw ML, Kelley B, Camarata P, Sokol JA. Collateral damage: heat transfer as a possible mechanism of optic nerve injury during neurosurgical intervention. *Ophthalmic Plast Reconstr Surg.* (2012) 28:328–30. doi: 10.1097/IOP.0b013e31825 ca5b2

18. Michael CB, Lee AG, Patrinely JR, Stal S, Blacklock JB. Visual loss associated with fibrous dysplasia of the anterior skull base. Case report and review of the literature. *J Neurosurg.* (2000) 92:350–4. doi: 10.3171/jns.2000.92. s2.0350

19. Pan KS, FitzGibbon EJ, Vitale S, Lee JS, Collins MT, Boyce SM. Utility of optical coherence tomography in the diagnosis and management of optic neuropathy in patients with fibrous dysplasia. *J Bone Miner Res.* (2020) 35:2199–210. doi: 10.1002/jbm r.4129

20. Weisman JS, Hepler RS, Vinters HV. Reversible visual loss caused by fibrous dysplasia. *Am J Ophthalmol.* (1990) 110:244–9. doi: 10.1016/S0002-9394(14)76338-X

21. Lin CG, Wells Porrmann J, Paz M, Moshel YA, LeBenger J, Benitez RP. Organized hematoma of the sphenoid sinus with acute blindness: insight into pathogenesis of disease. *Ear Nose Throat J.* (2020) 99:605–9. doi: 10.1177/0145561320941959

22. Cutler CM, Lee JS, Butman JA, FitzGibbon EJ, Kelly MH, Brillante BA, et al. Long-term outcome of optic nerve encasement and optic nerve decompression in patients with fibrous dysplasia: risk factors for blindness and safety of observation. *Neurosurgery.* (2006) 59:1011–7. doi: 10.1227/01.NEU.0000254440.02736.E3

23. Lee JS, FitzGibbon E, Butman JA, Dufresne CR, Kushner H, Wientroub S, et al. Normal vision despite narrowing of the optic canal in fibrous dysplasia. *N Engl J Med.* (2002) 347:1670–6. doi: 10.1056/NEJMoa020742

24. Messaoud R, Zaouali S, Ladjimi A, Ben Yahia S, Jenzeri S, Hmidi K, et al. Compressive optic neuropathy caused by fibrous dysplasia. *J Fr Ophthalmol.* (2003) 26:631–6.

Publisher's Note: All claims expressed in this article are solely those of the authors and do not necessarily represent those of their affiliated organizations, or those of the publisher, the editors and the reviewers. Any product that may be evaluated in this article, or claim that may be made by its manufacturer, is not guaranteed or endorsed by the publisher.

Check for updates

Case Report: The First Reported Concurrence of Wilson Disease and Bilateral Retinitis Pigmentosa

Zifan Ye [1,2†], Xiuhua Jia [3†], Xin Liu [1,2], Qi Zhang [1,2], Kaijun Wang [1,2] and Min Chen [1,2]*

[1] Eye Center of the 2nd Affiliated Hospital, School of Medicine, Zhejiang University, Hangzhou, China, [2] Zhejiang Provincial Key Lab of Ophthalmology, Hangzhou, China, [3] Department of Ophthalmology, The 3rd Affiliated Hospital of Sun Yat-sen University, Guangzhou, China

Background: Wilson disease (WD) and retinitis pigmentosa (RP) are common genetic disorders in clinical practice, however, the concurrence of WD and RP has never been reported before. WD occurs due to mutations that cause copper metabolic abnormalities; in turn, change in copper metabolism has been suggested to be related with RP. Here, we report the first case of concurrent WD and bilateral RP, and investigate possible pathogenesis to illuminate whether the two genetic disorders are causality or coincidence.

Case Presentation: The patient was a 43-year-old Chinese female diagnosed with WD 12 years ago. She had suffered from night blindness since childhood and faced diminution of bilateral vision within 10 years, for which she was referred to our Eye Center during hospitalization for routine copper excretion treatment. The ceruloplasmin, skull magnetic resonance imaging (MRI), and abdominal ultrasound results accorded with hepatolenticular degeneration. Ocular examinations revealed corneal Kayser-Fleischer (K-F) ring, sunflower-like cataract, retinal osteocyte-like pigmentation, bilateral atrophy of outer retina, cystoid macular edema (CME), and tubular vision in both eyes. Phacoemulsification combined with intraocular lens implantation was performed in the right and left eye, but there was limited improvement in her visual acuity. Whole exome sequencing (WES) detected a deleterious homozygous mutation in the *ATP7B* gene related to WD, and a homozygous mutation in the *CNGA1* gene very likely to cause RP.

Conclusions: We reported the first case of concurrent WD and RP. WES detected two pathogenic gene mutations, *ATP7B* and *CNGA1.* Though we cannot completely rule out a causal effect of WD-related abnormal copper metabolism with RP, we speculate that the two gene mutations lead to the coincidence of the two genetic disorders, respectively.

Keywords: Wilson disease, retinitis pigmentosa, concurrence, gene mutation, abnormal copper metabolism

INTRODUCTION

Wilson disease (WD) is an autosomal-recessive disorder caused by mutations in the *ATP7B* gene, leading to abnormal copper metabolism. *ATP7B* encodes the copper transporter in the reverse Golgi network structure of liver cells, which is indispensable for biliary copper secretion and the synthesis of proceruloplasmin with copper atoms (1). Ceruloplasmin, the synthetic product, is then secreted

into the blood, mediating the transport of excess copper in cytoplasmic vesicles to prolysosomal vesicles and thereby discharging copper into the bile (1). The obstruction of copper excretion results in the accumulation of copper in the circulatory system and organs, especially the liver, central nervous system (CNS), and eyes. The age of WD onset varies from early childhood to young adulthood, though there are cases of late-onset WD (2). Clinical manifestations can differ according to different age groups. For instance, children are more likely to show hepatic symptoms (3), while older patients (15–17 years old and above) present neurological manifestations more often, including dysarthria, gait abnormalities, dystonia, tremor, and Parkinson's disease (4). The typical ocular manifestations of WD include Kayser-Fleischer (K-F) ring and sunflower-like cataract.

In turn, retinitis pigmentosa (RP) is a group of retina-degenerative diseases characterized by progressive degeneration of retinal pigmented epithelium (RPE) and photoreceptors. It affects ∼1 in every 4,000 persons on a global scale (5), making it one of the most common retinal degenerations that contribute to visual impairment in all age groups. There are 69 genes that have been mapped and identified to cause RP so far.[1] Various inheritance patterns have also been connected to RP, including sporadic, autosomal-dominant, autosomal-recessive, X-linked, mitochondrial, and digenic (6). Of these, autosomal-recessive inheritance accounts for ∼50–60% of all RP patients (7). Rod photoreceptor dysfunction is often the first system to occur, followed by injury to the cone photoreceptor cells. Therefore, night blindness, progressive vision loss, tunnel vision, and complete blindness are typical symptoms of RP. Subretinal injection of adeno-associated virus vector, inserting with RPE65 cDNA, may repair this genetic deficiency and may be the only therapy available and approved for RP (8). Whether copper metabolism was associated with RP remains controversial. As early as in 1976, Gahlot et al. reported that RP may be a condition caused by abnormal copper metabolism (9). While in 1978, Marmor et al. argued against a role for copper metabolism in ordinal retinitis pigmentosa (10).

For the first time, we reported a case with the concurrence of WD and bilateral RP in a patient from a consanguineous family. Whole exome sequencing (WES) detected separate gene mutations for the two genetic disorders.

CASE PRESENTATION

A 43-year-old female presented to the Department of Neurology of the Second Affiliated Hospital of Zhejiang University in March 2021. She was diagnosed with WD 12 years ago. Physical examination showed the patient had reduced facial expression and impaired articulation. The patient's left hand mildly trembled when she was asked to raise it flatly. She was also found to have increased extremity muscular tension, upper extremity tendon reflex ++++, and was unable to walk straight. Laboratory tests showed a low ceruloplasmin level (23 mg/L, reference 200–600 mg/L), and no abnormal serum copper concentration was found. Skull MRI showed hepatolenticular degeneration. Abdominal

ultrasound revealed liver cirrhosis and splenomegaly. The patient was hospitalized and given sodium dimercaptopropane sulfonate for copper removal, zinc gluconate to inhibit copper metabolism, and supportive treatment such as amantadine and vitamin C supplements. During hospitalization, the patient complained of progressive bilateral vision decrease over 10 years, for which she was referred to our Eye Center. She volunteered that the night blindness began in early childhood, and her parents were close relatives. Her parents and sister were healthy, denying a similar medical history. The patient's best corrected visual acuity (BCVA) at presentation was 0.8 (logarithm of the minimum angle of resolution, logMAR) in both eyes, and intraocular pressure (Non-contact tonometer, Topcon CT-80, Topcon Corporation, Tokyo, Japan) was 10.0 mmHg in the right eye (OD) and 13.5 mmHg in the left eye (OS), respectively. Slit lamp biomicroscopy (SL-D8Z; Topcon Corporation, Tokyo, Japan) revealed bilateral corneal K-F ring and sunflower-like cataract (**Figure 1A**). Fundus photography (TRC-NW8; Topcon Corporation, Tokyo, Japan) showed thinner retinal blood vessels and retinal osteocyte-like pigmentation in bilateral eyes (**Figure 1B**). Cystoid macular edema (CME) and outer retina atrophy was observed in both eyes via optical coherence tomography (OCT) (**Figure 1C**). Visual field examination (Octopus 900, Haag-Streit, USA) revealed binocular tunnel vision (**Figure 1D**). The patient was subsequently diagnosed with WD combined with binocular RP and complicated cataract.

After informed consent form the patient, phacoemulsification and posterior chamber intraocular lens implantation was performed in the right and left eye, respectively. Postoperatively, topical Tobradex (Tobramycin and Dexamethasone, Alcon) and Pranoprofen (Senju Pharmaceutical Co.Ltd, Japan) eyedrops were prescribed four times a day for anti-inflammatory treatment. Drug therapy for CME was not started before the surgery, and there was no significant change in the central retinal thickness (CRT) of both eyes during the 8-months follow-up. Unfortunately, there was limited improvement in her visual acuity. The BCVA remains 0.8 logMAR for both eyes at her last visit (**Supplementary Figure 1**).

Whole exome sequencing (WES, by Beijing Giantmed medical diagnostics Lab) was performed on the patient and her parents (**Figures 2A–E**). The results showed an *ATP7B* gene c.G2333T: p.R778L homozygous mutation, *CNGA1* gene c.C453A: p.Y151X homozygous mutation, *RP2* gene c.T248C: p.l83T heterozygous mutation, and *SNRNP200* gene c.C1898T: p.A633V heterozygous mutation in the patient (**Supplementary Table 1**). Both parents were heterozygous carriers of *ATP7B* and *CNGA1* genes. The mother was of the *RP2* heterozygous genotype, and the father was of the *SNRNP200* heterozygous genotype, which were both found in the patient. However, the parents did not show any WD or RP-related manifestations.

DISCUSSION

To our knowledge, this is the first report of concurrence of WD and RP in a patient from a consanguineous family. WES detected two separate pathogenic gene mutations: a homozygous
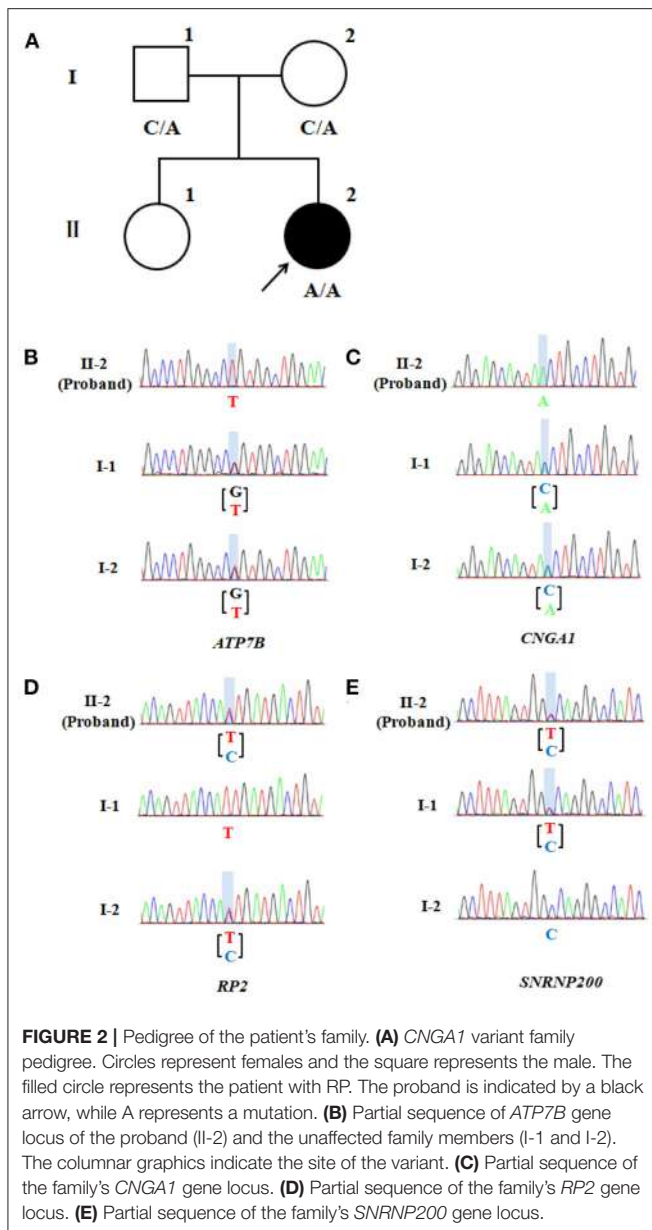
---

[1]RetNet: Summaries (uth.edu).
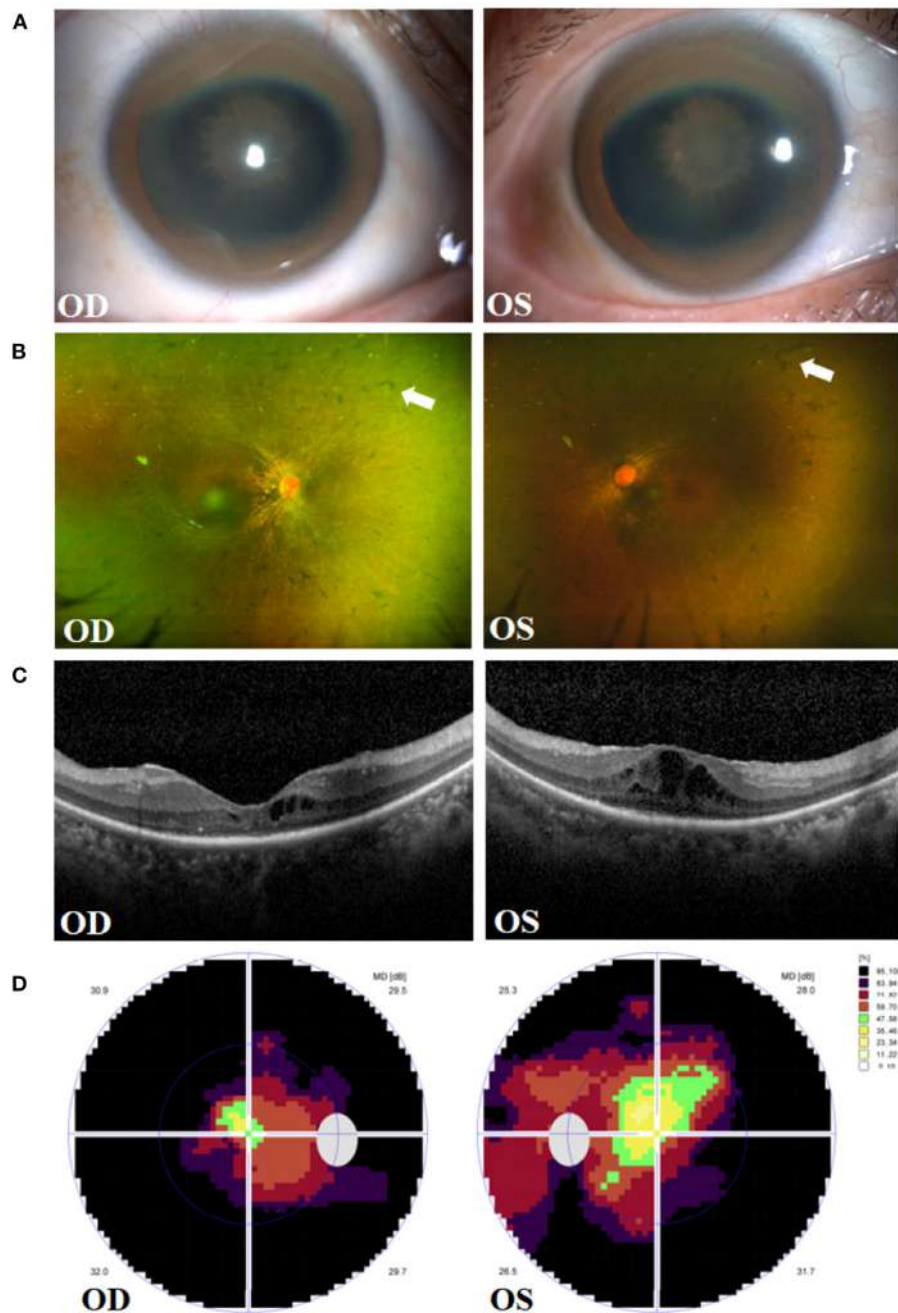
FIGURE 1 | Clinical presentations in the right eye (OD) and left eye (OS) of the patient. **(A)** Manifestation of Kayser-Fleischer (K-F) ring and sunflower-like cataract. **(B)** Fundus images of osteocyte-like pigmentation (white arrows) in bilateral retina. **(C)** Optical coherence tomography (**OCT**) showing outer retina atrophy and cystoid macular edema. **(D)** Vision detection featuring binocular tunnel vision.

mutation in the *ATP7B* gene related to WD, and a homozygous mutation in the *CNGA1* gene associated with RP.

WD is an autosomal-recessive disorder characterized by liver cirrhosis and basal ganglia lesions. Apart from liver and brain, copper also accumulates in other organs, for liver injury is supposed to cause secondary impairment in other tissues. Consequently, the clinical manifestations can include cardiac,

renal, dermatic, osteoarticular or endocrinologic conditions (11). Corneal K-F ring and sunflower-like cataract are common ocular manifestations of WD. K-F ring is formed by copper particles deposited in the Descemet membrane of the corneoscleral junction area which has been observed in ∼98% of patients with neurological WD symptoms and about 50% of patients with hepatic manifestations (12). Sunflower-like cataract is another

FIGURE 2 | Pedigree of the patient's family. **(A)** *CNGA1* variant family pedigree. Circles represent females and the square represents the male. The filled circle represents the patient with RP. The proband is indicated by a black arrow, while A represents a mutation. **(B)** Partial sequence of *ATP7B* gene locus of the proband (II-2) and the unaffected family members (I-1 and I-2). The columnar graphics indicate the site of the variant. **(C)** Partial sequence of the family's *CNGA1* gene locus. **(D)** Partial sequence of the family's *RP2* gene locus. **(E)** Partial sequence of the family's *SNRNP200* gene locus.

FIGURE 3 | Prediction of the protein structure of the *ATP7B(R778L)* mutant expression product.

ocular sign of WD. Compared with typical cataract leading to markedly reduced visual acuity, sunflower-like cataract seems to have a limited impact on vision (13), as it results from reversible copper deposition under the anterior lens capsule and can diminish after copper removal treatment.

Recent researches have pointed out that WD also affect the retina and optic nerve (14, 15). Especially in those patients who have obvious lesions in CNS, thickness of RNFL is found to have decreased, as is the macular thickness (16). Interestingly, disease duration and forms of neurological or hepatic manifestations do not influence RNFL thickness (17). In addition, the thickness of macula is discovered to get markedly thinner in the inferior quadrant (14). Therefore, retinal degeneration in WD is
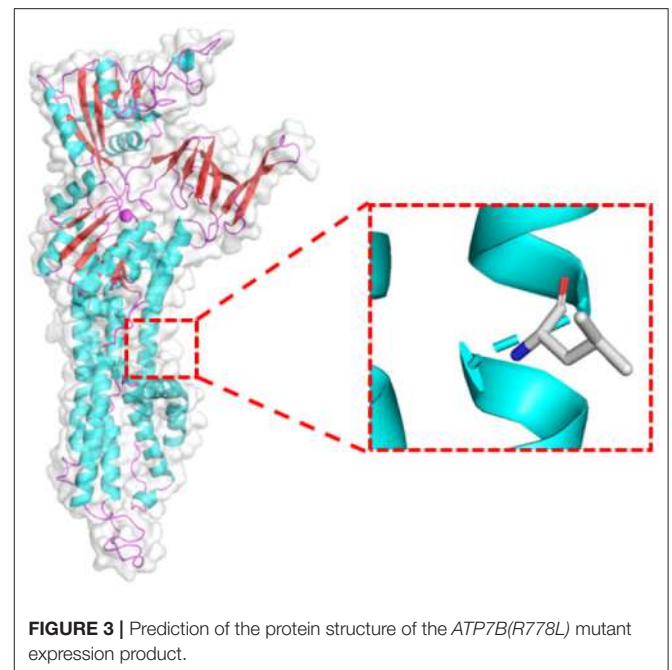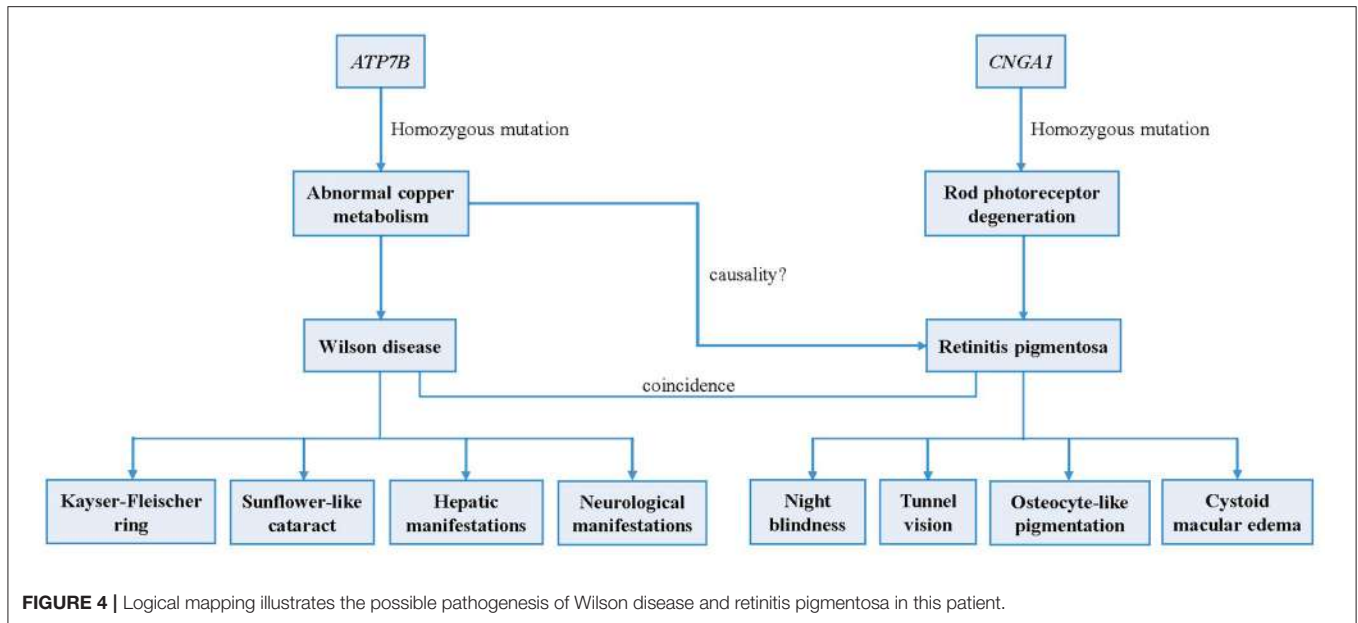
considered to be a marker of neural lesion and correlate with the degree of nerve injury.

ATP7B gene mutation has been recognized as the pathogenic genes of WD. The mutations affect the main elimination pathway of liver copper, resulting in copper deposition in various organs, though especially the liver, brain, and eyes. The prevalence rate is 1/10,000 to 1/30,000 worldwide (18) and it is observed to be higher in China (19, 20). Previous research showed that WD in China is seemingly resulted from some relatively common mutations and a large number of rare mutations (20). p.R778L, p.P992L, and p.T935M have been identified to be the top three mutations in China (19). In our case, WES detected the missense c.G2333T: p.R778L variant of *ATP7B*, and the candidate pathogenic mutation site was included in the ClinVar database.[2] The program Polyphen2 predicted the variant to be probably damaging. According to the American College of Medical Genetics and Genomics (ACMG) guidelines, the mutation was pathogenic and the grade was PM3-very strong. Swiss-Model software[3] predicted the 3D structure of the pathogenic protein sequence (**Figure 3**).

Meanwhile, RP is a group of hereditary retinal malnutrition diseases characterized by the progressive degeneration of RPE and photoreceptors (rods and cones). Night blindness, progressive loss of peripheral vision, tunnel vision, and even blindness in advanced stages are typical symptoms (21). CME can be one of its macular conditions and thus may relate to the loss of central vision (22). The prevalence of CME in RP patients varies from 11 to 50% according to different detection methods (23, 24). The etiology of CME in individuals with RP remains uncertain,

---

[2]https://www.ncbi.nlm.nih.gov/clinvar/variation/3852/
[3]http://swissmodel.expasy.org/

FIGURE 4 | Logical mapping illustrates the possible pathogenesis of Wilson disease and retinitis pigmentosa in this patient.

including (i) breakdown of the blood-retina barrier, (ii) impaired function of the RPE pumping mechanism, (iii) lesions on Müller cells, (iv) anti-retinal antibodies, and (v) vitreous traction (25). In this case, CME was found in both eyes, for which we speculate RP may be responsible.

Monogenic inheritance is responsible for the largest proportion of RP cases, yet the disease is highly heterogeneous. There are 69 genes that have been mapped and identified to cause RP so far,[4] most of which contribute to non-syndromic RP. Apart from the non-syndromic type, RP also occurs in diseases that affect other sensory nervous systems or multiple tissues, such as Usher syndrome, Bardet-Biedl syndrome, and Cohen syndrome (26).

With the current patient, WES identified three different mutations in genes related to RP. *RP2* and *SNRNP200* have been mapped to RP2 and RP33, respectively, but the pathogenesis remains ambiguous, and their ACMG pathogenic grades are both of "uncertain significance" (*RP2*: PM1 + PM2-supporting + PP3; *SNRNP200*: PM1 + PP3). *CNGA1* is one of the causative genes of autosomal-recessive RP (27), as related to RP 49 (autosomal-recessive). As a member of the cyclic nucleotide-gated cation channel subfamily, *CNGA1* encodes the α-subunit of the rod cGMP-gated channel (28). As an essential protein of the rod photoreceptors in the cascade reaction of light conduction, rod cGMP-gated channel is composed of three CNGA1 subunits and one CNGB1 subunit (29). Besides, CNGA1 is also required for the structure of the outer segment of rod photoreceptors (30). Several mutations to *CNGA1* have been identified to be deleterious and have a causal link to autosomal-recessive RP (31). Homozygous *CNGA1* variant c. C453A: p. Y151X has been reported once (32), though it was detected to be nonsense and has a prevalence of 0.00005 in a crowd. This pathogenic grade suggests the variant to

be "pathogenic" for the classification of evidential items assessed by ACMG guidelines shows PVS1 + PM2-supporting + PM3-very strong. Since the current patient's parents did not exhibit RP-related symptoms, we surmise that the homozygous *CNGA1* variant in the patient conformed to gene co-segregation and might be the variant leading to RP. 3D structure of the pathogenic protein sequence cannot be predicted owing to the nonsense mutation that caused excessive deletion of amino acid fragments.

Metal cations are required in numerous biological processes, as in the pathogenesis of RP. For example, the role of zinc cation in the development of RP has been illustrated to be related to the loss of thermostability of the rhodopsin protein and zinc coordination to amino acid residues (33). Severe brain iron deposition is also implicated in the pathogenesis of neurodegenerative disorders and inherited diseases. As a group of progressive extrapyramidal disorders, neurodegeneration with brain iron accumulation (NBIA) can present with RP in child cases which are classified as pantothenate kinase-associated degeneration (PKAN) and this can lead to significant visual impairment (34, 35). In addition, iron metabolic dysfunction, which cause iron accumulation or iron overload, has been reported in animal models, suggesting the potential involvement of ferroptosis in RP (8). Copper is also an essential trace that plays an important role in the structure and physiology of retina (36). Previous studies have tried to explore the relationship between copper metabolism and RP, but came out with contradictory results. In a study involving 15 primary RP patients from India, Gahlot et al. described the changes in copper metabolism including: (i) normal or slightly lower serum copper level, (ii) notably reduced ceruloplasmin concentration, and (iii) high urinary copper excretion (9). These finding serve as a sign of chronic copper toxicity. Moreover, liver biopsies from some RP patients suggested slight, non-specific changes, which indicated that copper metabolism in primary

---

[4]RetNet: Summaries (uth.edu).

RP may also be altered. Rao et al. also reported that copper metabolism changed in RP cases, but in different parameters, and the degree were not comparable in the severity to those of WD patients (37). On the contrary, the serum copper levels revealed by Karcioglu et al. were in an opposite tendency to that of Gahlot's study (38). Other results by Marmor et al. (10), Ehlers et al. (39), and Atmaca et al. (40) also did not support the existence of copper metabolic abnormalities in individuals with RP. Thus, hypothesis was proposed that exogenous factors such as diet, overall nutrition and genetic isolation may account for the discrepancies between the normal results of copper metabolism and the striking Indian findings (10). By far, there is still lack of convincing evidence to indicate that RP is related to abnormal copper metabolism (**Supplementary Table 2**).

CONCLUSION

In summary, a case of concurrent WD and binocular RP was reported for the first time. We identified a deleterious homozygous mutation in the patient's *ATP7B* gene that caused WD, as well as a homozygous mutation in *CNGA1* that conformed to gene co-segregation that potentially led to RP (**Figure 4**). Since there remains no sufficient evidence to support that the occurrence of RP is associated with WD or abnormal copper metabolism, we speculate that the two pathogenic gene mutations lead to the coincidence of the two genetic disorders, respectively.

DATA AVAILABILITY STATEMENT

The original contributions presented in the study are included in the article/**Supplementary Materials**, further inquiries can be directed to the corresponding author/s.

ETHICS STATEMENT

The studies involving human participants were reviewed and approved by Ethics Committee of the Second Affiliated Hospital of Zhejiang University. The patients/participants provided their written informed consent to participate in this study. Written informed consent was obtained from the individual(s) for the publication of any potentially identifiable images or data included in this article.

AUTHOR CONTRIBUTIONS

ZY wrote the first draft. XJ guided the genetic analysis and revised the manuscript. XL and QZ recorded the medical information. KW and MC contributed to the treatment of the patient and made revisions of the manuscript. All authors contributed to the critical revision and provided final approval of the submitted version of this article.

FUNDING

ACKNOWLEDGMENTS

SUPPLEMENTARY MATERIAL

The Supplementary Material for this article can be found online at: https://www.frontiersin.org/articles/10.3389/fmed.2022.877752/full#supplementary-material

REFERENCES

1. Cater MA, La Fontaine S, Shield K, Deal Y, Mercer JF. ATP7B mediates vesicular sequestration of copper: insight into biliary copper excretion. *Gastroenterology.* (2006) 130:493–506. doi: 10.1053/j.gastro.2005.10.054
2. Zigrai M, Vyskocil M, Tothova A, Veres P, Bluska P, Valkovic P. Late-Onset Wilson's Disease. *Front Med.* (2020) 7:26. doi: 10.3389/fmed.2020.00026
3. Saito T. Presenting symptoms and natural history of Wilson disease. *Eur J Pediatr.* (1987) 146:261–5. doi: 10.1007/BF00716470
4. Lorincz MT. Neurologic Wilson's disease. *Ann N Y Acad Sci.* (2010) 1184:173–87. doi: 10.1111/j.1749-6632.2009.05109.x
5. Pagon RA. Retinitis pigmentosa. *Surv Ophthalmol.* (1988) 33:137–77. doi: 10.1016/0039-6257(88)90085-9
6. Kajiwara K, Berson EL, Dryja TP. Digenic retinitis pigmentosa due to mutations at the unlinked peripherin/RDS and ROM1 loci. *Science.* (1994) 264:1604–8. doi: 10.1126/science.8202715
7. Hartong DT, Berson EL, Dryja TP. Retinitis pigmentosa. *Lancet.* (2006) 368:1795–809. doi: 10.1016/S0140-6736(06)69740-7
8. Yang M, So KF, Lam WC, Lo ACY. Cell ferroptosis: new mechanism and new hope for retinitis pigmentosa. *Cells.* (2021) 10:2153. doi: 10.3390/cells10082153

9. Gahlot DK, Khosla PK, Makashir PD, Vasuki K, Basu N. Copper metabolism in retinitis pigmentosa. *Br J Ophthalmol.* (1976) 60:770–4. doi: 10.1136/bjo.60.11.770
10. Marmor MF, Nelson JW, Levin AS. Copper metabolism in American retinitis pigmentosa patients. *Br J Ophthalmol.* (1978) 62:168–71. doi: 10.1136/bjo.62.3.168
11. Dziezyc K, Litwin T, Czlonkowska A. Other organ involvement and clinical aspects of Wilson disease. *Handb Clin Neurol.* (2017) 142:157–69. doi: 10.1016/B978-0-444-63625-6.00013-6
12. Cozma I, Atherley C, James NJ. Influence of ethnic origin on the incidence of keratoconus and associated atopic disease in Asian and white patients. *Eye.* (2005) 19:924–5; author reply 5–6. doi: 10.1038/sj.eye.6701677
13. Langwinska-Wosko E, Litwin T, Dziezyc K, Czlonkowska A. The sunflower cataract in Wilson's disease: pathognomonic sign or rare finding? *Acta Neurol Belg.* (2016) 116:325–8. doi: 10.1007/s13760-015-0566-1
14. Albrecht P, Muller AK, Ringelstein M, Finis D, Geerling G, Cohn E, et al. Retinal neurodegeneration in Wilson's disease revealed by spectral domain optical coherence tomography. *PLoS ONE.* (2012) 7:e49825. doi: 10.1371/journal.pone.0049825
15. Langwińska-Wośko E, Litwin T, Szulborski K, Członkowska A. Optical coherence tomography and electrophysiology of retinal

and visual pathways in Wilson's disease. *Metab Brain Dis.* (2016) 31:405–15. doi: 10.1007/s11011-015-9776-8

16. Langwińska-Wośko E, Litwin T, Dziezyc K, Karlinski M, Członkowska A. Optical coherence tomography as a marker of neurodegeneration in patients with Wilson's disease. *Acta Neurol Belg.* (2017) 117:867–71. doi: 10.1007/s13760-017-0788-5

17. Svetel M, Bozic M, Vitkovic J, Jovanovic C, Dragasevic N, Pekmezovic T, et al. Optical coherence tomography in patients with Wilson's disease. *Acta Neurol Scand.* (2021) 144:149–54. doi: 10.1111/ane.13431

18. Bandmann O, Weiss KH, Kaler SG. Wilson's disease and other neurological copper disorders. *Lancet Neurol.* (2015) 14:103–13. doi: 10.1016/S1474-4422(14)70190-5

19. Dong Y, Ni W, Chen WJ, Wan B, Zhao GX, Shi ZQ, et al. Spectrum and classification of ATP7B variants in a large cohort of Chinese Patients with Wilson's Disease Guides Genetic Diagnosis. *Theranostics.* (2016) 6:638–49. doi: 10.7150/thno.14596

20. Xie JJ, Wu ZY. Wilson's disease in China. *Neurosci Bull.* (2017) 33:323–30. doi: 10.1007/s12264-017-0107-4

21. Gao Q, Liu Y, Lei X, Deng Q, Tong Y, Du L, et al. A novel CNGA1 gene mutation (c.G622A) of autosomal recessive retinitis pigmentosa leads to the CNGA1 protein reduction on membrane. *Biochem Genet.* (2019) 57:540–54. doi: 10.1007/s10528-019-09907-3

22. Fahim AT, Daiger SP, Weleber RG. Nonsyndromic retinitis pigmentosa overview. In: Adam MP, Ardinger HH, Pagon RA, Wallace SE, Bean LJH, Mirzaa G, et al, editors. *GeneReviews(®).* Seattle, WA: University of Washington, Seattle Copyright © 1993-2021, University of Washington, Seattle. GeneReviews is a registered trademark of the University of Washington, Seattle. All rights reserved (1993).

23. Adackapara CA, Sunness JS, Dibernardo CW, Melia BM, Dagnelie G. Prevalence of cystoid macular edema and stability in oct retinal thickness in eyes with retinitis pigmentosa during a 48-week lutein trial. *Retina.* (2008) 28:103–10. doi: 10.1097/IAE.0b013e31809862aa

24. Iovino C, Au A, Hilely A, Violanti S, Peiretti E, Gorin MB, et al. Evaluation of the choroid in eyes with retinitis pigmentosa and cystoid macular edema. *Invest Ophthalmol Vis Sci.* (2019) 60:5000–6. doi: 10.1167/iovs.19-27300

25. Triolo G, Pierro L, Parodi MB, De Benedetto U, Gagliardi M, Manitto MP, et al. Spectral domain optical coherence tomography findings in patients with retinitis pigmentosa. *Ophthalmic Res.* (2013) 50:160–4. doi: 10.1159/000351681

26. Makiyama Y, Oishi A, Otani A, Ogino K, Nakagawa S, Kurimoto M, et al. Prevalence and spatial distribution of cystoid spaces in retinitis pigmentosa: investigation with spectral domain optical coherence tomography. *Retina.* (2014) 34:981–8. doi: 10.1097/IAE.0000000000000010

27. Strong S, Liew G, Michaelides M. Retinitis pigmentosa-associated cystoid macular oedema: pathogenesis and avenues of intervention. *Br J Ophthalmol.* (2017) 101:31–7. doi: 10.1136/bjophthalmol-2016-309376

28. Verbakel SK, van Huet RAC, Boon CJF, den Hollander AI, Collin RWJ, Klaver CCW, et al. Non-syndromic retinitis pigmentosa. *Prog Retin Eye Res.* (2018) 66:157–86. doi: 10.1016/j.preteyeres.2018.03.005

29. Dryja TP, Finn JT, Peng YW, McGee TL, Berson EL, Yau KW. Mutations in the gene encoding the alpha subunit of the rod cGMP-gated channel in autosomal recessive retinitis pigmentosa. *Proc Natl Acad Sci USA.* (1995) 92:10177–81. doi: 10.1073/pnas.92.22.10177

30. Wang L, Zou T, Lin Y, Li L, Zhang P, Gong B, et al. Identification of a novel homozygous variant in the CNGA1 gene in a Chinese family with autosomal recessive retinitis pigmentosa. *Mol Med Rep.* (2020) 22:2516–20. doi: 10.3892/mmr.2020.11331

31. Zhong H, Molday LL, Molday RS, Yau KW. The heteromeric cyclic nucleotide-gated channel adopts a 3A:1B stoichiometry. *Nature.* (2002) 420:193–8. doi: 10.1038/nature01201

32. Bai Z, Xie Y, Liu L, Shao J, Liu Y, Kong X. Genetic investigation of 211 Chinese families expands the mutational and phenotypical spectra of hereditary retinopathy genes through targeted sequencing technology. *BMC Med Genom.* (2021) 14:92. doi: 10.1186/s12920-021-00935-w

33. Kircheva N, Dobrev S, Nikolova V, Angelova S, Dudev T. Zinc and its critical role in retinitis pigmentosa: insights from DFT/SMD calculations. *Inorg Chem.* (2020) 59:17347–55. doi: 10.1021/acs.inorgchem.0c02664

34. Kurian MA, McNeill A, Lin JP, Maher ER. Childhood disorders of neurodegeneration with brain iron accumulation (NBIA). *Dev Med Child Neurol.* (2011) 53:394–404. doi: 10.1111/j.1469-8749.2011.03955.x

35. Gregory A, Hayflick SJ. Neurodegeneration with brain iron accumulation. *Folia Neuropathol.* (2005) 43:286–96. doi: 10.1016/B978-0-444-63233-3.00019-1

36. Ugarte M, Osborne NN, Brown LA, Bishop PN. Iron, zinc, and copper in retinal physiology and disease. *Surv Ophthalmol.* (2013) 58:585–609. doi: 10.1016/j.survophthal.2012.12.002

37. Rao SS, Satapathy M, Sitaramayya A. Copper metabolism in retinitis pigmentosa patients. *Br J Ophthalmol.* (1981) 65:127–30. doi: 10.1136/bjo.65.2.127

38. Karcioglu ZA, Stout R, Hahn HJ. Serum zinc levels in retinitis pigmentosa. *Curr Eye Res.* (1984) 3:1043–8. doi: 10.3109/02713688409011750

39. Ehlers N, Bulow N. Clinical copper metabolism parameters in patients with retinitis pigmentosa and other tapeto-retinal degenerations. *Br J Ophthalmol.* (1977) 61:595–6. doi: 10.1136/bjo.61.9.595

40. Atmaca LS, Arcasoy A, Cavdar AO, Ozmert E. Levels of zinc in plasma, erythrocytes, and hair, and levels of serum copper in patients with retinitis pigmentosa in Turkey. *Br J Ophthalmol.* (1989) 73:29–31. doi: 10.1136/bjo.73.1.29

frontiers | Frontiers in Medicine

A Novel Algorithm for the Evaluation of Corneal Nerve Beadings by *in vivo* Confocal Microscopy in Patients With Type 1 Diabetes Mellitus

Irene Abicca[1]*, Daniela Giannini[1], Marta Gilardi[2], Anna Maria Roszkowska[3],
Mariacristina Parravano[1], Fabiana Picconi[4], Simona Frontoni[4,5] and
Domenico Schiano-Lomoriello[1]

[1] IRCCS–Fondazione Bietti, Rome, Italy, [2] Ophthalmic Hospital of Rome, Rome, Italy, [3] Ophthalmology Clinic, Department of Biomedical Sciences, University of Messina, Messina, Italy, [4] Unit of Endocrinology, Diabetes and Metabolism, S. Giovanni Calibita, Fatebenefratelli Hospital, Rome, Italy, [5] Department of Systems Medicine, University of Rome Tor Vergata, Rome, Italy

Purpose: Peripheral neuropathy could complicate diabetes mellitus (DM). *In vivo* confocal microscopy (IVCM) is an ocular examination for the diagnosis of small fiber neuropathies and the detection of the earliest corneal sub-basal nerve plexus (SBP) alterations. Corneal SBP characteristics include focal enlargement along with the nerve fiber, called corneal beadings. These dilatations represent a mitochondrial accumulation induced by the reactive oxygen stress, as a consequence of hyperglycemia. For this reason, corneal beadings are considered indicative of metabolic activity. This study aimed to describe the corneal characteristics of a population of type 1 diabetes mellitus (T1DM) well metabolically controlled, using a new algorithm for the analysis of corneal beading size (BS).

Methods: Patients aged ≥ 18 years affected by T1DM were compared with healthy subjects who underwent IVCM (Confoscan 4; Nidek Technologies Padova, Italy). Starting from the coordinates of the beadings detected by the IVCM, we implemented a new algorithm for automatically measuring BS in corneal SBP images.

Results: We compared 20 eyes of T1DM patients with 26 healthy controls. The corneal nerves' fiber length ($p = 0.008$), corneal nerves' fiber length density ($p = 0.008$), and the number of fibers ($p = 0.017$) were significantly lower in the diabetic group compared with controls. There was no difference between diabetic and healthy eyes in the mean number of corneal beadings both in the frame of analysis ($p = 0.606$) and for 0.1 mm of SBP nerve ($p = 0.145$). Regarding the BS, patients with T1DM had corneal beadings larger than controls ($p = 0.036$).

Conclusions: We found that the corneal beadings parameters are similar in healthy and T1DM individuals. Nevertheless, measuring the BS with our algorithm, we showed that corneal beadings are enlarged in patients affected by T1DM when compared with healthy controls. Identifying beading expansion in corneal nerve fiber using IVCM should become a useful tool to predict peripheral neuropathy at an early stage.

Keywords: beading, corneal confocal microscopy, diabetes mellitus, corneal nerve, peripheral neuropathy

INTRODUCTION

Type 1 diabetes mellitus (T1DM) is one of the most common metabolic disorders worldwide. A severe complication, which causes disability and reduces the quality of life (1), is represented by diabetic peripheral neuropathy (DPN), which is frequently diagnosed at a late stage. DPN should include corneal sensitivity alteration, with corneal sub-basal nerve plexus (SBP) modifications (2, 3). Furthermore, SBP damages have been described to be related to the duration of the disease and unsuitable glycemic control (4, 5).

Skin biopsy is considered the gold standard for the evaluation of morphological change in small nerve fibers and diabetic neuropathy progression (6). Unfortunately, this procedure is characterized by invasive nature and increased costs and can lead to delayed healing of the bioptic area (7). Therefore, it cannot be used as a screening test for all patients with diabetes. Alternatively, *in vivo* confocal microscopy (IVCM) is a rapid and reproducible ophthalmic application that allows studying of all corneal layers, such as cellular elements and small nerve fibers in the corneal SBP (2, 8, 9).

It has been proven that intraepidermal nerve fiber density and corneal nerve fiber morphology, evaluated by IVCM, are both correlated to neuropathy stages (10). Due to this, IVCM is considered an efficient non-invasive, and reliable alternative to skin biopsy, able to diagnose and track the progression of peripheral neuropathy in patients with diabetes (11).

In particular, the SBP analysis carried out by IVCM revealed a significant reduction in corneal parameters, specifically for nerve fibers length, nerve fibers length density, number of fibers, bifurcations, and beadings in patients with diabetes (12). Glycosylated hemoglobin levels in patients with diabetes showed an inverse relationship with nerve fibers length, nerve fibers length density, branches, and number of beadings (12).

The pathogenetic mechanism of the onset of diabetic neuropathy seems to be the reactive oxygen stress induced by hyperglycemia.

One of the consequences of reactive oxygen stress is to induce the accumulation of mitochondria along with the nerves fibers (13). In particular, beadings are enlargements (beads) along nerve fibers, which appear hyper-reflective at the IVCM examination. These dilatations are considered indicative of metabolic activity (14, 15).

Several studies reported the corneal nerve fibers changes in patients with diabetes (16–19), compared with healthy controls and described the beadings characteristics as number and density. Some of these studies suggested a direct correlation between the decrease of beading frequency (17–19) and metabolic activity of nerve fibers in patients with diabetes. Furthermore, the beading size (BS) resulted in being altered in diabetes, as described by Ishibashi et al. (17), using their specific algorithm. They reported a beading frequency reduction associated with a bead enlargement in a patient with type 2 diabetes, compared with healthy subjects. In addition, the number and size of beads were found to be related to changes in the mitochondrial distribution along corneal nerve fibers. Altered beading structures may have a relationship with peripheral nerve

changes, therefore, the BS might be a new biomarker for the detection of DPN at its earliest stage.

Nowadays, despite the evidence in the literature regarding the potential role of the beading dimension in predicting diabetic neuropathy evolution, a reproducible method for evaluating this characteristic is not in use.

This study aimed to apply a new algorithm for the measurement of corneal BS in the corneas of a T1DM population and compare it with a healthy control group.

MATERIALS AND METHODS

Study Population

We enrolled patients aged ≥ 18 years affected by T1DM according to the American Diabetes Association (ADA) criteria (20), referring to the Unit of Endocrinology, Diabetes, and Metabolism, Department of Systems Medicine in S. Giovanni Calibita Fatebenefratelli Hospital, University of Rome Tor Vergata, Rome, Italy, and we compared them with a control group of healthy adults, matched by age. All patients underwent a general medical examination, anthropometric parameters, and laboratory measurements. Blood and urinary samples were analyzed as previously described by our group (16). Triglycerides (TG), plasma total cholesterol (TC), high and low-density lipoprotein cholesterol (HDL-C and LDL-C), glycosylated hemoglobin (HbA1c), creatinine and microalbuminuria (urinary albumin/creatinine ratio) were performed in all T1DM, to rule out the confounding effect of high lipid values or renal failure on corneal nerves parameters.

We excluded diabetic patients with microalbuminuria >30 mg/g and diabetic autonomic neuropathy (DAN) evaluated by Ewing battery (21).

Regarding the healthy subjects, we performed an oral glucose tolerance test to exclude diabetes and impaired glucose tolerance. In addition, we excluded subjects with dyslipidemia, chronic renal failure, and hypertension based on their medical history.

In both groups (T1DM and control), we included patients with no history of possible confounding diseases (inflammatory diseases, alcohol abuse, vitamin deficiency, malignancy treated with chemotherapy agents, recent history of heart or respiratory failure, chronic liver or renal failure central nervous system diseases, entrapment mononeuropathies, and cervical or lumbosacral radiculopathies). Ocular exclusion criteria in all subjects were contact lens wearing, ocular trauma, ocular medications (except for artificial tears), clinical history of eye surgery, and ocular inflammation.

In vivo Confocal Microscopy

In vivo confocal microscopy (Confoscan 4; Nidek Technologies Padova, Italy) was performed bilaterally on the central cornea of all patients that included with a Z-ring adapter.

The same experienced operator (DSL) achieved all examinations. We used a sterile and transparent gel (dexpanthenol 5%) on the top of the instrumental lens to eliminate optical interfaces and to keep no-contact examination with invasiveness. After auto-alignment, a full-thickness scan of the cornea was performed, as previously described (22). The
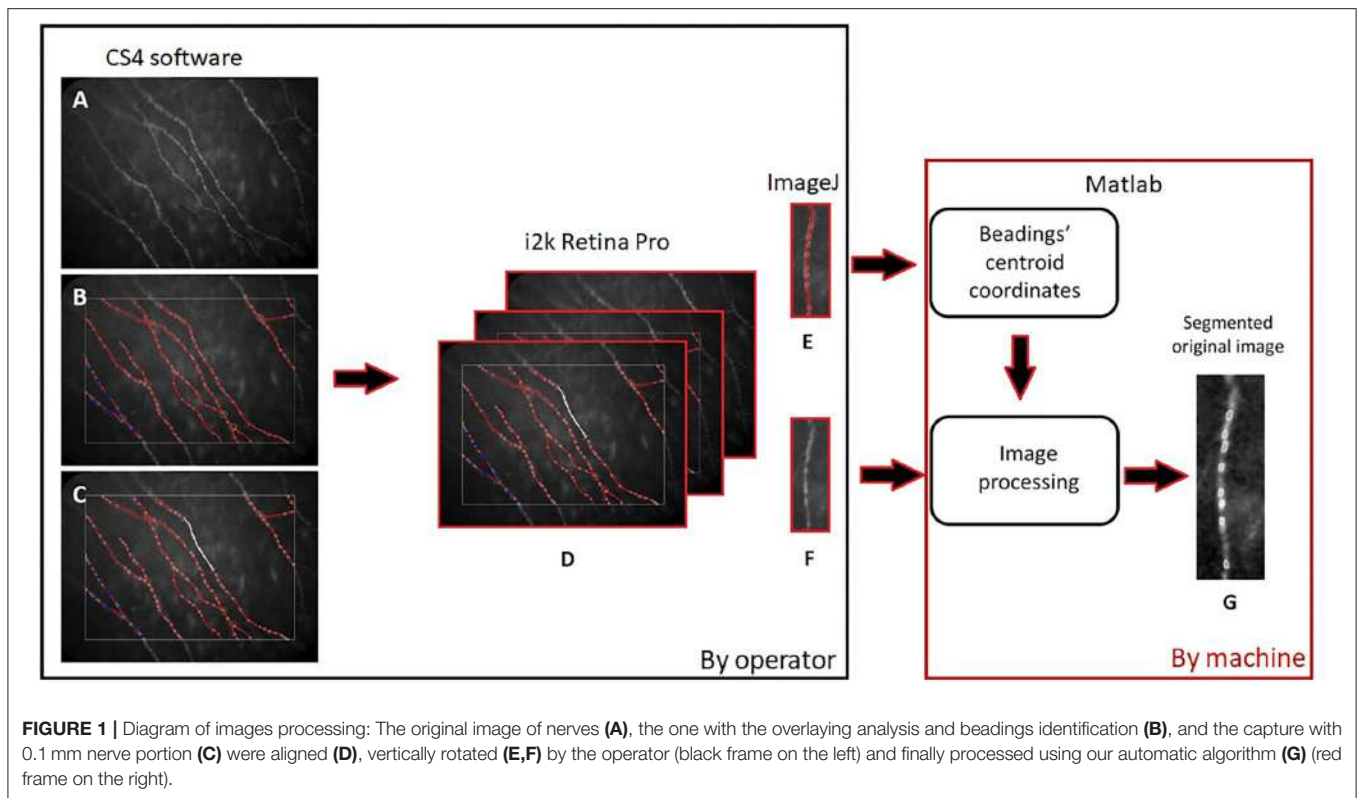
FIGURE 1 | Diagram of images processing: The original image of nerves **(A)**, the one with the overlaying analysis and beadings identification **(B)**, and the capture with 0.1 mm nerve portion **(C)** were aligned **(D)**, vertically rotated **(E,F)** by the operator (black frame on the left) and finally processed using our automatic algorithm **(G)** (red frame on the right).

overall time for the examination was up to 3 min. Some patients complained of ocular symptoms or visual complications.

Two experienced researchers (IA and MG), masked by the group assignment of images, carefully examined the images. One eye for each patient was considered, choosing the best-focused frame of the SBP for each patient. They discarded images with motions and/or with more than one layer.

The CS4 software (Nerves Tracking Tool v1.3.0) was used to automatically identify corneal fibers and beadings in each frame and review them. Errors were manually edited. In the case of a mismatch, a third operator (DG) chose the best option.

The following SBP parameters were available by the instrument for the analysis:

1. Nerve fiber length (μm/frame): the total length of all fibers and branches in a frame;
2. Nerve fiber length density (μm/mm^2): the total density of the nerve fibers in mm^2;
3. Number of fiber: the total number of nerve fibers, including main nerves and branches;
4. Number of branching: points where nerve branches arise from the main nerve;
5. Nerve fiber tortuosity using Nidek Nerve index, a unitless measure that represents the degree of the twistedness of a curved structure;
6. Number of beadings: the total number of beadings identified in the main nerves (trunks, long fibers that crossed the borders of the area of analysis);

7. Beadings density (beadings/mm): the total number of beadings divided by the total length of nerve trunks in millimeters.
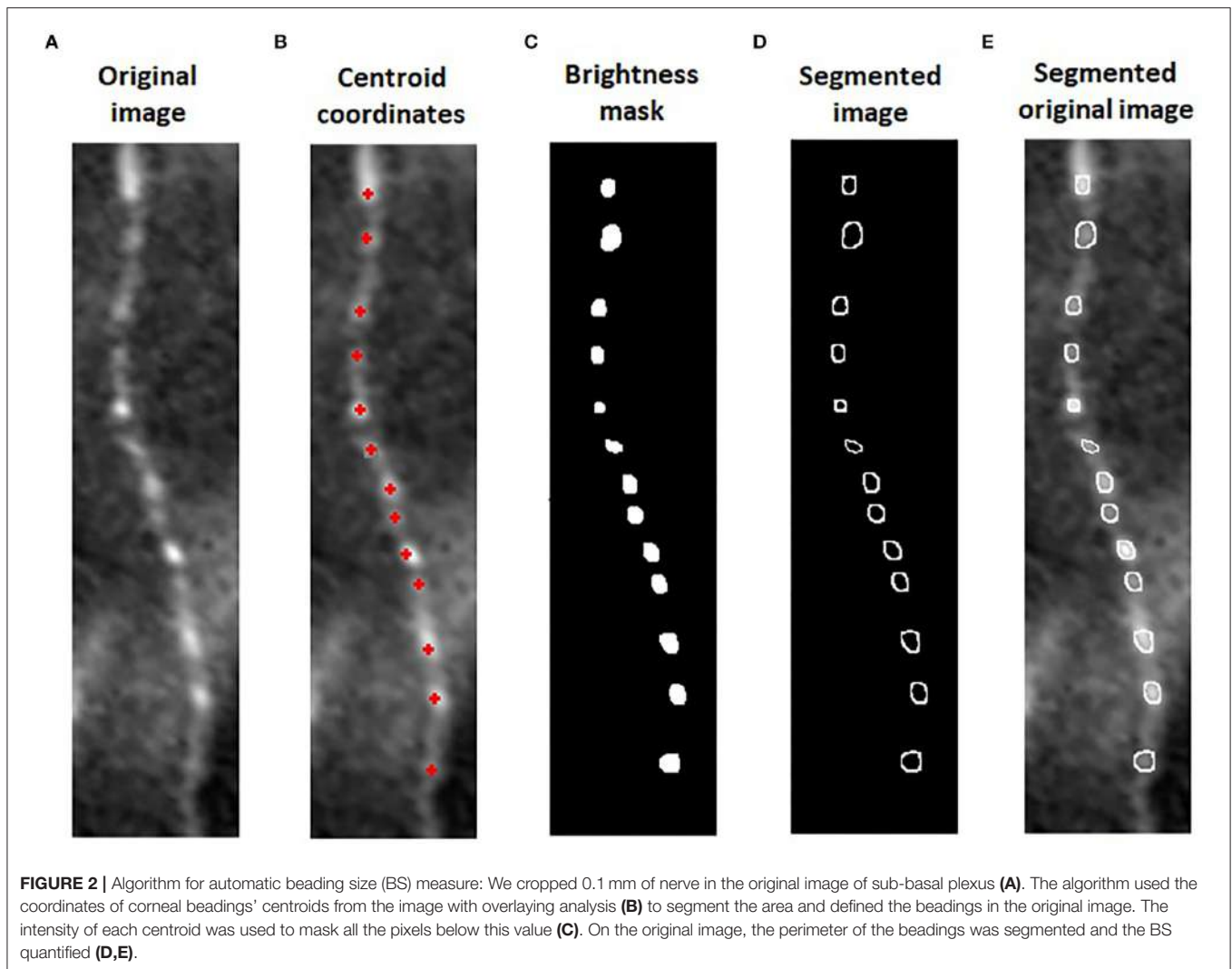
After the SBP detection using CS4 software, as described above, we processed the images to obtain a new morphological characterization of the beadings. To achieve this we saved three different images of the same capture of fibers:

1. The original image of nerves (**Figure 1A**);
2. The image with the overlaying analysis of the nerves and beadings identification (**Figure 1B**);
3. The capture with a manual selection of 0.1 mm nerve portion using the caliper tool (**Figure 1C**).

We aligned these three images (**Figure 1D**), using i2k Retina Pro (version 3.1), and we vertically rotated the fiber and cropped 0.1 mm of corneal nerve, using ImageJ (**Figures 1E,F**). After this preparation of images, a customized algorithm was applied to automatically measure BS in corneal nerves (**Figure 1G**). The algorithm was developed using Matlab (version R2015a; The Mathworks, Inc., Natick, MA, USA). Previously, the operator, using *imtool* (Image Processing Toolbox Matlab), extracted the coordinates of corneal beadings' centroids (defined as the geometric center of a plane figure) from the image with overlaying beadings analysis. The algorithm used these coordinates from the image with overlaying analysis to automatically segment the area and defined the BS in the original image (**Figures 2A,B**).

On one beading at a time, the intensity of each centroid was used by the algorithm as a threshold to filter all the pixels with a

FIGURE 2 | Algorithm for automatic beading size (BS) measure: We cropped 0.1 mm of nerve in the original image of sub-basal plexus **(A)**. The algorithm used the coordinates of corneal beadings' centroids from the image with overlaying analysis **(B)** to segment the area and defined the beadings in the original image. The intensity of each centroid was used to mask all the pixels below this value **(C)**. On the original image, the perimeter of the beadings was segmented and the BS quantified **(D,E)**.

brightness below this value. Finally, a mask overlap was created on the original image to automatically border the perimeter of the beadings (**Figures 2C,D**). The beading area was quantified from this segmentation (**Figure 2E**). For each patient, we calculated the BS, defined as the sum of all areas divided by the number of corneal beadings identified on 0.1 mm of the nerve fiber.

Statistical Analysis

The SPSS (IBM SPSS Statistics 25) was used for statistical evaluation. All results were expressed as the mean $\pm$ standard deviations (SDs). The independent sample t-test or the Mann–Whitney test was used for statistical analysis, as appropriate. In all analyses, $p < 0.05$ was considered to be statistically significant.

RESULTS

We included twenty eyes of 20 patients affected by T1DM, and we compared them to 26 healthy controls. The groups were similar in age ($p = 0.583$). The clinical and demographic characteristics of the study population are described in **Table 1**.

All patients underwent IVCM and, using CS4 software (CS4 Nerves Tracking Tool v1.3.0), we analyzed their SBP. The corneal nerves' fiber length, the length density, and the number of fibers were lower in the diabetic group and these differences were statistically significant (**Table 2**).

There was no difference between diabetic and healthy eyes in a mean number of corneal beadings in the frame analyzed ($p = 0.606$).

We cropped 0.1 mm of SBP nerve for the analysis in our new algorithm. Using the corneal beadings' detection of CS4 software with the manual correction (as described in the Materials and methods Section), we found that, even in this case, the mean number of corneal beadings was similar between the two groups (T1DM = 7.8 $\pm$ 2.17 vs. control = 8.85 $\pm$ 1.69, $p = 0.145$).

Then we applied our new algorithm to all images for the automatic measurement of BS both in T1DM and in the control group. We found that, in patients with T1DM, BS was higher than in healthy controls and this difference was statistically significant (T1DM = 12.94 $\pm$ 3.05 μm^2 vs. control = 11.11 $\pm$ 2.5 μm^2, $p = 0.031$).

TABLE 1 | Demographic and metabolic characteristics of study population (SD, standard deviation; T1DM, type 1 diabetes mellitus; DM, diabetes mellitus; BMI, body mass index; HBA1c, glycosylated hemoglobin; TC, total cholesterol; HDL-C, high-density lipoprotein cholesterol; LDL-C, low-density lipoprotein; TG, triglycerides).

	Healthy (n = 26)	T1DM (n = 20)
Age (mean ± SD)	42.73 ± 12.18	40.50 ± 15.15
Sex (male/female)	13/13	9/11
Age at diagnosis of DM (y)	–	25.15 ± 14.20
Duration of DM (y)	–	15.35 ± 12.66
BMI (Kg/m^2)	–	23.39 ± 3.10
HBA1c (%)	–	7.74 ± 1.00
TC (mg/dl)	–	165.60 ± 34.26
HDL-C (mg/dl)	–	58.75 ± 13.22
LDL-C (mg/dl)	–	91.46 ± 26.78
TG (mg/dl)	–	76.50 ± 38.18
Creatinine (mg/dl)	–	0.78 ± 0.11
Microalbuminuria/creatininuria (mg/g)	–	7.93 ± 7.11

TABLE 2 | Sub-basal plexus corneal nerves parameters of study population (SD, standard deviation; T1DM, type 1 diabetes mellitus; *statistically significant).

Nerve parameters (mean ± SD)	Healthy (n = 26)	T1DM (n = 20)	P-value
Nerve fibers length (μm/frame)	1216.03 ± 378.05	965.40 ± 233.52	0.008*
Nerve fibers length density (μm /mm^2)	13690.3 ± 4246.7	10863.24 ± 2627.64	0.008*
Number of fibers (n°/mm^2)	6.65 ± 2.56	5.15 ± 1.53	0.017*
Number of branching	2.69 ± 1.83	1.75 ± 1.25	0.085
Nerve nerve fiber tortuosity	5.48 ± 1.61	5.31 ± 1.33	0.973
Beadings density (n°/mm)	68.92 ± 13.96	63.87 ± 14.75	0.278
Beadings number (n°/frame)	20.65 ± 11.46	16.85 ± 3.91	0.606
Beading size (μm^2)	11.11 ± 2.5	12.94 ± 3.05	0.036*

TABLE 3 | Comparison of sub-basal plexus demographic, metabolic and corneal nerves parameter of T1DM with and without diabetic peripheral neuropathy (DPN) (SD, standard deviation; T1DM, type 1 diabetes mellitus; DM, diabetes mellitus; BMI, body mass index; HBA1c, glycosylated hemoglobin; TC, total cholesterol; HDL-C, high-density lipoprotein cholesterol; LDL-C, low-density lipoprotein; TG, triglycerides).

Nerve parameters	T1DM without DPN (n = 12)	T1DM with DPN (n = 8)	P-value
Age (mean ± SD)	41.08 ± 15.22	39.63 ± 16.06	0.842
Sex (male/female)	2/10	6/2	
Age at onset of DM (y)	30.08 ± 15.99	17.75 ± 6.41	0.157
Duration of DM (y)	11.00 ± 6.31	21.88 ± 17.07	0.181
BMI (Kg/m^2)	23.05 ± 2.06	23.91 ± 4.34	0.615
HBA1c (%)	7.53 ± 0.89	8.06 ± 1.12	0.277
TC (mg/dl)	169.83 ± 35.41	159.25 ± 33.74	0.678
HDL-C (mg/dl)	64.67 ± 13.01	49.88 ± 7.64	0.005
LDL-C (mg/dl)	90.92 ± 28.96	92.28 ± 25.04	0.624
TG (mg/dl)	70.50 ± 32.5	85.50 ± 46.28	0.384
Creatinine (mg/dl)	0.75 ± 0.11	0.83 ± 0.09	0.135
Microalbuminuria/ creatininuria (mg/g)	9.34 ± 7.81	5.82 ± 5.71	0.260
Nerve fibers length (μm/frame)	957.65 ± 257.42	977.03 ± 208.86	0.855
Nerve fibers length density (μm /mm^2)	10776.04 ± 2896.63	10994.04 ± 2350.15	0.855
Number of fibers (n°/mm^2)	5.5 ± 1.68	4.63 ± 1.19	0.189
Number of branching	2.08 ± 1.51	1.25 ± 0.46	0.270
Nerve fiber tortuosity	5.23 ± 1.52	5.43 ± 1.08	0.735
Beadings density (n°/mm)	64.55 ± 18.22	62.86 ± 8.16	0.270
Beadings number (n°/frame)	16.17 ± 4.59	17.88 ± 2.53	0.300
Beading size (μm^2)	13.25 ± 3.50	12.47 ± 2.36	0.560

Comparing T1DM without and with DPN (12 eyes vs. 8 eyes, respectively), we found that they were similar in age and metabolic characteristics. Furthermore, we did not find any difference in corneal parameters between T1DM and BS (**Table 3**).

DISCUSSION

Peripheral neuropathy is a severe complication of both type 1 and type 2 diabetes mellitus (T1DM and T2DM). The recommendations of the American Diabetes Association are to assess annually for DPN in all patients with T2DM and patients with a diagnosis of T1DM for more than 5 years (23).

In vivo confocal microscopy is a reliable, non-invasive method for the detection of DPN, including small nerve fiber lesions, even in patients without symptoms (10, 24).

The cornea is one of the most richly innervated body tissues, with a sensitive innervation provided by the ophthalmic branch of the trigeminal nerve. The corneal nerves allow for protecting, restoring, and supporting the ocular surface (25). Consequently, IVCM, which enables the *in vivo* analysis of corneal innervation, is a useful tool both for the study of the peripheral nerves involvement and for the identification of risk factors for ocular surface disorders in patients with diabetes.

Hyperglycemia induces reactive oxygen stress, playing an important role in diabetic neuropathy onset and leading to the accumulation of mitochondria along with the nerves fiber. At IVCM, mitochondria are visualized as corneal beadings. In T1DM, when the increase in superoxide induces the activation of the polyol pathway and the accumulation of glycosylation products, damage of ocular surface and corneal nerves occurs (26). The long-term effects of the metabolic and vascular disorders in diabetes are neural function impairment and loss of neurotrophic support, which induces apoptosis of neurons, Schwann cells, and glial cells of the peripheral nervous system, resulting in corneal nerves reduction.

Our group already reported early alterations in SBP even in a small population of T1DM adults without DPN and diabetic retinopathy (16). However, we did not find any difference in the

number and density of beadings compared with healthy controls. According to these results, beadings should be excluded as a parameter for the early detection of corneal nerve alterations in T1DM patients with good metabolic control. Nevertheless, we inquired about another beading parameter that should be speculated as well: the size. For this reason, the purpose of the present study was to investigate the beading size in a population of T1DM. We chose patients who had good glycemic and lipid control because we aimed to eliminate confounding factors of the metabolism.

First, in our study, we analyzed the corneal nerve parameters at IVCM and we found that corneal fiber length, length density, and number of fibers were significantly lower in our patients with T1DM compared with controls. These results confirm that corneal nerves appeared altered even in a well metabolically controlled population of T1DM, as already reported by our group and in literature (16, 27).

As far as corneal beadings are concerned, we did not find differences in the number and density of corneal beadings between T1DM and controls.

According to the literature, patients affected by T1DM showed a lower beading frequency when compared with healthy controls (5, 17) and this seemed to be in contrast with our results. However, different methods for the analysis were applied. The "beading frequency" was defined as frequency/0.1 mm of beading, using ImageJ (Texelcraft, Tokyo, Japan), while we described in our studies the "beading density," defined as the total number of beadings divided by the total length of nerve trunks in millimeters, using the automatic count of CS4 software (12) and manually corrected.

In our opinion, the lack of alteration in beading number and density should be the consequence of the good glycemic and lipid control of our diabetic population. However, we applied our new algorithm to speculate the size of beadings. We found that corneal beadings were bigger in patients affected by T1DM than in healthy controls and this difference was statistically significant.

Ishibashi et al. (17) already described the BS in a large cohort study of T2DM. They found that, even in absence of DPN, the worsening of peripheral neuropathy follows an enlargement of bead size.

To our knowledge, our study is the first to describe the enlargement of the new parameter BS in a T1DM population well metabolically controlled and without number and density alteration.

Hishibashi's group (5) already hypothesized that beadings alterations could be the consequence of changes in the distribution of mitochondria during diabetes mellitus.

Mitochondrial loss in the early stages of small fiber neuropathies was reported (28, 29).

The new and interesting result of our study was that, even in a group of patients with diabetes with a similar number and density of beadings compared with healthy controls, we had an alteration in bead size. This finding should be the consequence of mitochondrial dysfunction. The advantage of our new algorithm is the completely automatic measurement of BS, based on the

previous analysis of beadings using the reproducible method of CS4 software (12).

The main limitation of our research was the small number of patients included, due to the strict inclusion criteria for the analysis. Therefore, a longitudinal study with a larger group should be further investigated.

Our goal for future developments is the application of our algorithm for the bead detection, making the analysis of the new BS parameter easier. Now, the limits of this analysis of corneal nerves are that a lot of time and specifically trained operators are needed. Furthermore, the study of corneal innervation allows us to speculate on the pathogenic mechanism of ocular surface alteration in diabetes. Due to the report on the impact of age on density and morphology of SBP in healthy adults (30), it should be interesting, in future studies, to evaluate the correlation between the age of patients with diabetes and the progression of corneal damage. The deepening of the analysis of the nerves and specifically of the corneal beadings, which are associated with metabolic activity in diabetes, could help to better understand these alterations.

In our opinion, identifying beading expansion in corneal nerve fiber using IVCM should become a useful tool for predicting peripheral neuropathy at an early stage.

DATA AVAILABILITY STATEMENT

The original data used and analyzed to support the findings of this study are included in the **Supplementary Material**, further inquiries can be directed to the corresponding author/s.

ETHICS STATEMENT

The studies involving human participants were reviewed and approved by Sezione IRCCS I.F.O-Fondazione G.B. Bietti. The patients/participants provided their written informed consent to participate in this study.

AUTHOR CONTRIBUTIONS

IA, DG, and DSL: conception and design. IA, MP, FP, and SF: collection and assembly of data. IA, DG, MG, and AMR: data analysis and interpretation. All authors wrote the manuscript and final approval of the manuscript.

ACKNOWLEDGMENTS

SUPPLEMENTARY MATERIAL

The Supplementary Material for this article can be found online at: https://www.frontiersin.org/articles/10.3389/fmed.2022.897259/full#supplementary-material

REFERENCES

1. Van Acker K, Bouhassira D, De Bacquer D, Weiss S, Matthys K, Raemen H, et al. Prevalence and impact on quality of life of peripheral neuropathy with or without neuropathic pain in type 1 and type 2 diabetic patients attending hospital outpatients clinics. *Diabetes Metab.* (2009) 35:206–13. doi: 10.1016/j.diabet.2008.11.004

2. Rosenberg ME, Tervo TM, Immonen IJ, Müller LJ, Grönhagen-Riska C, Vesaluoma MH. Corneal structure and sensitivity in type 1 diabetes mellitus. *Invest Ophthalmol Vis Sci.* (2000) 41:2915–21.

3. Cai D, Zhu M, Petroll WM, Koppaka V, Robertson DM. The impact of type 1 diabetes mellitus on corneal epithelial nerve morphology and the corneal epithelium. *Am J Pathol.* (2014) 184:2662–70. doi: 10.1016/j.ajpath.2014.06.016

4. Dehghani C, Pritchard N, Edwards K, Vagenas D, Russell AW, Malik RA, et al. Natural history of corneal nerve morphology in mild neuropathy associated with type 1 diabetes: development of a potential measure of diabetic peripheral neuropathy. *Invest Ophthalmol Vis Sci.* (2014) 55:7982–90. doi: 10.1167/iovs.14-15605

5. Ishibashi F, Okino M, Ishibashi M, Kawasaki A, Endo N, Kosaka A, et al. Corneal nerve fiber pathology in Japanese type 1 diabetic patients and its correlation with antecedent glycemic control and blood pressure. *J Diabetes Investig.* (2012) 3:191–8. doi: 10.1111/j.2040-1124.2011.00157.x

6. England JD, Gronseth GS, Franklin G, Carter GT, Kinsella LJ, Cohen JA, et al. Evaluation of distal symmetric polyneuropathy: the role of autonomic testing, nerve biopsy, and skin biopsy (an evidence-based review). *Muscle Nerve.* (2009) 39:106–15. doi: 10.1002/mus.21227

7. Ahmed A, Bril V, Orszag A, Paulson J, Yeung E, Ngo M, et al. Detection of diabetic sensorimotor polyneuropathy by corneal confocal microscopy in type 1 diabetes: a concurrent validity study. *Diabetes Care.* (2012) 35:821–8. doi: 10.2337/dc11-1396

8. Hossain P, Sachdev A, Malik RA. Early detection of diabetic peripheral neuropathy with corneal confocal microscopy. *Lancet.* (2005) 366:1340–3. doi: 10.1016/S0140-6736(05)67546-0

9. Oliveira-Soto L, Efron N. Morphology of corneal nerves using confocal microscopy. *Cornea.* (2001) 20:374–84. doi: 10.1097/00003226-200105000-00008

10. Quattrini C, Tavakoli M, Jeziorska M, Kallinikos P, Tesfaye S, Finnigan J, et al. Surrogate markers of small fiber damage in human diabetic neuropathy. *Diabetes.* (2007) 56:2148–54. doi: 10.2337/db07-0285

11. Hertz P, Bril V, Orszag A, Ahmed A, Ng E, Nwe P, et al. Reproducibility of *in vivo* corneal confocal microscopy as a novel screening test for early diabetic sensorimotor polyneuropathy. *Diabet Med.* (2011) 28:1253–60. doi: 10.1111/j.1464-5491.2011.03299.x

12. Batawi H, Shalabi N, Joag M, Koru-Sengul T, Rodriguez J, Green PT, et al. Sub-basal corneal nerve plexus analysis using a new software technology. *Eye Contact Lens.* (2018) 44(Suppl. 1):S199–205. doi: 10.1097/ICL.0000000000000375

13. Tummanapalli SS, Issar T, Kwai N, Poynten A, Krishnan AV, Willcox M, et al. Association of corneal nerve loss with markers of axonal ion channel dysfunction in type 1 diabetes. *Clin Neurophysiol.* (2020) 131:145–54. doi: 10.1016/j.clinph.2019.09.029

14. Patel DV, McGhee CNJ. Contemporary *in vivo* confocal microscopy of the living human cornea using white light and laser scanning techniques: a major review. *Clin Exp Ophthalmol.* (2007) 35:71–88. doi: 10.1111/j.1442-9071.2007.01423.x

15. Patel DV, McGhee CNJ. *In vivo* confocal microscopy of human corneal nerves in health, in ocular and systemic disease, and following corneal surgery: a review. *Br J Ophthalmol.* (2009) 93:853–60. doi: 10.1136/bjo.2008.150615

16. Schiano Lomoriello D, Abicca I, Parravano M, Giannini D, Russo B, Frontoni S, et al. Early alterations of corneal subbasal plexus in uncomplicated type 1 diabetes patients. *J Ophthalmol.* (2019) 2019:9818217. doi: 10.1155/2019/9818217

17. Ishibashi F, Kojima R, Taniguchi M, Kosaka A, Uetake H, Tavakoli M. The expanded bead size of corneal C-nerve fibers visualized by corneal confocal microscopy is associated with slow conduction velocity of the peripheral nerves in patients with type 2 diabetes mellitus. *J Diabetes Res.* (2016) 2016:3653459. doi: 10.1155/2016/3653459

18. Midena E, Brugin E, Ghirlando A, Sommavilla M, Avogaro A. Corneal diabetic neuropathy: a confocal microscopy study. *J Refract Surg.* (2006) 22:S1047–52. doi: 10.3928/1081-597X-20061102-08

19. Maddaloni E, Sabatino F, Del Toro R, Crugliano S, Grande S, Lauria Pantano A, et al. *In vivo* corneal confocal microscopy as a novel non-invasive tool to investigate cardiac autonomic neuropathy in Type 1 diabetes. *Diabet Med.* (2015) 32:262–6. doi: 10.1111/dme.12583

20. American Diabetes Association. Diagnosis and classification of diabetes mellitus. *Diabetes Care.* (2013) 36(Suppl. 1):S67–74. doi: 10.2337/dc13-S067

21. Tesfaye S, Boulton AJM, Dyck PJ, Freeman R, Horowitz M, Kempler P, et al. Diabetic neuropathies: update on definitions, diagnostic criteria, estimation of severity, and treatments. *Diabetes Care.* (2010) 33:2285–93. doi: 10.2337/dc10-1303

22. McLaren JW, Bourne WM, Patel SV. Standardization of corneal haze measurement in confocal microscopy. *Invest Ophthalmol Vis Sci.* (2010) 51:5610–6. doi: 10.1167/iovs.10-5614

23. Pop-Busui R, Boulton AJM, Feldman EL, Bril V, Freeman R, Malik RA, et al. Diabetic neuropathy: a position statement by the American Diabetes Association. *Diabetes Care.* (2017) 40:136–54. doi: 10.2337/dc16-2042

24. Edwards K, Pritchard N, Vagenas D, Russell A, Malik RA, Efron N. Utility of corneal confocal microscopy for assessing mild diabetic neuropathy: baseline findings of the LANDMark study. *Clin Exp Optom.* (2012) 95:348–54. doi: 10.1111/j.1444-0938.2012.00740.x

25. Belmonte C, Aracil A, Acosta MC, Luna C, Gallar J. Nerves and sensations from the eye surface. *Ocul Surf.* (2004) 2:248–53. doi: 10.1016/S1542-0124(12)70112-X

26. Babizhayev MA, Strokov IA, Nosikov VV, Savel'yeva EL, Sitnikov VF, Yegorov YE, et al. The role of oxidative stress in diabetic neuropathy: generation of free radical species in the glycation reaction and gene polymorphisms encoding antioxidant enzymes to genetic susceptibility to diabetic neuropathy in population of type i diabetic patients. *Cell Biochem Biophys.* (2015) 71:1425–43. doi: 10.1007/s12013-014-0365-y

27. Petropoulos IN, Green P, Chan AWS, Alam U, Fadavi H, Marshall A, et al. Corneal confocal microscopy detects neuropathy in patients with type 1 diabetes without retinopathy or microalbuminuria. *PLoS ONE.* (2015) 10:e0123517. doi: 10.1371/journal.pone.0123517

28. Casanova-Molla J, Morales M, Garrabou G, Solà-Valls N, Soriano A, Calvo M, et al. Mitochondrial loss indicates early axonal damage in small fiber neuropathies. *J Peripher Nerv Syst.* (2012) 17:147–57. doi: 10.1111/j.1529-8027.2012.00396.x

29. Roszkowska AM, Licitra C, Tumminello G, Postorino EI, Colonna MR, Aragona P. Corneal nerves in diabetes-the role of the *in vivo* corneal confocal microscopy of the subbasal nerve plexus in the assessment of peripheral small fiber neuropathy. *Surv Ophthalmol.* (2021) 66:493–513. doi: 10.1016/j.survophthal.2020.09.003

30. Roszkowska, AM, Wylegała A, Gargano R, Spinella R, Inferrera L, et al. Impact of corneal parameters, refractive error and age on density and morphology of the subasal nerve plexus fibers in healthy adults. *Sci. Rep.* (2021) 11:6076. doi: 10.1038/s41598-021-85597-5

Neurotrophic Keratopathy in Systemic Diseases: A Case Series on Patients Treated With rh-NGF

Alessandro Meduri[1], Giovanni William Oliverio[1]*, Antonio Valastro[1], Claudia Azzaro[1], Umberto Camellin[1], Francesco Franchina[1], Leandro Inferrera[2], Anna Roszkowska[1,3] and Pasquale Aragona[1]

[1] Department of Biomedical Sciences, Ophthalmology Clinic, University of Messina, Messina, Italy, [2] Department of Medical, Surgical Sciences and Health, Eye Clinic, University of Trieste, Trieste, Italy, [3] Department of Ophthalmology, Faculty of Medicine and Health Sciences, Andrzej Frycz Modrzewski Krakow University, Kraków, Poland

Purpose: To evaluate the prevalence, clinical ocular presentation and corneal healing in moderate and severe neurotrophic keratopathy (NK) caused by systemic diseases and treated with rh-NGF.

Setting: Department of Biomedical and Dental Sciences and Morphofunctional Imaging, Ophthalmology Clinic, University of Messina, Italy.

Design: Retrospective observational study of case series.

Materials and Methods: In this retrospective observational study 11 patients (five female and six males) aged from 24 to 88 years (55.4 ± 21.3 years) with moderate and severe NK caused by systemic diseases were enrolled. The VAS questionnaire was dispensed. The ocular examination comprised slit lamp evaluation, ocular surface assessment with Keratograph 5M (Oculus, Germany), corneal sensitivity with Cochet-Bonnet esthesiometer (Lunneaux, France) and corneal thickness measurement with AC-OCT (DRI, Triton, Topcon, Japan). The underlying systemic causes of NK were determined.

Results: The main cause of NK was post-neuroma surgery (36%), followed by diabetes (18%). The remaining causes were rheumatoid arthritis (9%), post-traumatic (9%), post-surgery (9%), atopia (9%), Graves' disease (9%). Seven eyes presented severe grade of NK with corneal ulcer and in four a moderate grade was registered. The rh-NGF (Cenegermin) was administered with a standard protocol one drop six times daily for 8 weeks. The complete healing of all corneal defects was registered at the end of the treatment.

Conclusions: The post-neuroma surgery was the most common cause of NK and severe grade was clinically more represented. The rh-NGF proved effective to promote corneal recovery with all defects healed after the treatment.

Keywords: neurotrophic keratopathy, rh-NGF, neurotrophic keratitis, Cenegermin, nerve growing factor

INTRODUCTION

Neurotrophic keratopathy (NK) is a degenerative corneal disease that affects the health and integrity of the ocular surface, resulting from impairment of corneal nerves that causes alterations in their sensory and trophic function (1). When the corneal epithelium is damaged, a coordinated and collaborative system of communication between epithelial and neuronal cells is required to promote the resynthesis of the damaged matrix, cell migration, and the restoration of architectural integrity (2, 3). As a result of permanent impairment of epithelial repair, the exposed stroma becomes subject to enzymatic deterioration, melting, and in severe forms perforation, which are all characteristics of NK (2). NK is defined as a rare disease with a prevalence estimated between 1.6 and 4.2/10,000 individuals. However, the recent studies demonstrated that this condition is commonly underestimated (4).

The etiology of corneal nerves alteration in NK could be linked to numerous ocular or systemic conditions (4, 5).

The main local causes reported are herpetic infections, chemical injuries, while the corneal surgery could directly damage the corneal nerves (5).

Although the etiology of neurotrophic keratitis is commonly related to primary ocular diseases, there are several systemic or genetic diseases, and central nervous disorders that may underlie this corneal affection (4–6).

Recent knowledge in pathogenesis of NK and the introduction of topical recombinant human Nerve Growth factor (rh-NGF) has significantly changed the natural history of the disease (1, 2).

The purpose of this study is to analyze the prevalence of moderate and severe NK resulting from systemic diseases in affected patients treated in our center with rh-NGF, aiming to identify the most frequent cause and the grade of corneal involvement. The additional aim is to assess the corneal healing process during the treatment.

MATERIALS AND METHODS

In this retrospective observational cohort study, 21 eyes of 21 patients with moderate and severe NK treated with rh-NGF between January 2017 and March 2020 at Excellence Regional Center for Ocular Surface diseases of the Ophthalmology Clinic of the University Hospital of Messina were enrolled. The study was conducted with respect of tenets of Declaration of Helsinki and obtained approval of the Ethical Committee of the University Hospital of Messina. For the study purposes only patients with underlying systemic diseases that caused NK were included with the aim to determine the percentage of presentation of moderate and severe forms accordingly to the underlying pathology. Therefore, 10 patients were excluded from the study as they were affected by NK which had an ocular pathology as the primary cause. The enrolled sample comprised 11 patients with systemic diseases. Five patients were female and 6 were male and their age ranged from 24 to 88 years (mean 55.4 ± 21.3 years).

All patients underwent ocular examination that included slit lamp evaluation, ocular surface assessment with Keratograph

5M (Oculus, Germany), corneal sensitivity with Cochet-Bonnet esthesiometer (Lunneaux, France) and corneal thickness measurement with AS-OCT (DRI, Triton, Topcon). Dua classification for NK severity determination was used (1) and moderate form defined as persistent epithelial defects (PED) was differentiated from severe one (ulcer) in relation to the corneal involvement. The corneal surface was analyzed with Keratograph 5M using fluorescein staining.

Corneal sensitivity was measured in the center of the cornea three times with the Cochet-Bonnet esthesiometer and reported in filament length (cm). The average of the three measurements was used. In cases of severe NK, the thinnest point in the ulcer bed was measured using Swept source AS-OCT (DRI Triton, Topcon, Japan). The ocular discomfort was assessed using the Visual Analog Scale (VAS). All patients received Cenegermin drops (20 μg/ml) (Oxervate ®, Dompè, farmaceutici Spa, Milan, Italy) accordingly to the standardized protocol with one drop for six times daily for 8 weeks.

Corneal healing was defined as <0.5 mm fluorescein staining in the lesion area, according to REPARO 2 (7).

RESULTS

In a total of 21 patients, 11 (52.4%) presented NK related to systemic diseases, and 10 (47.6%) to ocular affections.

Furthermore, the group with underlying systemic causes was evaluated. The main cause of NK was post-neuroma surgery (36%), followed by diabetes (18%), previous surgery (9%), complications of Graves' disease (9%), previous trauma (9%), ocular complications of rheumatoid arthritis (9%) and severe atopic dermatitis (9%).

Severe NK (ulcer) was observed in seven patients (mean age 62.3 ± 21.7 years) and moderate NK (PED) in four patients (mean age 43.3 ± 16.1 years). The causes and severity distribution of NK are shown in **Figure 1**. Moderate NK was related to post-neuroma surgery (75%) and Graves' disease (25%), whereas severe NK to diabetes (30%), and other causes (**Figure 1**). Total VAS score was 20.27 ± 4.11 mm before the treatment, 20.98 ± 3.63 mm after 4 weeks and 10.92 ± 7.19 mm after 8 weeks (**Table 1**). Corneal sensitivity improved in all eyes. The changes of sensitivity and VAS score from baseline to 8 weeks after rh-NGF administration are shown in (**Tables 1, 2**).

As to the corneal surface recovery after 4 weeks of the treatment a complete healing was registered in 100% of ulcers and 50% of PED. After 8 weeks a complete corneal recovery was observed in all patients.

Corneal thinnest location pachymetry in patients with severe NK was 285.25 ± 71.83 μm before treatment, 385.5 ± 16.33 μm at 4 weeks, and 448.25 ± 37.71 μm at 8 weeks (**Table 2**).

DISCUSSION

In our series there was a higher prevalence of NK resulted from several systemic diseases (52.4%); whereas the ocular causes of NK were related mainly to herpetic infections (47.6%).
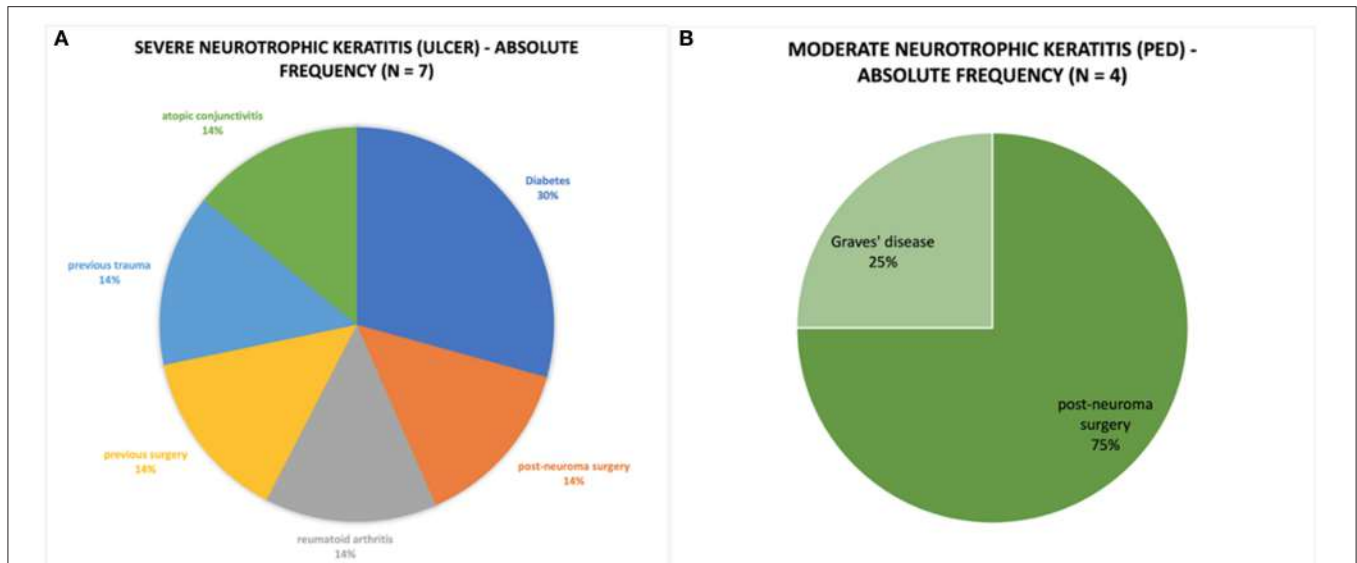
FIGURE 1 | (A) Pie chart represent the absolute frequency of cases of severe neurotrophic keratitis caused by systemic pathology. (B) Pie chart representing the absolute frequency of cases of moderate neurotrophic keratitis caused by systemic pathology.

TABLE 1 | Corneal sensibility in severe and moderate neurotrophic keratitis.

Presentation	Baseline	4 weeks	8 weeks
Severe NK	1.9 ± 1.8	4.5 ± 0.7	4.6 ± 0.5
Moderate NK	1.1 ± 0.5	3.3 ± 2	3.9 ± 1.9
Total	1.6 ± 1.5	3.6 ± 1.7	4.25 ± 1.3

All data are reported as mean ± standard deviation.

TABLE 2 | Visual analog scores in severe and moderate neurotrophic keratitis.

Presentation	Baseline	4 weeks	8 weeks
Severe NK	23.36 ± 4.38	21.28 ± 3.87	11.91 ± 7.80
Moderate NK	20.27 ± 4.11	20.98 ± 3.63	10.92 ± 7.19
Total	21.81 ± 4.24	21.13 ± 3.75	11.41 ± 7.49

All data are reported as mean ± standard deviation.

Systemic diseases such as diabetes, multiple sclerosis, central nervous system diseases, genetic syndromes and autoimmune diseases could be associated with NK (1, 4–12).

A recent epidemiologic study on 335 patients showed that central nervous systems diseases followed by diabetes are the main causes of NK due to the systemic conditions (13).

In our study, the main systemic causes of NK were post neuroma surgery (36%) and diabetes (18%) and such finding confirms these recently published data.

As to the central nervous system diseases, intracerebral tumors play a primary role, and they could be represented by both head and neck cancers with intracranial spreading and trigeminal involvement (14–18).

The effects of the different therapies of cerebral tumors such as surgery (19–22) radiotherapy, (23) and systemic chemotherapy (24, 25) may also alter the nerve fibers or induce limbal stem cell deficiency (26, 27) resulting clinically in NK.

Association between diabetes and NK was identified already in 1977, as a consequence of the neuropathy of ophthalmic branch of trigeminal nerve due to microvascular damages of myelinated fibers (6, 28, 29).

The severity and progression of NK in diabetic patients are related to peripheral neuropathy, so the corneal nerve plexus is considered as an important marker of this latter's evolution and management effectiveness (6, 30). In particular NFL is considered a good parameter to evaluate the diabetic sensorimotor polyneuropathy (8).

Additionally, diabetes has further negative effects on the ocular surface inducing tear film instability and ocular surface microbiome alterations, that increase corneal erosion and infection susceptibility (31–33).

As to the other systemic diseases that may induce NK, the autoimmune diseases such as rheumatoid arthritis, Grave's disease are reported and were observed in 9% of patients in our group (34, 35).

Other systemic causes of NK are rare and are represented by amyloidosis, leprosis, CIPD, disseminated lymphangiomatosis, T-cell lymphoma, syringomyelia, vitamin B12 deficiency, HIV, and ischemic conditions like Wallenberg syndrome or cocaine snorting (36–50).

Furthermore, in pediatric patients with NK different genetic syndromes were described.

They comprehend above all HSN, congenital insensitivity to pain with anhidrosis, Gómez-López-Hernández syndrome, Goldenhar syndrome, congenital trigeminal nerve aplasia, and other more infrequent conditions like APS, familial dysautonomia, and Crisponi/CISS1 syndrome (34, 50–67).

In our study the severity of neurotrophic keratopathy interestingly appeared to be related to the patients' age. The patients with PED were younger with respect to the patients with ulcers. In a previous study, Roszkowska et al. (6, 8) demonstrated that the age is the most important element that influence corneal sub-basal nerve plexus (SBNP) nerves length, tortuosity and density. This could explain the finding that more severe corneal defects were registered in older patients who already have lower SBNP parameters. We therefore speculate that at the basis of the severity of NK there is a component of cellular tropism linked to the age and general condition of the patient.

The diagnosis of NK is based firstly on medical and surgical history of the patient to investigate all those conditions that may underlie the pathology (9, 68). Indeed, it is mandatory to consider both ocular and systemic treatments which the patient is undergoing, focusing on those that could damage corneal sensory innervation. Since NK is characterized by damage to the trigeminal sensory innervation, patients commonly do not experience any symptoms, making the diagnosis of NK particularly challenging (67). It is for the same reason that patients often see the specialist only in late phases of the disease when the pathology is already at an advanced stage (69, 70). It is important to perform a complete neurological assessment to reveal any cranial nerve damage, because a trigeminal nerve impairment may be associated with other cranial nerves injuries (1). NK's treatment consists of medical therapies, non-surgical and surgical intervention, depending on disease's stage (1, 10, 71–77).

Cenegermin is a recombinant human nerve growth factor, and it is the first EMA and FDA approved medication for moderate and severe NK in adults. It acts by promoting the growth of corneal nerves, differentiation, proliferation, and migration of corneal epithelial cells and maintaining corneal epithelial limbal stem cells (72–74).

Cenegermin resulted effective in different clinical studies on NK, but only few reports discussed its efficacy in disease related to systemic causes (72, 75–77). In this study, Cenegermin was effective in promoting corneal healing in both moderate and severe NK related to systemic diseases, with improvement of corneal sensitivity and complete recovery of the surface defects. Interestingly the severe forms healed faster with respect to PED. We reported the same results in our recent study when we analyzed the efficacy of Cenegermin in all patients with NK

independently of underlying cause. About this we hypothesized that in ulcers the rh-NGF promotes better stromal healing with restore of the corneal thickness that induces the faster epithelial resurfacing as compared to PED (78–81).

This interesting finding needs further investigation to be confirmed on higher number of treated patients.

It can be concluded that this study emphasizes the crucial relation between NK and systemic diseases and particularly neurological diseases and diabetes emerged as main conditions. Given the high prevalence of these systemic diseases and their socio-economic impact, the prevention and a proper early management of NK is of high importance. We believe that accurate preventing, managing and monitoring of these systemic diseases, can help to reduce the risk of presenting of moderate and severe forms of NK.

Additionally, we demonstrated on our sample that despite the associated systemic pathology, the use of rh-NGF was equally effective in all studied subjects. However, further studies with a larger number of participants are necessary to understand better the relationships between NK presentation and systemic diseases.

DATA AVAILABILITY STATEMENT

The raw data supporting the conclusions of this article will be made available by the authors, without undue reservation.

ETHICS STATEMENT

The studies involving human participants were reviewed and approved by Ethical Committee of the University Hospital of Messina. The patients/participants provided their written informed consent to participate in this study.

AUTHOR CONTRIBUTIONS

GO: conceptualization, writing, review, editing, and data analysis. AM: conceptualization, data collection, and supervisor. AV: data collection and analysis. LI: data collection and original draft preparation. CA, FF, and UC: conceptualization, writing, review, and editing. PA: conceptualization, writing, review and editing, original draft preparation, data analysis, and supervision. All authors contributed to the article and approved the submitted version.

REFERENCES

1. Dua HS, Said DG, Messmer EM, Rolando M, Benitez-Del-Castillo JM, Hossain PN, et al. Neurotrophic keratopathy. *Prog Retin Eye Res.* (2018) 66:107-31. doi: 10.1016/j.preteyeres.2018.04.003

2. Fini ME, Cook JR, Mohan R. Proteolytic mechanisms in corneal ulceration and repair. *Arch Dermatol Res.* (1998) 290:S12-23. doi: 10.1007/PL00007449

3. Tan MH, Bryars J, Moore J. Use of nerve growth factor to treat congenital neurotrophic corneal ulceration. *Cornea.* (2006) 25:352-5. doi: 10.1097/01.ico.0000176609.42838.df

4. Feroze K, Patel B. *StatPearls.* (2019). Available online at: https://www.ncbi.nlm.nih.gov/books/NBK431106/ (accessed November 2, 2021).

5. Bonini S, Rama P, Olzi D, Lambiase A. Neurotrophic keratitis. *Eye.* (2003) 17:989–95. doi: 10.1038/sj.eye.6700616

6. Roszkowska AM, Licitra C, Tumminello G, Postorino EI, Colonna MR, Aragona P. Corneal nerves in diabetes-the role of the *in vivo* corneal confocal microscopy of the subbasal nerve plexus in the assessment of peripheral small fiber neuropathy. *Surv Ophthalmol.* (2021) 66:493–513. doi: 10.1016/j.survophthal.2020.09.003

7. Bonini S, Lambiase A, Rama P, Sinigaglia F, Allegretti M, et al. Phase II randomized, double-masked, vehicle-controlled trial of recombinant human nerve growth factor for neurotrophic keratitis. *Ophthalmology.* (2018) 125:1332–43. doi: 10.1016/j.ophtha.2018.02.022

8. Roszkowska AM, Wylegała A, Gargano R, Spinella R, Inferrera L, Orzechowska-Wylegała B, et al. Impact of corneal parameters, refractive error

and age on density and morphology of the subbasal nerve plexus fibers in healthy adults. *Sci Rep.* (2021) 11:6076. doi: 10.1038/s41598-021-85597-5

9. Sacchetti M, Lambiase A. Diagnosis and management of neurotrophic keratitis. *Clin Ophthalmol.* (2014) 8:571-9. doi: 10.2147/OPTH.S45921

10. Groos EB Jr. Neurotrophic keratitis. In: Krachmer JH, Mannis MJ, Holland EJ, editors. *Cornea: Clinical Diagnosis and Management.* Mosby: St Louis (1997). p. 1340

11. Puca A, Meglio M, Vari R, Tamburrini G, Tancredi A. Evaluation of fifth nerve dysfunction in 136 patients with middle and posterior cranial fossae. *Eur Neurol.* (1995) 35:33–7. doi: 10.1159/000117086

12. Al-Aqaba MA, Dhillon VK, Mohammed I, Said DG, Dua HS. Corneal nerves in health and disease. *Prog Retin Eye Res.* (2019) 73:100762. doi: 10.1016/j.preteyeres.2019.05.003

13. Saad S, Abdelmassih Y, Saad R, Guindolet D, Khoury SE, Doan S, et al. Neurotrophic keratitis: frequency, etiologies, clinical management and outcomes. *Ocul Surf.* (2020) 18:231–6. doi: 10.1016/j.jtos.2019.11.008

14. Ableman TB, Newman SA. Perineural spread of head and neck cancer: ophthalmic considerations. *J Neurol Surg B Skull Base.* (2016) 77:131–9. doi: 10.1055/s-0036-1582239

15. Sánchez Orgaz M, Gonzalez Pessolani T, Pozo Kreilinger JJ, Zamora P, Martí Álvarez C, Boto-de-Los-Bueis A. Orbital and conjunctival metastasis from lobular breast carcinoma. *Orbit.* (2017) 36:197-200. doi: 10.1080/01676830.2017.1310255

16. Solari HP, Ventura MP, Cheema DP, Odashiro AN, Burnier MN Jr. Orbital metastasis from breast carcinoma presenting as neurotrophic keratitis. *Can J Ophthalmol.* (2006) 41:93–6. doi: 10.1016/S0008-4182(06)80075-X

17. Bonzano C, Bonzano E, Cutolo CA, Scotto R, Traverso CE. A case of neurotrophic keratopathy concomitant to brain metastasis. *Cureus.* (2018) 10:e2309. doi: 10.7759/cureus.2309

18. Ibáñez Flores N, Sanz Moreno S. Queratopatía neurotrófica bilateral secundaria a metastasis en tronco del encéfalo [Bilateral neurotrophic keratitis secondary to encephalic trunk metastasis]. *Arch Soc Esp Oftalmol.* (2002) 77:681–4. doi: 10.4321/S0365-66912002001200008

19. Newman SA. Prospective study of cavernous sinus surgery for meningiomas and resultant common ophthalmic complications (An American Ophthalmological Society Thesis) Trans. *Am Ophthalmol Soc.* (2007) 105:392–447.

20. Lam BC, Saboo US, Kheirkhah A. Acute neurotrophic keratitis with trigeminal trophic syndrome after craniotomy. *J AAPOS.* (2020) 24:376–9 doi: 10.1016/j.jaapos.2020.07.011

21. Galvis V, Nino V, Tello A, Grice JM, Gómez MA. Topical insulin in neurotrophic keratopathy after resection of acoustic neuroma *Arch Soc Esp Oftalmol.* (2019) 94:100–4. doi: 10.1016/j.oftale.2018.06.012

22. Kloek CE, Jeng-Miller KW, Jacobs DS, Dunn IF. Prosthetic replacement of the ocular surface ecosystem treatment of ocular surface disease after skull base tumor resection. *World Neurosurg.* (2018) 110:e124–8. doi: 10.1016/j.wneu.2017.10.111

23. Ting DSJ, Rana-Rahman R, Ng JY, Wilkinson DJP, Ah-Kine D, Patel T. Clinical spectrum and outcomes of ocular and periocular complications following external-beam radiotherapy for inoperable malignant maxillary sinus tumors. *Ocul Oncol Pathol.* (2021) 7:36–43. doi: 10.1159/000511011

24. Gozzi F, Tiseo M, Facchinetti F, Gandolfi S, Rubino P. Bilateral severe corneal ulcer in a patient with lung adenocarcinoma treated with gefitinib. *Case Rep Ophthalmol.* (2021) 12:288-92. doi: 10.1159/000514696

25. Sekhon A, Wang JYF, Tan JCH, Holland SP, Yeung SN. Limbal stem cell deficiency secondary to systemic paclitaxel (Taxol) for breast cancer: a case report. *BMC Ophthalmol.* (2020) 20:e400. doi: 10.1186/s12886-020-01672-x

26. Ellies P, Anderson DF, Topuhami A, Tseng SC. Limbal stem cell deficiency arising from systemic chemotherapy. *Br J Ophthalmol.* (2001) 85:373–4. doi: 10.1136/bjo.85.3.371c

27. Ding X, Bishop RJ, Herzlich AA, Patel M, Chan CC. Limbal stem cell deficiency arising from systemic chemotherapy with hydroxycarbamide. *Cornea.* (2009) 28:221–3. doi: 10.1097/ICO.0b013e318183a3bd

28. Hyndiuk RA, Kazarian EL, Schultz RO, Seideman S. Neurotrophic corneal ulcers in diabetes mellitus. *Arch Ophthalmol.* (1977) 95:2193–6. doi: 10.1001/archopht.1977.04450120099012

29. Kara-corlu MA, Cakiner T, Saylan T. Neurotrophic corneal ulcers in diabetes mellitus. *Arch Ophthalmol.* (1977) 95:2193–96.

30. Mansoor H, Tan HC, Lin MT, Mehta JS, Liu YC. Diabetic corneal neuropathy. *J Clin Med.* (2020) 9:3956. doi: 10.3390/jcm9123956

31. Markoulli M, Flanagan J, Tummanapalli SS, Wu J, Willcox M. The impact of diabetes on corneal nerve morphology and ocular surface integrity. *Ocul Surf.* (2018) 16:45–57. doi: 10.1016/j.jtos.2017.10.006

32. Margolis TP. Neurotrophic keratopathy: ophthalmology's diabetic foot problem. *Eye Contact Lens.* (2021) 47:136–9. doi: 10.1097/ICL.0000000000000774

33. Patel SN, Shetlar DJ, Pflugfelder SC. Bilateral candida parapsilosis infiltration of nonhealing indolent epithelial defects in a diabetic patient with neurotrophic keratopathy. *Can J Ophthalmol.* (2018) 53:e224–6. doi: 10.1016/j.jcjo.2018.01.025

34. Wu PY, Chang HW, Chen WL. Neurotrophic keratitis in autoimmune polyglandular syndrome type 1: a case report. *BMC Ophthalmol.* (2021) 21:e17. doi: 10.1186/s12886-020-01770-w

35. Roszkowska AM, Oliverio GW, Aragona E, Inferrera L, Severo AA, Alessandrello F, et al. Ophthalmologic manifestations of primary sjögren's syndrome. *Genes.* (2021) 12:365. doi: 10.3390/genes12030365

36. Nguyen VT, Hwang TN, Shamie N, Chuck RS, McCulley TJ. Amyloidosis-associated neurotrophic keratopathy precipitated by overcorrected blepharoptosis. *Cornea.* (2009) 28:575–6. doi: 10.1097/ICO.0b013e318191bdae

37. Reynolds MM, Veverka KK, Gertz MA, Dispenzieri A, Zeldenrust SR, Leung N, et al. Ocular manifestations of familial transthyretin amyloidosis. *Am J Ophthalmol.* (2017) 183:156.f f doi: 10.1016/j.ajo.2017.09.001

38. de Carvalho Mendes Castenheira AM, Pujol Vives P, Asaad Ammaar M. Neurotrophic keratopathy in a patient with familial amyloidosis. *Arch Soc Esp Oftalmol.* (2017) 92:447–50. doi: 10.1016/j.oftale.2017.07.004

39. Iraha S, Kondo S, Yamaguchi T, Inoue T. Bilateral corneal perforation caused by neurotrophic keratopathy associated with leprosy: a case report. *BMC Ophthalmol.* (2022) 22:e42. doi: 10.1186/s12886-022-02265-6

40. Grzybowski A, Nita M, Virmond M. Ocular leprosy. *Clin Dermatol.* (2015) 33:79–89. doi: 10.1016/j.clindermatol.2014.07.003

41. Bansal S, Myneni AA, Mu L, Myers BH, Patel SP. Corneal sensitivity in chronic inflammatory demyelinating polyneuropathy. *Cornea.* (2014) 33:703–6. doi: 10.1097/ICO.0000000000000145

42. Knickelbein JE, Stefko ST, Charukamnoetkanok P. Neurotrophic keratitis in a patient with disseminated lymphangiomatosis. *Eye Brain.* (2009) 1:1-4. doi: 10.2147/EB.S6957

43. Lin TC, Lin PY, Wang LC, Chen SJ, Chang YM, Lee SM. Intraocular involvement of T-cell lymphoma presenting as inflammatory glaucoma, neurotrophic keratopathy, and choroidal detachment. *J Chin Med Assoc.* (2014) 77:385oc. doi: 10.1016/j.jcma.2014.04.002

44. Amalric P, Bessou P, Vergnes H. Syringomyelia and bilateral corneal perforation caused by neurotrophic keratitis. *Rev Otoneuroophtalmol.* (1964) 36:62–4.

45. Nassiri N, Assarzadegan F, Shahriari M, Norouzi H, Kavousnezhad S, Nassiri N, et al. Vitamin B12 deficiency as a cause of neurotrophic keratopathy. *Open Ophthalmol J.* (2018) 12:7-11. doi: 10.2174/1874364101712010007

46. Paz Moreno-Arrones J, Benítez-Herreros J, Drake-Rodríguez P, Romero-García Tenorio A. Neurotrophic corneal ulcer in an HIV patient. *Arch Soc Esp Oftalmol.* (2011) 86:27–30. doi: 10.1016/S2173-5794(11)70006-8

47. Mandarà E, Brocca D, Pellegrini F, Interlandi E. Topical nerve growth factor for the treatment of neurotrophic keratopathy caused by wallenberg syndrome. *Cornea.* (2021) 41:647–8. doi: 10.1097/ICO.0000000000002928

48. Hipps WM, Wilhelmus KR. Persistent visual loss from neurotrophic corneal ulceration after dorsolateral medullary infarction (Wallenberg syndrome). *J Neuroophthalmol.* (2004) 24:345–6. doi: 10.1097/00041327-200412000-00015

49. Pellegrini F, Interlandi E, Cuna A, Mandarà E, Lee AG. Corneal involvement in wallenberg syndrome: case report and literature review. *Neuroophthalmology.* (2019) 44:54olo doi: 10.1080/01658107.2019.1602147

50. Mantelli F, Lambiase A, Sacchetti M, Orlandi V, Rosa A, Casella P, et al. Cocaine snorting may induce ocular surface damage through corneal sensitivity impairment. *Graefes Arch Clin Exp Ophthalmol.* (2015) 253:765–72. doi: 10.1007/s00417-015-2938-x

51. Donaghy M, Hakin RN, Bamford JM, Garner A, Kirkby GR, Noble BA, et al. Hereditary sensory neuropathy with neurotrophic keratitis. Description of an autosomal recessive disorder with a selective reduction of small myelinated

nerve fibres and a discussion of the classification of the hereditary sensory neuropathies. *Brain*. (1987) 110:563-83. doi: 10.1093/brain/110.3.563

52. Bhaskar PA. Hereditary sensory neuropathy (HSN) type I with neurotrophic keratitis. *J Assoc Physicians India*. (1986) 34:379–81.

53. Bowe BE, Levartovsky S, Eiferman RA. Neurotrophic corneal ulcers in congenital sensory neuropathy. *Am J Ophthalmol*. (1989) 107:303-4. doi: 10.1016/0002-9394(89)90324-3

54. Sethi A, Ramasubramanian S, Swaminathan M. The painless eye: neurotrophic keratitis in a child suffering from hereditary sensory autonomic neuropathy type IV. *Indian J Ophthalmol*. (2020) 68:2270–2. doi: 10.4103/ijo.IJO_2101_19

55. Jarade EF, El-Sheikh HF, Tabbara KF. Indolent corneal ulcers in a patient with congenital insensitivity to pain with anhidrosis: a case report and literature review. *Eur J Ophthalmol*. (2002) 12:60–5. doi: 10.1177/112067210201200112

56. John D, Thomas M, Jacob P. Neurotrophic keratitis and congenital insensitivity to pain with anhidrosis–a case report with 10-year follow-up. *Cornea*. (2011) 30:100–2. doi: 10.1097/ICO.0b013e3181e458e4

57. Yagev R, Levy J, Shorer Z, Lifshitz T. Congenital insensitivity to pain with anhidrosis: ocular and systemic manifestations. *Am J Ophthalmol*. (1999) 127:322–6. doi: 10.1016/S0002-9394(98)00370-5

58. Indo Y. NTRK1 congenital insensitivity to pain with anhidrosis. In: Adam MP, Ardinger HH, Pagon RA, Wallace SE, Bean LJH, Gripp KW, et al. editors. *GeneReviews®*. Seattle, WA: University of Washington (1993–2022).

59. Chao J, Rao R, Gupta C. Gómez-López-Hernández syndrome: a case report on pediatric neurotrophic corneal ulcers and review of the literature. *J AAPOS*. (2021) 25:373–5. doi: 10.1016/j.jaapos.2021.08.299

60. Pastor-Idoate S, Carreño E, Tesón M, Herreras JM. Gómez-López-Hernández syndrome: another consideration in corneal neurotrophic ulcers. *Eur J Ophthalmol*. (2012) 22:826–9. doi: 10.5301/ejo.5000138

61. Rollon-Mayordomo A, Mataix-Albert B, Espejo-Arjona F, Herce-Lopez J. Lledo- Villar L, Caparros-Escudero C, et al. Neurotrophic keratitis in a pediatric patient with goldenhar syndrome and trigeminal aplasia successfully treated by corneal neurotization. *Ophthalmic Plast Reconstr Surg*. (2022) 38:e49–51. doi: 10.1097/IOP.0000000000002086

62. Olavarri González G, García-Valcarcel González B, Baeza Autillo A, Balado Vazquez P. Neurotrophic keratopathy secondary to trigeminal nerve aplasia in patient with goldenhar syndrome. *Arch Soc Esp Oftalmol*. (2016) 91:191–4. doi: 10.1016/j.oftale.2016.03.002

63. Kamal SM, Riccobono K, Kwok A, Edmond JC, Pflugfelder SC. Unilateral pediatric neurotrophic keratitis due to congenital left trigeminal nerve aplasia with PROSE (prosthetic replacement of the ocular surface ecosystem) treatment. *Am J Ophthalmol Case Rep*. (2020) 20:100854. doi: 10.1016/j.ajoc.2020.100854

64. Ohana M, Lipsker D, Chaigne D, Speeg-Schatz C, Sauer A. Unilateral ulceration of the cornea secondary to congenital trigeminal nerve agenesis. *Eur J Ophthalmol*. (2015) 25:e35–7. doi: 10.5301/ejo.5000552

65. Scanzera AC, Shorter E. Case series: management of neurotrophic keratitis from familial dysautonomia. *Optom Vis Sci*. (2018) 95:678–81. doi: 10.1097/OPX.0000000000001255

66. Agresta A, Fasciani R, Padua L, Petroni S, La Torraca I, Dickmann A, et al. Corneal alterations in Crisponi/CISS1 syndrome: a slit-lamp biomicroscopy and *in vivo* confocal microscopy corneal report. *Ophthalmic Genet*. (2017) 38:83–7. doi: 10.3109/13816810.2015.1137326

67. Jabbour S, Harissi-Dagher M. Recessive mutation in a nuclear-encoded mitochondrial tRNA synthetase associated with infantile cataract, congenital neurotrophic keratitis, and orbital myopathy. *Cornea*. (2016) 35:894–6. doi: 10.1097/ICO.0000000000000847

68. Inferrera L, Aragona E, Wylegała A, Valastro A, Latino G, Postorino EI, et al. The role of Hi-Tech devices in assessment of corneal healing in patients with neurotrophic keratopathy. *J Clin Med*. (2022) 11:1602. doi: 10.3390/jcm11061602

69. Feroze KB, Patel BC. Neurotrophic keratitis. In: Hauber S, editor. *StatPearls*. Treasure Island, FL: StatPearls Publishing (2022).

70. Dhillon VK, Elalfy MS, Al-Aqaba M, Gupta A, Basu S, Dua HS. Corneal hypoesthesia with normal sub-basal nerve density following surgery for trigeminal neuralgia. *Acta Ophthalmol*. (2016) 94:e6–10. doi: 10.1111/aos.12697

71. Oliverio GW, Spinella R, Postorino EI, Inferrera L, Aragona E, Aragona P, et al. Safety and tolerability of an eye drop based on 0.6% povidone-iodine nanoemulsion in dry eye patients. *J Ocul Pharmacol Ther*. (2021) 37:90–6. doi: 10.1089/jop.2020.0085

72. Blanco-Mezquita T, Martinez-Garcia C, Proença R, Zieske JD, Bonini S, Lambiase A, et al. Nerve growth factor promotes corneal epithelial migration by enhancing expression of matrix metalloprotease-9. *Investig Ophthalmol Vis Sci*. (2013) 54:3880–90. doi: 10.1167/iovs.12-10816

73. Joo MJ, Yuhan KR, Hyon JY, Lai H, Hose S, Sinha D, et al. The effect of nerve growth factor on corneal sensitivity after laser in situ keratomileusis. *Arch Ophthalmol*. (2004) 122:1338–41. doi: 10.1001/archopht.122.9.1338

74. Lambiase A, Bonini S, Aloe L, Rama P, Bonini S. Antiinflammatory and healing properties of nerve growth factor in immune corneal ulcers with stromal melting. *Arch Ophthalmol*. (2000) 118:1446–49. doi: 10.1001/archopht.118.10.1446

75. Roszkowska AM, Inferrera L, Aragona E, Gargano R, Postorino EI, Aragona P. Clinical and instrumental assessment of the corneal healing in moderate and severe neurotrophic keratopathy treated with rh-NGF (Cenegermin). *Eur J Ophthalmol*. (2022) 27:11206721221097584. doi: 10.1177/11206721221097584

76. Lambiase A, Rama P, Bonini S, Caprioglio G, Aloe L. Topical treatment with nerve growth factor for corneal neurotrophic ulcers. *N Engl J Med*. (1998) 338:1174cal doi: 10.1056/NEJM199804233381702

77. Pflugfelder SC, Massaro-Giordano M, Perez VL, Hamrah P, Deng SX, Espandar L, et al. Topical recombinant human nerve growth factor (cenegermin) for neurotrophic keratopathy: a multicenter randomized vehicle-controlled pivotal trial. *Ophthalmology*. (2020) 127:14phic doi: 10.1016/j.ophtha.2019.08.020

78. Scorolli L, Meduri A, Morara M, Scalinci SZ, Greco P, Meduri RA, et al. Effect of cysteine in transgenic mice on healing of corneal epithelium after excimer laser photoablation. *Ophthalmologica*. (2008) 222:380–5. doi: 10.1159/000151691

79. Scalinci SZ, Scorolli L, Meduri A, Grenga PL, Corradetti G, Metrangolo C. Effect of basic fibroblast growth factor and cytochrome c peroxidase combination in transgenic mice corneal epithelial healing process after excimer laser photoablation. *Clin Ophthalmol*. (2011) 5:215–21. doi: 10.2147/OPTH.S16866

80. Meduri A, Scorolli L, Scalinci SZ, Grenga PL, Lupo S, Rechichi M, et al. Effect of the combination of basic fibroblast growth factor and cysteine on corneal epithelial healing after photorefractive keratectomy in patients affected by myopia. *Indian J Ophthalmol*. (2014) 62:424–8. doi: 10.4103/0301-4738.119420

81. Meduri A, Aragona P, Grenga PL, Roszkowska AM. Effect of basic fibroblast growth factor on corneal epithelial healing after photorefractive keratectomy. *J Refract Surg*. (2012) 28:220–3. doi: 10.3928/1081597X-20120103-02

Conflict of Interest: The authors declare that the research was conducted in the absence of any commercial or financial relationships that could be construed as a potential conflict of interest.

Publisher's Note: All claims expressed in this article are solely those of the authors and do not necessarily represent those of their affiliated organizations, or those of the publisher, the editors and the reviewers. Any product that may be evaluated in this article, or claim that may be made by its manufacturer, is not guaranteed or endorsed by the publisher.

Check for updates

Challenges in Age-Related Macular Degeneration: From Risk Factors to Novel Diagnostics and Prevention Strategies

Marco Lombardo [1,2]*, Sebastiano Serrao [1,2] and Giuseppe Lombardo [2,3]*

[1] *Studio Italiano di Oftalmologia, Rome, Italy,* [2] *Vision Engineering Italy srl, Rome, Italy,* [3] *CNR-IPCF, Istituto per i Processi Chimico-Fisici, Messina, Italy*

Age-related macular degeneration (AMD) is a chronic multifactorial eye disease representing the primary cause of vision loss in people aged 60 years and older. The etiopathogenesis of the disease remains uncertain, with several risk factors contributing to its onset and progression, such as genotype, aging, hypertension, smoking, overweight, and low dietary intake of carotenoids. Since the aging populations of the industrialized world are increasing rapidly, the impact of AMD in the socio-economical life-developed countries is expected to increase dramatically in the next years. In this context, the benefits of prevention and early disease detection for prompt and effective treatment can be enormous to reduce the social and economic burden of AMD. Nutritional and lifestyle changes, including dietary intake of xanthophyll pigments, such as lutein and zeaxanthin, no smoking, and regular exercise, are known to protect from risk of AMD progression from early to advanced disease stages. In this review, we present the clinical outcomes of a pilot study on trans-scleral iontophoresis delivery of lutein in patients with AMD. Topical delivery of lutein directly to the macula may provide a more efficient method for enriching the macular pigment and for achieving greater patient compliance to therapy than oral administration and thus enhancing prevention strategies. Modern diagnostic methodologies shall address the major problem of accurately detecting the risk of transition from intermediate AMD to advanced AMD stages. Adaptive optics retinal imaging and resonance Raman spectroscopy are two highly promising technologies for the objective assessment of patients with AMD. In this review, we present some of their clinical applications for collecting quantitative measurements of retinal cellular changes and macular content of xanthophyll pigments, respectively. In conclusion, there is great expectation that technological advancements in AMD management will deliver improved screening, therapeutic prevention, and diagnostic systems in the coming decade through a pro-active strategy of "treatment for prevention" that will aim to reduce the global burden of vision loss caused by AMD in the elderly.

Keywords: age-related macular degeneration (AMD), lutein, adaptive optics, Resonance Raman (RR) spectroscopy, prevention

INTRODUCTION

An aging population is much more susceptible than younger people to many health problems, including eye diseases. The aging of the population in the world will experience a substantial increase in the size of the population aged 65 years or over by 2030, a population that accounts for the highest incidence and prevalence of eye diseases (1).

Age-related macular degeneration (AMD) is a chronic progressive disease and among the leading causes of low vision and legal blindness worldwide in people older than 60 years (2). Clinically, AMD is classified in early (Stages 1 and 2), intermediate (Stage 3), and late (Stage 4) stages according to the signs and symptoms complained by the subjects (3). Impairment of visual function starts in intermediate AMD and progresses to late AMD with vision-threatening complications like neovascularization (neovascular or "wet" AMD) or "geographic atrophy" ("dry" AMD) of the central retina (i.e., the macula). Late-stage AMD, the most severe form of the pathology, is present in about 5% of the over 65's and 12% of the over 80's (4, 5). According to the *Retinal Disease Panel of the National Plan for Eye and Vision Research* (6), AMD represents ∼90% of cases of blindness in people aged 60 years or older. Vision loss caused by advanced stages of AMD has profound human and socioeconomic consequences in all societies. The costs of productivity loss and of rehabilitation for blindness constitute a significant economic burden for an individual, the family, and society globally (7–9). Of note, 30% of persons with advanced AMD also have clinical depression (10).

The focus of most research and development activities on AMD is aimed at evaluating the cost effectiveness of treatments of the neovascular forms. On the other hand, more effective strategies of secondary prevention for slowing down or halting AMD progression would be highly desirable. To be clinically efficient, such activities should require:

1) the identification of patients at higher risk of disease progression, and
2) the development of novel diagnostic technologies and treatment for preventing progression from intermediate to advanced AMD stages.

Addressing both issues can greatly benefit patients and society.

AMD is a multifactorial eye disease with several risk factors contributing to its onset and progression, such as genotype, aging, hypertension, hypercholesterolemia, smoking, overweight, and low dietary intake of vegetables, fish, and fruits. However, it has been shown that almost all patients with AMD could benefit from a healthy lifestyle, with those with a high genetic risk, showing the strongest risk reduction (10, 11). A high dietary intake of vegetables, fish, and fruits and no smoking have been shown to halve the risk of progression to late AMD in comparison with patients with an unfavorable lifestyle (11, 12). Current knowledge of the beneficial role of lifestyle on AMD progression shall drive clinicians and local authorities to more rigorous measures for prevention through behavioral change of populations. For example, high plasma concentration of xanthophyll pigments, such as lutein and zeaxanthin, has been associated with a 37% reduced risk to progress to late stage AMD in a prospective study (*Alienor study*) on 609 patients followed up to 7 years (13). Lutein and zeaxanthin accumulate physiologically in the macula and, by absorbing blue light, prevent the generation of reactive oxygen species (ROS) that can damage photoreceptor and retinal pigment epithelium (RPE) cells (14). Several clinical trials, including the *AREDS2*, *CAREDS*, and *Blue Mountain Eye Study*, have reported that regular and high dietary lutein and zeaxanthin intake reduces the risk of AMD progression (15–17). On the other hand, there are some barriers that halt clinicians to support prevention strategies that promote xanthophylls supplementation mainly caused by limits of current oral supplementation methodologies as well as of diagnostics technologies for measuring macular pigments. Efficacy of prevention strategies shall be assessed by sensitive and accurate diagnostic methodologies in order to measure objectively their beneficial action on disease progression along a clinically relevant time scale. For example, high-resolution ophthalmic devices for imaging the retina at the cellular level would be desirable for investigating pathologic tissue changes with micrometer accuracy and for tracking response to prevention strategies in advance with respect to current diagnostic tools. Adaptive optics retinal imaging has the potential to establish a novel methodology for screening patients at risk of AMD progression and to monitor the therapeutic effect of prevention strategies (18). In addition, diagnostic tools for measuring the xanthophyll pigments *in situ* would be desirable for elucidating and assessing the protective effect of prevention strategies based upon supplementation with lutein.

In this review, we provided the state-of-the-art knowledge about risk factors and prevention strategies for AMD and further presented former clinical outcomes on novel diagnostic and prevention methodologies for addressing one of the major needs in the management of AMD, which is to prevent vision loss in patients at higher risk of AMD progression.

GLOBAL IMPACT OF AMD

According to World Health Organization (WHO), more than 8 million people suffer from vision impairment caused by age-related macular degeneration (2); since AMD prevalence is directly related to age, and since the aging populations of the industrialized world are increasing rapidly, the impact of AMD on the socio-economical life in developed countries is expected to increase dramatically in the next years.

The prevalence and potential risk factors in late-stage AMD are similar across western and eastern countries, with higher prevalence in Chinese people than other ethnic groups (19). In a meta-analysis study (4), AMD has been estimated to be present in 0.2% of the population aged 55–64 years, rising to 13% of the population older than 85 years. Prevalence of neovascular AMD increases from 0.1% among subjects younger than 64 years to about 6% for those older than 85 years. Prevalence of pure geographic atrophy (GA) increases from 0.04 to 4.2% for these age groups. Based on the results of a systematic review (20), 30–50 million people suffer from any type of AMD globally.

Conservatively, Europe accounts for 31% of global cases of AMD with a mean projected number of 17 million people that are living with AMD, of which 2.5 million cases have AMD Stages 3 and 4, and the number is expected to rise more than 30% by 2040 (21). A multinational study on AMD economic burden found that the average annual total cost for single patient with neovascular AMD varied from €5.300 in the United Kingdom to about €12.500 in Germany (9). Global cost of visual impairment due to AMD has been estimated to be €343 billion, excluding home health care costs and productivity losses (22, 23). A specific study estimating the productivity loss (i.e., loss of employment and loss of salary) caused by AMD has estimated that the total loss in gross domestic profit in the US due to dry AMD is, averagely, $24 billion (24). In the next decades, these values are expected to largely increase with projected demographic shifts (25). According to the United Nations predictions, the number of people aged over 60 will triple from 600 million worldwide in 2000 to 2 billion by 2050. The increase in the population aged over 80 is expected to be more than 5-fold, from 70 million in 2000 to 380 million by 2050 (26). In this context, the socioeconomic benefits of effective strategies for primary and secondary prevention of AMD could be enormous.

RISK FACTORS

AMD is a multifactorial disease with numerous inherited and environmental risk factors contributing to its onset and progression. The non-modifiable risk factors include the inheritance of major genetic loci of AMD-associated genetic variants, local traits, such as darker iris pigmentation and hyperopic refraction, and aging (27–31). Overall, genes influence several pathological processes related to AMD, including the mechanisms involving collagen and glycosaminoglycans synthesis, angiogenesis, and the immune processes. All these factors have been associated with the onset and progression from early to intermediate, and advanced stages of AMD (27, 28). There are several known AMD-associated genetic variants (29), and some of them have been targeted by interventional clinical trials (30). The genetic contribution of the complement pathway (CFH, CFI, C9, C2, TMEM97/VTN, and C3 genes) and ARMS2 to AMD Stage 4 has been found to explain 90% of the overall genetic risk in a population of 17,000 patients (31). Gene therapy for AMD Stage 4 (either for treating "dry" or "wet" AMD) is, indeed, currently being explored. Several clinical trials are testing safety and efficacy of gene augmentation for endogenous production of soluble inhibitors of vascular endothelial growth factors (VEGFs), utilizing viral vectors delivered *via* an intravitreal injection. Genetic susceptibility is, however, influenced by the environmental factors; together, both factors can be highly predictive of the onset, progression, and response to treatments (32). In this view, strategies to minimize the influence and impact of environmental factors can greatly benefit to reduce the social burden of AMD. The modifiable risk factors include cardiovascular diseases, obesity, smoking, and sunlight exposure (33). Lack or poor physical activity rises the risk for several metabolic and vascular diseases and has been correlated with the progression of some cases of AMD (34). Several clinical trials have evidenced the beneficial role of nutrition (fish, fruits, and vegetables) and nutritional supplements (35). A healthy diet, avoiding food rich in sugar, fat, alcohol, and oils, was associated with reduced occurrence of early and/or advanced AMD (36). Absence of smoking and moderate physical activity (i.e., regular low-intensity exercise) have been also demonstrated to provide a protective role in AMD disease progression. In conclusion, the adoption of healthy lifestyles may benefit significantly populations, particularly those at genetic/family risk. Public health interventions promoting plant-rich diets, physical activity, and avoiding smoking and sedentary behavior would be highly recommendable strategies for AMD prevention. Current scientific and clinical evidence shows that supplementation with xanthophylls, lutein, and zeaxanthin can be of particular importance to prevent progression from early- to late-stage AMD (34). The protective effect of daily intake of several other supplements, which may have a role in slowing down disease progression, such as zinc (with xanthophylls), folate, curcumin, saffron, and goji berry, is under study (35). The protective role of beta-carotene, omega-3 fatty acids (DHA, EPA), vitamin A, vitamin C, and vitamin E against AMD progression has not been supported by epidemiological studies (14, 35).

PREVENTION STRATEGIES

Antioxidant and Protective Effect of Lutein

Lutein is a dietary carotenoid from the xanthophyll family of carotenoids. Lutein and its isomer zeaxanthin are the main components of human retina's macular pigment. In the normal human retina, the concentration of these carotenoids is the highest across the foveal area, decreasing exponentially as distance increases from the fovea. The ratio of lutein to zeaxanthin is 1:2 in the macula and 2:1 in the peripheral retina; lutein is, therefore, 2.5–3 times more concentrated in the macula than the peripheral retinal region.

The main physiological functions ascribed to the macular carotenoids are:

1) a shielding effect protecting the retinal photoreceptor's membrane system against potentially harmful, short-wavelength radiation.
2) protection against photo-induced damage of the retinal photoreceptor's membrane system.

Nature has used xanthophyll pigments as an effective protector, capable of both absorbing damaging blue light and inhibiting the formation of ROS and neutralizing photosensitizers (37–39). The reason why xanthophylls accumulate selectively in these areas of the central retina is not yet fully elucidated. According to the most supported hypothesis, xanthophylls transversely incorporate in the lipid-bilayer portion of membranes of the human retina through xanthophyll-binding proteins (40, 41). These membrane-associated, xanthophyll-binding proteins bind lutein (and zeaxanthin) with high specificity and affinity. The highest concentration of lutein and zeaxanthin is detected in the Henle fiber layer in the foveal region (2/3 of total) and

in the photoreceptors' outer segment (1/3 of total) (42–44). The precise location of macular xanthophylls across the retina has been associated with specific functions aiming at protecting the retinal photoreceptors from oxidative damage (45, 46). The main physiological function ascribed to the inner retinal macular carotenoids is the protection of the retinal photoreceptors from photo-induced damage caused by harmful short-wavelength radiation by means of a shielding effect. The function of the outer retinal xanthophyll pigments as antioxidants and quenchers of ROS has been related to their physical interaction with the cell membrane lipid-bilayer and their membrane localization and accumulation in the bulk domain of the photoreceptor outer segment (POS) membrane.

Lutein absorbs blue light, with a maximum absorption peak at 460 nm (37, 47). This is the most phototoxic visible light to which the retina is routinely exposed, rendering lutein and zeaxanthin efficient physical quenchers of this harmful light, blocking the production of singlet oxygen and related ROS (38). Therefore, the oxygen deactivation property of lutein is a consequence of its ability to absorb blue light *via* the unconjugated double bonds present in the molecule. In addition, xanthophylls are selectively accumulated in the bulk domain of the POS membrane, which is rich in long-chain polyunsaturated fatty acids, including docosahexaenoic acid (DHA). Rhodopsin, which is the main protein of POS membranes (90% of all proteins in these membranes) and is responsible for the first stages of visual signal transduction, is also located in the POS membrane bulk domain. Rhodopsin requires the presence of polyunsaturated lipids for its activity; on the other hand, co-localization of rhodopsin with polyunsaturated phospholipids creates a dangerous situation for both, especially during illumination, when ROS are produced by photosensitizers (i.e., all-trans-retinal) (48). Such a selective accumulation of macular xanthophylls in domains rich in vulnerable unsaturated lipids is, therefore, ideal, given their photoprotective action. Reacting as antioxidant with free radicals and ROS, lutein protects the retinal photoreceptors against peroxidation and photo-damage.

Beyond acting as a blue-light filter and efficient quenchers of ROS, macular xanthophylls may also enhance vision contrast by reducing chromatic aberrations, glare disability, and light scattering (49–52).

According to current knowledge, the antioxidant and protective activities of lutein could be related to its effects on the physical properties of lipid bilayer membranes in the Henle fiber layer and the bulk domain of the POS in the foveal region (41, 45, 48, 50). Lutein is able to quench singlet oxygen by two different mechanisms. The first mechanism, which involves energy transfer, is called *physical quenching*. According to this mechanism, lutein deactivates singlet oxygen to the non-reactive triplet state. The second mechanism, which, however, contributes <0.05% to the overall singlet oxygen quenching by carotenoids, is called *chemical quenching* and involves a chemical reaction between carotenoid and singlet oxygen, which results in pigment auto-oxidation.

Oral Supplementation of Lutein

Lutein is not synthetized by the human body and can only be absorbed from a vegetable-rich diet. The daily dietary intake of lutein ranges from 0.5 to 4 mg in the western world (53, 54). Following normal dietary ingestion, the plasma lutein concentration ranges between 0.13 and 0.18 µM (i.e., between 0.07 and 0.10 µg/ml).

In several controlled epidemiological studies, dietary intake of lutein and its isomer zeaxanthin was associated with protection from risk of AMD progression. The *Eye Disease Case Control Study* has found the risk for advanced AMD was reduced by more than 40% in patients in the highest quintile of dietary carotenoid intake (> 6 mg/day) when compared to those in the lowest quintile (Odd Ratio, OR:0.57) (55, 56). The *Carotenoids in Age-Related Eye Disease Study* (*CAREDS*) concluded that lutein- and zeaxanthin-rich diets could protect against intermediate AMD in female participants <75 years of age (19). The *Blue Mountain Eye Study* reported that high dietary xanthophylls intake reduces the risk of AMD progression over 5–10 years (18, 57), patients in the top tertile of intake (≥1 mg/day) had a decreased risk of incident neovascular AMD, and those with above median intakes (743 µg/day) had a reduced risk of indistinct soft or reticular drusen when compared with the remaining population. In the *Age-Related Eye Disease Study* (*AREDS*), dietary xanthophylls intake (as determined by a food habit questionnaire at enrollment) was inversely associated with neovascular AMD (OR: 0.65), geographic atrophy (OR: 0.45), and large or extensive intermediate drusen (OR: 0.73) when the highest vs. lowest quintiles were compared (58).

An increase in dietary intake of lutein has been shown to raise its level in the plasma, which could provide a higher protection against photo-damage in human subjects at risk of AMD progression (16, 59). There is evidence that, after 1–2 months of daily supplementation, plasma levels of lutein stay at a higher level than the baseline while the supplementation continues; as supplementation is discontinued, plasma concentration of lutein decreases within 1–4 months to the pre-treatment level (60). Following 10-mg daily oral supplementation of lutein (the most common dose in commercial product), lutein plasma concentration has been shown to increase 3–5 times more than baseline values in healthy adults and subjects suffering from AMD (48, 60, 61). The increase of plasma lutein concentration has shown a significant correlation with the macular pigment optical density (MPOD), which has been estimated to increase to 5% (over a 1.5-degree area) in comparison with baseline measurements (**Table 1**). The MPOD is a measurement of the attenuation of blue light by macular pigments and is considered as an indirect measure of the amount of macular lutein and zeaxanthin in the macula.

AREDS2 study enrolled 4.203 participants, aged 50–85, with intermediate AMD in both eyes, or intermediate AMD in one eye and advanced AMD in the fellow eye. The main study outcome has shown that lutein and zeaxanthin intake resulted in a 10% reduction of progression to advanced AMD (Hazard Ratio; HR: 0.90; $p = 0.04$) (62). Further analysis has shown that the participants with low dietary intake of lutein and zeaxanthin at

TABLE 1 | Clinical data on the effect of regular oral daily supplementation of lutein (10 mg).

Baseline plasma concentration of lutein	Plasma concentration of lutein after 1–2 months of oral supplementation	Increase of Macular Pigment Optical Density (MPOD; 400 × 400 μm area) after oral supplementation
0.13–0.18 μM (0.07–0.10 mg)	0.3–0.9 μM (0.17–0.5 mg)	5% greater than baseline

the start of the study, supplemented with an AREDS formulation, were 25% less likely to develop AMD Stage 4 than the patients with similar dietary intake who did not receive lutein and zeaxanthin (4). In a pre-specified comparison between patients with AMD receiving lutein/zeaxanthin vs. those who did not receive this supplementation, a 10% reduction in the risk for progression to late AMD has been recorded (4, 63).

Considering the overall supporting science on safety of dietary supplements of lutein (10–20 mg/day) for reducing the risk of progression from early to advanced AMD stages, supplementation may be a cost-effective approach for patients with AMD to reduce future impairment and disability. Nevertheless, compliance of patients to oral supplementation is still limited (64). This is mainly due to the type of administration and the requirement of daily intake of the therapy for prolonged time (theoretically, the supplementation should not be stopped). Another factor that significantly affects the efficacy of oral supplementation in increasing macular lutein content is the limited absorption of this carotenoid through the digestive route. Lutein is transported in the plasma *via* lipoproteins, primarily HDLs (52%) and, secondarily, by LDLs (22%) (64, 65). Lutein and zeaxanthin associate more closely with HDL, and it has been theorized that only a small proportion (2.5%) of HDL might be responsible for transporting lutein and zeaxanthin to the retina (66). The plasma concentration varies considerably among individuals and may be influenced by several factors involved in its absorption and plasma transport (type of lutein, duration of lutein intake, amount of fat in the diet, concomitant ingestion of fibers, genetic factors, age, etc.). In addition, it has been shown that substantial increase in macular pigments can be found only after at least 3 months of oral supplementation (38, 62, 67), so it would be important to implement new strategies to enrich the macular pigment faster than current mainstream method and to improve patients' compliance to therapy.

Topical Delivery of Lutein

Iontophoresis is a non-invasive technique widely used in medical practice to deliver a charged molecule from a liquid formulation to a target tissue through the application of a low-intensity electric current (68). During iontophoresis, the current applied to an active electrode located in the ocular (either corneal or scleral) applicator flows to a passive electrode placed on the periorbital skin, thus promoting the movement of the charged liquid formulation and enabling the therapeutic molecule to penetrate in the ocular tissues (69).

Recent studies (70, 71) have provided preclinical and clinical data on a novel scleral iontophoresis device for delivering a lutein-enriched liquid formulation directly to the retina. The 0.1% lutein ophthalmic formulation was composed of FloraGLO® crystalline lutein (Kemin Food L.C., Des Moines, IA, USA) encapsulated in positively charged liposomes using phospholipon 90H (Lipoid GmbH, Ludwigshafen, Germany), octadecylamine (Sigma-Aldrich, Saint Louis, MO, USA), and distilled water. The scleral iontophoresis device consisted of a generator, an applicator with the active electrode, which is filled with the lutein liquid formulation, and a return, passive, electrode. The generator's current was set at 2.5 mA and was delivered for a total 4 min.

In a first *ex vivo* study (70), two-photon microscopy has been used to quantify the amount of lutein, reaching the macular region in the human retina of eye bank donor eyes after scleral iontophoresis. Analysis of the two-photon emission fluorescence (TPEF) intensity signal collected in the fluorescence band spectrum of lutein was done in order to evaluate the increase of such a signal in samples that underwent iontophoresis in comparison with controls. Six eye globes, from different donors, were used for experiments, four of which underwent trans-scleral iontophoresis delivery of lutein and two eyes were used as controls. Details of study methodology can be found in **Supplementary Material** (72).

One hour after iontophoresis, features consistent with lutein-enriched liposomes were found both in the central and peripheral retina of treated eyes (**Figure 1**). Imaging of retinal pigment epithelial (RPE) cells and choroid did not show any lutein-enriched liposomes (**Figure 2**). A higher TPEF intensity level in the fluorescence band spectra of lutein was found in the macular region of treated eyes in comparison with controls (**Figure 3**); the greater differences between treated eyes and controls were found in the retinal layers between the photoreceptors and Henle's fibers. This was not surprising, because, in normal eyes, lutein is mainly concentrated in the photoreceptors' outer segments (both in the peripheral retina and macula) and the inner retina (only in the macula).

The concentration of lutein was estimated to be 21 μM in controls; this value was equated to the integral of the TPEF intensity signal of controls (i.e., the area under the orange curve in **Figure 3**). The increase of lutein after scleral iontophoresis was calculated as the ratio between the two areas, which were subtended by the TPEF signals of treated eyes (the area under the blue curve in **Figure 3**) and controls (the area under the orange curve in **Figure 3**). The concentration of macular lutein was 40 μM 1 h after iontophoresis, thus increasing the amount of lutein in the macula of 1.9 times in comparison with the baseline. The results are summarized in **Table 2**.

In a second *ex vivo* experiment (71), resonant Raman spectroscopy (RRS) was used to confirm efficacy of scleral iontophoresis delivery of the positively charged lutein solution to the human retina in eye bank donor human eye globes. Resonance Raman spectroscopy is a vibrational spectroscopy technique that is commonly used to identify and quantify chemical compounds. Carotenoid molecules are especially suitable for Raman measurements since they can be excited with
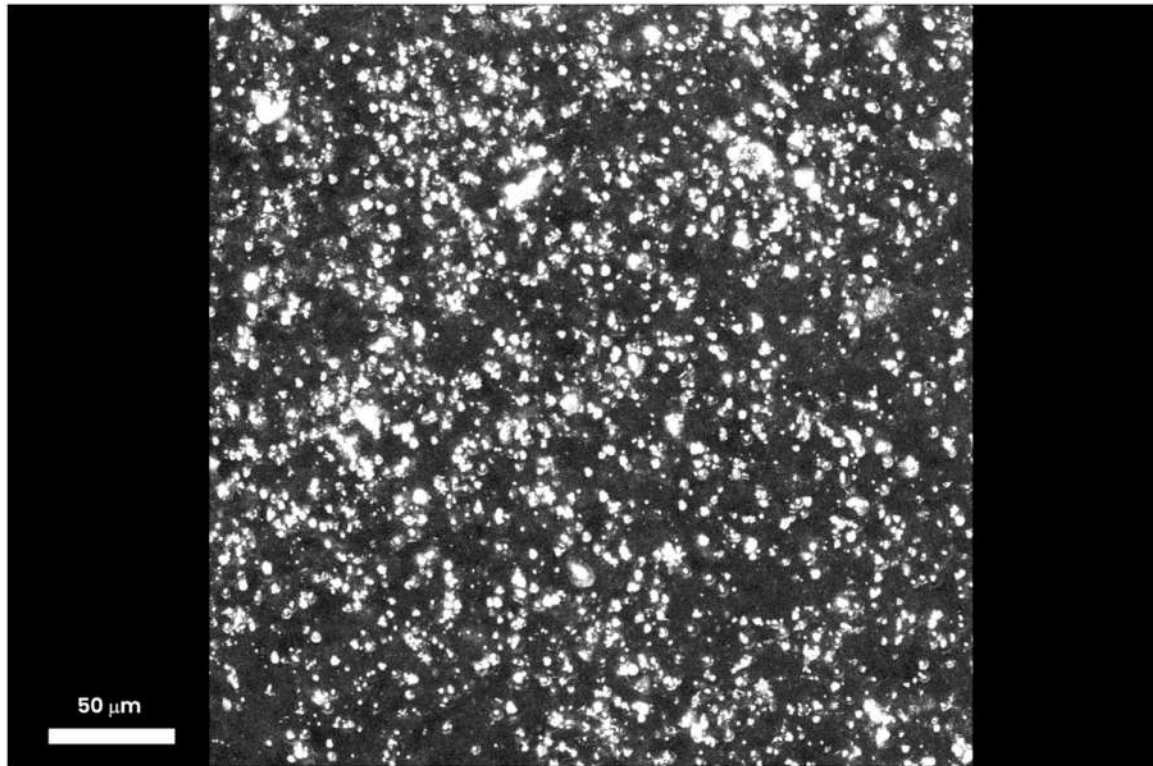
FIGURE 1 | Three-dimensional projection stack of the macular area, showing several particles ($\geq 5\,\mu m$), which emit a TPEF signal corresponding to lutein-enriched liposomes. One hour after trans-scleral iontophoresis, the lutein-enriched liposomes were spread throughout the outer and inner retinal depth; the major differences of the TPEF signal generated by exogenous lutein were found in the retinal layers between the photoreceptors and Henle's fibers. Scale bar: $50\,\mu m$.

light overlapping their visible absorption bands (73, 74). When excited by blue light, these molecules exhibit a strong resonance Raman scattering response, enabling to detect their characteristic vibrational energy levels through their corresponding spectral fingerprint signature even in living human tissues.

In this study, a purpose-developed RRS was used for detecting lutein in human ocular tissues. Eight eye globes from different donors were used for experiments; six of which underwent trans-scleral iontophoresis delivery of lutein, and the remaining two eyes were used as controls. Details of study methodology can be found in **Supplementary Material**.

One hour after iontophoresis, the inner sclera, choroid, and retinal periphery were greatly enriched with lutein in treated eyes ($p < 0.05$); no lutein was found in the same ocular regions of non-treated samples. In the same period, the average concentration of lutein in the macula of treated samples was 1.3 times greater than controls (**Figure 4**). The results are summarized in **Table 3**.

In conclusion, both *ex vivo* studies on eye bank human donor eyes have provided clear indication that scleral iontophoresis of a positively charged lutein liquid formulation could be effective in enriching the macular pigment of the human eye in few minutes.

Pilot Clinical Study on Scleral Iontophoresis Delivery of Lutein

A pilot study was performed by the present authors to confirm safety and to assess tolerability in patients with AMD. The study followed the tenets of the declaration of Helsinki, and all the patients signed written informed consent after full explanation of the procedure. The study was granted exemption because no investigational method or device was used on patients (i.e., the scleral iontophoresis and the lutein liquid formulation were already CE certified before commencing the study). The inclusion criteria were the patients older than 40 years old, both genders, with a diagnosis of AMD with drusen (Stages 2 and 3) or neovascular AMD (Stage 4) in either eye and a corrected distance visual acuity (CDVA) ≤ 0.1 LogMAR. AMD severity was classified using *Age-Related Eye Disease Study* (*AREDS*) criteria (75). The exclusion criteria included heavy smokers (more than 20 cigarettes per day); pregnancy; presence of corneal scars or cataract; glaucoma; dry eye syndrome, Stage 4; and any additional eye disease other than AMD. Assessment of safety of scleral iontophoresis of lutein was determined by assessing CDVA using the EDTRS chart and central retinal thickness (a 1-mm ETDRS sector) using Optical Coherence Tomography (Canon HST-100, Japan) at the baseline and 1 week, 1 month, and 3 months after treatment. In addition, the patients were asked to fill a patient outcome report for self-assessment of ocular itching, lacrimation, photophobia, and ocular discomfort at 1 week postoperatively. At the baseline, each patient received one application of scleral iontophoresis, which consisted of (1) applying a drop of anesthetics (0.4% oxybuprocaine, Novesina, Novartis, US) onto the eye to treat and the return electrode
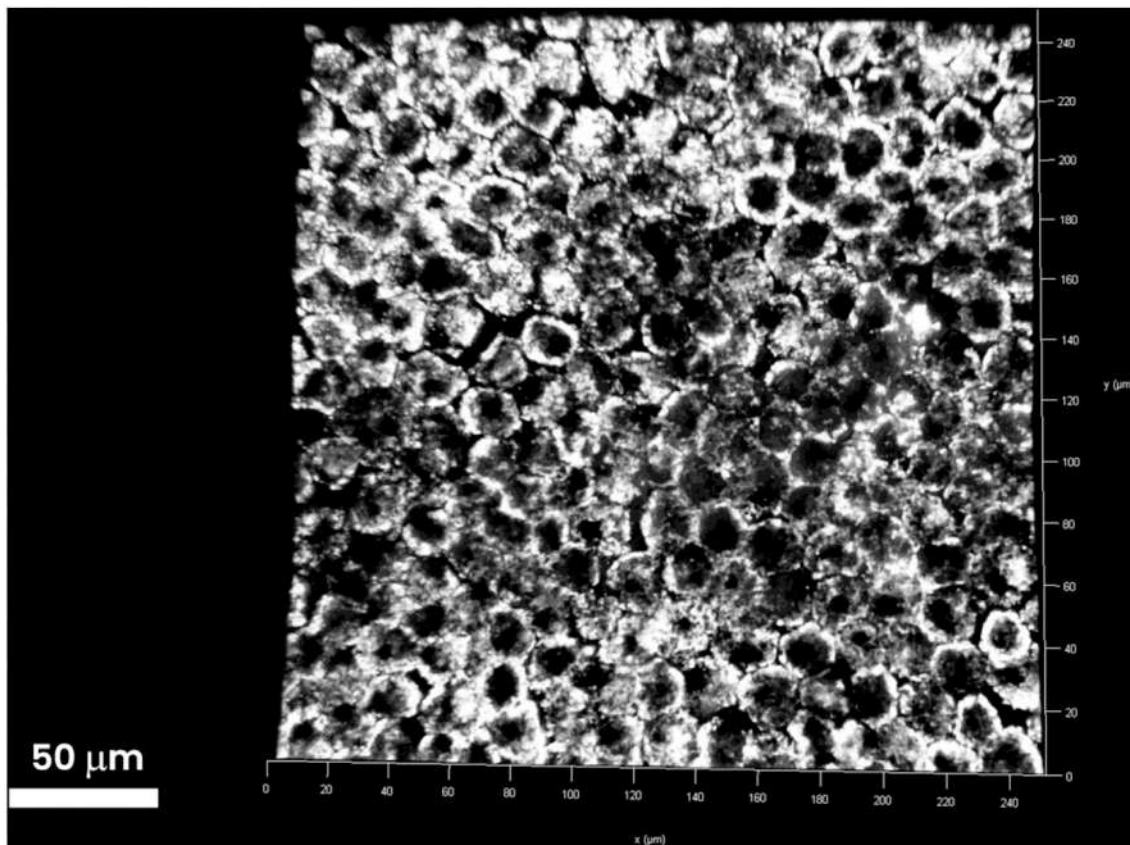
FIGURE 2 | Three-dimensional stack of the RPE layer underlying the retinal periphery. RPE cells are tightly attached to one another and form a barrier between the choroid and retina. The RPE layer is increasingly impermeable to passive diffusion of molecules >400 Da. No extra-cellular particles emitting TPEF signals were found in the RPE layer. The TPEF coming from the intracellular content of RPE cells is generated by lipofuscin (1-μm particles). Scale bar: 50 μm.

onto the forehead after cleaning the area with 70% alcohol; (2) connecting the power supply battery (K-IONO, Offhealth SpA, Italy) to the ocular applicator *via* a cable; (3) applying the ocular application to the eye to treat and fill it with the lutein liquid formulation (Lipo+, Offhealth SpA, Italy); (4) setting the current intensity at 2.5 mA for 4 min. At the end of the procedure, after removing the ocular application and rinsing the eye with balanced salt solution, the patient was invited to rest lying down on the operating bed for 5 min. The main treatment steps of scleral iontophoresis of lutein are summarized in **Figure 5**.

Clinical data were summarized as mean and standard deviation; the Wilcoxon test was used to compare baseline and postoperative values at each examination interval. Statistical significance will be set at 0.05. All the analysis will be performed using the statistical software SPSS.

Nine ($n = 9$) patients, with mean age, 69 ± 9 years (range; 57–73 years; six females and three males), were enrolled in this pilot study. Three patients had diagnosis of AMD Stage 2, three patients had diagnosis of AMD Stage 3, and three patients had diagnosis of AMD Stage 4. The clinical outcomes of the pilot study are summarized in **Table 4**. The CDVA improved significantly from 0.20 ± 0.19 LogMAR to 0.11 ± 0.18 LogMAR ($p = 0.01$) at 1 week postoperatively, and then returning toward

preoperatively value during follow-up. The 1-mm EDTRS sector retinal thickness did not change during follow-up (from 263 μm at the baseline to 262 μm at 3 months; $p = 0.52$).
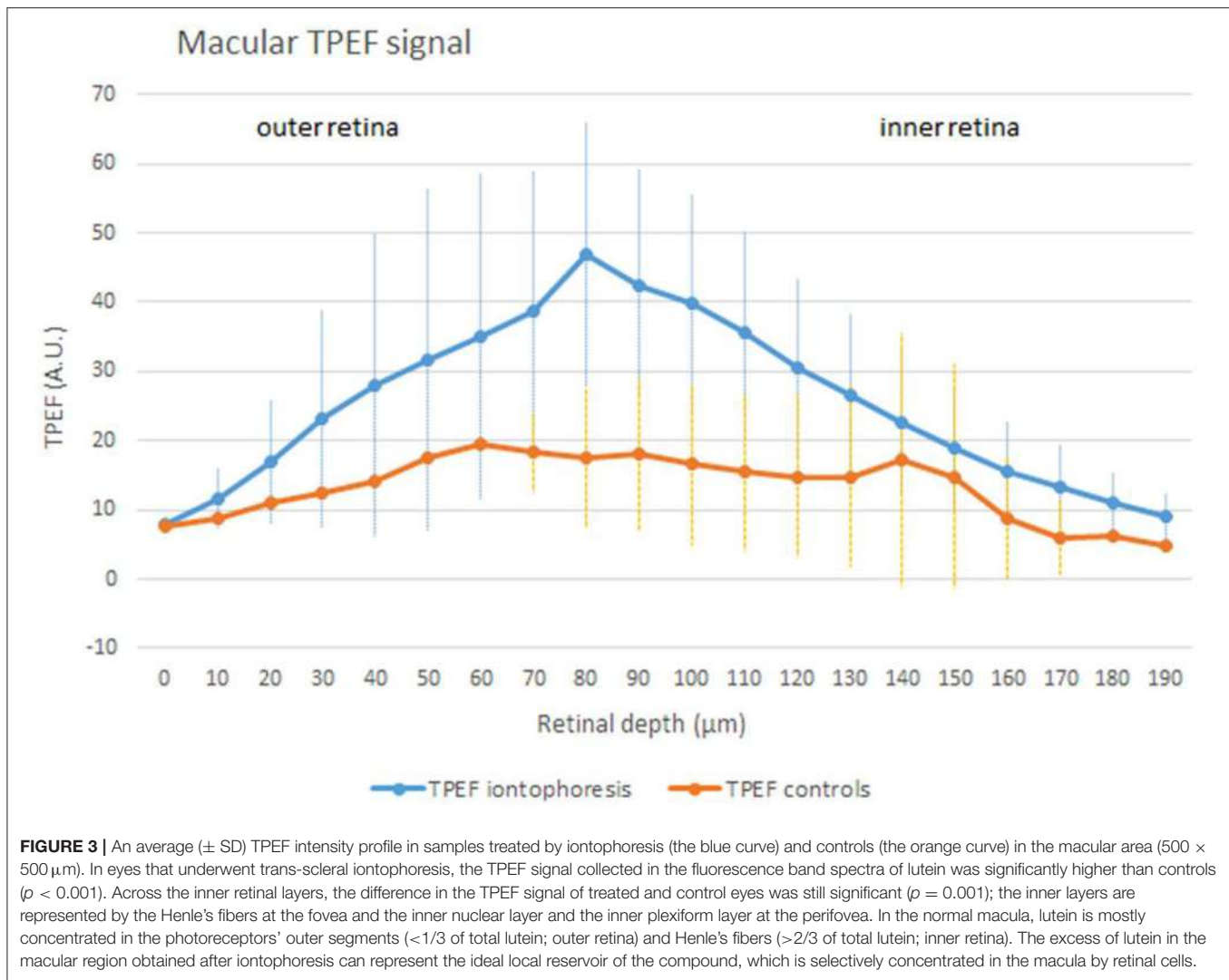
The patients did not complain of pain or discomfort during the treatment. At 1 week, the patient outcome report score for tolerability was low for all symptoms, as summarized in **Table 5**. Overall, the clinical data from the pilot study demonstrated that scleral iontophoresis for topical delivery of lutein is safe and well-tolerated; randomized controlled clinical studies will be helpful to support evidence on efficacy of this novel secondary prevention strategy in patients with higher risk of AMD progression from early to advanced stages.

NOVEL DIAGNOSTICS

In the last decade, ophthalmic imaging has advanced from simple photography of the eye disease to an advanced investigation tool, enabling clinicians to better understand disease phenotype and to make quantitative assessments of the eye.

AMD is usually investigated by assessment of visual acuity, optical coherence tomography (OCT), and retinal/choroidal angiography using fluorescein/indocyanine green dyes. Currently, clinical diagnosis of established cases of AMD
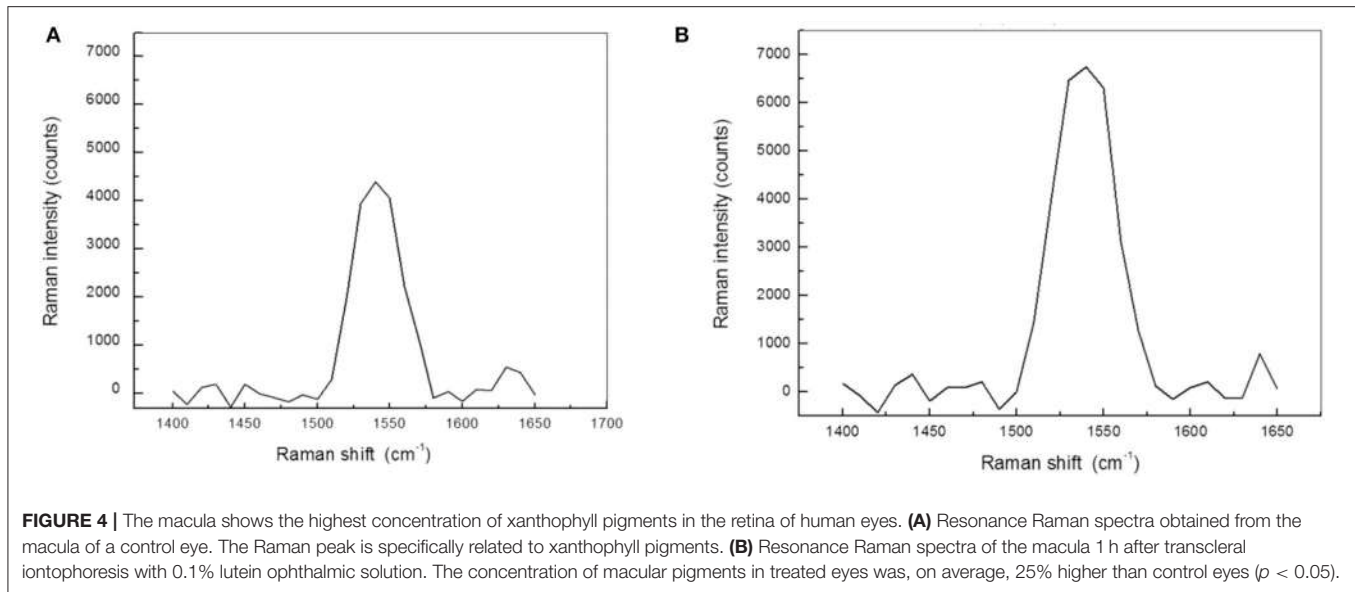
FIGURE 3 | An average (± SD) TPEF intensity profile in samples treated by iontophoresis (the blue curve) and controls (the orange curve) in the macular area (500 × 500 μm). In eyes that underwent trans-scleral iontophoresis, the TPEF signal collected in the fluorescence band spectra of lutein was significantly higher than controls ($p < 0.001$). Across the inner retinal layers, the difference in the TPEF signal of treated and control eyes was still significant ($p = 0.001$); the inner layers are represented by the Henle's fibers at the fovea and the inner nuclear layer and the inner plexiform layer at the perifovea. In the normal macula, lutein is mostly concentrated in the photoreceptors' outer segments (<1/3 of total lutein; outer retina) and Henle's fibers (>2/3 of total lutein; inner retina). The excess of lutein in the macular region obtained after iontophoresis can represent the ideal local reservoir of the compound, which is selectively concentrated in the macula by retinal cells.

TABLE 2 | Estimation of lutein concentration in the macular area of eyes after scleral iontophoresis of lutein and controls.

Macular lutein in controls (n = 2 eyes)	Macular lutein in iontophoresis (n = 4 eyes)	Increase of lutein in macula (500 × 500 μm area) after iontophoresis
21 μM (12 mg)	40 μM (23 mg)	90% greater than controls

is evident on clinical examination when gross macroscopic alterations occur at the retina, such as drusen larger than 65 μm, hemorrhages, serous or hemorrhagic retinal or RPE detachment, RPE atrophy etc. With the advent of the anti-VEGF therapy, OCT retinal imaging has been increasingly used for the early diagnosis of choroidal neovascularization (CNV) and for the treatment and re-treatment management. OCT imaging is currently the paradigm of the diagnostic procedure to diagnose retinal diseases; in particular, analysis of SD-OCT and OCT-angiography retinal images has shown to provide clinically significant information on both disease progression and functional outcomes after anti-VEGF treatment (76, 77). Nevertheless, OCT is not sensitive enough to identify early signs or those patients with higher risk of disease progression from intermediate to late AMD stages because of relatively poor spatial resolution and lack of intrinsic functional information from retinal and RPE cells and retinal/choroidal microvasculature. There is, therefore, need to develop reliable methods for detecting specific signs of disease progression in the retinal tissue in a much shorter time frame than current state-of-the-art technologies.

The prerequisite for successful patients care in this age-related disease area is the development of diagnostic devices to facilitate definition of new and appropriate label-free clinical endpoints with high sensitivity and specificity. Such endpoints need to be meaningful to clinicians and patients and not limited to visual acuity, which is, currently, the only generally accepted functional clinical endpoint in retinal diseases, although it does not have enough sensitivity to reliably and consistently monitor disease progression. There is need for objective and sensitive clinical

FIGURE 4 | The macula shows the highest concentration of xanthophyll pigments in the retina of human eyes. **(A)** Resonance Raman spectra obtained from the macula of a control eye. The Raman peak is specifically related to xanthophyll pigments. **(B)** Resonance Raman spectra of the macula 1 h after transcleral iontophoresis with 0.1% lutein ophthalmic solution. The concentration of macular pigments in treated eyes was, on average, 25% higher than control eyes ($p < 0.05$).

endpoints, assessing both the structural (e.g., drusen volume and characteristics) and functional (e.g., photoreceptors reflectance, choriocapillary blood flow) macular abnormalities. In addition, the ideal clinical outcome metrics should be able to establish sub-phenotypes of intermediate AMD with high risk to develop late-stage AMD and to early detect the response to therapy. Such assessments could greatly contribute to reduce the incidence of AMD progression from intermediate to late AMD stages. For example, progression from early AMD to the advanced stage of AMD has been related to a set of signs, such as the number and type of (soft) drusen in the macula, drusen size, the presence of pigment irregularities in the macular, age > 65 years, previous cataract surgery, cigarette smoking, and family history of AMD (mostly due to genetic variants of CHF and ARMS2 genes). More knowledge of additional and, possibly, more specific risk factors of AMD progression, such as those related to the macular xanthophyll pigments, would also contribute to improve more appropriate patients' management and care.

Among the novel diagnostic tools, adaptive optics ophthalmic imaging can resolve the retinal microscopy *in vivo* with unprecedented spatial resolution for detection of details smaller than $3\,\mu$m, and resonance Raman spectroscopy is a promising technology for the measurement of macular carotenoid levels in the living human retina.

Adaptive Optics Retinal Imaging

It has been clear for long time that, by the time pathology is visible with current imaging tools, significant neuro-retinal cellular damage has already occurred. The resolution at which retinal images could be recovered *in vivo* by current retinal cameras is limited to the macroscopic scale (lateral resolution is $\geq 12\,\mu$m). In order to bring the lateral resolution of ophthalmoscopes to the microscopic scale (i.e., lateral resolution $\leq 4\,\mu$m), it is necessary to compensate both for low- and high-order optical aberrations of the eye.

**TABLE 3 |** Concentration of lutein in ocular tissues (ng/mm^2, M ± SD).

	Inner sclera	Choroid	Peripheral retina	Macula
Controls ($n = 2$)	0	0	0	3.7 ± 1.0
Iontophoresis ($n = 6$)	16 ± 9.0*	1.2 ± 0.3*	2.5 ± 1.3*	4.8 ± 1.7

*$P < 0.05$ between study and control groups.

Adaptive optics (AO) is a technology used to improve the performance of optical systems by reducing the effects of optical distortions. It provides considerable improvements in the contrast and sharpness of retinal images that are normally degraded by ocular aberrations when combined with any one of the known imaging modalities (e.g., fundus camera, SLO, OCT) (18). The benefit of AO for high-resolution retinal imaging has been clearly shown in numerous reports with the discovery of differences in the pattern of the cone/rod mosaic in various diseases, including AMD, diabetic retinopathy, inherited retinal dystrophies, and glaucoma (78).

Adaptive optics retinal imaging systems have demonstrated the capability to resolve numerous microstructural aspects of the living human retina. They make possible to resolve photoreceptor cells, including cones and rods, retinal nerve fibers and microvasculature; the improved resolution provides a more sensitive tool with which to study, detect, and track retinal diseases (78). Given the prevalence of AMD, it is likely that this will be one of the more active growth areas in clinical AO imaging. The availability to combine complementary AO imaging, such as *en face* and axial scanning of the retina, and detection, such as bright- and dark-field modality, options at the same time can provide a holistic approach to in-depth investigation of the retinal photoreceptors, capillaries, and nerve fiber bundles.
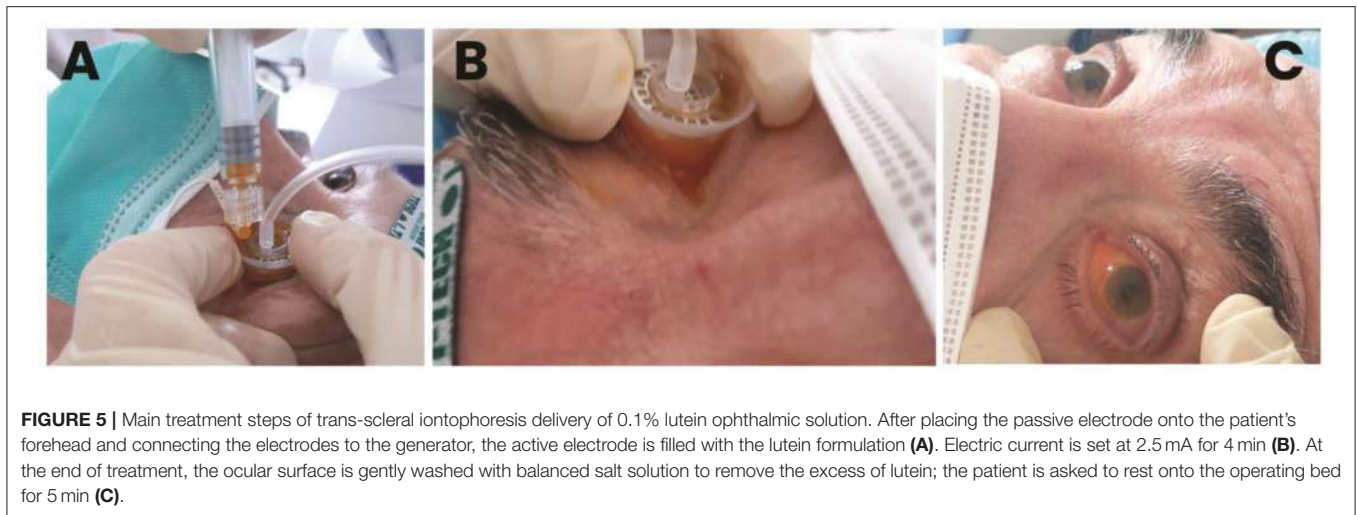
FIGURE 5 | Main treatment steps of trans-scleral iontophoresis delivery of 0.1% lutein ophthalmic solution. After placing the passive electrode onto the patient's forehead and connecting the electrodes to the generator, the active electrode is filled with the lutein formulation **(A)**. Electric current is set at 2.5 mA for 4 min **(B)**. At the end of treatment, the ocular surface is gently washed with balanced salt solution to remove the excess of lutein; the patient is asked to rest onto the operating bed for 5 min **(C)**.

In early stages of AMD (i.e., stages from 1 to 3), the ability to predict the rate of progression is currently limited. By monitoring drusen over time, *en face* and axial AO imaging could be used to monitor drusen progression in terms of number and size, and assess their direct effect on the overlying photoreceptor mosaic (79). Preservation of cones over the drusen (either large colloid drusen or basal laminar drusen) could be clearly observed in patients (79). In a study of early AMD, the authors identified several additional small drusen deposits that were not observed with wide field fundus imaging or SD-OCT in early AMD stages (80). AO-SLO imaging also revealed a decrease in photoreceptor density and increased cone spacing in patients with AMD Stages 1 to 3, as well as a spectrum of photoreceptor changes, ranging from variability in cell reflectivity to decreased cell density (81). The increased reflectivity of photoreceptors associated with the drusen could be attributed to increased scatter from the RPE (due to decreased melanin or accumulation of some waste material) and to loss of outer segment pigments or loss of the photoreceptor outer segment. Significant decrease in visible photoreceptor density was also found in large coalescent drusen and areas of GA in advanced stages of dry AMD. A 30% decrease in cone counts was found (at 5–7 degrees eccentricity) in eyes with later stages in comparison with eyes with earlier stages of AMD progression. In addition, AO imaging has been shown to visualize reliably disruptions to the photoreceptor mosaic even outside the clinically visible GA lesions and to track the progression of the GA lesions over time (82). As such, a sensitive, non-invasive, high-resolution imaging tool could help to better recognize the earliest retinal changes and to identify patients who could progress rapidly and may benefit from a more intensive observation and management (83, 84). Furthermore, a better diagnostic approach of the macular disease could have an important role in the evaluation of the effectiveness of new prevention strategies at the cellular level.

These authors tested different AO imaging modalities *in vivo*, providing former clinical data on patients using either flood illumination or line scanning laser ophthalmoscopy (LSO) imaging modalities (18). The advantage of the line scanning

TABLE 4 | Clinical data outcome of the pilot study on scleral iontophoresis delivery of lutein.

	CDVA (LogMAR)	ETDRS letters (n.)	1-mm ETDRS sector (μm)
Baseline	0.20 ± 0.19	45 ± 10	263 ± 32
1-week	0.11 ± 0.18*	50 ± 10*	263 ± 32
1-month	0.13 ± 0.22	50 ± 11*	263 ± 32
3-months	0.16 ± 0.19	48 ± 10*	262 ± 32

*$p < 0.05$ between post-operative and baseline values.

TABLE 5 | Patient outcome report on tolerability.

	Ocular itching	Lacrimation	Photophobia	Ocular discomfort
Patient 01	1	0	0	1
Patient 02	0	0	0	1
Patient 03	1	1	0	0
Patient 04	0	1	0	0
Patient 05	1	0	0	1
Patient 06	0	0	0	0
Patient 07	1	0	0	1
Patient 08	0	1	0	1
Patient 09	1	0	0	1

For each symptom, score ranges from 0 (any symptom) to 4 (highest intensity for the symptom).

approach is that it multiplexes the illumination and detection in one dimension, while rejecting scattered light outside of the confocal range gate defined by the pixel size in a similar fashion as a flying-spot SLO; nevertheless, the line scanning approach reduces the hardware complexity by elimination of a high-speed scanner and associated mirror or lens relays. A multimodal AO-LSO-OCT system (PSI Corp., MA, USA) has been operated in both bright-field and dark-field detection modalities for imaging

FIGURE 6 | Montage of AO images in a 45-year-old female patient (scale bar: 100 µm). The photoreceptor mosaic can be clearly resolved across the central retina. Image processing and analysis of AO retinal images allow the clinicians to detect and track pathologic changes of the cone mosaic with cellular resolution.
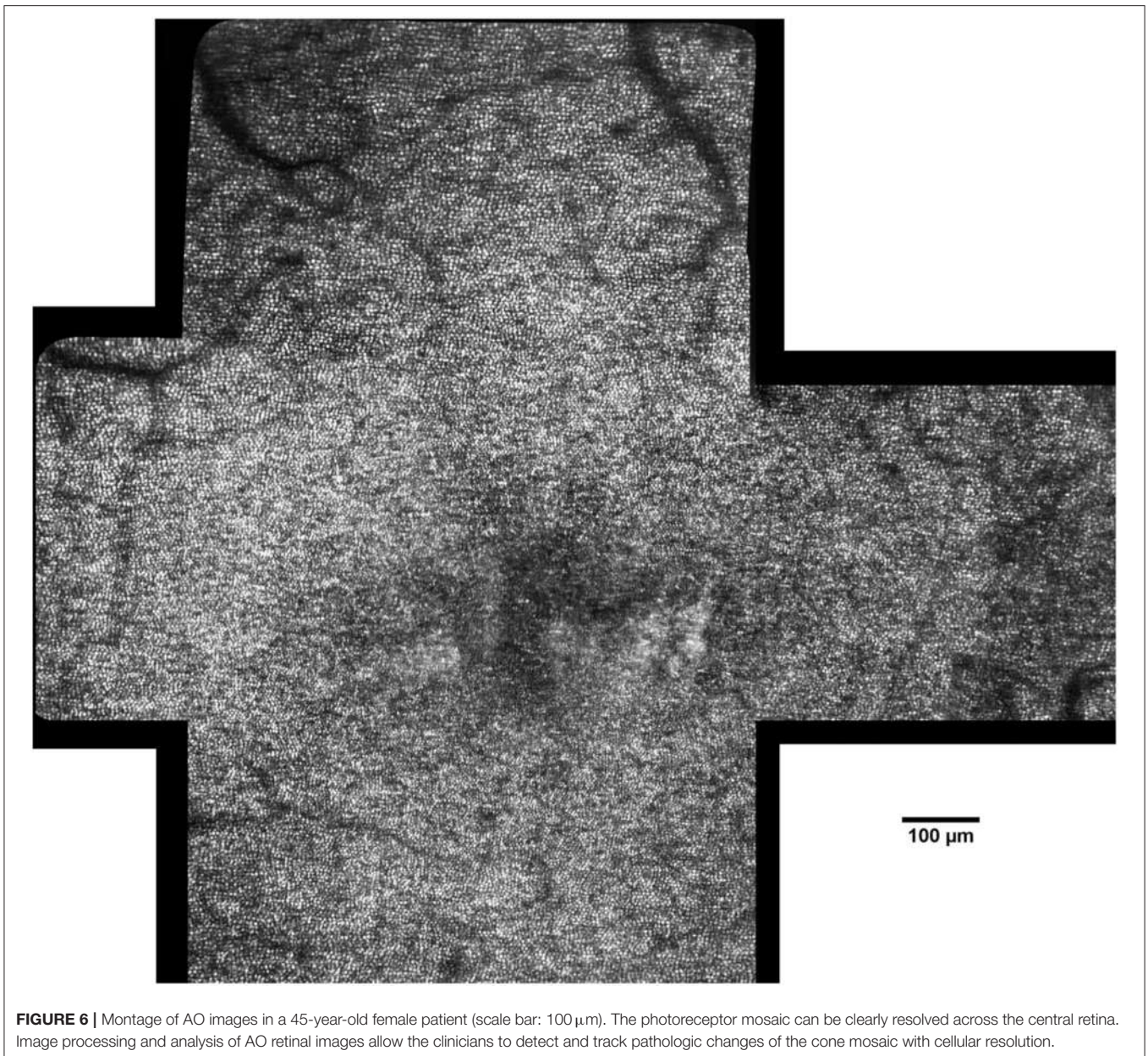
the retina. In the bright-field mode, quasi-confocal imaging was obtained by illuminating the retina with a scanning light source, which is collected by a line-array CMOS sensor for high contrast imaging of the retinal photoreceptors. Using this mode, images of the photoreceptor mosaic could be collected across the central and peripheral retina at high resolution; even the foveal cones within 1 degree from the foveal center could be clearly visualized (**Figure 6**). Polarized detection could be achieved within the bright-field modality by illuminating the eye with linearly polarized light and by filtering the light exiting the eye with a linear polarizer (or analyzer). Images of the retinal nerve fiber layer (RNFL) bundles could be acquired with the polarizer oriented for maximum through output (i.e., parallel to the major axis of bundles), and then at 45° and 90° relative to

that orientation (**Figure 7**). In the dark-field detection mode, the light back scattered from the retina is collected by a time-domain integration (TDI) line camera in order to improve resolution of acquired images of the retinal vascular structures (**Figure 8**). High-resolution OCT could be performed simultaneously during LSO imaging of the retina (synchronous image acquisition). The complementary AO-OCT imaging modality does offer additional technical advantages compared to AO-LSO, providing a high-resolution cross-sectional view through the living retina, comparable to a histological section (**Figure 9**) (85).

The possibility to analyze retinal photoreceptors in AO images allows for assessing their density and arrangement as well as their waveguide and reflectance properties. Clinical studies have demonstrated how AO technology is sensitive enough to
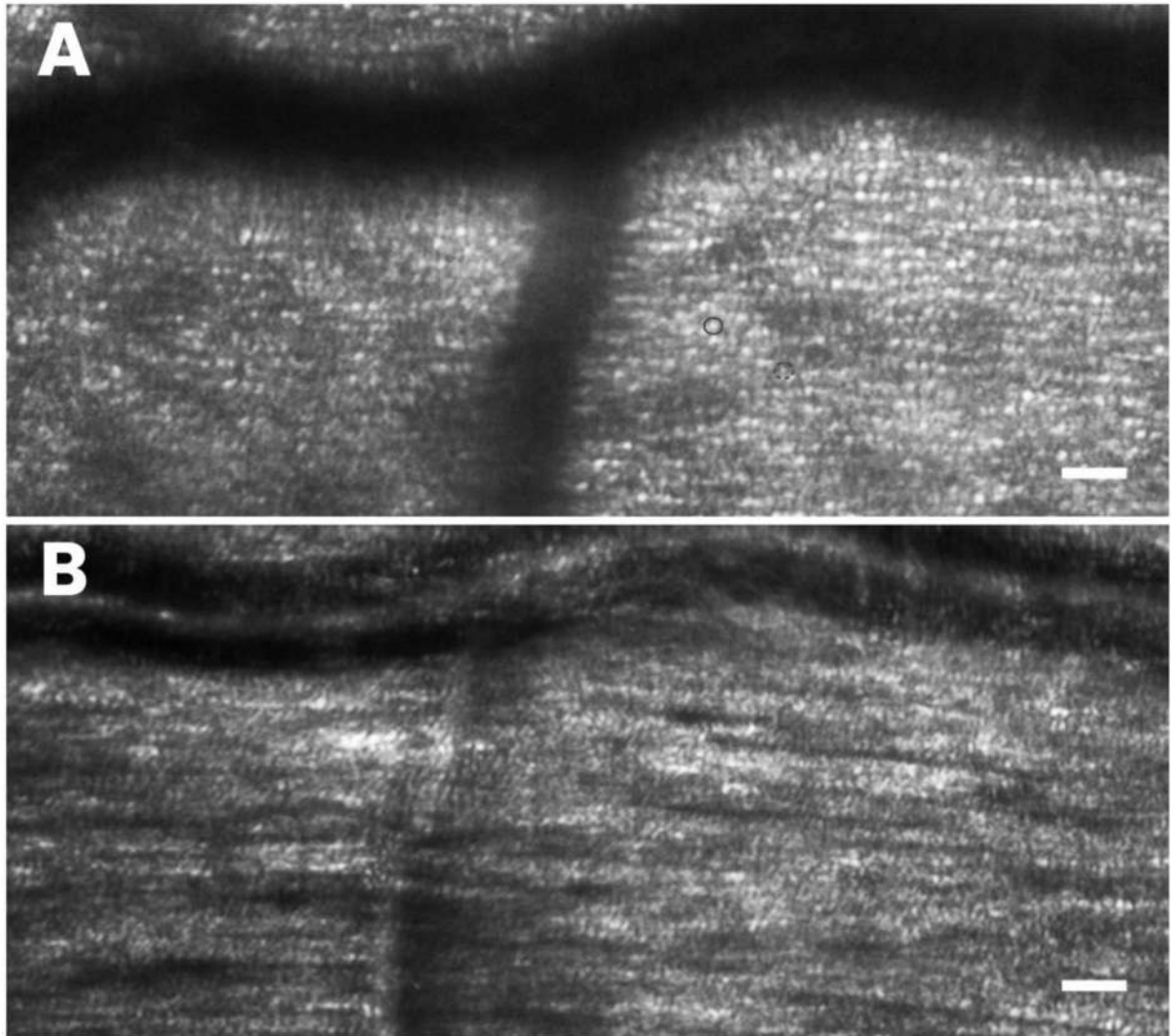
FIGURE 7 | High-resolution AO imaging allows the clinicians to scan the retinal microstructures easily for rapid screening of health and integrity of the outer and inner retinal layers. In **(A)** the photoreceptor mosaic, including cones (brighter and bigger dots; the full circle) and rods (dimmer dots surrounding the cones; the dotted circle), is shown. In **(B)** the nerve fiber bundles, overlapping the cell mosaic is well-resolved. Scale bars: 50 μm.

detect retinal tissue abnormalities with unprecedented spatial resolution, providing clinical information that is invisible to a current diagnostics tool (86, 87).

There are currently few barriers to a wide adoption of AO technology in clinical ophthalmology: the main obstacles are the high cost of sensing and correcting elements and the system complexity. A user-friendly AO instrument that can be used by ophthalmologists will facilitate the introduction of this technology into clinical practice.

Resonance Raman Spectroscopy

Although the protective effect of dietary lutein/zeaxanthin on slowing down progression and severity of AMD is under intensive investigation, there is no commercially available diagnostic tool able to detect the amount of xanthophyll pigments in the macula and to monitor for their effect on preventing AMD progression from intermediate to advanced stages in response to dietary intake or emerging topical administration.

Resonance Raman spectroscopy (RRS) is one of the most promising technologies for the measurement of macular carotenoid levels from the human retina (71). It is precise, sensitive, specific, reproducible, and objective. It has also the potential to be translated to clinical applications in order to collect quantitative, direct, measurement of macular content of xanthophyll pigments.

To date, the macular carotenoid levels could be measured only indirectly using the macular pigment optical density (MPOD) measurement (88). There is a variety of methods currently in use that claim to measure the MPOD *in vivo*. Technically, the MPOD is a measurement of the attenuation of blue light by macular
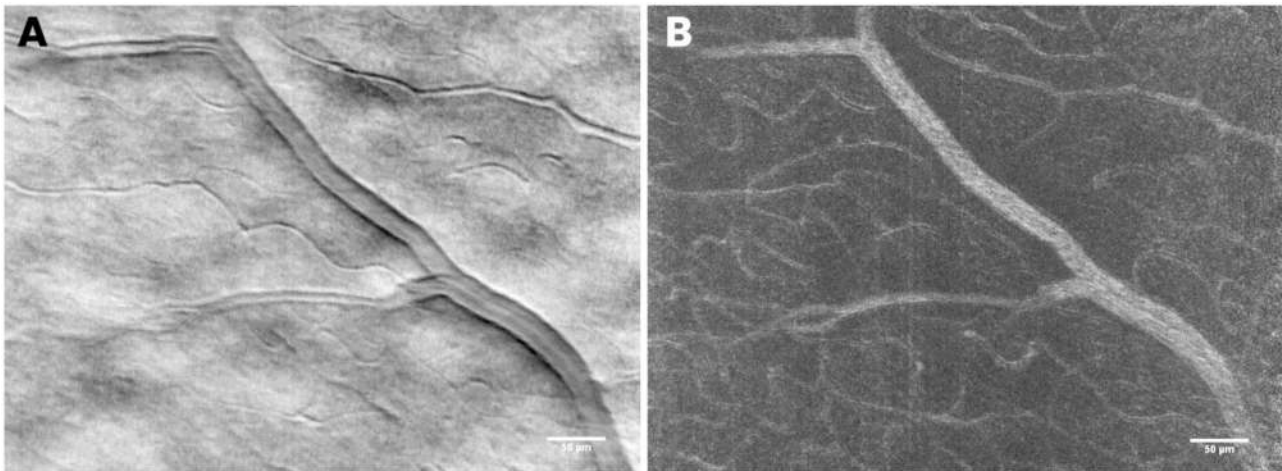
FIGURE 8 | In the dark-field detection mode, retinal vascular structures can be resolved with high resolution. The use of a time-domain integration (TDI) line camera allows the user to exploit the split field imaging modality, which consists of collecting two shifted images on the camera, subtracted and divided by their sum. In **(A)** the mean TDI image and in **(B)** the standard variation, TDI image showing details of the retinal vessel walls and beds, respectively. Scale bars: 50 μm.
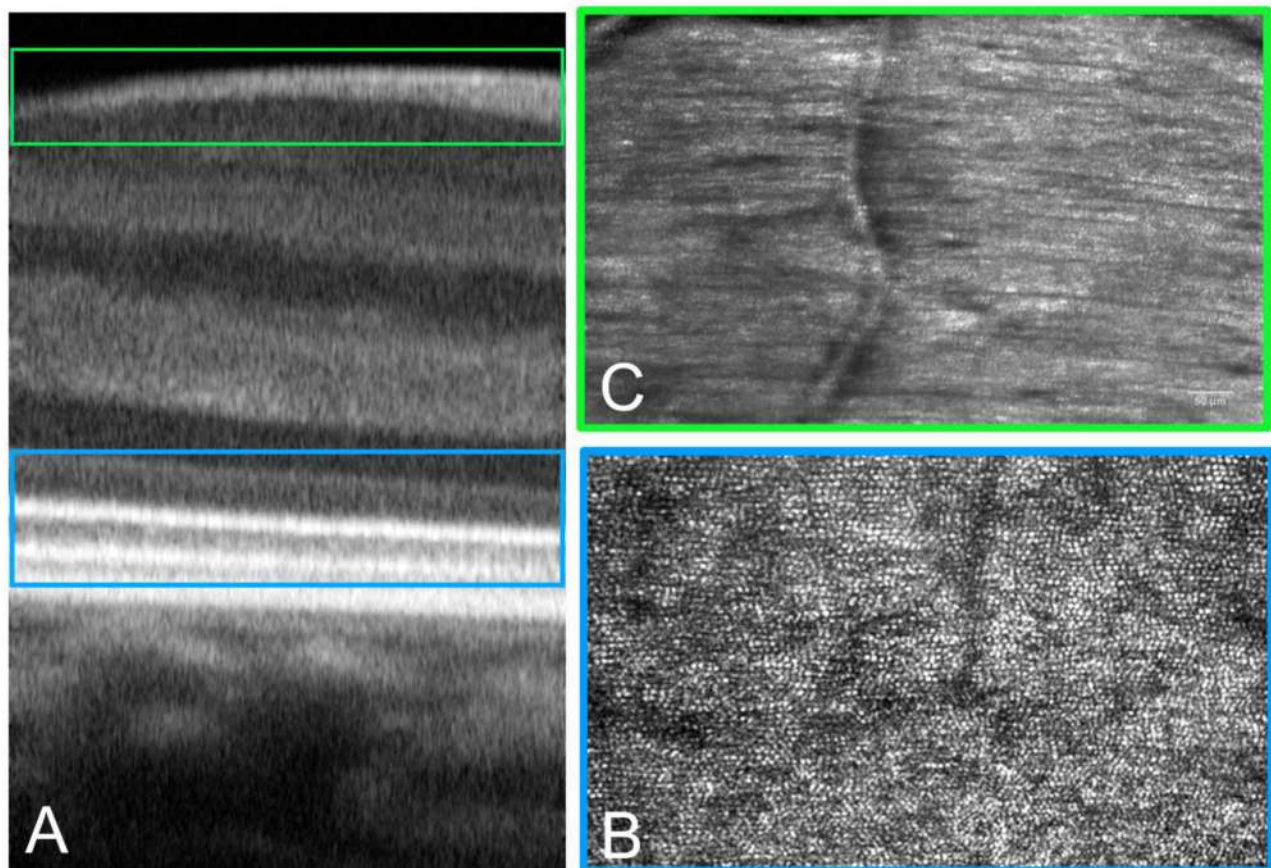
FIGURE 9 | Adaptive optics technology can be implemented in a multimodal imaging system to acquire images of the retina, showing details of the tissue with histologic resolution *in vivo*. Multimodal imaging provides spatial co-localization of complementary information on structure (and function). Cross-sectional **(A)** and enface **(B,C)** AO images of the retina. **(A)** The AO-OCT scan provides detailed information on tissue layers from the choriocapillaris to the inner limiting membrane. **(B)** The same retinal area scanned at the IS-OS layer showing the photoreceptor mosaic. **(C)** High-resolution images of the retinal nerve fiber bundles are acquired with the polarizer oriented for maximum through output (paralleled to the major axis of bundles).

pigments and could be somewhat indirectly related to the amount of lutein and zeaxanthin in the macula; however, uncertainties exist on whether the MPOD may be reliably correlated with the amount of xanthophyll pigments in the retina. The methods to measure MPOD are divided into psychophysical (sometimes referred to as "subjective") and physical (sometimes referred to as "objective"). The psychophysical techniques available include heterochromatic flicker photometry and color matching; the physical techniques include Fundus AutoFluorescence (FAF) and fundus reflectance. Validation of macular pigment subjective measurement techniques is still the subject of lively debate, and, due to their intrinsic technical limits, these methodologies are not gaining popularity among ophthalmologists and retinal specialists. Current physical methods are based on a variety of assumptions and are vulnerable to several technical limits. These methods shall (1) take into account single- and double-path light traversal through deeper retinal layers, (2) eliminate image contrast, diminishing fluorescence and scattering from the optical media (via confocal detection techniques, filtering, etc.), (3) bleach the photoreceptors, and (4) use a location in the peripheral retina as a reference point. For these reasons, auto-fluorescence and reflectance patterns hold poor specificity and are not sensitivity enough to follow AMD disease progression.

Contrary to all existing methods, RRS has no assumptions other than approximating the spectrally broad background fluorescence with the fluorescence response at a wavelength that is slightly offset from the macular xanthophylls Raman response (71). It directly measures absolute amounts of carotenoids in the illuminated region; in addition, it provides a measure of the absolute xanthophylls concentration distribution in the macular region since it does not use a reference point in the peripheral retina.

Resonance Raman detection of xanthophyll molecules is highly specific and can be established as a label-free tool for reliably evaluating the amount of macular pigments in patients. Xanthophyll molecules have been reliably detected in the living human retina (89–91), and the Raman signature of the xanthophyll molecules has been shown to be identical to the isolated carotenoid molecule. The authors have demonstrated feasibility and safety of RSS of macular xanthophylls on excised retina and human subjects, showing different patterns of macular pigment distribution (peaked, plateaued, ring shaped) (71, 89, 92, 93). It remains to be understood how the technique could be translated in clinical practice for monitoring and tracking the concentration of macular xanthophyll pigments in patients at risk of AMD progression. Overall, the advantages of RSS can be summarized in the following features:

- *objective measurement*: resonance Raman spectroscopy is a non-invasive technology able to directly measure and monitor the concentration of macular xanthophyll pigments in the living human retina;
- *molecular contrast*: excitation of the retina with a blue laser source enables the generation of a characteristics resonance Raman scattering response from xanthophyll molecules and allows for their accurate measurement from

their corresponding spectral fingerprint signature in the living human retina;
- *spatial mapping*: scanning the blue light over the central retina allows for depicting and tracking over the same area a bi-dimensional map of the macular xanthophyll pigments content in the living human retina.

The limit consists in the implementation of a quantitative, reliable, method for data analysis and for eliminating the influence of the crystalline lens absorbance, which increases with aging and varies among populations.

CONCLUSION

Age-related macular degeneration is the major eye disease in the aging populations worldwide. Knowing that the total cost savings derived from avoided AMD events for the same population is, on average, €4 billion per year, both novel diagnostic approaches aiming at identifying patients at risk of AMD progression and effective secondary prevention strategies to halt disease progression would greatly benefit society worldwide. Currently, the most indorsed pathophysiologic pathway of AMD includes a relationship with genotype, age, and lesions to the photoreceptor/RPE/Bruch's membrane/choriocapillaris complex, which have been associated with light-induced oxidative damage (*blue light hazard*). Systemic risk factors, such as smoking, hypercholesterolemia, overweight, and cardiovascular diseases, likely contribute to increased oxidative stress in the choriocapillaris complex. A healthy lifestyle, including a type of diet rich in vegetables, fruits and fish, and regular exercise are recommended to counteract the effect of aging and oxidative stress. In this context, there is increasing evidence that xanthophyll pigments may play an important role in maintaining the health and function of the macula. Their levels are known to decrease with aging and are significantly lower in patients with AMD, making the retina more vulnerable to light-induced damage with advancing age. Several clinical trials, including the *CAREDS*, the *Blue Mountain Eye Study*, and the *AREDS2*, have reported that higher dietary lutein and zeaxanthin intake reduces the risk of AMD progression. On the other hand, there are some barriers that halt clinicians to support prevention strategies that promote xanthophylls supplementation, mainly due to the low patient adherence to therapy and the limits of current diagnostics technologies for measuring macular pigments. New prevention strategies may involve topical delivery of lutein directly into the eye in order to allow clinicians to test directly the effect of xanthophylls on slowing down or halting disease progression in patients at higher risk. On the other hand, because the rate of disease progression is typically slow, it is estimated that patients have a clinical loss of visual function years after the onset of early signs of AMD. For this reason, both the early diagnosis and the monitoring of treatment efficacy at a cellular level represent two of the greatest needs in the management of AMD. If AO imaging succeeds in entering the clinical practice to provide high-resolution, objective, measures of the cone photoreceptor

structure, RPE, and micro-vasculature in patients, it will open a new frontier for establishing effective patient care with novel prevention and treatment strategies.

Efforts will be also needed for improving management of patients suffering from AMD Stage 4. Although gene therapies have potential and are promising, there are significant obstacles, such as safety, long-term efficacy, and cost, to these therapeutic options for AMD becoming mainstream (94, 95).

AUTHOR CONTRIBUTIONS

All authors listed have made a substantial, direct, and intellectual contribution to the work and approved it for publication.

ACKNOWLEDGMENTS

SUPPLEMENTARY MATERIAL

The Supplementary Material for this article can be found online at: https://www.frontiersin.org/articles/10.3389/fmed.2022.887104/full#supplementary-material

REFERENCES

1. United Nations. *World Population Ageing 2019. Highlights.* United Nations (2019).
2. WHO. *Global Data on Visual Impairments 2010.* Geneva: WHO (2012).
3. Ferris FL, Wilkinson CP, Bird A, Chakravarthy U, Chew E, Csaky K, et al. Clinical classification of age-related macular degeneration. *Ophthalmology.* (2013) 120:844–51. doi: 10.1016/j.ophtha.2012.10.036
4. Smith W, Assink J, Klein R, Mitchell P, Klaver CC, Klein BE, et al. Risk factors for age-related macular degeneration: Pooled findings from three continents. *Ophthalmology.* (2001) 108:697–704. doi: 10.1016/S0161-6420(00)00580-7
5. Owen CG, Jarrar Z, Wormald R, Cook DG, Fletcher AE, Rudnicka AR. The estimated prevalence and incidence of late stage age related macular degeneration in the UK. *Br J Ophthalmol.* (2012) 96:752–6. doi: 10.1136/bjophthalmol-2011-301109
6. NIH. *National Plan for Eye and Vision Research. NIH Publication n. 04-4288.*
7. Moshfeghi AA, Lanitis T, Kropat G, Kuznik A, Gibson A, Feng H, et al. Social cost of blindness due to AMD and diabetic retinopathy in the United States in 2020. *Ophthalmic Surg Lasers Imaging Retina.* (2020) 51:S6–14. doi: 10.3928/23258160-20200401-01
8. Jeffery RCH, Mukhtar SA, Lopez D, Preen DB, McAllister IL, Mackey DA, et al. Incidence of newly registered blindness from age-related macular degeneration in australia over a 21-year period: 1996-2016. *Asia Pac J Ophthalmol.* (2021) 10:442–9.
9. Alan F, Cruess AF, Zlateva G, Xu X, Soubrane G, Pauleikhoff D, et al. Economic burden of bilateral neovascular age-related macular degeneration: multi-country observational study. *Pharmacoeconomics.* (2008) 26:57–73. doi: 10.2165/00019053-200826010-00006
10. Casten RJ, Rovner BW, Tasman W. Age-related macular degeneration and depression: a review of recent research. *Curr Opin Ophthalmol.* (2004) 15:181–3. doi: 10.1097/01.icu.0000120710.35941.3f
11. Ho L, van Leeuwen R, Witteman JC, van Dujin CM, Uiterlinden AG, Hofman A, et al. Reducing the genetic risk of age-related macular degeneration with dietary antioxidants, zinc, and omega-3 fatty acids: the Rotterdam study. *Arch Ophthalmol.* (2011) 129:758e766. doi: 10.1001/archophthalmol.2011.141
12. de Koning-Backus APM, Buitendijk GHS, Kiefte-de Jong JC, Coljin JM, Hofman A, Vingerling JR, et al. Intake of vegetables, fruit, and fish is beneficial for age-related macular degeneration. *Am J Ophthalmol.* (2019) 198:70–9. doi: 10.1016/j.ajo.2018.09.036
13. Merle BMJ, Cougnard-Grégoire A, Korobelnik J-F, Schalch W, Etheve S, Rougier M-B, et al. Plasma lutein, a nutritional biomarker for development of advanced age-related macular degeneration: the alienor study. *Nutrients.* (2021) 13:2047. doi: 10.3390/nu13062047
14. Bernstein PS. Nutritional interventions against age-related macular degeneration. *Acta Hortic.* (2009) 841:103–12. doi: 10.17660/ActaHortic.2009.841.10

15. Tan JS, Wang JJ, Flood V, Rochtchina E, Smith W, Mitchell P. Dietary antioxidants and the long-term incidence of age-related macular degeneration: the Blue Mountains Eye Study. *Ophthalmology.* (2008) 115:334–41. doi: 10.1016/j.ophtha.2007.03.083
16. Moeller SM, Parekh N, Tinker L, Ritenbaugh C, Blodi B, Wallace RB, et al. Associations between intermediate age-related macular degeneration and lutein and zeaxanthin in the Carotenoids in Age-related Eye Disease Study (CAREDS): ancillary study of the Women's Health Initiative. *Arch Ophthalmol.* (2006) 124:1151–62. doi: 10.1001/archopht.124.8.1151
17. The Age-Related Eye Disease Study 2 Research Group. Lutein-zeaxanthin and omega-3 fatty acids for age-related macular degeneration. the age-related eye disease study 2 (AREDS2) randomized clinical trial. *J Am Med Assoc.* (2013) 309:2005–015. doi: 10.1001/jama.2013.4997
18. Lombardo M, Serrao S, Devaney N, Parravano M, Lombardo G. Adaptive optics technology for high-resolution retinal imaging. *Sensors.* (2013) 13:334–66. doi: 10.3390/s130100334
19. Klein R, Klein BE, Knudtson MD, Wong TY, Cotch MF, Liu K, et al. Prevalence of age-related macular degeneration in 4 racial/ethnic groups in the multi-ethnic study of atherosclerosis. *Ophthalmology.* (2006) 113:373–80. doi: 10.1016/j.ophtha.2005.12.013
20. Colijn JM, Buitendijk GHS, Prokofyeva E, Alves D, Cachulo ML, Khawaja AP, et al. European Eye Epidemiology (E3) consortium. Prevalence of age-related macular degeneration in Europe: the past and the future. *Ophthalmology.* (2017) 2017:S0161–6420. doi: 10.1016/j.ophtha.2017.05.035
21. Wong WL, Su X, Li X, Cheung CM, Klein R, Cheng CY, et al. Global prevalence of age-related macular degeneration and disease burden projection for 2020 and 2040: a systematic review and meta-analysis. *Lancet Glob Health.* (2014) 2:e106–116. doi: 10.1016/S2214-109X(13)70145-1
22. Rein DB, Zhang P, Wirth KE, Lee PP, Hoerger TJ, McCall N, et al. The economic burden of major adult visual disorders in the United States. *Arch Ophthalmol.* (2006) 124:1754–60. doi: 10.1001/archopht.124.12.1754
23. Rein DB, Wittenborn JS, Zhang X, Honeycutt AA, Lesesne SB, Saaddine J, et al. Forecasting age-related macular degeneration through the year 2050: the potential impact of new treatments. *Arch Ophthalmol.* (2009) 127:533–40. doi: 10.1001/archophthalmol.2009.58
24. Brown GC, Brown MM, Sharma S, Stein JD, Roth Z, Campanella J, et al. The burden of age-related macular degeneration: a value-based medicine analysis. *Trans Am Ophthalmol Soc.* (2005) 103:173–84.
25. Friedman DS, O'Colmain BJ, Munoz B, Tomany SC, McCarty C, de Jong PTVM, et al. Prevalence of age-related macular degeneration in the United States. *Arch Ophthalmol.* (2004) 122:564–72. doi: 10.1001/archopht.122.4.564
26. Chopdar A, Chakravarthy U, Verma D. Age related macular degeneration. *BMJ.* (2003) 326:485–8. doi: 10.1136/bmj.326.7387.485
27. Maller JB, Fagerness JA, Reynolds RC, Neale BM, Daly MJ, Seddon JM. Variation in complement factor 3 is associated with risk of age-related macular degeneration. *Nat Genet.* (2007) 39:1200–1. doi: 10.1038/ng2131

28. Sobrin L, Ripke S, Yu Y, Fagerness J, Bhangale TR, Tan PL, et al. Heritability and genome-wide association study to assess genetic differences between advanced Age-Related Macular Degeneration subtypes. *Ophthalmology.* (2012) 119:1874–85. doi: 10.1016/j.ophtha.2012.03.014

29. Fritsche LG, Igl W, Bailey JN, Grassman F, Sengupta S, Bragg-Gresham JL, et al. A large genome-wide association study of age-related macular degeneration highlights contributions of rare and common variants. *Nat Genet.* (2016) 48:134e143. doi: 10.1038/ng.3448

30. Wu J, Sun X. Complement system and age-related macular degeneration: drugs and challenges. *Drug Des Devel Ther.* (2019) 13:2413e2425. doi: 10.2147/DDDT.S206355

31. Colijn JM, Meester-Smoor M, Verzijden T, de Breuk A, Silva R, Merle BMJ, et al. Genetic risk, lifestyle, and age-related macular degeneration in europe: the EYE-RISK consortium. *Ophthalmology.* (2021) 128:1039–49. doi: 10.1016/j.ophtha.2020.11.024

32. Seddon JM, Reynolds R, Yu Y, Daly MJ, Rosner B. Risk models for progression to advanced age-related macular degeneration using demographic, environmental, genetic, and ocular factors. *Ophthalmology.* (2011) 118:2203–11. doi: 10.1016/j.ophtha.2011.04.029

33. Chakravarthy U, Wong TY, Fletcher A, Piault E, Evans C, Zlateva G, et al. Clinical risk factors for age-related macular degeneration: a systematic review and meta-analysis. *BMC Ophthalmol.* (2010) 10:31. doi: 10.1186/1471-2415-10-31

34. Loprinzi PD, Swenor BK, Ramulu PY. Age-related macular degeneration is associated with less physical activity among US adults: cross-sectional study. *PLoS ONE.* (2015) 10:e0125394. doi: 10.1371/journal.pone.0125394

35. Carneiro Â, José Paulo Andrade JP. Nutritional and lifestyle interventions for age-related macular degeneration: a review. *Oxid Med Cell Longev.* (2017) 2017:6469138. doi: 10.1155/2017/6469138

36. Mares JA, Voland RP, Sondel SA. Healthy lifestyles related to subsequent prevalence of age-related macular degeneration. *Arch Ophthalmol.* (2011) 129:470–80. doi: 10.1001/archophthalmol.2010.314

37. Koushan K, Rusovici R, Li W, Ferguson LR, Chalam KV. The role of lutein in eye-related disease. *Nutrients.* (2013) 5:1823–39. doi: 10.3390/nu5051823

38. Qingning Bian, Gao S, Zhou J, Qin J, Taylor A, Johnson EJ, et al. Lutein and zeaxanthin supplementation reduces photo-oxidative damage and modulates the expression of inflammation-related genes in retinal pigment epithelial cells. *Free Radic Biol Med.* (2012) 53:1298–307. doi: 10.1016/j.freeradbiomed.2012.06.024

39. Subczynski WK, Wisniewska A, Widomska J. Location of macular xanthophylls in the most vulnerable regions of photoreceptor outer-segment membranes. *Arch Biochem Biophys.* (2010) 504:61–6. doi: 10.1016/j.abb.2010.05.015

40. Bhosale P, Li B, Sharifzadeh M, Gellermann W, Frederick JM, Tsuchida K, et al. Purification and partial characterization of a lutein-binding protein from human retina. *Biochemistry.* (2009) 48:4798–807. doi: 10.1021/bi9004478

41. Yemelyanov AY, Katz NB, Bernstein PS. Ligand-binding characterization of xanthophyll carotenoids to solubilized membrane proteins derived from human retina. *Exp Eye Res.* (2001) 72:381–92. doi: 10.1006/exer.2000.0965

42. Bone RA, Landrum JT, Fernandez L, Tarsis SL. Analysis of the macular pigment by HPLC: retinal distribution and age study. *Invest Ophthalmol Vis Sci.* (1988) 29:843–9.

43. Chen SF, Chang Y, Wu JC. The spatial distribution of macular pigment in humans. *Curr Eye Res.* (2001) 23:422–34. doi: 10.1076/ceyr.23.6.422.6963

44. Trieschmann M, van Kuijk FJ, Alexander R, Hermans P, Luthert P, Bird AC, et al. Macular pigment in the human retina: histological evaluation of localization and distribution. *Eye.* (2008) 22:132–7. doi: 10.1038/sj.eye.6702780

45. Widomska J, Subczynski WK. Why has Nature chosen Lutein and Zeaxanthin to protect the retina? *J Clin Exp Ophthalmol.* (2014) 5:326. doi: 10.4172/2155-9570.1000326

46. Rapp LM, Maple SS, Choi JH. Lutein and zeaxanthin concentrations in rod outer segment membranes from perifoveal and peripheral human retina. *Invest Ophthalmol Vis Sci.* (2000) 41:1200–9.

47. Landrum JT, Bone RA. Lutein, zeaxanthin, and the macular pigment. *Arch Biochem Biophys.* (2001) 385:28–40. doi: 10.1006/abbi.2000.2171

48. Ratnayake K, Payton JL, Meger ME, Godage NH, Gionfriddo E, Karunarathne A. Blue light-triggered photochemistry and cytotoxicity of retinal. *Cell Signal.* (2020) 69:109547. doi: 10.1016/j.cellsig.2020.109547

49. Kijlstra A, Tian Y, Kelly ER, Berendschot TSJM. Lutein: more than just a filter for blue light. *Prog Ret Eye Res.* (2012) 31:303e315. doi: 10.1016/j.preteyeres.2012.03.002

50. Rodriguez-Carmona M, Kvansakul J, Harlow JA, Köpcke W, Schalch W, Barbur JL. The effects of supplementation with lutein and/or zeaxanthin on human macular pigment density and colour vision. *Ophthal Physiol Opt.* (2006) 26:137–47. doi: 10.1111/j.1475-1313.2006.00386.x

51. Sasaki M, Yuki K, Kurihara T, Miyake S, Noda K, Kobayashi S, et al. Biological role of lutein in the light-induced retinal degeneration. *J Nutr Biochem.* (2012) 23:423–9. doi: 10.1016/j.jnutbio.2011.01.006

52. Liu R, Wang T, Zhang B, Qin L, Wu C, Li Q, et al. Lutein and zeaxanthin supplementation and association with visual function in age-related macular degeneration. *Invest Ophthalmol Vis Sci.* (2015) 56:252–8. doi: 10.1167/iovs.14-15553

53. Granado F, Blázquez S, Olmedilla B. Changes in catotenoid intake from fruit and vegetables in the spanish population over the period 1964 2004. *Public Health Nutr.* (2007) 10:1018–23. doi: 10.1017/S1368980007662314

54. Lucarini M, Lanzi S, D'Evoli L, Aguzzi A, Lombardi-Boccia G. Intake of vitamin A and carotenoids from the Italian population. *Int J Vitam Nutr Res.* (2006) 76:103–9. doi: 10.1024/0300-9831.76.3.103

55. Seddon JM, Ajani UA, Sperduto RD, Hiller R, Blair N, Burton TC, et al. Dietary carotenoids, vitamins A, C, and E, and advanced age-related macular degeneration. Eye disease case-control study group. *J Am Med Assoc.* (1994) 272:1413–20. doi: 10.1001/jama.272.18.1413

56. Seddon JM, Ajani UA, Sperduto RD, Hiller R, Blair N, Burton TC, et al. Dietary carotenoids, vitamins A, C, and E, and advanced age-related macular degeneration. Eye disease case-control study group. *J Am Med Assoc.* (1994) 272:1413–20. doi: 10.1001/jama.1994.03520180037032

57. Joachim N, Mitchell P, Burlutsky G, Kifley A, Wang JJ. The incidence and progression of age-related macular degeneration over 15 years: the blue mountains eye study. *Ophthalmology.* (2015) 122:2482–9. doi: 10.1016/j.ophtha.2015.08.002

58. Age-Related Eye Disease Study Research Group. The relationship of dietary carotenoids and vitamin A, E, and C intake with age-related macular degeneration in a case-control study: AREDS report no. 22. *Arch Ophthalmol.* (2007) 125:1225–123. doi: 10.1001/archopht.125.9.1225

59. Weigert G, Kaya S, Pemp B, Sacu S, Lasta M, Werkmeister RM, et al. Effects of lutein supplementation on macular pigment optical density and visual acuity in patient with age-related macular degeneration. *Invest Ophthalmol Vis Sci.* (2011) 52:8174–8. doi: 10.1167/iovs.11-7522

60. Berendschot TJM. Influence of lutein supplementation on macular pigment, assessed with two objective techniques. *Invest Ophthalmol Vis Sci.* (2000) 41:3322–6.

61. Khachik F, de Moura FF, Chew EY, Douglass LW, Ferris FL, Kim J, et al. The effect of lutein and zeaxanthin supplementation on metabolites of these carotenoids in the serum of persons aged 60 or older. *Invest Ophthalmol Vis Sci.* (2006) 47:5234–42. doi: 10.1167/iovs.06-0504

62. The Age-Related Eye Disease Study 2 Research Group. The age-related eye disease study 2 (AREDS2): study design and baseline characteristics (AREDS2 report number 1). *Ophthalmology.* (2012) 119:2282–9. doi: 10.1016/j.ophtha.2012.05.027

63. Musch DC. Evidence for including lutein and zeaxanthin in oral supplements for age-related macular degeneration. *J Am Med Assoc.* (2013) 2013:E1–3. doi: 10.1001/jamaophthalmol.2013.7443

64. Loane E, McKay GJ, Nolan JM, Beatty S. Apolipoprotein E genotype is associated with macular pigment optical density. *Invest Ophthalmol Vis Sci.* (2010) 51:2636–43. doi: 10.1167/iovs.09-4397

65. Renzi LM, Hammond BR Jr, Dengler M, Roberts R. The relation between serum lipids and lutein and zeaxanthin in the serum and retina: results from cross-sectional, case-control and case study designs. *Lipid Health Dis.* (2012) 11:33. doi: 10.1186/1476-511X-11-33

66. Thomson LR, Toyoda Y, Langner A, Delori FC, Garnett KM, Craft N, et al. Elevated retinal zeaxanthin and prevention of light-induced photoreceptor cell death in quail. *Invest Ophthalmol Vis Sci.* (2002) 43:3538–49.

67. Murray IJ, Makridaki M, van der Veen RL, Carden D, Parry NR, Berendschot TT. Lutein supplementation over a 1 year period in early AMD might have a mild beneficial effect on visual acuity - the CLEAR study. *Invest Ophthalmol Vis Sci.* (2013) 54:1781–8. doi: 10.1167/iovs.12-10715

68. Eljarrat-Binstock E, Domb AJ. Iontophoresis: a non-invasive ocular drug delivery. *J Controlled Release.* (2006) 110:479–89. doi: 10.1016/j.jconrel.2005.09.049

69. Myles ME, Neumann DM, Hill JM. Recent progress in ocular drug delivery for posterior segment disease: emphasis on transscleral iontophoresis. *Adv Drug Delivery Rev.* (2005) 57:2063–79. doi: 10.1016/j.addr.2005.08.006

70. Sousa-Martins D, Sousa S, Duarte J, Marta M, Lombardo M, Lombardo G. Lutein reaches the retina following iontophoresis application. *Invest Ophthalmol Vis Sci.* (2016) 57:106.

71. Lombardo M, Villari V, Micali N, Roy P, Sousa SH, Lombardo G. Assessment of trans-scleral iontophoresis delivery of lutein to the human retina. *J Biophotonics.* (2018) 11:jbio.201700095. doi: 10.1002/jbio.201700095

72. Lombardo G, Micali NL, Villari V, Serrao S, Lombardo M. All-optical method to assess stromal concentration of riboflavin in conventional and accelerated UV-A irradiation of the human cornea. *Invest Ophthalmol Vis Sci.* (2016) 57:476–83. doi: 10.1167/iovs.15-18651

73. Hammond BR, Wooten BR. Resonance Raman spectroscopic measurement of carotenoids in the skin and retina. *J Biomed Opt.* (2005) 10:054002. doi: 10.1117/1.2116767

74. Bernstein PS, Yoshida MD, Katz NB, McClane RW, Gellermann W. Raman detection of macular carotenoid pigments in intact human retina. *Invest Ophthalmol Vis Sci.* (1998) 39:2003–11.

75. Age-Related Eye Disease Study Research Group. A simplified severity scale for age-related macular degeneration: AREDS Report No. 18. *Arch Ophthalmol.* (2005) 123:1570–4. doi: 10.1001/archopht.123.11.1570

76. Damian I, Nicoara SD. SD-OCT biomarkers and the current status of artificial intelligence in predicting progression from intermediate to advanced AMD. *Life.* (2022) 12:454. doi: 10.3390/life12030454

77. Arrigo A, Romano F, Aragona E, Di Nunzio C, Battista M, Bandello F, et al. Optical coherence tomography angiography can categorize different subgroups of choroidal neovascularization secondary to age-related macular degeneration. *Retina.* (2020) 40:2263–9. doi: 10.1097/IAE.0000000000002775

78. Carroll J, Kay D, Scoles D, Dubra A, Lombardo M. Adaptive optics retinal imaging – clinical opportunities and challenges. *Curr Eye Res.* (2013) 38:709–21. doi: 10.3109/02713683.2013.784792

79. Godara P, Siebe C, Rha J, Michaelides M, Carroll J. Assessing the photoreceptor mosaic over drusen using adaptive optics and SD-OCT. *Ophthalmic Surg Lasers Imaging.* (2010) 41(Suppl.): S104–8. doi: 10.3928/15428877-20101031-07

80. Boretsky A, Khan F, Burnett G, Hammer DX, Ferguson RD, van Kuijk F, et al. *In vivo* imaging of photoreceptor disruption associated with age-related macular degeneration: a pilot study. *Lasers Surg Med.* (2012) 44:603–10. doi: 10.1002/lsm.22070

81. Land ME, Cooper RF, Young J, Berg E, Kitchner T, Xiang Q, et al. Cone structure in subjects with known genetic relative risk for AMD. *Optom Vis Sci.* (2014) 91:939–49. doi: 10.1097/OPX.0000000000000323

82. Gocho K, Sarda V, Falah S, Sahel JA, Sennlaub F, Benchaboune M, et al. Adaptive optics imaging of geographic atrophy. *Invest Ophthalmol Vis Sci.* (2013) 54:3673–80. doi: 10.1167/iovs.12-10672

83. Baraas RC, Horjen Å, Gilson SJ, Pedersen HR. The relationship between perifoveal L-cone isolating visual acuity and cone photoreceptor spacing-understanding the transition between healthy aging and early AMD. *Front Aging Neurosci.* (2021) 13:732287. doi: 10.3389/fnagi.2021.732287

84. Xu X, Wang X, Sadda SR, Zhang Y. Subtype-differentiated impacts of subretinal drusenoid deposits on photoreceptors revealed by adaptive optics scanning laser ophthalmoscopy. *Graefes Arch Clin Exp Ophthalmol.* (2020) 258:1931–40. doi: 10.1007/s00417-020-04774-w

85. Mujat M, Ferguson RD, Patel AH, Iftimia N, Lue N, Hammer DX. High resolution multimodal clinical ophthalmic imaging system. *Opt Express.* (2010) 18:11607–21. doi: 10.1364/OE.18.011607

86. Mariotti L, Devaney N, Lombardo G, Lombardo M. Understanding the changes of cone reflectance in adaptive optics flood illumination retinal images over 3 years. *Biomed Opt Expr.* (2016) 7:2807–22. doi: 10.1364/BOE.7.002807

87. Cooper RF, Lombardo M, Carroll J, Sloan KR, Lombardo G. Methods for investigating the local spatial anisotropy and the preferred orientation of cones in adaptive optics retinal images. *Vis Neurosci.* (2016) 33:e005. doi: 10.1017/S0952523816000018

88. Werner JS, Bieber ML, Schefrin BE. Senescence of foveal and parafoveal cone sensitivities and their relations to macular pigment density. *J Opt Soc Am A.* (2000) 17:1918–32. doi: 10.1364/JOSAA.17.001918

89. Gellermann W, Ermakov IV, Ermakova MR, McClane RW, Da-You Zhao, Bernstein PS. *In vivo* resonant Raman measurement of macular carotenoid pigments in the young and the aging human retina. *J Opt Soc Am A.* (2002) 19:1172–86. doi: 10.1364/JOSAA.19.001172

90. Ermakov IV, Sharifzadeh M, Ermakova M, Gellermann W. Resonance Raman detection of carotenoid antioxidants in living human tissue. *J Biomed Opt.* (2005) 10:064028. doi: 10.1117/1.2139974

91. Bernstein PS, Zhao DY, Sharifzadeh M, Ermakov IV, Gellermann W. Resonance Raman measurement of macular carotenoids in the living human eye. *Arch Biochem Biophys.* (2004) 430:163–9. doi: 10.1016/j.abb.2004.07.004

92. Mohsen S, Zhao DY, Bernstein PS, Gellermann W. Resonance Raman imaging of macular pigment distributions in the human retina. *J Opt Soc Am A.* (2008) 25:947–57. doi: 10.1364/JOSAA.25.000947

93. Ermakov IV, Ermakova MR, Gellermann W. Simple Raman instrument for *in vivo* detection of macular pigments. *Appl Spectrosc.* (2005) 59:861–7. doi: 10.1366/0003702054411616

94. Tan T-E, Fenner BJ, Barathi VA, Tun SBB, Wey YS, Tsai ASH, et al. Gene-based therapeutics for acquired retinal disease: opportunities and progress. *Front Genet.* (2021) 12:795010. doi: 10.3389/fgene.2021.795010

95. Tan CS, Ngo WK, Chay IW, Ting DS, Sadda SR. Neovascular age-related macular degeneration (nAMD): a review of emerging treatment options. *Clin Ophthalmol.* (2022) 16:917–33. doi: 10.2147/OPTH.S231913

Conflict of Interest: ML and GL are co-founders of Vision Engineering Italy srl. Vision Engineering Italy srl has no commercial or financial interest in the methods and products described herein.

The remaining author declares that the research was conducted in the absence of any commercial or financial relationships that could be construed as a potential conflict of interest.

Publisher's Note: All claims expressed in this article are solely those of the authors and do not necessarily represent those of their affiliated organizations, or those of the publisher, the editors and the reviewers. Any product that may be evaluated in this article, or claim that may be made by its manufacturer, is not guaranteed or endorsed by the publisher.

Giant Cell Arteritis Presenting With Ocular Symptoms: Clinical Characteristics and Multimodal Imaging in a Chinese Case Series

Qian Chen[1†], Weimin Chen[2†], Chaoyi Feng[1†], Deshan Gong[3], Jiong Zhang[4], Yingwen Bi[1], Ping Sun[1], Xinghuai Sun[1,5] and Guohong Tian[1,5*]

[1] Department of Ophthalmology, Eye Ear Nose and Throat Hospital of Fudan University, Shanghai, China, [2] Department of Neurology, Shanghai Deji Hospital, Shanghai, China, [3] Department of Neurosurgery, Shanghai Deji Hospital, Shanghai, China, [4] Department of Rheumatology, Huashan Hospital, Fudan University, Shanghai, China, [5] State Key Laboratory of Medical Neurobiology, Institutes of Brain Science, Fudan University, Shanghai, China

Purpose: To evaluate demographic and clinical characteristics of a Chinese population with giant cell arteritis using multimodal imaging focusing on ophthalmic examinations.

Design: Retrospective observational case series.

Materials and Methods: In the neuro-ophthalmology division of the Eye, Ear, Nose, and Throat Hospital, Shanghai, we evaluated the demographic and clinical characteristics of patients diagnosed with giant cell arteritis between January 2016 and June 2021. Results of routine ophthalmic examinations including fundus examination, optical coherence tomography, color duplex ultrasonography of ocular and superficial temporal arteries, orbital magnetic resonance imaging, and superficial temporal artery biopsy were evaluated.

Results: A total of 15 patients (22 eyes; ten male and five female) were evaluated with a mean age of 77.0 ± 8.5 years. Among them, seven had bilateral involvement that occurred simultaneously or sequentially. Twelve patients presented with arteritic anterior ischemic optic neuropathy, two with arteritic anterior ischemic optic neuropathy combined with cilioretinal artery occlusion, and one with cotton-wool spots. In acute stages of optic neuropathy and retinopathy, optical coherence tomography revealed optic disc edema, thickening of the inner retinal nerve fiber layer and ganglion cell layer, and loss of layer structure. In late stages, optical coherence tomography revealed diffuse atrophy of the inner retina. The "halo" sign was observed in 12 patients in the superficial temporal artery ultrasound, and seven out of eight patients who underwent biopsy demonstrated classic giant cell arteritis pathological changes. Most patients having poor visual acuity but ability to perceive light; 10/22 eyes had permanent vision loss.

Conclusion: Although rare in Asians, giant cell arteritis may be underdiagnosed among elderly Chinese patients presenting with anterior ischemic optic neuropathy.

Non-invasive superficial temporal artery ultrasound detecting inflammatory thickening of the intima as the "halo" sign combined with routine elevated erythrocyte sedimentation rate and C-reactive protein may be helpful in diagnosing patients with a high probability of having giant cell arteritis.

INTRODUCTION

Giant cell arteritis (GCA) is a type of systemic vasculitis that mainly affects medium-sized and large arteries. The incidence of GCA in Asians is 20 times less than that in Caucasians [1]. Although rare, an increasing number of Asian GCA cases, with typical clinical features that are commonly observed among Caucasians, has been reported [2–6]; however, only one nationwide survey has addressed that the prevalence of GCA in patients aged > 50 years in 1997 was 1.47 per 100,000 persons in Japan [7].

In 2018, we reported the case of a Chinese patient with biopsy-proven GCA, presenting with simultaneous anterior ischemic optic neuropathy (AION) with no light perception [6]. To our knowledge, this is the first Chinese case report on the ophthalmic involvement in this disease. In the subsequent years, >15 patients presenting with AION and profound visual loss accompanied with headache have been diagnosed in our neuro-ophthalmology clinic, which indicates that GCA might be underdiagnosed among elderly Asian patients. The permanent visual loss associated with this neuro-ophthalmic condition requires careful vigilance.

In this case series, we utilized multimodal imaging techniques, especially non-invasive color duplex ultrasonography (CDUS), in elderly patients with ocular artery ischemic conditions who were at a high risk of GCA and for whom biopsy was not straightforward or available.

MATERIALS AND METHODS

Patients

Between January 2016 and June 2021, patients with newly diagnosed GCA were admitted to the neuro-ophthalmology division of the Eye, Ear, Nose, and Throat Hospital in Shanghai, China.

The criteria for diagnosing GCA were as follows [8]: (1) age of onset, >50 years; (2) new onset headache; (3) temporal artery abnormality on examination (tenderness or reduced pulsation); (4) elevated erythrocyte sedimentation rate (ESR) (> 50 mm/h); and (5) abnormal temporal artery biopsy, revealing necrotizing vasculitis with predominant mononuclear cell infiltration or granulomatous inflammation.

Patients who presented with at least three of these five criteria were enrolled.

Exclusion criteria included: (1) polyarteritis nodosa or other conditions suspicious of systemic vasculitis [9], (2) inability to cooperate for examination to diagnose GCA, (3) incomplete clinical data, and (4) refusal to sign the consent form.

Demographic Data and Ophthalmic Examinations

Data regarding age, sex, lateral involvement of the involved eye, history of headache, jaw claudication, transient monocular visual loss (TMVL), and diplopia were collected. Neuro-ophthalmologic examinations included dilated fundus examination, standard Snellen visual acuity, visual field test, fundus fluorescein angiography, and optical coherence tomography (OCT). Laboratory tests included complete blood count, liver and renal function tests, ESR, C-reactive protein (CRP), rheumatoid factor, anti-streptomycin antibody, and other rheumatology panel tests such as anti-nuclear antibody, anti-extractable nuclear antibodies, and anti-neutrophil cytoplasmic antibody. An infectious disease panel was also included.

Ultrasound Imaging

Color duplex ultrasonography (CDUS) was performed with MyLab 90 (Esaote, Genova, Italy) to detect ocular arteries [ophthalmic artery (OA), central retinal artery (CRA), and posterior ciliary artery (PCA)]. A high-frequency (6–18 MHz) linear probe was used to detect the superficial cutaneous temporal artery in cooperating patients. The detection site of the superficial cutaneous temporal artery is located in the main trunk of the artery bilaterally in front of the ear.

Temporal Artery Biopsy

Patients scheduled for superficial temporal artery biopsy were referred to a neurosurgeon. The biopsy was performed in the operating room under local anesthesia, and the severely involved side guided by CDUS was chosen for the biopsy. Long-segment arteries > 3 cm were used for the biopsy to prevent skip lesions [10].

Statistical Analysis

Descriptive statistics (e.g., means, percentage) were used to summarize the demographic characteristics and clinical features of this case series.

Abbreviations: AION, anterior ischemic optic neuropathy; CDUS, color duplex ultrasonography; CLAO, cilioretinal artery occlusion; CRA, central retinal artery; CRAO, central retinal artery occlusion; CRP, C-reactive protein; ESR, erythrocyte sedimentation rate; GCA, Giant cell arteritis; OA, ophthalmic artery; OCT, optical coherence tomography; PCA, posterior ciliary artery; TMVL, transient monocular visual loss.

TABLE 1 | Demographic and clinical characteristics of giant cell arteritis Chinese patients.

No.	Age (y)	Sex	Eye (lateral)	Presenting symptom	HA	TMVL	WL	BCVA	Fundus	ESR (mm/h)	CRP (mg/L)	CDUS	STAU	Biopsy
1	64	M	OS	AION	+	+	−	NLP	Pallid edema	53	77.54	CRA + PCA +	Halo sign Stenosis	P
2	69	M	OD	AION	+	+	−	LP	Pallid edema hemorrhage	33	4.6	CRA + PCA + OA +	Halo sign Segmental stenosis	P
3	66	M	OU	NA	+	−	−	20/40 20/30	Cotton-wool spots	113	80.96	CRA + PCA +	Halo sign Segmental occlusion	P
4	81	M	OD	AION + CLAO	−	+	−	20/100	Pallid edema	65	35.8	CRA + OA +	Halo sign	P
5	76	M	OS	AION	+	+	−	HM	Pallid edema	65	13.1	CRA + PCA + OA +	Normal	N
6	88	F	OS	AION	+	+	−	NLP	Pallid edema	49	8.6	CRA + PCA + OA +	Halo sign Stenosis	N
7	86	M	OD	AION + CLAO	+	+	−	NLP	Pallid edema	22	21.8	PCA + OA +	Halo sign	P
8	79	M	OS	AION	+	+	−	20/400	Pallid edema hemorrhage	50	55	CRA + PCA + OA +	Halo sign Diffuse stenosis	P
9	71	F	OU	AION	+	+	−	NLP NLP	Pallid edema hemorrhage	68	62.8	PCA +	Halo sign	P
10	71	M	OU	AION	+	+	−	LP 20/400	Pallid edema Cotton-wool spots	69	129.5	CRA + PCA + OA +	NA	NA
11	68	M	OD	AION	+	−	−	LP	Pallid edema	27	7.64	PCA +	Halo sign	NA
12	84	F	OU	AION	+	+	−	20/200 20/400	Pallid edema	59	42.8	CRA +	Halo sign	NA
13	90	F	OU	AION	+	+	−	LP NLP	Pallid edema Peripapillary atrophy	63	74	CRA + PCA + OA +	Halo sign Steno sis	NA
14	77	M	OU	AION	+	+	−	NLP NLP	Pallid edema Peripapillary atrophy	90	105	CRA + PCA +	Halo sign	P
15	85	F	OU	AION	+	+	−	NLP NLP	Pallid edema	77	57.3	CRA + PCA + OA +	Halo sign Occlusion	NA

HA, headache; TMVL, transient monocular visual loss; WL, weight loss; BCVA, best-corrected visual acuity; ESR, erythrocyte sedimentation rate; CRP, C-reactive protein; CDUS, color duplex ultrasonography; STAU, superficial temporal artery ultrasound; M, male; F, female; OS, oculus sinister (left eye); OD, oculus dexter (right eye); OU, oculus uterque (both eyes); AION, anterior ischemic optic neuropathy; CLAO, cilioretinal artery occlusion; HM, hand motion; LP, light perception; NLP, no light perception; CRA, central retinal artery; PCA, posterior ciliary artery; OA, ophthalmic artery; P, positive; N, negative; NA, not available.
+In the CDUS column indicates decreased blood flow.
CRP normal limit (0–3 mg/L).
ESR normal limit (0–15 mm/h).

FIGURE 1 | Color fundus photographs in patients with giant cell arteritis showing chalky-white swollen discs **(A,B,D)** with retina exudate and cotton-wool spots **(A)**, late-stage optic atrophy and cupping **(C)**, peripapillary hemorrhage with atrophy **(D)**, and cilioretinal artery occlusion **(B,C,E,F)** are the same eye.
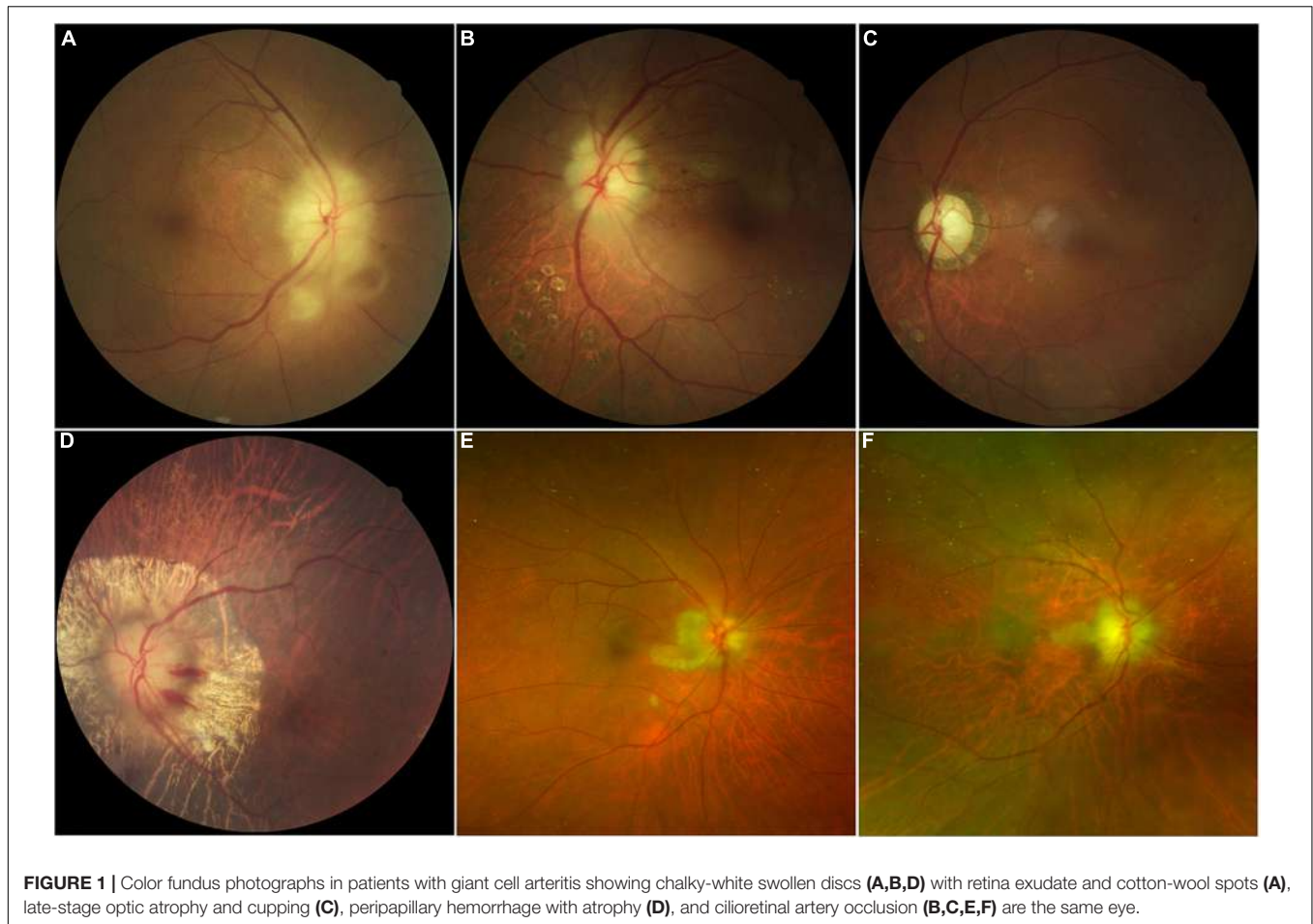
Ethics Approval and Informed Consent

The Institutional Ethics Review Board of the Eye Ear Nose and Throat Hospital of the Fudan University Shanghai approved all the experimental protocols, and written informed consent was obtained from all participants and/or their legal guardians (KJ-2011-04). The methods were carried out in accordance with the relevant guidelines and regulations. The study was performed in accordance with the Declaration of Helsinki.

RESULTS

Demographic and Clinical Features

A total of 15 patients (22 eyes; 10 male, 5 female) were assessed. The mean age was 77.0 ± 8.5 y. Among them, seven patients had bilateral involvement that occurred simultaneously or sequentially. The presenting ophthalmic manifestations included AION ($n = 12$), AION combined with cilioretinal artery occlusion (CLAO) ($n = 2$), and cotton-wool spots ($n = 1$).

Headache was the most common accompanying systemic symptom ($n = 14$, 99.3%) and could be the only presenting symptom. TMVL was the common aura attack ($n = 13$, 86.7%), a detail that was provided by the patient only when asked

specifically. Other systemic symptoms included weight loss ($n = 8$, 53.3%), joint pain ($n = 2$, 13.3%), scalp tenderness ($n = 2$), jaw claudication ($n = 1$, 6.7%), and stroke ($n = 1$). None of the patients had diplopia in our case series. There was only one patient with no systemic symptoms.
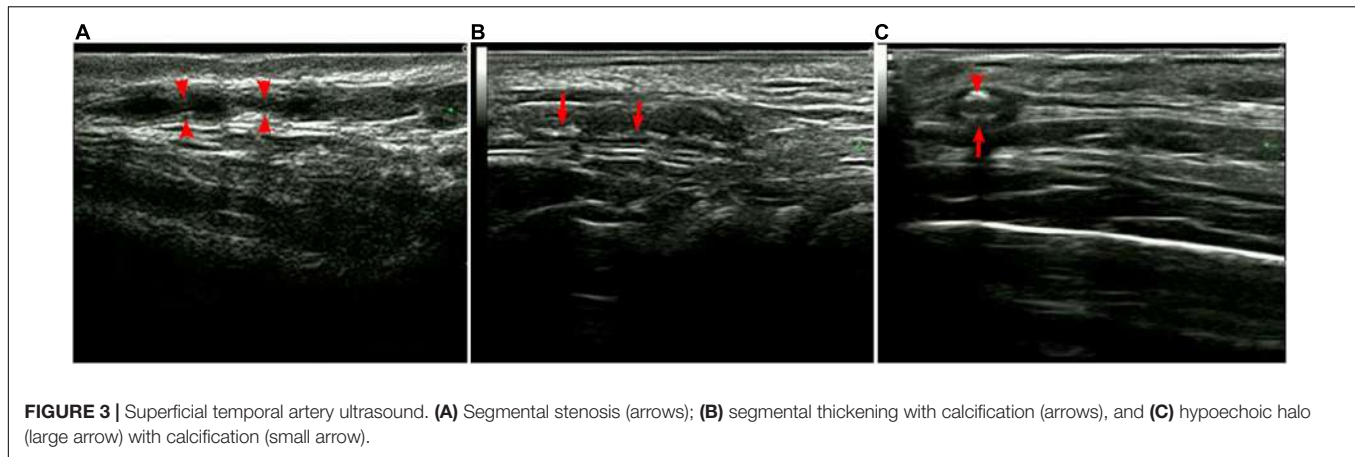
Visual acuity was very poor, except in patient 3, who presented with only headache without ocular ischemic attack. Most patients having poor visual acuity but ability to perceive light. The visual acuity results are shown in **Table 1**.

Fundus examination of most AION eyes (15/22 eyes) revealed a classic chalky-white disc swollen due to GCA, and some with peripapillary hemorrhage (4/22 eyes), retinal exudates, and cotton-wool spots (4/22 eyes). CLAO was observed in two patients; both cases were combined with AION. Peripapillary atrophy (6/22 eyes) was also common in patients with severe disease and bilateral involvement. Optic atrophy with cupping was observed in cases of late-stage AION or in eyes with history of previous attack (**Figure 1**). Details of demographic and clinical features are shown in **Table 1**.

The main findings of OCT performed in 11 eyes were ischemic retinopathy or neuropathy. Eight eyes were in the acute stage and showed optic disc edema with a loss of layer structure in the inner retina and extreme edematous thickening of the peripapillary retinal nerve fiber layer and
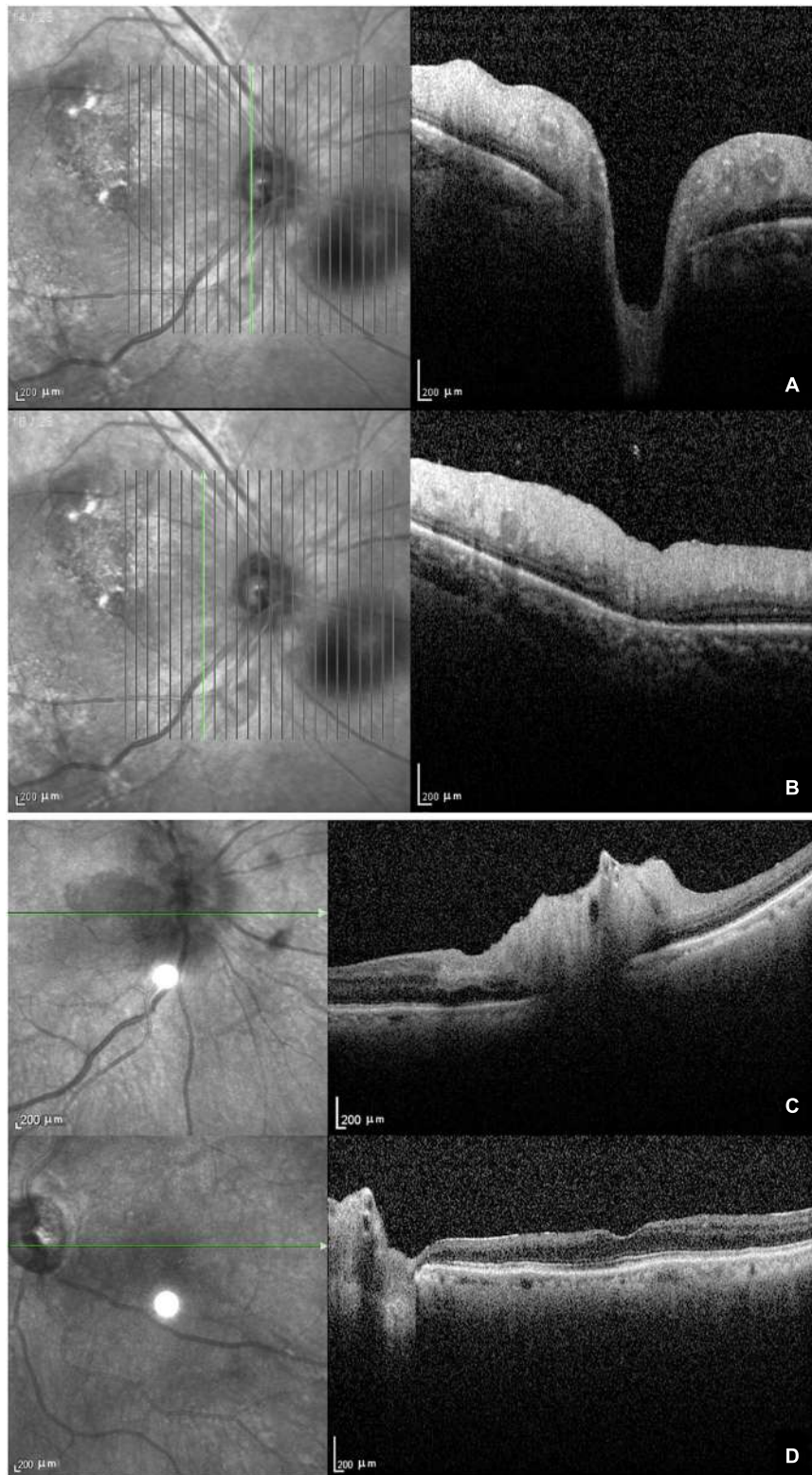
FIGURE 2 | Optical coherence tomography in patients with giant cell arteritis. **(A)** Optic disc edema with a loss of layer structure in the inner retina; **(B)** edematous thickening of the peripapillary retinal nerve fiber layer and ganglion cell layer; **(C)** arteritic anterior ischemic optic neuropathy combined with ciliary vascular obstruction showing edema of the optic disc, thickening, and a loss of layer structure in the inner retina; **(D)** atrophy and thinning of the retinal nerve fiber layer and ganglion cell layer with epiretinal membrane at the late stage.

FIGURE 3 | Superficial temporal artery ultrasound. **(A)** Segmental stenosis (arrows); **(B)** segmental thickening with calcification (arrows), and **(C)** hypoechoic halo (large arrow) with calcification (small arrow).

ganglion cell layer (**Figures 2A,B**). In patients with arteritic AION combined with CLAO, OCT showed edema of the optic disc, thickening of the inner retinal nerve fiber layer and ganglion cell layer, and loss of layer structure (**Figure 2C**). Patients with late-stage bilateral involvement and no light perception had peripapillary atrophy with extremely thin retinal nerve fiber and ganglion cell layers and epiretinal membranes (**Figure 2D**). Due to their poor systemic condition, only two patients underwent fundus fluorescein angiography, which revealed a delay in optic disc and choroidal artery perfusion.

Routine Blood Test

The ESR and CRP levels in all patients are listed in **Table 1**. According to the American College of Rheumatology 1990 criteria for GCA, the ESR was elevated in 11 patients (73.3%), and the CRP was substantially elevated in all 15 patients. The results of the rheumatologic panel were unremarkable, including the rheumatoid, anti-streptomycin antibody, anti-nuclear antibody, and anti-neutrophil cytoplasmic antibody. The complete blood count showed a considerable increase in white blood cell count ($n = 9$) and decrease in red blood cell count and hemoglobin ($n = 12$). The platelet count was elevated in four patients, with increased thrombocytes in nine patients.

Ultrasonography Imaging

Color duplex ultrasonography (CDUS) detected that almost all patients had varying degrees of ophthalmic ischemic conditions associated with the CRA, PCA, and OA. Among the 15 patients, 14 underwent superficial temporal artery ultrasound with a high-frequency linear probe. The results demonstrated bilateral thickening of the vessel wall with the hypoechoic halo sign, consistent with mural inflammation, in 12 (92.9%) patients. The mural showed rough signals with segmental thickening and stenosis, and some had diffuse stenosis or occlusion. Non-specific calcification was also observed in some individuals (**Figure 3**). The mean thickness of the intima was 0.49 ± 0.12 mm (0.25-0.75 mm), and the mean vessel diameter was 1.36 ± 0.42 mm (0.74-2.5 mm).

Magnetic Resonance Imaging Orbit/Brain

Fat-suppressed contrast-enhanced T1-weighted magnetic resonance imaging (MRI) of the orbit, available for only nine patients demonstrated bilateral optic nerve sheath enhancement. The cranial vessels, including the internal/external carotid arteries and some scalp arteries, showed enhancement of the thickened intima with luminal stenosis or occlusion (**Figure 4**). Brain MRI showed non-specific diffuse brain atrophy with enlarged ventricles in 11 patients.

Temporal Artery Biopsy

Among the eight patients who underwent temporal artery biopsy, seven (87.5%) demonstrated positive results in terms of classic GCA pathological changes, such as arterial wall inflammation with mononuclear cell infiltration, multinucleated giant cells, and luminal stenosis or occlusion (**Figure 5**).

Treatment and Prognosis

All patients underwent cortical steroid treatment after GCA diagnosis. Intravenous methylprednisolone 500 mg/d to 1 g/d were administered to 11 patients and low dose methylprednisolone 120 mg/d or oral prednisone 60 mg/d was prescribed for patients with intolerance due to contraindications and old age. Immunosuppressive agents such as methotrexate were added while oral prednisone was tapered to a low dosage around 5 to 15 mg/d. Tocilizumab was prescribed and well tolerated in two patients. Final visual functions were very poor in most patients, except in one patient who initially presented with only a headache.

DISCUSSION

The low incidence of GCA among Asians is considered to be associated with the different type of human leukocyte antigen observed in this population [11, 12]. In a comparative study by Pereira et al., only one Asian case was reported during an 8-year period [1], whereas in our territory eye center division of neuro-ophthalmology in Shanghai, 15 consecutive
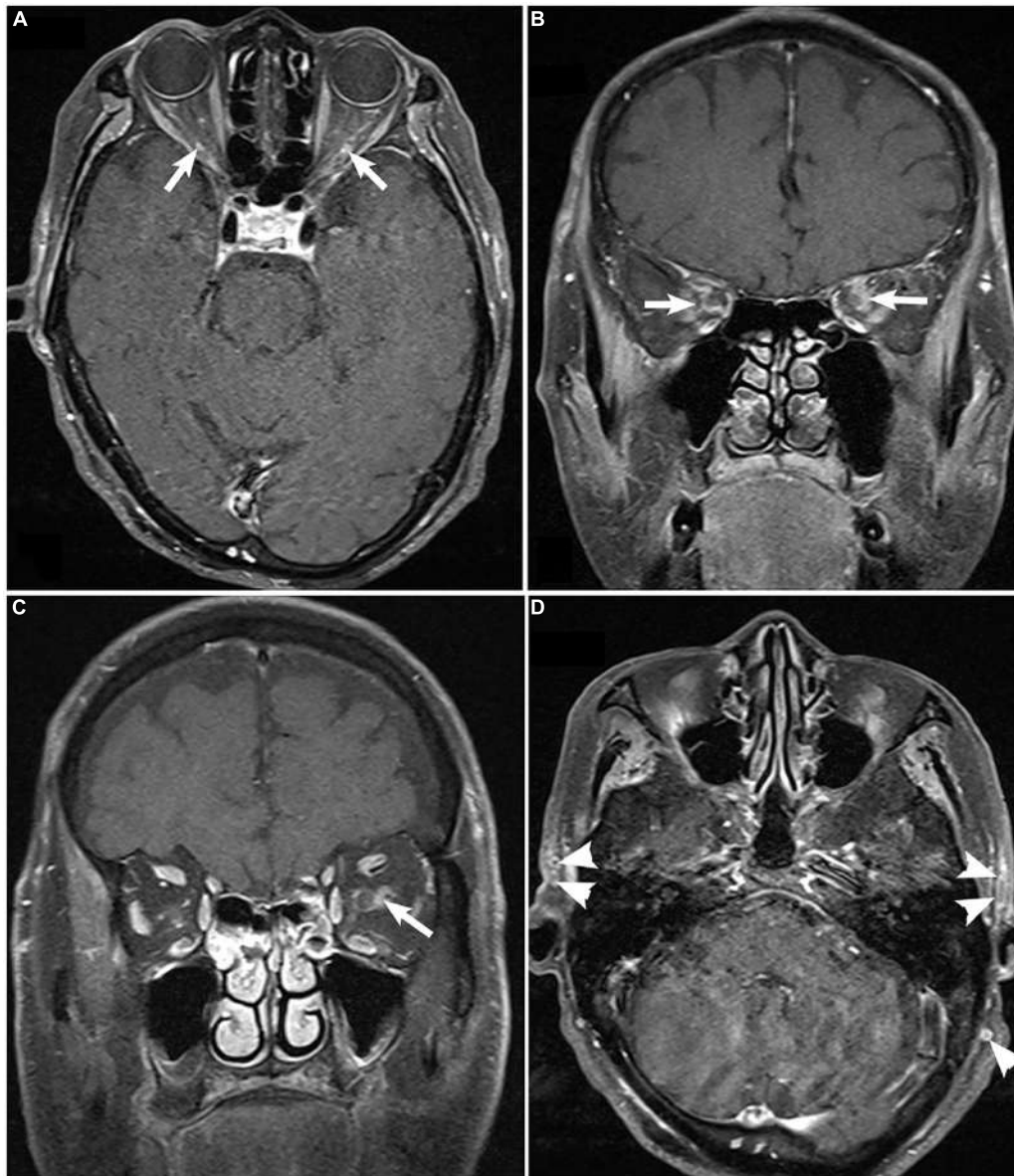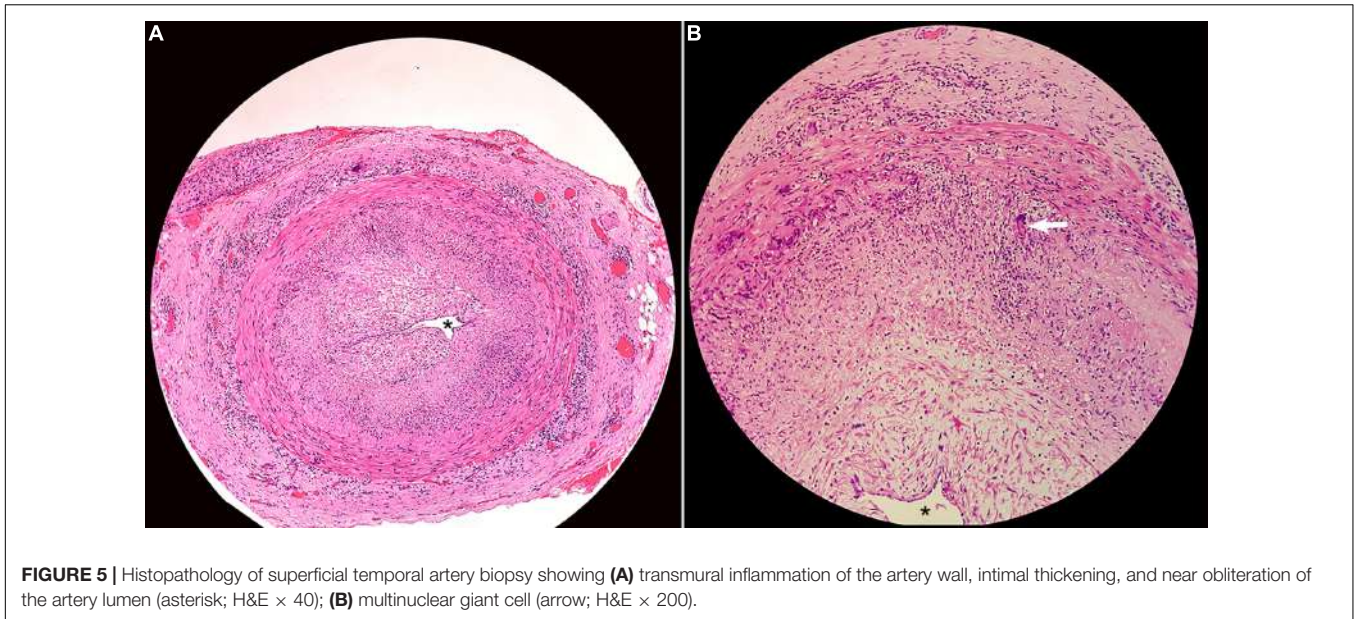
FIGURE 4 | Fat-suppressed contrast-enhanced T1-weighted magnetic resonance imaging of the orbit demonstrating enhancement of bilateral optic nerve sheaths [arrow; **(A)**, axial; **(B)**, coronal], unilateral enhancement of optic nerve sheaths [**(C)**, arrow], and enhancement and thickening superficial temporal artery [**(D)**, arrowhead].

cases have been diagnosed within the last 5 years. To date, this is the only case series report on GCA presenting with ocular manifestations in China. It is also a notably large case series report on Asian populations. Our data suggested that ophthalmologists need to remain vigilant about GCA being potentially underdiagnosed among elderly Asian patients with ischemic conditions such as ophthalmic ischemia, central retinal artery occlusion (CRAO)/AION, and AION combined with CLAO; in particular, the latter was highly indicative of a PCA occlusion. There were no cases of branch retinal artery occlusion in this series since they lack the internal elastic lamina (13, 14).

Female predominance has been reported in the literature among both Caucasian and Asian ethnicities (1, 7, 15). The male/female ratio in our case series was 2:1, which was consistent with the ratio found in a small case series with Thai patients (2); both of these case series were composed mainly of patients with AION.

Systemic symptoms such as headache, TMVL, weight loss, and scalp tenderness were common complaints in this study of which headache could be the only presenting symptom. Although TMVL was also very common, it was reported only when the patients were specifically asked. Diplopia and visual hallucinations were not reported by any patient. Unlike

FIGURE 5 | Histopathology of superficial temporal artery biopsy showing **(A)** transmural inflammation of the artery wall, intimal thickening, and near obliteration of the artery lumen (asterisk; H&E × 40); **(B)** multinuclear giant cell (arrow; H&E × 200).

Caucasians, Asian patients with GCA usually present with non-specific symptoms such as headache, weight loss, malaise, fatigue, and fever, rather than jaw claudication or double vision. This results in delayed diagnosis by physicians or rheumatologists.

Due to a lack of specific blood biomarkers for the diagnosis of GCA, routine complete blood count, ESR, and CRP are very useful ancillary tests that can quickly distinguish patients with arteritic AION from those with non-arteritic AION. Elevated ESR and CRP levels, combined with anemia, are highly indicative of the necessity for further work-up.

According to the literature, the incidence of visual symptoms in GCA can be as high as 70%, and 20% of patients may experience permanent visual loss (15, 16). In our case series, he visual acuity most tested in the affected eye was light perception, and the outcome was also very poo. The fundus appearance revealed classic chalky-white swelling in the acute stage, and retinal cotton-wool spots might have been an early sign of arterial ischemia. Peripapillary atrophy is another feature in patients with chronic ischemia, which can be observed in the acute stage. The simultaneous presence of AION and CRAO indicates PCA involvement and is highly indicative of GCA causing arteritic AION rather than non-arteritic AION. In addition, AION combined with CRAO/branch retinal artery occlusion, which indicates OA involvement, was not observed in our series.

Due to the considerably low temporal artery biopsy rate in China, GCA is rarely reported by ophthalmologists in this country; therefore, GCA remains underdiagnosed among the AION population, especially in the elderly. Temporal artery ultrasonography, which is non-invasive and cost-effective, is recommended by the European League Against Rheumatism as the first-line study for evaluating large-vessel vasculitis and has been widely utilized in our clinic recently for evaluating high-risk GCA patients (17–19). CDUS can detect the blood flow in ocular arteries, including the OA, CRA, and PCA, and the high-frequency linear probe can detect the superficial cutaneous temporal artery. The hypoechoic halo sign is indicative of inflammatory thickening of the intima with stenosis/occlusion of the lumen; these phenomena are consistent with pathological changes in GCA. According to our data, the halo sign is a highly specific indicator for GCA diagnosis and can also guide the side for biopsy. However, a limitation associated with using ultrasound for detection of temporal artery vasculitis is operator dependence.

MRI is another non-invasive technique for evaluating arteries and determining a diagnosis (17, 20). In addition to the cranial arteries, enhancement of the optic nerve sheath in orbit MRI has been reported as one characteristic of GCA, which was observed in our case series as well (20, 21). Although perineural enhancement is a non-specific phenomenon which can also be observed in infectious and other autoimmune optic neuropathies such as sarcoidosis, MRI on a patient with potential GCA is still crucial to exclude malignant conditions.

The limitations of the study include the short follow-up of patients which limited our ability to obtain long-term effects of immune therapies like Tocilizumab. Furthermore, future research should focus on identifying specific biomarkers of GCA pathogenesis in the Chinese population.

In summary, GCA may be underdiagnosed in elderly Chinese patients with ocular ischemic conditions. The profound visual loss associated with AION/CRAO in elderly patients is highly indicative of GCA in cases of elevated ESR or CRP levels. The hypoechoic halo sign found on ultrasound of the temporal artery is a very sensitive and specific indicator for diagnosis and should be utilized to guide biopsy.

DATA AVAILABILITY STATEMENT

The datasets used and/or analyzed during the current study are available from the corresponding author on reasonable request.

ETHICS STATEMENT

AUTHOR CONTRIBUTIONS

QC and GT conceived the study. DG and YB performed the biopsy and pathology. WC and JZ participated in the diagnosis. CF and PS collected and interpreted data. QC and CF drafted the manuscript. GT revised the manuscript. XS sponsored by funding. All authors have approved the final manuscript.

FUNDING

ACKNOWLEDGMENTS

REFERENCES

1. Pereira LS, Yoon MK, Hwang TN, Hong JE, Ray K, Porco T, et al. Giant cell arteritis in Asians: a comparative study. *Br J Ophthalmol.* (2011) 95:214–6. doi: 10.1136/bjo.2009.177220

2. Attaseth T, Vanikieti K, Poonyathalang A, Preechawat P, Jindahra P, Wattanatranon D. Anterior ischemic optic neuropathy due to biopsy-proven giant cell arteritis in Thai patients. *Clin Ophthalmol.* (2015) 9:1071–5. doi: 10.2147/OPTH.S82898

3. Cha DM, Lee T, Choe G, Yang HK, Hwang JM. Silent giant cell arteritis in an elderly Korean woman. *Korean J Ophthalmol.* (2013) 27:224–7. doi: 10.3341/kjo.2013.27.3.224

4. Liou LM, Khor GT, Lan SH, Lai CL. Giant cell arteritis with multiple cranial nerve palsy and reversible proptosis: a case report. *Headache.* (2007) 47:1451–3. doi: 10.1111/j.1526-4610.2007.00952.x

5. Wang X, Hu Z, Lu W, Tang X, Zeng L, Zhang J, et al. Giant cell arteritis: a rare disease in Asians. *J Clin Rheumatol.* (2009) 15:48. doi: 10.1097/RHU.0b013e31819632e1

6. Tian G, Chen W, Chen Q, Wang M, Zhao G, Li Z, et al. Giant cell arteritis presenting as bilateral anterior ischemic optic neuropathy: a biopsy-proven case report in Chinese patient. *BMC Ophthalmol.* (2018) 18:282. doi: 10.1186/s12886-018-0953-5

7. Kobayashi S, Yano T, Matsumoto Y, Numano F, Nakajima N, Yasuda K, et al. Clinical and epidemiologic analysis of giant cell (temporal) arteritis from a nationwide survey in 1998 in Japan: the first government-supported nationwide survey. *Arthritis Rheum.* (2003) 49:594–8. doi: 10.1002/art.11195

8. Hunder GG, Bloch DA, Michel BA, Stevens MB, Arend WP, Calabrese LH, et al. The American College of Rheumatology 1990 criteria for the classification of giant cell arteritis. *Arthritis Rheum.* (1990) 33:1122–8. doi: 10.1002/art.1780330810

9. Zhang Y, Wang D, Chu X, Zhang W, Zeng X. Differences in clinical manifestations and prognosis of Chinese giant cell arteritis patients with or without polymyalgia rheumatica. *Ir J Med Sci.* (2019) 188:713–20. doi: 10.1007/s11845-018-1903-1

10. Liu T, Volpe JN, Galetta LS. *Neuro-Ophthalmology: Diagnosis and Management.* 2nd ed. Amsterdam: Elsevier Inc (2001).

11. Hunder GG, Lie JT, Goronzy JJ, Weyand CM. Pathogenesis of giant cell arteritis. *Arthritis Rheum.* (1993) 36:757–61. doi: 10.1002/art.1780360604

12. Hashimoto H. Takayasu's arteritis and giant cell (temporal or cranial) arteritis. *Intern Med.* (2000) 39:4–5. doi: 10.2169/internalmedicine.39.4

13. Vodopivec I, Rizzo JF III. Ophthalmic manifestations of giant cell arteritis. *Rheumatology.* (2018) 57:ii63–72. doi: 10.1093/rheumatology/kex428

14. Hayreh SS. Acute retinal arterial occlusive disorders. *Prog Retin Eye Res.* (2011) 30:359–94. doi: 10.1016/j.preteyeres.2011.05.001

15. Chen JJ, Leavitt JA, Fang C, Crowson CS, Matteson EL, Warrington KJ. Evaluating the incidence of arteritic ischemic optic neuropathy and other causes of vision loss from giant cell arteritis. *Ophthalmology.* (2016) 123:1999–2003. doi: 10.1016/j.ophtha.2016.05.008

16. Glutz von Blotzheim S, Borruat FX. Neuro-ophthalmic complications of biopsy-proven giant cell arteritis. *Eur J Ophthalmol.* (1997) 7:375–82. doi: 10.1177/112067219700700412

17. Ninan JV, Lester S, Hill CL. Diagnosis and management of giant cell arteritis: an Asia-Pacific perspective. *Int J Rheum Dis.* (2019) 22:28–40. doi: 10.1111/1756-185X.13297

18. Serling-Boyd N, Stone JH. Recent advances in the diagnosis and management of giant cell arteritis. *Curr Opin Rheumatol.* (2020) 32:201–7. doi: 10.1097/BOR.0000000000000700

19. Dejaco C, Ramiro S, Duftner C, Besson FL, Bley TA, Blockmans D, et al. EULAR recommendations for the use of imaging in large vessel vasculitis in clinical practice. *Ann Rheum Dis.* (2018) 77:636–43. doi: 10.1136/annrheumdis-2017-212649

20. Klink T, Geiger J, Both M, Ness T, Heinzelmann S, Reinhard M, et al. Giant cell arteritis: diagnostic accuracy of MR imaging of superficial cranial arteries in initial diagnosis-results from a multicenter trial. *Radiology.* (2014) 273:844–52. doi: 10.1148/radiol.14140056

21. Liu TY, Miller NR. Giant cell arteritis presenting as unilateral anterior ischemic optic neuropathy associated with bilateral optic nerve sheath enhancement on magnetic resonance imaging. *J Neuroophthalmol.* (2015) 35:360–3. doi: 10.1097/WNO.0000000000000269

The Role of Corticosteroids in Treating Acute Ocular Toxoplasmosis in an Immunocompetent Patient: A Case Report

Hung-Yi Lin[1] and Wan-Ju Annabelle Lee[2,3,4]*

[1] Medical Education Center, Chi Mei Medical Center, Tainan, Taiwan, [2] Department of Ophthalmology, Chi Mei Medical Center, Tainan, Taiwan, [3] Institute of Clinical Pharmacy and Pharmaceutical Sciences, College of Medicine, National Cheng Kung University, Tainan, Taiwan, [4] Department of Optometry, Chung Hwa University of Medical Technology, Tainan, Taiwan

Background: This study aimed to report a case who was treated with corticosteroids and anti- parasitic agents for ocular toxoplasmosis, but who progressed to acute retinal necrosis, and finally retinal detachment.

Case Presentation: A 42-year-old man presented to the ophthalmology clinic with a 1-month history of progressive blurred vision and floaters in his right eye. His best visual acuity (VA) was 20/20 in both eyes. The anterior segment was unremarkable. Funduscopic examination of the right eye revealed active lesions of whitish foci of chorioretinitis with surrounding edema along the superonasal vessels, and retinal vasculitis with perivascular sheathing. Serologic testing was positive for *Toxoplasma gondii* IgM and IgG, but negative for other virus- and syphilis infections. Ocular toxoplasmosis was diagnosed. Corticosteroids and anti-parasitic agents were given simultaneously, but his right eye VA became 20/100. Funduscopic examination revealed retinal necrosis with localized retinal breaks. We immediately performed focal photocoagulation, however, his right eye progressed to retinal detachment and required vitrectomy.

Conclusion: Early administration of systemic corticosteroids in patients with acquired acute ocular toxoplasmosis may lead to complications that impair vision. Intensive observation should be arranged after corticosteroid use.

Keywords: ocular toxoplasmosis, corticosteroid, retinal necrosis, retinal detachment, choroidoretinitis

INTRODUCTION

Toxoplasmosis is an infection caused by the intracellular protozoan parasite *Toxoplasma gondii*. Primary infection in immunocompetent persons is usually asymptomatic and self-limited. The most common manifestations of acute toxoplasmosis in immunocompetent patients are cervical lymphadenopathy and flu-like symptoms. Toxoplasmosis may also present as ocular disease, which is the most frequent etiology of infectious posterior uveitis (1). In immune intact patients, typical clinical manifestations of ocular toxoplasmosis have been described as a nidus of fluffy,

Abbreviations: PCR, polymerase chain reaction; DNA, deoxyribonucleic acid; VA, visual acuity; OCT, optical coherence tomography; HSV, herpes simplex virus; CMV, cytomegalovirus; TB, tuberculosis; M. tuberculosis, mycobacterium tuberculosis; VZV, varicella-zoster virus; IgG, immunoglobulin G; IgM, immunoglobulin M.

white, necrotizing retinitis or choroidoretinitis adjacent to a variably pigmented chorioretinal scar. Clinical diagnosis in most cases is based on typical presentation upon funduscopic examination. Serological analysis may be helpful in recently-acquired cases (2). In atypical cases, such as the absence of a retinochoroidal scar, analyzing antibody levels and parasitic DNA in the aqueous humor and serum specimen may be necessary to confirm the diagnosis (3). The current treatment regimen with anti-parasitic agents has been discussed widely without reaching consensus. Corticosteroid therapy is used as a part of the therapeutic regimen to regulate the immune response, however, this strategy may lead to damage to the ocular tissues. A combination of anti-parasitic agents and corticosteroids is suggested in most clinical scenarios, but the timing for commencement of corticosteroids has been subject to some controversy (4).

Here, we report an ocular toxoplasmosis case of an immunocompetent young male who presented with acute focal choroidoretinitis without the typical scarring lesion, and who progressed to localized retinal detachment soon after simultaneous use of anti-parasitic agents and corticosteroids.

CASE PRESENTATION

A 42-year-old man presented to the ophthalmology clinic with a 1-month history of progressive blurred vision and floaters in his right eye. He had no medical history. On ocular examination, the visual acuity (VA) was 20/20 in both eyes. The anterior segment was unremarkable. Funduscopic examination of the right eye revealed active lesions with whitish foci of choroidoretinitis with surrounding edema along the superonasal vessels, and retinal vasculitis with perivascular sheathing (**Figures 1A,B**). Serologic testing was positive for *Toxoplasma gondii* IgM and IgG, HSV-1 IgG, HSV-2 IgG, and CMV IgG, and negative for syphilis and Anti-HIV. Optical coherence tomography (OCT) of the macula revealed mild perifoveal edema in the right eye. Fluorescein angiography of the right eye showed obliteration of the blood flow with a non-perfusion area and leakage at the vessel wall (**Figure 1C**).

Based on the patient's history, ophthalmic findings, and serology results, an infectious cause was highly suspected. We performed aqueous humor tapping for viral and tuberculosis polymerase chain reaction (PCR) testing to exclude possible causative agents. The PCR result showed no evidence of any viral or TB infection. We also performed a serum quantiferon gold test for the patient in case of recurrent tuberculosis, but the result was negative.

Thus, ocular toxoplasmosis was diagnosed. We consulted an infection specialist regarding the survey and management of potential systemic toxoplasmosis. The infection was initially managed by the infection specialist with sulfamethoxazole-trimethoprim (400/80 mg) twice per day, and one dose of dexamethasone 5 mg intravenously, on the first day. Five days later, the patient complained of significantly increasing photophobia in the lesioned eye, so we titrated sulfamethoxazole-trimethoprim (400/80 mg) to 3 times per

day and added prednisolone 15 mg per day, simultaneously. Two days later, his right eye visual acuity (VA) declined to 20/100. Funduscopic examination revealed severe vitritis complicated with progressive localized retinal necrosis and multiple localized retinal breaks. Although we performed focal retinal photocoagulation immediately, he progressed to localized rhegmatogenous retinal detachment 5 days later. He then underwent a successful pars plana vitrectomy. During the surgery, we sent the vitreous samples for PCR to detect other possible pathogens, including HSV, CMV, and TB, but the results were negative. His vision improved to 20/80 after the surgery, and he has been treated with pyrimethamine plus sulfadiazine since then. The retina was attached but his VA remained at 20/80. **Figure 2** showcases the timeline with relevant data from the period of care.

DISCUSSION

Ocular toxoplasmosis typically affects the posterior pole of a single eye and lesions may be single, multiple, or satellites adjacent to retinal pigmented scars. Active lesions present as grayish-white spots of retinal necrosis adjacent to choroiditis, in addition to vasculitis, hemorrhage, and/or vitritis. Healing occurs from the periphery toward the center of the lesion, with variable pigmentary changes. The retina is the primary site of ocular infection by *T. gondii*, but the choroid, vitreous, and anterior chamber may also be involved (5). Anterior uveitis is a common finding, with mutton-fat keratic precipitates, cells, flare, and posterior synechiae. Retinal vasculitis and associated inflammatory reactions may be the only ophthalmic signs during the early stages of acquired ocular toxoplasmosis. The later development of retinitis or scars in the same eye, consistent with ocular toxoplasmosis, suggests parasites as the cause of the initial inflammation. The involvement of the underlying choroid is termed "choroidoretinitis" and describes the clinical image. Ocular complications include choroidal neovascularization, cataract, glaucoma, optic nerve atrophy, and retinal detachment (6, 7).

The diagnosis of ocular toxoplasmosis is usually clinical. With regard to the active lesions, vitritis is mostly the first factor causing visual symptoms. A considerable vision deterioration may manifest due to macular involvement, whereas peripheral lesions may not have an obvious effect on vision. Choroidoretinitis is the most prevalent feature of active intraocular inflammation in patients with ocular toxoplasmosis. However, many cases may present with substantial clinical variations leading to diagnostic difficulties (3, 8–10).

In immunocompetent patients, the active lesions tend to heal automatically within 2–4 months, leaving an atrophic area (resolving from the periphery to the center) that gradually leads to a hyper-pigmented scar due to disruption of the retinal pigment epithelium (RPE). The presence of *T. gondii* IgG antibodies cannot confirm a diagnosis of eye infection, but IgG negativity generally rules it out. Ocular toxoplasmosis may be diagnosed pathologically by way of histology (identifying cysts in biopsies stained with hematoxylin and eosin), by
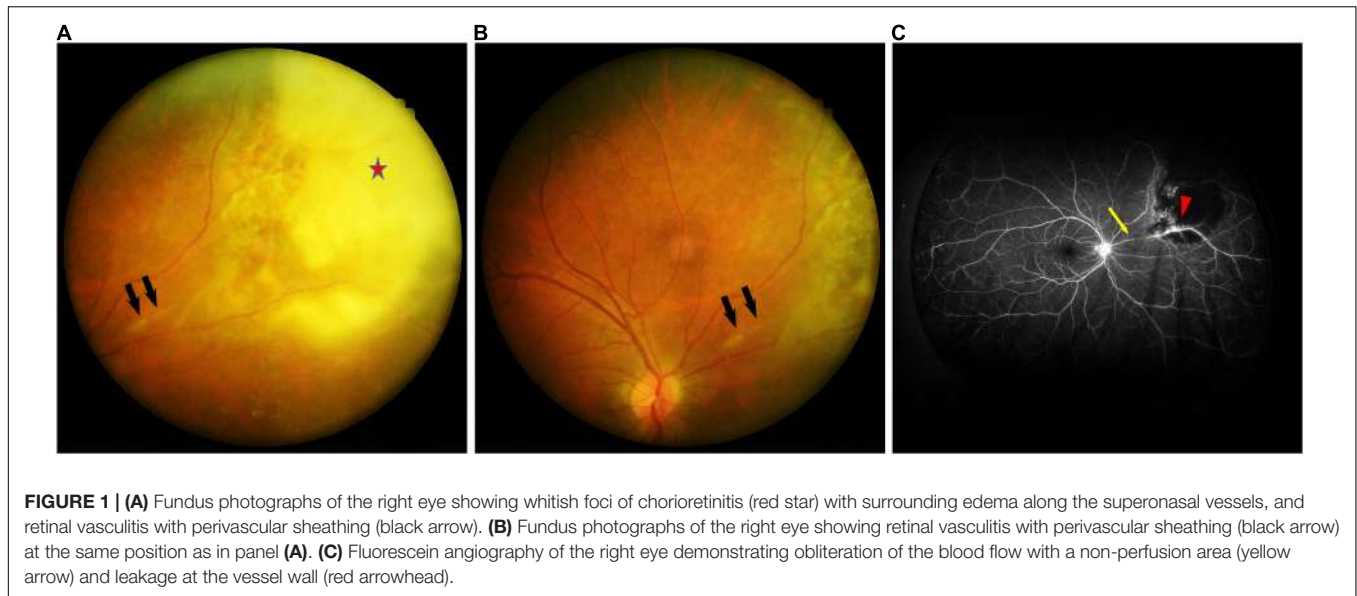
FIGURE 1 | (A) Fundus photographs of the right eye showing whitish foci of chorioretinitis (red star) with surrounding edema along the superonasal vessels, and retinal vasculitis with perivascular sheathing (black arrow). (B) Fundus photographs of the right eye showing retinal vasculitis with perivascular sheathing (black arrow) at the same position as in panel (A). (C) Fluorescein angiography of the right eye demonstrating obliteration of the blood flow with a non-perfusion area (yellow arrow) and leakage at the vessel wall (red arrowhead).
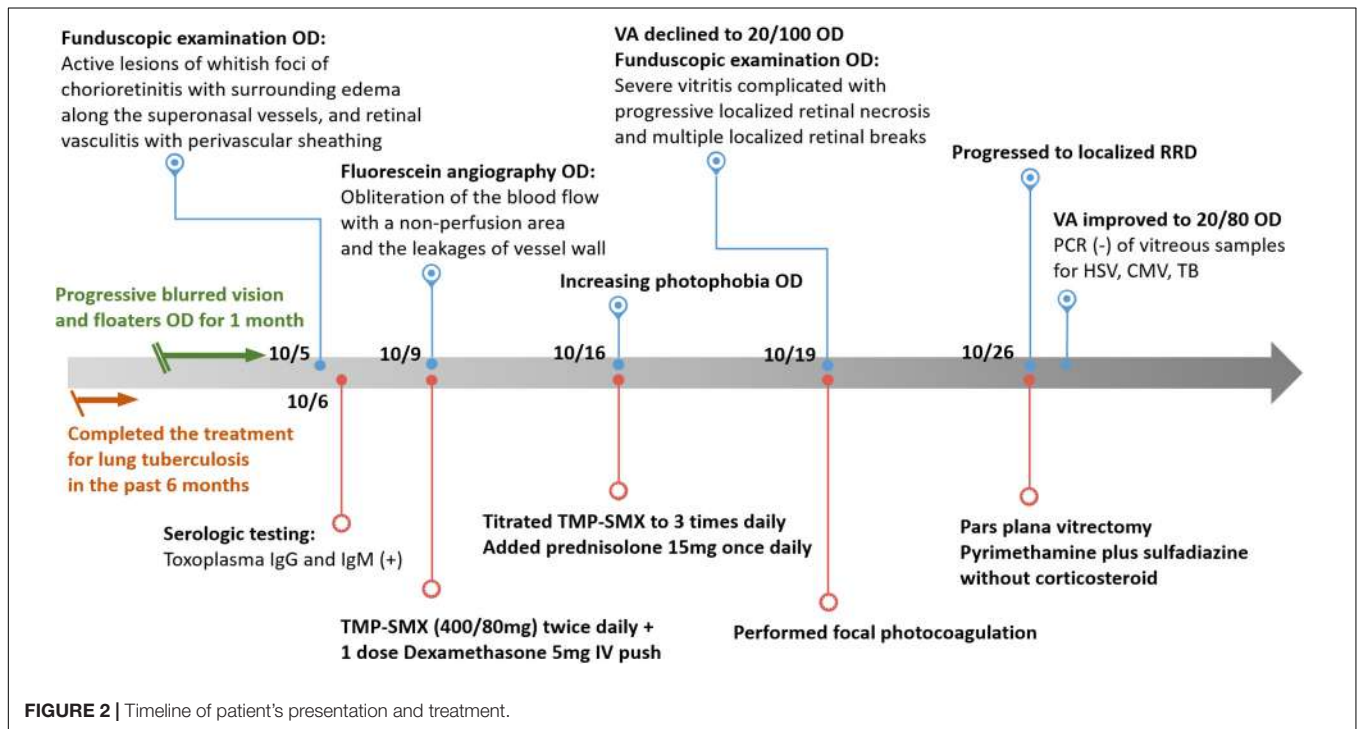
FIGURE 2 | Timeline of patient's presentation and treatment.

immunohistochemistry (detecting monoclonal or polyclonal antibodies), or by polymerase chain reaction (PCR) (10–12).

We report on an immunocompetent patient with progressive blurry vision whose initial differential diagnoses included acute retinal necrosis, ocular tuberculosis, and ocular toxoplasmosis. Acute retinal necrosis, which is commonly caused by VZV, HSV-1, HSV-2, and rarely CMV, generally occurs in immunocompetent patients and may develop without a systemic prodrome. PCR testing of the vitreous or aqueous humor is sufficient for diagnosis, and the serology test is rarely helpful (13). Ocular tuberculosis, which usually follows hematogenous

spread, should also be considered, especially if the patient has had previous tuberculous infection. Definitive diagnosis of tuberculosis needs cultures or DNA amplification from the involved tissue. However, culture or biopsy from the involved tissues in cases of ocular tuberculosis is unpractical, because aqueous and vitreous paracentesis commonly fails to produce positive bacterial culture results (14). Our patient denied any respiratory symptoms, and his recent pulmonary radiographic exam showed no suspected lesion. Recently-acquired ocular toxoplasmosis may present as focal choroidoretinitis without a visible chorioretinal scar (15). Some studies also report that the

sensitivity of PCR ranges from 27 to 36% in patients diagnosed with ocular toxoplasmosis (11). Since there were no positive results from either aqueous or vitreous samples, we made our diagnosis based on the ocular findings and the positive anti-toxoplasma IgM titer.

The treatment and prophylaxis of active ocular toxoplasmosis have been widely discussed. Typically, toxoplasmic choroidoretinitis in immunocompetent patients is expected to resolve within 1–2 months, since most infections with active ocular toxoplasmosis are thought to be self-limiting over the course of 1–2 months. Taking into account the benign natural course and the possibility of toxicity from anti-parasitic drugs, the therapeutic approach for each individual with active infection should seek to avoid unnecessarily high rates of drug-induced morbidity. Anti-parasitic agents are suggested for acquired immunocompetent patients with active toxoplasmic choroidoretinitis whenever the optic disc or fovea is involved, or if there is severe vitritis or vasculitis, giant diameter size, multiple active lesions, and prolonged clinical course (16). Treatment is also warranted for patients with atypical presentations (17). Current therapeutic strategy for ocular toxoplasmosis aims to stop the parasite reproducing and to eradicate it, while suppressing inflammation to control tissue damage from the immune response. The anti-parasitic agents pyrimethamine and sulfadiazine plus corticosteroid form the classical triple-treatment for ocular toxoplasmosis (17). Trimethoprim-sulfamethoxazole has been put forward as another therapeutic option because of lower cost, comparable efficacy, and safety for the prophylaxis of recurrent toxoplasmic choroidoretinitis (18). One currently used approach (except in individuals who are allergic to sulphonamides) involves systemic treatment with a combination of trimethoprim (800 mg) and sulfamethoxazole (160 mg), administered twice daily for 6 weeks, which is generally well-tolerated. This strategy is equivalent to the standard daily treatment with pyrimethamine (50 mg) in combination with sulfadiazone (1000 mg) 4 times a day and folinic acid (15 mg) twice weekly (to prevent anemia), for 6 weeks (19). Corticosteroids were thought to be beneficial for patients by suppressing the intraocular inflammation (16). However, corticosteroid monotherapy has been reported to worsen the clinical course and cause serious complications (15). Despite several published articles proposing various dosages of adjunctive corticosteroids, there is still no strong evidence from randomized controlled trials to support this adjuvant therapy being helpful for patients with ocular toxoplasmosis, especially as regards improvement of their vision (20, 21). The combined antibiotic and steroid approach should be limited to patients with an exaggerated inflammatory response, since it remains unclear whether supplementary treatment with corticosteroids does indeed effect an improvement in the outcome over and above that achieved with anti-parasitic agents alone.

This case is noteworthy because it shows how, even in an immunocompetent patient under proper management with anti-parasitic agents accompanied with corticosteroids, the severe inflammation still led to retinal detachment and impaired vision. Corticosteroids might minimize the inflammatory damage in most cases, but the route, dosage, and timing of administration are still subject to controversy. Early administration of corticosteroids together with the anti-parasitic agents, as in our case, might not be beneficial but might actually lead to advanced complications in the ocular tissues. We should keep in mind that iatrogenic immunosuppression by corticosteroids may cause aggressive choroidoretinitis and further complications such as retinal detachment. Detailed ophthalmic examinations are required to prevent future vision loss.

DATA AVAILABILITY STATEMENT

The original contributions presented in the study are included in the article/supplementary material, further inquiries can be directed to the corresponding author.

ETHICS STATEMENT

Ethical review and approval was not required for the study on human participants in accordance with the local legislation and institutional requirements. The patients/participants provided their written informed consent to participate in this study.

AUTHOR CONTRIBUTIONS

H-YL contributed to writing the original manuscript. Both authors contributed to the literature research and preparation of the manuscript and figures, were responsible for the design of the case report, and read and approved the final manuscript.

FUNDING

REFERENCES

1. Frenkel JK. Ocular toxoplasmosis. *JAMA*. (1994) 272:356. doi: 10.1001/jama.1994.03520050034024
2. Rothova A. Ocular manifestations of toxoplasmosis. *Curr Opin Ophthalmol.* (2003) 14:384–8. doi: 10.1097/00055735-200312000-00011
3. Englander M, Young LH. Ocular toxoplasmosis: advances in detection and treatment. *Int Ophthalmol Clin.* (2011) 51:13–23. doi: 10.1097/IIO.0b013e31822d663b
4. Lima GS, Saraiva PG, Saraiva FP. Current therapy of acquired ocular toxoplasmosis: a review. *J Ocular Pharmacol Therapeut.* (2015) 31:511–7. doi: 10.1089/jop.2015.0059
5. Commodaro AG, Belfort RN, Rizzo LV, Muccioli C, Silveira C, Burnier MN Jr., et al. Ocular toxoplasmosis: an update and review of the literature. *Mem Inst Oswaldo Cruz.* (2009) 104:345–50. doi: 10.1590/s0074-02762009000200030
6. Delair E, Latkany P, Noble AG, Rabiah P, McLeod R, Brézin A. Clinical manifestations of ocular toxoplasmosis. *Ocular Immunol Inflamm.* (2011) 19:91–102.doi: 10.3109/09273948.2011.564068

7. Cunningham ET Jr., Belfort R Jr., Muccioli C, Arevalo JF, Zierhut M. Ocular toxoplasmosis. *Ocular Immunol Inflamm.* (2015) 23:191–3. doi: 10.3109/09273948.2015.1051360

8. Butler NJ, Furtado JM, Winthrop KL, Smith JR. Ocular toxoplasmosis II: clinical features, pathology and management. *Clin Exp Ophthalmol.* (2013) 41:95–108. doi: 10.1111/j.1442-9071.2012.02838.x

9. Furtado JM, Winthrop KL, Butler NJ, Smith JR. Ocular toxoplasmosis I: parasitology, epidemiology and public health. *Clin Exp Ophthalmol.* (2013) 41:82–94. doi: 10.1111/j.1442-9071.2012.02821.x

10. Pleyer U, Schlüter D, Mänz M. Ocular toxoplasmosis: recent aspects of pathophysiology and clinical implications. *Ophthalmic Res.* (2014) 52:116–23. doi: 10.1159/000363141

11. Ozgonul C, Besirli CG. Recent developments in the diagnosis and treatment of ocular toxoplasmosis. *Ophthalmic Res.* (2017) 57:1–12.

12. Smith JR, Ashander LM, Arruda SL, Cordeiro CA, Lie S, Rochet E, et al. Pathogenesis of ocular toxoplasmosis. *Prog Retinal Eye Res.* (2021) 81:100882. doi: 10.1016/j.preteyeres.2020.100882

13. Pleyer U, Metzner S, Hofmann J. [Diagnostics and differential diagnosis of acute retinal necrosis]. *Ophthalmologe.* (2009) 106:1074–82. doi: 10.1007/s00347-009-2049-3

14. Thompson MJ, Albert DM. Ocular tuberculosis. *Arch Ophthalmol.* (2005) 123:844–9. doi: 10.1001/archopht.123.6.844

15. Oray M, Ozdal PC, Cebeci Z, Kir N, Tugal-Tutkun I. Fulminant Ocular Toxoplasmosis: the Hazards of Corticosteroid Monotherapy. *Ocul Immunol Inflamm.* (2016) 24:637–46. doi: 10.3109/09273948.2015.1057599

16. Holland GN, Lewis KG. An update on current practices in the management of ocular toxoplasmosis. *Am J Ophthalmol.* (2002) 134:102–14. doi: 10.1016/s0002-9394(02)01526-x

17. Rothova A, Meenken C, Buitenhuis HJ, Brinkman CJ, Baarsma GS, Boen-Tan TN, et al. Therapy for ocular toxoplasmosis. *Am J Ophthalmol.* (1993) 115:517–23. doi: 10.1016/S0002-9394(14)74456-3

18. Opremcak EM, Scales DK, Sharpe MR. Trimethoprim-sulfamethoxazole therapy for ocular toxoplasmosis. *Ophthalmology.* (1992) 99:920–5.doi: 10.1016/S0161-6420(92)31873-1

19. Garweg JG, Stanford MR. Therapy for ocular toxoplasmosis–the future. *Ocular Immunol Inflamm.* (2013) 21:300–5. doi: 10.3109/09273948.2013.779724

20. Kim SJ, Scott IU, Brown GC, Brown MM, Ho AC, Ip MS, et al. Interventions for toxoplasma retinochoroiditis: a report by the American Academy of Ophthalmology. *Ophthalmology.* (2013) 120:371–8. doi: 10.1016/j.ophtha.2012.07.061

21. Jasper S, Vedula SS, John SS, Horo S, Sepah YJ, Nguyen QD. Corticosteroids as adjuvant therapy for ocular toxoplasmosis. *Cochrane Database Syst Rev.* (2017) 1:Cd007417. doi: 10.1002/14651858.CD007417.pub

Varying Clinical Phenotypes of Mitochondrial DNA T12811C Mutation: A Case Series Report

Qingdan Xu[1†], Ping Sun[1†], Chaoyi Feng[2], Qian Chen[2], Xinghuai Sun[1,2,3], Yuhong Chen[1,2*] and Guohong Tian[1,2*]

[1] Department of Ophthalmology, Eye and ENT Hospital, Fudan University, Shanghai, China, [2] NHC Key Laboratory of Myopia, Chinese Academy of Medical Sciences, and Shanghai Key Laboratory of Visual Impairment and Restoration, Fudan University, Shanghai, China, [3] State Key Laboratory of Medical Neurobiology, Institute of Brain Science, Fudan University, Shanghai, China

The T12811C mitochondrial DNA (mtDNA) mutation has been reported in Leber hereditary optic neuropathy (LHON) previously, with vision loss as the main manifestation. The involvement of other organ systems, including the central and peripheral nervous system, heart, and extraocular muscles, has not been well described. This case series report investigated four patients with T12811C mtDNA mutation, verified through a next generation sequencing. Two male patients presented with bilateral subacute visual decrease combined with involvement of multiple organ systems: leukoencephalopathy, hypertrophic cardiomyopathy, neurosensory deafness, spinal cord lesion and peripheral neuropathies. Two female patients presented with progressive ptosis and ophthalmoplegia, one of whom also manifested optic atrophy. This study found out that patients harboring T12811C mtDNA mutation manifested not only as vision loss, but also as a multi-system disorder affecting the nervous system, heart, and extraocular muscles.

Keywords: Leber hereditary optic neuropathy, mitochondrial disorder, mitochondrial DNA, ophthalmoplegia, optic atrophy

INTRODUCTION

Leber hereditary optic neuropathy (LHON) is a maternally inherited ocular disease leading to painless, progressive, bilateral loss of central vision in young adults, predominately affecting males (1–5). Although visual dysfunction is the most common symptom of LHON, other systemic abnormalities can also occur. These include dystonia, Parkinsonism, extra-pyramidal motor symptoms, peripheral neuropathy, cardiac conduction abnormalities, spinal cord disease, and skeletal muscle abnormalities (6–13). The maternal transmission indicates that mutations in the mitochondrial DNA (mtDNA) play key roles in the development of LHON. Three mtDNA variants are considered as primary mutations causing LHON, namely, ND4 G11778A, ND1 G3460A, and ND6 T14484C (14, 15). These three mtDNA mutations account for over 95% of LHON cases worldwide, while the remaining LHON cases may be caused by other variants (4).

The T12811C (Y159H) mutation is located in highly conserved residues in ND5 that encodes the subunit of respiratory chain complex I (16). This missense mutation results in the substitution from tyrosine to histidine. In previous investigations, Huoponen et al. reported that the ND5

T12811C mutation acted as a secondary mutation that increased the penetrance of the ND4 G11778A mutation in LHON (17). Here, we investigated the clinical phenotypes of the T12811C mutation in four Chinese patients diagnosed with LHON and other systemic diseases. The detailed clinical manifestations and genetic characteristics were evaluated. Our study reveals the genetic heterogeneity of mitochondrial diseases and expands the phenotypic spectrum of T12811C mutation.

MATERIALS AND METHODS

Patients

This study was approved by the Institutional Review Board of Eye, Ear, Nose, and Throat Hospital of Fudan University (KJ2011-04). Written consent forms were obtained from all participants or their guardians. Four Han Chinese patients who had ND5 T12811C mutation were enrolled at the Neuro-Ophthalmology Division of the Eye, Ear, Nose, and Throat Hospital of Fudan University, Shanghai, China.

Clinical Investigation

Detailed medical histories were recorded for all the patients, especially the family histories as well as histories of smoking and drinking. All the patients underwent complete neuro-ophthalmologic evaluations including assessment of best-corrected visual acuity (BCVA), color vision using Ishihara plates, relative afferent papillary defect (RAPD), slit-lamp biomicroscopy, fundoscopy, Goldmann/Octopus visual field perimetry, and spectral-domain optical coherence tomography (OCT). Other ancillary tests focused on neurological system, heart, and hearing were performed according to the patients' different symptoms. Ophthalmic examinations and neurological evaluations were also conducted for all the parents.
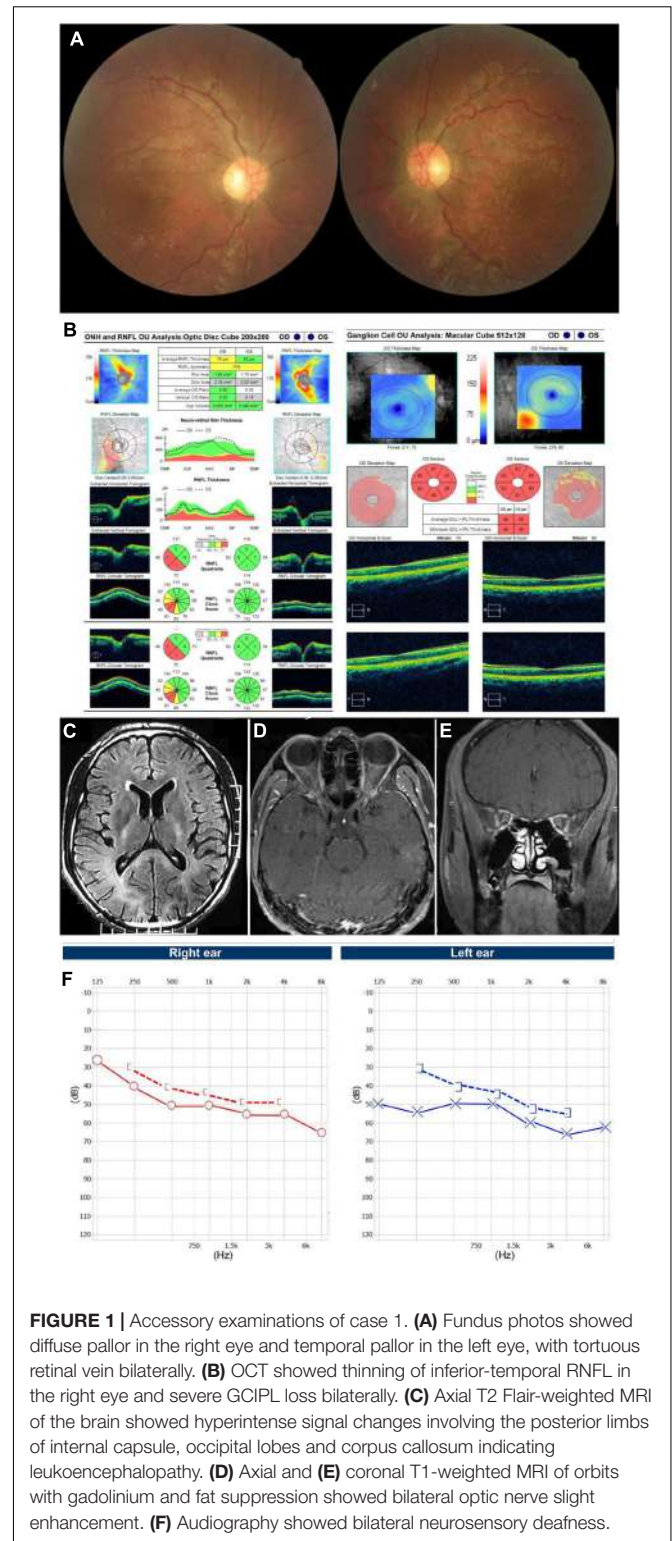
Genetics Analysis

The total DNA was isolated from peripheral blood of the four patients. For case 1, case 3, and case 4, next generation sequencing was utilized and a panel of 194 optic-atrophy associated genes were sequenced using the Illumina HiSeq 2000 (Illumina, Inc., San Diego, CA, United States) sequencing system. The panel covered the whole mtDNA genome and the nucleus genes related to mitochondrial disorders. The average coverage depth was 300 times. Ninety nine percent of the target region received 20 times coverage or more. For case 2, a small panel covering nine optic-atrophy associated nucleus genes (*RTN4IP1*, *YME1L1*, *OPA1*, *OPA3*, *TMEM126A*, *DNM1L*, *ACO2*, *WFS1*, *CISD2*) and the whole mtDNA genome were sequenced.

RESULTS

Case 1

A 25-year-old man presented with painless vision loss in both eyes for 1 month. He noticed he could not see clearly in the right eye for 10 days and when first examined, both eyes' visual acuity was abnormal. He was diagnosed with hypertrophic

FIGURE 1 | Accessory examinations of case 1. **(A)** Fundus photos showed diffuse pallor in the right eye and temporal pallor in the left eye, with tortuous retinal vein bilaterally. **(B)** OCT showed thinning of inferior-temporal RNFL in the right eye and severe GCIPL loss bilaterally. **(C)** Axial T2 Flair-weighted MRI of the brain showed hyperintense signal changes involving the posterior limbs of internal capsule, occipital lobes and corpus callosum indicating leukoencephalopathy. **(D)** Axial and **(E)** coronal T1-weighted MRI of orbits with gadolinium and fat suppression showed bilateral optic nerve slight enhancement. **(F)** Audiography showed bilateral neurosensory deafness.

cardiomyopathy 7 years ago. He complained of hearing loss for years and the pure tone audiometry demonstrated moderate neurosensory hearing loss for both ears. He had no family history of similar diseases and denied smoking or drinking alcohol. The

TABLE 1 | Clinical manifestations of the four cases.

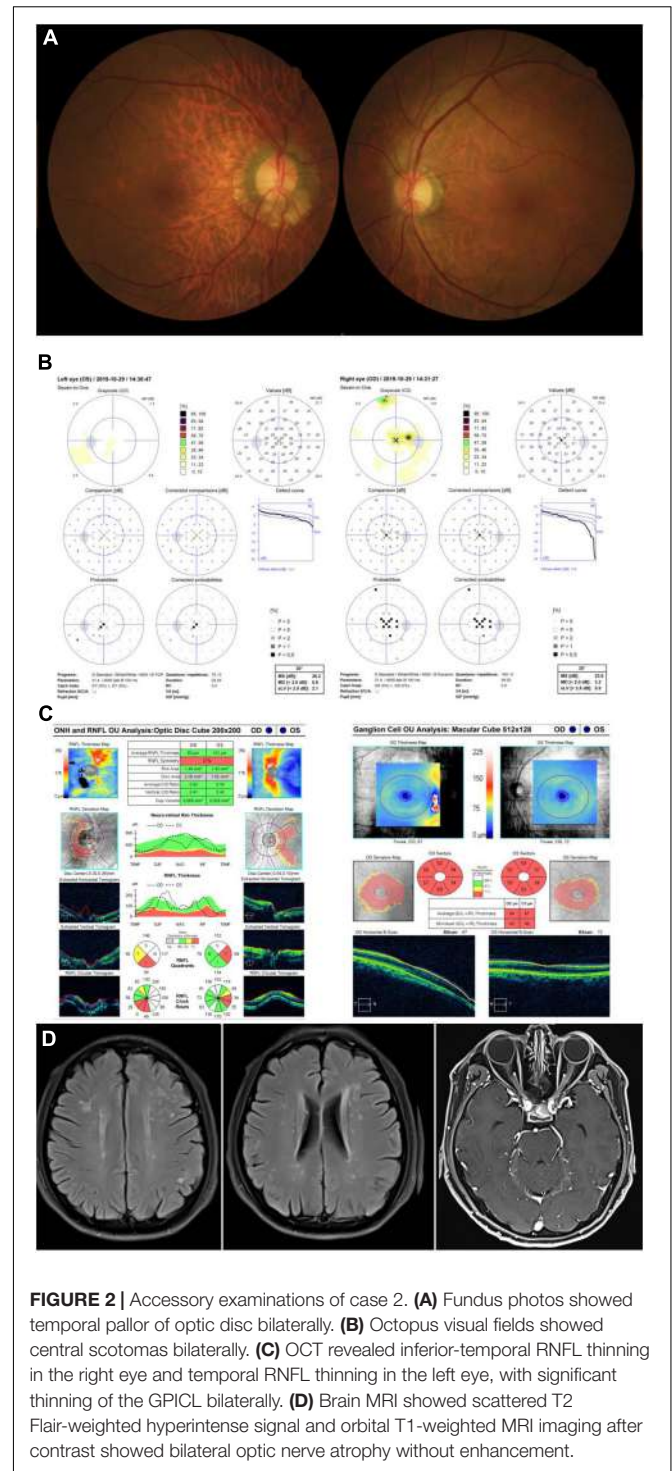|	Sex	Age (year)	Presenting symptoms	Neuro-ophthalmologic examination						Other systems involvement	MRI brain/orbit
				BCVA	Color	Fundus	Visual field	Eye movement	OCT		
Case 1	M	25	Visual decrease Heart disease Hearing loss	HM OD	0/8 OD	Diffuse pallor, tortuous retinal vein OD	Central scotoma OD	Normal OD	Thinning of inferior-temporal RNFL OD and severe GCIPL loss OU	Leukoencephalopathy Hypertrophic cardiomyopathy Neurosensory deafness	Leukoencephalopathy, bilateral optic nerve atrophy
				20/400 OS	0/8 OS	Temporal pallor, tortuous retinal vein OS	Central scotoma OS	Normal OS			
Case 2	M	58	Visual decrease Low limb paraplegia Numbness of arms and legs	20/200 OU	0/8 OU	Temporal pallor OU	Central scotomas OU	Normal OU	Thinning of RNFL and severe GCIPL loss OU	Peripheral neuropathies Spinal cord lesion	Bilateral optic nerve atrophy without spinal cord lesion
Case 3	F	32	Progressive ptosis Eye movement disorders Visual decrease	20/60 OD	4/8 OD	Temporal pallor OD	Normal OD	Ptosis, horizontal and vertical movement deficient OU	Thinning of RNFL OD and severe GCIPL loss OU		Thinning of extraocular muscles without other brain lesion
				20/30 OS	6/8 OS	Normal OS	Normal OS				
Case 4	F	16	Progressive ptosis Eye movement disorders	20/20 OU	8/8 OU	Normal OU	Normal OU	Ptosis, horizontal and vertical movement deficient OU	Normal OU		Thinning of extraocular muscles without other brain lesions

BCVA was hand motion in his right eye and 20/400 in his left eye. Color vision was 0/8 in both eyes. There was no RAPD in the right eye. Funduscopic examination showed diffuse pallor in his right eye and temporal atrophy of optic disc in his left eye, with bilateral tortuous retinal vein (**Figure 1A**). Goldmann visual field tests revealed central scotomas in both eyes. OCT demonstrated thinning of inferior-temporal retinal nerve fiber layer (RNFL) in the right eye and severe ganglion cell-inner plexiform layer (GCIPL) loss in both eyes (**Figure 1B**). T2 Flair-weighted magnetic resonance imaging (MRI) of the brain showed hyperintense signal changes involving the posterior limbs of internal capsule, occipital lobes and corpus callosum indicating leukoencephalopathy (**Figure 1C**). T1-weighted MRI of the orbits with gadolinium and fat suppression showed slight enhancement of the bilateral optic nerves in both axial (**Figure 1D**) and coronal (**Figure 1E**) views. The audiography demonstrated bilateral neurosensory deafness (**Figure 1F**). Genetic testing results showed the T12811C mutation with the heteroplasmy at the level of 99.81%. Another variant of G3946A in ND1 with the heteroplasmy of 16.45% was also detected. The patient was diagnosed with Leber plus syndrome and prescribed coenzyme Q 10 together with idebenone. His visual acuity stabilized at Snellen 20/400 for both eyes after 1 year of follow-up (**Table 1**).

Case 2

A 58-year-old man presented with bilateral progressive visual decrease within 2 months, accompanied by weakness and numbness of his legs. He noticed both eyes blurry in the morning without periorbital pain or headache. He did not have any family history of similar diseases. He denied taking any neurotoxic medication, smoking or drinking alcohol. The BCVA was 20/200 and color vision was 0/8 in both eyes. The fundus showed temporal pallor of the bilateral optic discs (**Figure 2A**). The neurological examination only showed bilateral peripheral neuropathies. Muscle strength was level IV but with paresthesia of both arms and legs. Octopus visual fields showed central scotomas in both eyes (**Figure 2B**). The OCT showed inferior-temporal RNFL thinning in the right eye and temporal RNFL thinning in the left eye, with significant thinning of the GCIPL in both eyes (**Figure 2C**). The brain MRI showed scattered T2 Flair-weighted hyperintense signal and orbital MRI only showed bilateral optic nerve atrophy without enhancement in T1-weighted imaging after contrast (**Figure 2D**). A small pituitary tumor was reported which was irrelevant to optic neuropathy. There was no reported spinal cord lesion. Genetic testing revealed the T12811C mutation with the heteroplasmy at the level of 98.93%. The patient was diagnosed with Leber plus syndrome and prescribed cobamamide together with coenzyme Q 10 and idebenone. His visual acuity was stabilized at Snellen 20/200 for both eyes during follow-up (**Table 1**).
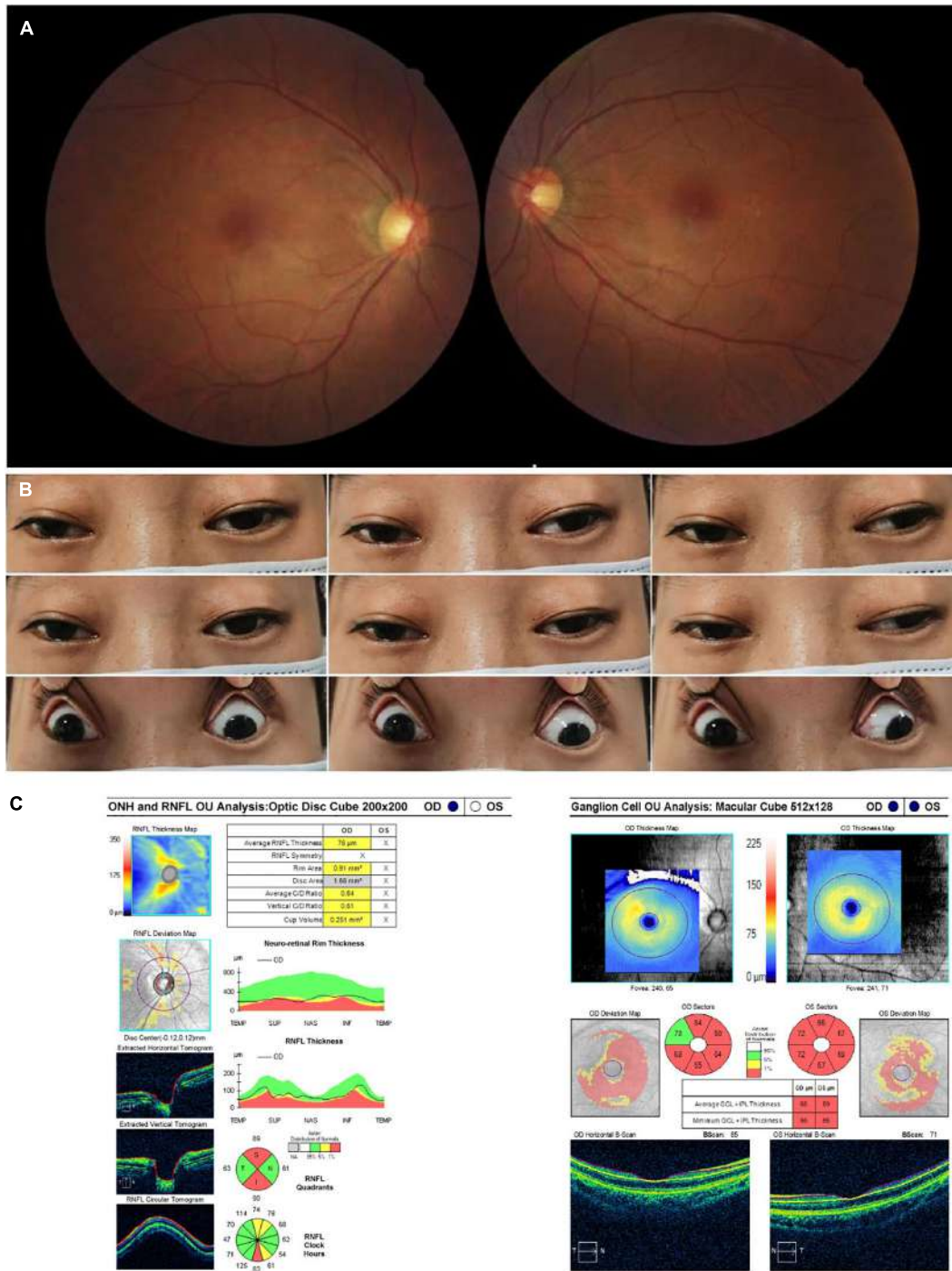
Case 3

A 32-year-old woman complained of progressive bilateral ptosis and strabismus since she was 20 years old. She underwent strabismus surgery 10 years ago. She had no family history

FIGURE 2 | Accessory examinations of case 2. **(A)** Fundus photos showed temporal pallor of optic disc bilaterally. **(B)** Octopus visual fields showed central scotomas bilaterally. **(C)** OCT revealed inferior-temporal RNFL thinning in the right eye and temporal RNFL thinning in the left eye, with significant thinning of the GPICL bilaterally. **(D)** Brain MRI showed scattered T2 Flair-weighted hyperintense signal and orbital T1-weighted MRI imaging after contrast showed bilateral optic nerve atrophy without enhancement.

of similar diseases and denied smoking or drinking alcohol. Tests for ocular myasthenia gravis, including acetylcholine receptors antibody, single-fiber electromyography, repetitive nerve stimulation, and chest computed tomography scan were all negative. The BCVA was 20/60 in her right eye and 20/30 in her left eye. Color vision was 4/8 in her right eye and 6/8 in her left eye. Funduscopic examination revealed temporal
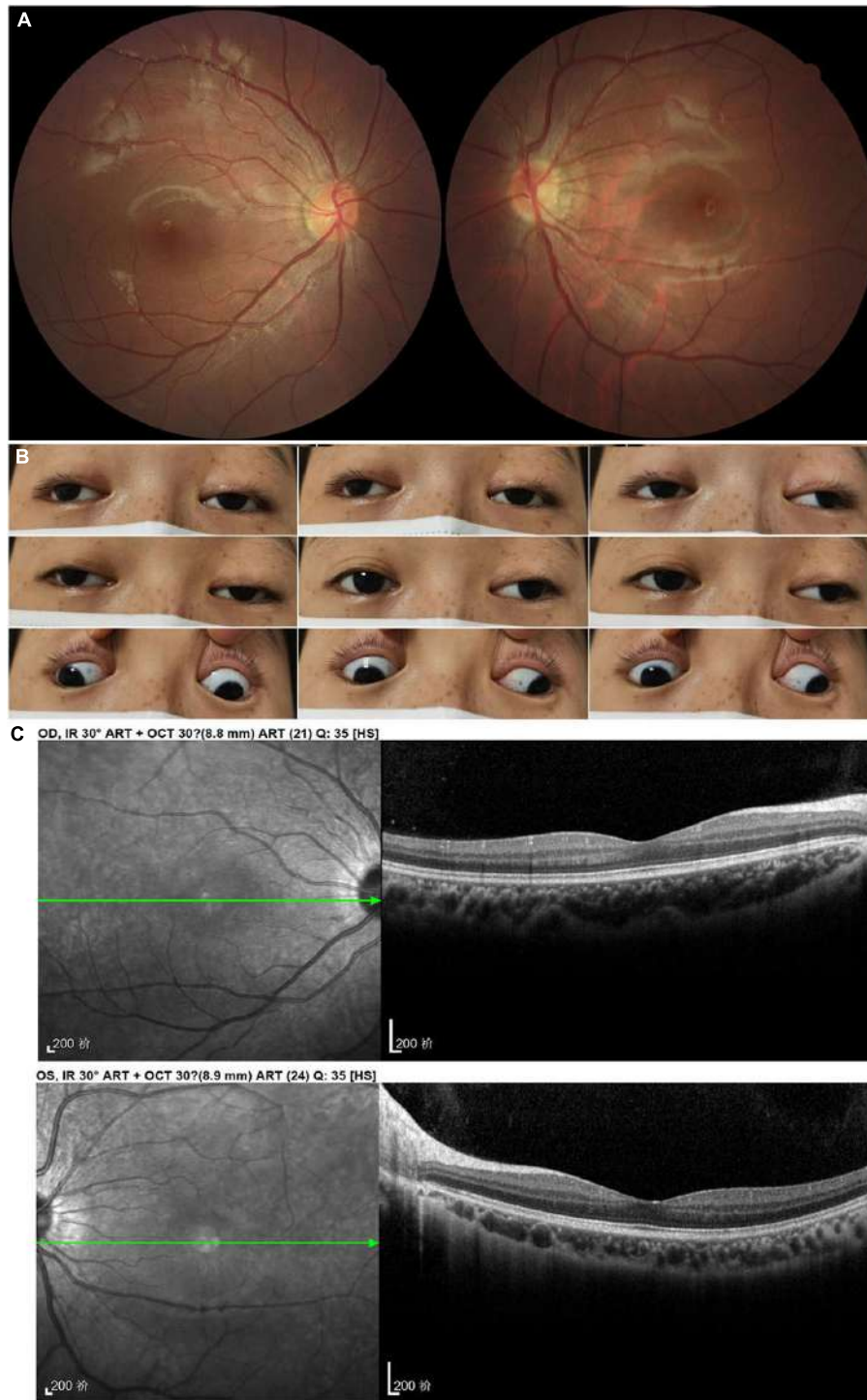
FIGURE 3 | Accessory examinations of case 3. **(A)** Fundus photos showed temporal pallor in the right eye. **(B)** Nine cardinal eye positions showed impaired mobility in both eyes, including adduction, abduction, elevation, and depression. **(C)** OCT showed thinning of RNFL superiorly and inferiorly in the right eye, with diffuse thinning of GCIPL bilaterally. The RNFL thickness of the left eye was not available due to poor cooperation.

pallor of the optic disc in her right eye (**Figure 3A**). Eye movement was impaired in both eyes, including adduction, abduction, elevation, and depression (**Figure 3B**). The OCT demonstrated 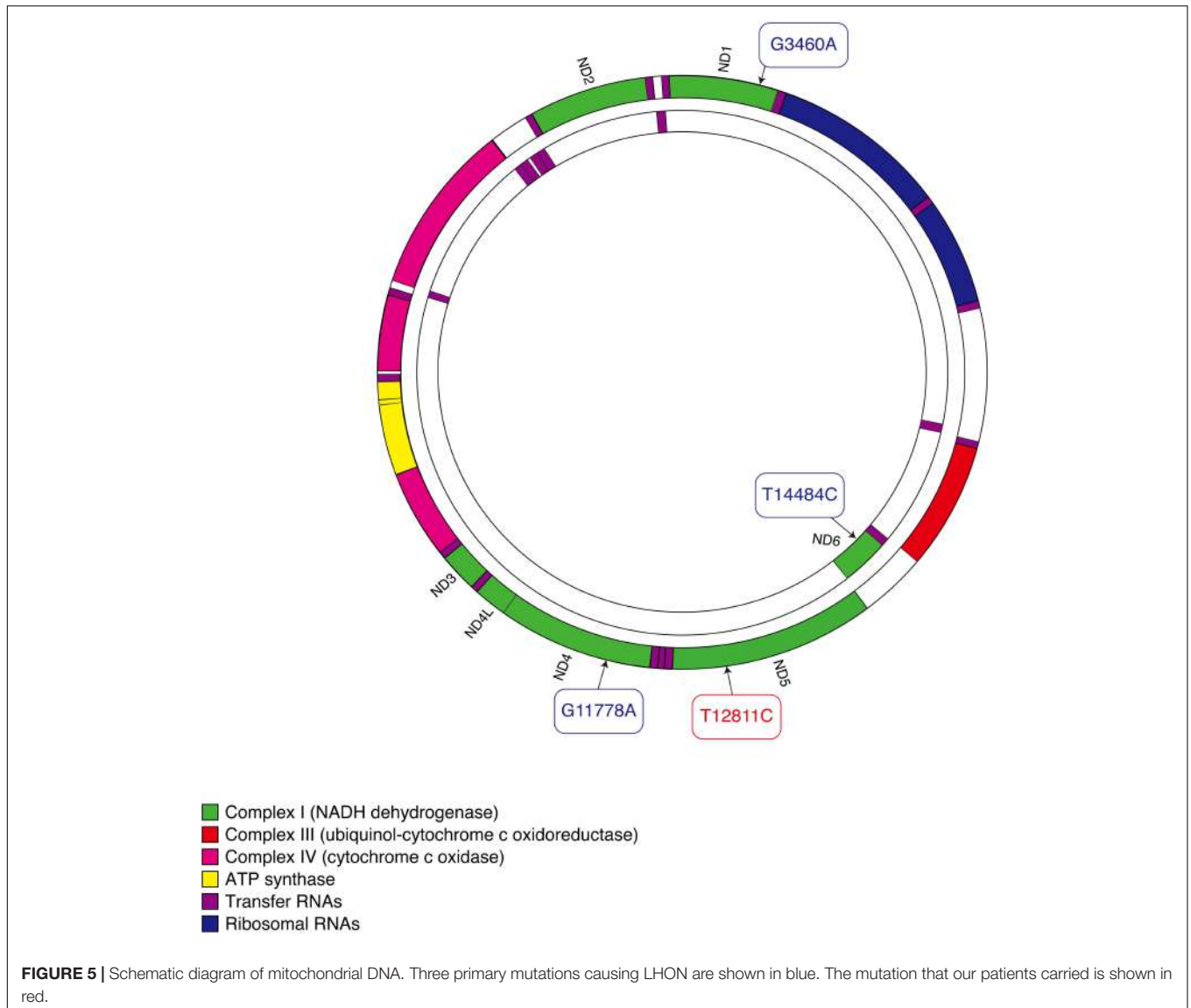thinning of the RNFL superiorly and inferiorly in the right eye and diffuse bilateral thinning of GCIPL (**Figure 3C**). The brain and orbital MRI showed thinning of extraocular muscles without other brain lesions. Genetic testing results detected the T12811C mutation only with

FIGURE 4 | Accessory examinations of case 4. **(A)** Fundus photos showed normal optic disc and retina bilaterally. **(B)** Nine cardinal eye positions revealed adduction, elevation, and depression were moderately reduced bilaterally, and abduction was slightly reduced in the right eye and almost full in the left eye. **(C)** OCT showed normal retina thickness and macular structure bilaterally.

the heteroplasmy at the level of 99.49%. No gene fragment deletion that was responsible for chronic progressive external ophthalmoplegia (CPEO) syndrome was found. She was finally diagnosed with mitochondrial disease with LHON and CPEO syndrome and prescribed coenzyme Q 10 together with idebenone (**Table 1**).

FIGURE 5 | Schematic diagram of mitochondrial DNA. Three primary mutations causing LHON are shown in blue. The mutation that our patients carried is shown in red.

Case 4

A 16-year-old woman presented with bilateral droopy eyelids and extraocular muscle weakness for about 5 years. She had no family history of similar diseases and denied smoking or drinking alcohol. The BCVA was 20/20 and color vision was 8/8 in both eyes. The fundoscopy revealed normal optic discs without retinopathy in both eyes (**Figure 4A**). Ophthalmic examination only revealed bilateral ptosis and exotropia. Adduction, elevation, and depression were moderately reduced in both eyes. Abduction was slightly reduced in the right eye and almost full in the left eye (**Figure 4B**). The OCT revealed normal retina thickness in both eyes (**Figure 4C**). The brain and orbital MRI showed thinning of extraocular muscles without other brain lesions. Genetic testing results showed the T12811C mutation with the heteroplasmy at the level of 99.94%. No gene fragment deletion which was usually found in CPEO patients was detected in this patient. She was finally diagnosed as ophthalmoplegia with

mitochondrial disease and prescribed coenzyme Q 10 together with idebenone (**Table 1**).

DISCUSSION

This case series study reported the multi-system phenotypes caused by the T12811C mutation. Our patients with an identical T12811C mutation in ND5 showed different clinical symptoms: vision loss, hypertrophic cardiomyopathy, hearing loss, paraplegia, ptosis, and extraocular muscle weakness. These clinical findings showed the broad phenotypic spectrum of the single point mutation of T12811C in mtDNA. It involved multiple systems, such as optic atrophy, cardiac abnormality, leukoencephalopathy, cochlea lesion, spinal cord lesion, peripheral neuropathies, and extraocular ophthalmoplegia.

The pathophysiology of LHON is complex. It typically manifests as an acute or subacute loss of central vision, a result of optic atrophy secondary to severe damage of retinal ganglion cells (18). The accompanying abnormalities, mainly neurological disorders, have also been reported in some patients (19). Three particular variants of G11778A, T14484C, G3460A in mtDNA are confirmed as primary mutations and explain over 95% of LHON patients worldwide (20–22). T12811C was initially published as a secondary LHON-associated mutation exacerbating the visual loss of LHON (16, 17). Recently, T12811C was reported as a primary mutation for the first time in one case, who presented as isolated LHON (23). Our group of patients manifested as multi-system disorders, thereby expanding the phenotypes in association with the T12811C mutation.

The T12811C mutation changes an evolutionarily conserved tyrosine to a histidine in the transmembrane region of ND5, the core subunit of complex I (16) (**Figure 5**). This mutation was predicted to alter the structure of the transmembrane region of the ND5 protein (24). ND5 plays an important role in the stability and activity of complex I (25). Researches have revealed that ND5 protein synthesis is the rate-limiting step for complex I activity and the highest rate of ND5 protein synthesis is just sufficient to maintain a normal respiratory rate (26–28). This may explain the experimental results that defects in ND5 can lead to a significant decrease in rates of mitochondrial respiration (28, 29). Hence, we consider the mutation T12811C in the ND5 gene to be pathogenic and responsible for the clinical phenotypes in our patients.

Furthermore, previous studies suggested that mutations in the ND5 gene were more likely to be associated with an extended phenotype rather than isolated visual dysfunction (30). Diseases caused by the mutations in ND5 would exhibit various degrees of clinical heterogeneity, such as Leigh syndrome (31), Idiopathic Parkinson's disease (32), mitochondrial encephalomyopathy, lactic acidosis and stroke-like episodes (MELAS) (33), myoclonic epilepsy with ragged-red fibers (MERRF) (34), and hypertrophic cardiomyopathy (35). Strikingly, neurological and muscular disorders are the main problems caused by the mutations in ND5 gene, which were also observed in our patients. Besides, deafness (36), paraplegia (37), ptosis (38), strabismus (39), and ophthalmoplegia (40) have also been occasionally seen in patients with mutations in the ND5 gene. To the best of our knowledge, our study is the first report describing ophthalmoplegia as the only symptom in such patients. Since no gene fragment deletion responsible for CPEO syndrome was found in our cases, ophthalmoplegia is most likely a phenotype of T12811C. Unfortunately, the biopsy of muscle was rejected in the two patients with opthalmoplegia according to patients' will. The histochemistry of COX and SDH together with detected mtDNA variants in muscle sample would be a great help in the diagnosis of mitochondrial CPEO.

Some researchers have proposed hypotheses explaining how the same gene mutation can cause different phenotypes. Patients with mitochondrial diseases harbor both mutant and wild-type mtDNAs. During mitosis, the mtDNA is divided and stochastically distributed to the next generation. If the mutation load surpasses the threshold in the tissue, affected patients will present corresponding clinical manifestations (41). Since

tissues with high demand for energy metabolism have lower thresholds, organs like brain, heart, skeletal muscle, optic nerve, and retina are more vulnerable to the pathogenic effects of mtDNA mutations (42). Other modifier factors including nuclear modifier genes (43), epigenetic phenomena (44), secondary mtDNA mutations (45), mitochondrial haplogroup (46), or environmental factors (47), also get involved in modifying the clinical expression and consequently cause differences in phenotypes among patients.

Similarly, additional factors may play a role in the phenotypic manifestation of the T12811C mutation as well. Here, all of our patients denied smoking and drinking alcohol, which were considered as the major environmental factors for LHON (47). However, in addition to T12811C, another variant G3946A was detected in case 1, although with relatively low heteroplasmy. The G3946A mutation can affect the assembly or turnover of complex I. It was reported to be associated with MELAS and hearing loss and the case 1 happened to have leukoencephalopathy and hearing loss as well (48). This mtDNA variant might interact with T12811C, triggering or exacerbating the expression of the phenotype. Meanwhile, all our patients harbored a single nucleotide polymorphism of A10398G, which was previously reported to increase the penetrance of primary G11778A mutation of LHON (49). However, due to its high frequency in Asian population (66%) (50), the effect of A10398G mutation on our patients remains unclear. Thus, there are still possibilities that the involved additional genetic and/or environmental factors were unrevealed in our patients.

CONCLUSION

In summary, we reported four patients with T12811C mtDNA mutation presenting with various clinical phenotypes as LHON, hypertrophic cardiomyopathy, leukoencephalopathy, cochlea lesion, spinal cord lesion, peripheral neuropathies, and ophthalmoplegia. Mitochondrial disease should be considered as one of the differential diagnoses in patients manifesting with optic atrophy or ophthalmoplegia.

ETHICS STATEMENT

The studies involving human participants were reviewed and approved by the Institutional Review Board of Eye, Ear, Nose, and Throat Hospital of Fudan University. Written informed consent was obtained from the individual(s), and minor(s)' legal guardian/next of kin, for the publication of any potentially identifiable images or data included in this article.

AUTHOR CONTRIBUTIONS

YC and GT conceptualized and designed the study. GT recruited the patients and collected the data. CF and QC obtained patients' consent, examined, and followed-up the patients. QX and PS

REFERENCES

1. Newman NJ, Wallace DC. Mitochondria and Leber's hereditary optic neuropathy. *Am J Ophthalmol.* (1990) 109:726–30.

2. Yu-Wai-Man P, Griffiths PG, Hudson G, Chinnery PF. Inherited mitochondrial optic neuropathies. *J Med Genet.* (2009) 46:145–58. doi: 10.1136/jmg.2007.054270

3. Carelli V, La Morgia C, Valentino ML, Barboni P, Ross-Cisneros FN, Sadun AA. Retinal ganglion cell neurodegeneration in mitochondrial inherited disorders. *Biochim Biophys Acta.* (2009) 1787:518–28. doi: 10.1016/j.bbabio.2009.02.024

4. Man PYW, Turnbull DM, Chinnery PF. Leber hereditary optic neuropathy. *J Med Genet.* (2002) 39: 162–9. doi: 10.1136/jmg.39.3.162

5. Sadun AA, La Morgia C, Carelli V. Leber's hereditary optic neuropathy. *Curr Treat Option Neurol.* (2011) 13:109–17. doi: 10.1007/s11940-010-0100-y

6. Hanemann CO, Hefter H, Schlaug G, Seitz RJ, Freund HJ, Benecke R. Characterization of basal ganglia dysfunction in Leber 'Plus' disease. *J Neurol.* (1996) 243:297–300. doi: 10.1007/Bf00868531

7. Chu CC, Huang CC, Kao LY, Kuo HC, Yu TN, Tso DJ, et al. Clinical phenotype and the G11778A mutation of mitochondrial DNA in patients with Leber's hereditary optic neuropathy in Taiwan. *Neuro Ophthalmology.* (2001) 26:207–16. doi: 10.1076/noph.26.4.207.15871

8. Bruyn GW, Vielvoye GJ, Went LN. Hereditary spastic dystonia - a new mitochondrial encephalopathy - putaminal necrosis as a diagnostic sign. *J Neurol Sci.* (1991) 103:195–202. doi: 10.1016/0022-510x(91)90164-3

9. Harding AE, Sweeney MG, Miller DH, Mumford CJ, Kellarwood H, Menard D, et al. Occurrence of a multiple sclerosis-like illness in women who have a Lebers hereditary optic neuropathy mitochondrial-DNA mutation. *Brain.* (1992) 115:979–89. doi: 10.1093/brain/115.4.979

10. Johns DR, Smith KH, Savino PJ, Miller NR. Lebers hereditary optic neuropathy - clinical manifestations of the 15257 mutation. *Ophthalmology.* (1993) 100:981–6.

11. Newman NJ. Lebers hereditary optic neuropathy - new genetic considerations. *Arch Neurol Chicago.* (1993) 50:540–8. doi: 10.1001/archneur.1993.00540050082021

12. Nikoskelainen EK, Marttila RJ, Huoponen K, Juvonen V, Lamminen T, Sonninen P, et al. Lebers plus - neurological abnormalities in patients with Lebers hereditary optic neuropathy. *J Neurol Neurosurg Psychiatry.* (1995) 59:160–4. doi: 10.1136/jnnp.59.2.160

13. Nikoskelainen EK, Savontaus ML, Wanne OP, Katila MJ, Nummelin KU. Leber's hereditary optic neuroretinopathy, a maternally inherited disease. A genealogic study in four pedigrees. *Arch Ophthalmol.* (1987) 105:665–71. doi: 10.1001/archopht.1987.01060050083043

14. Brown MD, Torroni A, Reckord CL, Wallace DC. Phylogenetic analysis of Lebers hereditary optic neuropathy mitochondrial DNAs indicates multiple independent occurrences of the common mutations. *Human Mutation.* (1995) 6:311–25. doi: 10.1002/humu.1380060405

15. Mackey DA, Oostra RJ, Rosenberg T, Nikoskelainen E, BronteStewart J, Poulton J, et al. Primary pathogenic mtDNA mutations in multigeneration pedigrees with Leber hereditary optic neuropathy. *Am J Hum Genet.* (1996) 59:481–5.

16. Cai W, Fu Q, Zhou X, Qu H, Tong Y, Guan MX. Mitochondrial variants may influence the phenotypic manifestation of Leber's hereditary optic neuropathy-associated ND4 G11778A mutation. *J Genet Genomics.* (2008) 35:649–55. doi: 10.1016/S1673-8527(08)60086-7

17. Huoponen K, Lamminen T, Juvonen V, Aula P, Nikoskelainen E, Savontaus ML. The spectrum of mitochondrial-DNA mutations in families with Leber hereditary optic neuroretinopathy. *Hum Genet.* (1993) 92:379–84. doi: 10.1007/Bf01247339

18. Sundaramurthy S, SelvaKumar A, Ching J, Dharani V, Sarangapani S, Yu-Wai-Man P. Leber hereditary optic neuropathy-new insights and old challenges. *Graefes Arch Clin Exp Ophthalmol.* (2021) 259:2461–72. doi: 10.1007/s00417-020-04993-1

19. de Weerdt CJ, Went LN. Neurological studies in families with Leber's optic atrophy. *Acta Neurol Scand.* (1971) 47:541–54. doi: 10.1111/j.1600-0404.1971.tb07507.x

20. Kim JY, Hwang JM, Chang BL, Park SS. Spectrum of the mitochondrial DNA mutations of Leber's hereditary optic neuropathy in Koreans. *J Neurol.* (2003) 250:278–81. doi: 10.1007/s00415-003-0985-4

21. Mashima Y, Yamada K, Wakakura M, Kigasawa K, Kudoh J, Shimizu N, et al. Spectrum of pathogenic mitochondrial DNA mutations and clinical features in Japanese families with Leber's hereditary optic neuropathy. *Curr Eye Res.* (1998) 17:403–8. doi: 10.1080/02713689808951221

22. Houshmand M, Sharifpanah F, Tabasi A, Sanati MH, Vakilian M, Lavasani S, et al. Leber's hereditary optic neuropathy: the spectrum of mitochondrial DNA mutations in Iranian patients. *Ann N Y Acad Sci.* (2004) 1011:345–9. doi: 10.1196/annals.1293.035

23. Zhou HP, Ishikawa H, Yasumoto R, Sakurai K, Sawamura H. Leber hereditary optic neuropathy harboring a rare m.12811 T>C mitochondrial DNA mutation. *Can J Ophthalmol.* (2021) 56:e82–4. doi: 10.1016/j.jcjo.2020.12.022

24. Bi R, Zhang AM, Jia X, Zhang Q, Yao YG. Complete mitochondrial DNA genome sequence variation of Chinese families with mutation m.3635G>A and Leber hereditary optic neuropathy. *Mol Vis.* (2012) 18:3087–94.

25. Perales-Clemente E, Fernandez-Vizarra E, Acin-Perez R, Movilla N, Bayona-Bafaluy MP, Moreno-Loshuertos R, et al. Five entry points of the mitochondrially encoded subunits in mammalian complex I assembly. *Mol Cell Biol.* (2010) 30:3038–47. doi: 10.1128/Mcb.00025-10

26. Bai YD, Hu PQ, Park JS, Deng JH, Song XF, Chomyn A, et al. Genetic and functional analysis of mitochondrial DNA-encoded complex I genes. *Ann N Y Acad Sci.* (2004) 1011:272–83. doi: 10.1196/annals.1293.026

27. Chomyn A. Mitochondrial genetic control, of assembly and function of complex I in mammalian cells. *J Bioenerg Biomembr.* (2001) 33:251–7. doi: 10.1023/A:1010791204961

28. Bai YD, Shakeley RM, Attardi G. Tight control of respiration by NADH dehydrogenase ND5 subunit gene expression in mouse mitochondria. *Mol Cell Biol.* (2000) 20:805–15. doi: 10.1128/Mcb.20.3.805-815.2000

29. Bao HG, Zhao CJ, Li JY, Wu C. Association of MT-ND5 gene variation with mitochondrial respiratory control ratio and NADH dehydrogenase activity in tibet chicken embryos. *Anim Genet.* (2007) 38:514–6. doi: 10.1111/j.1365-2052.2007.01622.x

30. Kolarova H, Liskova P, Tesarova M, Kucerova Vidrova V, Forgac M, Zamecnik J, et al. Unique presentation of LHON/MELAS overlap syndrome caused by m.13046T>C in MTND5. *Ophthalmic Genet.* (2016) 37:419–23.

31. Petruzzella V, Di Giacinto G, Scacco S, Piemonte F, Torraco A, Carrozzo R, et al. Atypical leigh syndrome associated with the D393N mutation in the

mitochondrial ND5 subunit. *Neurology.* (2003) 61:1017–8. doi: 10.1212/01. Wnl.0000080363.10902.E9

32. Parker WD, Parks JK. Mitochondrial ND5 mutations in idiopathic Parkinson's disease. *Biochem Bioph Res Commun.* (2005) 326:667–9. doi: 10.1016/j.bbrc. 2004.11.093

33. Panades-de Oliveira L, Montoya J, Emperador S, Ruiz-Pesini E, Jerico I, Arenas J, et al. A novel mutation in the mitochondrial MT-ND5 gene in a family with MELAS. The relevance of genetic analysis on targeted tissues. *Mitochondrion.* (2020) 50:14–8. doi: 10.1016/j.mito.2019.10.001

34. Naini AB, Lu JS, Kaufmann P, Bernstein RA, Mancuso M, Bonilla E, et al. Novel mitochondrial DNA ND5 mutation in a patient with clinical features of MELAS and MERRF. *Arch Neurol Chicago.* (2005) 62:473–6. doi: 10.1001/ archneur.62.3.473

35. Wei YL, Yu CA, Yang P, Li AL, Wen JY, Zhao SM, et al. Novel mitochondrial DNA mutations associated with chinese familial hypertrophic cardiomyopathy. *Clin Exp Pharmacol Physiol.* (2009) 36:933–9. doi: 10.1111/j. 1440-1681.2009.05183.x

36. Kolarova H, Liskova P, Tesarova M, Vidrova VK, Forgac M, Zamecnik J, et al. Unique presentation of LHON/MELAS overlap syndrome caused by m.13046T>C in MTND5. *Ophthalmic Genet.* (2016) 37:419–23. doi: 10.3109/ 13816810.2015.1092045

37. Wei YP, Huang Y, Yang YM, Qian M. MELAS/LS overlap syndrome associated with mitochondrial DNA mutations: clinical, genetic, and radiological studies. *Front Neurol.* (2021) 12:648740. doi: 10.3389/fneur.2021.648740

38. Ng YS, Lax NZ, Maddison P, Alston CL, Blakely EL, Hepplewhite PD, et al. MT-ND5 mutation exhibits highly variable neurological manifestations at low mutant load. *Ebiomedicine.* (2018) 30:86–93. doi: 10.1016/j.ebiom.2018.02.010

39. Han J, Lee YM, Kim SM, Han SY, Lee JB, Han SH. Ophthalmological manifestations in patients with leigh syndrome. *Brit J Ophthalmol.* (2015) 99:528–35. doi: 10.1136/bjophthalmol-2014-305704

40. Ayalon N, Flore LA, Christensen TG, Sam F. Mitochondrial encoded NADH dehydrogenase 5 (MT-ND5) gene point mutation presents as late onset cardiomyopathy. *Int J Cardiol.* (2013) 167:E143–5. doi: 10.1016/j.ijcard.2013. 04.018

41. DiMauro S. A brief history of mitochondrial pathologies. *Int J Mol Sci.* (2019) 20:5643. doi: 10.3390/ijms20225643

42. DiMauro S, Schon EA. Mechanisms of disease: mitochondrial respiratory-chain diseases. *N Engl J Med.* (2003) 348:2656–68. doi: 10.1056/NEJMra022567

43. Gropman A, Chen TJ, Perng CL, Krasnewich D, Chernoff E, Tifft C, et al. Variable clinical manifestation of homoplasmic G14459A mitochondrial DNA mutation. *Am J Med Genet A.* (2004) 124a:377–82. doi: 10.1002/ajmg.a.2 0456

44. McFarland R, Clark KM, Morris AAM, Taylor RW, Macphail S, Lightowlers RN, et al. Multiple neonatal deaths due to a homoplasmic mitochondrial DNA mutation. *Nat Genet.* (2002) 30:145–6. doi: 10.1038/ng819

45. Jancic J, Rovcanin B, Djuric V, Pepic A, Samardzic J, Nikolic B, et al. Analysis of secondary mtDNA mutations in families with Leber's hereditary optic neuropathy: four novel variants and their association with clinical presentation. *Mitochondrion.* (2020) 50:132–8. doi: 10.1016/j.mito.2019.10. 011

46. Ji Y, Zhang AM, Jia X, Zhang YP, Xiao X, Li S, et al. Mitochondrial DNA haplogroups M7b1'2 and M8a affect clinical expression of Leber hereditary optic neuropathy in Chinese families with the m.11778G–>A mutation. *Am J Hum Genet.* (2008) 83:760–8. doi: 10.1016/j.ajhg.2008.11.002

47. Caporali L, Maresca A, Capristo M, Del Dotto V, Tagliavini F, Valentino ML, et al. Incomplete penetrance in mitochondrial optic neuropathies. *Mitochondrion.* (2017) 36:130–7. doi: 10.1016/j.mito.2017.07.004

48. Kirby DM, McFarland R, Ohtake A, Dunning C, Ryan MT, Wilson C, et al. Mutations of the mitochondrial ND1 gene as a cause of MELAS. *J Med Genet.* (2004) 41:784–9. doi: 10.1136/jmg.2004.020537

49. Sudoyo H, Suryadi H, Lertrit P, Pramoonjago P, Lyrawati D, Marzuki S. Asian-specific mtDNA backgrounds associated with the primary G11778A mutation of Leber's hereditary optic neuropathy. *J Hum Genet.* (2002) 47:594–604. doi: 10.1007/s100380200091

50. van der Walt JM, Nicodemus KK, Martin ER, Scott WK, Nance MA, Watts RL, et al. Mitochondrial polymorphisms significantly reduce the risk of Parkinson disease. *Am J Hum Genet.* (2003) 72:804–11. doi: 10.1086/373937

Diabetic retinopathy as a predictor of cardiovascular morbidity and mortality in subjects with type 2 diabetes

Joan Barrot[1,2,3,4], Jordi Real[2,3], Bogdan Vlacho[2,5]*,
Pedro Romero-Aroca[6], Rafael Simó[7,8,9], Didac Mauricio[2,9,10,11],
Manel Mata-Cases[2,9,12], Esmeralda Castelblanco[2,13],
Xavier Mundet-Tuduri[2,4]* and Josep Franch-Nadal[2,9,14]

[1]Primary Health Care Center Dr. Jordi Nadal i Fàbregas (Salt), Gerència d'Atenció Primária, Institut
Català de la Salut, Girona, Spain, [2]Diabetis des de l'Atenció Primária (DAP)-Cat Group, Unitat
de Suport a la Recerca Barcelona, Fundació Institut Universitari per a la Recerca a l'Atenció Primária
de Salut Jordi Gol i Gurina (IDIAPJGOL), Barcelona, Spain, [3]Fundació Institut Universitari per a la
Recerca a l'Atenció Primária de Salut Jordi Gol i Gorina (IDIAPJGOL), Barcelona, Spain,
[4]Departament of Medicine, Universitat Autònoma de Barcelona, Barcelona, Spain, [5]Hospital de la
Santa Creu i Sant Pau, Barcelona, Spain, [6]Ophthalmology Service, University Hospital Sant Joan,
Institut de Investigacio Sanitaria Pere Virgili (IISPV), University of Rovira and Virgili, Reus, Spain,
[7]Diabetes and Metabolism Research Unit, Department of Endocrinology, Vall d'Hebron University
Hospital, Vall d'Hebron Research Institute, Barcelona, Spain, [8]Department of Medicine, Faculty
of Medicine, Autonomous University of Barcelona, Barcelona, Spain, [9]Centro de Investigación
Biomédica en Red de Diabetes y Enfermedades Metabólicas Asociadas (CIBERDEM), Barcelona,
Spain, [10]Department of Endocrinology and Nutrition, Hospital de la Santa Creu i Sant Pau,
Barcelona, Spain, [11]Departament of Medicine, University of Vic—Central University of Catalonia, Vic,
Spain, [12]Centre d'Atenció Primária La Mina, Gerència d'Àmbit d'Atenció Primária de Barcelona,
Institut Català de la Salut, Barcelona, Spain, [13]Division of Endocrinology, Metabolism and Lipid
Research, John T. Milliken Department of Medicine, School of Medicine, Washington University
in St. Louis, St. Louis, MO, United States, [14]Primary Health Care Center Raval Sud, Gerència d'Àmbit
d'Atenció Primaria, Institut Català de la Salut, Barcelona, Spain

This study aimed to evaluate the predictive value of diabetic retinopathy (DR) and its stages with the incidence of major cardiovascular events and all-cause mortality in type 2 diabetes mellitus (T2DM) persons in our large primary healthcare database from Catalonia (Spain). A retrospective cohort study with pseudo-anonymized routinely collected health data from SIDIAP was conducted from 2008 to 2016. We calculated incidence rates of major cardiovascular events [coronary heart disease (CHD), stroke, or both—macrovascular events] and all-cause mortality for subjects with and without DR and for different stages of DR. The proportional hazards regression analysis was done to assess the probability of occurrence between DR and the study events. About 22,402 T2DM subjects with DR were identified in the database and 196,983 subjects without DR. During the follow-up period among the subjects with DR, we observed the highest incidence of all-cause mortally. In the second place were the macrovascular events among the subjects with DR. In the multivariable analysis, fully adjusted for DR, sex, age, body mass index (BMI), tobacco, duration of T2DM, an antiplatelet or antihypertensive drug, and HbA1c, we observed that subjects with any stage of DR had higher risks for all of the study events, except for stroke. We observed the highest probability

of all-cause death events (adjusted hazard ratios, AHRs: 1.34, 95% CI: 1.28; 1.41). In conclusion, our results show that DR is related to CHD, macrovascular events, and all-cause mortality among persons with T2DM.

Introduction

Diabetes mellitus has become one of the major public health challenges globally, both in developed and developing countries (1). The increasing prevalence of diabetes worldwide is caused by a complex interplay of socioeconomic, demographic, environmental, and genetic factors. The International Diabetes Federation (IDF) estimates that 10.5% of adults between 20 and 79 years have diabetes, equating to 537 million people (2). The IDF also estimates that 643 million adults will live with diabetes in 2030 (11.3% of the population), and the number will reach 783 million (12.2%) by 2045.

The main burden of diabetes results from its complications. Diabetic retinopathy (DR) is a microvascular and neurodegenerative complication whose prevalence increases with disease duration and causes a high risk of severe visual impairment and blindness (3, 4). According to recently published studies, there is considerable variability in the prevalence of DR. The meta-analysis of Yau et al. reports that one in every three subjects with diabetes will present some degree of DR (5) compared to 27% in the last review and the analysis of the IDF from the studies published in recent years (6).

Diabetes can cause numerous complications that weaken health, lower quality of life, and cause early death. People with diabetes are two to three times more likely to develop cardiovascular disease, and the risk of death doubles compared to people without diabetes (7).

The consequences of late detection of DR go beyond the resulting suboptimal visual acuity (8, 9). We have extensive evidence that associates DR with other micro- and macrovascular complications of diabetes. Recently, it was reported that DR is associated with subclinical atherosclerosis (10–14), macrovascular comorbidities such as coronary disease (15–20) and cerebrovascular accident (21–26). Of interest, some studies have reported an association between cognitive impairment and the incidence of dementia [risk ratio (RR), 1.3; 95% confidence interval (CI), 1.27–1.58] (27, 28), and the relation between DR and neurodegeneration diseases such as Parkinson's disease has been proposed but remains unclear (29). In addition, a recent meta-analysis with observational studies found that subjects with diabetes who have DR have an increased

risk of mortality from all causes compared to subjects with diabetes who do not have retinopathy (RR: 2.33, 95% CI: 1.92; 2.81) (30–32).

So far, to the best of our knowledge, there is a lack of studies evaluating the relation between DR and major cardiovascular events from primary healthcare settings. In this study, we aimed to evaluate the predictive value of DR, its severity with the incidence of major cardiovascular events [coronary heart disease (CHD) and stroke], and all-cause mortality in subjects with T2DM in a Mediterranean region.

Materials and methods

The study included a retrospective cohort of subjects with T2DM from the SIDIAP database (Sistema de Información para el desarrollo de la Investigación en Atención Primaria). The SIDIAP database routinely collects pseudo-anonymized health data from users who attend the primary healthcare centers of the Catalonian Health Institute (Institut Català de la Salut, ICS). The ICS is the primary healthcare provider in Catalonia (Spain), covering about 80% (5,564,292 persons) of the Catalonian population. The SIDIAP database contains comprehensive patient data, such as visits with healthcare professionals, diagnoses, demographic information, clinical variables, laboratory test results, prescriptions, referrals to specialists and hospitals, and medication obtained from pharmacies. For this analysis, data were extracted covering a 10-year period. The inclusion period was defined from 1 January 2008 to 31 December 2012. The follow-up period was until the data extraction end date (31 December 2017) or a discontinuation event (death or any other database dropout).

Participants

All subjects aged between 30 and 89 years with a diagnosis of T2DM, defined as the presence of International Classification of Diseases, 10th Revision (ICD-10) diagnostic codes: E11, E14 (and their subcodes), and screening for fundus photography (to determine the presence of DR), were included in the analysis. We excluded those subjects with other types of

diabetes (type 1 diabetes, gestational diabetes, secondary, or other), without diagnostic codes for T2DM, subjects with cardiovascular events, and/or absence of fundus photography. The eligible participants were followed up for at least 5 years or until the discontinuation event.

Variables

For all the included subjects, the presence or absence of DR was assessed using reports pertaining to digital 45° color fundus images. Two photographs were taken for each eye, the macula-centered and between the macula and the optic nerve. We only included fundus photography from patients screened at primary healthcare centers. DR was classified into different stages according to the Early Treatment Diabetic Retinopathy Study (ETDRS) classification (33) as no apparent retinopathy (NDR), mild non-proliferative retinopathy (NPDR), moderate NPDR, severe NPDR, proliferative diabetic retinopathy (PDR), and diabetic macular edema (DME). The DR diagnosis was taken from the worst-affected eye, and from the most recent photograph in case there was more than one screening during the inclusion period. Also, at inclusion, we collected socio-demographic variables (age, gender), toxic habits (current tobacco use), and clinical variables related to diabetes [age at diagnosis of diabetes, diabetes duration, and glycated hemoglobin levels (HbA1c)]. Data on cardiovascular risk factors [body mass index (BMI), blood lipids, total cholesterol, low-density lipoprotein (LDL) cholesterol, high-density lipoprotein (HDL) cholesterol, non-HDL cholesterol, blood pressure, pulse pressure] were collected. Additional data were gathered on medication. Obesity was defined as a BMI $\geq$ 30 kg/m^2. The estimated glomerular filtration rate (eGFR) was calculated according to the CKD Epidemiology Collaboration (CKD-EPI) equation. Chronic kidney disease (CKD) was defined as an estimated glomerular filtration rate (eGFR) < 60 ml/min/1.73 m^2 calculated using the CKD-EPI equation and/or a ratio of albumin/creatinine (CAC) in urine $\geq$ 30 mg/g.

During the follow-up period, we collected data on mortality by any cause and by severe cardiovascular events such as stroke (defined by ICD-10 codes and subcodes for "cerebral infarctions" and/or "transient cerebral ischemic attacks and related syndromes") or CHD defined by ICD-10 codes and subcodes for "angina pectoris" and/or "acute myocardial infarction and/or subsequent myocardial infarction" and/or "certain current complications following acute myocardial infarction" and/or "chronic ischemic heart disease." Additionally, we created a composite event as a combination of stroke and/or CHD, named as "macrovascular events." The definition of the study variables and codes are summarized in **Supplementary Table 1**.

Statistical analysis

A descriptive statistical analysis was carried out, summarizing the quantitative parameters with the mean and its standard deviation (SD), median or interquartile range, and the qualitative variables with frequency and percentage. We used an opportunistic sampling technique to capture all persons meeting the study inclusion criteria. To assess the association of the main study events considering the time of follow-up, a time-to-event complete case analysis (CCA) was performed, adjusting Cox proportional hazards models (34). Unadjusted hazard ratios (UnAHRs) and adjusted hazard ratios (AHRs), 95% CI, and *p*-value were estimated and summarized. We used Kaplan–Meier survival curves to graphically visualize the cumulative incidence for study events during the follow-up period in each group. Different study events were fully adjusted considering potentially confounding clinical variables such as DR, sex, age, BMI, tobacco, duration of T2DM, antiplatelet or antihypertensive drug treatment, and HbA1c. Additionally, we performed a model adding lipid-lowering and antidiabetic drugs to the previous model. To treat missing data, a multiple imputation analysis (MICE) was performed with the statistical package (35) using ten replicates and five iterations. The CCA and MICE analyses were compared in a sensitivity analysis, adjusting the models for different variables (Model 1: unadjusted; Model 2: adjusted for age and sex; Model 3: adjusted for sex, smoking, antiplatelet or antihypertensive drug treatment, and BMI; Model 4: fully adjusted). *P*-values less than 0.05 were considered statistically significant without using the correction for multiple comparisons for the multiple events analyzed. We used the cox.zph function in the survival package (R statistical software) to check the proportional hazards assumption of Cox models (34). Statistical analysis was performed with R statistical software, version 3.6.1.[1]

Institutional review board statement

This study was approved by the Institutional Review Board (or Ethics Committee) of IDIAP Jordi Gol i Gurina Foundation (protocol code P13/028 and date of approval 03/04/2013).

Results

At the end of the inclusion period, 219,385 (86.5%) subjects met the study inclusion criteria and were included in the analysis. We identified 22,402 (10.2%) persons with any stage DR. **Figure 1** shows the study flow diagram. The mean age (SD) of the subjects was 64.6 ($\pm$ 11.6) years; the cohort

---

1 https://www.r-project.org

FIGURE 1
Study flow chart.
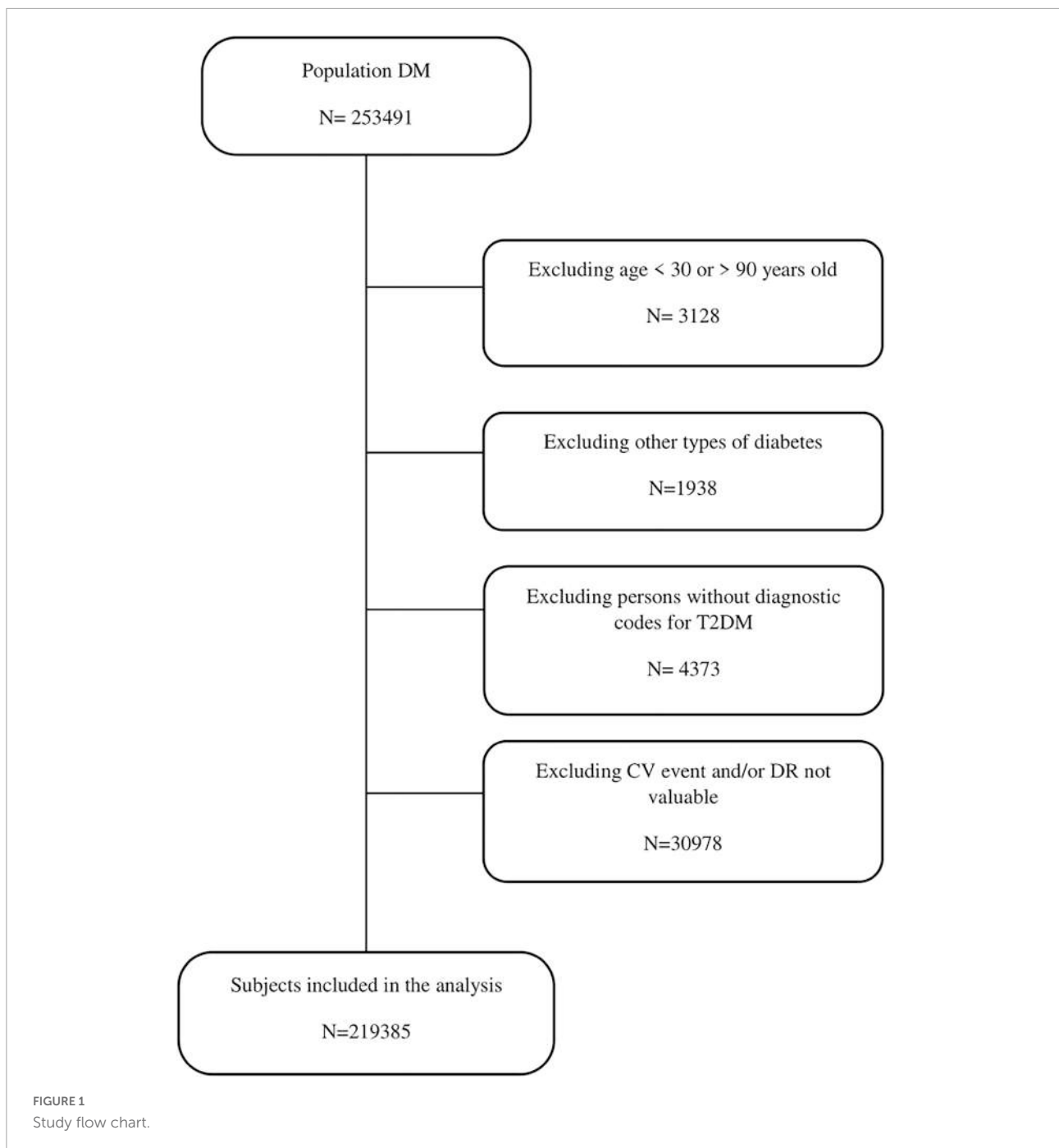
contained a slightly higher proportion of men than women (55.7%) (Table 1).

Compared to those with normal fundus photography, subjects who had DR (any stage) were older and had 1.6 times longer diabetes duration. Moreover, the DR group had a smaller proportion of smokers and a higher proportion (53.4%) of subjects with BMI < 30 kg/m^2. Furthermore, the lipid profile was better in the DR group, with lower total cholesterol, triglycerides, and LDL cholesterol levels, and a

higher proportion (28.3%) of subjects with LDL < 100 mg/dl and higher mean HDL (HDL cholesterol). Subjects with DR had a poorer renal profile than subjects without DR (eGFR, 70.9 (22.4) ml/min/1.73 m^2 vs. 78.8 (19.7) ml/min/1.73 m^2, respectively). The proportions of subjects (32.4%) with eGFR < 60 ml/min/1.73 m2 were higher than those without DR. We observed 1.6 times higher CKD prevalence among the subjects with DR than the subjects without DR. Regarding good glycemic control (HbA1c < 7%), statistically significant

differences were observed among the groups, in favor of subjects without DR (61.3%) compared with subjects with DR (42.0%).

Association between diabetic retinopathy and study events

Table 2 shows the epidemiology for different study events for both subjects with or without DR. During the follow-up period among the subjects with DR, mortality (all cause) was the most common event, followed by macrovascular events, CHD, and then stroke. The same pattern was observed among persons without DR, but with a lower incidence. The

shortest time until the event was observed among the subjects with CHD and DR.

In the bivariate analysis, we observed statistically significant, unadjusted hazard ratios for all of the events, with the risk for the study events being higher among the subjects with DR. When stratified for the stage of DR, the same tendency was observed. The highest risk for the study events was observed among the subjects with proliferative DR. We did not observe statistically significant HRs among the persons with DME and stroke events.

In the multivariable CCA, fully adjusted for DR, sex, age, BMI, tobacco use, duration of T2DM, an antiplatelet or antihypertensive drug, and HbA1c, we observed that subjects with any stage of DR had higher risks for all of the study events.

TABLE 1   Clinical characteristics of the subjects at inclusion.

	All N = 219,385	Without diabetic retinopathy N = 196,983	With diabetic retinopathy N = 22,402
Male sex (%)	122,280 (55.7)	109,984 (55.8)*	12,296 (54.9)*
Age (years), mean (*SD*)	64.6 (11.6)	64.4 (11.5)*	67.0 (11.6)*
Current tobacco use (%)	58,602 (26.0)	52,839 (28.1)*	5,763 (26.9)*
Clinical variables, mean (*SD*)			
Diabetes duration (years)	5.18 (5.27)	4.84 (4.95)*	8.10 (6.81)*
BMI (kg/m^2)	30.6 (5.22)	30.7 (5.20)*	30.2 (5.33)*
SBP (mmHg)	134 (14.8)	134 (14.5)*	137 (16.3)*
DBP (mmHg)	77.1 (9.59)	77.3 (9.51)*	76.0 (10.2)*
Heart rate (beat/min)	76.5 (12.3)	76.4 (12.2)*	77.4 (12.4)*
Laboratory variables, mean (*SD*)			
HbA1c (%)	7.18 (1.53)	7.12 (1.49)*	7.76 (1.75)*
Total cholesterol (mg/dL)	198 (40.3)	198 (40.1)*	192 (41.5)*
HDL cholesterol (mg/dL)	49.0 (12.8)	49.0 (12.8)*	49.5 (13.4)*
LDL cholesterol (mg/dL)	117 (33.8)	118 (33.7)*	112 (34.4)*
Triglycerides (mg/dL)	168 (122)	169 (123)*	160 (112)*
GFR (CKD-EPI; ml/min/1.73 m^2)	78.0 (20.1)	78.8 (19.7)*	70.9 (22.4)*
Albumin-to-creatinine ratio	32.9 (131)	28.9 (114)*	67.5 (226)*
Comorbidities (%)			
Dyslipidemia	104,442 (47.6)	93,347 (47.4)*	11,095 (49.5)*
Hypertension	132,756 (60.5)	117,830 (59.8)*	14,926 (66.6)*
CKD	31,584 (14.4)	26,623 (13.5)*	4,961 (22.1)*
Concomitant treatment (%)			
Antihypertensive drugs	131,967 (60.2)	117,143 (59.5)*	14,824 (66.2)*
Antiplatelet drugs	52,396 (23.9)	44,581 (22.6)*	7,815 (34.9)*
Antidiabetics drugs	160,166 (73.0)	141,309 (71.9)*	18,857 (84.2)*
Lipid-lowering drugs	103,059 (47.0)	92,143 (46.8)*	10,916 (48.7)*

BMI, body mass index; CKD, chronic kidney disease; GFR, glomerular filtration rate; HbA1c, glycosylate hemoglobin; SD, standard deviation. *$p < 0.001$.

TABLE 2   The overall incidence for the study events between both groups.

Events	Groups of subjects	Patients/year	Event-free survival time (median in years)	Events (number)	Event rate (1,000 patients/year)
Mortality	No DR	1017964.6	4.950	17,527	17.2
	DR	112524.5	4.750	3,364	29.9
CHD	No DR	998687.0	4.846	6,360	6.3
	DR	109527.5	4.586	1,058	9.7
Stroke	No DR	1006859.7	4.893	3,637	3.6
	DR	110843.5	4.652	563	5.1
Macrovascular	No DR	988167.7	4.786	9,758	9.9
	DR	107933.7	4.498	1,584	14.7

CHD, coronary heart disease; stroke, macrovascular: CHD and/or stroke; event rate, incidence per 1,000 person-year.

The probability of an event occurring was highest for all-cause death (AHR: 1.34, 95% CI: 1.28; 1.41) and lowest for stroke (AHR: 1.09, 95% CI: 0.97; 1.24). Similar results were observed when adding the lipid-lowering and antidiabetic drugs to the additional model. The Kaplan–Meier survival curves for study events are shown in **Figure 2**, and the results for the unadjusted and adjusted HR are summarized in **Table 3**.

Sensitivity analysis

Figure 3 and **Supplementary Table 2** show the HR observed in the sensitivity analysis. In the MICE, similar HRs for different study events were observed to those from the CCA. When comparing the two analyses for different adjusted models, we observed that HRs for the different events in the MICE analysis were going in the same direction as the CC analysis.

Discussion

The results of our analysis with data collected from primary healthcare centers in Catalonia show a positive association between the DR and major cardiovascular events (CHD and stroke) and all-cause mortality.

Coronary heart disease, stroke, and DR have common risk factors, such as hyperglycemia, hyperlipidemia, and hypertension. Several studies have observed an association between DR and macrovascular disease and subclinical atherosclerosis (10–14). Some studies have reported that DR is a strong determinant of carotid intima-media thickness and arterial stiffness in patients with T2DM (12, 13). In the Atherosclerosis Risk in Communities (ARIC) cohort study based on a population of 1,524 people with T2DM without

cardiovascular events at inclusion, during the follow-up of 7.8 years, the authors observed that the presence of DR was associated with the occurrence of CHD events (HR: 2.07, 95% CI: 1.38; 3.11) and fatal CHD (HR: 3.35, 95% CI: 1.40; 8.01) (16). Compared with the results observed in our study, during the follow-up over an average of 4.8 years, we observed lower but statistically significant adjusted risks for CHD (HR:1.27, 95% CI: 1.16; 1.39). In a recently reported systematic review and meta-analysis of cohort studies, including 17,611 patients without a previous history of CV disease at baseline, DR was associated with an increased risk of CV disease (relative risk (RR): 2.42, 95% CI: 1.77; 3.31) in diabetes (17). This risk was especially elevated among the T1DM persons (RR: 3.59, 95% CI: 1.79; 7.20) compared with T2DM persons (RR: 1.81, 95% CI: 1.47; 2.23) (17). Regarding the severity of DR, only a few studies have evaluated the association between the stage of DR and CV events. The studies done by Gimeno-Orna et al. and Targher et al. reported an increased risk between NPDR and RDP and the incidence of non-fatal or fatal cardiovascular events, independently of other known cardiovascular risk factors (HR:1.71, 95% CI: 1.1; 2.66 and HR: 2, 95% CI: 1.1; 3.56, respectively) (18, 19). Additionally, the Japan Diabetes Complications Study (JDCS) that included 2,033 subjects with T2DM with an 8-year follow-up period found an increased risk for CHD even during the initial stages of DR (mild-to-moderate NPDR) after adjusting for traditional CV risk factors (HR:1.69, 95% CI: 1.17; 2.97) (20). Our study observed a similar tendency but with a lower HR for NPDR and CHD in a fully adjusted model.

Evidence suggests that subjects with diabetes and DR seem to be at a high risk of ischemic stroke, with a meta-analysis that included 19 observational cohort studies of 81,452 diabetic patients reporting that the presence of

FIGURE 2

Survival curves and different study events and stages of diabetic retinopathy. **(A1)** All-cause mortality; **(B1)** coronary heart disease; **(C1)** stroke; **(D1)** macrovascular complications; **(A2)** all-cause mortality and different states of DR; **(B2)** coronary heart disease and different states of DR; **(C2)** stroke and different states of DR; **(D2)** and different states of DR and different states of DR.

TABLE 3 Hazard ratios for events among the study groups complete cases analysis.

	General		Stage of DR			
	Group without DR $N = 196,983$	Group with DR $N = 22,402$	Non-proliferative diabetic retinopathy (NPDR) $N = 19,048$	Proliferative diabetic retinopathy (PRD) $N = 663$	Diabetic macular edema (DME) $N = 475$	Unknown stage* $N = 2,216$
Mortality, *n* (%)	17,527 (8.90)	3,364 (15.0)	2,794 (14.7)	144 (21.7)	76 (16.0)	350 (15.8)
Unadjusted HR 95% CI [LL; UL]	Ref.	1.75 [1.69;1.82]	1.69 [1.62;1.76]	2.82 [2.39;3.32]	2.44 [1.95;3.06]	1.91 [1.72;2.12]
**Adjusted HR 95% CI [LL; UL]	Ref.	1.34 [1.28;1.41]	1.34 [1.27;1.42]	1.68 [1.31;2.15]	1.71 [1.27;2.31]	1.19 [1.03;1.38]
***Adjusted HR 95% CI [LL; UL]	Ref.	1.34 [1.27;1.41]	1.34 [1.26;1.41]	1.66 [1.30;2.13]	1.69 [1.25;2.28]	1.19 [1.03;1.38]
CHD, *n* (%)	6,360 (3.23)	1,058 (4.72)	904 (4.75)	38 (5.73)	22 (4.63)	94 (4.24)
Unadjusted HR 95% CI [LL; UL]	Ref.	1.84 [1.70;1.99]	1.51 [1.41;1.62]	2.00 [1.45;2.75]	1.82 [1.20;2.76]	1.39 [1.13; 1.70]
**Adjusted HR 95% CI [LL; UL]	Ref.	1.27 [1.16;1.39]	1.30 [1.19;1.43]	1.17 [0.71;1.92]	0.80 [0.38; 1.68]	1.11[0.86;1.44]
***Adjusted HR 95% CI [LL; UL]	Ref.	1.28 [1.17;1.40]	1.31 [1.19;1.44]	1.18 [0.72;1.92]	0.81 [0.38; 1.69]	1.11[0.86;1.44]
Stroke, *n* (%)	3,637 (1.85)	563 (2.51)	468 (2.46)	26 (3.92)	9 (1.89)	60 (2.71)
Unadjusted HR 95% CI [LL; UL]	Ref.	1.75 [1.64;1.86]	1.36 [1.24;1.50]	2.41 [1.64;3.55]	1.30 [0,68;2.50]	1.56 [1.20;2.01]
**Adjusted HR 95% CI [LL; UL]	Ref.	1.09 [0.97;1.24]	1.11 [0.97;1.26]	1.65[0.95;2.86]	0.74 [0.27;1.99]	0.93[0.65;1.33]
***Adjusted HR 95% CI [LL; UL]	Ref.	1.09 [0,97;1,24]	1.11 [0.97;1.26]	1.65[0.95;2.85]	0.74 [0.28;1.98]	0.93[0.65;1.33]
Macrovascular, *n* (%)	9,758 (4.95)	1,584 (7.07)	1,341 (7.04)	61 (9.02)	30 (6.32)	152 (6.86)
Unadjusted HR 95% CI [LL; UL]	Ref.	1.75 [1.64; 1.86]	1.47 [1.39; 1.55]	2.12 [1.65; 2.73]	1.62 [1.13; 2.31]	1.48 [1.26; 1.73]
**Adjusted HR 95% CI [LL; UL]	Ref.	1.22 [1.13; 1.31]	1.24 [1.15;1.34]	1.29 [0.88; 1.89]	0.79 [0.44; 1.44]	1.08 [0.87;1.33]
***Adjusted HR 95% CI [LL; UL]	Ref.	1.22 [1.14; 1.31]	1.25 [1.15;1.35]	1.30 [0.89; 1.90]	0.80 [0.44; 1.44]	1.08 [0.88;1.33]

DR, diabetic retinopathy; CHD, coronary heart disease; NDR, no apparent diabetic retinopathy; NPDR, non-proliferative diabetic retinopathy; PDR, proliferative diabetic retinopathy; DME, diabetic macular edema; ref, reference group; HR, hazard ratio; 95% CI, 95% confidence interval; LL, lower limit; UL, upper limit.
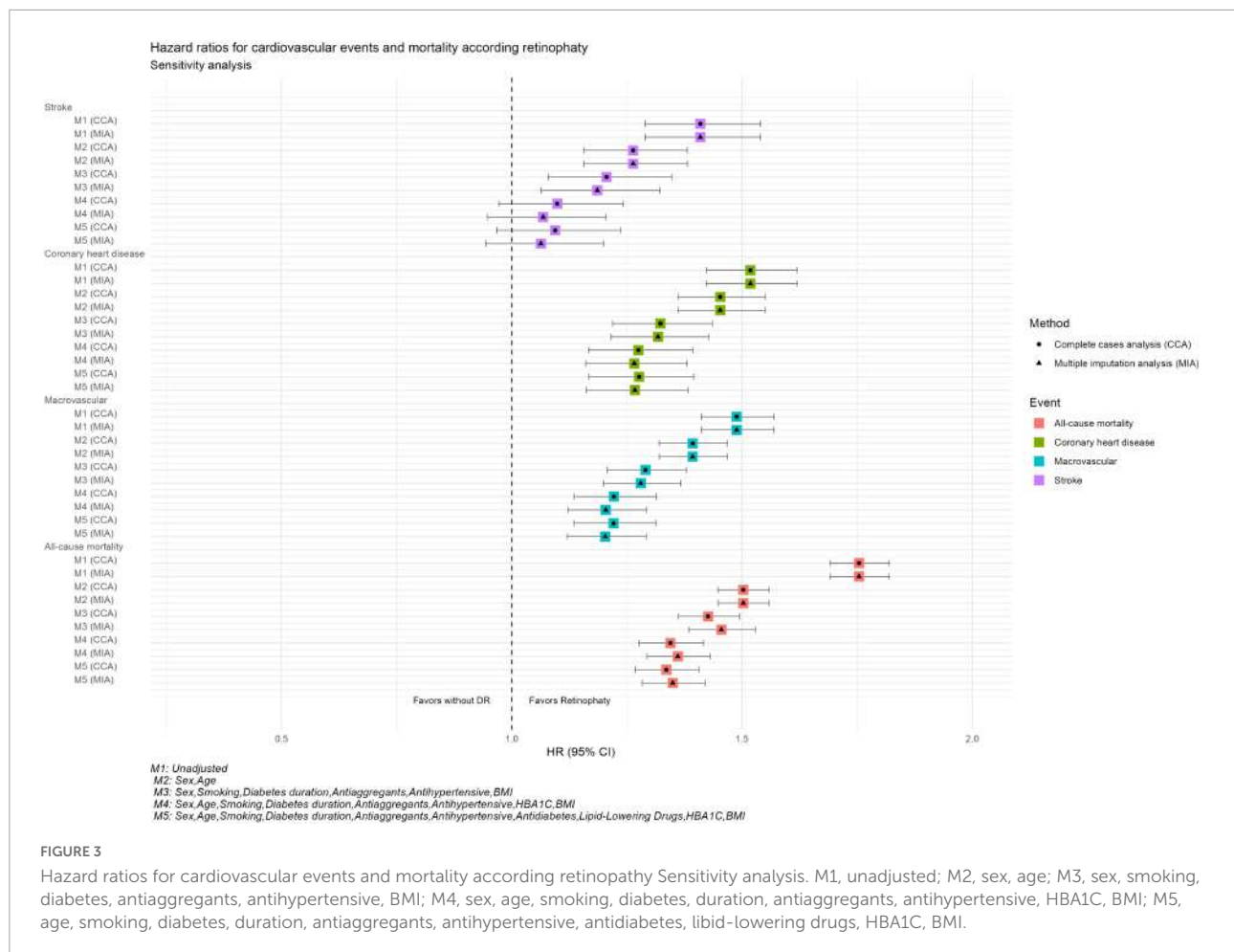*Subjects having diabetic retinopathy by diagnostic code but without fundus photography/stage of DR.
**Adjusted for DR, sex, age, BMI, tobacco, duration of T2DM, an antiplatelet or antihypertensive drug, and HbA1c.
***Adjusted for DR, sex, age, BMI, tobacco, duration of T2DM, an antiplatelet, antihypertensive, lipid-lowering, or antidiabetic drugs, and HbA1c.

DR was associated with an increased risk of stroke (HR: 1.25, 95% CI: 1.12; 1.39). Subgroup analysis for the type of diabetes yielded a pooled HR of 1.29 and 95% CI: 1.10; 1.50 in T2DM (21). In a secondary analysis of patients enrolled in the Action to Control Cardiovascular Risk in Diabetes (ACCORD) Eye Study in an adjusted Cox regression model, DR was independently associated with incident stroke (HR:1.52, 95% CI:1.05; 2.20) (22). Another prospective cohort study with 1,617 middle-aged people with diabetes observed that during a follow-up of 7.8 years, DR was associated with an increased risk of ischemic stroke (HR: 2.34, 95% CI: 1.13; 4.86) (24). In our study, we did not observe associations between DR or stage of DR and stroke in fully adjusted models, which could be due to the

methodological differences or diagnostic codes used to identify the cases with stroke.

Regarding all-cause mortality, our study shows that the presence of any degree of DR is correlated with an increased risk of this event. In a study from the United States with 4,777 adults, the authors found that those persons with mild and moderate/severe retinopathy had an increased risk of all-cause mortality (HR: 1.81, 95% CI: 1.29; 2.55 and HR: 4.14, 95% CI: 1.77; 9.69, respectively) (30). In another meta-analysis from ten observational studies with 11,239 diabetic patients, the authors reported a doubling in the risk of mortality due to CVD in subjects with diabetes and severe DR (31). Similar results were also obtained in the analysis of other studies with similar follow-up periods in a meta-analysis of 19 studies

FIGURE 3

Hazard ratios for cardiovascular events and mortality according retinopathy Sensitivity analysis. M1, unadjusted; M2, sex, age; M3, sex, smoking, diabetes, antiaggregants, antihypertensive, BMI; M4, sex, age, smoking, diabetes, duration, antiaggregants, antihypertensive, HBA1C, BMI; M5, age, smoking, diabetes, duration, antiaggregants, antihypertensive, antidiabetes, libid-lowering drugs, HBA1C, BMI.

encompassing 142,625 participants; the risk ratio (RR) for all-cause mortality with DR was 2.33 (95% CI: 1.92; 2.81) compared to subjects without DR. According to the different degrees of DR in subjects with T2DM, the RR of all-cause mortality varied. The RDNP risk was 1.38 (1.11–1.70), while the risk of PDR was 2.32 (1.75; 3.06) (32). Our analysis only observed statistically significant risks for all-cause mortality stratified for different stages of DR; this risk was highest among the persons who had PDR.

Our study has some potential limitations inherent in observational studies with routinely collected healthcare data. Firstly, missing data for the study variables is an important limitation. We used pseudo-anonymized routinely collected health data, where patients were visited as part of the regular healthcare surveillance. To test the effect of this limitation, we did a CCA and multiple imputations of missing data, and the results were consistent. Due to the database characteristics, there is a possibility of registering errors related to the diagnostic code for DR. Therefore, we used the fundus photography results and combined them with diagnostic codes. This limitation could also be applied to the study events. We used a wide spectrum of codes to define each study event. Another limitation is the numerical imbalance between the different groups due to the study design and lack of randomization. Moreover, we should acknowledge there is an inherent possibility of a certain risk of detection bias related to the frequency of medical visits. To minimize this bias, we designed the study to include only DM subjects who had at least one visit. We included the subjects in the study on the day of diabetic eye screening. Therefore, all the subjects were active users of the system. The main strength of our study was the large study population which increases the statistical power and external validity. Similarly, the results of our study confirm the results of previous studies.

In conclusion, our results show that DR is associated with an increased risk of cardiovascular disease and death among persons with T2DM. These findings indicate the importance of early screening, identification, and proper treatment of subjects with DR to reduce the risk of macrovascular disease and death. Further functional studies are needed to evaluate the biological background of these complications of diabetes and the potential use of stages of DR as an early marker for major adverse cardiovascular events.

Data availability statement

The data analyzed in this study is subject to the following licenses/restrictions: Restrictions apply to the availability of some or all data generated or analyzed during this study because they were used under a license. The corresponding author will, on request, detail the restrictions and any conditions under which access to some data may be provided. Requests to access these datasets should be directed to XM-T, mundetx@gmail.com.

Ethics statement

This study was approved by the Institutional Review Board (or Ethics Committee) of IDIAP Jordi Gol i Gurina Foundation (protocol code P13/028 and date of approval 03/04/2013). Written informed consent for participation was not required for this study in accordance with the national legislation and the institutional requirements.

Author contributions

JB: conceptualization. XM-T: methodology and resources. JR: software, formal analysis, and data curation. JR, BV, and JB: validation. JB and BV: writing—original draft preparation and review and editing. DM, PR-A, RS, JR, EC, JB, MM-C, and JF-N: supervision. All authors have read and agreed to the published version of the manuscript.

Acknowledgments

We thank Amanda Prowse for her editorial support of this manuscript.

Conflict of interest

JB has received speaking fees from Boehringer Ingelheim, Astra-Zeneca, Lilly, MSD, Novo Nordisk, Sanofi. DM has received advisory and/or speaking fees from Astra-Zeneca, Ascensia, Boehringer Ingelheim, GSK, Lilly, MSD, Novartis, Novo Nordisk and Sanofi; he has received research grants to the institution from Astra-Zeneca, GSK, Lilly, MSD, Novartis, Novo Nordisk, Sanofi and Boehringer. JF-N has received advisory and/or speaking fees from Astra-Zeneca. Ascensia, Boehringer Ingelheim, GSK, Lilly, MSD, Novartis, Novo Nordisk and Sanofi; he has received research grants to the institution from Astra-Zeneca, GSK, Lilly, MSD, Novartis, Novo Nordisk, Sanofi and Boehringer. XM-T has received advisory and/or speaking fees from Boehringer Ingelheim, Lilly, MSD, Novartis. MM-C has received advisory honorarium from Astra-Zeneca, Bayer, Boehringer Ingelheim, GSK, Lilly, MSD, Novartis, Novo Nordisk, and Sanofi; he has received speaker honorarium from Astra-Zeneca, Bayer, Boehringer Ingelheim, GSK, Lilly, Menarini, MSD, Novartis, Novo Nordisk, and Sanofi; he has received research grants to the institution from Astra-Zeneca, GSK, Lilly, MSD, Novartis, Novo Nordisk and Sanofi.

The remaining authors declare that the research was conducted in the absence of any commercial or financial relationships that could be construed as a potential conflict of interest.

Publisher's note

All claims expressed in this article are solely those of the authors and do not necessarily represent those of their affiliated organizations, or those of the publisher, the editors and the reviewers. Any product that may be evaluated in this article, or claim that may be made by its manufacturer, is not guaranteed or endorsed by the publisher.

Supplementary material

The Supplementary Material for this article can be found online at: https://www.frontiersin.org/articles/10.3389/fmed.2022.945245/full#supplementary-material

References

1. Zimmet P, Alberti KG, Magliano DJ, Bennett PH. Diabetes mellitus statistics on prevalence and mortality: Facts and fallacies. *Nat Rev Endocrinol.* (2016) 12:616–22. doi: 10.1038/nrendo.2016.105

2. International Diabetes Federation. *IDF diabetes atlas*. 10th ed. Brussels: International Diabetes Federation (2021).

3. Solomon SD, Chew E, Duh EJ, Sobrin L, Sun JK, VanderBeek BL, et al. Diabetic retinopathy: A position statement by the American diabetes association. *Diabetes Care.* (2017) 40:412–8. doi: 10.2337/dc16-2641

4. Simó R, Hernández C. Neurodegeneration in the diabetic eye: New insights and therapeutic perspectives. *Trends Endocrinol Metab.* (2014) 25:23–33. doi: 10.1016/j.tem.2013.09.005

5. Yau JW, Rogers SL, Kawasaki R, Lamoureux EL, Kowalski JW, Bek T, et al. Global prevalence and major risk factors of diabetic retinopathy. *Diabetes Care.* (2012) 35:556–64. doi: 10.2337/dc11-1909

6. Thomas RL, Halim S, Gurudas S, Sivaprasad S, Owens DR. IDF diabetes atlas: A review of studies utilising retinal photography on the global prevalence of diabetes-related retinopathy between 2015 and 2018. *Diabetes Res Clin Pract.* (2019) 157:107840. doi: 10.1016/j.diabres.2019.107840

7. Almdal T, Scharling H, Jensen JS, Vestergaard H. The independent effect of type 2 diabetes mellitus on ischemic heart disease, stroke, and death: A population-based study of 13,000 men and women with 20 years of follow-up. *Arch Intern Med.* (2004) 164:1422–6. doi: 10.1001/archinte.164.13.1422

8. Scanlon PH, Aldington SJ, Stratton IM. Delay in diabetic retinopathy screening increases the rate of detection of referable diabetic retinopathy. *Diabet Med.* (2014) 31:439–42. doi: 10.1111/dme.12313

9. Klein R, Klein BE, Moss SE. Epidemiology of proliferative diabetic retinopathy. *Diabetes Care.* (1992) 15:1875–91. doi: 10.2337/diacare.15.12.1875

10. Cheung N, Wong TY. Diabetic retinopathy and systemic vascular complications. *Prog Retin Eye Res.* (2008) 27:161–76. doi: 10.1016/j.preteyeres.2007.12.001

11. Liu Y, Teng X, Zhang W, Zhang R, Liu W. Association between diabetic retinopathy and subclinical atherosclerosis in China: Results from a community-based study. *Diab Vasc Dis Res.* (2015) 12:366–72. doi: 10.1177/1479164115591744

12. Saif A, Karawya S, Abdelhamid A. Retinopathy is a strong determinant of atherosclerosis in type 2 diabetes: Correlation with carotid intima-media thickness. *Endocr Pract.* (2015) 21:226–30. doi: 10.4158/EP14390

13. Rema M, Mohan V, Deepa R, Ravikumar R. Association of carotid intima-media thickness and arterial stiffness with diabetic retinopathy: The Chennai urban rural epidemiology study (CURES-2). *Diabetes Care.* (2004) 27:1962–7. doi: 10.2337/diacare.27.8.1962

14. Alonso N, Traveset A, Rubin E, Ortega E, Alcubierre N, Sanahuja J, et al. Type 2 diabetes-associated carotid plaque burden is increased in patients with retinopathy compared to those without retinopathy. *Cardiovasc Diabetol.* (2015) 14:33. doi: 10.1186/s12933-015-0196-1

15. Pearce I, Simó R, Lövestam-Adrian M, Wong DT, Evans M. Association between diabetic eye disease and other complications of diabetes: Implications for care. A systematic review. *Diabetes Obes Metab.* (2019) 21:467–78. doi: 10.1111/dom.13550

16. Cheung N, Wang JJ, Klein R, Couper DJ, Sharrett AR, Wong TY. Diabetic retinopathy and the risk of coronary heart disease: The atherosclerosis risk in communities study. *Diabetes Care.* (2007) 30:1742–6. doi: 10.2337/dc07-0264

17. Guo VY, Cao B, Wu X, Lee JJW, Zee BC. Prospective association between diabetic retinopathy and cardiovascular disease-a systematic review and meta-analysis of cohort studies. *J Stroke Cerebrovasc Dis.* (2016) 25:1688–95. doi: 10.1016/j.jstrokecerebrovasdis.2016.03.009

18. Gimeno-Orna JA, Faure-Nogueras E, Castro-Alonso FJ, Boned-Juliani B. Ability of retinopathy to predict cardiovascular disease in patients with type 2 diabetes mellitus. *Am J Cardiol.* (2009) 103:1364–7. doi: 10.1016/j.amjcard.2009.01.345

19. Targher G, Bertolini L, Zenari L, Lippi G, Pichiri I, Zoppini G, et al. Diabetic retinopathy is associated with an increased incidence of cardiovascular events in type 2 diabetic patients. *Diabet Med.* (2008) 25:45–50. doi: 10.1111/j.1464-5491.2007.02327.x

20. Kawasaki R, Tanaka S, Tanaka S, Abe S, Sone H, Yokote K, et al. Risk of cardiovascular diseases is increased even with mild diabetic retinopathy: The Japan diabetes complications study. *Ophthalmology.* (2013) 120:574–82. doi: 10.1016/j.ophtha.2012.08.029

21. Hu K, Jiang M, Zhou Q, Zeng W, Lan X, Gao Q, et al. Association of diabetic retinopathy with stroke: A systematic review and meta-analysis. *Front Neurol.* (2021) 12:626996. doi: 10.3389/fneur.2021.626996

22. Wong KH, Hu K, Peterson C, Sheibani N, Tsivgoulis G, Majersik JJ, et al. Diabetic retinopathy and risk of stroke: A secondary analysis of the ACCORD eye study. *Stroke.* (2020) 51:3733–6. doi: 10.1161/STROKEAHA.120.030350

23. Petitti DB, Bhatt H. Retinopathy as a risk factor for nonembolic stroke in diabetic subjects. *Stroke.* (1995) 26:593–6. doi: 10.1161/01.str.26.4.593

24. Cheung N, Rogers S, Couper DJ, Klein R, Sharrett AR, Wong TY. Is diabetic retinopathy an independent risk factor for ischemic stroke? *Stroke.* (2007) 38:398–401. doi: 10.1161/01.STR.0000254547.91276.50

25. Hägg S, Thorn LM, Putaala J, Liebkind R, Harjutsalo V, Forsblom CM, et al. Incidence of stroke according to presence of diabetic nephropathy and severe diabetic retinopathy in patients with type 1 diabetes. *Diabetes Care.* (2013) 36:4140–6. doi: 10.2337/dc13-0669

26. Hankey GJ, Anderson NE, Ting RD, Veillard AS, Romo M, Wasik M, et al. Rates and predictors of risk of stroke and its subtypes in diabetes: A prospective observational study. *J Neurol Neurosurg Psychiatry.* (2013) 84:281–7. doi: 10.1136/jnnp-2012-303365

27. Hugenschmidt CE, Lovato JF, Ambrosius WT, Bryan RN, Gerstein HC, Horowitz KR, et al. The cross-sectional and longitudinal associations of diabetic retinopathy with cognitive function and brain MRI findings: The action to control cardiovascular risk in diabetes (ACCORD) trial. *Diabetes Care.* (2014) 37:3244–52. doi: 10.2337/dc14-0502

28. Exalto LG, Biessels GJ, Karter AJ, Huang ES, Quesenberry CP Jr., Whitmer RA. Severe diabetic retinal disease and dementia risk in type 2 diabetes. *J Alzheimers Dis.* (2014) 42 Suppl 3:S109–17. doi: 10.3233/JAD-132570

29. Mauricio D, Vlacho B, Barrot de la Puente J, Mundet-Tudurí X, Real J, Kulisevsky J, et al. Associations between diabetic retinopathy and Parkinson's disease: Results from the catalonian primary care cohort study. *Front Med (Lausanne).* (2022) 8:800973. doi: 10.3389/fmed.2021.800973

30. Frith E, Loprinzi PD. Retinopathy and mortality. *Diabetes Spectr.* (2018) 31:184–8. doi: 10.2337/ds17-0010

31. Xu XH, Sun B, Zhong S, Wei DD, Hong Z, Dong AQ. Diabetic retinopathy predicts cardiovascular mortality in diabetes: A meta-analysis. *BMC Cardiovasc Disord.* (2020) 20:478. doi: 10.1186/s12872-020-01763-z

32. Zhu XR, Zhang YP, Bai L, Zhang XL, Zhou JB, Yang JK. Prediction of risk of diabetic retinopathy for all-cause mortality, stroke and heart failure: Evidence from epidemiological observational studies. *Medicine (Baltimore).* (2017) 96:e5894. doi: 10.1097/MD.0000000000005894

33. Wu L. Classification of diabetic retinopathy and diabetic macular edema. *World J Diabetes.* (2013) 4:290. doi: 10.4239/wjd.v4.i6.290

34. Therneau TM, Grambsch PM. *Modeling survival data: Extending the cox model.* New York, NY: Springer (2000). doi: 10.1007/978-1-4757-3294-8

35. Buuren S, Groothuis-Oudshoorn C. MICE: multivariate imputation by chained equations in R. *J Stat Softw.* (2011) 45:1–67. doi: 10.18637/jss.v045.i03

Serous retinal detachment secondary to an unsuccessful transarterial embolization in a post-traumatic carotid-cavernous sinus fistula patient: A case report

Chia-Yi Lee[1] and Wan-Ju Annabelle Lee[1,2,3]*

[1]Department of Ophthalmology, Chi Mei Medical Center, Tainan, Taiwan, [2]Institute of Clinical Pharmacy and Pharmaceutical Sciences, College of Medicine, National Cheng Kung University, Tainan, Taiwan, [3]Department of Optometry, Chung Hwa University of Medical Technology, Tainan, Taiwan

A carotid-cavernous sinus fistula (CCF) is an abnormal communication between the cavernous sinus and the carotid arterial system. Direct CCFs arise from a direct connection between the cavernous sinus and the cavernous portion of the internal carotid artery. Nowadays, endovascular neurosurgery has become the first-line treatment modality for direct CCFs owing to the high complete obliteration rate. However, reversal of the clinical symptoms may not always be congruous after the endovascular intervention. Herein, we present a 50-year-old patient who manifested diplopia, ophthalmoplegia, and orbital congestion after a traffic accident. He had suffered head injury with right side frontal intracranial hemorrhage 1 month before the ophthalmic presentation. He came to our department primarily because of declining vision and for the above symptoms, and was diagnosed with direct type CCF, for which he received transarterial coil embolization. Unexpectedly, he later presented with serous retinal detachment accompanied by ocular ischemic syndrome secondary to recurrent CCF 1 month after the intervention, so repeat coil embolization was performed.

Introduction

Carotid-cavernous sinus fistula (CCF) refers to an abnormal communication from the carotid artery or any of its branches to the cavernous sinus. CCFs can be classified by velocity of blood flow (high/low), etiology (traumatic/spontaneous), and anatomy of the shunt (direct/dural, internal carotid/external carotid/both). Studies from

D. Parkinson in the 1960s and 1970s have been shown to be of great value in assessing CCF features (1). The Barrow classification has been the most widely adopted system so far (2, 3). However, other classification systems have been proposed since the Barrow classification may not precisely reflect correlations between etiology, symptomatology, therapeutic approaches and outcomes. CCFs are always direct fistulas between the cavernous segment of the internal carotid artery and the cavernous sinus. They can be post-traumatic or due to the rupture of an aneurysm of the carotid syphon. On the other hand, the cavernous sinus, as well as all other dural sinuses, can be affected by a dural arteriovenous fistula (DAVF). They are distinguished by multiple small arterial feeders from dural branches going into the cavernous sinus and they have completely different etiology from CCFs.

Direct fistulas are characterized by a direct connection between the ICA and the cavernous sinus. They are usually high-flow fistulas. Causes include penetrating or blunt trauma, rupture of an ICA aneurysm within the cavernous sinus, Ehlers–Danlos syndrome type IV, or iatrogenic interventions. Posteriorly draining fistulas into the petrosal sinuses can be asymptomatic or present with painful, isolated cranial nerve palsies, sometimes with minimal or absent ophthalmic signs. Hemorrhagic complications such as subarachnoid hemorrhage and intracerebral hemorrhage have been reported and warrant prompt surgical intervention.

Anteriorly draining fistulas are more likely to cause ocular symptoms. Direct CCFs are usually associated with trauma, with high flow properties, and often lead to acute presentation of ocular or orbital symptoms and signs (4). Proptosis, lid swelling, conjunctival injection and chemosis and corkscrew vessels are all clinical signs associated with direct CCFs. Intra-ocular pressure (IOP) elevation can follow from a raised episcleral venous pressure or an angle closure mechanism when venous congestion in the iris and choroid causes the lens iris diaphragm to move forward (5). These above presentations raise major concerns of blindness and future ophthalmic complications.

Comprehensive obliteration of the shunt between ICA and cavernous sinus is the treatment goal of direct CCFs. The application of endovascular embolization techniques is currently the mainstay of clinical practice. Endovascular embolization (transarterial embolization, transvenous embolization, or a combination of both) has achieved high rates (> 80%) of CCF closure (6). While symptom improvement is frequently robust following successful endovascular management, some clinical symptoms, especially neurological deficits, may remain unresolved. In cases where there is either spontaneous or post-treatment thrombosis in the superior ophthalmic vein, normal venous dynamics are interrupted, contributing to venous congestion, and subsequent impairment in arterial perfusion and ischemic optic neuropathy.

Treatment of ocular complications is required if there is deterioration of vision. However, the treatment of the underlying CCF should be a priority. Anatomical closure by endovascular embolization may leave residual ocular symptoms. However, only limited literature has reported about failed endovascular embolization and its possible consequences (7). Serous retinal detachment has been noted as a very rare ocular presentation of CCFs. Careful examination and detailed history intake are important to record and describe recurrence. Herein, we present a case of serous retinal detachment with ocular ischemic syndrome due to recurrent post-traumatic CCF after an unsuccessful transarterial embolization (TAE) with coil. To the best of our knowledge, this is the first case report of serous retinal detachment and ocular ischemia syndrome secondary to a recurrent CCF.

Case presentation

A 50-year-old Asian male with no significant medical history presented to our department with a 1-month history of horizontal double vision with progressive eyeball protrusion, periorbital ecchymosis, and redness in his left eye. He had been involved in a traffic accident 1 month prior involving head injury with right frontal intracranial hemorrhage. He had received conservative treatment at that time in another hospital.

At the first visit, the best-corrected visual acuity (BCVA) and intraocular pressure (IOP) in the right eye were 20/20 (on a Snellen chart) and 13 mmHg, respectively, and the corresponding values for the left eye were 20/30 and 18 mmHg. The ophthalmologic examination was notable in the left eye which presented as exophthalmos (with 2 mm of protrusion compared with the fellow eye), ptosis (Margin Reflex Distance-1, MRD-1, was 1.5 mm), conjunctival injection and chemosis with corkscrew vessels, and a relative afferent pupillary defect.
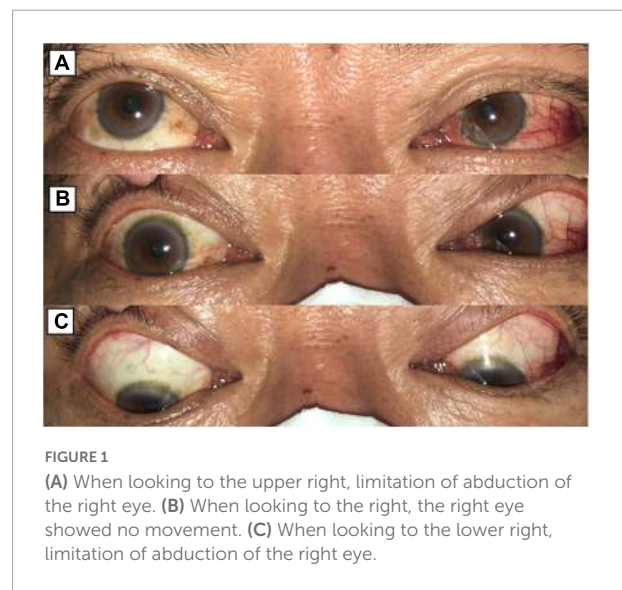
FIGURE 1
(A) When looking to the upper right, limitation of abduction of the right eye. (B) When looking to the right, the right eye showed no movement. (C) When looking to the lower right, limitation of abduction of the right eye.
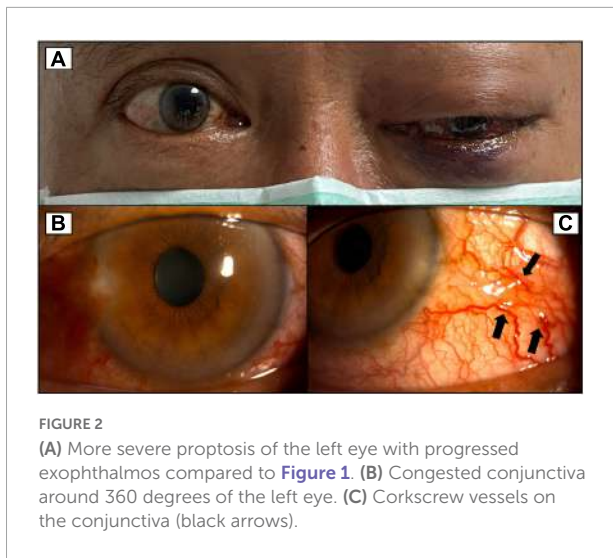
FIGURE 2
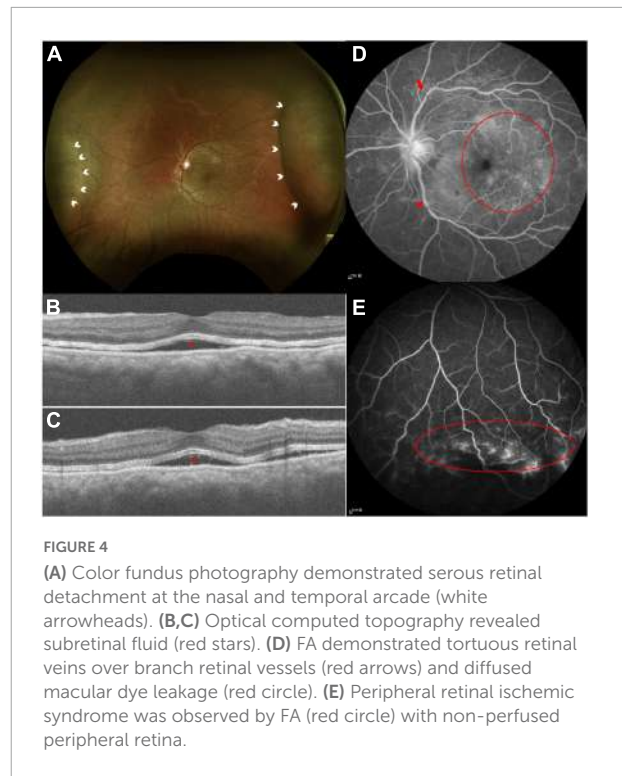(A) More severe proptosis of the left eye with progressed exophthalmos compared to **Figure 1**. (B) Congested conjunctiva around 360 degrees of the left eye. (C) Corkscrew vessels on the conjunctiva (black arrows).

FIGURE 4
(A) Color fundus photography demonstrated serous retinal detachment at the nasal and temporal arcade (white arrowheads). (B,C) Optical computed topography revealed subretinal fluid (red stars). (D) FA demonstrated tortuous retinal veins over branch retinal vessels (red arrows) and diffused macular dye leakage (red circle). (E) Peripheral retinal ischemic syndrome was observed by FA (red circle) with non-perfused peripheral retina.

Extraocular movements of the right eye revealed limitation of abduction. Extraocular movements of the left eye were normal (**Figure 1**). On the Ishihara color test, all plates were identified correctly (15/15) in both eyes. At that time, on suspicion of low-flow CCF, we arranged brain magnetic resonance imaging through the outpatient department.

Unfortunately, 2 weeks later, the patient suffered from left eye ophthalmoplegia (**Figure 2**) with elevated IOP. He also complained of vision decline (BCVA: 20/40) with intermittent eye pain in his left eye. Under suspicion of a post-traumatic direct type CCF, emergent orbital and brain magnetic resonance angiography (MRA) was arranged. MRA revealed an engorged left superior ophthalmic vein and dilatation of bilateral cavernous sinuses, which favored the diagnosis of CCF (**Figure 3**). The patient was expediently referred to the neurology department where

digital subtraction angiography confirmed right side direct CCF. After embolization of the fistula through the use of transarterial coil by the neuro-radiologist, the patient's IOP gradually decreased after stopping anti-glaucoma medications. Furthermore, the extraocular movements of his right eye improved gradually. No more binocular diplopia presented. His left eye BCVA returned to 20/30 at that time, but he still had left eye proptosis and a relative afferent pupillary defect.
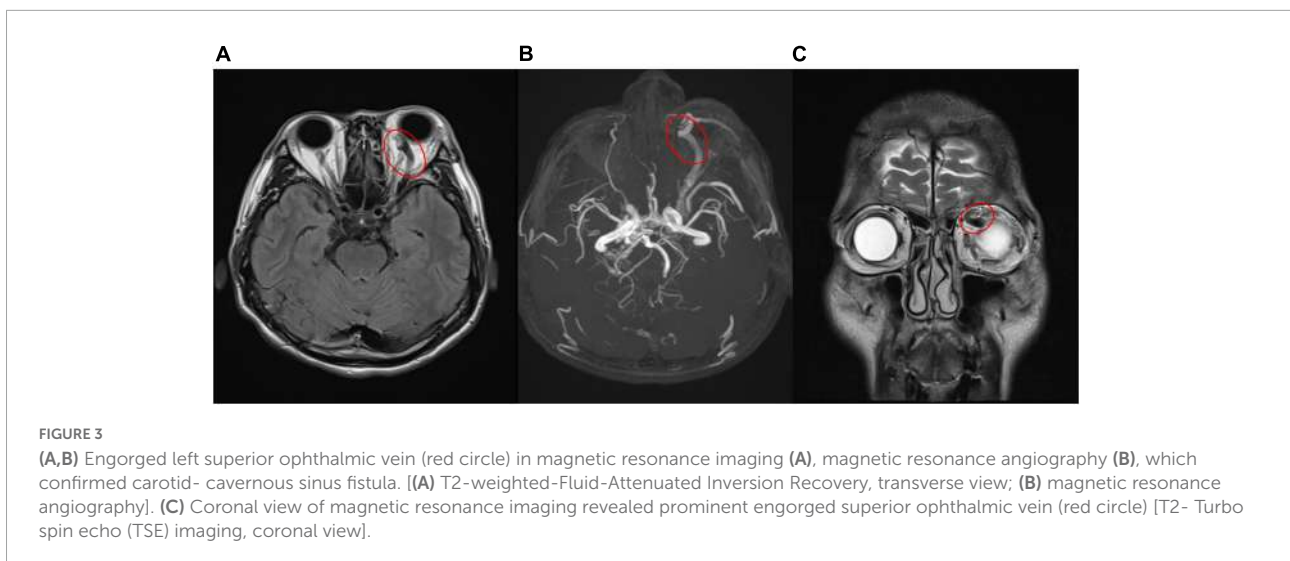
FIGURE 3
(A,B) Engorged left superior ophthalmic vein (red circle) in magnetic resonance imaging (A), magnetic resonance angiography (B), which confirmed carotid- cavernous sinus fistula. [(A) T2-weighted-Fluid-Attenuated Inversion Recovery, transverse view; (B) magnetic resonance angiography]. (C) Coronal view of magnetic resonance imaging revealed prominent engorged superior ophthalmic vein (red circle) [T2- Turbo spin echo (TSE) imaging, coronal view].
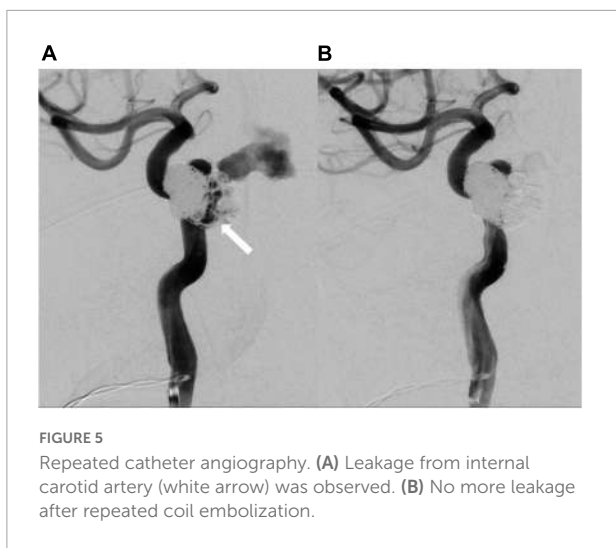
FIGURE 5
Repeated catheter angiography. **(A)** Leakage from internal carotid artery (white arrow) was observed. **(B)** No more leakage after repeated coil embolization.

FIGURE 7
(A) Before successful transarterial embolization (TAE). Severe congested conjunctiva with corkscrew vessels of the left eye. **(B)** After successful TAE. Congested conjunctiva improved and without corkscrew vessels. **(C)** Before successful TAE. Left eye ophthalmoplegia was observed. **(D)** After successful TAE. Left eye ophthalmoplegia improved.

One month after the TAE, the patient's left eye showed severe congestion with corkscrew vessels on the conjunctiva again without diplopia, associated with progressed exophthalmos (three mm of protrusion compared with the fellow eye) and reduced vision (20/200) in the left eye. Fundus photography of the left eye revealed serous retinal detachment, retinal vein tortuosity and mild choroidal detachment throughout the periphery (Figure 4). Suspecting ocular ischemic syndrome, we performed fluorescein angiography (FA), which revealed peripheral diffuse retinal ischemia with central macular edema. Therefore, emergent focal photocoagulation was performed at the periphery in his left eye and the patient was referred again, emergently, to the neuro-radiologist. A repeat catheter angiogram revealed insufficient coil compaction with a leak in ICA which failed to achieve complete fistula obliteration (Figure 5). Recurrent CCF was diagnosed and treated by repeated transarterial coil embolization. Three weeks later, the BCVA of the left eye had returned to 20/50. The serous retinal detachment and macular edema had resolved, too. The timeline of the patient's clinical course is shown in Figure 6.

Discussion

Most CCFs drain into the ophthalmic veins (typical venous drainage pattern), leading to the pathogenic ocular clinical triad associated with a CCF. Presenting symptoms of CCFs may include a subjective bruit, diplopia, tearing, red eye, ocular foreign body sensation, blurred vision and sometimes headache (8–10). Neurogenic strabismus most commonly presents as a sixth nerve palsy. The frequency of sixth nerve involvement is due to the central location of the sixth nerve, adjacent to the ICA within the cavernous sinus, putting it at higher risk of injury than other cranial nerves that are located in the deep layer of the lateral wall of the sinus. Patients with suspected CCFs require neuroimaging that includes non-invasive computed
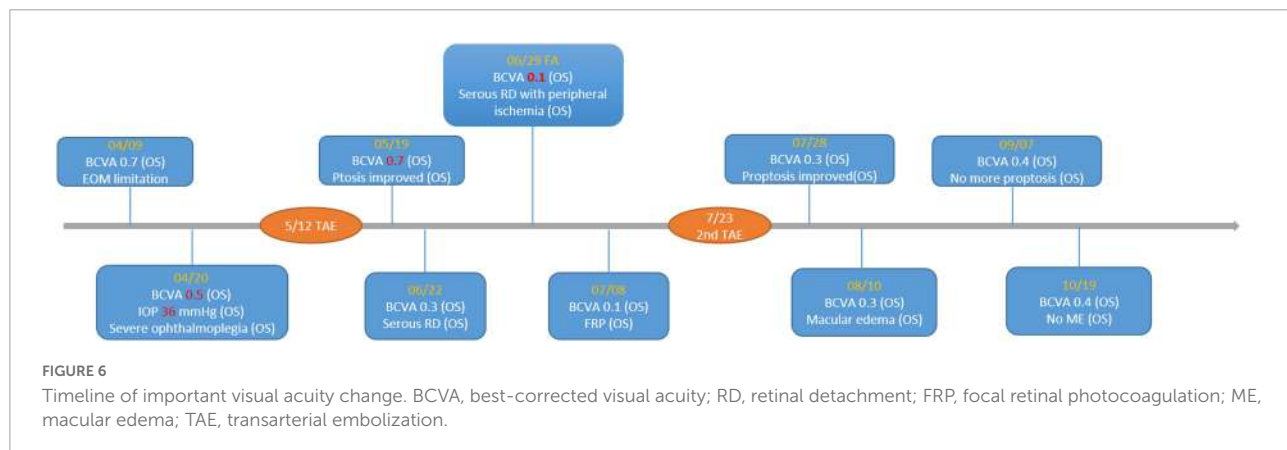
FIGURE 6
Timeline of important visual acuity change. BCVA, best-corrected visual acuity; RD, retinal detachment; FRP, focal retinal photocoagulation; ME, macular edema; TAE, transarterial embolization.

tomographic angiography (CTA) or MRA. However, the definitive diagnostic tool is digital subtraction angiography (DSA), which may be diagnostic and therapeutic (11).

With the development of endovascular interventional techniques, open surgical procedures are no longer preferred. A transarterial approach *via* the ICA is most commonly used. Detachable balloons have been used worldwide in the past for fistula repair. Transarterial balloon placement is accomplished by directing the collapsed balloon through the fistula and into the cavernous sinus, inflating the balloon to a size large enough to completely occlude the fistulous connection, and then releasing the balloon (11, 12). In some countries where balloons have been withdrawn from the market, coiling has replaced them as the endovascular treatment of choice for direct CCFs. A meta-analysis reported high success rates in both transarterial- and transvenous approaches (13).

Despite the high success rate of either transarterial- or transvenous embolization for CCFs, residual ocular symptoms occasionally occur. A patient based review demonstrated that these residual deficits included eye movement deficits, decreased visual acuity and persistent elevated IOP (5, 14). However, ocular ischemic syndrome or even retinopathy were very rare ocular complications following CCFs treated by TAEs. One case report presented a young man with traumatic direct CCF, treated by TAE, who developed ocular ischemic syndrome afterward. Fortunately, this case recovered spontaneously with reversal of the ocular ischemic syndrome and complete recovery of the patient's vision (15).

In our case, when the patient first received TAE, his visual acuity and extraocular movement limitations improved dramatically. Though he still had proptosis and a relative afferent pupil defect in his injured eye, his BCVA improved quickly after the procedure. At that time, the patient was concerned more with recovery of his vision, thus, he could tolerate those residual ophthalmic complications (proptosis and mild chemosis of the conjunctiva). However, when he returned to our department 1 month after the first TAE, he had much more severely congested conjunctiva and more prominent proptosis, but the most important sign was the decline of his vision. Unexpectedly, he developed left eye serous retinal detachment with peripheral choroidal detachment, which probably worsened within a short period. In fact, his vision had decreased in a short time (20/30–20/200) when we performed FA for him (7 days after this visit). The FA and following macular optical coherence tomography (OCT) revealed subretinal fluid with peripheral ischemic syndrome and serous retinal detachment, which was compounded by recurrent CCF due to unsuccessful TAE. Although we did perform focal photocoagulation laser treatment for his ischemic retina, his vision remained poor. It was not until the second TAE was performed that his vision improved. During the second catheter angiography, a leakage site was found in the ICA, whereby the high flow in the ICA from the fistula resulted in clinical

deterioration. Though spontaneous closure of fistulae has been reported in many circumstances, our patient's rapid decline of visual acuity and ocular ischemic syndrome both warranted an emergent procedure. After the second successful TAE with coil treatment, his left eye vision recovered from 20/200 to 20/50. Moreover, his proptosis and congested corkscrew vessels in the conjunctiva recovered gradually. Five months from the second TAE, his BCVA remained 20/50, but he had no more proptosis, and his conjunctiva became normal without diplopia (**Figure 7**). The relative pupillary defect remained positive in his left eye, but the subsequent visual field examination and disk OCT showed no evidence of left eye optic neuropathy. We surmised the relative pupillary defect may have been associated with the sequelae of serous retinal detachment and ocular ischemic syndrome.

Conclusion

Recurrence of ocular symptoms and signs heralds the recurrence of the fistula, and patients in whom manifestations recur require repeated angiography and consideration of further treatment. Persistence or recurrence of symptoms due to venous stasis (proptosis or chemosis) should trigger an early angiographic follow-up because they can be related to the recurrence of the fistula. If the fistula is completely occluded, any preexisting bruit immediately disappears, and intraocular pressure will gradually return to normal. However, the clinical conundrum is whether these symptoms are related to the recurrence or are merely inconsistent with the degree of recovery. Visual decline may predict a poor clinical outcome. Nevertheless, patients with visual impairment or even vision loss caused by retinal damage usually suffer from permanently poor visual function. This is exemplified by our case, who did not have profound visual loss, but whose BCVA remained 20/50 because of transient serous retinal detachment and ocular ischemic syndrome caused by recurrent CCF.

Data availability statement

The original contributions presented in this study are included in the article/supplementary material, further inquiries can be directed to the corresponding author.

Ethics statement

Ethical review and approval was not required for the study on human participants in accordance with the local legislation and institutional requirements. The patients/participants provided their written informed consent to participate in this study. Written informed consent was obtained from the

individual(s) for the publication of any potentially identifiable images or data included in this article.

Author contributions

C-YL and W-JL contributed to the writing the manuscript, literature research, preparation of the manuscript and figures, and responsible for the design. Both authors contributed to the article and approved the submitted version.

Funding

Conflict of interest

The authors declare that the research was conducted in the absence of any commercial or financial relationships that could be construed as a potential conflict of interest.

Publisher's note

All claims expressed in this article are solely those of the authors and do not necessarily represent those of their affiliated organizations, or those of the publisher, the editors and the reviewers. Any product that may be evaluated in this article, or claim that may be made by its manufacturer, is not guaranteed or endorsed by the publisher.

References

1. Parkinson D. A surgical approach to the cavernous portion of the carotid artery. Anatomical studies and case report. *J Neurosurg.* (1965) 23:474–83. doi: 10.3171/jns.1965.23.5.0474

2. Henderson AD, Miller NR. Carotid-cavernous fistula: Current concepts in aetiology, investigation, and management. *Eye.* (2018) 32:164–72.

3. Boyes TL, Ralph FT. Carotid-cavernous fistula. *Am J Ophthalmol.* (1954) 37:262–6.

4. Fattahi TT, Brandt MT, Jenkins WS, Steinberg B. Traumatic carotid-cavernous fistula: Pathophysiology and treatment. *J Craniofac. Surg.* (2003) 14:240–6.

5. Grumann AJ, Boivin-Faure L, Chapot R, Adenis JP, Robert PY. Ophthalmologic outcome of direct and indirect carotid cavernous fistulas. *Int Ophthalmol.* (2012) 32:153–9.

6. Gemmete JJ, Ansari SA, Gandhi DM. Endovascular techniques for treatment of carotid-cavernous fistula. *J Neuroophthalmol.* (2009) 29:62–71.

7. Luo CB, Teng MM, Chang FC, Lin CJ, Guo WY, Chang CY. Transarterial detachable coil embolization of direct carotid-cavernous fistula: Immediate and long-term outcomes. *J Chin Med Assoc.* (2013) 76:31–6. doi: 10.1016/j.jcma.2012.09.007

8. McManus NM, Offman RP, Provatas TL, Sievertsen EE. An eye with a heartbeat: Carotid cavernous fistula-a case report. *J Emerg Med.* (2018) 55:e75–6. doi: 10.1016/j.jemermed.2018.05.015

9. Robert T, Botta D, Blanc R, Fahed R, Ciccio G, Smajda S, et al. Ocular signs caused by dural arteriovenous fistula without involvement of the cavernous sinus: A case series with review of the literature. *AJNR Am J Neuroradiol.* (2016) 37:1870–5. doi: 10.3174/ajnr.A4831

10. Tan AC, Farooqui S, Li X, Tan YL, Cullen J, Lim W, et al. Ocular manifestations and the clinical course of carotid cavernous sinus fistulas in Asian patients. *Orbit.* (2014) 33:45–51. doi: 10.3109/01676830.2013.851253

11. Prasad SN, Singh V, Boruah DK, Phadke RV, Sharma K, Kannaujia V. Endovascular management of direct carotid-cavernous fistula: Evolution of cost effective sandwich technique. *J Neurosci Rural Pract.* (2020) 11:558–64. doi: 10.1055/s-0040-1714447

12. Hou K, Li G, Luan T, Xu K, Yu J. Endovascular treatment of the cavernous sinus dural arteriovenous fistula: Current status and considerations. *Int J Med Sci.* (2020) 17:1121–30. doi: 10.7150/ijms.45210

13. Texakalidis P, Tzoumas A, Xenos D, Rivet DJ, Reavey-Cantwell J. Carotid cavernous fistula (CCF) treatment approaches: A systematic literature review and meta-analysis of transarterial and transvenous embolization for direct and indirect CCFs. *Clin Neurol Neurosurg.* (2021) 204:106601. doi: 10.1016/j.clineuro.2021.106601

14. Kısabay Ak A, Çınar C, Doğan GN, Ataç C, Gökçay F, Çelebisoy N. Clinical improvement in indirect carotid cavernous fistulas treated endovascularly: A patient based review. *Clin Neurol Neurosurg.* (2021) 207:106750. doi: 10.1016/j.clineuro.2021.106750

15. Gunna NT, Paritala A, Takkar B, Sheth J. Ocular ischaemic syndrome following coil embolisation for direct carotid cavernous fistula. *BMJ Case Rep.* (2021) 14:e242121. doi: 10.1136/bcr-2021-242121

Evaluation of retina and microvascular changes in the patient with Parkinson's disease: A systematic review and meta-analysis

Yu Deng, Chuanhong Jie*, Jianwei Wang, Ziqiang Liu, Yuanyuan Li and Xiaoyu Hou

Eye Hospital China Academy of Chinese Medical Sciences, Beijing, China

Background: Parkinson's disease (PD) is a multifaceted neurodegenerative disease. The optic nerve, as a window into the central nervous system (CNS), is known to be an important part of the CNS and can be detected non-invasively. With the widespread availability of optical coherence tomography (OCT) devices, an increasing number of studies have paid attention to the neuropathological disorders in the retina of PD patients in recent years. However, it is still controversial whether OCT can be used as a complementary tool for PD diagnosis.

Methods: This review is registered with PROSPERO, number CRD42022301258. The Embase, PUBMED, and The Cochrane Library databases were independently retrieved by 2 investigators to identify relevant papers published from 1 January 2017 to 24 January 2022. These studies used OCT or OCTA to evaluate the difference in the retinal nerve fiber layer (RNFL) thickness, ganglion cell layer(GCL) thickness, macula thickness, Cup and disk area superficial retinal capillary plexus (SCP), and deep retinal capillary plexus(DCP). The standard mean difference (SMD) with the 95% confidence interval (CI) was pooled for continuous outcomes.

Results: In total, 26 studies had been enrolled in this meta-analysis with a total number of 2,790 eyes, including 1,343 eyes from the PD group along with 1,447 eyes from the HC group. The results revealed that the RNFL thickness (SMD: -0.53; 95%CI, $-0.71\sim-0.35$; $P < 0.00001$), GCL thickness (SMD: -0.43; 95%CI, -0.66 to -0.19; $P = 0.0003$), macula thickness (SMD: -0.22; 95%CI, -0.22 to -0.11; $P < 0.0001$) were significantly thinner in patients with PD. The SCP (SMD: -0.61; 95%CI, -1.31 to -0.10; $P = 0.02$) was significantly lower in PD patients. The DCP (SMD: -0.48; 95%CI, -1.02 to -0.06; $P = 0.08$) is lower in PD patients, but the difference was statistically insignificant.

Conclusion: Retinal nerve fiber layer thickness, GCL thickness, macular thickness, and SVD of PD patients are lower than those of healthy control. OCT and OCTA could detect morphological retinal changes in PD and might be objective and reproducible auxiliary tools to assist clinician diagnosis.

Systematic review registration: [https://www.crd.york.ac.uk/prospero/], identifier [CRD42022301258].

Introduction

Parkinson's disease (PD) is often accompanied by severe degeneration of dopaminergic neurons within the substantia nigra pars compacta (1) and pathological changes such as Lewy body formation (2). The clinical symptoms encompass motor and non-motor symptoms such as dyslexia and diplopia (3). Due to the complexity of the pathological process and clinical manifestations of PD, diagnosis of PD and the assessment methods of its progression mainly rely on the clinician's empirical judgment. However, there is still a lack of diagnostic biological markers (4). Currently, the key challenge is to find a reliable, easily applicable, and well-tolerated diagnostic marker for the diagnosis of PD.

The optic nerve, as part of the CNS (5), has a similar anatomical structure, and physiological characteristics, as well as the same origin of the embryo as the CNS. As the only part of the CNS which can be detected non-invasively, the retina is known as the window into the CNS (6). The structural changes in the retina are the material basis of visual symptoms in PD patients. Results of the post-mortem autopsy showed that PD patients had photoreceptor edema in the retinal plexus layer, loss of retinal ganglion cells (7), decreased retinal dopamine concentration (8), and α –synaptic protein deposition (9). OCT is a non-invasive imaging technique that allows rapid assessment of retinal structural and blood flow changes. Because of its high sensitivity, accuracy, reproducibility, and low cost, it can be used as a potential diagnostic tool for neurodegenerative disorders. However, it is still controversial whether OCT can be used as a biomarker for PD diagnosis. There has been a range of results owing to variations in instruments and research subjects.

Thus, the main purpose of the present systematic review and meta-analysis was to evaluate the difference in the RNFL, macular, GCL, vessel density, and optic disk area between PD patients and health control. The study aimed to provide evidence for the reliability of OCT in the screening and diagnosis of patients with Parkinson's disease.

Materials and methods

Search strategy

This review was registered at PROSPERO (CRD42022301258), and conducted with reference to the Preferred Reporting Items for Systematic Reviews and Meta-Analyses (PRISMA) guidelines (10). EMBASE, PUBMED, the Cochrane library databases were retrieved, while relevant papers were identified from 1 January 2017 to 24 January 2022. Keywords used in the search were "Parkinson's Disease," "Lewy Body Parkinson's Disease," "Lewy Body Parkinson's Disease," Idiopathic Parkinson's Disease," "Paralysis Agitans," "Parkinson's Disease, Idiopathic," "Parkinson's Disease, Idiopathic," "Parkinson's Disease," "Parkinsonism, Primary," "Idiopathic Parkinson's Disease," "Parkinson's Disease, Lewy Body," "Primary Parkinsonism," "Tomography, Optical Coherence," "Tomography, OCT," Optical Coherence Tomography" Coherence Tomography, Optical," "OCT Tomography,". Using Endnote X20 as a preliminary sieve, references were imported and duplicates removed. Furthermore, references from former related articles were collected to make sure a comprehensive search was conducted.

Study selection and extraction

Under the guidance of the PICOS statement (participants, interventions, comparisons, outcomes, and study design), two review authors (DY and LZQ) independently determined study eligibility using a standardized inclusion form. Only articles written in English-language were included. Inclusion criteria consisted of: (1) Original article. (2) All patients were clinically diagnosed with Parkinson's disease and without the medical histories of neither glaucoma, retinal vein obstruction, or other eye diseases. OCT or OCTA was used to observe RNFL thickness as well as other morphological changes. People who matched

the subjects for age, and gender were recruited as the healthy control group (HC). (3) Outcome indicators: RNFL thickness, GCL thickness, macular nerve fiber layer thickness, optic disk area. All measurement data are mean ± standard deviation (ME ± SD). (4) The study must be a randomized controlled trial, cross-sectional study, prospective cohort study, or retrospective cohort study. Exclusion criteria were as follows:(1) unclear research question, undefined study object, (2) basic experiments, case series, case reports, meta-analyses, systematic reviews, and commentaries, (3) unable to extract key information from the literature, (4) no control group or incomplete data, (5) did not match the purpose of this article.

Based on the inclusion and exclusion criteria, each piece of literature was independently screened by 2 reviewers(DY and LZQ)and cross-checked. When meeting disagreement, it is necessary to discuss with another reviewer(WJW)to decide whether or not to include studies. The specific screening steps comprised three steps. Firstly, the reviewers would evaluate whether the title and abstract meet the inclusion and exclusion criteria. Secondly, the full text of the remaining articles would be further screened to evaluate whether they meet the eligibility criteria. Finally, two reviewers would check the literature included with each other. When meeting inconsistencies, another reviewer would resolve this problem and determine the inventory of the literature finally included. The extracted information from each study, including the first author, year of publication, study design type, sample size, the mean age of the patients, outcome,

FIGURE 1
Flow diagram of the study selection process.
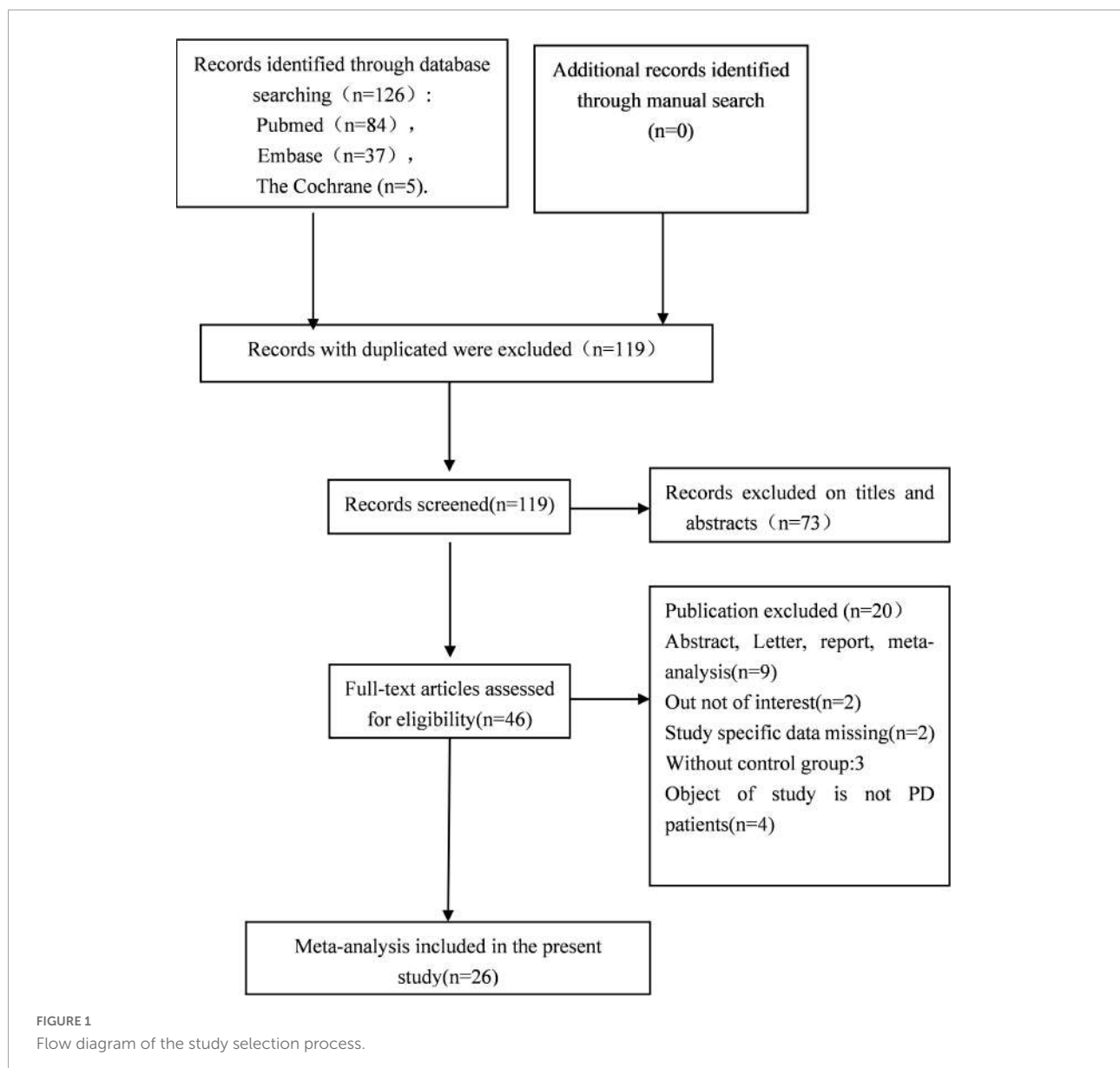
and so on, would be carefully and independently extracted by two reviewers.

Statistical analysis and quality assessment

RevMan version 5.3 software[1] was used to perform the meta-analysis and draw the risk of bias plots. Instead of mean difference (MD), standardized mean difference (SMD) alone with a 95% confidence interval (95%CI) will be used to assess the continuous outcome, because measurement scales of OCT equipment were consistent between studies. $p < 0.05$ indicated a significant difference, on the other hand, testing for heterogeneity among the included studies was evaluated by the chi-square-based Q test and the I^2 statistics. When $P \geq 0.1$ and $I^2 \leq 50\%$, the possibility of heterogeneity was low and the fixed effect model was adopted. When $P < 0.1$ and $I^2 > 50\%$, the possibility of heterogeneity was high, and the random effect model was adopted. Using egger's test to judge publication bias when $P > 0.1$ indicated that there was no publication bias. The Newcastle-Ottawa Scale (NOS) was used to evaluate the quality of the included studies for cohort studies.

Results

The initial search strategy of the four databases retrieved 126 publications in English. A flow diagram of the study selection process is summarized in **Figure 1**, as well as the basic information of the included studies is shown in **Table 1**. A total of 119 articles were obtained after removing the duplicates. After screening the titles and abstracts, there are still 46 articles left. Finally, after reviewing the full text 26 articles initially remained: 1 RCT, 3 cohort studies, and 22 cross-section studies. There are a total number of 1,795 participants with 2,790 eyes (PD for 1,343 eyes and HC for 1,447 eyes) extracted from included studies. The sample size ranged from 19 to 137 PD participants, while the average ages of the participants ranged from 52 to 70.72 years old. All studies explicitly described that no statistically significant difference was found in age or gender between the two groups. The average duration of Parkinson's disease patients ranged from 2.04 to 13.53 years. Out of the 26 studies included in the present meta-analysis, 25 studies explicitly reported the type of the OCT devices, which consisted of Zeiss, Optovue, Heidelberg, Topcon, NIDEK, and VG200. The quality of the included 26 studies was assessed using the Newcastle-Ottawa Scale (NOS) tool, and the quality scores ranged from 7 to 9.

---

1 www.cochrane.org

Retinal nerve fiber layer thickness

In total, 21 studies had been enrolled in this meta-analysis with a total number of 2,094 eyes, including 999 eyes from the PD group, while 1,095 eyes from the HC group (**Figure 2**). First, the heterogeneity test was conducted. The result shows that there was high heterogeneity in the study ($I^2 = 74\%$). After removing articles one by one, the *heterogeneity* remained substantial, therefore a random-effects model was used for the analysis. The results indicated that RNFL thickness in the PD group was significantly thinner than in the HC group (SMD: −0.53; 95%CI, −0.71∼−0.35; $P < 0.00001$). Additionally, the result is consistent with that of the most included studies (11, 13, 16, 17, 19–21, 25–27, 29–31, 33). However, seven studies showed no statistically significant difference in RNFL between PD and HC groups (14, 15, 22–24, 34, 36). Furthermore, the meta-analysis of RNFL thickness in superior, inferior, nasal, and temporal quadrants showed that RNFL thickness in the PD group of all quadrants, especially in superior and inferior quadrants, was thinner than HC group [(RNFL-S: SMD: 0.53; 95%CI, 0.81–0.26; $P = 0.0001$);(RNFL-I: SMD: 0.53; 95%CI, 0.80–0.26; $P = 0.0001$); (RNFL-N: SMD: 0.22; 95%CI, 0.37–0.07; $P = 0.003$);(RNFL-T: SMD:−0.25; 95%CI,−0.45 to −0.06; $P = 0.009$)] (**Table 2**). The Egger test was used to evaluate the publication bias, and the result showed P = 0.2977, indicating no obvious publication bias.

Ganglion cell layer thickness

In total, 11 studies had been enrolled in this meta-analysis with a total number of 1,391 eyes, including 677 eyes from the PD group, while 714 eyes from the HC group (**Figure 3**). First, the heterogeneity test was conducted. The result shows that there was high heterogeneity in the studies ($I^2 = 76\%$). After removing articles one by one, the *heterogeneity* remained substantial, therefor a random-effects model was used for the analysis. The results indicated that GCL thickness in the PD group was significantly thinner than in the HC group (SMD: −0.43; 95%CI, −0.66 to −0.19; $P = 0.0003$). Additionally, the result is consistent with the 4 included studies (16, 21, 23, 30). Nevertheless, seven studies showed no statistically significant difference in GCL between PD and HC groups (11, 14, 20, 22, 28, 34, 36). The Egger test was used to evaluate the publication bias, and the result showed $P = 0.4285$, indicating no obvious publication bias.

Cup and disk area

In total, 2 studies had been enrolled in this meta-analysis with a total number of 144 eyes, including 69 eyes from the PD group, and 75 eyes from the HC group (**Figures 4**, **5**). First, the

TABLE 1 Main characteristics of included studies.

References	Country	Year	Design	Monocular/ Binocular	Group	Sample size (M/F)	Nu of eyes	Age	Mean medical history (Year/ month)	OCT Device	NOS Quality score
Eraslan et al. (11)	Turkey	2016	Cross-section	Binocular	PD	16/9	50	58.64 ± 10.31	53.65 ± 44.13(M)	Zeiss	8
					HC	15/8	46	56.65 ± 9.61	–		
Eraslan et al. (12)	Turkey	2016	Cross-section	Binocular	PD	14/8	44	60.45 ± 9.1	71.41 ± 53.6(M)	Optovue	8
					HC	12/14	50	60.56 ± 9.9	–		
Pilat et al. (13)	Iran	2016	Cross-section	Monocular	PD	19/6	25	60.79 ± 9.24	6.02 ± 1.97(Y)	Optopol	8
					HC	19/6	25	60.58 ± 8.95	–		
Polo et al. (14)	Spain	2016	Cross-section	Monocular	PD	24/14	38	69 (58–74)	13.2 ± 5.77(Y)	Zeiss	8
					HC	24/13	37	68 (60–76)	–		
Satue et al. (15)	Spain	2016	cohort studies	Binocular	PD	17/13	60	69.54 ± 6.6	13.53 ± 6.22(Y)	Heidelberg	8
					HC	17/13	60	68.34 ± 8.45	–		
Ucak et al. (16)	Turkey	2016	Cross-section	Binocular	PD	19/11	58	68.5 ± 7.63	4.87 ± 4.07(Y)	Zeiss	8
					HC	16/14	60	66.23 ± 8.94	–		
Aydin et al. (17)	Turkey	2018	Cross-section	Monocular	PD	17/8	25	70 (50–82)	48(2–192)(M)	Heidelberg	9
					HC	19/10	29	68 (59–78)	–		
Kwapong et al. (18)	China	2018	cohort studies	Monocular	PD	38	49	62.95 ± 7.97	3.84 ± 2.80(Y)	Optovue	8
					HC	28	34	61.18 ± 5.74	–		
Ma et al. (19)	China	2018	Cross-section	Binocular	PD	21/16	74	60.43 ± 8.43	34.95 ± 29.18(M)	Zeiss	7
					HC	23/19	84	57.31 ± 9.54	–		
Matlach et al. (20)	Germany	2018	Cross-section	Binocular	PD	21/9	46	64.1 ± 8.3	9.8 ± 6.9(Y)	Zeiss	8
					HC	18/22	40	64.1 ± 8.2	–		
Moschos et al. (21)	Greece	2018	Cross-section	Monocular	PD	17/14	31	67.8 ± 3.9	–	Heidelberg	9
					HC	14/11	25	68.0 ± 4.1	–		

(Continued)

TABLE 1 (Continued)

References	Country	Year	Design	Monocular/ Binocular	Group	Sample size (M/F)	Nu of eyes	Age	Mean medical history (Year/ month)	OCT Device	NOS Quality score
Satue et al. (22)	Spain	2018	Cross-section	Monocular	PD	35/15	50	70.72 ± 6.20	13.53 ± 6.22(Y)	Topcon	8
					HC	35/19	54	69.57 ± 8.13	–		
Unlu et al. (23)	Turkey	2018	Cross-section	Binocular	PD	15/13	56	59.06 ± 9.41	10.80 ± 6.15(Y)	Heidelberg	8
					HC	15/15	60	60.22 ± 13.41	–		
Visser et al. (24)	Netherlands	2018	Cross-section	Binocular	PD	15/5	39	65 (54–70)	8.0 (4, 15)(Y)	Heidelberg	8
					HC	9/11	39	52 (63–75)	–		
Elkhatib et al. (25)	Egypt	2019	cohort studies	Binocular	PD	10/10	40	63.2 ± 5.50	6.53 ± 3.07(Y)	NIDEK	9
					HC	11/9	40	62.4 ± 6.96	–		
Gulmez Sevim et al. (26)	Turkey	2019	Cross-section	Monocular	PD	20/20	41	59.64 ± 9.94	4(Y)	Heidelberg	7
					HC	19/16	35	59.44 ± 7.59	–		
Hasanov et al. (27)	Turkey	2019	RCT	Binocular	PD	19	38	54.39 ± 5.71	47.21 ± 41.15(M)	Topcon	7
					HC	19	38	55.53 ± 6.48	–		
Murueta-Goyena et al. (28)	Spain	2019	cross section	Binocular	PD	41/22	126	61.91 ± 8.56	8.81 ± 5.15(Y)	Heidelberg	8
					HC	16/18	68	59.79 ± 6.22	–		
Shafiei et al. (29)	Iran	2019	Cross-section	Monocular	PD	18/5	23	61.30 ± 11.57	–	–	8
					HC	18/5	23	61.22 ± 11.39	–		
Sung et al. (30)	Korea	2019	Cross-section	Monocular	PD	25/49	74	65.30 ± 8.38	–	Zeiss	9
					HC	18/35	53	64.68 ± 6.64	–		
Rascuna et al. (31)	Italy	2020	Cross-section	Binocular	PD	12/9	41	59.3 ± 7.0	27.4 ± 14.3(M)	Zeiss	8
					HC	9/8	33	/			
Shi et al. (32)	China	2020	Cross-section	Binocular	PD	12/13	50	61.9 ± 7.6	3.7 ± 2.4(Y)	Optovue	9
					HC	12/13	50	59.0 ± 5.8	–		

(Continued)

155

TABLE 1 (Continued)

References	Country	Year	Design	Monocular/Binocular	Group	Sample size (M/F)	Nu of eyes	Age	Mean medical history (Year/month)	OCT Device	NOS Quality score
Tugcu et al. (33)	Turkey	2020	Cross-section	Binocular	PD	12/9	42	62.48 ± 9.76	5.02 ± 3.25(Y)	Heidelberg	9
					HC	12/10	43	62.41 ± 6.99	–		
Robbins et al. (34)	Singapore	2021	Cross-section	Binocular	PD	39/30	124	71.7 ± 7.0	–	Zeiss	8
					HC	77/60	248	70.9 ± 6.7	–		
Zhang et al. (35)	China	2021	Cross-section	Binocular	PD	45	75	55.92 ± 7.53	2.04 ± 1.23(Y)	VG200	9
					HC	75	150	54.68 ± 6.66			
Zhou et al. (36)	China	2021	Cross-section	Monocular	PD	18/6	24	65.88 ± 6.50	5.3 ± 4.2(Y)	Zeiss	8
					HC	11/12	23	63.43 ± 7.11			

heterogeneity test was conducted. The result shows that there was heterogeneity in the study (I^2 = 49%), so the random-effects model was used for the analysis. The results indicated that there was no statistically significant difference in a cup and disk area among the PD group and the HC group (P = 0.45; P = 0.39).

Macula thickness

In total, 11 studies had been enrolled in this meta-analysis with a total number of 1,346 eyes, including 621 eyes from the PD group, while 725 eyes from the HC group (Figure 6). First, the heterogeneity test was conducted. The result shows that there was no heterogeneity in the study (I^2 = 0%), so the fixed-effects model was used for the analysis. The results indicated that macula thickness in the PD group was significantly reduced compared with the HC group (SMD: −0.22; 95%CI, −0.22 to −0.11; P < 0.0001). Nevertheless, there were only two studies consistent with our finds (30, 34). No statistically significant difference was found between the PD and HC groups in the other nine studies (11, 14, 15, 19, 27, 31, 33, 36). The Egger test was used to evaluate the publication bias, and the result showed P = 0.0688, indicating the existence of publication bias.

Vessel density in superficial retinal capillary plexus

Six studies had been enrolled in this meta-analysis with a total number of 901 eyes, including 363 eyes from the PD group, and 538 eyes from the HC group (Figure 7). First, the heterogeneity test was conducted. The result shows that there was high heterogeneity in the study (I^2 = 91%). After removing articles one by one, the *heterogeneity* remained substantial, therefore the random-effects model was used for the analysis. The results indicated that SCP in the PD group was significantly lower than in the HC group (SMD: −0.61; 95%CI, −1.31 to −0.10; P = 0.02). Furthermore, a meta-analysis of SCP in superior, inferior, nasal, and temporal quadrants showed that SCP in the PD group of all quadrants, especially in nasal quadrants, was significantly lower than in the HC group [(SCP-S: SMD: −0.45; 95%CI, −0.75 to −0.15; P = 0.003);(SCP-I: SMD:−0.59; 95%CI, −1.17 to −0.02; P < 0.0001); (SCP-N: SMD: −0.92; 95%CI, −1.34 to −0.50; P < 0.0001);(SCP-T: SMD:−0.59; 95%CI,−0.79 to −0.40; P < 0.0001) (Table 3). The Egger test was used to evaluate the publication bias, and the result showed P = 0.1397, indicating no obvious publication bias.

Vessel density in deep retinal capillary plexus

Three studies had been enrolled in this meta-analysis with a total number of 482 eyes, including 215 eyes from the PD
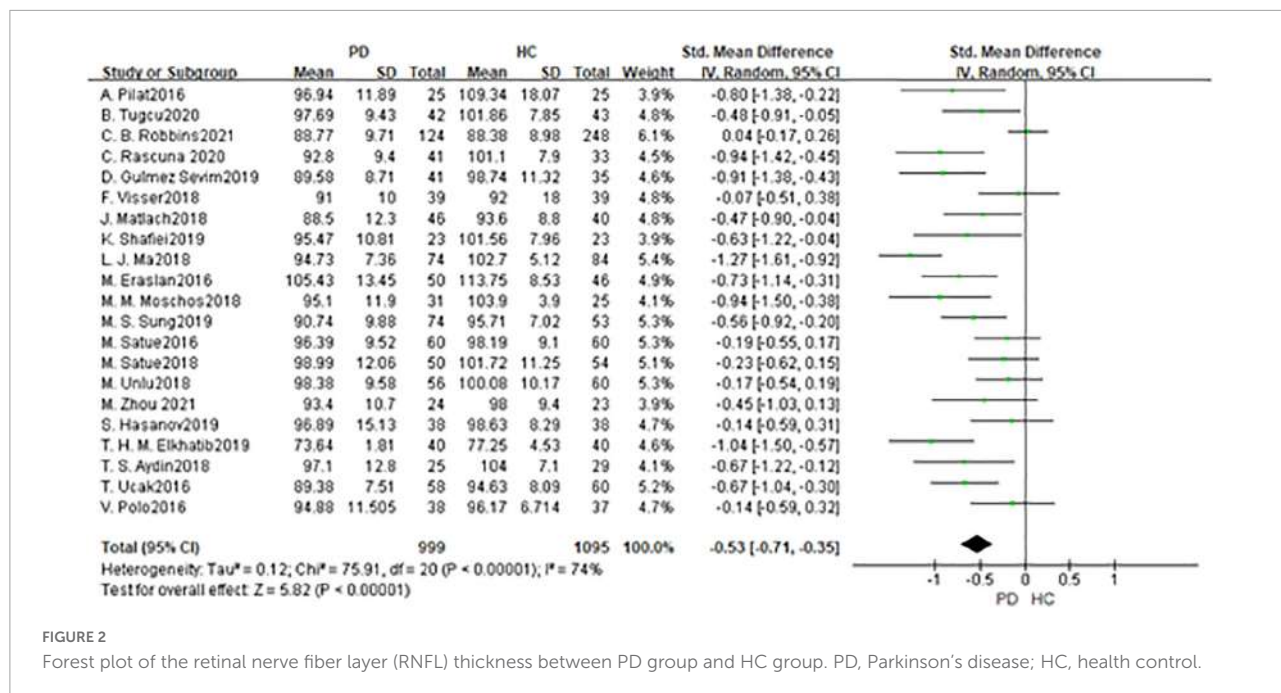
FIGURE 2
Forest plot of the retinal nerve fiber layer (RNFL) thickness between PD group and HC group. PD, Parkinson's disease; HC, health control.

TABLE 2   The results of the meta-analysis of the RNFL thickness in different quadrants.

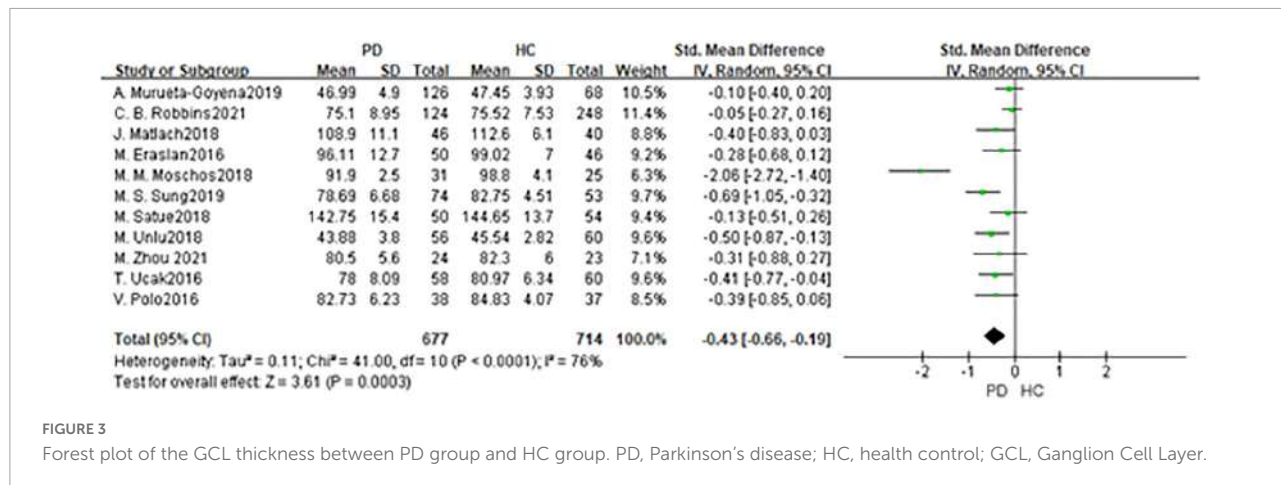|	No of studies	N (PD/HC)	I^2(%)	P	Model	SMD&95%CI	Eggers test
RNFL-S	14	619/594	81%	=0.0001	Random(IV)	−0.53 [−0.81, −0.26]	0.0590
RNFL-I	14	578/561	81%	=0.0001	Random(IV)	−0.53 [−0.80, −0.26]	0.0137
RNFL-N	16	719/710	51%	=0.003	Random(IV)	−0.22[−0.37, −0.07]	0.1811
RNFL-T	15	694/681	69%	=0.009	Random(IV)	−0.25[−0.45, −0.06]	0.2114

FIGURE 3
Forest plot of the GCL thickness between PD group and HC group. PD, Parkinson's disease; HC, health control; GCL, Ganglion Cell Layer.

group, and 267 eyes from the HC group (Figure 8). First, the heterogeneity test was conducted. The result shows that there was heterogeneity in the study (I^2 = 87%). After removing articles one by one, the *heterogeneity* remained substantial, so the random-effects model was used for the analysis. The results indicated that DCP in the PD group was no statistical difference from that in the HC group (SMD: −0.48; 95%CI, −1.02 to −0.06; P = 0.08). Furthermore, the meta-analysis of DCP in superior, inferior, nasal, and temporal quadrants showed that DCP of superior, inferior, and nasal quadrants in the PD group were significantly reduced compared with HC group [(DCP-S: SMD: −0.91; 95%CI, −1.82 to 0.00; P = 0.05);(DCP-I: SMD: −0.75; 95%CI, −1.48 to −0.02; P = 0.04); (DCP-N: SMD: −0.45; 95%CI, −0.88 to −0.01; P = 0.04)] (Table 4). However, there was

FIGURE 4
Forest plot of the disk area between PD group and HC group. PD, Parkinson's disease; HC, health control.
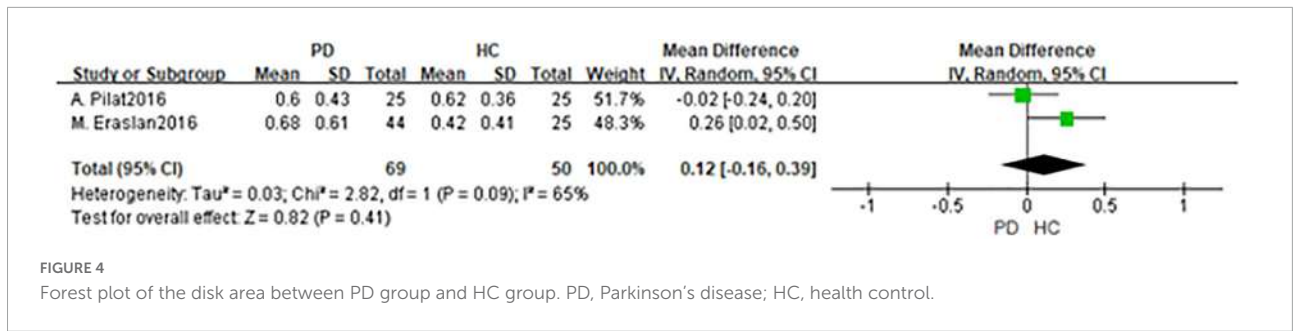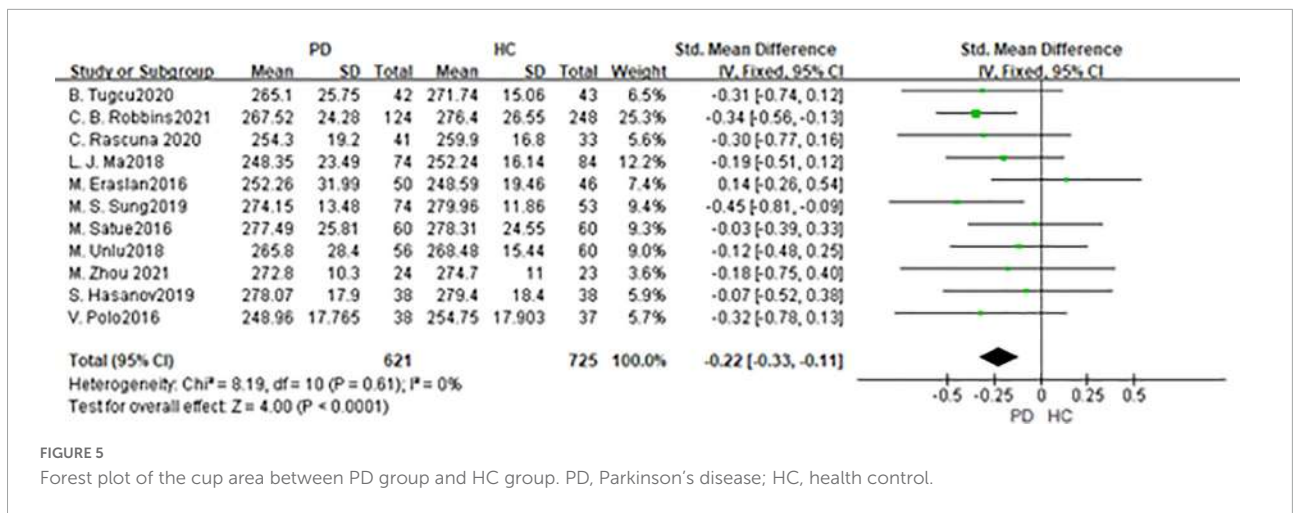

FIGURE 5
Forest plot of the cup area between PD group and HC group. PD, Parkinson's disease; HC, health control.
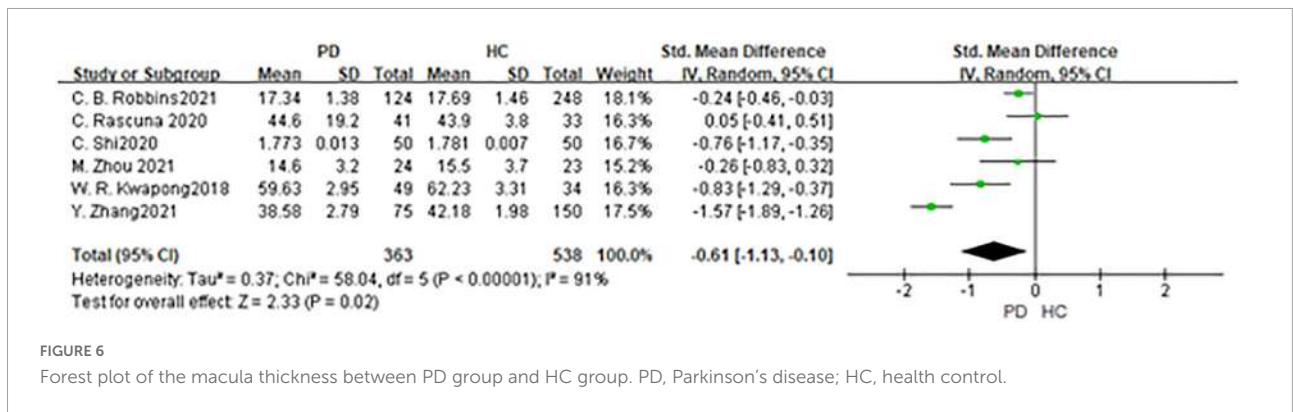

FIGURE 6
Forest plot of the macula thickness between PD group and HC group. PD, Parkinson's disease; HC, health control.
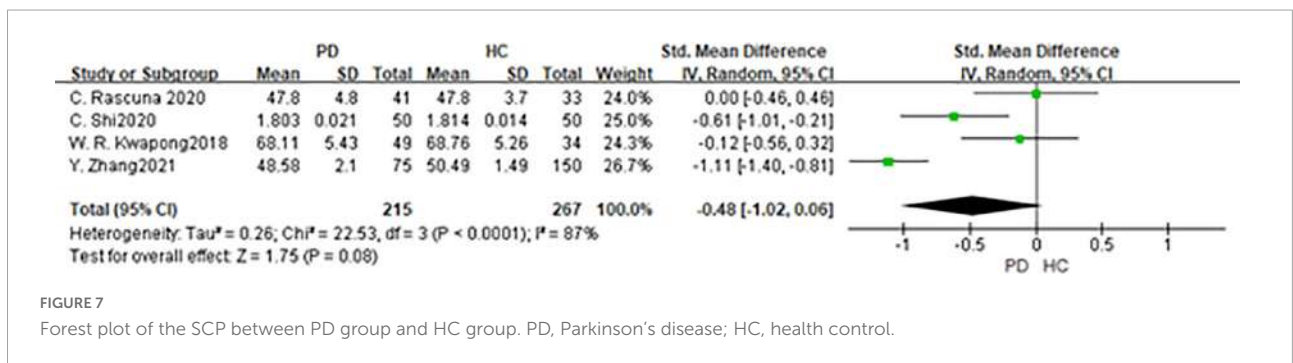

FIGURE 7
Forest plot of the SCP between PD group and HC group. PD, Parkinson's disease; HC, health control.

TABLE 3 The results of the meta-analysis of the SCP in different quadrants.

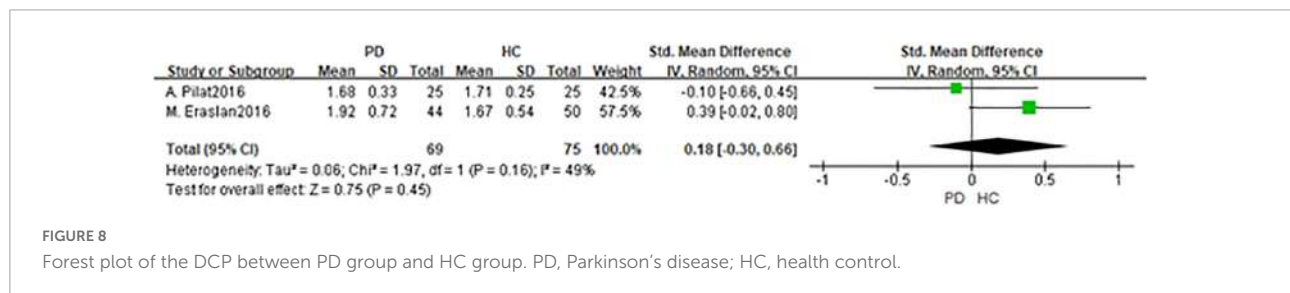|	No of studies	N (PD/HC)	I^2(%)	P	Model	SMD&95%CI	Eggers test
SCP-S	4	239/290	62%	=0.003	Random (IV)	−0.45 [−0.75, −0.15]	0.1654
SCP-I	4	239/290	89%	<0.00001	Random (IV)	−0.59 [−1.17, −0.02]	0.2848
SCP-N	4	198/257	74%	<0.00001	Random (IV)	−0.92 [−1.34, −0.50]	0.1545
SCP-T	4	198/257	0%	<0.00001	Fixed (IV)	−0.59 [−0.79, −0.40]	0.0735

FIGURE 8

Forest plot of the DCP between PD group and HC group. PD, Parkinson's disease; HC, health control.

no statistically significant difference between the PD group and the HC group in the temporal quadrant (DCP-T: SMD:−0.59; 95%CI,−1.28 to 0.10; P = 0.09) (Table 3). The Egger test was used to evaluate the publication bias, and the result showed P = 0.3848, indicating no obvious publication bias.

Discussion

In the present meta-analysis, we directly assessed OCT parameters such as the RNFL thickness, GCL thickness, macula thickness, etc., to evaluate neuropathological changes in PD patients. PD patients are often accompanied by visual symptoms such as visual illusions and minor hallucinations. A post-mortem study revealed that retinal dopamine content was reduced in PD patients (37), and the GCL, inner plexiform layer (IPL) as well as RNFL thinning were also found in PD patients (38). Decreased dopamine secretion and degeneration of retinal dopaminergic neurons are directly related to visual impairment and retinal nerve changes in PD patients (39). The neuropathological disorders in the retina of PD patients have gradually attracted more attention in recent years (40). RNFL thickness thinning in PD patients was first reported in 2004 by Martin et al. (41), they used OCT to demonstrate neuropathological changes in PD patients. Yet, other publications come to varying conclusions.

Aaker et al. (42) reported no significant difference in RNFL thickness among the groups. Robbins et al. (34) reported that RNFL thickness in PD patients was a little bit higher than HC group but there was still no statistical difference. Nevertheless, Satue et al. (43) used OCT to evaluate retinal changes in eyes of PD patients and the results showed that PD led to RNFL, GCL, and macula thinning. Because of the discrepancy between former studies, whether OCT scan was able to identify retinal changes in PD patients and classify patients reliably into the patient group is still controversial.

The present study found that RNFL, GCL, and macula thickness are thinning in PD patients, moreover, OCT can reliably classify the PD patients according to retinal changes. Structural and functional retinal changes, such as thinning in RNFL thickness, have been described in a variety of neurodegenerative diseases like multiple sclerosis and Alzheimer's disease (44), suggesting that retinal degeneration may occur simultaneously with central neurodegenerative changes. Therefore retina has been suggested to be the window to the neuropathological changes of the central nervous system (45). Garcia et al. (46) found that the thickness of RNFL in PD patients was negatively correlated with the severity of PD. Powell et al. (47) found that RNFL gradually became thinner by using an OCT device, and RNFL thickness was negatively correlated with the severity and duration of PD. Thus, using

TABLE 4 The results of the meta-analysis of the DCP in different quadrants.

	No of studies	N (PD/HC)	I^2(%)	P	Model	SMD&95%CI	Eggers test
DCP-S	3	215/267	95%	0.05	Random (IV)	−0.91 [−1.82, 0.00]	0.3738
DCP-I	3	215/267	91%	0.04	Random (IV)	−0.75 [−1.48, −0.02]	0.4211
DCP-N	3	174/234	75%	0.04	Random (IV)	−0.45 [−0.88, −0.01]	0.3848
DCP-T	3	174/234	90%	0.09	Random (IV)	−0.59 [−1.28, 0.10]	0.4795

OCT to monitor dynamic retinal changes of PD patients is of Therefore, monitoring RNFL thickness in PD patients is of great importance in the early diagnosis as well as monitoring the development of the PD patients. Since only 1/10 of the retinal nerves are dopaminergic neurons (48), the loss of dopaminergic neurons has little influence on the thickness of RNFL. That may be the reason for the absence of statistical significance in RNFL changes in some studies. In this study, it was found that the thinning of RNFL was most obvious in the superior and inferior quadrants of PD patients, which may be related to the gradual degeneration of dopaminergic neurons in the retinal ganglion cells and amacrine cells, and eventually leading to the apoptosis of retinal ganglion cells (49). Finally led to the gradual atrophy of the optic nerve. The macula is the most sensitive part of the retina, where more than 50% of the retinal ganglion cells are concentrated. The changes in contrast sensitivity and color vision of PD patients are related to the thinning of GCL in the macula (50). Garcia et al. (46) reported that the GCL thickness of PD patients was negatively correlated with PD severity, while Polo et al. (14) found that GCL thickness was moderately correlated with color vision and contrast sensitivity. The clinical manifestations of PD are complex and varied, meanwhile different patients often suffer from different combinations of motor and non-motor symptoms. At present, there is a lack of reliable and easily detected biological markers (51). On the one hand for complicated PD patients who are unable to undergo lumber puncture pathological diagnosis and cannot be diagnosed and differentiated, OCT can be an important and useful adjunct for early diagnosis. On the other hand, for patients definitively diagnosed with PD, OCT is also an important adjunct to monitoring disease progression. In general, retinal changes play an important role in the progress of PD, on the other hand, OCT scan is a useful adjunct to differentiate people with PD from healthy controls.

As a promising non-invasive technique that can be used for imaging the microvasculature of the retina, optical coherence tomography angiography (OCTA) enables doctors to get a quantitative and rapid characterization of the retinal capillary in different layers (52). OCTA can provide not only structural and functional images of retinal vasculatures without using contrast agents but also better visibility (53). OCTA can detect retinal microvascular abnormalities of superficial and deep layers in patients who have no detectable clinical retinopathy (54). Former studies have shown that the retinal microvascular density decreased in PD patients (18), meanwhile, OCTA can be used as one of the biological indicators for the early diagnosis of PD (55). The SCP and DCP can be measured by OCTA scanning. Robbins et al. (34) found that vessel density (VD) decreased in PD patients, however, no structure changes such as tinning in RNFL were found in their study. Kwapong et al. (18) found that the SCP of PD patients decreased significantly, however, there was no statistically significant difference in

the DCP. Rascuna et al. (31) found there was no significant difference in the SCP among the groups.

There is limited literature on retinal microvascular disorders in patients with PD, by OCTA scanning. As far as we know, this paper is the first systematic review of retinal microvascular density in patients with PD by OCTA scanning. The present study found that the SCP in PD patients was lower than that of the HC group. The result is in good agreement with former studies (18, 32, 34, 36). Additionally, two studies are inconsistent with our finds, Zhou et al. (36) found that the SVD of PD patients was a little bit lower than HC group, but the difference was not statistically significant, Rascuna et al. (31) found that the SVD was slightly higher in PD group, however, the difference was not statistically significant. A further meta-analysis of VD in different quadrants showed that SCP in PD patients in all quadrants was lower than that in the HC group, with the greatest reduction in nasal-SCP, with statistical significance ($P < 0.05$). Inflammation is the key pathogenesis and potential therapeutic target of PD (56); α-synuclein (α-syn), which also called Lewy bodies or Lewy neurites, is the core pathological feature of PD (57). The decreased VD and FAZ perimeter in PD patients are closely related to retinal neuroinflammation and gliosis (34). Ortuno et al. (58) reported retinal α –syn deposition around the retinal artery in mice with PD. Decreased retinal thickness and VD can also be observed in other degenerative neuropathies like multiple sclerosis (59), and the retinal microvascular degenerative pathologies, characterized by abnormal changes in VD, reflect processes of retinal degeneration (34). Compared with RNFL and other indicators, SCP may be an earlier and more sensitive indicator for PD patients (35). OCT in combination with OCTA can improve the diagnostic accuracy of PD (36). Meta-analysis of the DCP indicated that there was no significant difference between PD and HC groups. Further analysis of DCP in each quadrant showed that inferior and nasal DCP were lower than HC group, and the difference was statistically significant ($P < 0.05$), while superior and temporal DCP had no significant difference. DVD is greatly affected by projection artifacts and different OCTA devices are probable to have different OCTA algorithms (60), this could be the reason why the changes in the DCP in PD patients were not obvious.

Accounting for decreased RNFL thickness with advancing age, the average RNFL thickness decreased at a range of 0.4 µm per year (61). There was a large difference in the age between the included studies, for example, the mean age of the study by Eraslan et al. (11) is 10 years older than that reported by Polo et al. (14), while the mean duration was 7 years longer in the study by Eraslan et al. (11). The right and left sides of the brain are asymmetrically affected in PD patients (62), Shriert et al. (63) and Cubo et al. (64) found that there was intraocular asymmetry in macular retina thickness.10 studies of the included 26 studies randomly selected one eye from each patient for the analysis, on the contrary, 16 studies selected two eyes for the analysis. The difference in the selection of eyes might be an important reason for the heterogeneity. It

is worth noting that a single retinal parameter may not be discriminative enough to serve as an independent biomarker with a predefined cutoff value to define disease presence or absence. However, these OCT and OCTA image findings may enhance clinician confidence in the diagnosis of PD when combined with clinical history and other existing tests. There is a need for future long-term studies that characterize the natural history of microvascular and structural changes in retinal tissue across the clinical spectrum of Parkinson's disease. The results of such studies may provide insight into whether they can be used to assess the onset or rapid progression of PD.

However, the following limitations still exist in this study. First, retinal thickness is correlated with retinal dopamine concentrations. It is unclear whether dopaminergic medications have any effect on measurements obtained from OCT or OCTA. As an effective treatment for PD patients, dopaminergic medications are the drug of choice to relieve motor and non-motor symptoms of PD patients. Additionally, a majority of the included studies didn't illustrate whether PD patients take dopaminergic medications, which may lead to bias in the results and consequently affect the accuracy of it. This may be the reason for the differences in the results of different studies. Second, different OCT devices of different manufacturers have different scanning strategies (65) which led to different scanning artifacts (66). Inter-device differences may cause bias in the present meat-analysis. Finally, refractive media opacity may affect the result of VD measured by OCTA (67), most of the included studies don't illustrate whether all participants have clear refractive media. Limited by the existing devices as well as algorithm, the VD of DCP can be disturbed by SCP (68). Further studies must consider these limits (69).

Conclusion

Retinal nerve fiber layer thickness, GCL thickness, macular thickness, and SVD of PD patients are lower than those of healthy control. Serving as supplementary diagnostic tools, OCT and OCTA could detect early morphological retinal changes in PD and might be objective and reproducible auxiliary tools to assist clinician diagnosis. In the future, OCT and OCTA can be used to judge the progression of PD.

Data availability statement

The original contributions presented in this study are included in the article/supplementary material, further inquiries can be directed to the corresponding author.

Author contributions

CJ contributed to the conception and design of the study. JW, ZL, XH, and YL retrieved the articles and organized the database. YD performed the statistical analysis and wrote sections of the manuscript. All authors contributed to manuscript revision, read, and approved the submitted version.

Funding

Conflict of interest

The authors declare that the research was conducted in the absence of any commercial or financial relationships that could be construed as a potential conflict of interest.

Publisher's note

All claims expressed in this article are solely those of the authors and do not necessarily represent those of their affiliated organizations, or those of the publisher, the editors and the reviewers. Any product that may be evaluated in this article, or claim that may be made by its manufacturer, is not guaranteed or endorsed by the publisher.

References

1. Lee A, Gilbert RM. Epidemiology of Parkinson disease. *Neurol Clin.* (2016) 34:955–65. doi: 10.1016/j.ncl.2016.06.012

2. Copeland RL Jr, Leggett YA, Kanaan YM, Taylor RE, Tizabi Y. Neuroprotective effects of nicotine against salsolinol-induced cytotoxicity: implications for Parkinson's disease. *Neurotox Res.* (2005) 8:289–93. doi: 10.1007/BF0303 3982

3. Urwyler P, Nef T, Killen A, Collerton D, Thomas A, Burn D, et al. Visual complaints and visual hallucinations in Parkinson's disease. *Parkinsonism Relat Disord.* (2014) 20:318–22. doi: 10.1016/j.parkreldis.2013.12.009

4. Rizzo G, Copetti M, Arcuti S, Martino D, Fontana A, Logroscino G. Accuracy of clinical diagnosis of Parkinson disease: a systematic review and meta-analysis. *Neurology.* (2016) 86:566–76. doi: 10.1212/WNL.0000000000002350

5. Newman EA. Functional hyperemia and mechanisms of neurovascular coupling in the retinal vasculature. *J Cereb Blood Flow Metab.* (2013) 33:1685–95. doi: 10.1038/jcbfm.2013.145

6. Patton N, Aslam T, Macgillivray T, Pattie A, Deary IJ, Dhillon B. Retinal vascular image analysis as a potential screening tool for cerebrovascular disease: a rationale based on homology between cerebral and retinal microvasculatures. *J Anat.* (2005) 206:319–48. doi: 10.1111/j.1469-7580.2005.00395.x

7. Devos D, Tir M, Maurage CA, Waucquier N, Defebvre L, Defoort-Dhellemmes S, et al. ERG and anatomical abnormalities suggesting retinopathy in dementia with Lewy bodies. *Neurology.* (2005) 65:1107–10. doi: 10.1212/01.wnl.0000178896. 44905.33

8. Tatton WG, Kwan MM, Verrier MC, Seniuk NA, Theriault E. MPTP produces reversible disappearance of tyrosine hydroxylase-containing retinal amacrine cells. *Brain Res.* (1990) 527:21–31. doi: 10.1016/0006-8993(90)91056-m

9. Beach TG, Carew J, Serrano G, Adler CH, Shill HA, Sue LI, et al. Phosphorylated alpha-synuclein-immunoreactive retinal neuronal elements in Parkinson's disease subjects. *Neurosci Lett.* (2014) 571:34–8. doi: 10.1016/j.neulet. 2014.04.027

10. Page MJ, McKenzie JE, Bossuyt PM, Boutron I, Hoffmann TC, Mulrow CD, et al. The PRISMA 2020 statement: an updated guideline for reporting systematic reviews. *BMJ.* (2021) 372:n71. doi: 10.1136/bmj.n71

11. Eraslan M, Balci SY, Cerman E, Temel A, Suer D, Elmaci NT. Comparison of optical coherence tomography findings in patients with primary open-angle glaucoma and Parkinson disease. *J Glaucoma.* (2016) 25:e639–46. doi: 10.1097/IJG. 0000000000000239

12. Eraslan M, Cerman E, Yildiz Balci S, Celiker H, Sahin O, Temel A, et al. The choroid and lamina cribrosa is affected in patients with Parkinson's disease: enhanced depth imaging optical coherence tomography study. *Acta Ophthalmol.* (2016) 94:e68–75. doi: 10.1111/aos.12809

13. Pilat A, McLean RJ, Proudlock FA, Maconachie GD, Sheth V, Rajably YA, et al. In vivo morphology of the optic nerve and retina in patients with Parkinson's disease. *Invest Ophthalmol Vis Sci.* (2016) 57:4420–7. doi: 10.1167/iovs.16-2 0020

14. Polo V, Satue M, Rodrigo MJ, Otin S, Alarcia R, Bambo MP, et al. Visual dysfunction and its correlation with retinal changes in patients with Parkinson's disease: an observational cross-sectional study. *BMJ Open.* (2016) 6:e009658. doi: 10.1136/bmjopen-2015-009658

15. Satue M, Rodrigo MJ, Obis J, Cipres Alastuey M, Vilades E, Garcia-Martin E. Evaluation of progressive visual dysfunction and degeneration of the retinal nerve fiber layer and macular thickness in patients with Parkinson disease. *Acta Ophthalmol.* (2016) 94:350. doi: 10.1167/iovs.16-20460

16. Ucak T, Alagoz A, Cakir B, Celik E, Bozkurt E, Alagoz G. Analysis of the retinal nerve fiber and ganglion cell – Inner plexiform layer by optical coherence tomography in Parkinson's patients. *Parkinsonism Relat Disord.* (2016) 31:59–64. doi: 10.1016/j.parkreldis.2016.07.004

17. Aydin TS, Umit D, Nur OM, Fatih U, Asena K, Nefise OY, et al. Optical coherence tomography findings in Parkinson's disease. *Kaohsiung J Med Sci.* (2018) 34:166–71. doi: 10.1016/j.kjms.2017.11.006

18. Kwapong WR, Ye H, Peng C, Zhuang X, Wang J, Shen M, et al. Retinal microvascular impairment in the early stages of Parkinson's disease. *Invest Ophthalmol Vis Sci.* (2018) 59:4115–22. doi: 10.1167/iovs.17-23230

19. Ma LJ, Xu LL, Mao CJ, Fu YT, Ji XY, Shen Y, et al. Progressive changes in the retinal structure of patients with Parkinson's disease. *J Parkinsons Dis.* (2018) 8:85–92. doi: 10.3233/JPD-171184

20. Matlach J, Wagner M, Malzahn U, Schmidtmann I, Steigerwald F, Musacchio T, et al. Retinal changes in Parkinson's disease and glaucoma. *Parkinsonism Relat Disord.* (2018) 56:41–6. doi: 10.1016/j.parkreldis.2018.06.016

21. Moschos MM, Chatzirallí IP. Evaluation of choroidal and retinal thickness changes in Parkinson's disease using spectral domain optical coherence tomography. *Semin Ophthalmol.* (2018) 33:494–7. doi: 10.1080/08820538.2017. 1307423

22. Satue M, Obis J, Alarcia R, Orduna E, Rodrigo MJ, Vilades E, et al. Retinal and choroidal changes in patients with Parkinson's disease detected by swept-source optical coherence tomography. *Curr Eye Res.* (2018) 43:109–15. doi: 10. 1080/02713683.2017.1370116

23. Unlu M, Gulmez Sevim D, Gultekin M, Karaca C. Correlations among multifocal electroretinography and optical coherence tomography findings in patients with Parkinson's disease. *Neurol Sci.* (2018) 39:533–41. doi: 10.1007/ s10072-018-3244-2

24. Visser F, Vermeer KA, Ghafaryasl B, Vlaar AMM, Apostolov V, van Hellenberg Hubar J, et al. In vivo exploration of retinal nerve fiber layer morphology in Parkinson's disease patients. *J Neural Transm.* (2018) 125:931–6. doi: 10.1007/s00702-018-1872-6

25. Elkhatib THM, Hashim NA, Emad EM, Zein H, El-aidy L. Optical coherence tomography and cognitive dysfunction in Parkinson disease. *Egypt J Neurol Psychiatry Neurosurg.* (2019) 55:52. doi: 10.1186/s41983-019-0097-4

26. Gulmez Sevim D, Unlu M, Sonmez S, Gultekin M, Karaca C, Ozturk Oner A. Retinal vessel diameter obtained by optical coherence tomography is spared in Parkinson's disease. *Int Ophthalmol.* (2019) 39:813–9. doi: 10.1007/s10792-018-0873-7

27. Hasanov S, Demirkilinc Biler E, Acarer A, Akkın C, Colakoglu Z, Uretmen O. Functional and morphological assessment of ocular structures and follow-up of patients with early-stage Parkinson's disease. *Int Ophthalmol.* (2019) 39:1255–62. doi: 10.1007/s10792-018-0934-y

28. Murueta-Goyena A, Del Pino R, Reyero P, Galdós M, Arana B, Lucas-Jiménez O, et al. Parafoveal thinning of inner retina is associated with visual dysfunction in Lewy body diseases. *Mov Disord.* (2019) 34:1315–24. doi: 10.1002/mds.27728

29. Shafiei K, Iranmanesh F, Sharifi A, Saliminiya N, Dehesh T. The retinal nerve fiber layer thickness is related to severity of Parkinson's disease. *J Kerman Univ Med Sci.* (2019) 26:479–87.

30. Sung MS, Choi SM, Kim J, Ha JY, Kim BC, Heo H, et al. Inner retinal thinning as a biomarker for cognitive impairment in de novo Parkinson's disease. *Sci Rep.* (2019) 9:11832. doi: 10.1038/s41598-019-48388-7

31. Rascuna C, Russo A, Terravecchia C, Castellino N, Avitabile T, Bonfiglio V, et al. Retinal thickness and microvascular pattern in early Parkinson's disease. *Front Neurol.* (2020) 11:533375. doi: 10.3389/fneur.2020.533375

32. Shi C, Chen Y, Kwapong WR, Tong Q, Wu S, Zhou Y, et al. Characterization by fractal dimension analysis of the retinal capillary network in Parkinson disease. *Retina.* (2020) 40:1483–91. doi: 10.1097/IAE.0000000000002641

33. Tugcu B, Melikov A, Yildiz GB, Gökcal E, Ercan R, Uysal O, et al. Evaluation of retinal alterations in Parkinson disease and tremor diseases. *Acta Neurol Belg.* (2020) 120:107–13. doi: 10.1007/s13760-019-01228-x

34. Robbins CB, Thompson AC, Bhullar PK, Koo HY, Agrawal R, Soundararajan S, et al. Characterization of retinal microvascular and choroidal structural changes in Parkinson disease. *JAMA Ophthalmol.* (2021) 139:182–8. doi: 10.1001/ jamaophthalmol.2020.5730

35. Zhang Y, Zhang D, Gao Y, Yang L, Tao Y, Xu H, et al. Retinal flow density changes in early-stage parkinson's disease investigated by swept-source optical coherence tomography angiography. *Curr Eye Res.* (2021) 46:1886–91. doi: 10. 1080/02713683.2021.1933054

36. Zhou M, Wu L, Hu Q, Wang C, Ye J, Chen T, et al. Visual impairments are associated with retinal microvascular density in patients with Parkinson's disease. *Front Neurosci.* (2021) 15:718820. doi: 10.3389/fnins.2021.718820

37. Harnois C, Di Paolo T. Decreased dopamine in the retinas of patients with Parkinson's disease. *Invest Ophthalmol Vis Sci.* (1990) 31:2473–5.

38. Chrysou A, Jansonius NM, van Laar T. Retinal layers in Parkinson's disease: a meta-analysis of spectral-domain optical coherence tomography studies. *Parkinsonism Relat Disord.* (2019) 64:40–9. doi: 10.1016/j.parkreldis.2019.04.023

39. Inzelberg R, Ramirez JA, Nisipeanu P, Ophir A. Retinal nerve fiber layer thinning in Parkinson disease. *Vision Res.* (2004) 44:2793–7. doi: 10.1016/j.visres. 2004.06.009

40. Archibald NK, Clarke MP, Mosimann UP, Burn DJ. The retina in Parkinson's disease. *Brain.* (2009) 132(Pt. 5):1128–45.

41. Garcia-Martin E, Satue M, Fuertes I, Otin S, Alarcia R, Herrero R, et al. Ability and reproducibility of Fourier-domain optical coherence tomography to detect retinal nerve fiber layer atrophy in Parkinson's disease. *Ophthalmology.* (2012) 119:2161–7. doi: 10.1016/j.ophtha.2012.05.003

42. Aaker GD, Myung JS, Ehrlich JR, Mohammed M, Henchcliffe C, Kiss S. Detection of retinal changes in Parkinson's disease with spectral-domain optical coherence tomography. *Clin Ophthalmol.* (2010) 4:1427–32. doi: 10.2147/OPTH. S15136

43. Satue M, Garcia-Martin E, Fuertes I, Otin S, Alarcia R, Herrero R, et al. Use of fourier-domain OCT to detect retinal nerve fiber layer degeneration in Parkinson's disease patients. *Eye.* (2013) 27:507–14. doi: 10.1038/eye.2013.4

44. Moreno-Ramos T, Benito-Leon J, Villarejo A, Bermejo-Pareja F. Retinal nerve fiber layer thinning in dementia associated with Parkinson's disease, dementia with Lewy bodies, and Alzheimer's disease. *J Alzheimers Dis.* (2013) 34:659–64. doi: 10.3233/JAD-121975

45. Lampert EJ, Andorra M, Torres-Torres R, Ortiz-Perez S, Llufriu S, Sepulveda M, et al. Color vision impairment in multiple sclerosis points to retinal ganglion cell damage. *J Neurol.* (2015) 262:2491–7. doi: 10.1007/s00415-015-7876-3

46. Garcia-Martin E, Larrosa JM, Polo V, Satue M, Marques ML, Alarcia R, et al. Distribution of retinal layer atrophy in patients with Parkinson disease and association with disease severity and duration. *Am J Ophthalmol.* (2014) 157:470–8. doi: 10.1016/j.ajo.2013.09.028

47. Powell A, Muller AJ, O'Callaghan C, Sourty M, Shine JM, Lewis SJG. Dopamine and functional connectivity in patients with Parkinson's disease and visual hallucinations. *Mov Disord.* (2020) 35:704–5. doi: 10.1002/mds.27995

48. Djamgoz MB, Hankins MW, Hirano J, Archer SN. Neurobiology of retinal dopamine in relation to degenerative states of the tissue. *Vision Res.* (1997) 37:3509–29. doi: 10.1016/S0042-6989(97)00129-6

49. Shin HY, Park HL, Jung KI, Choi JA, Park CK. Glaucoma diagnostic ability of ganglion cell-inner plexiform layer thickness differs according to the location of visual field loss. *Ophthalmology.* (2014) 121:93–9. doi: 10.1016/j.ophtha.2013.06.041

50. Hajee ME, March WF, Lazzaro DR, Wolintz AH, Shrier EM, Glazman S, et al. Inner retinal layer thinning in Parkinson disease. *Arch Ophthalmol.* (2009) 127:737–41. doi: 10.1001/archophthalmol.2009.106

51. Lin CH, Wu RM. Biomarkers of cognitive decline in Parkinson's disease. *Parkinsonism Relat Disord.* (2015) 21:431–43. doi: 10.1016/j.parkreldis.2015.02.010

52. Spaide RF, Fujimoto JG, Waheed NK, Sadda SR, Staurenghi G. Optical coherence tomography angiography. *Prog Retin Eye Res.* (2018) 64:1–55. doi: 10.1016/j.preteyeres.2017.11.003

53. Savastano MC, Federici M, Falsini B, Caporossi A, Minnella AM. Detecting papillary neovascularization in proliferative diabetic retinopathy using optical coherence tomography angiography. *Acta Ophthalmol.* (2018) 96:321–3. doi: 10.1111/aos.13166

54. Copete S, Flores-Moreno I, Montero JA, Duker JS, Ruiz-Moreno JM. Direct comparison of spectral-domain and swept-source OCT in the measurement of choroidal thickness in normal eyes. *Br J Ophthalmol.* (2014) 98:334–8. doi: 10.1136/bjophthalmol-2013-303904

55. Zou J, Liu K, Li F, Xu Y, Shen L, Xu H. Combination of optical coherence tomography (OCT) and OCT angiography increases diagnostic efficacy of Parkinson's disease. *Quant Imaging Med Surg.* (2020) 10:1930–9. doi: 10.21037/qims-20-460

56. Tansey MG, Goldberg MS. Neuroinflammation in Parkinson's disease: its role in neuronal death and implications for therapeutic intervention. *Neurobiol Dis.* (2010) 37:510–8. doi: 10.1016/j.nbd.2009.11.004

57. Braak H, Del Tredici K. Neuropathological staging of brain pathology in sporadic Parkinson's disease: separating the wheat from the chaff. *J Parkinsons Dis.* (2017) 7:S71–85. doi: 10.3233/JPD-179001

58. Ortuno-Lizaran I, Beach TG, Serrano GE, Walker DG, Adler CH, Cuenca N. Phosphorylated alpha-synuclein in the retina is a biomarker of Parkinson's disease pathology severity. *Mov Disord.* (2018) 33:1315–24. doi: 10.1002/mds.27392

59. Gupta VB, Chitranshi N, den Haan J, Mirzaei M, You Y, Lim JK, et al. Retinal changes in Alzheimer's disease- integrated prospects of imaging, functional and molecular advances. *Prog Retin Eye Res.* (2021) 82:100899. doi: 10.1016/j.preteyeres.2020.100899

60. Spaide RF, Fujimoto JG, Waheed NK. Image artifacts in optical coherence tomography angiography. *Retina.* (2015) 35:2163–80. doi: 10.1097/IAE.0000000000000765

61. Alamouti B, Funk J. Retinal thickness decreases with age: an OCT study. *Br J Ophthalmol.* (2003) 87:899–901. doi: 10.1136/bjo.87.7.899

62. Wang J, Yang QX, Sun X, Vesek J, Mosher Z, Vasavada M, et al. MRI evaluation of asymmetry of nigrostriatal damage in the early stage of early-onset Parkinson's disease. *Parkinsonism Relat Disord.* (2015) 21:590–6. doi: 10.1016/j.parkreldis.2015.03.012

63. Shrier EM, Adam CR, Spund B, Glazman S, Bodis-Wollner I. Interocular asymmetry of foveal thickness in Parkinson disease. *J Ophthalmol.* (2012) 2012:728457. doi: 10.1155/2012/728457

64. Cubo E, Tedejo RP, Rodriguez Mendez V, Lopez Pena MJ, Trejo Gabriel YGJM. Retina thickness in Parkinson's disease and essential tremor. *Mov Disord.* (2010) 25:2461–2. doi: 10.1002/mds.23215

65. Xiao H, Liu X, Liao L, Tan K, Ling Y, Zhong Y. Reproducibility of foveal avascular zone and superficial macular retinal vasculature measurements in healthy eyes determined by two different scanning protocols of optical coherence tomography angiography. *Ophthalmic Res.* (2020) 63:244–51. doi: 10.1159/000503071

66. Zhang J, Tang FY, Cheung CY, Chen H. Different effect of media opacity on vessel density measured by different optical coherence tomography angiography algorithms. *Transl Vis Sci Technol.* (2020) 9:19. doi: 10.1167/tvst.9.8.19

67. Yu JJ, Camino A, Liu L, Zhang X, Wang J, Gao SS, et al. Signal strength reduction effects in OCT angiography. *Ophthalmol Retina.* (2019) 3:835–42. doi: 10.1016/j.oret.2019.04.029

68. Gao SS, Jia Y, Liu L, Zhang M, Takusagawa HL, Morrison JC, et al. Compensation for reflectance variation in vessel density quantification by optical coherence tomography angiography. *Invest Ophthalmol Vis Sci.* (2016) 57:4485–92. doi: 10.1167/iovs.16-20080

69. Parrulli S, Corvi F, Cozzi M, Monteduro D, Zicarelli F, Staurenghi G. Microaneurysms visualisation using five different optical coherence tomography angiography devices compared to fluorescein angiography. *Br J Ophthalmol.* (2021) 105:526–30. doi: 10.1136/bjophthalmol-2020-316817

Check for updates

Reduced serum magnesium is associated with the occurrence of diabetic macular edema in patients with diabetic retinopathy: A retrospective study

Xiaoli Xiang[1], Zijia Ji[2], Tingwang Jiang[3], Zhengru Huang[1]* and Jing Yan[4]*

[1]Department of Ophthalmology, The Affiliated Changshu Hospital of Xuzhou Medical University, Changshu, China, [2]Department of Ultrasonography, The Affiliated Changshu Hospital of Xuzhou Medical University, Changshu, China, [3]Department of Key Laboratory, The Affiliated Changshu Hospital of Xuzhou Medical University, Changshu, China, [4]School of Health Service Management, Anhui Medical University, Hefei, China

Serum magnesium levels have been reported to reflect the risk of diabetic retinopathy (DR); however, the effect of serum magnesium level on diabetic macular edema (DME) remains unclear. Here, we investigated the association between the serum magnesium levels and DME in patients with DR. Patients with DR were recruited between January 2018 and June 2021. A total of 519 such patients were included in this study. All patients underwent a standardized clinical ophthalmic examination by an experienced ophthalmologist, and an assay was conducted to determine the serum magnesium concentration. Compared with the non-DME group, the DME group had a higher proportion of insulin use and a higher level of serum ischemia-modified albumin and fasting plasma glucose. The serum magnesium and calcium levels were lower in the DME group than in the non-DME group ($P < 0.05$). Higher magnesium levels were negatively associated with DME after adjustment for relevant covariates. Compared with the participants in the lowest magnesium quartile, those in the fourth quartile showed a significantly lower risk of DME after adjustment [odds ratio (OR), 0.294; 95% confidence interval, 0.153–0.566; $P < 0.0001$]. Considering the potentially different effects of serum magnesium on the development of DME in patients with DR based on age, DR staging and insulin use, stratified analysis was performed by considering these factors. Among insulin-using patients with non-proliferative DR who were < 66 years of age, those in the third and fourth quartile of serum magnesium were less likely to develop DME than those in the lowest quartile of serum magnesium [OR (95% CI), 0.095 (0.014–0.620), 0.057 (0.011–0.305); $P = 0.014, 0.001$]. Overall, a higher serum magnesium level was associated with a lower risk of DME in patients with DR. Furthermore, patients with DR who used insulin were more likely to

develop DME. Long-term studies on oral magnesium supplements are needed to determine whether maintaining the serum magnesium levels in a higher physiological range can reduce the risk of DME in patients with DR.

Introduction

Diabetes is a global health problem with high incidence (1) and can lead to several complications. Diabetic retinopathy (DR) is a unique diabetic microvascular complication that is the main cause of adult vision loss in many countries (2). Diabetic macular edema (DME), a buildup of fluid in the central retina, can occur at various stages of DR. DME is the main cause of central vision loss in patients with diabetes and can affect activities of daily living, such as reading and driving, and severely decrease their quality of life (3). Increased retinal vascular permeability, followed by edema and hard exudate, are the main clinical features (4). The prevalence of DR and DME in patients with diabetes has been reported to be 35.4 and 7.4%, respectively (5).

Serum magnesium levels have been reported to reflect the risk of DR (6). Magnesium is the second largest intracellular cation in the human body, after potassium. It is a cofactor of more than 600 enzymes and an activator of more than 200 enzymes (7). Moreover, magnesium plays a role in many metabolic pathways, including glycolysis, β-oxidation, and insulin signal transduction (8, 9). However, the effect of serum magnesium level on DME remains unclear. Therefore, the purpose of this study was to determine the clinical value of serum magnesium levels in the diagnosis of DME by analyzing the relationship between the serum magnesium levels and DME in patients with DR.

Materials and methods

Study population

This was a single-center retrospective study. A total of 519 patients with type 2 diabetes diagnosed with DR using color fundus imaging or fluorescein angiography who were admitted to the Department of Ophthalmology of the Affiliated Changshu Hospital of Xuzhou Medical University between January 2018 and June 2021 were enrolled in this study.

The exclusion criteria were as follows: (1) a history of eye trauma and eye surgery; (2) macular degeneration, macular anterior membrane, vitreomacular traction syndrome, and other fundus diseases; (3) pregnancy; (4) systemic diseases (neurological diseases; tumors; infections; severe hepatic, cardiac, and renal insufficiency; history of malignant tumors; history of hematology; history of autoimmune diseases; history of malabsorption; history of chronic diarrhea; and history of chronic kidney disease); (5) neuropsychiatric disorders leading to inability to cooperate with the examination; and (6) intake of thiazide diuretics, aminoglycoside antibiotics, amphotericin B, and other drugs that may affect serum magnesium excretion.

This study was approved by the Ethics Committee of the Affiliated Changshu Hospital of Xuzhou Medical University (Changshu, China; approval number: 2019082). All patients provided written informed consent upon admission.

Baseline data collection

Clinical data, including age, sex, history of hypertension, systolic blood pressure, diastolic blood pressure, and use of hypoglycemic drugs, were collected. The height and weight of all patients were measured while being in the standing position at admission. The body mass index was calculated by dividing the weight by the height squared (kg/m^2). Blood pressure was read as the patient's sitting blood pressure measured in a quiet state by a professional nurse at admission. Fasting (> 8 h) blood samples were collected for analysis. Blood (cell) count and serum biochemical variables (i.e., urea, uric acid, calcium, magnesium, ischemia modified albumin, retinol binding protein, fasting blood glucose) were assessed using a conventional automated blood analyzer (AU5800 Series Chemistry Analyzers; Beckman Coulter, Brea, CA, USA).

Definition of diabetic macular edema and ophthalmic examination

Each patient underwent a standardized clinical ophthalmic examination by an experienced fundus surgeon, including a review of ophthalmic history, measurement of visual acuity, and intraocular pressure, slit-lamp examination, and dilated

fundus examination under a slit lamp. Color fundus imaging and optical coherence tomography were performed after pupil dilation, and fluorescein angiography was performed, where necessary. The diagnostic criteria for DR were based on the International Clinical Diabetic Retinopathy Disease Severity Scale (10). DME was defined according to the Early Treatment Diabetic Retinopathy Study report as any retinal thickening or hard exudate within the diameter of a disc in the fovea in the presence of DR features (11). Macular edema was confirmed by optical coherence tomography (Cirrus HD-OCT5000; Carl Zeiss, Jena, Germany) or fluorescein angiography (Spectralis HRA; Heidelberg, Germany).

Statistical analysis

The measurement data were normally distributed, represented by mean ± standard deviation values, and comparisons between the groups were made using the independent-sample t-test. The measurement data were skewness distribution data, represented by quartiles, and the Mann–Whitney U-test was used for intergroup comparison. Categorical variables are expressed as frequency (percentage) and were compared between groups using the χ^2-test. Spearman's rank correlation was used to analyze the correlation between serum magnesium levels and other clinical variables. A strong correlation was defined as a correlation coefficient > 0.4 and a P-value < 0.01. Binary logistic regression models were used to examine the relationship between serum magnesium levels and DME outcome. Variables with a P-value < 0.1 in univariate logistic regression were included in the multivariate logistic regression model. Statistical analyses were performed using SPSS 19.0 statistical software (IBM Corp., Armonk, NY, USA). All tests were two-sided, and statistical significance was set at $P < 0.05$.

Results

Baseline characteristics

In total, 519 patients with DR participated in this study. The patients in the DME group were older than those in the non-DME group. Although the proportion of men in the DME group was higher than that in the non-DME group, the proportion of women was still higher than that of men. Compared to the non-DME group, the DME group had a higher proportion of insulin use to control blood glucose and a higher level of serum ischemia-modified albumin and fasting plasma glucose. The serum magnesium and calcium levels were lower in the DME than in the non-DME group ($P < 0.05$). The clinical characteristics of all patients are listed in Table 1.

Frequency of diabetic macular edema among patients with different serum magnesium levels

The serum magnesium levels of patients were divided into four groups according to the following quartiles: Q1 (≤ 0.78 mmol/L), Q2 (0.78–0.85 mmol/L), Q3 (0.85–0.91 mmol/L), and Q4 (> 0.91 mmol/L), respectively. The incidence of DME in all groups (58.1, 41.5, 41.7, and 26.9%, respectively) decreased with increasing serum magnesium levels. Compared with Q1, groups Q2, Q3, and Q4 showed statistically significant differences ($P = 0.0051$, $P = 0.0121$, $P < 0.0001$, respectively) (Figure 1). There was also a difference in the incidence of DME between the Q2, Q3, and Q4 groups ($P = 0.0180$, $P < 0.0001$, $P = 0.0246$, respectively).

Comparison of risk for diabetic macular edema in patients with different serum magnesium levels

Table 2 shows the results from the univariate binary logistic regression model used to analyze the factors influencing DME, including serum magnesium, serum calcium, age, DR staging,

TABLE 1 Comparison of clinical characteristics between the diabetic macular edema (DME) and non-DME groups.

Variable	Non-DME ($n = 296$)	DME ($n = 223$)	P-value
Age (years)	61.17 ± 9.22	69.85 ± 8.46	<0.0001*
Male, n (%)	102 (45.7%)	144 (48.6%)	<0.0001*
PDR, n (%)	15 (15.1%)	104 (46.6%)	<0.0001*
BMI (kg/m²)	23.82 ± 2.85	23.98 ± 2.99	0.620
Hypertension, n (%)	233 (78.7%)	181 (81.2%)	0.492
SBP (mmHg)	146.26 ± 18.56	145.16 ± 19.97	0.243
DBP (mmHg)	82.87 ± 10.71	82.01 ± 10.55	0.249
Insulin, n (%)	89 (30.1%)	146 (65.5%)	<0.0001*
Laboratory findings			
Urea (mmol/L)	6.96 ± 2.97	7.35 ± 3.18	0.136
UA (μmol/L)	348.77 ± 114.05	345.10 ± 113.13	0.586
IMA (U/mL)	57.15 ± 14.23	58.82 ± 13.25	0.005*
RBP (μg/mL)	50.06 ± 17.65	48.92 ± 22.00	0.324
Calcium (mmol/L)	2.32 ± 0.12	2.30 ± 0.13	0.008*
Magnesium (mmol/L)	0.86 ± 0.14	0.79 ± 0.19	<0.0001*
FPG (mmol/L)	6.88 ± 2.02	7.09 ± 2.64	0.019*
Neutrophil ($\Diamond10^9$/L)	3.79 ± 1.40	3.89 ± 1.43	0.673
Lymphocyte ($\Diamond10^9$/L)	1.49 ± 0.56	1.47 ± 0.52	0.651
Blood platelet ($\Diamond10^9$/L)	171.00 ± 54.59	171.58 ± 54.49	0.466

DME, diabetic macular edema; PDR, proliferative diabetic retinopathy; BMI, body mass index; SBP, systolic blood pressure; DBP, diastolic blood pressure; UA, uric acid; IMA, ischemia modified albumin; RBP, retinol binding protein; FPG, fasting plasma glucose. *$P < 0.05$, significant difference.

FIGURE 1
Prevalence of diabetic macular edema (DME) in patients with diabetic retinopathy stratified by the serum magnesium levels.

TABLE 2   Univariate analysis of factors influencing DME.

Variable	Univariate analysis	
	OR (95% CI)	P-value
Age	0.897 (0.876–0.918)	<0.0001*
Sex	0.890 (0.628–1.261)	0.511
DR staging	16.372 (9.146–29.306)	<0.0001*
BMI	0.981 (0.924–1.041)	0.523
Hypertension	1.165 (0.753–1.802)	0.492
SBP	1.003 (0.994–1.012)	0.521
DBP	1.008 (0.991–1.024)	0.360
Insulin	4.410 (3.042–6.393)	<0.0001*
Laboratory findings		
Urea	1.043 (0.985–1.105)	0.149
UA	1.000 (0.998–1.001)	0.723
IMA	1. 008 (0.994–1.022)	0.247
RBP	0.996 (0.987–1.005)	0.369
Calcium	0.221 (0.057–0.859)	0.029*
Magnesium	0.043 (0.010–0.198)	<0.0001*
FPG	1.040 (0.964–1.121)	0.310
Neutrophil	1.050 (0.929–1.187)	0.434
Lymphocyte	0.939 (0.682–1.292)	0.698
Blood platelet	1.000 (0.997–1.003)	0.905

DME, diabetic macular edema; OR, odds ratio; CI, confidence interval; DR, diabetic retinopathy; BMI, body mass index; SBP, systolic blood pressure; DBP, diastolic blood pressure; UA, uric acid; IMA, ischemia modified albumin; RBP, retinol binding protein; FPG, fasting plasma glucose.
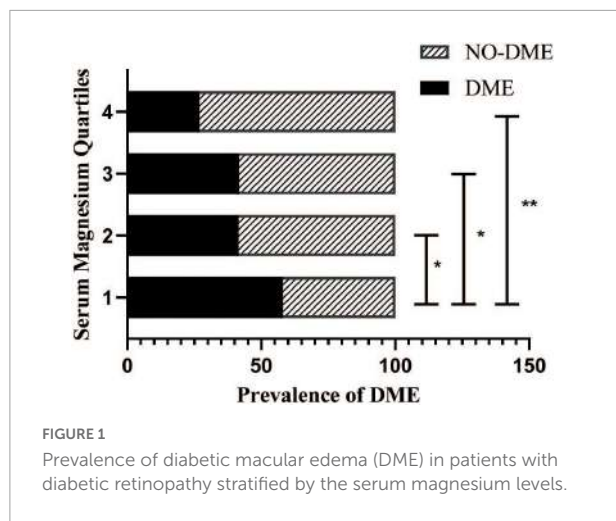*$P < 0.05$, significant difference.

and insulin use, in the multiple binary logistic regression model (Table 3). Multiple regression analysis (Table 3) showed that the serum magnesium levels in Q2 [odds ratio (OR), 0.512; 95% confidence interval (CI), 0.322–0.815], Q3 (OR, 0.515; 95% CI, 0.313–0.848), and Q4 (OR, 0.266; 95% CI, 0.153–0.461) were negatively correlated with the risk of DME compared with the serum magnesium levels in group Q1.

After adjusting for age, DR staging, and insulin use (Model 5), the negative correlation between serum magnesium and DME risk in the Q4 group was still statistically significant (Table 3). Higher serum magnesium levels were associated with a reduced risk of DME in patients with DR (OR, 0.310; 95% CI, 0.153–0.629). Insulin use (OR, 2.643; 95% CI, 1.683–4.152) and DR staging (OR, 9.308; 95% CI, 4.913–17.635) were associated with an increased risk of DME in patients with DR, whereas age was associated with a reduced risk of DME in patients with DR (OR, 0.918; 95% CI, 0.894–0.941).

Subgroup analyses based on age, diabetic retinopathy staging, and insulin

Considering the potentially different effects of serum magnesium on the development of DME in patients with DR based on age, DR staging, and insulin use, stratified analysis was performed based on these factors. Among insulin-using patients with non-proliferative DR who were < 66 years of age, those in the third and fourth quartile of serum magnesium were less likely to develop DME than those in the lowest quartile of serum magnesium [OR (95% CI), 0.095 (0.014–0.620) and 0.057 (0.011–0.305), respectively; $P = 0.014$ and 0.001, respectively].

The serum magnesium level prediction value for diabetic macular edema

As shown in Figure 2, marked Model 4 had the largest area under the curve (0.856; 95% CI, 0.823–0.890; Table 4) and a greater risk prediction value.

Clinical parameters correlated with serum magnesium levels

The serum magnesium levels were positively correlated with age, DR staging and retinol binding protein but negatively with body mass index, systolic blood pressure, diastolic blood pressure, fasting plasma glucose, and neutrophil count (all $P < 0.05$). There was no association between the serum magnesium levels and urea, uric acid, ischemia-modified albumin, calcium, lymphocyte count, platelet count (Table 5).

Discussion

Diabetes is a serious public health concern in China. In 2018, the estimated prevalence of diabetes mellitus in China was 12.4%. Approximately 36.7% of the Chinese adults with diabetes reported being aware of their condition, 32.9% reported

TABLE 3 Multivariate analysis of factors influencing DME.

Quartiles	Model 1		Model 2		Model 3		Model 4		Model 5	
	OR (95% CI)	P-value	OR (95% CI)	P-value	OR (95% CI)	P-value	OR (95% CI)	P-value	OR (95% CI)	P-value
Q1 (≤ 0.78)		<0.0001*		<0.0001*		<0.0001*		0.002*		0.012*
Q2 (0.78–0.85)	0.512 (0.322–0.815)	0.005*	0.526 (0.314–0.882)	0.015*	0.600 (0.349–1.030)	0.013	0.590 (0.343–1.016)	0.057	0.709 (0.396–1.269)	0.247
Q3 (0.85–0.91)	0.515 (0.313–0.848)	0.009*	0.621 (0.358–1.077)	0.090	0.824 (0.463–1.469)	0.104	0.828 (0.464–1.479)	0.523	0.767 (0.410–1.432)	0.405
Q4 (> 0.91)	0.266 (0.153–0.461)	<0.0001*	0.267 (0.144–0.494)	<0.0001*	0.295 (0.154–0.568)	<0.0001*	0.294 (0.153–0.566)	<0.0001*	0.310 (0.153–0.629)	0.001*
Age			0.897 (0.875–0.918)	<0.0001*	0.903 (0.881–0.925)	<0.0001*	0.902 (0.881–0.925)	<0.0001*	0.918 (0.894–0.941)	<0.0001*
Calcium					0.203 (0.045–0.927)	0.040	0.343 (0.072–1.647)	0.182	0.277 (0.052–1.464)	0.131
Insulin							3.449 (2.265–5.252)	<0.0001*	2.643 (1.683–4.152)	<0.0001*
DR staging									9.308 (4.913–17.635)	<0.0001*

DME, diabetic macular edema; OR, odds ratio; CI, confidence interval; DR, diabetic retinopathy. Logistic regression: Model 1, unadjusted for confounding variables; Model 2, adjusted for age; Model 3, adjusted for age and calcium; Model 4, adjusted for age, calcium, and insulin; Model 5, adjusted for age, calcium, insulin, and DR staging.
*$P < 0.05$, significant difference.

receiving treatment, and 50.1% of those receiving treatment had fully controlled disease. Compared with the United States, diabetes awareness, treatment, and control rates are lower in China (12). In many of our patients, diabetes was identified in the ophthalmology clinic after patients presented at the clinic with vision problems. Additionally, several patients with diabetes cannot be evaluated for fundus conditions due to severe cataract at the first ophthalmology visit. Without timely and effective treatment, DME may lead to severe vision loss or even blindness, which will impose a heavy economic burden on families and society. Therefore, timely detection and treatment of DME are important (3).

DME is a complex pathological condition caused by many factors. Retinal thickening in the macular area due to exudate accumulation (extracellular edema) caused by blood-retinal barrier dysfunction is considered the main pathological mechanism of DME (13). Magnesium is one of the major elements required to maintain normal metabolism and ionic balance in ocular tissues (14). A study involving 3,100 patients with diabetes with normal serum magnesium found that the incidence of diabetic retinopathy decreased with the increase of serum magnesium concentration. In patients with normal serum magnesium levels, the serum magnesium levels were negatively associated with the risk of diabetic microvascular complications (15). In another study involving 2,222 patients with diabetes, the authors stratified their serum magnesium levels into quartiles (Q1–Q4) and found that the group with low serum magnesium, Q1 (≤ 0.85 mmol/L), and Q2 (0.85–0.90 mmol/L), had significantly higher incidence rates of DR (50.9 and 30.2%, respectively) than the groups with high serum magnesium, Q3 (0.90–0.96 mmol/L), and Q4 (≥ 0.90 mmol/L) (23.5 and 21%, respectively). Lower serum magnesium levels were reportedly related to an increased risk of developing DR (9). However, the relationship between the serum magnesium levels and DME in patients with DR was not discussed in any of these studies. Our results suggest that within the normal range, higher serum magnesium level is a protective factor against DME in patients with DR, especially for those in non-proliferative DR period, aged < 66 years, who use insulin to control blood glucose.

Magnesium may protect against DME through systemic and local mechanisms. The serum magnesium concentration in normal adults is 0.70–1.10 mmol/L. Approximately 20% of this magnesium is protein bound, 65% is ionized, and the rest is combined with various anions, such as phosphates and citrates (16). Hypomagnesemia occurs in 13.5–47.7% of the patients with type 2 diabetes (17). Insulin resistance could reduce the TRPM6 channel activity of the intestinal
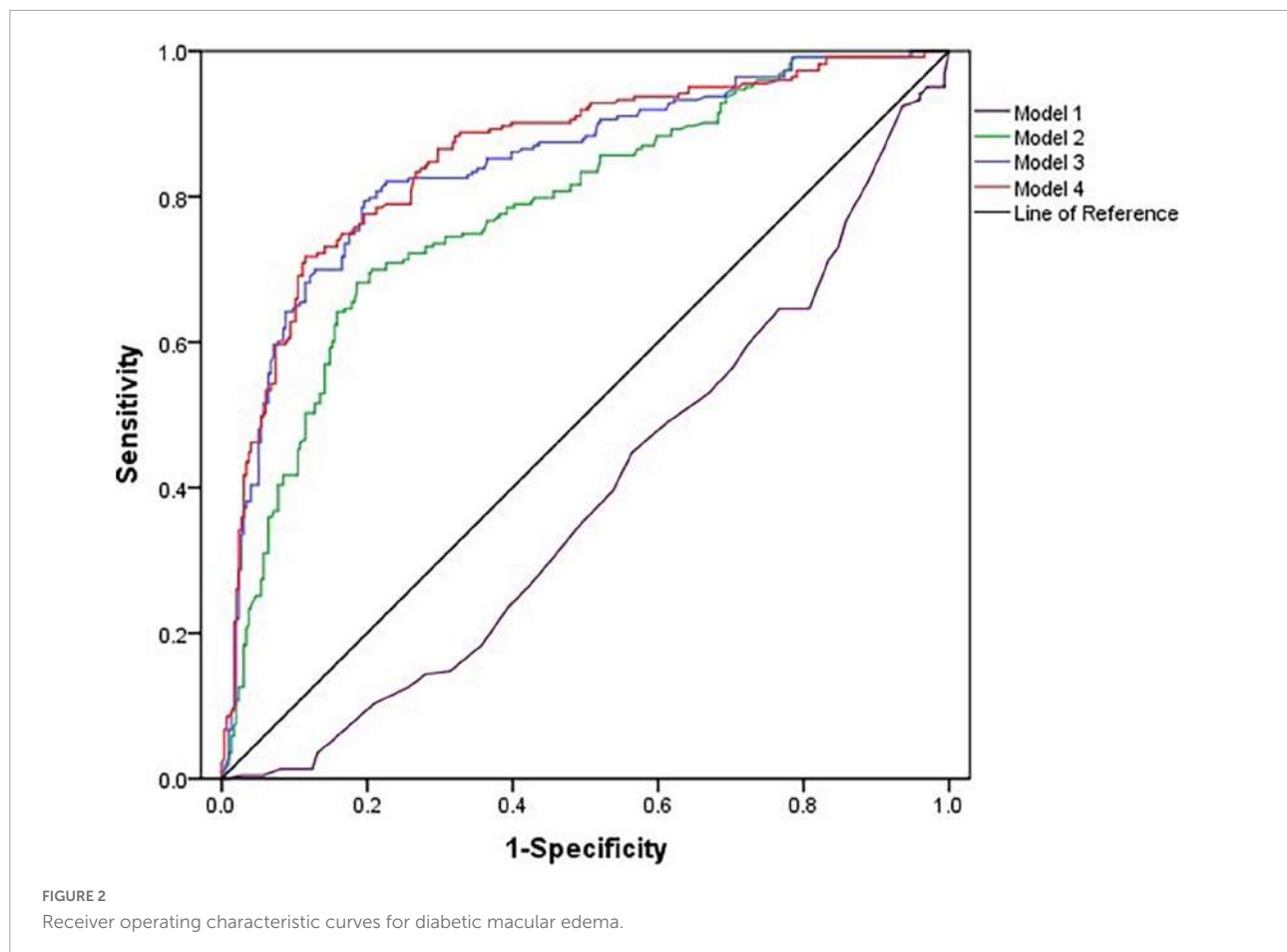
FIGURE 2
Receiver operating characteristic curves for diabetic macular edema.

TABLE 4 The predictive value of serum magnesium alone and combined with age, DR staging, and insulin for the occurrence of DME.

Variables	AUC (95% CI)	Youden index	Sensitivity	Specificity	P-value
Model 1*	0.388 (0.340–0.436)	−0.012	0.924	0.064	<0.0001
Model 2*	0.780 (0.740–0.820)	0.496	0.709	0.760	<0.0001
Model 3*	0.844 (0.808–0.879)	0.598	0.794	0.804	<0.0001
Model 4*	0.856 (0.823–0.890)	0.603	0.717	0.885	<0.0001

DME, diabetic macular edema; DR, diabetic retinopathy; AUC, area under the curve; CI, confidence interval. Model 1, unadjusted; Model 2, Model 1 + age; Model 3, Model 2 + DR Staging; Model 4, Model 3 + insulin.
*$P < 0.05$, significant difference.

and renal tubular epithelium and reduce the absorption of magnesium in the intestinal and renal epithelium, resulting in low serum magnesium (18). Simultaneously, hypomagnesemia can aggravate insulin resistance, and both of them are mutually pathogenic factors (19). Hyperglycemia is a systemic risk factor for DME (3). Magnesium intake reduces oxidative stress responses and improves insulin and glucose metabolism (20, 21). Therefore, patients with DR having high serum magnesium levels may have a reduced occurrence of DME because magnesium improves blood glucose and insulin resistance. Increased oxidative stress levels in the context of low serum magnesium levels may also contribute to DME progression.

Retinal nerve tissue is rich in polyunsaturated fatty acids and has the highest oxygen consumption among all tissues. During magnesium deficiency, insufficient antioxidant enzyme activity can damage membranes rich in lipid peroxidation by free radicals, consequently impairing retinal function (22).

Inflammation is another cause of DME. It has been reported that supplementation with MgO or Mg picolinate has the greatest impact on retinal function as it can improve lipid peroxidation and reduce the expression of pro-inflammatory cytokines, such as intercellular adhesion molecule and vascular endothelial growth factor, by preventing oxidative stress and lipid production (23). Magnesium can reduce retinal oxidative

TABLE 5 Clinical characteristics correlated with the serum magnesium levels.

Related variables	R	P-value
Age (years)	0.126	0.004*
DR staging	0.118	0.007*
BMI (kg/m^2)	−0.123	0.005*
SBP (mmHg)	−0.105	0.017*
DBP (mmHg)	−0.102	0.020*
Urea (mmol/L)	−0.007	0.868
UA (μmol/L)	−0.007	0.873
IMA (U/mL)	0.011	0.796
RBP (μg/mL)	0.092	0.036*
Calcium (mmol/L)	0.019	0.664
FPG (mmol/L)	−0.140	0.001*
Neutrophil (◇10^9/L)	−0.121	0.006*
Lymphocyte (◇10^9/L)	0.014	0.751
Platelet (◇10^9/L)	−0.078	0.077

DR, diabetic retinopathy; BMI, body mass index; SBP, systolic blood pressure; DBP, diastolic blood pressure; UA, uric acid; IMA, ischemia modified albumin; RBP, retinol binding protein; FPG, fasting plasma glucose.
*$P < 0.05$, significant difference.

stress and neuronal inflammation (22). However, deficiency in magnesium causes systemic and local inflammatory states that may predispose patients with DR to DME.

Moreover, magnesium has been shown to protect against heart failure in patients with type 2 diabetes. This protective effect is mediated, in part, by factors, such as the control of blood sugar by magnesium and the reduction of endothelial inflammation (24). Oral magnesium supplementation can improve vascular endothelial function and reduce vascular endothelial inflammation (25, 26). Destruction of retinal vascular endothelial cells is considered to be the initial cause of DME (13). Therefore, decreased serum magnesium levels may lead to the aggravation of retinal vascular endothelial inflammation, resulting in endothelial dysfunction and increased permeability, which may make patients with DR more prone to DME. In addition, hypomagnesemia causes an imbalance between vasoconstriction and dilation (24). Retinal vasospasm caused by magnesium deficiency leads to retinal ischemia and hypoxia, which further accelerate retinal damage (22).

Our data also suggest that insulin-treated patients with DR are at a higher risk of developing DME. Many people with type 2 diabetes require insulin therapy because of the gradual loss of islet beta cell function. Insulin use may also increase the risk of DR and DME in some patients (27). Among more than 300 patients treated with insulin, a 100% increased risk of DME was reported in those treated with insulin compared with those treated with oral medications (27). In addition, some studies have found that the macular thickness of patients with type 2 diabetes treated with insulin

was higher than that of people in the control group (28). Possible mechanisms of action include the upregulation of vascular endothelial growth factor expression, vascular activity of insulin itself, sudden improvement in glycemic control, and further damage to the already-impaired blood-retinal barrier (4). Insulin can also disrupt the tight junctions of retinal pigment epithelial cells by disrupting the outer barrier (29). Hypomagnesemia among diabetic patients was associated with diabetic retinopathy (30), and a decreased level of serum magnesium was associated with an increase in macular thickness and ellipsoid zone disruption in DME (31). However, the correlation between serum magnesium, DME, and insulin use was not discussed. Interestingly, in our data, elevated serum magnesium reduced the risk of DME in patients with non-proliferative DR aged < 66 years who were treated with insulin, but not in other age groups or in patients who were not treated with insulin. This may be related to the fact that in some of our patients, diabetes was discovered only after the first diagnosis in ophthalmology because of vision problems, and no standardized endocrine therapy had been previously performed. Nevertheless, in multiple quadratic regression, our data elucidated that the risk of DME was reduced in the highest quartile of serum magnesium compared with the lowest quartile, suggesting that maintaining adequate magnesium levels may reduce the risk of DME in patients with DR. Our results highlight the need for interventional studies to assess whether magnesium supplementation reduces the risk of DME in patients with DR.

However, our study had some limitations. First, this was a retrospective study, and further prospective studies are needed to investigate the association between the serum magnesium levels and microvascular complications in patients with diabetes. In this retrospective study, we investigated the serum magnesium levels in patients with DR, and the assessment of the systemic magnesium status was incomplete. Second, some of the enrolled patients did not know their specific diabetes history. Third, selection bias may have existed. Most patients in this study were residents of Changshu, China; therefore, caution should be exercised when applying the conclusions of this study to other patient groups. Prospective multicenter studies are needed to validate magnesium as a predictor of DME risk.

Conclusion

The higher the serum magnesium level, the lower the risk of DME in patients with DR. Furthermore, patients with DR who use insulin are more likely to develop DME. Long-term studies on oral magnesium supplements are needed to determine whether maintaining the serum magnesium levels within the physiological range can reduce the risk of DME in patients with DR.

Data availability statement

Ethics statement

The studies involving human participants were reviewed and approved by the Institutional Review Board of the Affiliated Changshu Hospital of Xuzhou Medical University (Changshu, China). The patients/participants provided their written informed consent to participate in this study.

Author contributions

XX: conception and design, data analysis and interpretation, and manuscript writing. ZJ and TJ: data collection and collation. ZH and JY: data interpretation and final review of the manuscript. All authors revised and approved the submitted manuscript.

Funding

Conflict of interest

The authors declare that the research was conducted in the absence of any commercial or financial relationships that could be construed as a potential conflict of interest.

Publisher's note

All claims expressed in this article are solely those of the authors and do not necessarily represent those of their affiliated organizations, or those of the publisher, the editors and the reviewers. Any product that may be evaluated in this article, or claim that may be made by its manufacturer, is not guaranteed or endorsed by the publisher.

References

1. Shaw JE, Sicree RA, Zimmet PZ. Global estimates of the prevalence of diabetes for 2010 and 2030. *Diabetes Res Clin Pract.* (2010) 87:4–14. doi: 10.1016/j.diabres.2009.10.007

2. Wong TY, Cheung CM, Larsen M, Sharma S, Simó R. Diabetic retinopathy. *Nat Rev Dis Primers.* (2016) 2:16012. doi: 10.1038/nrdp.2016.12

3. Diep TM, Tsui I. Risk factors associated with diabetic macular edema. *Diabetes Res Clin Pract.* (2013) 100:298–305. doi: 10.1016/j.diabres.2013.01.011

4. Matsuda S, Tam T, Singh RP, Kaiser PK, Petkovsek D, Zanella MT, et al. Impact of insulin treatment in diabetic macular edema therapy in type 2 diabetes. *Can J Diabetes.* (2015) 39:73–7. doi: 10.1016/j.jcjd.2014.06.005

5. Yau JW, Rogers SL, Kawasaki R, Lamoureux EL, Kowalski JW, Bek T, et al. Meta-analysis for eye disease (META-EYE) study group. Global prevalence and major risk factors of diabetic retinopathy. *Diabetes Care.* (2012) 35:556–64. doi: 10.2337/dc11-1909

6. Xing B, Xu X, Li C, Zhao Y, Wang Y, Zhao W. Reduced serum magnesium levels are associated with the occurrence of retinopathy in patients with type 2 diabetes mellitus: a retrospective study. *Biol Trace Elem Res.* (2021) 200:2025–32. doi: 10.1007/s12011-021-02824-w

7. de Baaij JH, Hoenderop JG, Bindels RJ. Magnesium in man: implications for health and disease. *Physiol Rev.* (2015) 95:1–46. doi: 10.1152/physrev.00012.2014

8. Pham PC, Pham PM, Pham SV, Miller JM, Pham PT. Hypomagnesemia in patients with type 2 diabetes. *Clin J Am Soc Nephrol.* (2007) 2:366–73. doi: 10.2215/CJN.02960906

9. Chutia H, Lynrah KG. Association of serum magnesium deficiency with insulin resistance in type 2 diabetes mellitus. *J Lab Physicians.* (2015) 7:75–8. doi: 10.4103/0974-2727.163131

10. Wilkinson CP, Ferris FL III, Klein RE, Lee PP, Agardh CD, Davis M, et al. Proposed international clinical diabetic retinopathy and diabetic macular edema disease severity scales. *Ophthalmology.* (2003) 110:1677–82. doi: 10.1016/S0161-6420(03)00475-5

11. Kinyoun J, Barton F, Fisher M, Hubbard L, Aiello L, Ferris F III. Detection of diabetic macular edema. Ophthalmoscopy versus photography–early treatment diabetic retinopathy study report number 5. The ETDRS research group. *Ophthalmology.* (1989) 96:746–50. doi: 10.1016/s0161-6420(89)32814-4

12. Wang L, Peng W, Zhao Z, Zhang M, Shi Z, Song Z, et al. Prevalence and treatment of diabetes in China, 2013-2018. *JAMA.* (2021) 326:2498–506.

13. Zhang X, Bao S, Lai D, Rapkins RW, Gillies MC. Intravitreal triamcinolone acetonide inhibits breakdown of the blood-retinal barrier through differential regulation of VEGF-A and its receptors in early diabetic rat retinas. *Diabetes.* (2008) 57:1026–33. doi: 10.2337/db07-0982

14. Kamińska A, Romano GL, Rejdak R, Zweifel S, Fiedorowicz M, Rejdak M, et al. Influence of trace elements on neurodegenerative diseases of the eye-the glaucoma model. *Int J Mol Sci.* (2021) 22:4323. doi: 10.3390/ijms22094323

15. Lu J, Gu Y, Guo M, Chen P, Wang H, Yu X. Serum magnesium concentration is inversely associated with albuminuria and retinopathy among patients with diabetes. *J Diabetes Res.* (2016) 2016:1260141. doi: 10.1155/2016/1260141

16. Saris NE, Mervaala E, Karppanen H, Khawaja JA, Lewenstam A. Magnesium. An update on physiological, clinical and analytical aspects. *Clin Chim Acta.* (2000) 294:1–26. doi: 10.1016/s0009-8981(99)00258-2

17. Gommers LM, Hoenderop JG, Bindels RJ, de Baaij JH. Hypomagnesemia in type 2 diabetes: a vicious circle?. *Diabetes.* (2016) 65:3–13. doi: 10.2337/db15-1028

18. Schlingmann KP, Weber S, Peters M, Niemann Nejsum L, Vitzthum H, Klingel K, et al. Hypomagnesemia with secondary hypocalcemia is caused by mutations in TRPM6, a new member of the TRPM gene family. *Nat Genet.* (2002) 31:166–70. doi: 10.1038/ng889

19. Kostov K. Effects of magnesium deficiency on mechanisms of insulin resistance in type 2 diabetes: focusing on the processes of insulin secretion and signaling. *Int J Mol Sci.* (2019) 20:1351. doi: 10.3390/ijms20061351

20. Castellanos-Gutiérrez A, Sánchez-Pimienta TG, Carriquiry A, da Costa THM, Ariza AC. Higher dietary magnesium intake is associated with lower body mass index, waist circumference and serum glucose in Mexican adults. *Nutr J.* (2018) 17:114. doi: 10.1186/s12937-018-0422-2

21. Jeong JW, Lee B, Kim DH, Jeong HO, Moon KM, Kim MJ, et al. Mechanism of action of magnesium lithospermate B against aging and obesity-induced ER stress, insulin resistance, and inflammsome formation in the liver. *Molecules.* (2018) 23:2098. doi: 10.3390/molecules23092098

22. Agarwal R, Iezhitsa L, Agarwal P. Pathogenetic role of magnesium deficiency in ophthalmic diseases. *Biometals.* (2013). [Epub ahead of print]. doi: 10.1007/s10534-013-9684-5

23. Orhan C, Er B, Deeh PBD, Bilgic AA, Ojalvo SP, Komorowski JR, et al. Different sources of dietary magnesium supplementation reduces oxidative stress by regulation Nrf2 and NF-κB signaling pathways in high-fat diet rats. *Biol Trace Elem Res.* (2021) 199:4162–70. doi: 10.1007/s12011-020-02 526-9

24. Oost LJ, van der Heijden AAWA, Vermeulen EA, Bos C, Elders PJM, Slieker RC, et al. Serum magnesium is inversely associated with heart failure, atrial fibrillation, and microvascular complications in type 2 diabetes. *Diabetes Care.* (2021) 44:1757–65. doi: 10.2337/dc21-0236

25. Darooghegi Mofrad M, Djafarian K, Mozaffari H, Shab-Bidar S. Effect of magnesium supplementation on endothelial function: a systematic review and meta-analysis of randomized controlled trials. *Atherosclerosis.* (2018) 273:98–105. doi: 10.1016/j.atherosclerosis.2018.04.020

26. Shechter M, Sharir M, Labrador MJ, Forrester J, Silver B, Bairey Merz CN. Oral magnesium therapy improves endothelial function in patients with coronary artery disease. *Circulation.* (2000) 102:2353–8. doi: 10.1161/01.cir.102.19. 2353

27. Henricsson M, Nilsson A, Janzon L, Groop L. The effect of glycaemic control and the introduction of insulin therapy on retinopathy in non-insulin-dependent diabetes mellitus. *Diabet Med.* (1997) 14:123–31. doi: 10.1002/(SICI) 1096-9136(199702)14:23.0.CO;2-U

28. Zapata MA, Badal J, Fonollosa A, Boixadera A, García-Arumí J. Insulin resistance and diabetic macular oedema in type 2 diabetes mellitus. *Br J Ophthalmol.* (2010) 94:1230–2. doi: 10.1136/bjo.2009.171702

29. Sugimoto M, Cutler A, Shen B, Moss SE, Iyengar SK, Klein R, et al. Inhibition of EGF signaling protects the diabetic retina from insulin-induced vascular leakage. *Am J Pathol.* (2013) 183:987–95. doi: 10.1016/j.ajpath.2013.05.017

30. Hamdan HZ, Nasser NM, Adam AM, Saleem MA, Elamin MI. Serum magnesium, iron and ferritin levels in patients with diabetic retinopathy attending Makkah Eye Complex, Khartoum, Sudan. *Biol Trace Elem Res.* (2015) 165:30–4. doi: 10.1007/s12011-015-0236-4

31. Ankita, Saxena, S, Ahmad MK, Nim DK, Mahdi AA, Kaur A, et al. Higher levels of serum ionic calcium are associated with macular edema in patients with diabetic retinopathy. *Clin Lab.* (2022) 68. doi: 10.7754/Clin.Lab.2021.210505

Check for updates

Case report: Findings of automated perimetry during a migraine episode in a patient with glaucoma

Shunsuke Nakakura[1]*, Satomi Oogi[1], Asaya Tanoue[2] and Teruyuki Miyoshi[2]

[1]Department of Ophthalmology, Saneikai Tsukazaki Hospital, Himeji, Japan, [2]Miyoshi Eye Clinic, Department of Ophthalmology, Fukuyama, Japan

Comorbidities like glaucoma and migraine are often observed among middle-aged individuals, especially women. Herein, we report a rare case of a patient who underwent automated perimetry during a migraine attack. A 52-year-old woman with a 1-year history of blurred vision in the nasal field of her right eye visited Miyoshi Eye Clinic. The intraocular pressures of the right and left eyes were 22 and 24 mm Hg, respectively. Retinal imaging revealed a retinal nerve fiber defect in the temporal superior macula with corresponding thinning of the superior ganglion cell complex in the right eye. The left eye appeared normal. Primary open-angle glaucoma was suspected, and the patient underwent a visual field examination on the same day. Perimetry showed that the mean deviations in the right and left eyes were -5.00 and -7.68 dB, respectively. A visual field defect in the inferior nasal aspect of the right eye corresponded to the retinal nerve fiber defect. However, right-sided homonymous hemianopia−like visual field defects were observed in both eyes. After the examination, the patient stated that a migraine attack had started 5 min before the examination and continued till after its end (attack duration was ~20 min). In the follow-up examinations without migraine, homonymous hemianopia-like visual field defects disappeared, and only a glaucomatous visual field defect in the right eye was observed. Hence, the initial visual field examination findings reflected the effects of a migraine attack alongside glaucoma. Detailed interviews with patients may be beneficial for understanding visual field findings and preventing their untimely examination.

Introduction

Migraine, a common neurological headache disorder, affects 10–15% of individuals worldwide, especially those of working age (1). Typical migraines are characterized by headache; nausea, vomiting, or both; photophobia and phonophobia; and mild blurring of vision (2). Glaucoma is also a common ocular disease whose prevalence increases with age. In 2020, glaucoma was responsible for 11% of all cases of blindness globally in adults aged ≥ 50 years (3). Some studies (4–6) have suggested that migraine increases the risk of developing glaucoma. However, there have been studies reporting no such findings (7, 8). Hence, the relationship between migraine and glaucoma is yet to be fully clarified. Visual field defects are characteristic of glaucoma and are also experienced by patients with migraine (9–17); furthermore, migraine and glaucoma often present as comorbidities. Here we report a case of primary open-angle glaucoma wherein automated perimetry during a migraine episode revealed unique visual field defects.

Case description

This case report was approved by the Institutional Review Board of Saneikai Tsukazaki Hospital, Himeji, Japan (No. 221002). All examinations were conducted according to the Declaration of Helsinki.

A 52-year-old woman visited Miyoshi Eye Clinic in Fukuyama, Japan, with complaints of blurred vision in the nasal field of her right eye persisting for 1 year. Visual acuities and intraocular pressures (according to Goldmann applanation tonometry) in the right and left eyes of the patient were 0.2 (1.0 × S−2.25D) and 0.2 (1.0 × S−2.75D) and 22 and 24 mm Hg, respectively.

Slit-lamp examination revealed no inflammation in both eyes, which exhibited normal anterior chamber depth. A Mirante Scanning Laser Ophthalmoscope (Nideck Co., Gamagori, Japan) was employed to capture retinal photographs. Additionally, the RS-3000 system of optical coherence tomography (Nideck Co.) was used to measure the thickness of the macular ganglion cell complex (Figure 1). The color image of the right eye revealed a defect of the retinal nerve fiber layer and a corresponding notch sign in the superior optic disk. Moreover, optical coherence tomography demonstrated thinning of the macular ganglion cell complex in the temporal superior aspect (Figure 1, left panel). The left eye of the patient exhibited no apparent glaucomatous alterations (Figure 1, right panel). The findings of the right eye indicated primary open-angle glaucoma, and a visual field examination using a Humphrey field analyzer (HFA; Carl Zeiss Meditec AG, Dublin, CA; 30-2 Swedish Interactive Threshold Algorithm standard) was performed on the same day. HFA was conducted from the right to the left eye without interval. The mean deviations of

the right and left eyes were −5.00 and −7.68 dB, respectively (Figure 2). A visual field defect in the nasal inferior aspect of the right eye corresponded to the retinal nerve fiber layer defect observed earlier. However, in both eyes, a right-sided homonymous hemianopia-like visual field defect was observed in both grayscale and pattern deviation images (Figure 2). Following perimetry, the patient stated that she experienced a migraine attack with an aura during the HFA examination. Consequently, a detailed medical interview regarding the migraine history of the patient was conducted.

The patient started experiencing migraines at the age of 17 years, with a frequency of several times per month. However, the frequency of the attacks and the headache during migraine attack decreased with age. Presently, the migraine symptom of the patient involved a visual disturbance aura almost without headache. She described the visual disturbance as dazzling white areas that emerged at various points in her visual field and spread across the whole field in a wave. The direction of the waves varied with each attack. The migraine aura and headache alternated between the right and left visual fields and frontal, lateral, or both hemispheres, respectively. As the patient did not exhibit vertigo or dizziness (18), her migraine was categorized as ICHD-code 1.2.1.2 "Typical aura without headache" (19).

The visual disturbance started 5 min before the HFA examination. The patient expressed that she was nervous during the examination. During the examination, the patient developed the visual disturbance. The migraine attack intensity peaked following the completion of the HFA examination of both eyes, and the attack lasted for ∼20 min.

The patient was started on antiglaucoma medication to prevent glaucoma progression. The intraocular pressure of the patient was controlled at approximately 18–20 mm Hg at the 11-month follow-up.

The HFA examination was repeated 1 and 10 months following the first examination (Figure 3), and mean deviations of −0.23 and −0.60 dB and −0.33 and 1.22 dB of the right and left eyes, respectively, were observed. During both examinations, the patient exhibited no migraine symptoms. The examination findings indicated no homonymous hemianopia–like visual field defects. The only abnormality was the visual field defect in the nasal inferior aspect of the right eye, corresponding to the retinal nerve fiber layer defect (Figure 3). Hence, the findings of the first HFA examination, which was performed during a migraine attack, reflected the effects of both glaucoma and migraine aura on the visual field.

Discussion

Here we reported a case of migraine-related visual field defect observed during perimetry in a patient with typical
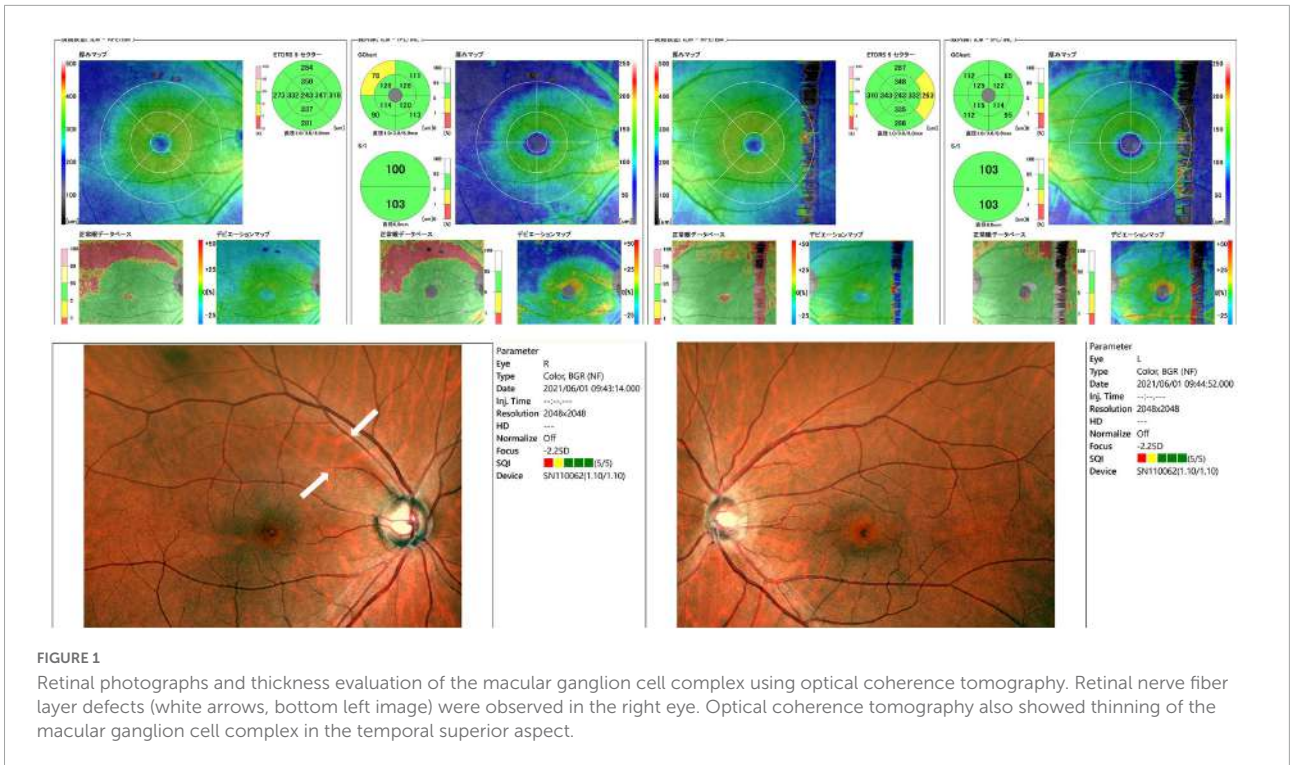
FIGURE 1

Retinal photographs and thickness evaluation of the macular ganglion cell complex using optical coherence tomography. Retinal nerve fiber layer defects (white arrows, bottom left image) were observed in the right eye. Optical coherence tomography also showed thinning of the macular ganglion cell complex in the temporal superior aspect.
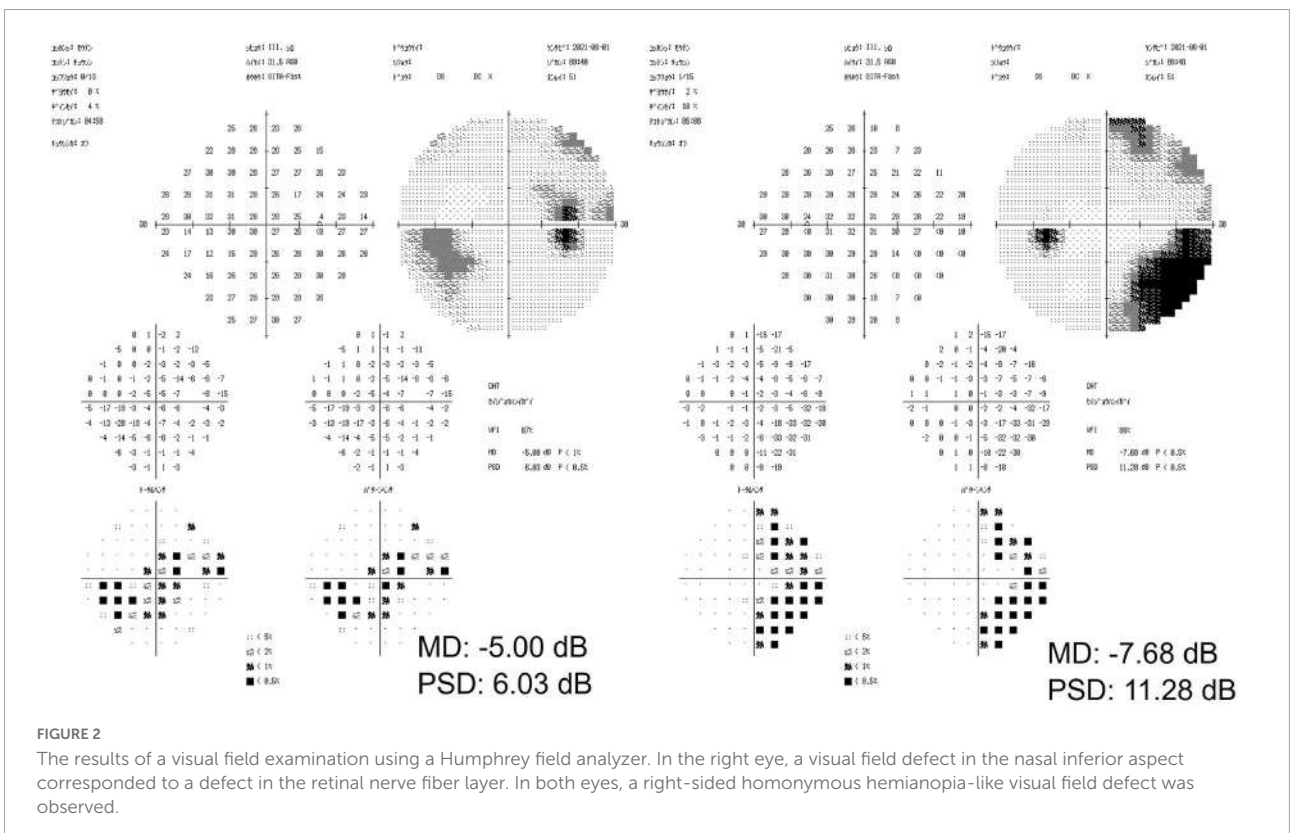
FIGURE 2

The results of a visual field examination using a Humphrey field analyzer. In the right eye, a visual field defect in the nasal inferior aspect corresponded to a defect in the retinal nerve fiber layer. In both eyes, a right-sided homonymous hemianopia-like visual field defect was observed.
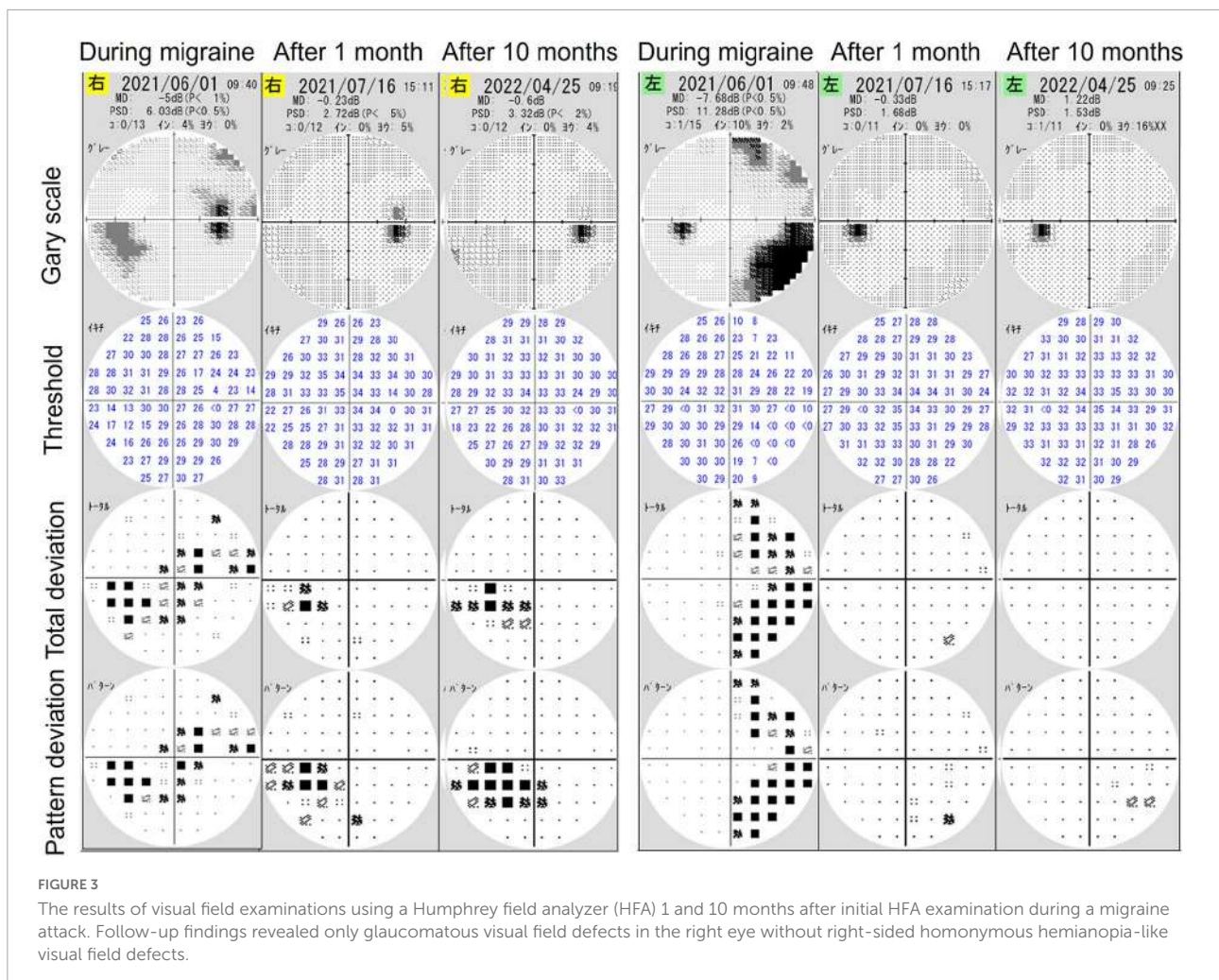
The results of visual field examinations using a Humphrey field analyzer (HFA) 1 and 10 months after initial HFA examination during a migraine attack. Follow-up findings revealed only glaucomatous visual field defects in the right eye without right-sided homonymous hemianopia-like visual field defects.

glaucoma. Luu et al. (9) reported a case of right-sided homonymous hemianopia assessed using HFA during a migraine attack; the HFA findings were similar to those of our patient. Furthermore, Yohannan and Jampel (10) reported a case of a left inferior quadrantanopsia using HFA during a migraine attack in a patient suspected of glaucoma. Both studies reported that repeated perimetry showed a resolution of anopia and a normal visual field (9, 10).

Yener and Korucu (11) compared HFA findings during attacks both in patients with migraine without aura and in those with tension-type headache and found no difference in their mean and pattern deviation values. Furthermore, the patients reportedly exhibited different patterns of non-specific visual field defects (11). Using automated perimetry (Dremel DigiLab 750; BioRad Laboratories, Hercules, CA, USA), Ebner (17) reported visual field depression, except in the central 5°, in a patient with homonymous type distribution during a migraine attack. During such an episode, aura, headache,

and a consequent decrease in the ability to concentrate may impact visual field findings. Migraine is considered to have a cortical origin because visual auras are homonymous and hemianopic (2). Visual auras comprise transient neurological disturbances of sight (90% of cases), disturbances of speech, or tingling/numbness of the face or body (2). Other visual field analyses using automated perimetry following a migraine attack have been reported (12–16). In these reports, a week after the attack, a decrease only in the sensitivity of the examination was observed (12–15). Additionally, a bilateral homonymous deficit was not observed in any case (12–15). Therefore, homonymous hemianopia visual field defect (9, 10, 17) can be considered as a common visual field characteristic of migraine attacks. Furthermore, this supports our HFA examination findings during a migraine attack. However, whether the homonymous hemianopia visual field defect reflects the ongoing visual auras or transient cerebral cortex paralysis remains unknown. A study reported that decreased sensitivity following the headache lasts 30–40 days on average, with a few cases showing durations of

up to 75 days (16). Fortunately, the visual field defects in our patient recovered after 1 month. However, ophthalmologists should consider migraine episodes while evaluating the visual fields of patients with glaucoma.

Conclusion

We described the findings of an automated visual field examination performed on a patient with typical glaucoma during a migraine attack. Detailed interviews with patients may be beneficial for understanding visual field findings and preventing their untimely examination.

Data availability statement

Data are available upon reasonable request. All data relevant to the study are accessed by the corresponding author. No additional data are available.

Ethics statement

The studies involving human participants were reviewed and approved by the Institutional Review Board of Saneikai Tsukazaki Hospital, Himeji, Japan (No. 221002). The patients/participants provided their written informed consent to participate in this study.

Author contributions

SN: data collection, study design and interpretation, manuscript drafting, and figures creation. SO: data collection, manuscript review, and editing. AT and TM: data collection and manuscript review. All authors contributed to the article and approved the submitted version.

Conflict of interest

The authors declare that the research was conducted in the absence of any commercial or financial relationships that could be construed as a potential conflict of interest.

Publisher's note

References

1. Stovner LJ, Hagen K, Jensen R, Katsarava Z, Lipton R, Scher A, et al. The global burden of headache: a documentation of headache prevalence and disability worldwide. *Cephalalgia.* (2007) 27:193–210. doi: 10.1111/j.1468-2982.2007.01288.x

2. Nguyen BN, Lek JJ, Vingrys AJ, McKendrick AM. Clinical impact of migraine for the management of glaucoma patients. *Prog Retin Eye Res.* (2016) 51:107–24. doi: 10.1016/j.preteyeres.2015.07.006

3. Gbd 2019 Blindness and Vision Impairment Collaborators, Vision Loss Expert Group of the Global Burden of Disease Study. Causes of blindness and vision impairment in 2020 and trends over 30 years, and prevalence of avoidable blindness in relation to VISION 2020: the Right to Sight: an analysis for the global burden of disease study. *Lancet Glob Health.* (2021) 9:e144–60. doi: 10.1016/S2214-109X(20)30489-7

4. Huang JY, Su CC, Wang TH, Tsai IJ. Migraine and increased risk of developing open angle glaucoma: a population-based cohort study. *BMC Ophthalmol.* (2019) 19:50. doi: 10.1186/s12886-019-1062-9

5. Cursiefen C, Wisse M, Cursiefen S, Jünemann A, Martus P, Korth M. Migraine and tension headache in high-pressure and normal-pressure glaucoma. *Am J Ophthalmol.* (2000) 129:102–4. doi: 10.1016/s0002-9394(99)00289-5

6. Funk RO, Hodge DO, Kohli D, Roddy GW. Multiple systemic vascular risk factors are associated with low-tension glaucoma. *J Glaucoma.* (2022) 31:15–22. doi: 10.1097/IJG.0000000000001964

7. Usui T, Iwata K, Shirakashi M, Abe H. Prevalence of migraine in low-tension glaucoma and primary open-angle glaucoma in Japanese. *Br J Ophthalmol.* (1991) 75:224–6. doi: 10.1136/bjo.75.4.224

8. Chen HY, Lin CL, Kao CH. Does migraine increase the risk of glaucoma?: a population-based cohort study. *Medicine.* (2016) 95:e3670. doi: 10.1097/MD.0000000000003670

9. Luu ST, Pesudovs K, Lee AW, Chen CS. Homonymous hemianopia captured on automated perimetry during a migraine episode. *Intern Med J.* (2010) 40:310–1. doi: 10.1111/j.1445-5994.2010.02194.x

10. Yohannan J, Jampel H. Progressing scintillating scotoma captured on automated visual field testing. *Ophthalmology.* (2016) 123:1395–6. doi: 10.1016/j.ophtha.2016.01.002

11. Yener AÜ, Korucu O. Visual field losses in patients with migraine without aura and tension-type headache. *Neuroophthalmology.* (2017) 41:59–67. doi: 10.1080/01658107.2016.1251466

12. Comoğlu S, Yarangümeli A, Köz OG, Elhan AH, Kural G. Glaucomatous visual field defects in patients with migraine. *J Neurol.* (2003) 250:201–6. doi: 10.1007/s00415-003-0975-6

13. Yenice O, Temel A, Incili B, Tuncer N. Short-wavelength automated perimetry in patients with migraine. *Graefes Arch Clin Exp Ophthalmol.* (2006) 244:589–95. doi: 10.1007/s00417-005-0083-7

14. McKendrick AM, Vingrys AJ, Badcock DR, Heywood JT. Visual dysfunction between migraine events. *Invest Ophthalmol Vis Sci.* (2001) 42:626–33.

15. McKendrick AM, Badcock DR. Decreased visual field sensitivity measured 1 day, then 1 week, after migraine. *Invest Ophthalmol Vis Sci.* (2004) 45:1061–70. doi: 10.1167/iovs.03-0936

16. McKendrick AM, Vingrys AJ, Badcock DR, Heywood JT. Visual field losses in subjects with migraine headaches. *Invest Ophthalmol Vis Sci.* (2000) 41:1239–47.

17. Ebner R. Visual field examination during transient migrainous visual loss. *J Clin Neuroophthalmol.* (1991) 11:114–7.

18. Nowaczewska M. Vestibular migraine - an underdiagnosed cause of vertigo. Diagnosis and treatment. *Neurol Neurochir Pol.* (2020) 54:106–15. doi: 10.1590/0004-282X20160037

19. Cephalalgia,. Headache classification committee of the international headache society (IHS) The international classification of headache disorders, 3rd edition. *Cephalalgia.* (2018) 38:1–211. doi: 10.1177/0333102417738202

Association between poor sleep quality and an increased risk of dry eye disease in patients with obstructive sleep apnea syndrome

Qi Pu[1†], Zhen Wu[2†], Ao-Ling Li[1], Xiao-Xiao Guo[1], Jing-Jie Hu[1] and Xin-Yu Li[1]*

[1]Department of Ophthalmology, Tongji Hospital, Tongji Medical College, Huazhong University of Science and Technology, Wuhan, China, [2]Department of Ear, Nose, and Throat, Changshu No. 2 People's Hospital, Changshu, China

Purpose: Obstructive sleep apnea (OSA) is related to an increased incidence of dry eye disease (DED). However, their exact relationship is unknown and requires further well-designed studies with advanced mechanisms detection.

Patients and methods: This case−control study included 125 OSA cases and 125 age−gender-matched controls enrolled in the hospital between 1 January and 1 October 2021. OSA diagnosis and classification were performed using a polysomnography (PSG) assay. Detailed ophthalmological examinations, including the Schirmer I test, corneal staining, and ocular surface disease index (OSDI), were used to detect DED-related parameters. A comprehensive ocular surface assay was performed to measure a series of parameters, including first non-invasive first tear film break-up time (f-NIBUT), average non-invasive first tear film break-up time (av-NIBUT), tear meniscus height (TMH), and loss of meibomian gland. In addition, the Pittsburgh Sleep Quality Index (PSQI) scale was used to assess sleep quality.

Results: Compared to the control, the OSA group showed an increased DED risk ($P = 0.016$) along with an increased PSQI score and a higher rate of poor quality sleep ($P < 0.001$ and $P = 0.007$, respectively). Stratification of OSA cases indicated that DED-related parameters were impaired in patients with severe OSA ($P < 0.05$). The analysis of DED-parameters-related factors showed significant correlations between OSA-related indexes and PSQI ($P < 0.05$). Moreover, the poor sleep quality group in the OSA cases showed worse DED-related parameters ($P < 0.05$), which was not observed in the control group.

Conclusion: OSA, especially the severe stage OSA, was related to an increased risk of DED. Also, sleep quality was correlated with the onset of both OSA and DED, where poor sleep quality revealed a relationship between OSA and the risk of DED. Overall, our findings provided evidence for advanced management of DED and OSA in future.

Introduction

Obstructive sleep apnea (OSA) syndrome is mainly manifested as snoring during sleep, accompanied by apnea and superficial breathing. OSA cases include the repeated occurrence of hypoxemia, hypercapnia, and sleep structure disorders at night, along with well-accepted related damages, such as cardiovascular, cerebrovascular, and metabolic dysfunctions (1). Understanding the potential pathological contributions of OSA to cancers, depression, and asthma can also update our knowledge of its biological effects (2, 3). In addition, a previous cross-sectional study involving 3,303 subjects showed that OSA was an independent risk factor for dry eye disease (DED) (4). Therefore, detecting the relationship between OSA and DED may provide information to manage both diseases.

Dry eye disease is regarded as one of the most common public health problems, with a prevalence rate of 5 to 50% (5). It leads to various symptoms, including a sensation of the presence of a foreign body, itching, and a burning sensation, and involves both physical and emotional discomforts described in ophthalmology (6). Currently, the management of DED includes eye drops targeting tear dysfunction, as well as abnormal inflammation in the ocular surface. However, the overall satisfaction degree for DED treatment is unsatisfactory (7). To provide better preventive and therapeutic strategies for DED patients, it is necessary to identify the risk factors of DED. Since OSA is a potentially harmful factor of DED, targeting OSA might provide advanced improvements in the management of DED. A study including both severe and mild/moderate OSA cases showed that OSA influenced meibomian gland alterations (8). Since meibomian gland dysfunction (MGD) is one of the structural bases of DED, OSA can be considered to harm the functioning of the meibomian gland, promoting the incidence of DED. Although OSA is relatively accepted as a potentially harmful risk factor for DED, its detailed pathological process remains unclear.

Mounting evidence demonstrates that sleep disorders are becoming prevalent health issues worldwide, with an estimate of 150 million people suffering from them (9). OSA is one of the most detected sleep disorders causing excessive daytime

sleepiness along with other potential sleep disorders (10). Yet, about 80% of moderate and severe OSA cases remain undiagnosed (11). Hence, the potential influences of poor sleep quality caused by OSA should be investigated by further advanced wide-range studies. Although sleep disorders are prominent, they are overlooked as serious comorbidities of DED, and there is also a lack of information on their detailed pathological connection (12). As poor sleep quality is related to both OSA and DED, we conjecture that poor quality of sleep might contribute to DED in patients with OSA. To verify this hypothesis, we conducted a case–control study with the following purposes: (1) recording and analyzing the detailed DED-related parameters and sleep quality among the OSA cases and age–gender-matched controls, and (2) detecting the association between poor sleep quality and DED incidence in OSA cases.

Materials and methods

Study design and participants

We conducted a hospital-based, case–control study involving OSA cases and healthy controls from Changshu Hospital between 1 January and 1 October 2021. The included participants were screened consecutively based on their history of the disease, drug use, and cooperation during the study period. After performing the polysomnography (PSG) examination in the Sleep Center, a total of 125 OSA cases and 125 age–gender-matched controls were included in the advanced experiments. The general information, DED-related examination records, and sleep quality assessments of all participants were collected, and after a series of processing, including OSA stratifications, DED scores, and sleep quality classifications, the data were used for statistical analyses. The detailed flow diagram of the study design and screening of participants is presented in **Figure 1**.

This case–control study was carried out as per the Declaration of Helsinki and was approved by the Institutional Review Board and Ethics Committee of the Changshu No. 2

FIGURE 1
Detailed flow diagram of study design and participants screening.
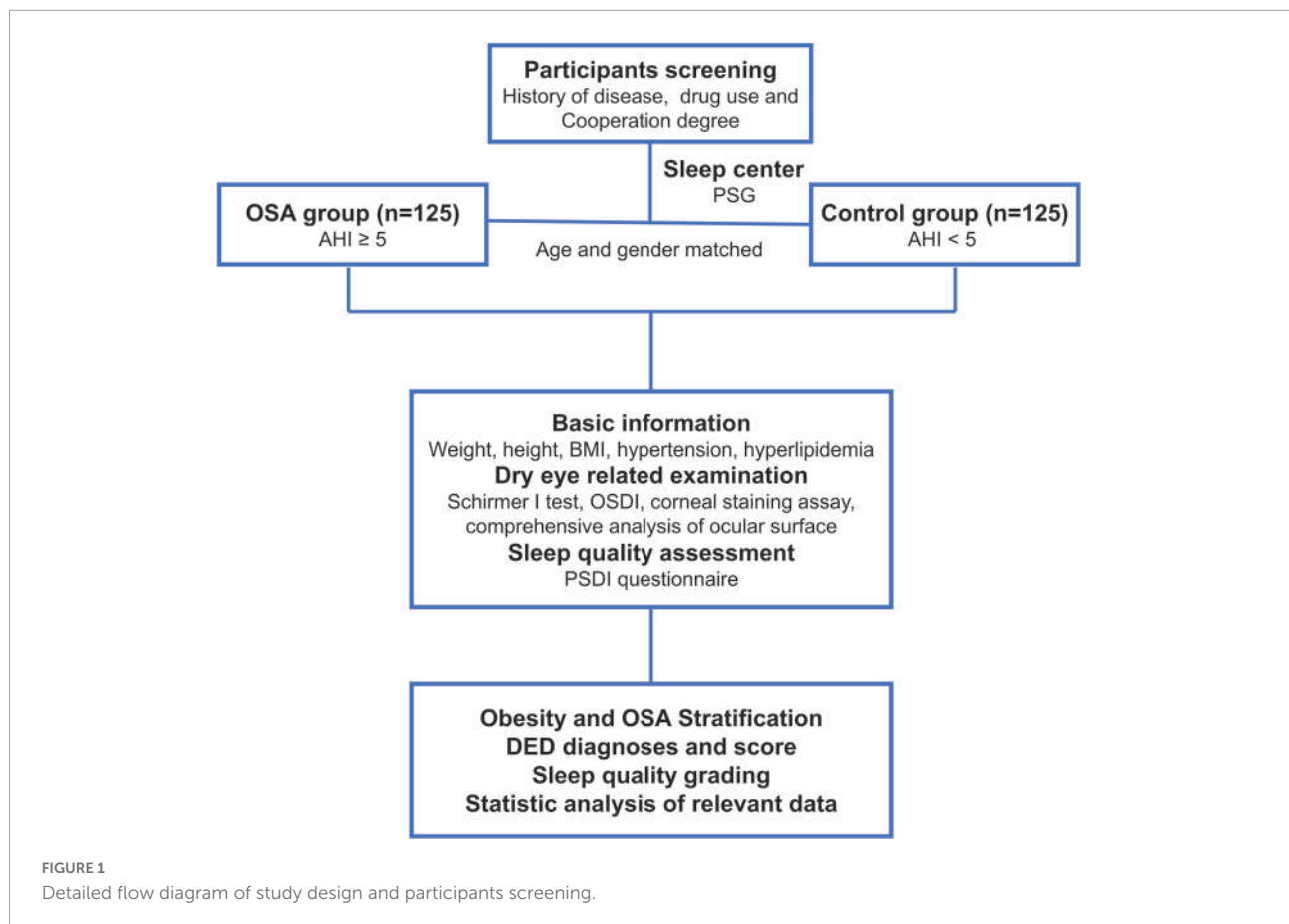
People's Hospital. Furthermore, written informed consent was obtained from all included participants.

The inclusion criteria included OSA cases confirmed by PSG, while the control group included the age–gender-matched participants without OSA. The age difference between OSA cases and matched controls was less than 2 years.

The exclusion criteria included OSA cases and relevant controls based on our team's related publications with slight modifications (13, 14). Participants were excluded from the OSA group if they met any of the following criteria: (1) patient with heart diseases, cerebrovascular diseases, autoimmune disorders, metabolic syndromes, malignant tumors, and psychological disorders; (2) patient with lacrimal diseases, systemic Sjogren's syndrome, or chemical injury in the cornea and conjunctiva; (3) history of the previous ocular surface, vitreoretinal, lacrimal canal, and tear gland surgeries in the recent 6 months; (4) patients with allergies or other conditions not able to finish the examination or treatments; (5) recent eye drops usage within 1 month; (6) history of sinusitis-nasal septum deviation and other diseases affecting sleep; (7) recently rotated night shift work for at least past 1 week; and (8) unwillingness to participate in the research.

Polysomnography examination

After performing a PSG examination using the Respironics Alice 5 system at the Sleep Center of the Department of Ear-Nose-Throat in Changshu No. 2 Hospital, all participants were divided into OSA and control groups. All detection procedures followed our previous research (13). The operation protocol included monitoring of at least 7 h of sleep time according to the patient's sleep habits, accompanied by the usage of PSG to monitor standard 3-lead electrocardiogram (EEG), electromyography (EMG) signal acquisition of heartbeat, eye movement, jaw movement, and leg movement. While the respiratory movement was automatically identified using the chest and abdomen respiratory induction plethysmography (RIP) belt, the respiratory airflow was intelligently identified by measuring the vitality and duration of the breath airflow in the nose and mouth. Subsequently, the following indicators were recorded: oral and nasal airflow; pulse saturation O_2 (SpO_2); sleep stages and the percentage of time in each period; the number of awakenings and other indicators; apnea-hypopnea index (AHI); obstructive apnea index (OAI); minimum blood oxygen saturation (lowest oxygen saturation, $LSpO_2$); oxygen desaturation index (ODI); mean oxygen saturation (MSpO2)

and percentage of time with $SpO_2 < 90\%$ (CT90%). On the day of the PSG examination, participants were not allowed to consume coffee/strong tea, alcohol, sedative drug, or sleep during the daytime. The cutoff value of OSA diagnosis was set at AHI = 5. A value of AHI 5–15, 15–30, and ≥30 events/hour indicated mild, moderate, and severe OSA cases, respectively [15].

Dry eye disease-related examinations

The basal DED detections were combined with a comprehensive inspection of the ocular surface to carry out DED-related examinations. The detailed process was modified based on the previous workflow of our recent publication [14], while DED was diagnosed based on non-invasive first tear film break-up time. Simultaneously, both f-NIBUT and av-NIBUT were measured as well. In addition, TMH and meibomian gland loss were detected using an Ocular Surface Comprehensive Analyzer (Sirius; CSO, Florence, Italy). The patient was instructed to place the mandible on the chin support while the forehead was maintained close to the forehead support, keeping their eyes open until the next blink. The instrument automatically captured the tear film image and displayed the measured values. The values from two repeats were used to obtain the average value. To a certain extent, TMH reflected the amount of tear secretion (Supplementary Figure 1). The Ocular Surface Comprehensive Analyzer was used to obtain a non-invasive TMH value by manually measuring the length between the corresponding points in the automatically presented tear film image. Sirius Anterior Segment Analysis System was used to obtain the imaging of upper and lower meibomian glands using the meibomian photography mode (Supplementary Figure 2). After capturing at least five images from the conjunctival surface of the upper and lower tarsal plates, the operator chose the clearest meibomian gland structure image and marked its boundary with equipment software. The device calculated the loss of the meibomian gland, and the results were classified according to the rate of loss. The mean values of two repeats were used for the final analyses.

Next, DED diagnosis and severity classification were performed using DED-related examinations, including the Schirmer I test, corneal fluorescein staining, and ocular surface disease index (OSDI) scales. The detailed operation process was achieved based on a previous publication [14]. Specifically, a folded Schirmer paper strip (5 mm × 35 mm) was placed at the outer third lower eyelid margin for 5 min while minutes and the wetting length of Schirmer paper were recorded as the Schirmer scores. The Oxford corneal staining score was used in the corneal fluorescein scale, and the ocular surface was divided into three parts, namely nasal conjunctiva, temporal conjunctiva, and cornea. Each part was scored from light to heavy, with points ranging between 0 and 5. The total score ranging between 0 and 15 points was used for the final analyses. Finally, DED was diagnosed based on the Expert Consensus on Clinical Management of Dry Eye (2020) [16].

Sleep quality assessment

The sleep quality of all participants was assessed using the Pittsburgh Sleep Quality Index (PSQI) scale [17]. The scale was compiled by Buysse of the University of Pittsburgh Medical Center in 1989, which included 19 self-evaluations and five other evaluation items. The items included seven components, namely subjective sleep quality, sleep duration, sleep latency, sleep efficacy, sleep disturbance, sleep aid medication, and sleep-related daytime problems. Each dimension was scored by a 4-level scoring method, that is, between 0 and 3 points, while the total score was calculated between 0 and 21 points. Based on a previous publication by Magno et al. [18], a PSQI score of <6 points indicated good sleep quality, while a PSQI score of ≥6 points indicated sleep disorder. The higher the PSQI score, the worse the sleep quality.

Statistical analysis

The statistical analysis was conducted using GraphPad Prism 8 software (GraphPad Software Inc., San Diego, CA, USA). The categorical variables were presented using frequency, while the continuous variables were expressed as mean ± standard deviation (SD). The Kolmogorov–Smirnov test was used to verify the normality of values, while the chi-square test was used to compare the differences in categorical variables among different groups. The t-test was used to compare the differences between two groups, while the analysis of variance (ANOVA) was used to compare the differences among multiple groups. For the *post-hoc* analyses of ANOVA, the Student–Newman–Keuls (SNK) method was used. The correlation analyses between OSA-related parameters, PSQI scores, and DED-related parameters were calculated using Pearson's correlation coefficient. The difference was considered statistically significant if the p-value was less than 0.05.

Results

Baseline characteristics

Table 1 presents the baseline information, including demographics, OSA-related parameters, clinic characteristics, and sleep quality, of the participants in both OSA and control groups. Since it was an age–gender-matched case–control study, there was consistency in the status of age and indiscriminate

gender distribution between OSA and relevant control groups ($P = 0.809$ and $P = 0.552$, respectively). To obtain OSA-related parameters, all participants were divided into two groups, namely OSA and control groups. Compared to the control groups, the OSA group showed significantly increased values of OSA-related parameters, including AHI, OAI, ODI, MSpO$_2$, LSpO$_2$, and CT90. Advanced analyses of the clinical characteristics showed higher incidences of hypertension and hyperlipidemia in the OSA cases ($P < 0.05$) along with an increased BMI value ($P < 0.001$). However, no significant difference was observed in the incidence of diabetes ($P = 0.105$). The OSA group showed a significantly higher incidence rate of DED ($P = 0.016$) than the control. Since sleep quality was reported to be related to OSA status, we examined the sleep quality in both OSA and relevant control groups using the PSQI score, which showed an increase in the PSQI score and a higher incidence rate of poor sleep quality in the OSA group ($P < 0.05$). Moreover, the detailed descriptions of PSQI contents in the OSA group showed higher scores in subjective sleep quality, sleep duration, sleep disturbance, sleep aid medication, and sleep-related daytime problems ($P = 0.004$, 0.010, 0.076, 0.002, 0.022, and 0.014, respectively).

Dry eye disease incidence and dry eye disease-related parameters in the obstructive sleep apnea and relevant control groups

Since our results suggested a higher DED incidence rate in the OSA group, the stratification of OSA groups provided a further detailed description of DED-related parameters. According to the AHI value of 5, 15, and 30 events/h, OSA cases were divided into mild, moderate, and severe groups, respectively. Generally, most DED-related parameters were significantly different in mild, moderate, and severe group between control and OSA cases; however, no significant difference was detected in their TMH values. The classic DED-related indexes, including Schirmer I test values, Oxford corneal staining score and OSDI, comprehensive ocular surface assay parameters, including f-NITBUT, av-NITBUT, TMH, and loss on eyelid meibography, can provide a better understanding of the relationship between OSA and DED. Generally, no significant difference was observed in any DED-related parameters between the mild/moderate OSA and control groups. Interestingly, most DED-related parameters were impaired in severe OSA cases, with no significant difference in Oxford corneal staining score and TMH between the control and severe OSA cases ($P = 0.0780$ and 0.064, respectively). The detailed data are presented in **Table 2**.

The correlations between general information, obstructive sleep apnea-related parameters, sleep quality, and dry eye disease-related parameters

Dry eye disease incidence and its related parameters were found to be significantly related to the risk and severity of OSA. In this case–control study, age and BMI were significantly associated with loss of lower eyelid meibography and Schirmer I test values, respectively ($P < 0.05$). The relationship analyses between DED-related parameters and OSA-related indexes, including AHI, OAI, ODI, MSpO$_2$, LSpO$_2$, and CT90, revealed a comprehensive correlation between them. Finally, the potential correlations between sleep quality and DED-related parameters were also analyzed, where sleep quality was assessed using the total PSQI score. The correlation analyses performed using the PSQI score showed negative linear correlations among Schirmer I test, f-NITBUT, av-NITBUT, and TMH values. However, positive correlations were detected among Oxford corneal staining score, OSDI score, loss on upper eyelid meibography, and lower eyelid meibography. The detailed correlation data are shown in **Table 3**.

Dry eye disease-related parameters of good and poor sleep groups belonging to obstructive sleep apnea and relevant control cases

As sleep quality was related to both OSA status and DED incidence, advanced analyses were used to detect the potential contributors of sleep quality in OSA-related DED incidence. Based on the PSQI score, the participants were further divided into good sleep quality and poor sleep quality groups. Interestingly, no significance was observed in any DED-related parameters between good sleep and poor sleep groups within the control participants ($P > 0.05$). However, in the poor sleep group in the OSA cases, a significantly increased incidence of DED was observed ($P = 0.002$). Advanced analyses included detailed classic DED-related parameters, including the Schirmer I test, corneal staining assay, and OSDI scores, which showed that OSA patients with poorer sleep tended to demonstrate less tear production and severe ocular surface damage with ocular discomfort ($P < 0.05$). Loss on both upper and lower eyelid meibography represented the meibomian gland structures and their potential biological function. Compared to the OSA cases with good sleep, the poor sleep ones demonstrated an increased rate of loss in eyelid meibography ($P < 0.001$). **Table 4** presents DED-related parameters of good and poor sleep groups belonging to the OSA cases and relevant controls.

TABLE 1 Demographics, clinical characteristics, OSA-related parameters, DED incidence, and sleep quality in OSA cases and relevant controls.

Variables	Control ($n = 125$)	OSA ($n = 125$)	P
Demographics			
Age (year)	53.72 ± 13.03	54.12 ± 12.99	0.809
Gender (no. of female, %)	48 (38.4)	48 (38.4)	0.552
OSA related parameters			
AHI (events/h)	1.58 ± 1.15	26.79 ± 17.07	**<0.001**
OAI (events/h)	0.40 ± 0.14	8.95 ± 8.55	**<0.001**
ODI (events/h)	3.30 ± 1.11	22.73 ± 15.05	**<0.001**
MSpO2 (%)	96.38 ± 1.05	94.02 ± 1.28	**<0.001**
LSpO2 (%)	90.17 ± 1.89	80.84 ± 4.21	**<0.001**
CT90 (%)	0.11 ± 0.05	4.91 ± 5.68	**<0.001**
Clinical characteristics			
Hypertension (n, %)	22 (17.6)	54 (43.2)	**<0.001**
Diabetes (n, %)	35 (28.0)	47 (27.6)	0.105
Hyperlipidemia (n, %)	26 (20.8)	44 (35.2)	**0.016**
BMI (kg/m^2)	26.58 ± 4.85	30.36 ± 5.46	**<0.001**
DED (n, %)	71 (56.8)	53 (42.4)	**0.016**
Sleep quality			
PSQI score	6.36 ± 3.77	8.10 ± 4.21	**<0.001**
Poor sleep quality (PSQI > 5, n, %)	80 (64.0)	58 (46.4)	**0.007**
Components of PSQI			
Subjective sleep quality	0.88 ± 0.88	1.20 ± 0.95	**0.004**
Sleep duration	0.89 ± 0.85	1.16 ± 0.88	**0.010**
Sleep latency	0.99 ± 1.00	1.08 ± 0.91	0.432
Sleep efficacy	0.86 ± 0.83	1.06 ± 0.98	0.076
Sleep disturbance	0.82 ± 0.81	1.15 ± 0.92	**0.002**
Sleep aid medication	0.84 ± 0.84	1.09 ± 0.86	**0.022**
sleep-related daytime problems	1.08 ± 0.91	1.36 ± 0.95	**0.014**

Comparison among groups was calculated using unpaired t-test and chi-square exact test. The comparisons with statistical differences were marked in bold.

TABLE 2 Incidence of DED, DED-related parameters, and comprehensive analysis of ocular surface among OSA cases in different stages and the relevant controls.

Variables	Control	OSA cases			P
		Mild OSA	**Moderate OSA**	**Severe OSA**	
DED incidence	53 (42.4)	13 (40.6)	30 (55.6)	28 (71.8)	**0.007**
Schirmer I test (mm/5 min)	15.61 ± 6.69	15.66 ± 6.68	15.17 ± 6.99	10.00 ± 6.56	**<0.001**
Oxford corneal staining score	0.70 ± 1.01	0.25 ± 0.43	0.39 ± 1.06	1.13 ± 1.45	**0.002**
OSDI	15.92 ± 10.09	15.41 ± 11.89	18.83 ± 13.94	33.10 ± 19.58	**<0.001**
f-NITBUT (s)	7.31 ± 2.39	7.25 ± 1.60	6.79 ± 1.99	5.85 ± 2.09	**0.003**
av-NITBUT (s)	10.55 ± 3.06	10.41 ± 1.89	10.08 ± 2.25	8.90 ± 2.50	**0.011**
TMH (mm)	0.38 ± 0.07	0.38 ± 0.07	0.38 ± 0.08	0.35 ± 0.08	0.588
Loss on upper eyelid meibography (%)	17.82 ± 8.44	17.49 ± 6.10	21.12 ± 10.15	26.20 ± 11.72	**<0.001**
Loss on lower eyelid meibography (%)	19.50 ± 8.52	18.69 ± 5.76	22.02 ± 9.36	27.87 ± 12.45	**<0.001**

Comparison among groups was calculated using unpaired t-test and chi-square exact test. The comparisons with statistical differences were marked in bold.

TABLE 3 Correlation analyses of DED-related ophthalmologic parameters and relevant factors, including general information, OSA parameters, and sleep quality among all the participants.

	Schirmer I test (mm/5 min)	Oxford corneal staining score	OSDI	f-NITBUT (s)	av-NITBUT (s)	TMH (mm)	Loss on upper eyelid meibography (%)	Loss on lower eyelid meibography (%)
Age	$r = 0.04$ ($-0.08\sim0.17$) $P = 0.505$	$r = -0.44$ ($-0.17\sim0.08$) $P = 0.492$	$r = -0.06$ ($-0.19\sim0.06$) $P = 0.316$	$r = -0.01$ ($-0.13\sim0.11$) $P = 0.873$	$r = 0.04$ ($-0.09\sim0.16$) $P = 0.562$	$r = 0.03$ ($-0.09\sim0.16$) $P = 0.619$	$r = 0.13$ ($0.01\sim0.25$) **$P = 0.039$**	$r = -0.04$ ($-0.06\sim0.18$) $P = 0.327$
BMI	$r = -0.15$ ($-0.27\sim-0.02$) **$P = 0.02$**	$r = 0.06$ ($-0.07\sim0.18$) $P = 0.344$	$r = 0.09$ ($-0.04\sim0.21$) $P = 0.172$	$r = -0.07$ ($-0.19\sim0.06$) $P = 0.302$	$r = -0.11$ ($-0.23\sim0.02$) $P = 0.099$	$r = -0.04$ ($-0.17\sim0.08$) $P = 0.502$	$r = 0.10$ ($-0.02\sim0.22$) $P = 0.135$	$r = 0.09$ ($0.01\sim0.26$) **$P = 0.031$**
AHI	$r = -0.28$ ($-0.39\sim-0.17$) **$P < 0.001$**	$r = 0.15$ ($0.03\sim0.27$) **$P = 0.016$**	$r = 0.44$ ($0.34\sim0.54$) **$P < 0.001$**	$r = -0.27$ ($-0.38\sim-0.15$) **$P < 0.001$**	$r = -0.24$ ($-0.35\sim-0.12$) **$P < 0.001$**	$r = -0.15$ ($-0.27\sim-0.02$) **$P = 0.019$**	$r = 0.33$ ($0.21\sim0.44$) **$P < 0.001$**	$r = 0.42$ ($0.23\sim0.45$) **$P < 0.001$**
OAI	$r = -0.29$ ($-0.40\sim-0.17$) **$P < 0.001$**	$r = 0.21$ ($0.09\sim0.32$) **$P = 0.001$**	$r = 0.47$ ($0.37\sim0.56$) **$P < 0.001$**	$r = -0.29$ ($-0.40\sim-0.18$) **$P < 0.001$**	$r = -0.27$ ($-0.38\sim-0.15$) **$P < 0.001$**	$r = -0.18$ ($-0.29\sim-0.05$) **$P = 0.005$**	$r = 0.36$ ($0.24\sim0.46$) **$P < 0.001$**	$r = 0.45$ ($0.26\sim0.47$) **$P < 0.001$**
ODI	$r = -0.29$ ($-0.40\sim-0.17$) **$P < 0.001$**	$r = 0.18$ ($0.06\sim0.30$) **$P = 0.004$**	$r = 0.42$ ($0.32\sim0.52$) **$P < 0.001$**	$r = -0.27$ ($-0.38\sim-0.15$) **$P < 0.001$**	$r = -0.24$ ($-0.35\sim-0.12$) **$P < 0.001$**	$r = -0.16$ ($-0.28\sim-0.03$) **$P = 0.013$**	$r = 0.32$ ($0.20\sim0.42$) **$P < 0.001$**	$r = 0.42$ ($0.19\sim0.42$) **$P < 0.001$**
MSpO$_2$	$r = 0.23$ ($0.11\sim0.34$) **$P < 0.001$**	$r = -0.08$ ($-0.21\sim0.04$) $P = 0.19$	$r = -0.33$ ($-0.44\sim0.22$) **$P < 0.001$**	$r = 0.17$ ($0.04\sim0.28$) **$P = 0.009$**	$r = 0.14$ ($0.01\sim0.26$) **$P = 0.03$**	$r = 0.16$ ($0.03\sim0.28$) **$P = 0.012$**	$r = -0.27$ ($-0.38\sim-0.15$) **$P < 0.001$**	$r = 0.29$ ($-0.40\sim-0.17$) **$P < 0.001$**
LSpO2	$r = 0.22$ ($0.10\sim0.34$) **$P < 0.001$**	$r = -0.09$ ($-0.21\sim0.04$) $P = 0.165$	$r = -0.33$ ($-0.43\sim-0.21$) **$P < 0.001$**	$r = 0.19$ ($0.07\sim0.31$) **$P = 0.003$**	$r = 0.16$ ($0.04\sim0.28$) **$P = 0.011$**	$r = 0.11$ ($-0.02\sim0.23$) $P = 0.086$	$r = 0.27$ ($-0.38\sim-0.15$) **$P < 0.001$**	$r = -0.41$ ($-0.39\sim-0.16$) **$P < 0.001$**
CT90	$r = -0.29$ ($-0.40\sim-0.17$) **$P < 0.001$**	$r = 0.24$ ($0.12\sim0.36$) **$P < 0.001$**	$r = 0.43$ ($0.33\sim0.53$) **$P < 0.001$**	$r = -0.26$ ($-0.37\sim-0.14$) **$P < 0.001$**	$r = -0.23$ ($-0.34\sim-0.11$) **$P < 0.001$**	$r = -0.13$ ($-0.25\sim-0.01$) **$P = 0.035$**	$r = 0.27$ ($0.15\sim0.38$) **$P < 0.001$**	$r = 0.38$ ($0.17\sim0.40$) **$P < 0.001$**
Total PSQI Score	$r = 0.31$ ($-0.42\sim-0.19$) **$P < 0.001$**	$r = 0.25$ ($0.13\sim0.36$) **$P < 0.001$**	$r = 0.47$ ($0.36\sim0.56$) **$P < 0.001$**	$r = -0.31$ ($-0.42\sim-0.19$) **$P < 0.001$**	$r = -0.26$ ($-0.38\sim-0.15$) **$P < 0.001$**	$r = -0.26$ ($-0.38\sim-0.14$) **$P < 0.001$**	$r = 0.37$ ($0.26\sim0.47$) **$P < 0.001$**	$r = 0.04$ ($0.27\sim0.48$) **$P < 0.001$**

The linear correlations with a significant difference were marked in bold. OSA, obstructive sleep apnea; AHI, apnea-hypopnea index; OAI, obstructive apnea index; MSpO2, mean nocturnal oxygen saturation; ODI, oxygen desaturation index; LSpO2, lowest oxygen saturation; TS90%, time spent below oxygen saturation of 90%.

TABLE 4 Dry eye disease (DED)-related parameters in good and poor sleep groups of OSA cases and relevant controls.

	Control			OSA		
	Good sleep (n = 67)	Poor sleep (n = 58)	P	Good sleep (n = 45)	Poor sleep (n = 80)	P
DED (n, %)	31 (46.3)	22 (37.9)	0.370	17 (37.8)	54 (67.5)	**0.002**
Schirmer I test(mm/5 min)	15.69 ± 6.97	15.52 ± 6.36	0.889	15.81 ± 5.34	15.72 ± 7.52	**0.001**
Oxford corneal staining score	0.76 ± 0.95	0.62 ± 1.08	0.444	0.09 ± 0.29	0.43 ± 0.85	**<0.001**
OSDI	15.71 ± 9.16	16.16 ± 11.05	0.806	12.31 ± 6.41	19.13 ± 14.36	**<0.001**
f-NITBUT (s)	7.29 ± 2.44	7.32 ± 2.32	0.948	7.87 ± 1.14	6.53 ± 2.00	**<0.001**
av-NITBUT (s)	10.31 ± 3.03	10.83 ± 3.06	0.342	11.11 ± 1.31	9.87 ± 2.31	**<0.001**
TMH (mm)	0.37 ± 0.07	0.39 ± 0.06	0.320	0.42 ± 0.05	0.37 ± 0.07	**<0.001**
Loss on upper eyelid meibography (%)	18.00 ± 8.44	17.62 ± 8.43	0.804	15.28 ± 3.03	21.24 ± 9.55	**<0.001**
Loss on lower eyelid meibography (%)	19.32 ± 8.25	19.70 ± 8.80	0.806	17.09 ± 3.80	21.96 ± 8.90	**<0.001**

Comparison among groups was calculated using unpaired t-test and chi-square exact test. The comparisons with statistical differences were marked in bold.

The association between sleep quality and dry eye disease-related parameters in the obstructive sleep apnea cases

As significant differences were detected in DED-related parameters, potential correlations were also found between PSQI scores and DED-related parameters. Among all the DED-related parameters, three parameters, including the Schirmer I test, OSDI score, and NIBUT, were selected for linear correlation analyses. As shown in Figure 2A, a negative correlation was found between the PSQI score and Schirmer I test value ($R^2 = 0.196$, $P < 0.001$). Besides, a positive correlation was demonstrated between PSQI score and OSDI value considering the clinical symptoms ($R^2 = 0.346$, $P < 0.001$, Figure 2B). NITBUT was regarded as an index for tear film quality and was also reported to be associated with an increased PSQI score ($R^2 = 0.223$, $P < 0.001$, Figure 2C).

To gain a better understanding of the association between sleep quality and DED-related parameters, the correlations were analyzed between detailed PSQI contents and all DED-related parameters, which are presented in Figure 3. An insignificant difference was only detected in the correlation between sleep aid medication and Schirmer I test values ($P = 0.086$). In the analysis of all correlation matrices between sleep quality scales and DED-related parameters, OSDI demonstrated the most significant correlation index ($R = 0.34$ to 0.59, $P \leq 0.001$).
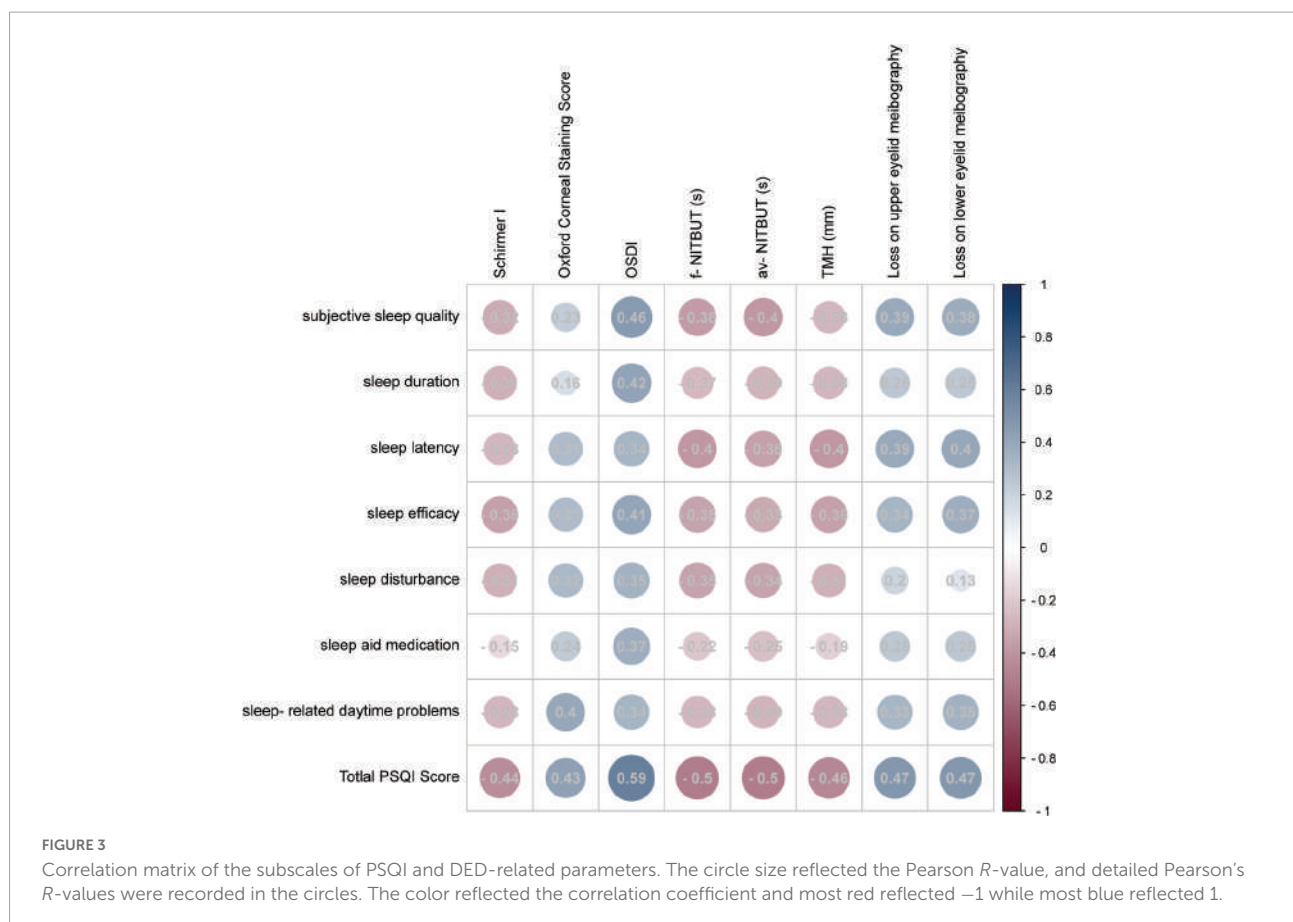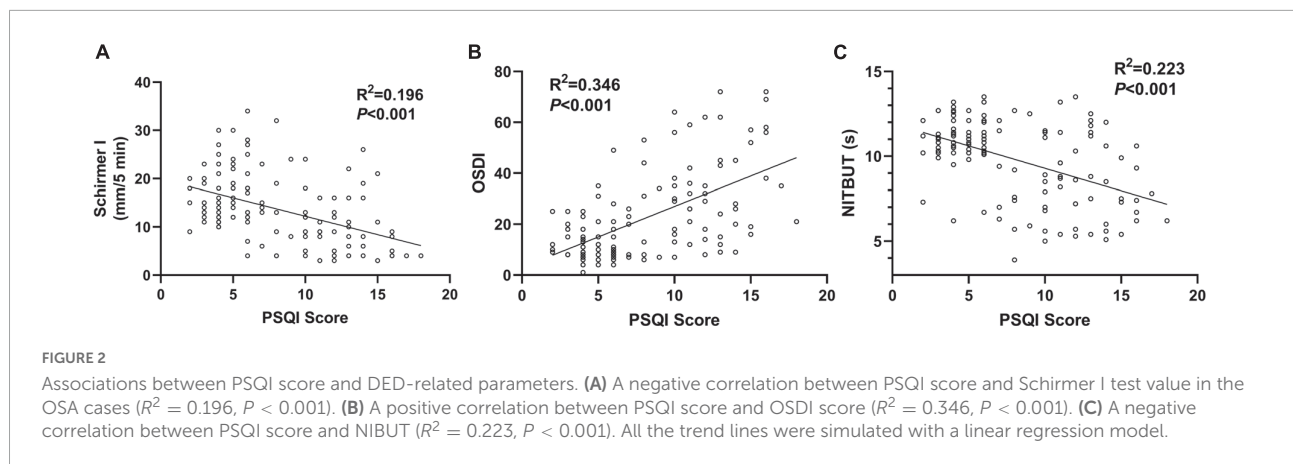
Discussion

Current observational studies demonstrated that OSA, sleep disorders, and DED are all prevalent disorders. However, the detailed relationship between these disorders and their potential biological mechanisms remains unclear. In this case–control study, DED and poor sleep quality were found to be more prevalent in OSA cases. Further classification of the OSA cases into mild, moderate, and severe groups showed that the DED incidence was found to be higher in the severe OSA group. Moreover, poor sleep quality was related to a higher risk of DED among all the participants, while worse sleep quality was related to severe DED. The analysis of the relationship between PSQI contents and DED-related parameters showed that PSQI scale contents were positively correlated with the OSDI score. Our study highlighted the potential role of sleep quality in the relationship between OSA status and DED risk.

Obstructive sleep apnea can reduce the quality of life, leading to multi-system disorders, including cognitive function impairment, systemic hypertension, cardiovascular diseases, and metabolic syndromes [19]. Even several therapies, including surgery, mandibular advancing device (MAD) and continuous positive airway pressure (CPAP), have been applied in OSA management [20, 21], and several accompanying diseases should be noticed. Recent studies illustrated that DED may be a comorbidity of OSA. This finding may provide an updated understanding of both pathological mechanisms and disease management. In a recent hospital-based cross-sectional study, OSA was found to be a risk factor for DED (OR = 4.36, 95% CI: 1.26 to 17.08) [22]. As indicated in our results, the OSA cases showed a higher risk of DED compared to the age–gender controls, which was consistent with the previous studies. Since the association between DED and OSA incidence has been indefinite, this study can provide new evidence on the topic. Moreover, our results demonstrated the incidence of DED and dysfunctions in DED-related parameters in severe OSA cases, suggesting the induction of DED risk by severe OSA status. Our results also illustrated that severe OSA might induce further pathological changes, indicating its involvement in the potential direct or indirect pathological mechanisms underlying the incidence of DED.

Although the association between OSA and DED incidence was revealed in previous studies, there is a need for further detailed knowledge of the contributions of OSA toward the

FIGURE 2

Associations between PSQI score and DED-related parameters. **(A)** A negative correlation between PSQI score and Schirmer I test value in the OSA cases ($R^2 = 0.196$, $P < 0.001$). **(B)** A positive correlation between PSQI score and OSDI score ($R^2 = 0.346$, $P < 0.001$). **(C)** A negative correlation between PSQI score and NIBUT ($R^2 = 0.223$, $P < 0.001$). All the trend lines were simulated with a linear regression model.

FIGURE 3

Correlation matrix of the subscales of PSQI and DED-related parameters. The circle size reflected the Pearson R-value, and detailed Pearson's R-values were recorded in the circles. The color reflected the correlation coefficient and most red reflected −1 while most blue reflected 1.

risk of DED. Among all DED subtype classifications, aqueous-deficient and evaporative DED subtypes are the most common ones (23). Generally, aqueous-deficient DED is related to reduced tear production, while evaporative DED is related to an abnormal lipid layer, which includes MGD. In the current study, the aqueous-deficient DED-related parameter, namely TMH, showed no significant difference between control and OSA groups at different stages. However, the severe OSA cases showed lower Schirmer I test values, suggesting an increased

risk of aqueous-deficient DED. Moreover, floppy eyelid syndrome was also a most frequently reported comorbidity of OSA, which affects tear film dynamics and contributes to a high rate of water evaporation (24, 25). These results demonstrated that OSA might contribute to the incidence of aqueous-deficient DED; however, well-designed studies may be required in future. Considering the evaporative DED-related parameters, NITBUT and meibography were found to be significantly impaired in the OSA cases, suggesting

the association of OSA with MGD-related evaporative DED. Several previous studies have reported a relationship between OSA and morphological alterations in the meibomian gland, while two independent case–control studies have highlighted the potential contributions of OSA in MGD-related DED (8, 26). Although the current study, along with other studies, has reported the relationship between OSA status and morphological alterations in the meibomian gland, the detailed biological mechanisms remain unclear. The physiological characteristics of OSA include partial or complete chronic upper airway obstruction, leading to intermittent hypoxia, sleep fragmentation during sleep, induced sympathetic nerve activation, oxidative stress, hypercoagulable state, inflammation, endothelial function damage, and metabolic abnormality (27). Intermittent hypoxia can lead to the production of reactive oxygen species, oxidative stress, endothelial function damage, and an increase in the activity of pro-inflammatory cytokines, adhesion molecules, and procoagulant factors. This leads to systemic inflammation through a series of transduction pathways (28). Inflammation plays an important role in the occurrence of both OSA and DED, with important inflammatory mediators in DED being interleukin 6 (IL-6) and C-reactive protein (CRP) (29). OSA is independently associated with elevated levels of CRP, IL-6, interleukin 8 (IL-8), interleukin 18 (IL-18), and tumor necrosis factor (TNF) (29, 30). In addition, the oxidative stress caused by OSA can upregulate inflammatory factors, cytokines, and adhesion molecules, in turn leading to circulatory and local inflammation. This can lead to dysfunctions of both the lacrimal and meibomian glands, thus, causing aqueous-deficient and evaporative DED, respectively. However, further clinical investigations and pathological experiments are required for a better understanding of the exact role of OSA in DED risk.

Obstructive sleep apnea is one kind of sleep disorder causing poor quality of sleep (31). Several recent studies reported the association between sleep quality and DED status. In a cross-sectional study, poor sleep quality was reported to be associated with the symptoms of DED (4). Several other independent studies have also reported the potential association between sleep quality and DED severity (12, 32, 33). In this case–control study, only the OSA group showed a relationship between poor sleep quality and higher DED risk and not the control group. The differences in the distribution of DED risk between the OSA and control groups indicated that poor sleep quality might contribute to the incidence of OSA-related-DED. In this observational study, we explored the correlations between all the subscales of PSQI for sleep quality analyses and DED-related parameters and interestingly found that OSDI scores were the most significant among all DED-related parameters. However, as the OSDI scale is a commonly used international questionnaire to quantify the subjective symptoms of DED, potential overlaps can be observed between DED-related clinical symptoms and sleep quality-related discomforts. Also, since

ocular discomfort scales are considered an important tool for primary care practice and earlier recognition, our study suggests further attention to the usage of the OSDI scale in OSA-related DED management.

The data in this study provided evidence of correlations between OSA status and DED risk and also proposed a hypothesis that poor sleep quality can contribute to the DED incidence in OSA cases. However, this study had several limitations. First, the amount of included participants was not large enough, and a deeper understanding may be needed through well-advanced and-designed studies with a larger population. Second, DED, OSA, and poor sleep quality are complex disorders, and understanding their interactions thoroughly is difficult. Although the preliminary conclusion in the current study revealed that poor sleep quality contributed to OSA-related DED incidence, further observational studies may be required. Third, we did not consider surgery, the usage of CPAP, or other nasal mask therapy devices in the treatment of OSA nor considered their effects on DED management. These devices are important since they may aggravate DED in severe OSAS cases. A contradictory conclusion on CPAP therapy in DED incidence was reported in previous studies. A previous study demonstrated a higher DED prevalence in patients with CPAP or other nasal mask therapy (34); however, another study reported that long-term (at least 1 year) use of CPAP improved the tear quality and overcame the ocular discomforts encountered in the early stage of CPAP (35). The exact effect of OSA treatment on the risk of DED needs further investigation in well-advanced studies. Finally, the confounding bias existed in the correlation between the OSA indexes and DED-related parameters. An ongoing study with more participants and relatively simple DED-related assay was conducted in our team and thus better statistical analyses using multiple regression analyses.

Conclusion

In conclusion, the OSA cases showed a higher prevalence of DED, while the severity of OSA was significantly correlated with the impairments in DED-related parameters. Moreover, sleep quality was found to be correlated with the onset of both OSA and DED, where poor sleep quality revealed a relationship between OSA and DED risk. Our study results suggest that clinicians engaged in DED and OSA management should pay attention to the interaction between DED and OSA. However, further investigations may be required to study the effects of sleep quality on the risks of DED and OSA, providing an understanding of both biological mechanism detection and clinical disease management. Moreover, further well-designed clinical studies may be required to analyze the relationships between OSA status, DED incidence, and sleep quality to provide better insights into improved therapeutic strategies.

Data availability statement

The original contributions presented in this study are included in the article/**Supplementary material**, further inquiries can be directed to the corresponding author.

Ethics statement

The studies involving human participants were reviewed and approved by Changshu No. 2 People's Hospital Medical Ethics Committee. The patients/participants provided their written informed consent to participate in this study.

Author contributions

X-YL: supervision, project administration, term, conceptualization, and writing—review and editing. QP and ZW: investigation, formal analysis, visualization, and writing—original draft preparation. A-LL, X-XG, and J-JH: data curation and validation. All authors contributed to manuscript revision, read, and approved the submitted version.

Acknowledgments

Conflict of interest

The authors declare that the research was conducted in the absence of any commercial or financial relationships that could be construed as a potential conflict of interest.

Publisher's note

All claims expressed in this article are solely those of the authors and do not necessarily represent those of their affiliated organizations, or those of the publisher, the editors and the reviewers. Any product that may be evaluated in this article, or claim that may be made by its manufacturer, is not guaranteed or endorsed by the publisher.

Supplementary material

The Supplementary Material for this article can be found online at: https://www.frontiersin.org/articles/10.3389/fmed.2022.870391/full#supplementary-material

SUPPLEMENTARY FIGURE 1
Image of TMH. TMH is the plane height formed by tears, margin of inferior eyelid and inferior bulbar conjunctiva, which can reflect the amount of lacrimal gland secretion. The normal value of TMH is 0.4∼1 mm, and TMH less than 0.35 mm indicates the possibility of DED.

SUPPLEMENTARY FIGURE 2
Image of meibomian gland. **(A)** Image of upper meibomian gland, and the loss of upper meibomian gland was 58.4%. **(B)** Image of lower meibomian gland, and the loss of lower meibomian gland was 5%.

References

1. Cao W, Luo J, Xiao Y. A review of current tools used for evaluating the severity of obstructive sleep apnea. *Nat Sci Sleep.* (2020) 12:1023–31. doi: 10.2147/NSS.S275252

2. Zhang D, Zhang Z, Li H, Ding K. Excessive daytime sleepiness in depression and obstructive sleep apnea: more than just an overlapping symptom. *Front Psychiatry.* (2021) 12:710435. doi: 10.3389/fpsyt.2021.710435

3. Althoff MD, Ghincea A, Wood LG, Holguin F, Sharma S. Asthma and three colinear comorbidities: obesity, OSA, and GERD. *J Allergy Clin Immunol Pract.* (2021) 9:3877–84. doi: 10.1016/j.jaip.2021.09.003

4. Lim EWL, Chee ML, Sabanayagam C, Majithia S, Tao Y, Wong TY, et al. Relationship between sleep and symptoms of tear dysfunction in Singapore Malays and Indians. *Invest Ophthalmol Vis Sci.* (2019) 60:1889–97. doi: 10.1167/iovs.19-26810

5. Storas AM, Strumke I, Riegler MA, Grauslund J, Hammer HL, Yazidi A, et al. Artificial intelligence in dry eye disease. *Ocul Surf.* (2021) 23:74–86. doi: 10.1016/j.jtos.2021.11.004

6. Craig JP, Nichols KK, Akpek EK, Caffery B, Dua HS, Joo CK, et al. TFOS DEWS II definition and classification report. *Ocul Surf.* (2017) 15:276–83. doi: 10.1016/j.jtos.2017.05.008

7. Mason L, Jafri S, Dortonne I, Sheppard JD Jr. Emerging therapies for dry eye disease. *Expert Opin Emerg Drugs.* (2021) 26:401–13. doi: 10.1080/14728214.2021.2011858

8. Karaca I, Yagci A, Palamar M, Tasbakan MS, Basoglu OK. Ocular surface assessment and morphological alterations in meibomian glands with meibography in obstructive sleep apnea Syndrome. *Ocul Surf.* (2019) 17:771–6. doi: 10.1016/j.jtos.2019.06.003

9. Chen CJ, Liu X, Chiou JS, Hang LW, Li TM, Tsai FJ, et al. Effects of Chinese herbal medicines on dementia risk in patients with sleep disorders in Taiwan. *J Ethnopharmacol.* (2021) 264:113267. doi: 10.1016/j.jep.2020.113267

10. Mehra R, Heinzer R, Castillo P. Current management of residual excessive daytime sleepiness due to obstructive sleep apnea: insights for optimizing patient outcomes. *Neurol Ther.* (2021) 10:651–72. doi: 10.1007/s40120-021-00289-6

11. Mendonca F, Mostafa SS, Morgado-Dias F, Ravelo-Garcia AG. An oximetry based wireless device for sleep apnea detection. *Sensors (Basel).* (2020) 20:888. doi: 10.3390/s20030888

12. Ayaki M, Tsubota K, Kawashima M, Kishimoto T, Mimura M, Negishi K. Sleep disorders are a prevalent and serious comorbidity in dry eye. *Invest Ophthalmol Vis Sci.* (2018) 59:DES143–50. doi: 10.1167/iovs.17-23467

13. Wan W, Wu Z, Lu J, Wan W, Gao J, Su H, et al. Obstructive sleep apnea is related with the risk of retinal vein occlusion. *Nat Sci Sleep.* (2021) 13:273–81. doi: 10.2147/NSS.S290583

14. Meng YF, Pu Q, Ma Q, Zhu W, Li XY. Neutrophil/lymphocyte ratio as an inflammatory predictor of dry eye disease: a case-control study. *Ther Clin Risk Manag.* (2021) 17:259–66. doi: 10.2147/TCRM.S298156

15. Ward Flemons W, Buysse D, Redline S, Pack A, Strohl K, Wheatley J, et al. Sleep-related breathing disorders in adults: recommendations for syndrome definition and measurement techniques in clinical research. (1999) The report of an american academy of sleep medicine task force. *Sleep.* 22:667–89.

16. Liu ZG. [Paying attention to the expert consensus on dry eye to standardize and promote the clinical diagnosis and treatment of dry eye]. *Zhonghua Yan Ke Za Zhi.* (2020) 56:726–9. doi: 10.3760/cma.j.cn112142-20200714-00476

17. Wang C, Xu WL, Li GW, Fu C, Li JJ, Wang J, et al. Impact of acupuncture on sleep and comorbid symptoms for chronic insomnia: a randomized clinical trial. *Nat Sci Sleep.* (2021) 13:1807–22. doi: 10.2147/NSS.S326762

18. Magno MS, Utheim TP, Snieder H, Hammond CJ, Vehof J. The relationship between dry eye and sleep quality. *Ocul Surf.* (2021) 20:13–9. doi: 10.1016/j.jtos.2020.12.009

19. Zolotoff C, Bertoletti L, Gozal D, Mismetti V, Flandrin P, Roche F, et al. Obstructive sleep apnea, hypercoagulability, and the blood-brain barrier. *J Clin Med.* (2021) 10:3099. doi: 10.3390/jcm10143099

20. Flores-Orozco EI, Tiznado-Orozco GE, Diaz-Pena R, Orozco EIF, Galletti C, Gazia F, et al. Effect of a mandibular advancement device on the upper airway in a patient with obstructive sleep apnea. *J Craniofac Surg.* (2020) 31:e32–5. doi: 10.1097/SCS.0000000000005838

21. Tapia IE, Shults J, Cielo CM, Kelly AB, Elden LM, Spergel JM, et al. Trial of intranasal corticosteroids to treat childhood OSA syndrome. *Chest.* (2022) 162:899–919. doi: 10.1016/j.chest.2022.06.026

22. Morsy NE, Amani BE, Magda AA, Nabil AJ, Pandi-Perumal SR, BaHammam AS, et al. Prevalence and predictors of ocular complications in obstructive sleep apnea patients: a cross-sectional case-control study. *Open Respir Med J.* (2019) 13:19–30. doi: 10.2174/1874306401913010019

23. Mittal R, Patel S, Galor A. Alternative therapies for dry eye disease. *Curr Opin Ophthalmol.* (2021) 32:348–61. doi: 10.1097/ICU.0000000000000768

24. Nijjar, M, Kotoulas SC, Kerr J, Riha RL. Floppy eyelid syndrome and obstructive sleep apnea: a unique phenotype? *Sleep Breath.* (2022). doi: 10.1007/s11325-022-02690-3 [Epub ahead of print].

25. Liu DT, Di Pascuale MA, Sawai J, Gao YY, Tseng SC. Tear film dynamics in floppy eyelid syndrome. *Invest Ophthalmol Vis Sci.* (2005) 46:1188–94. doi: 10.1167/iovs.04-0913

26. Muhafiz E, Olcen M, Erten R, Bozkurt E. Evaluation of meibomian glands in obstructive sleep apnea-hypopnea syndrome. *Cornea.* (2020) 39:685–90. doi: 10.1097/ICO.0000000000002252

27. Zhang X, Wang S, Xu H, Yi H, Guan J, Yin S. Metabolomics and microbiome profiling as biomarkers in obstructive sleep apnoea: a comprehensive review. *Eur Respir Rev.* (2021) 30:200220. doi: 10.1183/16000617.0220-2020

28. Stanek A, Brozyna-Tkaczyk K, Myslinski W. Oxidative stress markers among obstructive sleep apnea patients. *Oxid Med Cell Longev.* (2021) 2021:9681595. doi: 10.1155/2021/9681595

29. Bhatt SP, Guleria R, Kabra SK. Metabolic alterations and systemic inflammation in overweight/obese children with obstructive sleep apnea. *PLoS One.* (2021) 16:e0252353. doi: 10.1371/journal.pone.0252353

30. Qian X, Yin T, Li T, Kang C, Guo R, Sun B, et al. High levels of inflammation and insulin resistance in obstructive sleep apnea patients with hypertension. *Inflammation.* (2012) 35:1507–11. doi: 10.1007/s10753-012-9464-3

31. Ragnoli B, Pochetti P, Raie A, Malerba M. Interrelationship between obstructive sleep apnea syndrome and severe asthma: from endo-phenotype to clinical aspects. *Front Med (Lausanne).* (2021) 8:640636. doi: 10.3389/fmed.2021.640636

32. Negishi K, Ayaki M, Kawashima M, Tsubota K. Sleep and subjective happiness between the ages 40 and 59 in relation to presbyopia and dry eye. *PLoS One.* (2021) 16:e0250087. doi: 10.1371/journal.pone.0250087

33. Sayegh RR, Yu Y, Farrar JT, Kuklinski EJ, Shtein RM, Asbell PA, et al. Ocular discomfort and quality of life among patients in the dry eye assessment and management study. *Cornea.* (2021) 40:869–76. doi: 10.1097/ICO.0000000000002580

34. Shah PV, Zhu L, Kazi A, Zhu A, Shalshin A. The correlation between non-invasive ventilation use and the development of dry eye disease. *Cureus.* (2021) 13:e18280. doi: 10.7759/cureus.18280

35. Acar M, Firat H, Yuceege M, Ardic S. Long-term effects of PAP on ocular surface in obstructive sleep apnea syndrome. *Can J Ophthalmol.* (2014) 49:217–21. doi: 10.1016/j.jcjo.2013.11.010

Case report: Early onset Marin-Amat syndrome after receiving ChAdOx1 nCoV-19 vaccination

Ping-Feng Tsai[1,2,3] and Ying-Jen Chen[2,3]*

[1]Department of Medical Education, Taipei Veteran General Hospital, Taipei, Taiwan, [2]Department of Ophthalmology, Tri-Service General Hospital, Taipei, Taiwan, [3]School of Medicine, National Defense Medical Center, Taipei, Taiwan

While vaccination against COVID-19 is still ongoing, some rare adverse events temporally related to vaccinations have been reported, particularly with ChAdOx1 nCoV-19. Here, a 77-year-old male presented to our outpatient department with persistent ptosis of his left eye for 1 month. He initially received vaccination with ChAdOx1 nCoV-19 and developed symptoms of Bell's palsy 3 days later. He received a 14-day course of prednisolone, but the ptosis persisted. Marin-Amat syndrome was compatible with his symptoms of ptosis exacerbation during orbicularis oris exertion. A temporal correlation between ChAdOx1 nCoV-19 vaccination and Bell's palsy without infectious or autoimmune diseases was delineated. Further studies are needed to clarify the possible relationship between these two events.

KEYWORDS

ChAdOx1 nCoV-19, vaccine, Bell's palsy, facial synkinesis, AstraZeneca

Introduction

The coronavirus disease 2019 (COVID-19) global pandemic started in late 2019 and has recently been getting under control owing to the development of COVID-19 vaccines. One COVID-19 vaccine, ChAdOx1 nCoV-19, is an adenovirus-vectored vaccine and is nearly 100% effective in preventing serious events following COVID-19 infection (1). There are several commonly known side effects, including muscle pain, headache, and fever (1). However, there were no reports of Bell's palsy after ChAdOx1 nCoV-19 vaccination. Here, we report a case where the patient further developed a rare complication, Marin-Amat syndrome.

Case description

A 77-year-old man was referred to our clinic complaining of a left droopy eyelid. His medical history included hypertension, chronic obstructive pulmonary disease, and hyperlipidemia, which was followed at a local medical clinic. He initially received the first dose of ChAdOx1 nCoV-19 (AstraZeneca, AZ) and started noticing that his left eyelid gradually became ptotic 3 days later. Eleven days after the initial vaccination,
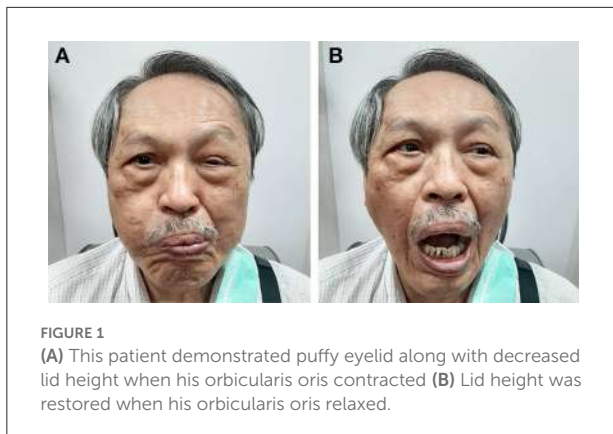
FIGURE 1
(A) This patient demonstrated puffy eyelid along with decreased lid height when his orbicularis oris contracted **(B)** Lid height was restored when his orbicularis oris relaxed.
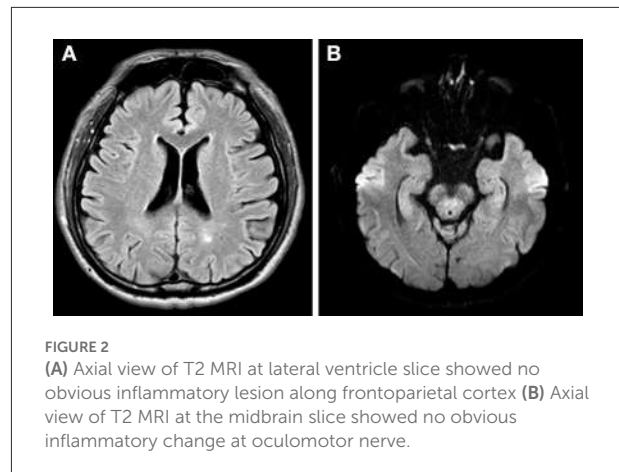
FIGURE 2
(A) Axial view of T2 MRI at lateral ventricle slice showed no obvious inflammatory lesion along frontoparietal cortex **(B)** Axial view of T2 MRI at the midbrain slice showed no obvious inflammatory change at oculomotor nerve.

he experienced weakness of the left facial muscle. Physical examination revealed left-sided blink reflex impairment, ptosis, and weakness of left side facial muscle including orbicularis oris. Extraocular movement and light reflex were intact on both eyes. There was no vesicle/blistering noted on his face and his extraocular movement as well as light reflex were intact on both sides. Lab tests including thyroid function, vitamin B_{12}, folate, glucose, cell count, electrolytes, renal function, liver function were within normal limits. Bell's palsy of his left side was diagnosed at our neurology clinic. He started prednisolone (40 mg QD) for 14 days; however, the left droopy eyelid showed little improvement. He then visited our ophthalmology clinic for persistent droopy eyelid despite a course of two-week prednisolone. His corrected visual acuity was 6/7.5 and 6/6 on his right and left eye, respectively. The intraocular pressure of both eyes was 18 mmHg. Slit-lamp examination was unremarkable except for puffy eyelids of his left eye with intermittent myokymic motion of his left upper and lower lids. Marginal reflex distance 1 (MRD1) of his left eye was 1 mm, in contrast to 3 mm on the right. His left eye was closed tightly as we asked him to open his mouth or smile (Figure 1). Note that his smile was symmetric at examination. Fundus imaging and optical coherence tomography of his macula and disc were unremarkable, and no obvious inflammatory lesions, including on the oculomotor and facial nerve region, were observed on the brain MRI (Figure 2). Marin-Amat syndrome was diagnosed.

Discussion

This paper reported a case of Bell's palsy in a patient who received the ChA-dOx1 nCoV-19 vaccine. The diagnosis of Bell's palsy presented after excluding the known etiology resulting in facial palsy. Although few studies have reported facial weakness after ChAdOx1 nCoV-19 vaccination, none have reported idiopathic Bell's palsy after ChAdOx1 nCoV-19 vaccination, to our knowledge. Diogo et al. (2) reported a patient

with facial weakness with geniculate ganglion enhancement on brain MRI after the first vaccination of ChAdOx1 nCoV-19 9 days later, along with symptoms of otalgia, implying Ramsey Hunt syndrome. Nicola et al. (3) reported a patient with facial palsy along with paraesthesia of the four limbs 10 days after the first vaccination. Electrophysiological findings were compatible with demyelinating motor polyneuropathy, which was diagnosed as Guillain Barre syndrome; the facial palsy was thought to stem from it (Table 1). In our case, a brain MRI revealed no obvious inflammatory changes or structural lesions compressing the facial nerve and oculomotor nerve, no obvious facial pain, vesicles, or other focal neurologic signs. However, the patient experienced an episode 3 days after vaccination, and symptoms culminated 11 days after vaccination; hence, the diagnosis of Bell's palsy.

The etiology of Bell's palsy is speculated to be multifactorial. Virus reactivation and inflammation may play a major role in the pathogenesis of Bell's palsy (4). However, the relationship between facial palsy and COVID-19 vaccination remains largely unclear. Cases of facial palsy after COVID-19 vaccination are seen more commonly in those who receive mRNA vaccinations, particularly with the BNT162b2 vaccine. A case-controlled study (5) conducted in Israel enrolled 37 patients with acute onset facial palsy after exposure to the BNT162b2 vaccine. They compared these patients with 74 participants in the control group who were matched with the date of admission to eliminate bias owing to the different prevalence of vaccination and different seasonal incidence of Bell's palsy. They described the time interval between the first vaccination to facial palsy ranged from 3 to 14 days, and yet no statistically significant increase in odds ratio was found after BNT162b2 vaccination. Another study set to compare the incidence of facial palsy after mRNA vaccination was similar, even slightly lower, compared to those after receiving influenza or other viral vaccines (6). ChAdOx1 nCoV-19 was differed from other mRNA COVID-19 vaccines in its excipient, drug vector, and, as expected, its pharmacovigilance profile. Given that most of the studies were conducted to explore the association between mRNA COVID-19

TABLE 1   Demonstrates possible facial palsy etiologies following ChAdOx1 nCoV-19 vaccination.

Case	Age/Sex	Time interval after AZ vaccination	Diagnosis	Treatment	Ref
1	77/M	3	Bell's palsy	Prednisolone 40mg/day for 14 days	NA
2	42/M	9	Ramsey Hunt syndrome	Prednisolone 60mg/day for 7 days	(2)
3	59/M	10	Guillain Barre syndrome	IVIG 0.4 mg/kg for 5 days	(3)

Case 1 in this table was the case we presented, while case 2 and 3 were cases reported previously. Note that the etiology of facial palsy following ChAdOx1 nCoV-19 vaccination was completely different which resulted in different treatment and a different clinical course.

vaccine and facial palsy, it remains largely unknown about the association between facial palsy and other COVID-19 vaccines, particularly ChAdOx1 nCoV-19.

Several disproportionality analyses were carried out *via* exploiting the information in the WHO pharmacovigilance database, VigiBase. Notably, cerebral venous thrombosis was found to have a high association with COVID-19 vaccines (7). COVID-19 vaccines were also found to be potentially associated with CNS demyelinating diseases, although a low association and was comparable with that of other viral vaccines (8). Our case highlighted a possible relationship between facial palsy and ChAdOx1 nCoV-19. Collectively, they demonstrate that COVID-19 vaccines may potentially lead to neurologic adverse events. The relationship between facial palsy and COVID-19 vaccines remained debatable, further epidemiological studies are warranted to clarify these observations.

This patient received a course of oral prednisolone and still experienced ptosis. Orbicularis oculi myokymia and synkinesis of the eyelid along with jaw motion were also observed, which is the key feature of Marin-Amat syndrome. Marin-Amat syndrome is a rare form of acquired facial synkinesis that manifests as involuntary eyelid closure with jaw movements. Ptosis is the most common complaint in these patients, followed by ptosis when eating. It is an overlooked etiology of ptosis and was traditionally thought as a late complication of the initial facial nerve injury. It is thought to result from aberrant facial regeneration (AFR) after an initial insult to the facial nerve (9). The pathogenesis of AFR is largely unknown, Celik et al. (10) demonstrated that the incidence of AFR following facial injury was related to the severity of injury and implied that the development of synkinesis would take place much earlier than 4 months. It is an imperative diagnosis to recognize in patients with persistent ptosis after initial facial injury.

Whether the aberrant facial regeneration is related to vaccination is unknown. The diagnosis of Marin-Amat syndrome is often overseen, and prudent evaluation for patients with ptosis, especially those with persistent ptosis after facial nerve injury, is needed. This case exhibits features of Marin-Amat syndrome, including intermittent orbicularis oculi myokymia, which was exacerbated by jaw movement. This feature implies a previous facial nerve insult, which is thought to be Bell's palsy, in our case.

Conclusion

This is the first case report delineating an episode of Bell's palsy complicated with Marin-Amat syndrome following ChAdOx1 nCoV-19 vaccination. Further studies are warranted to clarify the relationship between Bell's palsy and ChAdOx1 nCoV-19 vaccination.

Data availability statement

The original contributions presented in the study are included in the article/supplementary material, further inquiries can be directed to the corresponding author/s.

Ethics statement

The studies involving human participants were reviewed and approved by Institutional Review Board of Tri-Service General Hospital. The patients/participants provided their written informed consent to participate in this study. Written informed consent was obtained from the individual(s) for the publication of any potentially identifiable images or data included in this article.

Author contributions

Conceptualization: P-FT and Y-JC. Methodology, software, validation, formal analysis, investigation, resources, writing—review and editing, visualization, supervision, and project administration: Y-JC. Data curation and writing—original draft preparation: P-FT. All authors have read and agreed to the published version of the manuscript.

Conflict of interest

The authors declare that the research was conducted in the absence of any commercial or financial relationships that could be construed as a potential conflict of interest.

Publisher's note

All claims expressed in this article are solely those of the authors and do not necessarily represent those of their affiliated organizations, or those of the publisher, the editors and the reviewers. Any product that may be evaluated in this article, or claim that may be made by its manufacturer, is not guaranteed or endorsed by the publisher.

References

1. Voysey M, Clemens SAC. Safety and efficacy of the ChAdOx1 nCoV-19 vaccine (AZD1222) against SARS-CoV-2: an interim analysis of four randomised controlled trials in Brazil, South Africa, and the UK. *Lancet.* (2021) 397:99–111. doi: 10.1016/S0140-6736(20)32661-1

2. Corrêa DG, Cañete LAQ. Neurological symptoms and neuroimaging alterations related with COVID-19 vaccine: Cause or coincidence? *Clin Imaging.* (2021) S80:348–52. doi: 10.1016/j.clinimag.2021.08.021

3. Nasuelli NA, De Marchi F. A case of acute demyelinating polyradiculoneuropathy with bilateral facial palsy after ChAdOx1 nCoV-19 vaccine. *Neurol Sci.* (2021) 42:4747–9. doi: 10.1007/s10072-021-05467-w

4. Zhang W, Xu L. The etiology of Bell's palsy: a review. *J Neurol.* (2020) 267:1896–905. doi: 10.1007/s00415-019-09282-4

5. Shemer A, Pras E. Association of COVID-19 vaccination and facial nerve palsy: A case-control study. *JAMA Otolaryngol Head Neck Surg.* (2021) 147:739–43. doi: 10.1001/jamaoto.2021.1259

6. Renoud L, Khouri C. Association of facial paralysis with mRNA COVID-19 vaccines: A disproportionality analysis using the world health organization pharmacovigilance database. *JAMA Intern Med.* (2021) 181:1243–5.

7. Park J, Park MS. Association of cerebral venous thrombosis with mRNA COVID-19 vaccines: A disproportionality analysis of the world health organization pharmacovigilance database. *Vaccines (Basel).* (2022) 10:799. doi: 10.3390/vaccines10050799

8. Kim JE, Park J. A disproportionality analysis for the association of central nervous system demyelinating diseases with COVID-19 vaccination using the World Health Organization pharmacovigilance database. *Mult Scler.* (2022) 28:2112–23. doi: 10.1177/13524585221109397

9. Chao YJ, Tsai CC. Change of eyelid parameters in patients with marin-amat syndrome. *Ophthalmic Plast Reconstr Surg.* (2020) 36:298-301. doi: 10.1097/IOP.0000000000001538

10. Celik M, Forta H, Vural C. The development of synkinesis after facial nerve paralysis. *Eur Neurol.* (2000) 43:147–51. doi: 10.1159/000008154

Frontiers in Medicine

Translating medical research and innovation into improved patient care

A multidisciplinary journal which advances our medical knowledge. It supports the translation of scientific advances into new therapies and diagnostic tools that will improve patient care.

Discover the latest Research Topics

See more →

frontiers | Research Topics